



Investigating Halogen Bonding in Nitrogen Systems

A thesis submitted to the University of Manchester for the
Degree of Doctor of Philosophy in the Faculty of Science and
Engineering

2022

Sultan Salim Obaid Alkaabi

School of Natural Science

Department of Chemistry

Table of Contents

<i>List of Scheme</i>	5
<i>List of Figures</i>	6
<i>List of Tables</i>	17
<i>Abstract</i>	21
<i>Declaration</i>	23
<i>Copyright Statement</i>	23
<i>Acknowledgements</i>	25
<i>Abbreviations</i>	26
Chapter 1. Introduction	27
1.1. Thesis structure	27
1.2. Intermolecular forces	28
1.3. Halogen bonding	28
1.3.1. The role of the σ hole	29
1.3.2. Comparing halogen atoms	32
1.3.3. Halogen bond strength.....	33
1.3.4. Characteristics of halogen bonds	34
1.3.5. Applications of halogen bonds	35
1.3.6. Halogen –bonded systems	35
1.4. Growing crystals	44
1.4.1. Definition.....	44
1.4.2. Different methods for growing crystals	45
1.5. X-ray diffraction	47
1.5.1. Definition and generation of X-rays	48
1.5.2. Basic of crystal lattices	49
1.5.3. Bragg’s law.....	53
1.5.4. Single crystal X-ray diffraction	54

1.5.5. The steps followed to determine the crystal structure	55
1.6. Quantum chemical calculations	59
1.6.1. The quantum theory of atoms in molecules (QTAIM) analysis	60
1.7. Summary	64
<i>Chapter 2. Manuscript 1: Halogen bonding in a series of bromofluorobenzenes and 1,4-diazabicyclo[2.2.2]octane (DABCO)</i>	<i>69</i>
2.1. Abstract	69
2.2. Introduction	69
2.3. Experimental.....	72
2.3.1. Synthesis and crystallization	72
2.3.2. Refinement	73
2.4. Result and Discussion.....	75
<i>Chapter 3. Manuscript 2: A Crystallographic and QTAIM study of halogen bonding in a series of iodofluorobenzenes and hexamethylenetetramine and 1,3,5-triaza-phosphaadamantane</i>	<i>95</i>
3.1. Abstract	95
3.2. Introduction	95
3.3. Experimental.....	98
3.3.1. Synthesis and crystallization	99
3.3.2. Refinement	100
3.3.3. QTAIM experimental	102
3.4. Result and Discussion.....	102
<i>Chapter 4. Manuscript 3: Halogen bonds involving 1,4-diiodotetrafluorobenzene with a variety of nitrogen-based aromatic halogen bond acceptors 130</i>	
4.1. Abstract	130
4.2. Introduction	130
4.3. Experimental.....	133
4.3.1. Synthesis and crystallization	133
4.3.2. Refinement	134

4.4. Result and Discussion.....	136
<i>Chapter 5. Manuscript 4: Variety of halogen bonded adducts containing compounds using pyrimidine derivatives</i>	<i>151</i>
5.1. Abstract	151
5.2. Introduction	151
5.3. Experimental.....	153
5.3.1. Synthesis and crystallization	153
5.3.2. Refinement	154
5.4. Result and discussion.....	156
<i>Chapter 6. Manuscript 5: Crystallographic and QTAIM studies of variety of halogen bonded adducts containing compounds using piperazine</i>	<i>172</i>
6.1. Abstract	172
6.2. Introduction	172
6.3. Experimental.....	175
6.3.1. Synthesis and crystallization	175
6.3.2. Refinement	176
6.4. Result and Discussion.....	178
<i>Chapter 7. Conclusions and Future work</i>	<i>203</i>
<i>Chapter 8. Appendices</i>	<i>208</i>

Words count: 73863

List of Scheme

Scheme 1.1 Representation of the halogen bond (XB), where X = Cl, Br, or I and B = the halogen bond acceptor (base with lone pair), R = the covalently bonded atom or group, the red area represents the σ -hole.	29
Scheme 2.1 Compounds used in crystallization	71
Scheme 3.1 Compounds used in this study.....	98
Scheme 4.1 Compounds used in crystallisation.....	133
Scheme 5.1 Labelling notation of the compounds using in building XB halogen bonds adducts reported in this study	153
Scheme 6.1 Compounds used in this study.....	174

List of Figures

Figure 1.1 The two different regions of electron density that occur around the bonded halogen atom X.....	31
Figure 1.2 (i) Halogen-halogen type (I) $\theta_1 = \theta_2 \approx 120^\circ$ and (II) interactions $\theta_1 \approx 90^\circ$ and $\theta_2 \approx 180^\circ$; (ii) the directional Lewis base halogen bond interactions, where $\theta \approx 180^\circ$. Modified from reference ⁹	31
Figure 1.3 The molecular electrostatic potential, in Hartees, at the 0.001 electrons Bohr ⁻³ isodensity surface of CF ₄ , CF ₃ Cl, CF ₃ Br, and CF ₃ I. Taken from ⁶	33
Figure 1.4 Histogram of N...I, distance related to the 88 structures, less than the sum of the vdW radii 3.53 Å	36
Figure 1.5 Histogram of C-I...N angles between 150–180° for the 88 structures involving N...I	37
Figure 1.6 Packing diagram of halogen bonds in (a) 1,3,5-TITFB and DABCO, (b) 1,2-DITFB and DABCO ²⁸ . The colour key is as follows: gray, carbon; purple, iodine; blue, nitrogen; yellow, fluorine; white, hydrogen.....	38
Figure 1.7 Packing diagram of halogen bonds in (a) 1,3,5-TITFB and hexamethylenetetramine, (b) 1,3,5-TITFB and DABCO. The colour key is as follows: gray, carbon; purple, iodine; blue, nitrogen; yellow, fluorine; white, hydrogen. ³⁰	39
Figure 1.8 Fluoro-substituted iodobenzenes used in Catalano et al. ²⁵	40

Figure 1.9 Halogen-bonded structures found in Catlano and colleagues' study ²⁵ ,. The colour key is as follows: gray, carbon; purple, iodine; blue, nitrogen; yellow, fluorine; white, hydrogen.	41
Figure 1.10 Histogram of N...Br, distance related to the six structures, less than the sum of the vdW radii, 3.40 Å.	42
Figure 1.11 Packing diagram of halogen bonds in (a) 1,4-DITFB and DABCO, (b) 1,4-DITFB and piperazine in ²⁹ ; The colour key is as follows: gray, carbon; brown, bromine; blue, nitrogen; yellow, fluorine; white, hydrogen.	44
Figure 1.12 Slow evaporation	45
Figure 1.13 Slow cooling	46
Figure 1.14 Vapour diffusion	46
Figure 1.15 Liquid–liquid diffusion	47
Figure 1.16 Crystal dimensions and the electromagnetic spectrum ⁴¹	48
Figure 1.17 Difference in shape between amorphous (a) and crystalline (b) solids	49
Figure 1.18 Crystal lattice and unit cell	50
Figure 1.19 Fourteen possible Bravais lattices ⁴⁵	52
Figure 1.20 Miller indices <i>h</i> , <i>k</i> and <i>l</i> and their intercepts with the <i>a</i> , <i>b</i> , and <i>c</i> axes	53
Figure 1.21 Bragg's concept	54
Figure 1.22 X-ray single crystal instruments	55
Figure 1.23 Flow chart describing the steps to determine a crystal structure	56
Figure 1.24 Methods of mounting a crystal ³⁸	57
Figure 1.25 Local maxima, local minima, and saddle point curvatures taken from	61

Figure 1.26 Crystal structure of system studied in reference 54. ⁶⁵	63
Figure 1.27 Illustration of some types of critical points and XB bond paths.....	64
Figure 2.1 Views of the asymmetric unit of halogen-bonded adduct 1a , showing the atom numbering scheme, disordered in DABCO have been removed for clarity but carbon, nitrogen and hydrogen atoms in DABCO is half occupancy, each atom is therefore modelled with 0.5 occupancy. Ellipsoids are drawn at 50% probability level. The colour key is as follows: gray, carbon; brown, bromine; blue, nitrogen; green, fluorine; white, hydrogen.	75
Figure 2.2 A view of intermolecular N...Br halogen bonds and F...F interactions (stippled line) in crystal structure 1a . The colour key is as follows: grey, carbon; brown, bromine; blue, nitrogen; green, fluorine; white, hydrogen. [Symmetry codes :(i) +x, 1/2-y, 1/2+z (i) 1-x, -y, 1-z].	76
Figure 2.3 View of the asymmetric unit of halogen-bonded adduct 2a , showing the atom numbering. Ellipsoids are drawn at 50% probability level. The colour key is as follows: gray, carbon; brown, bromine; blue, nitrogen; green, fluorine; white, hydrogen.....	78
Figure 2.4 A view of intermolecular halogen bonds and F...H interactions in crystal structure 2a (Stippled line). [Symmetry codes :(i) 1/2+x,3/2-y,1/2+z]. The colour key is as follows: gray, carbon; brown, bromine; blue, nitrogen; green, fluorine; white, hydrogen.	79
Figure 2.5 View of the asymmetric unit of halogen-bonded adduct 3a , showing the atom numbering. Ellipsoids are drawn at 50% probability level. The colour key is as follows: gray, carbon; brown, bromine; blue, nitrogen; green, fluorine; white, hydrogen.....	81
Figure 2.6 Crystal packing of 3a showing N...Br halogen, bonds π - π stacking and Br...F between adjacent trimers. The colour key is as follows: gray, carbon; brown, bromine; blue, nitrogen; green, fluorine; white, hydrogen. Generic atom labels	

without symmetry codes have been used, Symmetry codes: (i) $+x, +y, 1+z$; (ii) $-1/2, 3/2-y, 1/2+z$ 82

Figure 2.7 View of the asymmetric unit of halogen-bonded adduct **4a**, the DABCO molecule is disordered across two sites and located about a special position (an inversion centre), each atom is therefore modelled with 0.25 occupancy to account for the doubling that occurs when applying the inversion symmetry operation to give an overall 2:1 ratio of $C_6F_4Br_2$:DABCO. Ellipsoids are drawn at 50% probability level, disordered DABCO have been removed for clarity..... 84

Figure 2.8 Crystal packing of **4a** showing N...Br halogen bonds, π - π stacking and Br...F between adjacent trimers. Symmetry codes: (i) $+x, +y, 1+z$; (ii) $1-x, 1-y, -z$. The colour key is as follows: grey, carbon; brown, bromine; blue, nitrogen; green, fluorine; white, hydrogen. Generic atom labels without symmetry codes have been used..... 85

Figure 2.9 The determined X-ray structure (left) and molecular graph (right) for trimers from adducts **1a**..... 89

Figure 2.10 The determined X-ray structure (left) and molecular graph (right) for trimers from adducts **2a**..... 90

Figure 2.11 The determined X-ray structure (left) and molecular graph (right) for trimers from adducts **3a**..... 90

Figure 2.12 The determined X-ray structure (left) and molecular graph (right) for trimers from adducts **4a**..... 91

Figure 3.1 Views of the asymmetric unit of halogen-bonded adduct **1a**, showing the atom numbering, Ellipsoids are drawn at 50% probability level. The colour key is as follows: gray, carbon; purple, iodine; blue, nitrogen; green, fluorine; white, hydrogen..... 103

Figure 3.2 View of intermolecular halogen bonds (red lines) and the other non-covalent interactions (dark blue lines) in **1a**. The colour key is as follows: gray, carbon; purple, iodine; blue, nitrogen; green, fluorine; white, hydrogen..... 104

Figure 3.3 The asymmetric unit of **2a.1** showing the atom numbering, Ellipsoids are drawn at 50% probability level. The colour key is as follows: gray, carbon; purple, iodine; blue, nitrogen; green, fluorine; white, hydrogen..... 106

Figure 3.4 View of one halogen bonded (red lines) and other weak F...F and F...H interactions (dark blue lines) in **2a.1**. The colour key is as follows: gray, carbon; purple, iodine; blue, nitrogen; yellow, fluorine; white, hydrogen..... 107

Figure 3.5 The asymmetric unit of **2a** and the atoms numbering. Ellipsoids are drawn at 50% probability level. The colour key is as follows: gray, carbon; purple, iodine; blue, nitrogen; green, fluorine; white, hydrogen..... 109

Figure 3.6 View of 2D halogen bonds (red lines), π - π stacking and other weak F...F and F...H interactions (dark blue lines) in **2a**. The colour key is as follows: gray, carbon; purple, iodine; blue, nitrogen; yellow, fluorine; white, hydrogen. .. 110

Figure 3.7 A view of the structure of halogen-bonded adduct **3a**, showing the atom numbering, Ellipsoids are drawn at 50% probability level, The colour key is as follows: gray, carbon; purple, iodine; blue, nitrogen; green, fluorine; white, hydrogen. [Symmetry codes: (i) $1/2-x, 3/2-y, +z$ (ii) $3/2-x, 3/2-y, +z$]...... 112

Figure 3.8 View of one halogen bonded (red lines) and I...I, F...F interactions (dark blue lines) in **3a**, The colour key is as follows: gray, carbon; purple, iodine; blue, nitrogen; yellow, fluorine; white, hydrogen..... 113

Figure 3.9 A view of halogen- bonded adduct **4b.1**, showing the atom numbering. Ellipsoids are drawn at 50% probability level, the colour key is as follows: gray, carbon; purple, iodine; blue, nitrogen; green, fluorine; white, hydrogen. [Symmetry codes: (i) $-x, 1-y, 2-z$ (ii) $+x, 3/2-y, +z$]. 115

Figure 3.10 View of the zigzag halogen bonded shape (red lines) and F...H weak interactions (dark blue lines) in 4b.1 , the colour key is as follows: gray, carbon; purple, iodine; blue, nitrogen; yellow, fluorine; white, hydrogen.....	117
Figure 3.11 View of halogen- bonded adduct 4b , showing the atom numbering. Ellipsoids are drawn at 50% probability level, The colour key is as follows: gray, carbon; purple, iodine; blue, nitrogen; green, fluorine; white, hydrogen. [Symmetry codes: (i) 1-x, 1-y, 1-z].....	118
Figure 3.12 View of halogen bonds (red lines) and C-H...O interactions (dark blue lines) display in 4b . The colour key is as follows: gray, carbon; purple, iodine; blue, nitrogen; yellow, fluorine; white, hydrogen; red, oxygen; orange, phosphorus. ...	118
Figure 3.13 Showing determined X-ray structure (left) and molecular graph (right) of adducts 1a	124
Figure 3.14 Showing determined X-ray structure (left) and molecular graph (right) of adducts 2a.1	124
Figure 3.15 Showing determined X-ray structure (left) and molecular graph (right) of adducts 2a	125
Figure 3.16 Showing determined X-ray structure (left) and molecular graph (right) of adducts 3a	125
Figure 3.17 Showing determined X-ray structure (left) and molecular graph (right) for adducts 4b.1	126
Figure 3.18 Showing determined X-ray structure (left) and molecular graph (right) of adducts 4b	126
Figure 4.1 A view of the structure of halogen-bonded adduct 1a , showing the atom numbering, Ellipsoids are drawn at 50% probability level, [Symmetry codes: (i) -x, 1-y, -z (ii) 2-x, 1-y, 1-z]. colour codes: Green, fluorine; blue, nitrogen; white, hydrogen and grey carbon.	136

Figure 4.2 Main N...I halogen bonds (a) and secondary F...H interactions (b) in 1a (stippled line), colour codes: purple, iodine; Green, fluorine; blue, nitrogen; white, hydrogen and grey carbon.	137
Figure 4.3 Views of the asymmetric unit of halogen-bonded adduct 2a , showing the atom numbering, ellipsoids are drawn at 50% probability level, colour codes: purple, iodine; Green, fluorine; blue, nitrogen; white, hydrogen and grey carbon	138
Figure 4.4 Main N...I halogen bonds (a) and secondary interactions (b) in 2a , (stippled line), colour codes: purple, iodine; Green, fluorine; blue, nitrogen; white, hydrogen and grey carbon	139
Figure 4.5 A view of the structure of halogen-bonded adduct 3a , showing the atom numbering, Ellipsoids are drawn at 50% probability level, [Symmetry codes :(i) 3/2-x, +y, 1-z (ii) 1/2-x, 3/2-y, 1/2 -z], colour codes: purple, iodine; Green, fluorine; blue, nitrogen; white, hydrogen and grey carbon.	140
Figure 4.6 A view of intermolecular N...I halogen bonds and F...H and N...H non-conventional hydrogen bond (stippled line) in 3a , colour codes: purple, iodine; Green, fluorine; blue, nitrogen; white, hydrogen and grey carbon.	141
Figure 4.7 Views of the asymmetric unit of halogen-bonded adduct 4a , showing the atom numbering, Ellipsoids are drawn at 50% probability level, colour codes: purple, iodine; Green, fluorine; blue, nitrogen; white, hydrogen and grey carbon.	142
Figure 4.8 A view of intermolecular N...I halogen bonds and N...H-N traditional hydrogen bond interaction (stippled line) in 4a , colour codes: purple, iodine; green, fluorine; blue, nitrogen; white, hydrogen and grey carbon.	143
Figure 4.9 Histogram shows the average bond distances of the 1a-4a and their position compared with the CSD reported structures for N...I containing structures reported until now.	145
Figure 4.10 The determined X-ray structure (left) and molecular graph (right) for adduct 1a	147

Figure 4.11 The determined X-ray structure (left) and molecular graph (right) for adduct 2a	147
Figure 4.12 The determined X-ray structure (left) and molecular graph (right) for adduct 3a	148
Figure 4.13 The determined X-ray structure (left) and molecular graph (right) for adduct 4a	148
Figure 5.1 Views of the asymmetric unit of halogen-bonded adduct 1a , showing the atom numbering. Ellipsoids are drawn at 50% probability level, colour codes: purple, iodine; green, fluorine; blue, nitrogen; white, hydrogen and grey carbon.	156
Figure 5.2 Crystal packing of 1a down the a axis, showing N...I halogen bonds beside the other weak intermolecular interactions (H...F, H...N and π ... π stacking), The colour key is as follows: gray, carbon; purple, iodine; blue, nitrogen; yellow, fluorine; white, hydrogen.	158
Figure 5.3 View of the asymmetric unit of halogen-bonded adduct 2a , showing the atom numbering. Ellipsoids are drawn at 50% probability level. The colour key is as follows: grey, carbon; blue, nitrogen; green, fluorine; white, hydrogen.....	159
Figure 5.4 Crystal packing of 2a down the b axis, showing N...I halogen bonds beside the other weak intermolecular interactions (H...F, H...N and π ... π stacking) colour codes: yellow, fluorine; blue, nitrogen; white, hydrogen and grey carbon; purple, iodine.....	160
Figure 5.5 Views of the asymmetric unit of halogen-bonded adduct 2c , showing the atom numbering. Ellipsoids are drawn at 50% probability level, colour codes: green, fluorine; blue, nitrogen; white, hydrogen and grey carbon, purple, iodine.....	161
Figure 5.6 crystal packing of 2c along a showing the N...I halogen bonds and the secondary interactions, colour codes: green, fluorine; blue, nitrogen; white, hydrogen and grey carbon, purple, iodine.....	162

Figure 5.7 Views of the asymmetric unit of halogen-bonded adduct 3b , showing the atom numbering. Ellipsoids are drawn at 50% probability level., colour codes: green, fluorine; blue, nitrogen; white, hydrogen and grey carbon, purple, iodine.	164
Figure 5.8 crystal packing of 3b along a showing the N...I halogen bonds and the secondary interactions, colour codes: yellow, fluorine; blue, nitrogen; white, hydrogen and grey carbon, purple, iodine.....	166
Figure 5.9 The determined X-ray structure (left) and molecular graph (right) for adduct 1a	168
Figure 5.10 The determined X-ray structure (left) and molecular graph (right) for adduct 2a	168
Figure 5.11 The determined X-ray structure (left) and molecular graph (right) for adduct 2c	169
Figure 5.12 The determined X-ray structure (left) and molecular graph (right) for adduct 3b	169
Figure 6.1 A view of intermolecular N...H hydrogen bonds (blue lines) in ITIZOA crystal structure reported by Parkin and his group, 2004. Generic atom labels without symmetry codes have been used.	178
Figure 6.2 Views of the structure of halogen-bonded adduct 1a , showing the atom numbering. Ellipsoids are drawn at 50% probability level. [Symmetry codes: (i) - $x+2, -y+2, -z+1$], colour codes: green, fluorine; blue, nitrogen; purple, iodine; white, hydrogen and grey carbon.	180
Figure 6.3 A view of intermolecular N...I halogen bonds (red lines), and F...F interactions in the crystal structure of 1a . Generic atom labels without symmetry codes have been used. colour codes: Yellow, fluorine; blue, nitrogen; white, hydrogen, purple, iodine and grey carbon.....	180
Figure 6.4 Views of the structure of halogen-bonded adduct 2a , showing the atom numbering. Ellipsoids are drawn at 50% probability level. colour codes: green,	

fluorine; blue, nitrogen;purple, iodine; white, hydrogen and grey carbon. [Symmetry codes: (i)1-x, 1-y, -1-z (ii) +x, 3/2-y, +z].....	181
Figure 6.5 A view of intermolecular N...I halogen bonds (red lines), and F...H interactions in crystal structure 2a , colour codes: Yellow, fluorine; blue, nitrogen; white, hydrogen; purple, iodine; and grey carbon.....	182
Figure 6.6 Views of the structure of halogen-bonded adduct 3a , showing the atom numbering- Ellipsoids are drawn at 50% probability level. colour codes: green, fluorine; blue, nitrogen; purple, iodine; white, hydrogen and grey carbon. [Symmetry codes: (i)2-x, -y, 2-z].....	184
Figure 6.7 A view of intermolecular N...I halogen bonds (red lines), F...H and I...H interactions in crystal structure 3a . Generic atom labels without symmetry codes have been used. colour codes: Yellow, fluorine; blue, nitrogen; white, hydrogen; purple, iodine; and grey carbon.....	186
Figure 6.8 Views of the structure of halogen-bonded adduct 4a , showing the atom numbering. Ellipsoids are drawn at 50% probability level. colour codes: brown, bromine; green, fluorine; blue, nitrogen; white, hydrogen and grey carbon. [Symmetry codes: (i) -x, 2-y, 1-z]	189
Figure 6.9 A view of intermolecular N...Br (red lines) halogen bonds, F...F and Br...H interactions in crystal structure 4a . Generic atom labels without symmetry codes have been used. colour codes: brown, bromine; yellow, fluorine; blue, nitrogen; white, hydrogen and grey carbon.....	190
Figure 6.10 Views of the structure of halogen-bonded adduct 5a , showing the atom numbering, the alternate disordered positions of atoms of the arene are shown shadowed .Ellipsoids are drawn at 50% probability level,colour codes: brown, bromine; green, fluorine; blue, nitrogen; white, hydrogen and grey carbon. [Symmetry codes: (i) -x, 1-y, 1-z].	192

Figure 6.11 A view of intermolecular N...Br halogen bonds (red lines), Br...Br and F...H interactions in crystal structure 5a . colour codes: brown, bromine; yellow, fluorine; blue, nitrogen; white, hydrogen and grey carbon.	193
Figure 6.12 The determined X-ray structure (left) and molecular graph (right) with the related electron density ρ BCP for adducts 1a	196
Figure 6.13 The determined X-ray structure (left) and molecular graph (right) with the related electron density ρ BCP for adducts 2a	196
Figure 6.14 The determined X-ray structure (left) and molecular graph (right) with the related electron density ρ BCP for adducts 3a	197
Figure 6.15 The determined X-ray structure (left) and molecular graph (right) with the related electron density ρ BCP for adducts 4a	197
Figure 6.16 The determined X-ray structure (left) and molecular graph (right) with the related electron density ρ BCP for adducts 5a	198

List of Tables

Table 1.1 Common halogen bond donors and acceptors ⁴	29
Table 1.2 The specific number of N...I structures and the search details using CSD	35
Table 1.3 15 CSD hits after searching specifically for structure 1 (interaction between 0–2.8 Å, angle range 150–180°), including DABCO as a halogen bond acceptor (for abbreviations see the text below).....	37
Table 1.4 The specific number of Br...N structures and the search details using CSD	42
Table 1.5 N...Br interactions less than the sum of the van der Waals radii (3.40 Å) in the CSD database	43
Table 1.6 The seven crystal systems and related cell dimensions.....	51
Table 2.1 Experimental details.	74
Table 2.2 Selected bond distances of 1a in Å.....	77
Table 2.3 Selected bond distances of 2a in Å.....	80
Table 2.4 Selected bond distances of 3a in Å.....	83
Table 2.5 Selected bond distances of 4a in Å.....	86
Table 2.6 N...Br halogen-bond distances (Å) and angles (°) in the current work and previously reported structures.	86
Table 2.7 Intermolecular interactions in (Å) less than the sum of the van der Waals radii observed in the current work and previously reported structures.	87
Table 2.8 Topological parameters calculated at B3LYP/6-311G** level of theory	89

Table 3.1 Experimental details of 1a-2a.1	100
Table 3.2 Experimental details of 3a-4b.1	101
Table 3.3 Hydrogen-bond geometry (Å, °) for 1a	105
Table 3.4 Selected bond distances (Å) in 1a	105
Table 3.5 Selected bond distances (Å) in 2a.1	108
Table 3.6 Hydrogen-bond geometry (Å, °) for 2a.1	108
Table 3.7 Selected bond distances (Å) in 2a	111
Table 3.8 Hydrogen-bond geometry (Å, °) for 2a	111
Table 3.9 Selected bond distances (Å) in 3a	114
Table 3.10 Hydrogen-bond geometry (Å, °) for 3a	114
Table 3.11 Selected bond distances (Å) in 4b.1	116
Table 3.12 Hydrogen-bond geometry (Å, °) for 4b.1	117
Table 3.13 Selected bond distances (Å) in 4b	120
Table 3.14 Hydrogen-bond geometry (Å, °) for 4b	120
Table 3.15 N...I halogen-bond distances (Å) and angles (°) in the current work and previously reported related structures.	121
Table 3.16 Intermolecular interactions in (Å) shorter than the sum of the van der Waals radii.....	121
Table 3.17 Summary of the C-H and C-F stretches found in adduct 1a-4b.1 compared with related amine and arene. Differences are given in brackets	122
Table 3.18 Topological parameters calculated at B3LYP/6-311G** level of theory	123

Table 4.1 Experimental details.	135
Table 4.2 Hydrogen-bond geometry (Å, °) for 1a	137
Table 4.3 Hydrogen-bond geometry (Å, °) for 2a	139
Table 4.4 Hydrogen-bond geometry (Å, °) for 3a	141
Table 4.5 Hydrogen-bond geometry (Å, °) for 4a	143
Table 4.6 N...I halogen-bond distances (Å) and C-I...N angles (°) in this study.	144
Table 4.7 Intermolecular interactions in (Å) less than the sum of the van der Waals radii.....	144
Table 4.8 Topological parameters calculated at B3LYP/6-311G** level of theory	146
Table 5.1 Experimental details.	155
Table 5.2 Hydrogen-bond geometry (Å, °) for 1a	157
Table 5.3 Hydrogen-bond geometry (Å, °) for 2a	160
Table 5.4 Hydrogen-bond geometry (Å, °) for 2c	162
Table 5.5 Different C-I bond distances detected in 3b	163
Table 5.6 Hydrogen-bond geometry (Å, °) for 3b	164
Table 5.7 C-I, N...I distances (Å) and C-I...N angles (°) related to the structures obtained in this study.....	166
Table 5.8 Topological parameters calculated at B3LYP/6-311G** level of theory using GAMESS and Multiwfn programmes	167
Table 6.1 Experimental details of 1a- 5a reported in this work.....	177
Table 6.2 Selected bond distances in Å for 1a	181

Table 6.3 Hydrogen-bond geometry (Å, °) for 2a	183
Table 6.4 Selected bond distances in Å for 2a	183
Table 6.5 N...I halogen-bond distances (Å) and angles (°) in the current work and previously reported structures.	185
Table 6.6 Hydrogen-bond geometry (Å, °) for 3a	186
Table 6.7 Selected bond distances in Å for 3a	187
Table 6.8 Intermolecular interactions in (Å) less than the sum of the van der Waals radii observed in iodine containing adducts and related structures.....	187
Table 6.9 Hydrogen-bond geometry (Å, °) for 4a	190
Table 6.10 Selected bond distances in Å for 4a	191
Table 6.11 N...Br halogen-bond distances (Å) and angles (°) in the current work and previously reported structures.	192
Table 6.12 Hydrogen-bond geometry (Å, °) for 5a	194
Table 6.13 Selected bond distances in Å for 5a	194
Table 6.14 Intermolecular interactions in (Å) less than the sum of the van der Waals radii observed.	195
Table 6.15 Topological parameters calculated at B3LYP/6-311G** level of theory	198

Abstract

This thesis reports an X-ray single crystallographic study of the solid-state halogen bonded adducts formed between a series of mono- and di-iodo- and bromo-fluorobenzenes with a variety of primary, secondary and tertiary nitrogen bases. As an extension of previous published work, 1,4-diazobicyclo[2.2.2]octane (DABCO) forms adducts with 4-bromo-tetrafluorobenzotrifluoride, 1,2-dibromo-tetrafluorobenzene and 1,3-dibromotetrafluoro-benzene to form trimers held by N...Br halogen bonds, while with 4,4'-dibromooctafluorobiphenyl a one-dimensional polymer is formed. The shortest N...Br distance was observed in the DABCO.1,3-dibromotetrafluorobenzene adduct of 2.667(15) Å, more than 20% shorter than the sum of the van der Waals radii.

Both hexamethylenetetramine and 1,3,5-triazina-7-phosphadamantane form adducts with iodopentafluorobenzene, 1,2-diiidotetrafluorobenzene, 1,3-diiidotetrafluorobenzene and 1,4-diiidofluorobenzene, although no halogen-bond formation was observed involving the phosphorus atom. The adducts containing iodopentafluorobenzene, 1,2-diiidotetrafluoro-benzene and 1,4-diiidofluorobenzene feature N...Br halogen bonds, while for 1,3-diiidotetrafluorobenzene an additional type II I...I interaction is detected. It is observed that the adduct with the shortest halogen bond displays the largest shift in C-F vibrational frequencies.

Combinations of pyrimidine, 4,6-dimethylpyrimidine, 1,3,5-triazine and pyrimidine-5-amine with 1,2-diiidotetrafluorobenzene, 1,3-diiidotetrafluorobenzene, 1,4-diiidotetrafluoroenzene, and 1,3,5-triidotrifluorobenzene have been investigated from which it is found consistently that pyrimidine forms the shortest N...I halogen bonds of ca. 2.85 Å, which are nearly 20% shorter than the sum of van der Waals radii of nitrogen and iodine.

The final experimental chapter describes the structures of halogen bonded adducts formed between piperazine and a series of iodo- and bromo-fluorobenzenes from which it is concluded that intermolecular N...I and N...Br halogen bonds are formed preferentially over N...H hydrogen bonds. In each chapter a comparison between the X-ray diffraction data and parameters obtained from QTAIM computational studies is made. These studies support the interpretation of the X-ray data, but also identify some additional weak interactions.

Declaration

No portion of the work referred to in this thesis has been submitted in support of an application for another degree or qualification of this or any other university or other university or other institute of learning.

Copyright Statement

- i. The author of this thesis (including any appendices and/or schedules to this thesis) own certain copyright or related rights in it (the “copyright”) and s/he has given The University of Manchester certain rights to use such Copyright, including for administrative purposes.
- ii. Copies of this thesis, either in full or in extracts and whether in hard or electronic copy,
may be made only in accordance with the copyright, Designs and Patents Act 1988 (as amended) and regulations issued under it or, where appropriate, in accordance with licensing agreements which the University has from time to time. This page must form part of any such copies made.
- iii. The ownership of certain Copyright , patents, designs, trademarks and other intellectual property (the “Intellectual Property”) and any reproductions of the copyright works in the thesis, for example graphs and tables (“Reproductions”), which may be described in this thesis, may not be owned by the author and may be owned by third parties. Such Intellectual Property and Reproductions cannot and must not be

made available for use without the prior written permission of the owner(s) of the relevant Intellectual property and/or Reproductions.

- iv. Further information on the conditions under which disclosure, publication and commercialisation of the thesis, the copyright and any Intellectual Property and/or Reproductions described in it may take place is available in the University IP Policy (see <http://documents.manchester.ac.uk/DocuInfo.aspx?DocID=24420>), in any relevant Thesis restriction declarations deposited in the University Library . The University Library's regulations(see <http://www.library.manchester.ac.uk/about/regulations/>) and in The University's policy on Presentation of Thesis.

Acknowledgements

I would like to offer my sincerest gratitude to Dr Alan Brisdon, my main supervisor who has given me the opportunity to work in this interesting field, supported me by his guidance, advice and valuable assistance during my study. I really appreciate his direction and valuable feedback.

I am thankful to my first year Co-supervisor Dr Robin Pritchard and his continuous encouragement during my X-ray lab work to analyse, refine structures. I would like also to thank the crystallography staff, Dr Inigo Vitorica-yerzabal and Dr George Whitehead for all the support and advice.

I would like to acknowledge the Government of Oman for their funding and support during my study.

Thanks to all the past and present members of Fluorine research group for their guidance and support throughout my study.

I am also grateful to Dr Mohammed Shazwan Shah Jamil for his welcoming from the first day of my study.

I would like to express my deepest gratitude to my children and wonderful wife, Raya, who always supporting, helping and also encouraging me in attain this level of education.

Abbreviations

°	Degree
ml	Millilitre
mmol	Millimole
vdW	van der Waals
IUPAC	International union of pure and applied chemistry
X	Halogen atom
Y or B	Halogen bond acceptor
R	Attached group to the halogen
HX	Hydrogen bond
R-X	Halogen bond donor
$V_{(r)}$	Electrostatic potential
XB	Halogen bond
C-X...X'-C	Halogen bond type(I)
C-X...B or XB	Halogen bond
K	Kelvin
HTMA	Hexamethylenetetramine
XRPD	X-ray powder diffraction
XRD	X-Ray Diffraction
ORTEP	Oak Ridge Thermal Ellipsoid Plot
α	Alpha
β	Beta
γ	Gamma
θ	Theta
λ	Wavelength
Å	Angstrom (10^{-10} m)
Z	Number of formula units per unit cell
CIF	Crystallographic Information Files
CSD	Cambridge Structural Database
CCDC	Cambridge crystallography data centre
NMR	Nuclear Magnetic Resonance
IR	Infrared
DABCO	1,4- diazabicyclo[2, 2, 2] octane
CD ₃ CN	Acetonitile-d ₃ , NMR solvent
TMS	Tetramethylsilane
1,2DBTFB	1,2-dibromotetrafluorobenzene
1,3DBTFB	1,3-dibromotetrafluorobenzene
4-B-2,3,5,6-TFBTF	4-bromo-2,3,5,6-tetrafluorobenzotrifluoride
DMSO	dimethyl sulfoxide-d ₆
QTAIM	Quantum theory of atoms in molecules
DFT	Density functional Theory

Chapter 1.

Introduction

1.1. Thesis structure

The presented thesis has been agreed to be in an alternative format consisting of 8 chapters. The first chapter describe the importance of halogen bond and related published work. This is followed by introducing the fields of crystal growth and the X-ray single crystal procedure in collecting the data related to each crystal and the process used in solving and refining the crystal structure. Then the basis of theoretical studies using QTAIM is described, which is used to support the existence of interactions in the solid state and to compare the strength of each XB interaction. In all of the research papers described, adduct formation, crystal growth, X-ray data collection and solution was performed by the thesis author. Manuscript preparation was primarily by thesis author, with assistance from supervisor. All research papers were prepared for submission to Acta Crystallographic Section C.

Chapter 2 “Halogen bonding in a series of bromofluorobenzene and 1,4-diazabicyclo[2.2.2]octane (DABCO)”

Chapter 3 “A Crystallographic and QTAIM study of halogen bonding in series of iodofluorobenzenes and hexamethylenetetramine and 1,3,5-triazaphosphaadamantane”

Chapter 4 “Halogen bonds involving 1,4-diiodotetrafluorobenzene with variety of nitrogen-based aromatic halogen bond acceptors”

Chapter 5 “Variety of halogen bonded adducts containing compounds using pyrimidine derivatives”

Chapter 6 “Crystallographic and QTAIM studies of variety of halogen bonded adducts containing compounds using piperazine”

Chapter 7 Conclusions and future work of the work presented in this thesis.

Chapter 8 Appendices

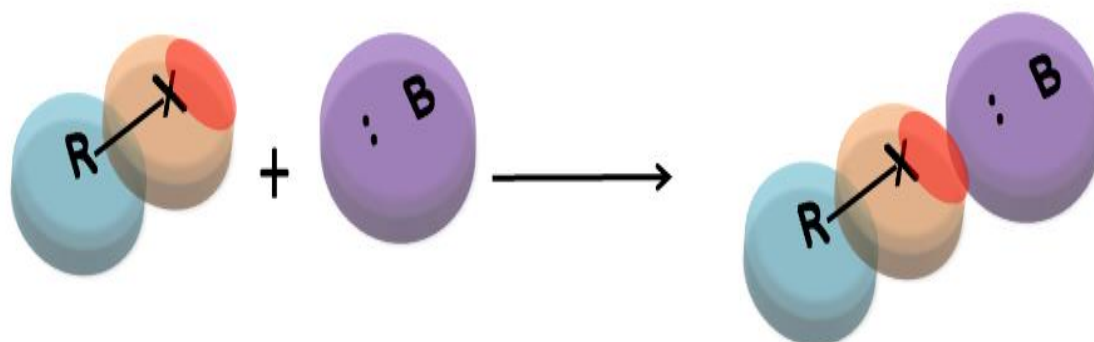
1.2. Intermolecular forces

Unlike intramolecular forces, which occur within a molecule, intermolecular forces arise between molecules. While intermolecular forces are much weaker than those within molecules, they function to keep matter in its phase, either solid or liquid. Our understanding of intermolecular forces has developed from early observations in the 1800s to the twentieth century, which featured high-resolution microscopy and X-ray diffraction techniques.¹ According to Stone¹, the classification of intermolecular forces mainly comes from the electrostatic nature of the attraction between molecules. This is divided into two main types: long-range attraction (e.g. dispersion or London interaction) and short-range attraction (e.g. such as is found in hydrogen and halogen bonding).¹

1.3. Halogen bonding

The first reported halogen bonded adduct was published by F. Guthrie in 1863, who synthesized the I₂...NH₃ complex.² By the middle of the nineteenth century, Hassel and colleagues introduced the phrase ‘halogen molecular bridge’ to describe the crystal structures formed in molecular halogen and Lewis base complexes.³ This kind of noncovalent interaction, represented by (R-X...B) and shown in **Scheme 1.1**, ‘occurs when there is evidence of a net attractive interaction between an electrophilic region associated with a halogen atom in a molecular entity and a nucleophilic region in another, or the same, molecular entity’,⁴ where R-X represents the halogen bond donor and B refers to the halogen bond acceptor. This attraction may result from electron density depletion on the outer side of the halogen, called the σ hole.⁴ **Table 1.1** lists some halogen bond donors and acceptors

suggested at the end of the International Union of Pure and Applied Chemistry (IUPAC) project (# 2009-032-1-100) in 2013.



Scheme 1.1 Representation of the halogen bond (XB), where X = Cl, Br, or I and B = the halogen bond acceptor (base with lone pair), R = the covalently bonded atom or group, the red area represents the σ -hole.

Table 1.1 Common halogen bond donors and acceptors⁴

Typical R-X (Halogen-bond donor)	Typical B (Halogen-bond acceptor)
Haloarene	Atom has lone pair
Haloalkane	π system
Dihalogen molecule	Anion
Haloalkyne	
Halonium ion	
Haloimide	

1.3.1. The role of the σ hole

Despite the high electronegativity of halogen atoms, when they bond covalently, a positive electrostatic potential region can appear on the outer surface of X and along the R-X axis, which can be explained with quantum mechanical, computational, and other studies.

The electrostatic potential $V(r)$ remains positive for all spherically symmetric ground state atoms.⁵ However, this differs in molecules (when atoms bond

covalently), where the charge distribution is affected by virtue of forming directional bonds to other atoms, particularly when the other atoms involved have greater electronegativity. This polarisation leads to places with negative $V(r)$ and others, on less electronegative atoms, having a positive electrostatic region on the far side of the outer sphere of X. This area becomes more positive when the halogen is attached to one or more highly electronegative atoms (e.g F). This will enhance electron withdrawing and increase the magnitude of the σ hole.⁶⁻⁸

In the case of halogen bonding, the formation of the σ hole can be explained in terms of the orbitals involved. The electronic configuration of a halogen atom X is $s^2px^2py^2pz^1$, in which there is one full s-orbital and two full p-orbitals ($px^2 py^2$). The third p orbital has only one electron and lies on the R-X axis.⁶ It is the electron density of this orbital that is involved in forming the sigma bond between the R-group and the halogen atom. Thus, in a spherical atom, the five p electrons in the three p orbitals result in an average orbital occupancy of 5/3. When the atom is covalently bonded, the electron occupancy of the px and py orbitals increases to 2, while in the pz orbital it decreases to 1, which is called polar flattening.^{5,7}

This polar flattening around the covalently bonded halogen C-X results in anisotropic distribution of electron density. An electrophilic region (σ hole) occurs along the extension of the R-X bond because of the depleted pz orbital and a nucleophilic region perpendicular to the covalent bond obtained from px and py electrons (Fig 1.1). The latter can form type II halogen-halogen contacts, which involves halogens with each other and can be simplified as C-X...X'-C, where X and X' are halogen atoms. Fig 1.2 illustrates the geometries of type I and type II halogen-halogen interactions beside the Lewis base halogen bond interaction.

1.3.2. Comparing halogen atoms

Studying the σ hole and how it forms for some methyl halides, based on molecular electrostatic potential $V(r)$, was undertaken by Brink et al. (1992) and revealed this region, which has a positive electrostatic potential.⁸ To differentiate between different halogen atoms, X, and their capability to form a σ hole, Clark et al. (2006) used the Molekel programme to produce coloured molecular electrostatic potential figures of the molecules CF_4 , CF_3Cl , CF_3Br , and CF_3I .⁶

It can be clearly seen in Fig 1.3 that the positive area develops in the order $F < Cl < Br < I$, with fluorine hardly showing any σ hole. This lack of a σ hole for fluorine was explained by its high electronegativity, which means it has more ability to pull the covalently shared electrons towards it, therefore causing neutralisation of the σ hole.¹⁰ Other studies have found that this becomes less effective when fluorine is bonded to other highly electron attracting groups, such as in F-CN, FOF, F_2 , and F-C (NO_3)₂.^{7,11}

A second factor that influences the occurrence of a σ hole in covalently bonded systems is related to sp hybridization.^{6,8} Clark et al. (2006) found that the contribution of the s orbital is low (< 12 %) when X = I, Br, or Cl; however it reaches 25% with fluorine.⁶

Furthermore, it has been noticed that the appearance of a σ hole is not limited to halogen atoms, but can also be seen in other covalently bonded atoms from groups V-VII.¹⁰

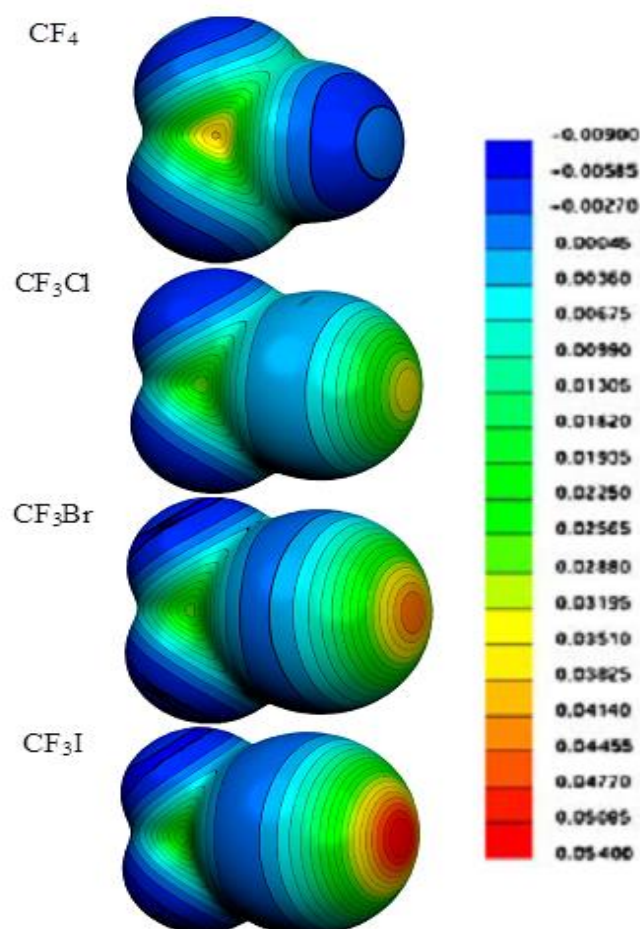


Figure 1.3 The molecular electrostatic potential, in Hartrees, at the 0.001 electrons Bohr⁻³ isodensity surface of CF₄, CF₃Cl, CF₃Br, and CF₃I. Taken from ⁶

1.3.3. Halogen bond strength

The strength of this kind of attraction increases as the halogen, X, changes in the order F < Cl < Br < I and is related to the increase of the size of the halogen.^{11,12} This in turn is related to the degree of polarization of atom X. As the halogen, X, becomes more polarizable, the strength of the halogen bond is enhanced¹³ because, as the electronegativity of the halogen atom X decreases, it becomes more able to form a sigma hole and, therefore, a halogen bond.¹³ The nature of R is also important; for example, the number of fluorine atoms attached to R has an influence on the amount of ‘pulling’ or withdrawing of the electron density involved in covalent bonding and consequently the size of the sigma hole that is formed.^{8,11}

Laurence and colleagues (2011) studied the basicity of Lewis bases (Y) that interacted with I₂ as a halogen bond donor. They developed and applied a basicity scale to compare the studied complexes that contain nitrogen and phosphorus. They found that the Lewis bases become weaker across the period and increase down the group when considering Lewis bases contain N, P, Se, S, I, O, Br, Cl, or F. Focusing on the nitrogen-containing bases, they found that the order observed is amine < pyridine < nitrile and related to the ‘decreasing of p-character of the nitrogen lone pair’.¹⁴

Lu and colleagues found that the strength of a halogen bond is also related to the solvent used.¹⁵ In the case of charged systems, the halogen bond length increases and strength tends to decrease when using chloroform, acetone, or water due to the solvation effect. In the case of neutral systems, the strength of the XB increases.¹⁵ Furthermore, the effects of different solvents can vary in the ability of the XB to compete and show priority over other noncovalent interactions.¹⁶ Computational studies have found that as the C-X...Lewis base angle reaches 180 °, the strength of the XB increases.^{17,18}

The more abundant hydrogen bond (X-H...Y-Z, where X-H represent the hydrogen bond donor and Y-Z the hydrogen bond acceptor) shows a similar concept. As the X-H...Y angle become close to linearity, the H...Y distance become shorter and the hydrogen bond become stronger.¹⁹

1.3.4. Characteristics of halogen bonds

In general, halogen bonds are characterised by two important parameters: the R-X...B angle, most commonly reaching 175 °, and the intermolecular distance between X and B, which should be less than the sum of the van der Waals radii. The bond energy of the XB may reach 200 kJ mol⁻¹,¹⁸ however, the actual values of these parameters are highly dependent on the identity of the halogen involved, the base involved in the interaction, and the type and number of electron withdrawing groups attached to the halogen bond donor.²⁰

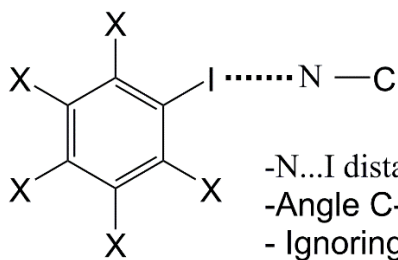
1.3.5. Applications of halogen bonds

Halogen bonds are uniquely important in many fields, especially in biological systems. Recently, it was found that a number of biological processes involve halogen bond formation.¹⁷ Auffinger et al. (2004) utilized the protein databank to investigate halogen bond contacts of the type C-X...O.²¹ Similarly, in 2009 Lu et al. carried out a survey involving data from the protein databank and found that the number of known halogenated structures increased 9-fold between 2004 and 2009.²² In addition, halogen bonds have applications in the area of drug design²¹ and crystal engineering, where crystal engineering is used to design co-crystals with specific required characteristics and applications, such as geometry, strength, and conductivity.⁷

1.3.6. Halogen –bonded systems

A search of the Cambridge Structure Database (CSD, version 5.43²³) for XB interactions involving iodo- and bromo- fluorinated benzene systems was conducted using Conquest.²⁴ A specific search for N...I interactions, as represented in **Table 1.2**, with a distance shorter than the sum of the N and I van der Waals radii (3.53 Å) and a C-I...N bond angle greater than 150°, yields 88 hits.

Table 1.2 The specific number of N...I structures and the search details using CSD

Structure 1	 <ul style="list-style-type: none">-N...I distance < 3.53 Å-Angle C-I...N >150- Ignoring ions- X is F, I or H
Hits shorter than the sum of vdW	88

Most of distances in these structures are shorter than 3.0 Å (Fig 1.4), which reflects the significance of N...I interactions.

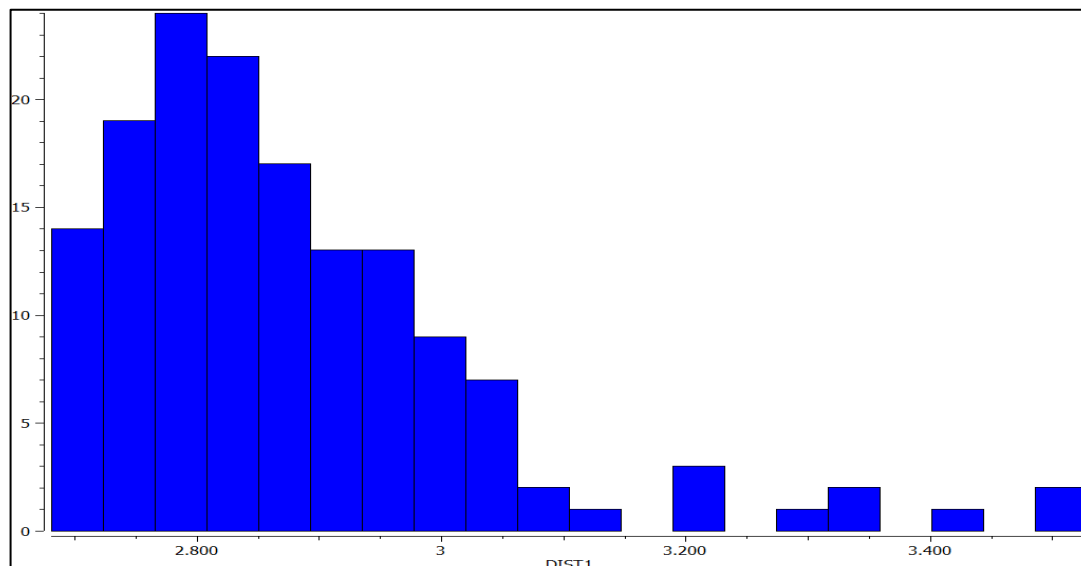


Figure 1.4 Histogram of N...I, distance related to the 88 structures, less than the sum of the vdW radii 3.53 Å

From Fig 1.5, which shows the angle histogram for the 88 hits, we can see that the structures tend to adopt linear arrangements with greater numbers of large C-I...N angles, which is a feature of halogen bonding. To concentrate on the most significant interactions, the search was directed towards interactions that were less than 2.80 Å (i.e. 20% less than the sum of the vdW radii); 25 hits were obtained, which mostly (15 hits) include the diamine, 1,4-diazabicyclo[2.2.2]octane (DABCO), as the halogen bond acceptor (Table 1.3).

This is not unusual since DABCO is a commonly used halogen bond acceptor that adopts a cylindrical shape with 3-fold symmetry, which packs in a way that decreases the potential energy barriers.²⁵⁻²⁷

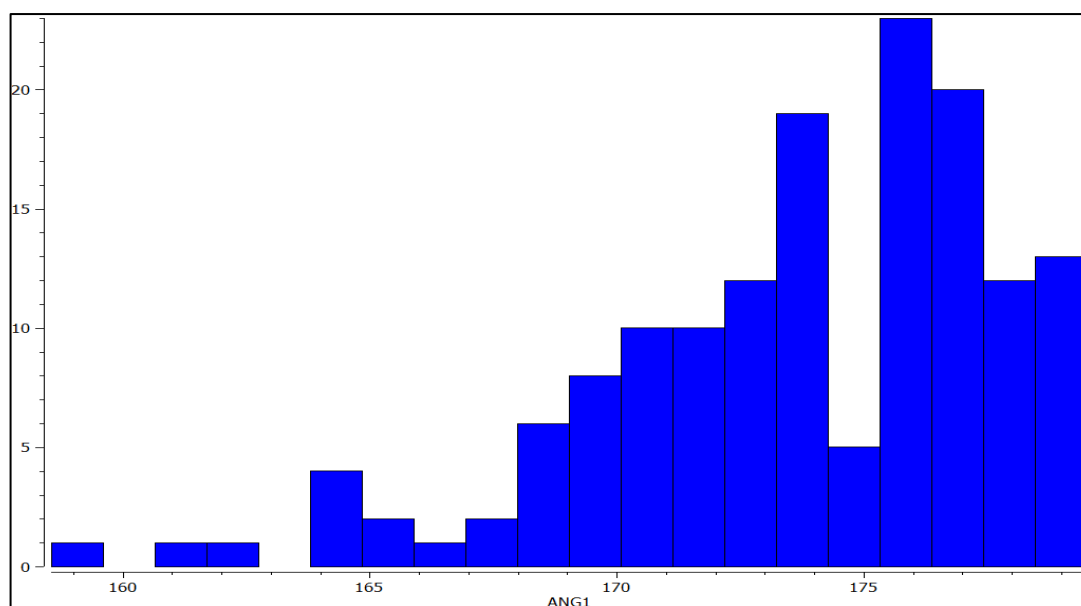


Figure 1.5 Histogram of C-I...N angles between 150–180° for the 88 structures involving N...I

Table 1.3 15 CSD hits after searching specifically for structure 1 (interaction between 0–2.8 Å, angle range 150–180°), including DABCO as a halogen bond acceptor (for abbreviations see the text below)

	Halogen bond Donor. Acceptor	CSD code	Shortest Interatomic distance N...I, Å	Average Angle, °	Reference
1	1,2ditfb. DABCO	DATCEI	2.77(2)	170.66(9)	28
2	1,3,5titfb. DABCO	DATCIM	2.757(3)	173.9(1)	28
3	1,4ditfb. DABCO	ISIHUN	2.744(5)	173.7(2)	29
		ISIHUN01	2.754(4)	173.5(2)	30
		ISIHUN02	2.769(3)	173.7(1)	31
		ISIHUN03	2.7350(8)	173.24(3)	
4	1itfb.DABCO	FUYFAI	2.718(6)	177.3(4)	25
		FUYFA103	2.694(1)	177.71(5)	25
		FUYFA104	2.699(3)	178.84(9)	25
		FUYFA105	2.709(5)	178.1(2)	25
		FUYFA106	2.714(5)	177.1(4)	25
5	1,iodo-2,6dfb .DABCO	FUYGOX	2.795(2)	176.49(8)	25
		FUYGOX01	2.859(3)	176.3(1)	25
		FUYGOX02	2.871(4)	176.4(1)	25
6	1,3-ditfb.DABCO	WIGVIU	2.79(3)	174.3(8)	32

Clear evidence of an attractive interaction between I and N in DATCEI and DATCIM was recognized by M. Pfrunder et al. (2012), where interactions were observed between both 1,2-diiodotetrafluorobenzene (1,2-DITFB) and 1,3,5-triiodotrifluorobenzene (1,3,5-TITFB) with (1,4-diazabicyclo[2.2.2]octane (DABCO), (Fig 1.6). They used slow evaporation to form the adducts from a mixture of ethanol and water solvents for the former and acetone for the latter. Even though a 1:1 molar ratio was used, both combinations produced colourless prismatic crystals containing a 1:2 ratio of DABCO and arene, respectively. One iodine from each 1,3,5-TITFB molecule was involved in conventional N...I halogen bond and I...I type II halogen-halogen interactions joining the adjacent N...I trimers (donor-acceptor-donor) in a 2D tape. However, when using dichloromethane as a solvent, a reaction occurred with DABCO, forming a quaternised nitrogen system, which in the solid state shows a network that includes halogen bonds.²⁸

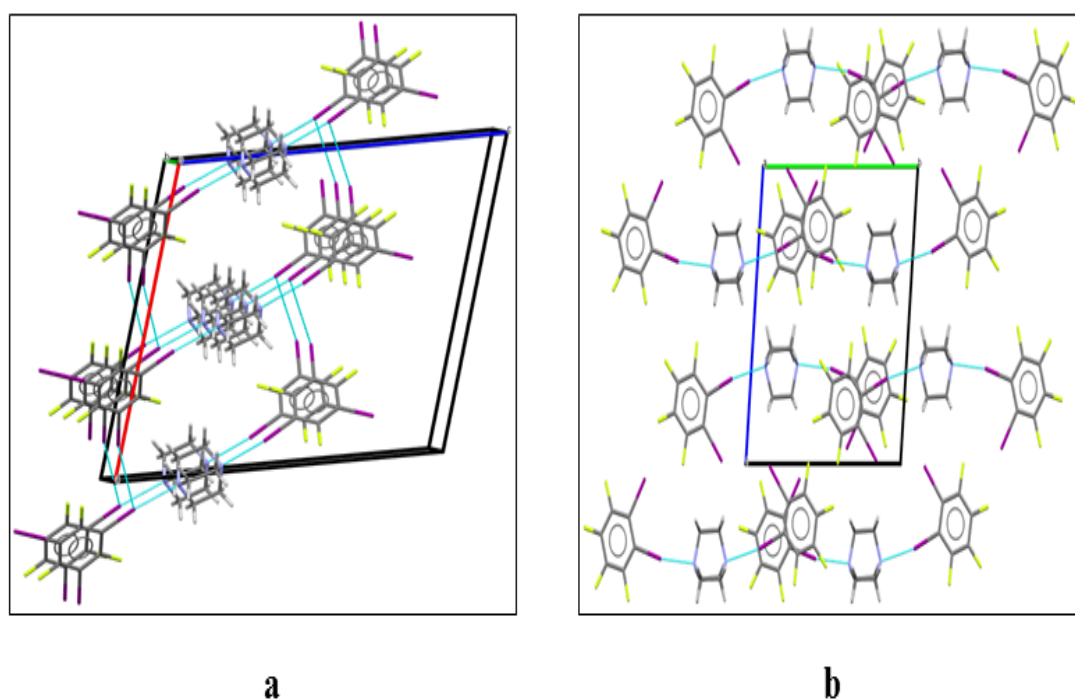


Figure 1.6 Packing diagram of halogen bonds in (a) 1,3,5-TITFB and DABCO, (b) 1,2-DITFB and DABCO²⁸. The colour key is as follows: gray, carbon; purple, iodine; blue, nitrogen; yellow, fluorine; white, hydrogen.

Jean and colleagues studied the halogen bond formed from a variety of tertiary amines, including DABCO, hexamethylenetetramine, and 4,4'-bipyridine. They co-crystallized a 1:1 stoichiometry of 1,4-diiodoperfluorobenzene and 1,3,5-triiodotrifluorobenzene (1,3,5-TITFB) with DABCO. Previously, Pfrunder et al. (2012) tried [1,3,5-triiodotrifluorobenzene (1,3,5-TITFB) with DABCO] combination using a similar 1:1 molar ratio, but this time Jean and colleagues produced structures with two of the three iodine atoms from 1,3,5-triiodotrifluorobenzene (1,3,5-TITFB) involved in N...I halogen bond with DABCO that exhibits a 2D zig-zag chain that propagate with 120° angles (Fig 1.7).^{28,30}

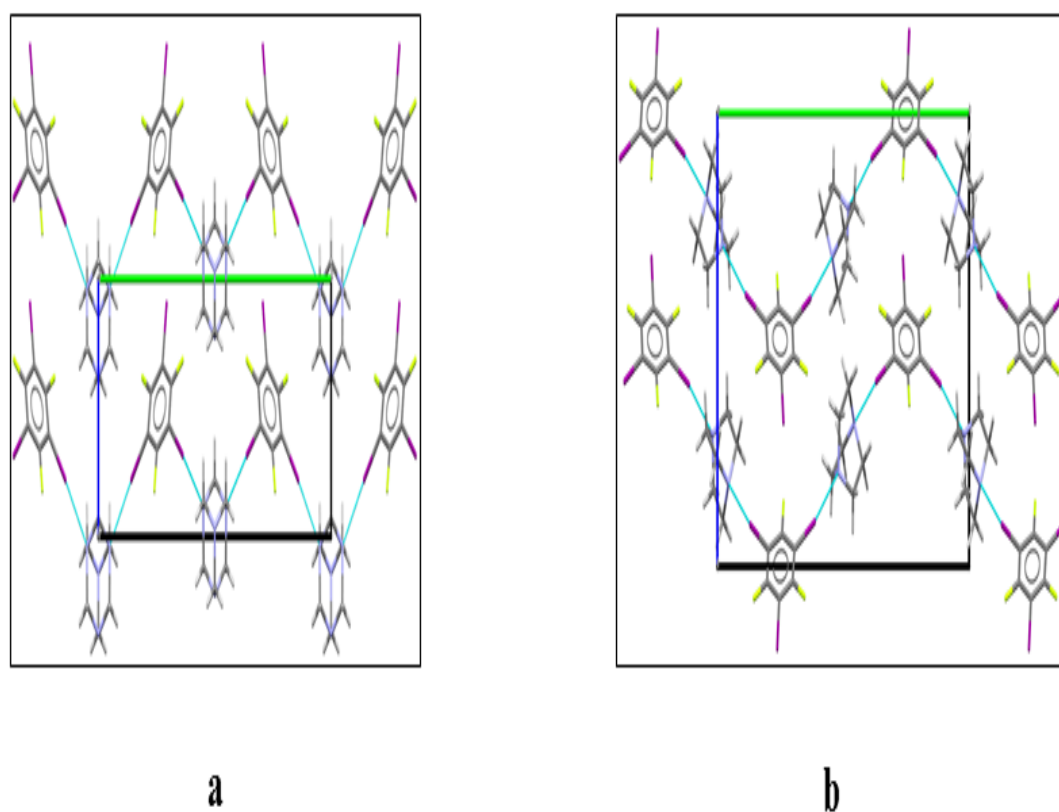


Figure 1.7 Packing diagram of halogen bonds in (a) 1,3,5-TITFB and hexamethylenetetramine, (b) 1,3,5-TITFB and DABCO. The colour key is as follows: gray, carbon; purple, iodine; blue, nitrogen; yellow, fluorine; white, hydrogen.³⁰

Later, in 2015, Luca Catalano and colleagues published their work on the preparation of crystals from DABCO and 5-fluoro-substituted iodobenzenes (Fig 1.8) using slow evaporation processes and acetone as a solvent. X-ray diffraction for all the crystals was accomplished at 103 K. Short I...N contact distances for all the samples were found at an average of approximately 2.79 Å and C-I...N angles averaged 176.6°. All the 2a-2e structures showed a 2:1 structure ratio of arene and DABCO, except 2c, which showed a 1:1 ratio. This resulted in trimeric (arene-DABCO-arene) N...I halogen bonded structures in 2a-2e, except 2c, which showed dimeric (arene-DABCO) structures (Fig 1.9). Reversible phase and rotational disorder were recorded when the temperature of the crystal reached room temperature.²⁵

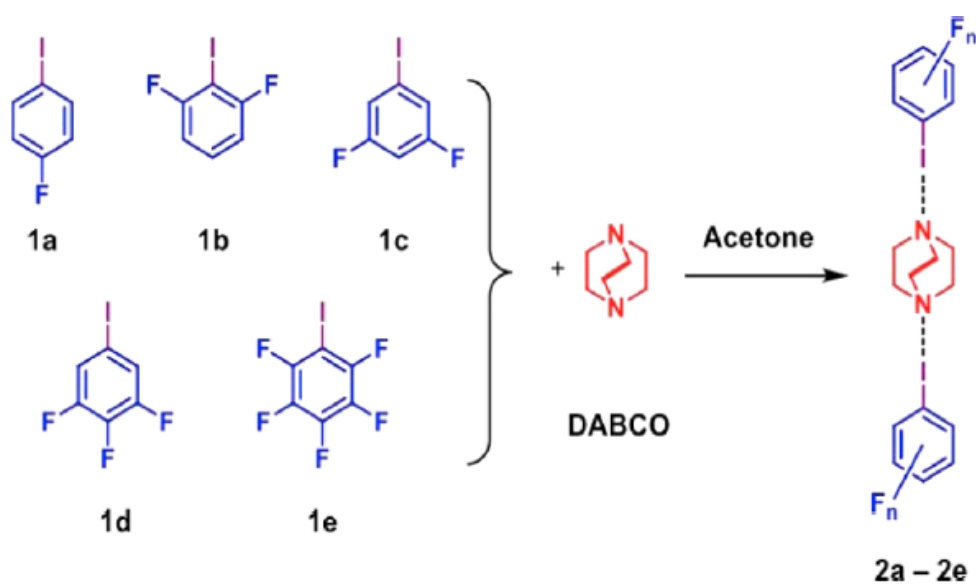


Figure 1.8 Fluoro-substituted iodobenzenes used in Catalano et al.²⁵

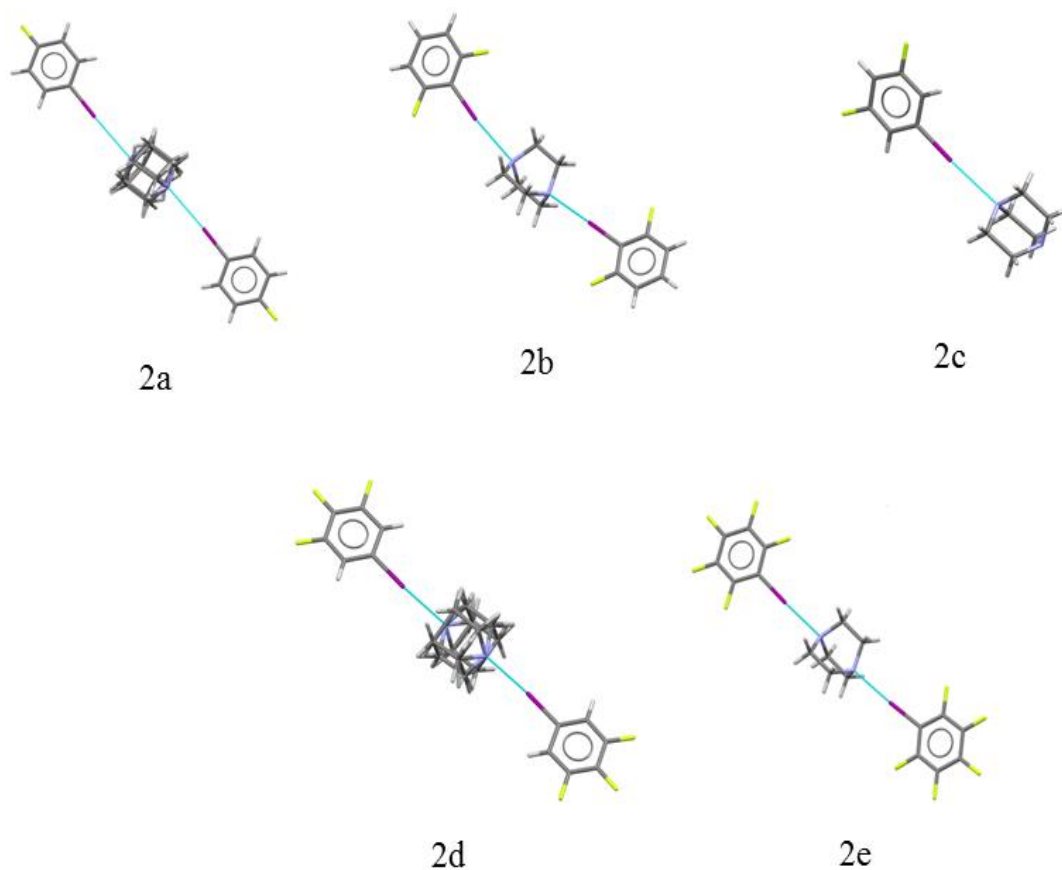
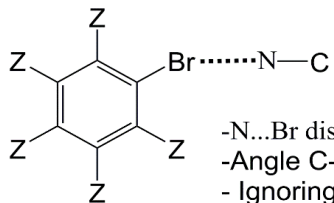


Figure 1.9 Halogen-bonded structures found in Catlano and colleagues' study²⁵, The colour key is as follows: gray, carbon; purple, iodine; blue, nitrogen; yellow, fluorine; white, hydrogen.

Repeating the CSD search, but this time investigating Br...N interactions, [Table 1.4](#) shows the data presented in the histogram in [Fig 1.10](#). This second search gives only six different structures that have an N...Br distance under the sum of the vdW radii of bromine and nitrogen atoms, 3.40 Å. We can conclude from the two previous CSD searches, that a higher number of structures involving N...I, XBs are known compared with N...Br interactions.

Table 1.4 The specific number of Br...N structures and the search details using CSD

<p>Structure 2</p>	 <p>-N...Br distance < 3.40 Å -Angle C-Br...N > 150 - Ignoring ions - Z is F, Br or H</p>
<p>Hits shorter than the sum of vdW</p>	<p>6</p>

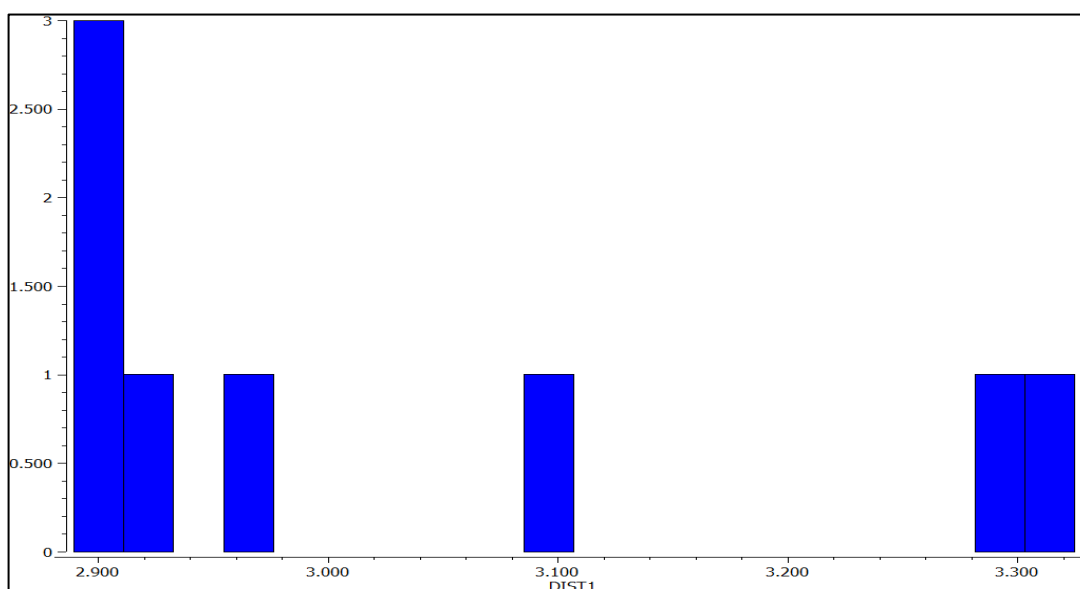


Figure 1.10 Histogram of N...Br, distance related to the six structures, less than the sum of the vdW radii, 3.40 Å.

Table 1.5 shows the six specific results found in the CSD database for N...Br interactions of the type shown by structure 2 in which the N...Br distance is less than the sum of the vdW radii, 3.40 Å. There are three structures with an N...Br interaction less than 3 Å and three have N...Br interaction distances above 3 Å.

Table 1.5 N...Br interactions less than the sum of the van der Waals radii (3.40 Å) in the CSD database

	Halogen bond donor. Acceptor	CSD Code	shortest Interatomic N...Br distance, Å	Average Angle °	Reference
1	1,4dbtfb.piperazine	DIVDOC	2.881(2)	177.72(7)	²⁹
2	1,4dbtfb.DABCO	DIVDUI	2.902(2)	168.7(1)	²⁹
3	1,4dbtfb.2,5-Diphenyl-1,3-oxazole	BACQII	2.965(3)	171.8(1)	³³
4	4,5-Dicyano-2-imidazolyl(phenyl)bromonium ylide	CIMPBR	3.094(2)	159.92(5)	³⁴
5	tbb.4,4'-azopyridine	NAVNAC	3.303(1)	170.05(5)	³⁵
6	1,4dbtfb.crown ether.thioureas	OQITUF	3.332(2)	165.22(9)	³⁶

Co-crystals of 1,4-dibromotetrafluorobenzene with piperazine gave an adduct, DIVDOC, with the N...Br shortest distance (2.881(2) Å) and the second highest angle (177.72°) documented in the CSD.²⁹ Cinic et al. also co-crystallised DABCO and 1,4-dibromotetrafluorobenzene (CSD Refcode DIVDUI) by mixing and grinding the starting material with nitromethane and using a shaker mill after grinding with grinding balls. XRPD analysis was used to investigate the complete conversion of the starting materials.²⁹ Because both DIVDOC and DIVDUI involve 1,4-dibromotetrafluorobenzene, the resulting shape was a long chain of alternate halogen bond donors and acceptors (Fig 1.11). More recently, and using vapour diffusion, one of our group was able to co-crystallize 1-bromotetrafluorobenzene with DABCO and obtained a shorter N...Br distance, 2.814(7) Å, making this the shortest N...Br halogen bond length currently known involving an aromatic bromofluorobenzene and DABCO.³⁷

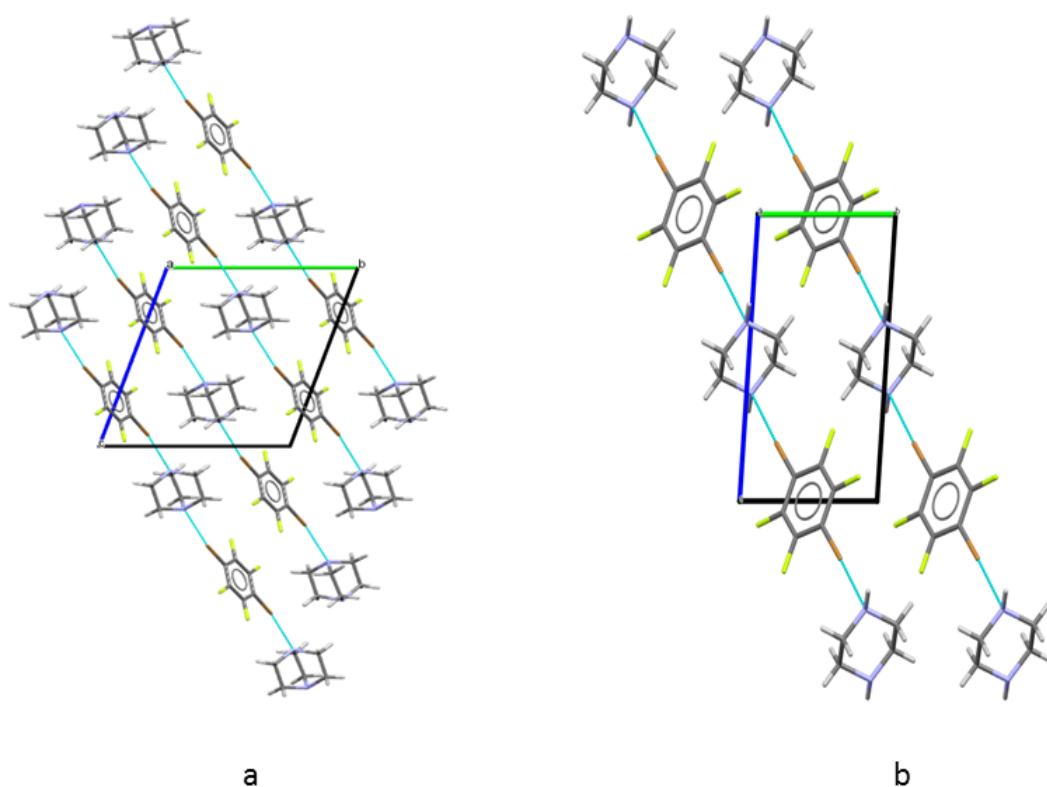


Figure 1.11 Packing diagram of halogen bonds in (a) 1,4-DITFB and DABCO, (b) 1,4-DITFB and piperazine in ²⁹; The colour key is as follows: gray, carbon; brown, bromine; blue, nitrogen; yellow, fluorine; white, hydrogen.

1.4. Growing crystals

1.4.1. Definition

Growing a good quality crystal is the first and one of the main steps leading to accurate determination of a crystal structure. This requires patience, and the crystal needs to be left to grow without disturbance. Theoretically speaking, crystallization will start with nucleation immediately after the concentration of the compound in the solvent becomes higher than its solubility product.³⁸ To form good quality crystals, the concentration should rise slowly near the nucleation site. Suitable crystal dimensions for X-ray study need to be in the range 0.1–0.3 mm.³⁸ There are several methods for growing crystals, and these will be outlined in the next section.

1.4.2. Different methods for growing crystals

The first method described is slow evaporation, an uncomplicated technique that involves making a saturated solution in a given solvent (Fig 1.12). The container should be covered, but not be entirely closed, to allow the solvent to evaporate. The container is allowed to stand undisturbed, because vibration causes nucleation. Too much nucleation produces many very small crystals that are unsuitable for single-crystal diffraction studies. This technique is not suitable for air-sensitive materials.³⁹

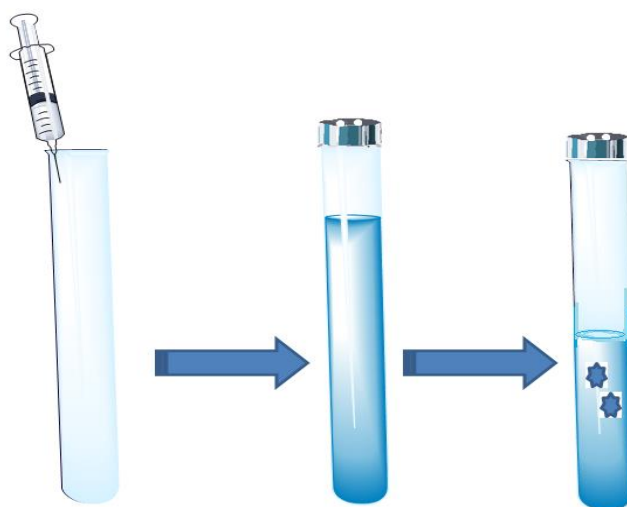


Figure 1.12 Slow evaporation

The second technique, which also requires a large amount of the saturated solvent, is slow cooling (Fig 1.13). A saturated solution is prepared near the boiling point of the solvent. The experiment is left to cool slowly until it reaches room temperature, and additional cooling can be used later to continue the cooling process. The main drawback of such a technique is the need for large quantities of the saturated solution.³⁹

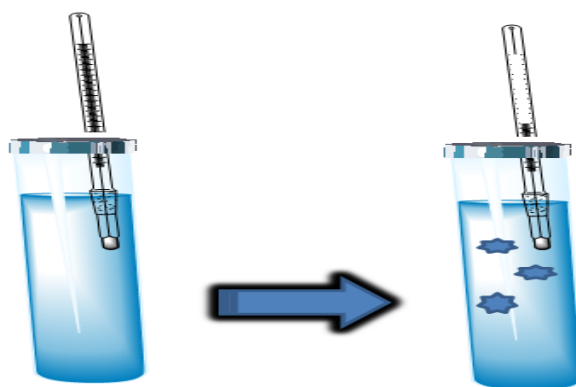


Figure 1.13 Slow cooling

The third method for growing crystals is based on vapour diffusion and uses two solvents that can mix well (Fig 1.14). Whereas the first solvent has a high boiling point, the second solvent—the precipitant—has a low boiling point. A solution created in the former solvent is placed in a small open container and put inside a larger one that contains the precipitant. Over time, the precipitant (more volatile) will diffuse into the solvent. Eventually, oversaturation, nucleation, and (hopefully) crystallization will occur. Varying the temperature can adjust the diffusion speed. To increase the possibility of getting good crystals, it is worthwhile to search for the right solvent. The advantages of this technique are the small amount of starting materials used and the high quality of the crystals that can be obtained.

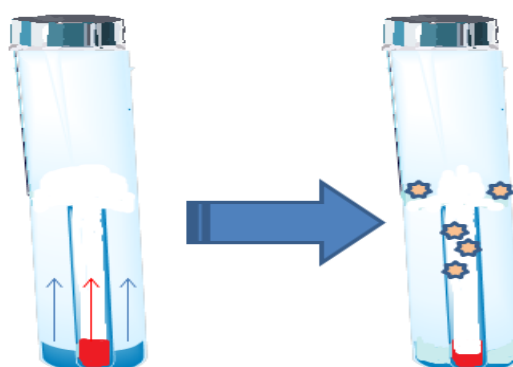


Figure 1.14 Vapour diffusion

Liquid–liquid diffusion (Fig 1.15) needs a binary solvent system comparable with vapour diffusion. In this case, density of the solvent has to be considered rather than the boiling point. The solution and precipitant are layered carefully in the same container. After a while, the two solvents mix via diffusion and, hopefully, crystals form. This technique is known to work with a small amount of solvent, but the challenge lies in choosing suitable solvents.³⁹

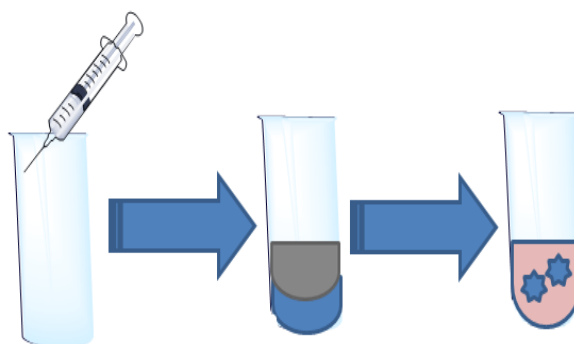


Figure 1.15 Liquid–liquid diffusion

When one or more suitable crystals has been grown, we may proceed to the next step of structure determination.

1.5. X-ray diffraction

The resolution of optical microscopes is limited by the wavelength of visible light (400–700 nm).⁴⁰ They cannot enable us to observe atoms in solid materials; consequently, a new technique was invented at the beginning of the twentieth century to overcome this weakness, based on shorter wavelength X-rays. Since then, X-ray crystallography has become a key technique in providing information about the structures and bonds between atoms and molecules.

1.5.1. Definition and generation of X-rays

After their discovery by Röntgen in 1895,³⁹ X-rays were recognised to be an electromagnetic wave, which occupy the wavelength range between 10^{-7} and 10^{-12} m in the electromagnetic spectrum (Fig 1.16).

Interatomic distances vary between 1–3 Å, and in 1912, Max von Laue noted that crystals scatter X-rays with wavelengths between 50–300 pm.⁴¹ X-ray crystallography is the procedure by which the various reflections by the crystal lattice are recorded.⁴¹

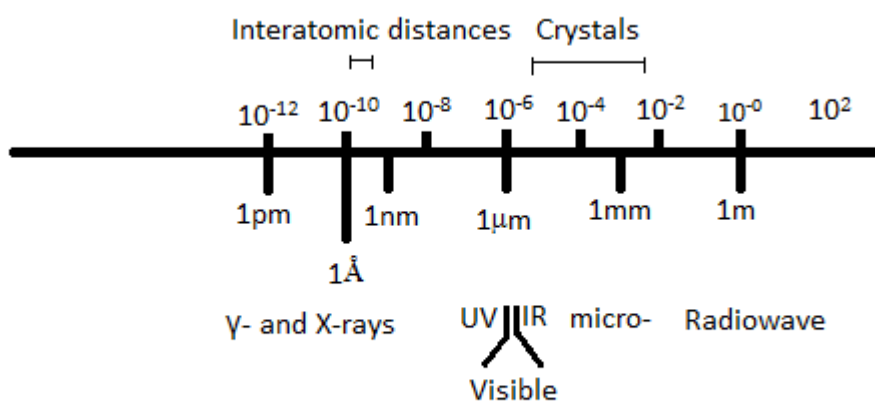


Figure 1.16 Crystal dimensions and the electromagnetic spectrum⁴¹

We can distinguish between two types of solids: amorphous, which do not have a definite geometrical shape and no long-range order, and crystalline materials that have a definite geometrical shape and long-range order (Fig 1.17).³⁹

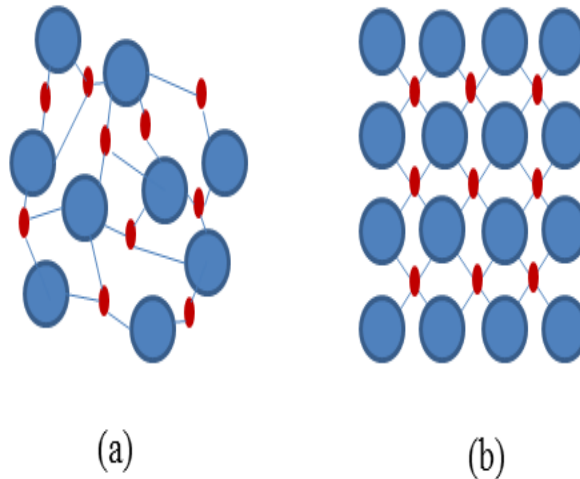


Figure 1.17 Difference in shape between amorphous (a) and crystalline (b) solids

The real breakthrough came when William Lawrence Bragg first used X-rays to determine the structure of NaCl, KBr, KCl, and KI.⁴²

1.5.2. Basic of crystal lattices

Atoms, molecules, or ions in crystalline solids are arranged repetitively in all three dimensions. This periodic arrangement of crystals creates an array of points called a crystal lattice (Fig 1.18A). Crystal lattices are distinct from the crystal structure, which is an array of atoms, molecules, and ions that comprises a crystal.⁴³ The crystal lattice points are selected so that they have the same repetitive view surrounding each point, and it is not necessary for the points to be located on specific atoms in the structure.

The basic building block is called a unit cell (Fig 1.18B). It is defined by selecting lattice points that give the smallest unit with the highest symmetry. As the symmetry of the unit cell increases, the higher is the symmetry of the crystal structure.⁴⁴ Each unit cell is defined by the a , b , and c vectors, which are separated by the angles α , β , and γ , such that α is the angle between b and c , β is the angle between a and c , and γ is the angle between a and b . Together, these are called unit cell parameters, and they can be easily defined by using right- or left-handed axes (Fig 1.18C).

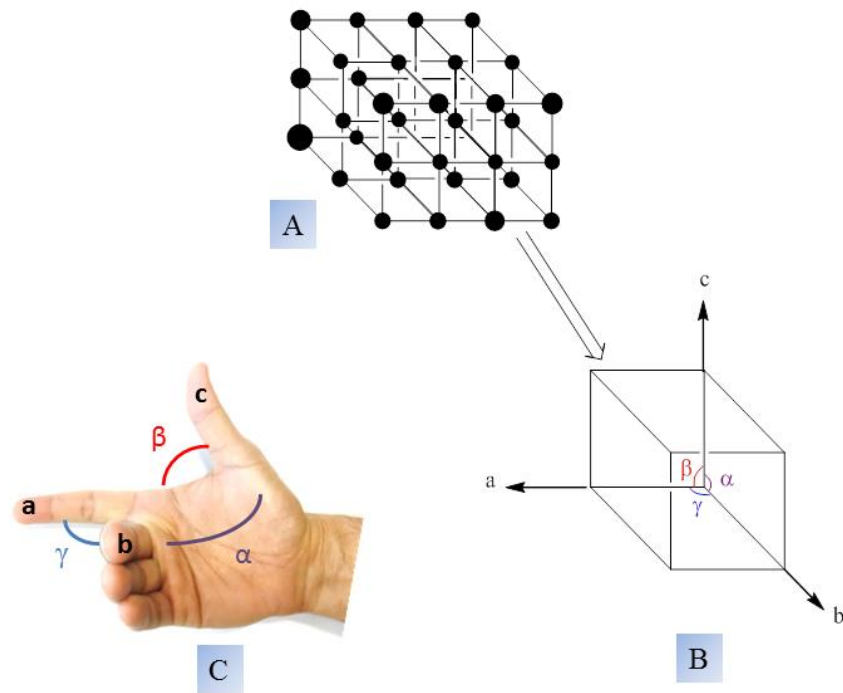


Figure 1.18 Crystal lattice and unit cell

Seven different crystal systems can be achieved by varying these vectors and angles (Table 1.6).⁴² The crystal systems are classified according to their rotational symmetry and cell conditions in terms of vector lengths and angles. Fourteen Bravais lattices can be defined, involving four different centring of the lattice points (Fig 1.19):

- 1- Primitive (P): where all the lattice points are at the corners of the unit cell;
- 2- Body centre (I): which includes the lattice points that are on the corners plus one in the middle of the cell;
- 3- Face centred (F): the primitive lattice points and the points occur in the middle of each face;
- 4- Centred (C): all the primitive lattice points plus lattice points in the middle of two opposite faces (A, B, or C).

Table 1.6 The seven crystal systems and related cell dimensions

Crystal System	Cell lengths	Cell Angles
Cubic	$a = b = c$	$\alpha = \beta = \gamma = 90^\circ$
Tetragonal	$a = b \neq c$	$\alpha = \beta = \gamma = 90^\circ$
Orthorhombic	$a \neq b \neq c$	$\alpha = \beta = \gamma = 90^\circ$
Rhombohedral	$a = b = c$	$\alpha = \beta = \gamma \neq 90^\circ$
Hexagonal	$a = b \neq c$	$\alpha = \beta = 90^\circ; \gamma = 120^\circ$
Monoclinic	$a \neq b \neq c$	$\alpha = \gamma = 90^\circ \neq \beta$
Triclinic	$a \neq b \neq c$	$\alpha \neq \beta \neq \gamma \neq 90^\circ$

Once the unit cell is defined, we can define the Miller indices h , k , and l . These are used fundamentally in X-ray crystallography to specify crystal planes, where they represent the faces of the crystal and intercepts with the a , b , and c vectors and are useful in explaining and understanding diffraction patterns (Fig 1.20).^{39,42}

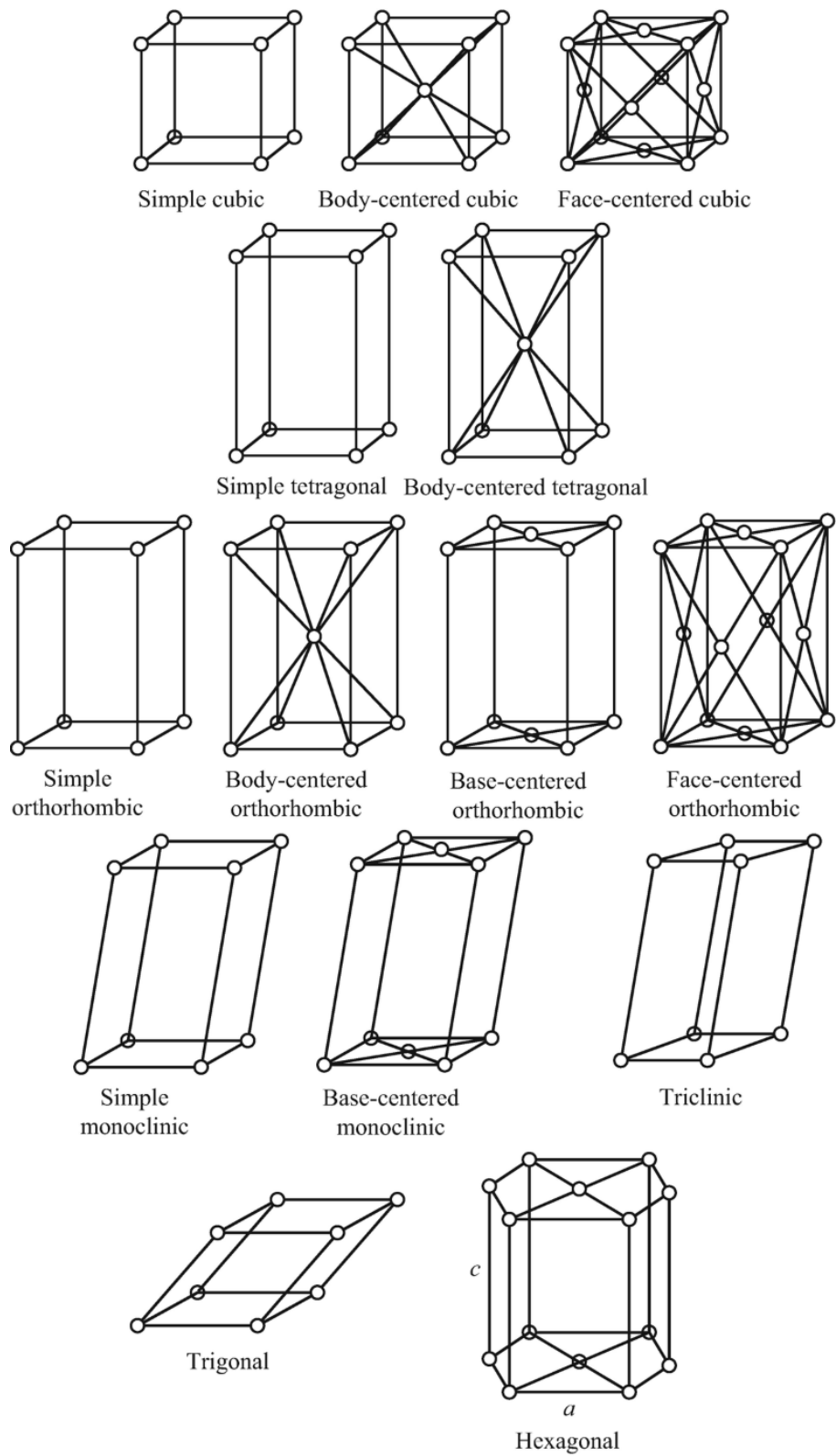


Figure 1.19 Fourteen possible Bravais lattices⁴⁵

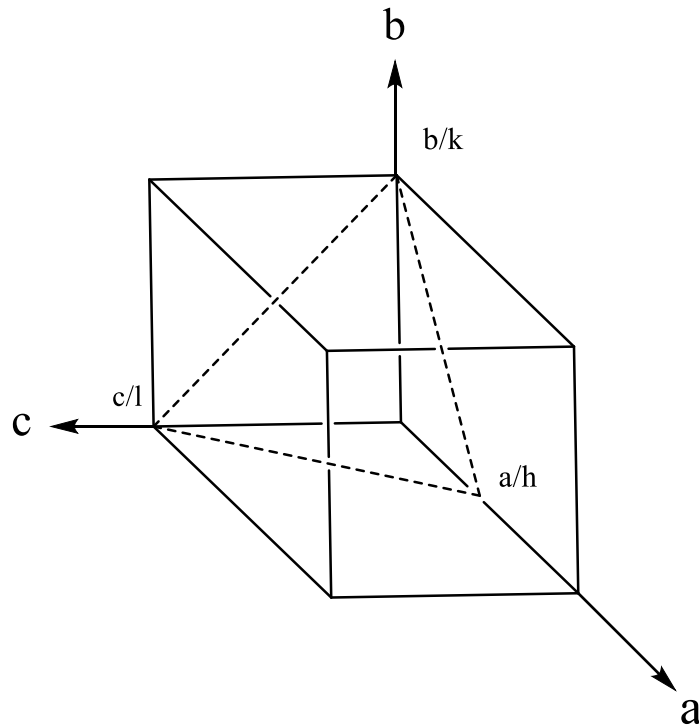


Figure 1.20 Miller indices h , k and l and their intercepts with the a , b , and c axes

1.5.3. Bragg's law

W. H. Bragg and his son W. L. Bragg worked out the first crystal structures by analysing Laue's hypothesis about crystals and the ability of X-rays to scatter from a regular array of atoms.⁴² Bragg's son expressed the Laue point of view in an intelligent way and solved a complete set of structures for NaCl, KBr, KCl, and KI.⁴² He deduced that the diffracted beams are reflected from the crystal planes by passing through certain crystal lattice points. He derived his famous equation, shown below, which is still used in modern crystallography. The geometry of the incident and diffracted beams are shown in Fig 1.21. The total path difference (ABC) between the two diffracted beams, which makes angles θ with respect to the diffraction planes, is expressed by the equation

$$n\lambda = 2d \sin \theta,$$

where λ is the wavelength of the X-ray beam, d is the plane spacing, and θ is the angle between the beam and the plane. The two diffracted beams will reinforce each other and show constructive interference if n is a whole number of wavelengths. Destructive interference occurs for all the other angles because the scattered beams cancel one another.⁴² This leads to absences in some reflections, which are used to determine the lattice type (general absence) and non-translational symmetry (systematic absence).³⁹

As θ is increased, the number of Bragg reflections increases, giving more detail about the structure. The single crystal will only diffract when the crystal plane is aligned correctly, and the Bragg condition is satisfied. This is no different to the powder condition, except that in powder diffraction, we do not have to rotate the crystal to get the planes aligned because there are millions of little crystallites that are in all possible orientations of the crystal.⁴²

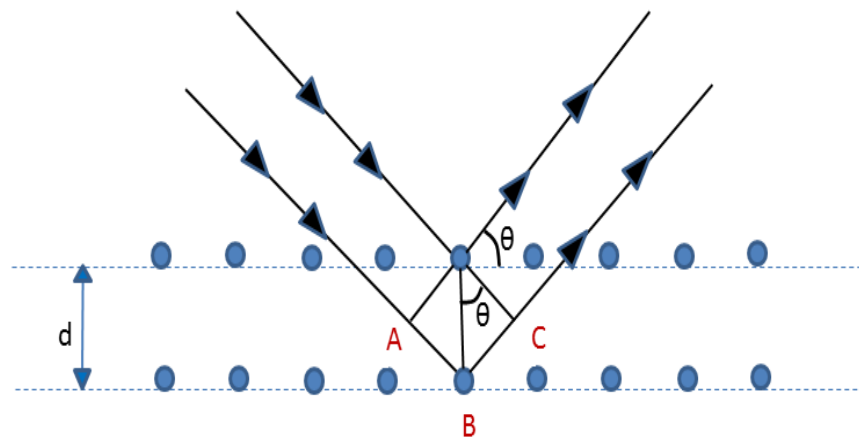


Figure 1.21 Bragg's concept

1.5.4. Single crystal X-ray diffraction

The two main X-ray diffraction methods used these days are powder and single crystal X-ray diffraction. Which technique is used depends on the kind of solid being analysed. What follows is a description of the processes for single crystal X-ray diffraction studies.

A single crystal X-ray instrument, as shown in Fig 1.22, consists of an X-ray source, goniometer, cold nitrogen source, CCD detector, and collimator.

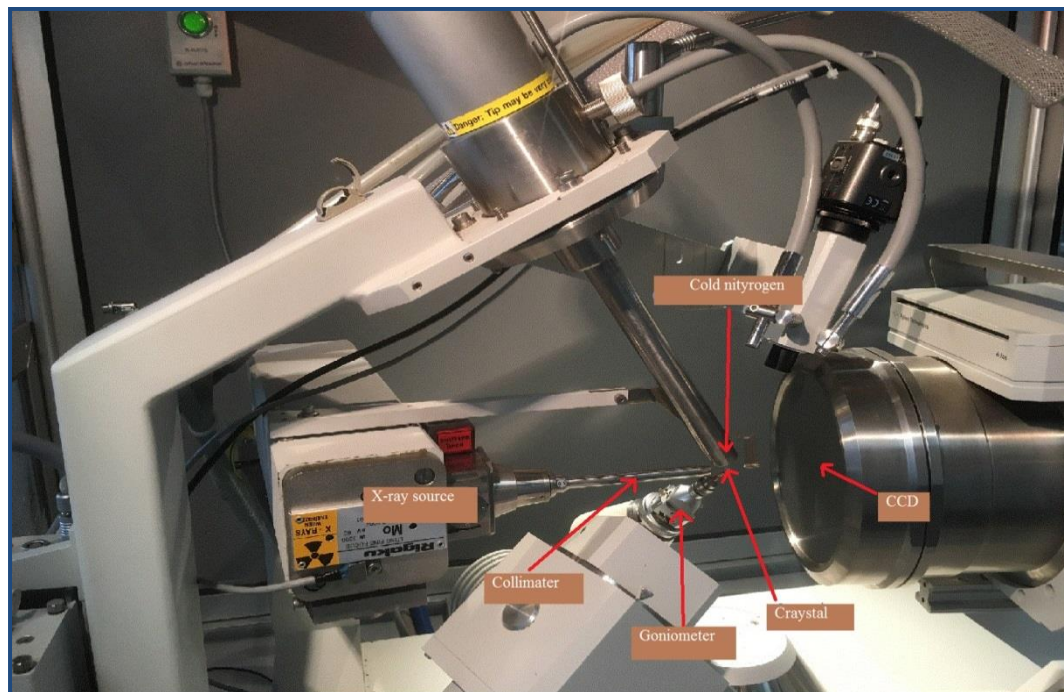


Figure 1.22 X-ray single crystal instruments

1.5.5. The steps followed to determine the crystal structure

The steps followed to determine a crystal's structure are illustrated in Fig 1.23. A suitable single crystal should be selected with dimensions between 0.1 and 0.3 mm. Selection of a crystal should be made with the aid of a polarizing microscope, in order to help choose a good quality single crystal.³⁹ Perfluoroether oil is used to attach the crystal to the glass fibre on the goniometer and to protect air sensitive crystals (Fig 1.24A).³⁹

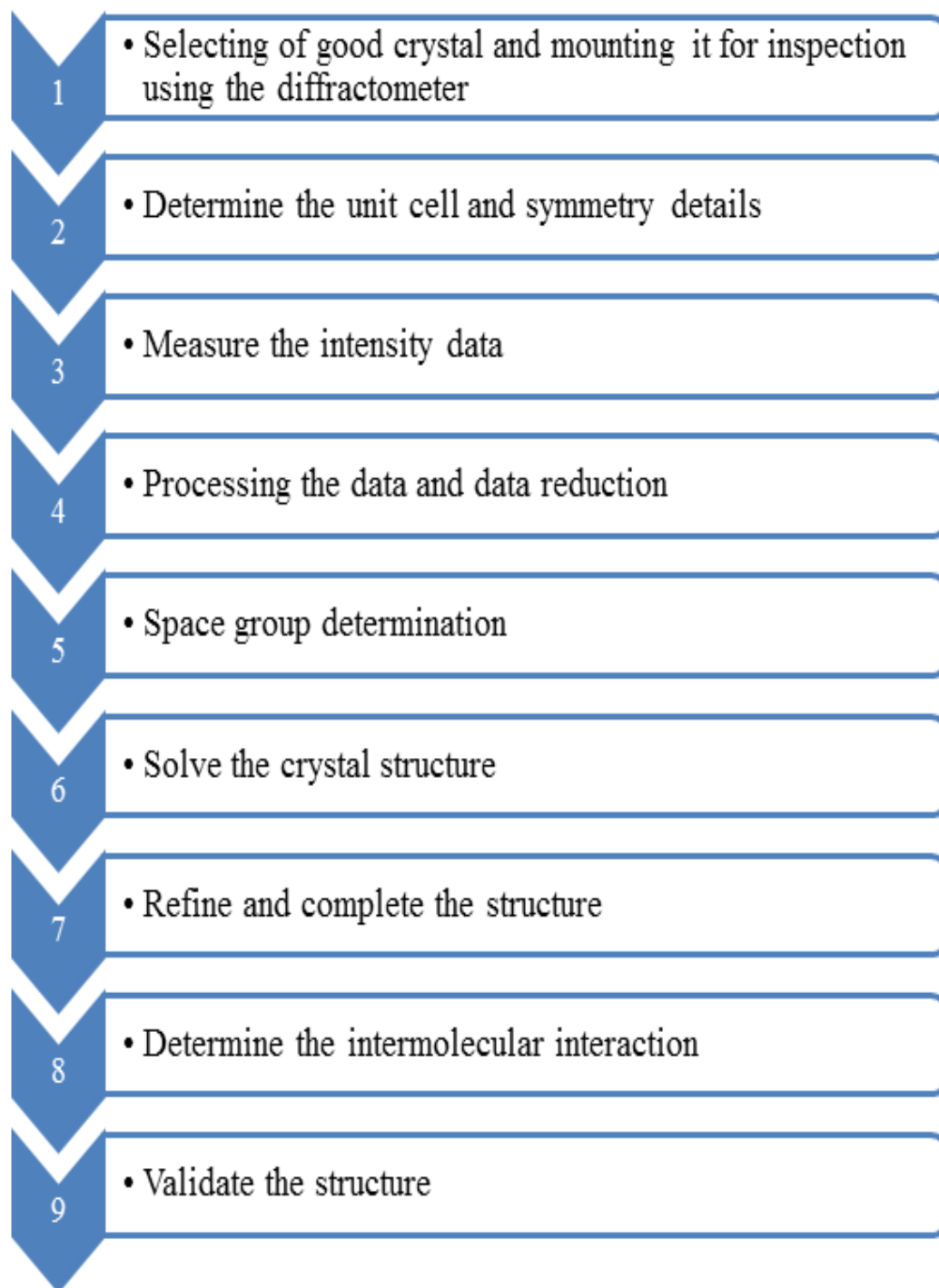


Figure 1.23 Flow chart describing the steps to determine a crystal structure

Alternatively, the crystal may be glued to the glass fibre (Fig 1.24B) or sealed in a glass capillary tube (Fig 1.24C) to avoid degrading the sample by losing solvent.⁴⁶

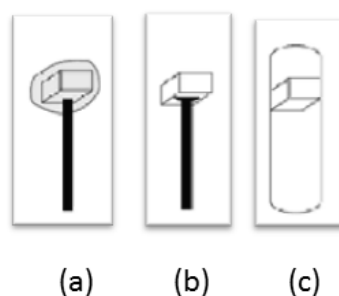


Figure 1.24 Methods of mounting a crystal³⁸

The crystal is then centred in the X-ray beam. This centring process is carried out by viewing the crystal via an inbuilt video microscope. A cold nitrogen gas stream is used to lower the temperature of the crystal in order to reduce the atomic vibration of the atoms and to reduce the possibility of radiation damage.⁴⁴

A quick scan follows to determine the unit cell and other symmetry details. This process defines how good the crystal is by showing clear sharp spots.

The next stage is to systematically measure the appropriate number of reflections to complete the data set for the particular crystal. This process may take minutes or hours depending on the crystal. The intensities of reflections with different (h, k, l) indices are obtained via a Charge-Coupled Device (CCD). Associated with every intensity is a standard uncertainty (s.u.), $\sigma(I)$, which approximates the precision of the measurement.⁴⁴

Afterwards, the data are processed and corrections applied related to the instrument geometry. Polarization corrections are carried out due to the slight polarization of the reflected X-rays, and Lorentz corrections account for how long the Miller plane spends in its diffraction position as the crystal is rotated. Absorption effects, related to the path lengths that X-rays travel through the crystal, are also known to be important. This includes the crystal shape, dimensions, path length calculation, and

other symmetry-related absorption corrections. All these corrections are done quickly with the aid of powerful computers.⁴⁴

From these data, unique .hkl and .ins (instruction) files are produced, followed by a determination of the space group by looking for systematic absences.^{46,39}

The electron density map can be obtained mathematically from the diffraction pattern using an inverse Fourier transform, represented by the equation.⁴⁴

$$\rho(xyz) = 1/V \sum_{hkl} |F(hkl)| \cdot \exp[i\Phi(hkl)] \cdot \exp[-2\pi i(hx + ky + lz)],$$

where $\rho(xyz)$ is the electron density at the unit cell location assigned by (x, y, z) , V is the volume of the unit cell, $|F(hkl)|$ is the amplitude of the structure factor related to the hkl Miller indices, and Φ is the phase.

While individual reflection intensities can be measured their phases cannot, to overcome the missing information or “phase problem”, two main methods are embedded in Olex2 software. The first and most commonly used is the direct method, which is used for structures containing similar atoms and uses the measured intensities to directly calculate the possible phase angles of the reflections.³⁹

The second method, the Patterson method, locates heavy atoms by carrying out a Fourier transform of F^2_{hkl} . The map looks similar to an electron density map, but Patterson peaks are described as ‘a map of vectors between pairs of atoms in the structure’.²⁹ One of the drawbacks of this method is that it shows the positions of atoms relative to each other but not to the unit cell.^{39,44}

After the electron density map has been produced based on one of the previous two methods, an initial structure model can be developed by assigning some atom types to the observed peaks. This is followed by refining this model using the least-squares method, and ends with a complete structure. The success of this process can be related to an agreement factor (residual factor R), which measures how well the

model matches the experimental (hkl) data. At this stage, the final crystallographic data can be generated and saved in the crystallographic information file (CIF) to carry out the final check for similar structures in the CSD.

The final and most important step for the crystallographer is to interpret and seek novelty in the geometrical information (bond lengths, bond angles, etc), and then publish the work.

1.6. Quantum chemical calculations

Computational chemistry is one way to describing the physical properties of the resulting structure and to support the work using quantum chemical calculations based on the well-known Schrödinger equation.

$$\hat{H}\Psi = E\Psi$$

Where Ψ represent the wave function, \hat{H} is the Hamiltonian operator and E is the total energy of the system.

A series of approaches or models have been implemented in quantum chemistry computer programmes to approximate the Schrodinger equation for many particles systems. Density Functional Theory (DFT) level of theory was developed by Kohn and Sham⁴⁷ by using the one-body density, rather than individual electron wave functions.

Various calculation analysis can be performed using the DFT method one of them is based on the three parameters hybrid functional B3LYP, which contains the Hartree-Fock exchange matrix.

Each calculation method including the B3LYP, requires a basis set to create an electron density maps. This basis sets can be selected when creating the input file in various software packages used to perform the computational chemistry. These basis sets can include additional parameters to better match observed properties.

One example is the 6-311G** basis set, which is equivalent to 6-311G(d,p) , where "**" and (d,p) are synonymous and both indicate that a polarization function has been added.

Computational calculations can be carried out using different software packages (GAMMESS⁴⁸ or Gaussian etc) to generate wavefunction files in the format .wfn.

The Multiwfn⁴⁹ wavefunction analysis programme can be used to perform the Quantum theory of atoms in molecules (QTAIM) electron density topological analysis and visualize the resulted structures.

1.6.1. The quantum theory of atoms in molecules (QTAIM) analysis

From X-ray diffraction studies the distances between pairs of atoms can be determined, from which bonds and interactions are implied by comparison with expected covalent and van der Waals radii. Quantum theory of atoms in molecules (QTAIM) analysis has been used to provide further evidence that distances observed that are less than the sum of the relevant van der Waals radii are significant interactions.

This theory was proposed by Bader and is based on calculating the electron density of the molecule, or set of molecules, followed by a topological analysis of the electron density distribution.⁵¹ If the electron density for a system is calculated and mapped, then for each atom, an area of high electron density is expected. If a bond exists between two atoms (atom A and atom B), then the electron density is expected to decrease when moving away from atom A towards atom B (but not to reach zero) before rising again when moving towards atom B. The point between the two atoms where the electron density stops falling (but is not zero) and then starts to rise in one direction is called a bond critical point (BCP).⁵²

Therefore, the presence of a BCP indicates the existence of a covalent or non-covalent interaction between two atoms.⁵² In addition to BCPs, other critical points are generated for nuclear (nuclear critical point, NCP) cages, (cage critical point, CCP), and rings (ring critical point, RCP).⁵²

The number of the different kinds of critical points should follow the Poincaré-Hopf relationship and be equal to one according to the Morse equation (Equation 1) for isolated molecules. ⁵²⁻⁵⁵

$$n_{\text{NCP}} - n_{\text{BCP}} + n_{\text{RCP}} - n_{\text{CCP}} = + 1 \quad (1)$$

where n represents the number of each critical point. Describing the topology analysis of electron density at each critical point of CP can be achieved by knowing the first derivative, $\nabla\rho$, which is known as the gradient of the electron density and vanishes at each CP:

$$\nabla\rho = i \frac{d\rho}{dx} + j \frac{d\rho}{dy} + k \frac{d\rho}{dz} \quad (i, j, \text{ and } k \text{ are vectors related to the gradient } \nabla\rho). \quad (2)$$

The second derivative, $(\nabla^2\rho)$, measures the change in the gradient and can be used to trace the local maxima, local minima, and saddle points (Fig 1.25) by identifying this change in electron concentration.

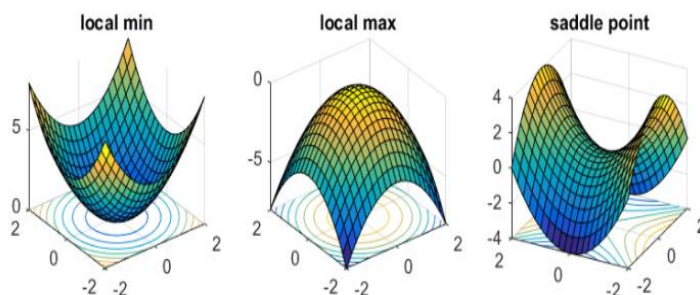


Figure 1.25 Local maxima, local minima, and saddle point curvatures taken from ⁵⁶

The sign of the Laplacian $\nabla^2\rho_{\text{BCP}}$ [< 0 covalent, and if > 0 close-shell interactions] and an energy related property called the total energy density, $H_{(r)}$ [< 0 covalent, and if > 0 non-covalent interaction] are used to characterise each BCP. $H_{(r)}$ is the sum of two related energy components, potential energy density V , and kinetic energy density G .

$$H_{(r)} = G_{(r)} + V_{(r)} \quad (3)$$

$H(r)$ at each bond critical point can be a good sign of the identity of the bond because the potential energy density $V(r)$ is always negative and so $H(r)$ is positive when $G(r)$ is positive and dominant.

If the interaction has a high degree of electron sharing, a negative sign of $H(r)$ is expected.⁵⁸

The strength of a bond or interaction can be related to the Laplacian $\nabla^2\rho_{\text{BCP}}$ of the electron density at the bond critical point and the energy density H_{BCP} ^{59,60}. Both of these parameters have been widely used in investigating the strength of intermolecular interactions.⁶⁰⁻⁶²

In 2004, Berski and colleagues used QTAIM calculations on complexes containing 4-amino-4H-1,2,4-triazole and 4-X-benzaldehyde to study the C-X...N (X = Cl, Br, I) halogen bonds and observed BCPs for each of these interactions; they found a small positive value of electron density ρ_{BCP} and $\nabla^2\rho_{\text{BCP}}$ in all studied structures, which confirmed closed-shell interactions.⁶³

In one study involving hydrogen bonded HX interactions, adducts revealed that when H_{BCP} and $\nabla^2\rho_{\text{BCP}} > 0$, the interaction is weak and when $H_{\text{BCP}} < 0$ and $\nabla^2\rho_{\text{BCP}} > 0$, the HX interaction is medium, while strong HX interactions are characterised by both H_{BCP} and $\nabla^2\rho_{\text{BCP}} < 0$.⁶⁰ These descriptions of HX interactions were subsequently used by Esrafili and colleagues in 2012 to describe XB in a series of dichloroacetic acid complexes.⁶² These complexes contain a variety of XH, Cl...O and Cl...Cl halogen bond interactions, and small positive ρ_{BCP} , $\nabla^2\rho_{\text{BCP}}$, and H_{BCP} values characterised the studied interactions. The shortest O-H...O (1.69 Å) interaction (37.9% shorter than the sum of van der Waals radii of oxygen and hydrogen atoms, 2.72 Å) has the highest electron density ρ_{BCP} and small negative H_{BCP} . Esrafili suggested that this was related to the strength of this XH compared with the other interactions.⁶⁴

Another QTAIM computational study conducted by Esrafili and colleagues in 2012 used GAMESS and AIM 2000 software to examine the existence of halogen bonds in F-Ar-X...N≡CY complexes where X = Cl, Br and Y = H, F, Cl, Br, OH, NH₂,

CH₃, and CN.⁶² Most of the bond critical points for Cl...N and Br...N interactions had a $\nabla^2\rho_{\text{BCP}} > 0$ and $H_{\text{BCP}} > 0$, which indicates a weak and electrostatic nature of the interactions.

One year later, Angelina and colleagues studied complexes containing Cl...N halogen bond interactions and found positive values for ρ_{BCP} and $\nabla^2\rho_{\text{BCP}}$ and a negative value for $H_{\text{BCP}} < 0$ for the shortest N...Cl halogen bond interactions. They concluded that this negative H_{BCP} can be taken as an indicator of the interaction strengthening.⁶⁵

The most recent QTAIM study⁶⁶ of N...I halogen bonds for systems contain 2,3,5,6-tetrafluoro-1,4-diiodobenzene and 4-(dimethylamino)pyridine (Fig 1.26) revealed a critical point between nitrogen and iodine associated with the short distance of 2.6622(4) Å (24.6% shorter than the sum of van der Waals radii for nitrogen and iodine atoms 3.53 Å).

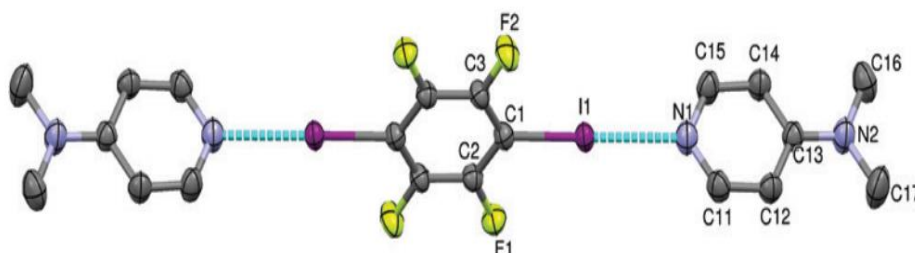


Figure 1.26 Crystal structure of system studied in reference 54.⁶⁶

They found that the BCP characterised by a large electron density (0.359(5) e.Å⁻³), a positive $\nabla^2\rho_{\text{BCP}}$ (1.95 e.Å⁻³), and a negative value for H_{BCP} (-0.0148 a.u.) corresponded to the shortest N...I halogen bonds, which can be taken as an indication of the strengthening of the related halogen bond.⁶⁶

Taken together a QTAIM study can therefore be used to support crystallographic determinations of the existence and characterisation of halogen bonds in the solid state via the observation of a BCP between a halogen bond donor and a halogen

bond acceptor. Fig 1.27 shows some types of critical points that can be observed in the structures of systems investigated in this work.

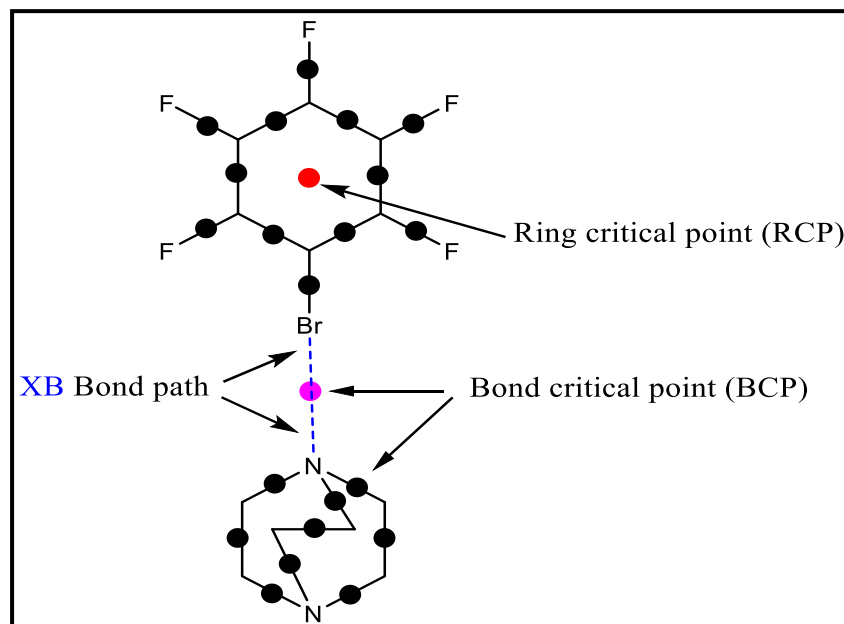


Figure 1.27 Illustration of some types of critical points and XB bond paths

1.7. Summary

Although the field of halogen bonding has expanded enormously over the past few decades, the combination of using crystallography and theoretical QTAIM calculations is under-developed.

Different mono- and di-iodo and bromo-fluorobenzene halogen bond donors will be used with different tertiary (chapter 2 + 3), secondary (chapter 6), and primary and aromatic nitrogen based XB acceptors (chapter 4 + 5).

The aim of this study is to grow halogen-bonded based crystals that are suitable for X-ray studies and determine their crystal structures. Secondly, by measuring the N...Br or N...I halogen bond distances and comparing them with the N...H hydrogen bonds other interactions that may appear within each structure. The final step will be to identify the related bond critical points and gather more information about their strength using QTAIM parameter analysis.

References

- 1 A. Stone, *The Theory of Intermolecular Forces*, OUP Oxford, 2013.
- 2 F. Guthrie, *J. Chem. Soc.*, 1863, **16**, 239–244.
- 3 P. Groth and O. Hassel, *ACTA Chem. Scand.*, 1964, **18**, 402–408.
- 4 G. R. Desiraju, P. S. Ho, L. Kloo, A. C. Legon, R. Marquardt, P. Metrangolo, P. Politzer, G. Resnati and K. Rissanen, *Pure Appl. Chem*, 2013, **85**, 1711–1713.
- 5 K. D. Sen and P. Politzer, *J. Chem. Phys.*, 1989, **90**, 4370–4372.
- 6 T. Clark, M. Hennemann, J. S. Murray and P. Politzer, *J. Mol. Model.*, 2007, **13**, 291–296.
- 7 P. Politzer and J. S. Murray, *ChemPhysChem*, 2013, **14**, 278–294.
- 8 T. Brinck, J. S. Murray and P. Politzer, *Int. J. Quantum Chem.*, 1992, **44**, 57–64.
- 9 M. Fourmigué, *Curr. Opin. Solid State Mater. Sci.*, 2009, **13**, 36–45.
- 10 P. Politzer, P. Lane, M. C. Concha, Y. Ma and J. S. Murray, *J. Mol. Model.*, 2007, **13**, 305–311.
- 11 M. Palusiak, *J. Mol. Struct. THEOCHEM*, 2010, **945**, 89–92.
- 12 K. E. Riley and K. M. Merz, *J. Phys. Chem. A*, 2007, **111**, 1688–1694.
- 13 P. Politzer, J. S. Murray and T. Clark, *Phys. Chem. Chem. Phys.*, 2010, **12**, 7748–7757.
- 14 C. Laurence, J. Graton, M. Berthelot and M. J. El Ghomari, *Chem. Eur. J.*, 2011, **17**, 10431–10444.
- 15 Y. Lu, H. Li, X. Zhu, W. Zhu and H. Liu, *J. Phys. Chem. A*, 2011, **115**, 4467–4475.
- 16 M. G. Sarwar, B. Dragisic, L. J. Salsberg, C. Gouliaras and M. S. Taylor, *J. Am. Chem. Soc.*, 2010, **132**, 1646–1653.
- 17 K. E. Riley, J. S. Murray, P. Politzer, M. C. Concha and P. Hobza, *J. Chem. Theory Comput.*, 2009, **5**, 155–163.

- 18 P. Metrangolo, F. Meyer, T. Pilati, G. Resnati and G. Terraneo, *Angew. Chemie - Int. Ed.*, 2008, **47**, 6114–6127.
- 19 E. Arunan, G. R. Desiraju, R. A. Klein, J. Sadlej, S. Scheiner, I. Alkorta, D. C. Clary, R. H. Crabtree, J. J. Dannenberg, P. Hobza, H. G. Kjaergaard, A. C. Legon, B. Mennucci and D. J. Nesbitt, *Pure Appl. Chem.*, 2011, **83**, 1637–1641.
- 20 L. C. Gilday, S. W. Robinson, T. A. Barendt, M. J. Langton, B. R. Mullaney and P. D. Beer, *Chem. Rev.*, 2015, **115**, 7118–7195.
- 21 P. Auffinger, F. A. Hays, E. Westhof and P. S. Ho, *Proc. Natl. Acad. Sci.*, 2004, **101**, 16789–16794.
- 22 Y. Lu, Y. Wang and W. Zhu, *Phys. Chem. Chem. Phys.*, 2010, **12**, 4543–4551.
- 23 C. R. Groom, I. J. Bruno, M. P. Lightfoot and S. C. Ward, *Acta Crystallogr. Sect. B Struct. Sci. Cryst. Eng. Mater.*, 2016, **72**, 171–179.
- 24 J. P. and R. T. Ian J. Bruno, Jason C. Cole, Paul R. Edgington, Magnus Kessler, Clare F. Macrae, Patrick McCabe, *Acta Crystallogr. Sect. B Struct. Sci.*, 2002, **58**, 389–397.
- 25 L. Catalano, S. Pérez-Estrada, G. Terraneo, T. Pilati, G. Resnati, P. Metrangolo and M. A. Garcia-Garibay, *J. Am. Chem. Soc.*, 2015, **137**, 15386–15389.
- 26 S. D. Karlen, H. Reyes, R. E. Taylor, S. I. Khan, M. Frederick Hawthorne and M. A. Garcia-Garibay, *pnas.org*, 2010, **107**, 14973–14977.
- 27 B. Rodríguez-Molina, S. Pérez-Estrada and M. A. Garcia-Garibay, *J. Am. Chem. Soc.*, 2013, **135**, 10388–10395.
- 28 M. C. Pfrunder, A. S. Micallef, L. Rintoul, D. P. Arnold, K. J. P. Davy and J. Mcmurtrie, *Cryst. Growth Des.*, 2012, **12**, 714–724.
- 29 D. Cinčić, T. Friščić and W. Jones, *Chem. Eur. J.*, 2008, **14**, 747–753.
- 30 J. L. Syssa-Magalé, K. Boubekour, J. Leroy, L. M. Chamoreau, C. Fave and B. Schöllhorn, *CrystEngComm*, 2014, **16**, 10380–10384.
- 31 R. Wang, J. George, S. K. Potts, M. Kremer, R. Dronskowski and U. Englert, *Acta Crystallogr. Sect. C*, 2019, **75**, 1190–1201.
- 32 N. Bedeković, V. Stilinović, T. Friščić and D. Cinčić, *New J. Chem.*, 2018, **42**, 10584–10591.
- 33 G. Fan, X. Yang, R. Liang, J. Zhao, S. Li and D. Yan, *CrystEngComm*, 2016, **18**, 240–249.

- 34 J. L. Atwood and W. A. Sheppard, *Acta Crystallogr. Sect. B*, 1975, **31**, 2638–2642.
- 35 C. M. Santana, E. W. Reinheimer, H. R. Krueger, L. R. MacGillivray and R. H. Groeneman, *Cryst. Growth Des.*, 2017, **17**, 2054–2058.
- 36 F. Topić and K. Rissanen, *J. Am. Chem. Soc.*, 2016, **138**, 6610–6616.
- 37 A. M. T. Muneer, PhD Thesis, The University of Manchester, 2018.
- 38 M. R. Jenny P. Glusker, Mitchell Lewis, *Crystal Structure Analysis for Chemists and Biologists*, John Wiley & Sons, 1994.
- 39 L. Ooi, *Principles of X-ray Crystallography*, OUP Oxford, 2010.
- 40 W. Clegg, *Crystal Structure Analysis: Principles and Practice*, Oxford, U.K, 2001.
- 41 W. Massa, *Crystal structure determination*, Springer, New York, 2004.
- 42 S. R. Cullity, B.D.; Stock, *Elements of X-ray Diffraction*, Prentice-Hall, New York, Third Edit., 2001.
- 43 J. P. Glusker, *Crystal structure analysis: a primer.*, Oxford University Press, 2010.
- 44 W. Clegg, *Crystal Structure Determination*, Oxford University Press, Oxford, U.K, 1998.
- 45 M. Razeghi, *Fundamentals of solid state engineering*, Springer, Cham, Switzerland, Fourth edi., 2019.
- 46 W. Clegg, *X-ray Crystallography*, Oxford University Press, 2015.
- 47 W. Kohn and L. J. Sham, *Phys. Rev.*, 1965, **140**, A1133
- 48 J. H. Jensen, S. Koseki, N. Matsunaga, K. A. Nguyen, S. Su, T. L. Windus, M. Dupuis, J. A. M. Jr, M. W. Schmidt, K. K. Baldrige, J. A. Boatz, S. T. Elbert and M. S. Gordon, *J. Comput. Chem.*, 1993, **14**, 1347–1363.
- 49 T. Lu and F. Chen, *J. Comput. Chem.*, 2012, **33**, 580–592.
- 50 M. R. Jenny P. Glusker, Mitchell Lewis, *Crystal Structure Analysis for Chemists and Biologists*, John Wiley & Sons, New York, 1994.
- 51 P. S. V. Kumar, V. Raghavendra and V. Subramanian, *J. Chem. Sci.*, 2016, **128**, 1527–1536.
- 52 R. J. Boyd, F. Matta and R. J. Boyd, *The Quantum Theory of Atoms in*

Molecules, 2007.

- 53 R. F. W. Bader, *Atoms in Molecules: A Quantum Theory*, Clarendon Press, Oxford, 1994.
- 54 V. Tognetti and L. Joubert, in *Challenges and Advances in Computational Chemistry and Physics*, Springer, 2016, vol. 22, pp. 435–459.
- 55 C. R. Wick and T. Clark, *J. Mol. Model.*, 2018, **24**, 142.
- 56 Escaping from Saddle Points,
<https://www.offconvex.org/2016/03/22/saddlepoints/>, (accessed March 2022)
- 57 R. Ge, Artificial Neural Networks- An intuitive approach Part 5 | by Niketh Narasimhan | Analytics Vidhya | Medium, <https://medium.com/analytics-vidhya/artificial-neural-networks-an-intuitive-approach-part-5-95da50a9cffd>, (accessed 2 October 2020).
- 58 D. Cremer and E. Kraka, *Angew. Chemie Int. Ed.*, 1984, **23**, 627–628.
- 59 R. F. W. Bader, *Atoms in Molecules: a Quantum Theory*, Oxford University Press, Oxford, U.K, 1990.
- 60 I. Rozas, I. Alkorta and J. Elguero, *J. Am. Chem. Soc.*, 2000, **122**, 11154–11161.
- 61 M. Jabłoński and M. Palusiak, *J. Phys. Chem. A*, 2012, **116**, 2322–2332.
- 62 M. D. Esrafilı and B. Ahmadi, *Comput. Theor. Chem.*, 2012, **997**, 77–82.
- 63 S. Berski, Z. Ciunik, K. Drabent, Z. Latajka and J. Panek, *J. Phys. Chem. B*, 2004, **108**, 12327–12332.
- 64 M. D. Esrafilı, *J. Mol. Model.*, 2012, **18**, 5005–5016.
- 65 E. L. Angelina, D. J. R. Duarte and N. M. Peruchena, *J. Mol. Model.*, 2013, **19**, 2097–2106.
- 66 R. Wang, D. Hartnick and U. Englert, *Zeitschrift für Krist. - Cryst. Mater.*, 2018, **233**, 733–744.

Chapter 2.

Manuscript 1: Halogen bonding in a series of bromofluorobenzenes and 1,4-diazabicyclo[2.2.2]octane (DABCO)

Alan K. Brisdon* and Sultan Alkaabi

Department of Chemistry, The University of Manchester, Oxford Road,
Manchester, M13 9PL, United Kingdom

Correspondence email: *alan.brisdon@manchester.ac.uk

2.1. Abstract

Studies of a series of bromo fluorobenzene halogen bond donors and 1,4-diazabicyclo[2.2.2]octane (DABCO) as a halogen bond acceptor yields 4 new adducts that have been characterised by X-ray single crystal diffraction. The structure of one of which has the shortest distance for an N...Br halogen bond that has been reported for this kind of systems. QTAIM computational calculations at the B3LYP/6-311G** level support the existence of bond critical points in all of the halogen bonded N...Br structures. Electron density ρ_{BCP} and Laplacian $\nabla^2\rho_{BCP}$ values for each N...Br interaction are in line with the expectations for halogen bonds.

Key words:- Halogen bonds, Crystal structure, bromofluorobenzene, iodofluorobenzene, DABCO, QTAIM, infrared, ^{19}F NMR , van der Waals radii

2.2. Introduction

Halogen bonds are one of the noncovalent interactions represented by R-X...Y that ‘occurs when there is evidence of a net attractive interaction between an electrophilic region associated with a halogen atom in a molecular entity and a nucleophilic region in another, or the same, molecular entity’. (Marquardt *et al.*, 2013) Where R-X represents the halogen bond donor, the dots represent a halogen bond and Y refers to a halogen bond acceptor.

There are many potential areas which might involve halogen bonds, such as biological process (Riley *et al.*, 2009; Auffinger *et al.*, 2004) drug design (Auffinger *et al.*, 2004) and the design of crystals with specific uses or characteristics. (Navarrini *et al.*, 2000) However, as described and discussed by many articles, most of the published XB systems have iodine as the halogen bond donor because of its high polarizability leading to large sigma hole (Brinck *et al.*, 1992; Palusiak, 2010)

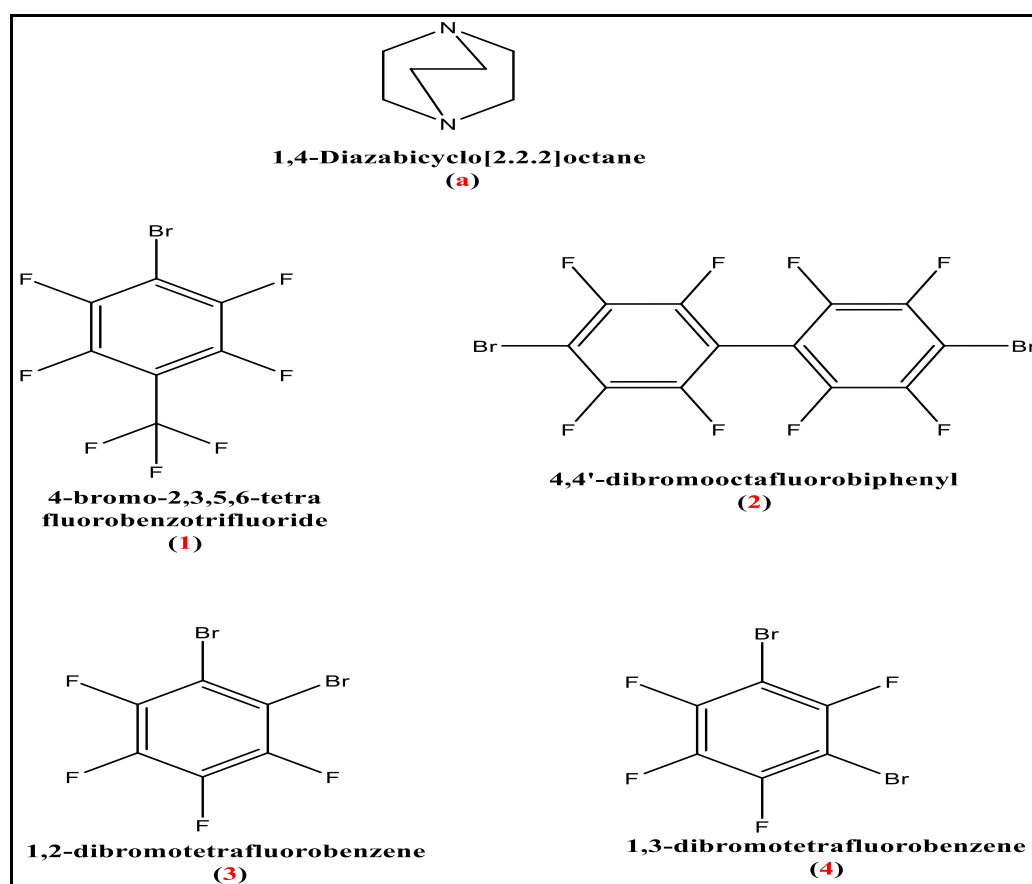
A study carried out by Dominik and his group in 2008, focused on the melting point of a variety of halogen-bonded crystals, formed using 1,4-diiodotetrafluorobenzene and 1,4-dibromotetrafluorobenzene as halogen-bond donors when they observed considerable differences in the melting point between the halogen bonded systems containing sulphur and oxygen compared with systems containing nitrogen acceptors. (Cinčić *et al.*, 2008)

One of the more frequently used nitrogen-containing compounds is the ditopic nitrogen base DABCO which is known to adopt a cylindrical shape, with 3-fold symmetry and often packs in a way leading to a low rotational barrier. (Metrangolo *et al.*, 2015; Karlen *et al.*, 2010; Rodríguez-Molina *et al.*, 2013) A comprehensive search using ConQuest revealed only 40 hits in the CCDC for structures involving DABCO as a halogen bond acceptor with iodine- and bromine-containing compounds (the search parameters used were C-X...N angle between 150-180° and N...X distance shorter than the sum of vdW radii). Of these 15 hits were for perfluorinated iodoaromatic structures and only 1 perfluorinated bromoaromatic adduct had been deposited in addition to the one recently prepared by our group. (Muneer, 2017)

A number of studies of halogen bonding have used the quantum theory of atoms in molecules (QTAIM) to examine the existence of bond critical points in intermolecular interactions (Rozas *et al.*, 2000; Jabłoński & Palusiak, 2012) and to provide evidence to support the observed interaction bonds distances from X-ray studies. According to Bader, 1994 the electron density at the bond critical point, ρ_{BCP} , of all electrons is expected to be small for "close-shell" interactions and halogen bonds derived from them.(Bader, 1994) Rozas and his group, in 2000,

focused on the energy density H_{BCP} , to differentiate between strong, medium and weak interactions (Rozas *et al.*, 2000). While in 2012 Esrafil and his group (Esrafil & Ahmadi, 2012) used the Laplacian, $\nabla^2\rho_{\text{BCP}}$, of the electron density at the bond critical point, combined with the total electron energy density, H_{BCP} , (Bader, 1994; Rozas *et al.*, 2000; Jabłoński & Palusiak, 2012) to describe the strength and the nature of N...Br halogen bonds in a series of F-Ar-Br...NCF complexes.

In this study 4-bromo-2,3,5,6-tetrafluorobenzotrifluoride (1), 4,4'-dibromooctafluorobiphenyl (2), 1,2-dibromotetrafluorobenzene (3) and 1,3-dibromotetrafluorobenzene (4) (Scheme 2.1) have been combined in different ratios with DABCO to investigate the ability of these bromine systems to engage in XB and to examine, where it is possible, the possibility to have more than one bromine centre involved as XB donors.



Scheme 2.1 Compounds used in crystallization

2.3. Experimental

Chemicals were purchased from commercial suppliers, and used without further purification.

2.3.1. Synthesis and crystallization

1a, **3a**, **4a** adducts were grown using the vapour diffusion technique, while **2a** was grown by slow evaporation from dried acetonitrile solutions of **2** and **a**.

In the vapour diffusion method a sealed system consisting of two different sized of vials were used. DABCO was placed in the small inner vial and the arene was placed in the larger, outer, vial. A 1:2 stoichiometric molar ratio of arene to DABCO was used to grow adducts **4a** [0.03 ml (0.097 mmol) of **4** and 0.049 g (0.438 mmol) of **a**], **3a** [0.03 ml of **3** (0.097 mmol) and 0.049 g of **a** (0.438 mmol)], and a 1:1 molar ratio for adduct **1a** [0.03 ml of **1** (0.175 mmol) and 0.020 g of **a** (0.179 mmol)].

The slow evaporation technique used in **2a**, where a 1:2 [0.03 ml (0.066 mmol) for **2** and 0.15 g (1.34 mmol) of **a**] molar ratio of 4,4'-dibromooctafluorobiphenyl and DABCO were dissolved separately in dried acetonitrile (0.4 ml).

Single crystals of the adducts suitable for X-ray analysis were obtained within 1 to 3 days at ambient temperature, whereas adduct **1a** was grown in a fridge over 15 days.

FT-IR spectra of the solid adducts were recorded using a Nicolet iS5 FT-IR instrument, (See S2.1- S2.4). IR $\nu(\text{cm}^{-1})$ data for adduct (**1a**), formed between DABCO and 4-bromo-2,3,5,6-tetrafluorobenzotrifluoride: 2937, 2871(C-H), 1325, 1148(C-F); for adduct (**2a**) formed between DABCO and 4,4-dibromooctafluorobiphenyl: 2936, 2870 (C-H), 1224 (C-F); for adduct (**3a**) formed between DABCO and 1,2-dibromotetrafluorobenzene: 2940, 2874(C-H), 1494, 1031(C-F); for adduct (**4a**) formed between DABCO and 1,3-dibromotetrafluorobenzene: 2940, 2874 (C-H), 1077, 1480(C-F).

^{19}F NMR spectra were recorded on a Bruker AMX 400 MHz spectrometer (See S 2.5-S 2.8) of the adducts dissolved in CD_3CN . However, the spectra showed no changes that might indicate the ability of the halogen bonding interaction to remain in solution.

Elemental analysis were performed for adducts by the microanalytical service at the University of Manchester. **(3a)**. Found C 29.69, H 1.52, N 3.83. Calc. for 2:1 adduct $\text{C}_{18}\text{H}_{12}\text{F}_8\text{Br}_4\text{N}_2$: C 29.68, H 1.66, N 3.87%; **(4a)**. Found C 29.82, H 1.51, N 3.85. Calc. for 2:1 adduct $\text{C}_{18}\text{H}_{12}\text{F}_8\text{Br}_4\text{N}_2$: C 29.68, H 1.66, N 3.87%

2.3.2. Refinement

Single crystals of the adducts were mounted on a thin glass fibre using paraffin oil. Data were collected at 150 K on a supernova Eos diffractometer, with a single source at offset, utilizing a monochromated Mo $\text{K}\alpha$ radiation source ($\lambda=0.710773$ Å). Structures were solved by direct methods followed by full matrix least squares refinement using SHELXL. (Sheldrick, 2015) All of the non-hydrogen atoms were refined anisotropically and the hydrogen atoms treated as riding atoms and added at their geometrically ideal positions. A summary of the crystallographic data related to the structures reported are listed in Table 2.1.

Table 2.1 Experimental details.

	(1a)	(2a)	(3a)	(4a)
Crystal data				
Chemical formula	2(BrC ₇ F ₇)·C ₆ H ₁₂ N ₂	Br ₂ C ₁₂ F ₈ ·C ₆ H ₁₂ N ₂	2(Br ₂ C ₆ F ₄)·C ₆ H ₁₂ N ₂	2(Br ₂ C ₆ F ₄)·C ₆ H ₁₂ N ₂
Mr	706.14	568.12	727.94	727.94
Crystal system, space group	Monoclinic, <i>P2₁/c</i>	Monoclinic, <i>P2₁/n</i>	Monoclinic, <i>P2₁/n</i>	Monoclinic, <i>C2/m</i>
Temperature (K)	150	150	150	150
<i>a</i> , <i>b</i> , <i>c</i> (Å)	9.4125 (12), 5.9434 (6), 20.7026 (19)	13.1452 (7), 10.8897 (7), 14.3039 (7)	7.0217 (6), 25.4798 (17), 12.7701 (9)	18.8934 (9), 6.8201 (3), 8.7971 (4)
β (°)	99.010 (11)	107.025 (5)	102.039 (8)	93.395 (4)
V (Å ³)	1143.9 (2)	1957.8 (2)	2234.5 (3)	1131.56 (9)
Z	2	4	4	2
Radiation type	Mo Kα	Mo Kα	Mo Kα	Mo Kα
μ (mm ⁻¹)	3.67	4.22	7.28	7.19
Crystal size (mm)	0.3 × 0.03 × 0.01	0.3 × 0.1 × 0.08	0.1 × 0.05 × 0.02	0.25 × 0.05 × 0.01
Data collection				
Diffractometer	SuperNova, Single source at offset/far, Eos detector	SuperNova, Single source at offset/far, Eos detector	SuperNova, Single source at offset/far, Eos detector	SuperNova, Single source at offset/far, Eos detector
Absorption correction	Multi-scan (<i>CrysAlis</i> PRO; Agilent, 2018)	Multi-scan (<i>CrysAlis</i> PRO; Agilent, 2018)	Multi-scan (<i>CrysAlis</i> PRO; Agilent, 2018)	Multi-scan (<i>CrysAlis</i> PRO; Agilent, 2018)
T _{min} , T _{max}	0.350, 1.000	0.512, 1.000	0.353, 1.000	0.693, 1.000
No. of measured, independent and observed [<i>I</i> > 2σ(<i>I</i>)] reflections	6217, 2469, 1682	10318, 3841, 2193	10422, 4373, 2763	4623, 1445, 1264
R _{int}	0.073	0.078	0.073	0.028
(sin θ/λ) _{max} (Å ⁻¹)	0.639	0.617	0.617	0.680
Refinement				
R[F ² > 2σ(F ²)], wR(F ²), S	0.057, 0.084, 1.02	0.058, 0.090, 0.98	0.072, 0.138, 1.04	0.036, 0.081, 1.08
No. of reflections	2469	3841	4373	1445
No. of parameters	208	271	289	145
H-atom treatment	H-atom parameters constrained	H-atom parameters constrained	H-atom parameters constrained	H-atom parameters constrained
Δ _{max} , Δ _{min} (e Å ⁻³)	0.62, -0.55	0.52, -0.58	0.99, -0.63	1.41, -0.60

Computer programs: *CrysAlis* PRO 1.171.39.4 (Rigaku OD, 2018), *ShelXT* (Sheldrick, 2015), *SHELXL* (Sheldrick, 2015) *Olex2* (Dolomanov *et al.*, 2009)

2.4. Result and Discussion

Following the successful preparation of the halogen-bonded adduct from the monotopic donor bromopentafluorobenzene with DABCO in our laboratories (Muneer, 2017), we decide to extend this work using a series of related bromofluorobenzenes, including those capable of forming more than one halogen-bond interaction.

Adduct **1a** was formed from the interaction between 4-bromo-2,3,5,6-tetrafluorobenzotrifluoride and DABCO. It crystallizes in the $P2_1/c$ space group and the asymmetric unit consists of one dynamically disordered DABCO molecule situated about an inversion centre and one molecule of 4-bromo-2,3,5,6-tetrafluorobenzotrifluoride (Fig. 2.1).

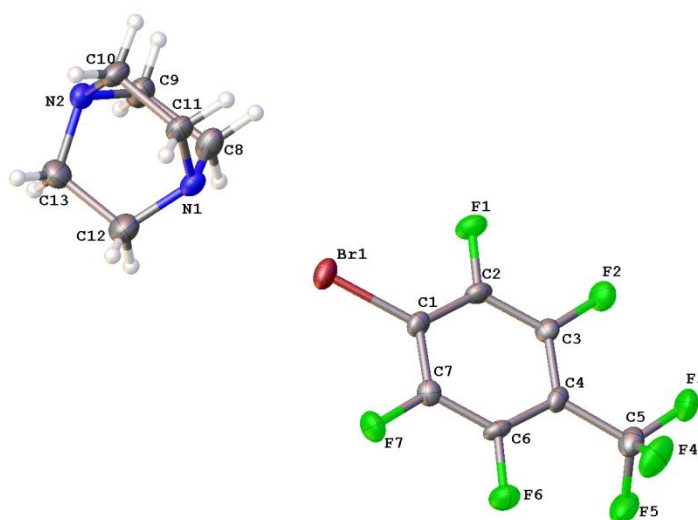


Figure 2.1 Views of the asymmetric unit of halogen-bonded adduct **1a**, showing the atom numbering scheme, disordered in DABCO have been removed for clarity but carbon, nitrogen and hydrogen atoms in DABCO is half occupancy, each atom is therefore modelled with 0.5 occupancy. Ellipsoids are drawn at 50% probability level. The colour key is as follows: gray, carbon; brown, bromine; blue, nitrogen; green, fluorine; white, hydrogen.

In the extended structure of **1a**, halogen bonds form with both nitrogen atoms of DABCO to give a trimeric unit of 1 DABCO and two arenes with 2.84(2) and

2.79(2) Å N...Br distances, an average of 2.82(2) Å. These distances are shorter than the sum of the van der Waals radii of nitrogen and bromine (3.4 Å) (Bondi, 1964; Alvarez, 2013) and also shorter than the distances observed for the halogen-bonded adduct of bromopentafluorobenzene with DABCO (average 2.844(7) Å) by 0.7%. (Muneer, 2017) The C-Br...N angles are nearly linear with values of 172.8(3) and 174.2(3) °, which is consistent with the nature of XB. These C-Br...N angles are also more linear than the corresponding ones in the previously reported structure involving bromopentafluorobenzene with DABCO, which ranged from 167.8(2) to 169.3(3) °. (Muneer, 2017)

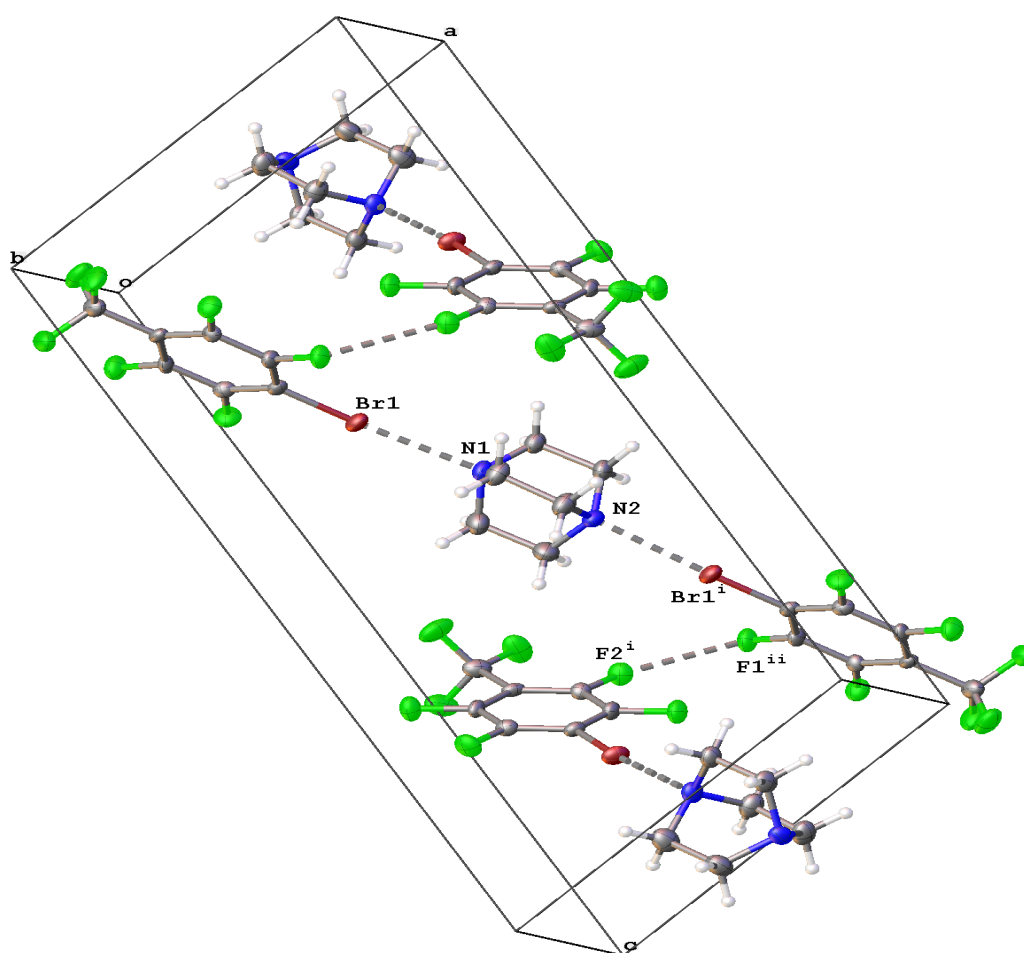


Figure 2.2 A view of intermolecular N...Br halogen bonds and F...F interactions (stippled line) in crystal structure **1a**. The colour key is as follows: grey, carbon; brown, bromine; blue, nitrogen; green, fluorine; white, hydrogen. [Symmetry codes : (i) +x, 1/2-y, 1/2+z (ii) 1-x, -y, 1-z].

In the crystal packing, the supermolecular trimers interact together through F...F interactions with a distance of 2.801(4) Å, which is 0.14 Å (4.7%) just shorter than double the van der Waals radii of fluorine 2.94 Å (Fig 2.2). (Bondi, 1964; Alvarez, 2013) However, the dominant interaction in this structure is the N...Br halogen bonds, which are 17.1% shorter than the sum of the van der Waals radii (3.4 Å) (Bondi, 1964; Alvarez, 2013).

Comparing some of the parameters of structure **1a** with similar structures, we find that the average C-Br bond distance for this structure is 1.885(4) Å, which is essentially the same as the average bond distance for structure [CSD refcode DIVDUI, 1.883(2) Å] reported in the structure contain 1,4-dibromotetrafluorobenzene and DABCO. (Cinčić *et al.*, 2008) The N-C and C-C bond distances in DABCO unit [1.466(12) and 1.567(13) Å respectively] are comparable with 1.483(10) and 1.536(10) Å reported for the low-temperature phase of DABCO. (Sauvajol, 1980) Unfortunately there are no reported structural data for 4-bromo-2,3,5,6-tetrafluorobenotrifluoride with which to make a direct comparison. The other bond distances in structure **1a** are listed in Table 2.2.

Table 2.2 Selected bond distances of **1a** in Å

Br1—C1	1.885 (5)	C6—C7	1.381 (6)
C1—C2	1.382 (6)	C6—F6	1.342 (5)
C1—C7	1.378 (6)	C7—F7	1.346 (5)
C2—C3	1.393 (6)	C8—C9	1.574 (13)
C2—F1	1.337 (5)	C8—N1	1.474 (12)
C3—C4	1.379 (6)	C9—N2	1.463 (12)
C3—F2	1.345 (5)	C10—C11	1.552 (12)
C4—C5	1.505 (6)	C10—N2	1.477 (12)
C4—C6	1.389 (6)	C11—N1	1.459 (11)
C5—F3	1.334 (6)	C12—C13	1.574 (13)
C5—F4	1.326 (6)	C12—N1	1.466 (11)
C5—F5	1.339 (5)	C13—N2	1.459 (11)

The structure of the second adduct, **2a**, crystallises in the $P2_1/n$ space group, similar to **1a**, with the asymmetric unit consisting of one DABCO and one 4,4-dibromooctafluorobiphenyl molecule (Fig. 2.3).

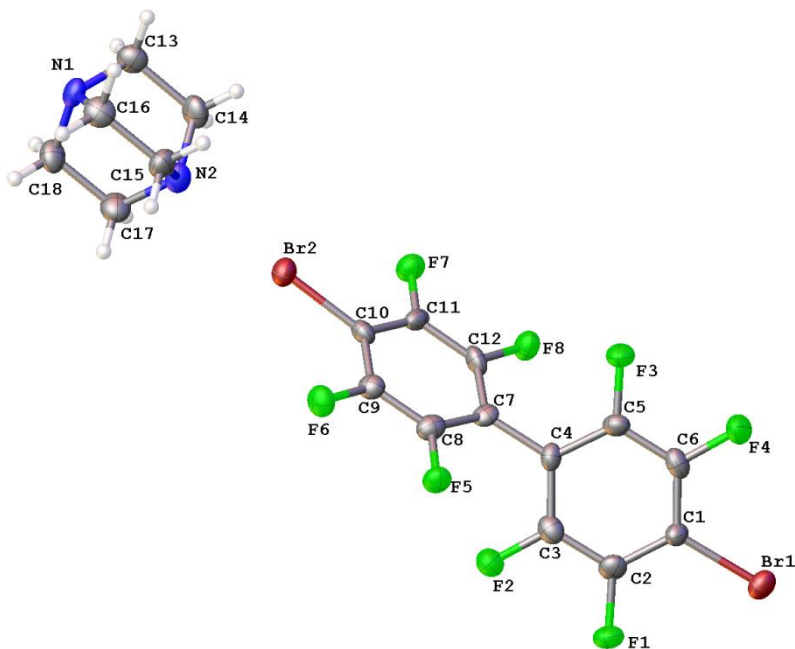


Figure 2.3 View of the asymmetric unit of halogen-bonded adduct **2a**, showing the atom numbering. Ellipsoids are drawn at 50% probability level. The colour key is as follows: gray, carbon; brown, bromine; blue, nitrogen; green, fluorine; white, hydrogen.

Both bromine atoms of 4,4-dibromooctafluorobiphenyl are involved in halogen bonding, thus forming one-dimensional chains of alternating donors and acceptors. The N...Br halogen bond distances of **2a** are 2.719(5) and 2.726(5) Å, with an average of 2.723(5) Å, 0.68 Å (19.9%) shorter than the sum of van der Waals radii, (3.4 Å). The C-Br...N bond angles are nearly linear and range between 175.6(2) and 175.8(2) °.

The dominant interactions in adduct **2a** are the N...Br halogen bonds, although there are other weak F...H interactions with distances (2.647 and 2.654 Å) which are approximately 0.02 Å (0.75%) less than the sum of the van der Waals radii of fluorine and hydrogen atoms (2.67 Å) (Fig. 2.4). (Bondi, 1964; Alvarez, 2013)

Furthermore, the crystal packing shows this XB interaction to be the main intermolecular interaction in this structure. The ring torsion angle of the fluorinated biphenyl rings changed from 60.7(4) ° in 4,4-dibromooctafluorobiphenyl (CSD ref code WOVYIP) to 55.5(8) ° in adduct **2a** which may be related to a packing effect on forming the supramolecular assembly of halogen bonded structures. (Pilati *et al.*, 2001)

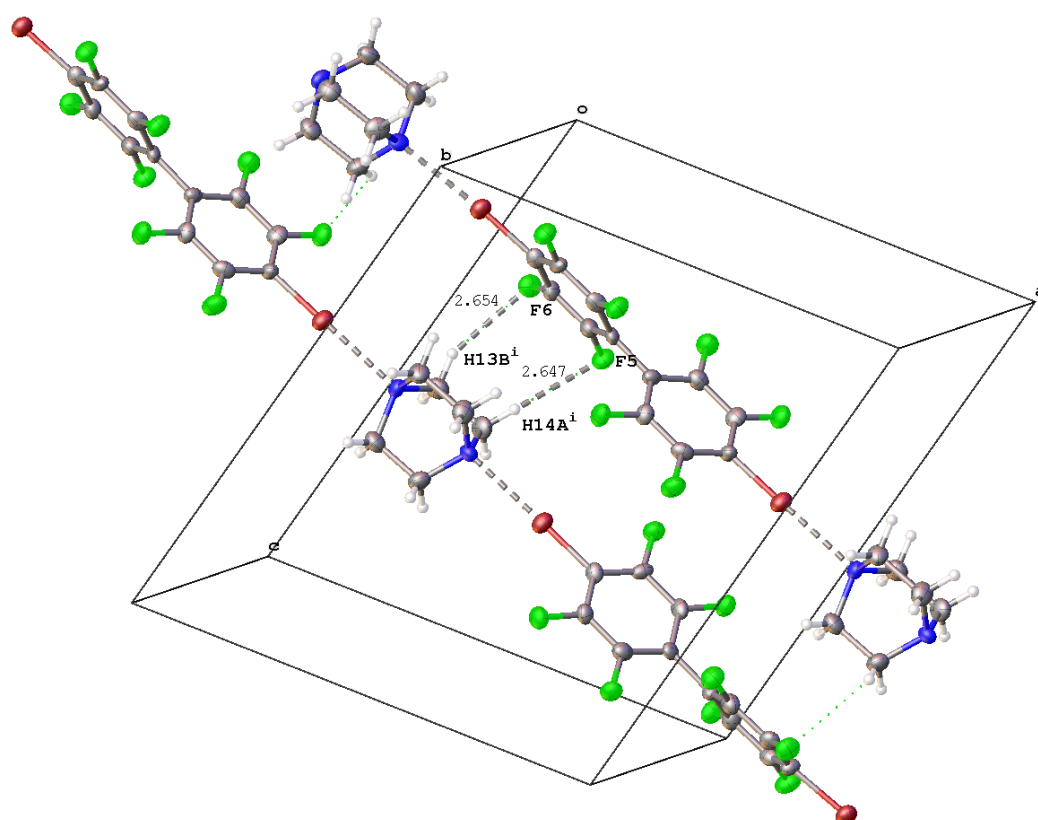


Figure 2.4 A view of intermolecular halogen bonds and F...H interactions in crystal structure **2a** (Stippled line). [Symmetry codes :(i) $1/2+x, 3/2-y, 1/2+z$]. The colour key is as follows: gray, carbon; brown, bromine; blue, nitrogen; green, fluorine; white, hydrogen.

Comparing some of the parameters for structure **2a** with previous structures revealed that the average C-Br bond distances for this structure 1.903(6) Å is longer than the average C-Br bond distance, 1.875(3) Å, for the pure 4,4-

dibromooctafluorobiphenyl (CSD refcode WOVYIP) collected at 291 K. (Pilati *et al.*, 2001) Similarly the average C-C and C-F parameters [1.387(8) and 1.352(6) Å] are comparable with [1.377(5) and 1.341(4) Å] reported in WOVYIP. The length of the C4-C7 bond between the two rings in **2a** is 1.488(7) Å, which is statistically the same as 1.483(4) Å recorded previously in pure 4,4-dibromooctafluorobiphenyl. (Pilati *et al.*, 2001) The average N-C and C-C distances [1.475(7) and 1.564(8) Å] in the DABCO unit are consistent with the values detected in **1a**. The remainder of the bond distances in structure **2a** are listed in Table 2.3.

Table 2.3 Selected bond distances of **2a** in Å

Br1—C1	1.902 (6)	C5—C6	1.380 (8)
Br2—C10	1.904 (6)	C7—C8	1.389 (8)
F1—C2	1.356 (6)	C7—C12	1.403 (8)
F2—C3	1.337 (6)	C8—C9	1.378 (8)
F3—C5	1.355 (6)	C9—C10	1.392 (8)
F4—C6	1.355 (6)	C10—C11	1.384 (7)
F5—C8	1.356 (6)	C11—C12	1.380 (8)
F6—C9	1.349 (6)	N1—C13	1.482 (7)
F7—C11	1.359 (6)	N1—C16	1.485 (7)
F8—C12	1.350 (6)	N1—C18	1.472 (7)
C1—C2	1.387 (8)	N2—C14	1.472 (7)
C1—C6	1.379 (8)	N2—C15	1.461 (6)
C2—C3	1.387 (8)	N2—C17	1.480 (7)
C3—C4	1.407 (8)	C13—C14	1.575 (8)
C4—C5	1.394 (8)	C15—C16	1.558 (7)
C4—C7	1.488 (7)	C17—C18	1.559 (8)

Only 2 structures involving 1,2-dibromotetrafluorobenzene in N...Br halogen bonding have been reported in CCDC until now. Adduct **3a** is the third one and it crystallises in the $P2_1/n$ space group and the asymmetric unit consists of one molecule of DABCO and 2 molecules of 1,2-dibromotetrafluorobenzene (Fig 2.5).

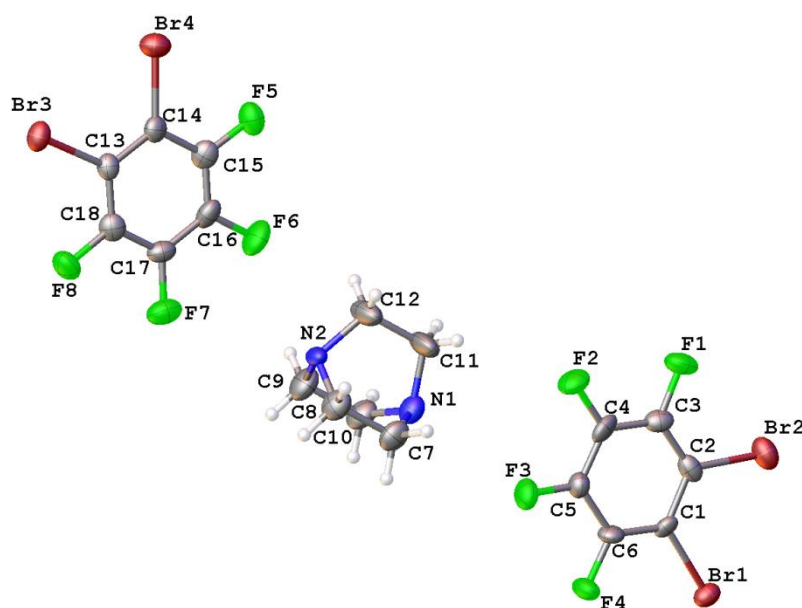


Figure 2.5 View of the asymmetric unit of halogen-bonded adduct **3a**, showing the atom numbering. Ellipsoids are drawn at 50% probability level. The colour key is as follows: gray, carbon; brown, bromine; blue, nitrogen; green, fluorine; white, hydrogen.

In the extended structure of adduct **3a**, the three molecules are halogen bonded by N...Br halogen bonds with a bow-like shape similar to the analogues iodine structure (DATCEI) reported previously. (M. C. Pfrunder et al, 2012) The N...Br distances range from 2.829(6) to 2.726(6) Å, which are 0.57 Å (16.8%) and 0.67 Å (20.6%) shorter than the sum of the van der Waals radii (3.40 Å) (Bondi, 1964; Alvarez, 2013). These distances are also shorter than the reported N...Br distances 2.894(2) and 2.910(2) Å, for the 1,4-dibromotetrafluorobenzene adduct with DABCO (CSD ref code DIVDUI). (Cinčić et al., 2008) The C-Br...N bond angles of **3a** were close to linear, ranging from 168.4(3) to 176.2(3) ° which is consistent with the expected angles for this kind of interaction.

Offset π - π stacking is seen in **3a** and characterized by a combination of alternate centroid-to-centroid distances of 3.735 and 4.188 Å (Fig 2.6), along with other non-covalent weak interactions such as a halogen-halogen type I interaction, between Br2...F2 formed by the second bromine with a distance of 3.240(5) Å, which is

0.08 Å (2.4%) Just slightly shorter than the sum of the van der Waals radii 3.32 Å.
(Bondi, 1964; Alvarez, 2013)

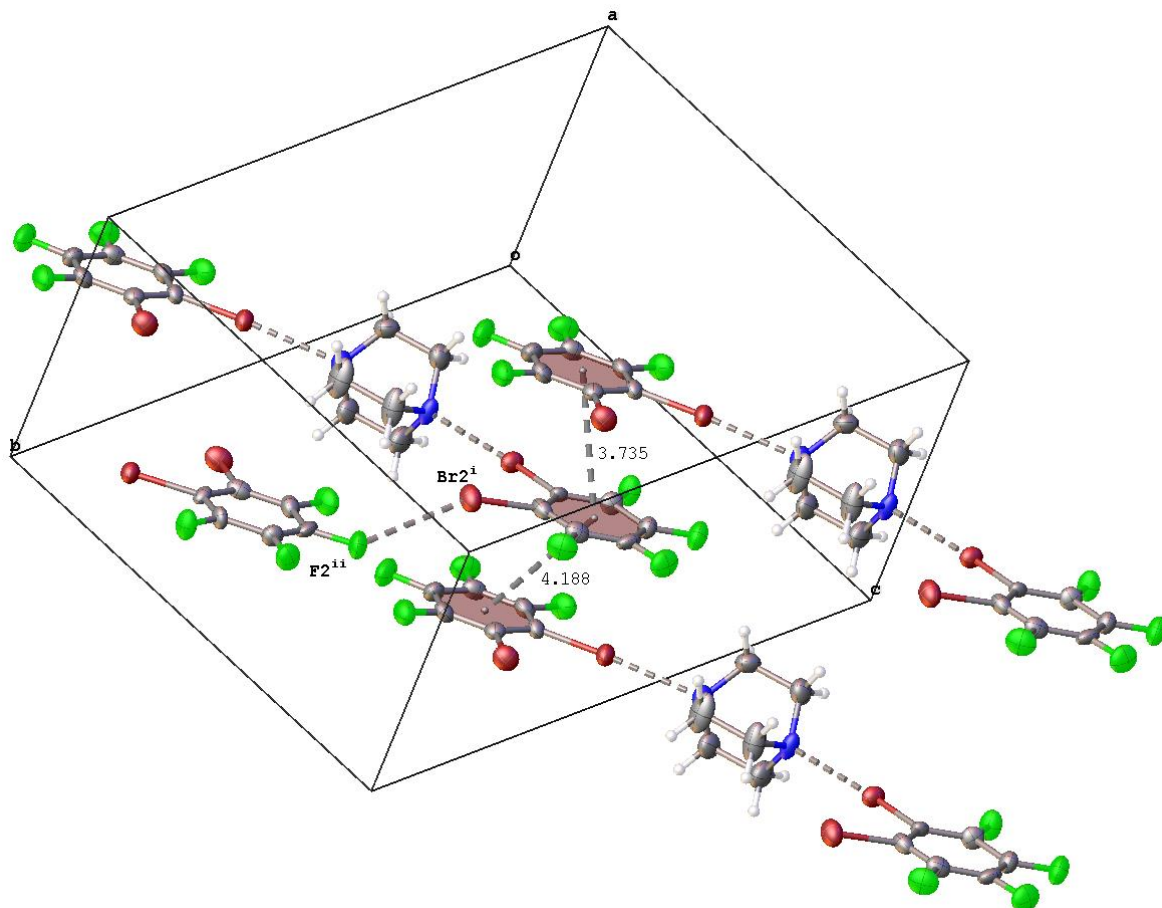


Figure 2.6 Crystal packing of **3a** showing N...Br halogen, bonds π - π stacking and Br...F between adjacent trimers. The colour key is as follows: gray, carbon; brown, bromine; blue, nitrogen; green, fluorine; white, hydrogen. Generic atom labels without symmetry codes have been used, Symmetry codes: (i) $+x, +y, 1+z$; (ii) $-1/2, 3/2-y, 1/2+z$.

Comparing some of the parameters related to structure **3a** with similar reported structures, revealed that the average C-Br bond distance for this structure is 1.894(8) Å, which is slightly longer but comparable with the average bond distance for structure DIVDUI, 1.883(2) Å. (Cinčić *et al.*, 2008) The average C-F bond

distances in the arene unit is 1.345(9) Å and within the range of the average bond distances in **1a**, 1.338(5) Å, and 1.352(6) Å in **2a**. Moving to the DABCO unit in **3a**, the average N-C and C-C bond distances are consistent with those found in **1a** and **2a**. The other bond distances in the structure of **3a** are listed in Table 2.4.

Table 2.4 Selected bond distances of **3a** in Å

Br1—C1	1.896 (8)	C15—C16	1.339 (12)
Br2—C2	1.892 (8)	C15—F5	1.352 (10)
C1—C2	1.398 (11)	C16—C17	1.386 (12)
C1—C6	1.381 (11)	C16—F6	1.333 (9)
C2—C3	1.357 (11)	C17—C18	1.385 (12)
C3—C4	1.352 (12)	C17—F7	1.351 (9)
C3—F1	1.357 (9)	C18—F8	1.359 (10)
C4—C5	1.372 (12)	C7—C8	1.547 (12)
C4—F2	1.354 (9)	C7—N1	1.448 (11)
C5—C6	1.397 (11)	C8—N2	1.468 (11)
C5—F3	1.325 (9)	C9—C10	1.536 (11)
C6—F4	1.330 (9)	C9—N2	1.474 (11)
Br3—C13	1.892 (8)	C10—N1	1.454 (11)
Br4—C14	1.881 (9)	C11—C12	1.552 (12)
C13—C14	1.395 (11)	C11—N1	1.479 (11)
C13—C18	1.372 (12)	C12—N2	1.466 (11)
C14—C15	1.400 (11)		

Adduct **4a** involves 1,3-dibromotetrafluorobenzene (**4**) for which the structure is already known (CSD refcode PASKUR) (Nayak *et al.*, 2012) and DABCO. Adduct **4a** crystallise in the *C2/m* space group and the asymmetric unit consists of one molecule of DABCO that displays dynamic disorder situated about an inversion center and 1 molecule of 1,3-dibromotetrafluorobenzene (Fig 2.7).

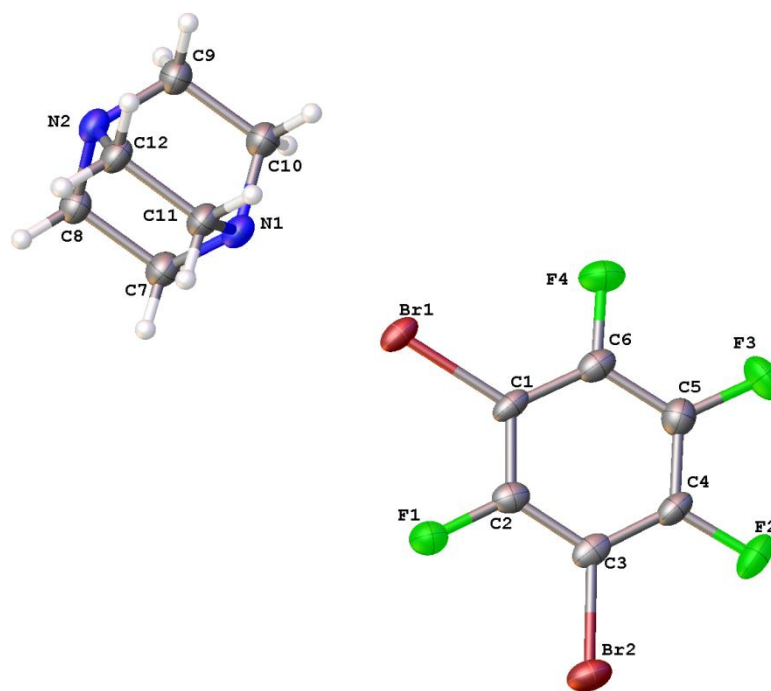


Figure 2.7 View of the asymmetric unit of halogen-bonded adduct **4a**, the DABCO molecule is disordered across two sites and located about a special position (an inversion centre), each atom is therefore modelled with 0.25 occupancy to account for the doubling that occurs when applying the inversion symmetry operation to give an overall 2:1 ratio of $C_6F_4Br_2$:DABCO. Ellipsoids are drawn at 50% probability level, disordered DABCO have been removed for clarity.

The extended structure of **4a** shows halogen bonds between one of the bromine atoms of the ring to DABCO. The N...Br distances are 2.667(15) and 2.745(15) Å, which are 0.73 Å (21.5%) and 0.66 Å (19.2%) shorter than the sum of the van der Waals radii (3.4 Å) and is the shortest N...Br distance recorded in this report. The halogen bond N...Br—C angles are near-linear at 176.3(4) and 179.5(3) ° with an average of 177.9(4) ° which is also the most linear N...Br—C angle reported here. In addition to the halogen bonds, and similar to **3a**, π - π stacking (Janiak, 2000) is seen and, in this case, characterised by only one centroid-to-centroid distance of 3.787 Å, Fig. 2.8. While the second bromine is involved in a type I Br...F halogen-halogen interaction 3.048(4) Å, which gives alternating chains of halogen bonded trimers with Br...F weak interactions between.

Comparing some of the parameters of structure **4a** with the other reported structures reveals that the average C-Br bond distance for this structure is 1.884(6) Å, which is the same as the average bond distance for structure [CSD refcode DIVDUI, 1.883(2) Å (Cinčić *et al.*, 2008)]. The other bond distances in the structure of **4a** are within the bond distances detected in **1a**, **2a** and **3a**, and are listed in Table 2.6.

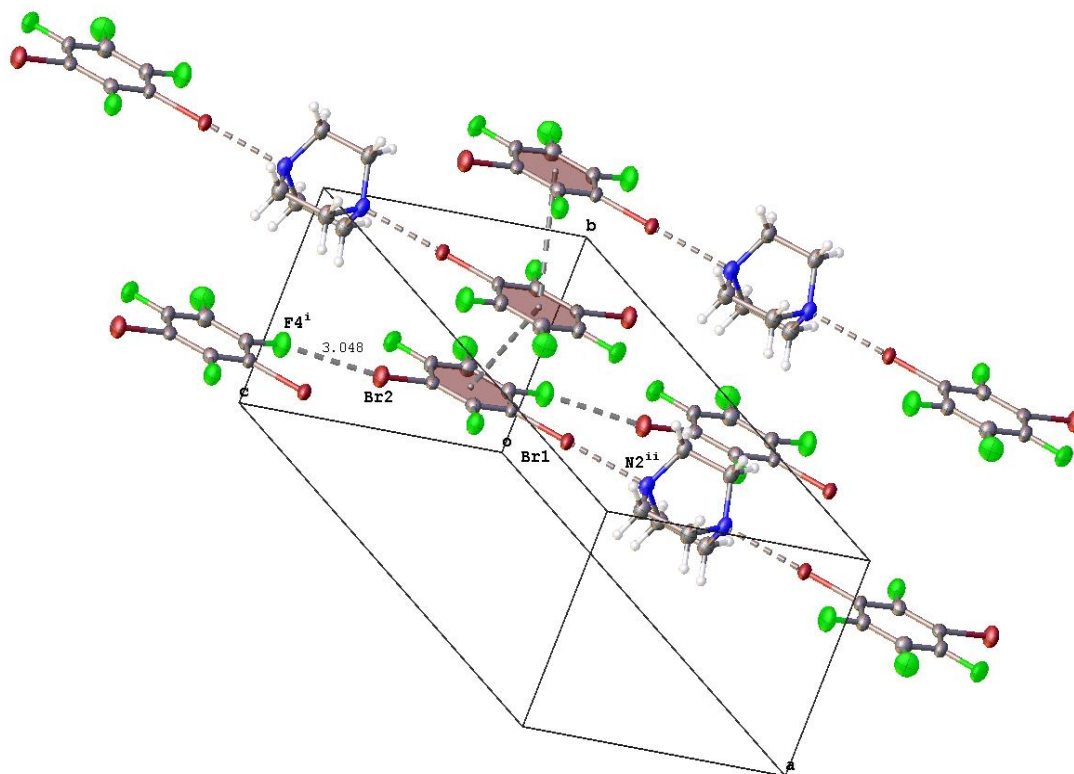


Figure 2.8 Crystal packing of **4a** showing N...Br halogen bonds, π - π stacking and Br...F between adjacent trimers. Symmetry codes: (i) $+x, +y, 1+z$; (ii) $1-x, 1-y, -z$. The colour key is as follows: grey, carbon; brown, bromine; blue, nitrogen; green, fluorine; white, hydrogen. Generic atom labels without symmetry codes have been used.

Table 2.5 Selected bond distances of **4a** in Å

Br1—C1	1.901 (5)	C6—F1	1.334 (6)
Br2—C3	1.866 (6)	C7—C8	1.546 (12)
C1—C2	1.375 (7)	C7—N1	1.479 (13)
C1—C6	1.387 (8)	C8—N2	1.467 (13)
C2—C3	1.389 (7)	C9—C10	1.556 (13)
C2—F4	1.348 (6)	C9—N2	1.470 (14)
C3—C4	1.366 (8)	C10—N1	1.470 (14)
C4—C5	1.372 (8)	C11—C12	1.550 (13)
C4—F3	1.342 (6)	C11—N1	1.469 (13)
C5—C6	1.393 (7)	C12—N2	1.468 (13)
C5—F2	1.365 (7)		

Comparing selected geometrical parameters of our work and the previously reported structures, reveals that the N...Br halogen bond distances in our structures are shorter, **Table 2.6**. The distances lie between 2.667(15) and 2.82(2) Å and the C-Br...N angles are more close to linearity and ranging from 179.5 to 172.8(3) °.

Table 2.6 N...Br halogen-bond distances (Å) and angles (°) in the current work and previously reported structures.

Entry	Donor	Acceptor	N...Br (Å)	N...Br-C (°)	Reference
1	4-B-2,3,5,6-TFBTF (1a)	DABCO	2.82(2) _(ave)	173.5(3) _(ave)	This work
2	4,4'-C ₁₂ Br ₂ F ₈ (2a)	DABCO	2.723(5) _(ave)	175.7(2) _(ave)	This work
3	1,2-C ₆ Br ₂ F ₄ (3a)	DABCO	2.778(6) _(ave)	177.9(3) _(ave)	This work
4	1,3-C ₆ Br ₂ F ₄ (4a)	DABCO	2.705(15) _(ave)	177.9 (4) _(ave)	This work
5	1-C ₆ BrF ₅	DABCO	2.844(7) _(ave)	168.4(3) _(ave)	(Muneer, 2017)
6	1,4-C ₆ Br ₂ F ₄ (DIVDUI)	DABCO	2.902(2) _(ave)	168.7(1) _(ave)	(Cinčić <i>et al.</i> , 2008)

However, the structure involve bromopentafluorobenzene with DABCO contain more fluorines on the ring (Muneer, 2017) which is expected to withdraw the electron density ending with more effectively, so resulting in a more more positively σ hole and shorter N...Br contacts, but this is not in line with the results reported here. This is may be due to the crystal packing and other weak contacts (ex π - π stacking, Janiak, 2000) which affect the measured N...Br distances Table 2.7.

Table 2.7 Intermolecular interactions in (Å) less than the sum of the van der Waals radii observed in the current work and previously reported structures.

Entry	Donor	C-Br (Å)	F...F (Å)	F...H (Å)	F...Br (Å)	π - π stacking (Å)	Reference
1	4-B-2,3,5,6-TFBTF (1a)	1.885(4)	2.801(4)	-	-	-	This work
2	4,4'-C ₁₂ Br ₂ F ₈ (2a)	1.903(6) _(ave)	-	2.651 _(ave)	-	-	This work
3	1,2-C ₆ Br ₂ F ₄ (3a)	1.894(8) _(ave)	2.890(7)	2.623 _(ave)	3.240(5)	3.735 4.188	This work
4	1,3-C ₆ Br ₂ F ₄ (4a)	1.884(6) _(ave)	-	2.660	3.048(4)	3.786	This work
5	1-C ₆ BrF ₅	1.882(7) _(ave)	2.810(5) _(ave)	2.613 _(ave)	-	-	(Muneer, 2017)
6	1,4-C ₆ Br ₂ F ₄ (DIVDUI)	1.883(2) _(ave)	2.813(3) _(ave)	2.621 _(ave)	-	-	(Cinčić <i>et al.</i> , 2008)

An infrared spectroscopic study of halogen bond formation confirmed changes in both ν_{C-H} and ν_{C-F} absorption bands which are consistent with those studied for a variety of halogen bonded adducts. (Esrafil, 2012; Politzer *et al.*, 2010)

The IR spectra recorded for adducts **1a-4a** (S 2.1-S 2.4) revealed differences in the DABCO C-H vibrational modes between structures containing two bromines on the fluorinated ring (adducts **3a-4a**) and adducts contain one bromine (**1a-2a**). The first group show a red shift of approximately 2 cm⁻¹, whereas the second group a blue shift by 2 cm⁻¹ (See Table in S 9). On the other hand, the C-F stretches seems to have the same trend of a blue shift in all of the adducts, similar to that previously

reported in a series of halogen bonded $\text{Br}(\text{CF}_2)_n\text{Br}$ molecules with DABCO from our group. (Brisdon *et al.*, 2017)

Further investigations were carried out using QTAIM and electron density for all the structures considered in this study. Atomic coordinates were taken from the X-ray structure. Electron densities were calculated at the B3LYP/6-311G** level of theory, using the GAMESS programme package (Schmidt *et al.*, 1993) and a topographical analysis of the bond critical points was carried out using Multiwfn programme (Lu & Chen, 2012)

The structures were examined and compared with their molecular graphs generated using the Multiwfn programme as shown in Fig (2.9-2.12).

A general comparison across all the structures shows that structure **4a** has the shortest bond distance in X-ray crystal structure and this is supported by QTAIM analysis where it has the corresponding highest electron density, ρ_{BCP} , and most positive value of Laplacian, $\nabla^2\rho_{\text{BCP}}$, for the bond critical points (Table 2.8). As expected for most reported intermolecular interactions, the energy density, H_{BCP} , is positive which corresponds to mainly electrostatic interactions (Rozas *et al.*, 2000).

It is also noteworthy that additional bond critical points were detected in the QTAIM analyses of adducts **1a** and **2a** between fluorine atoms within each arene substituent, F2...F3, 2.523 Å and [F2...F5, 2.830(6) and F3...F8, 2.800(4) Å] respectively, see Fig 2.9 and Fig 2.10. These intramolecular F...F interactions are shorter than the sum of van der Waals radii distance (2.94 Å), but that were not apparent from the original X-ray analysis.

Table 2.8 Topological parameters calculated at B3LYP/6-311G** level of theory

Trimer	Interaction	$X \dots B$ (Å)	ρ_{BCP} (a.u.)	$\nabla^2 \rho_{BCP}$ (a.u.)	$H(r)$ (a.u.)
1a	N2...Br1	2.79(2)	0.0226	0.0794	0.000904
	N1...Br1	2.84(2)	0.0208	0.0660	0.000907
2a	N1...Br1	2.719(5)	0.0266	0.0840	0.000615
	N2...Br2	2.726(5)	0.0262	0.0830	0.000639
3a	N1...Br3	2.726(6)	0.0261	0.0836	0.000704
	N2...Br1	2.829(6)	0.0214	0.0688	0.000927
4a	N2...Br1	2.667(15)	0.0293	0.0934	0.000424
	N1...Br1	2.747(15)	0.0250	0.0802	0.000722

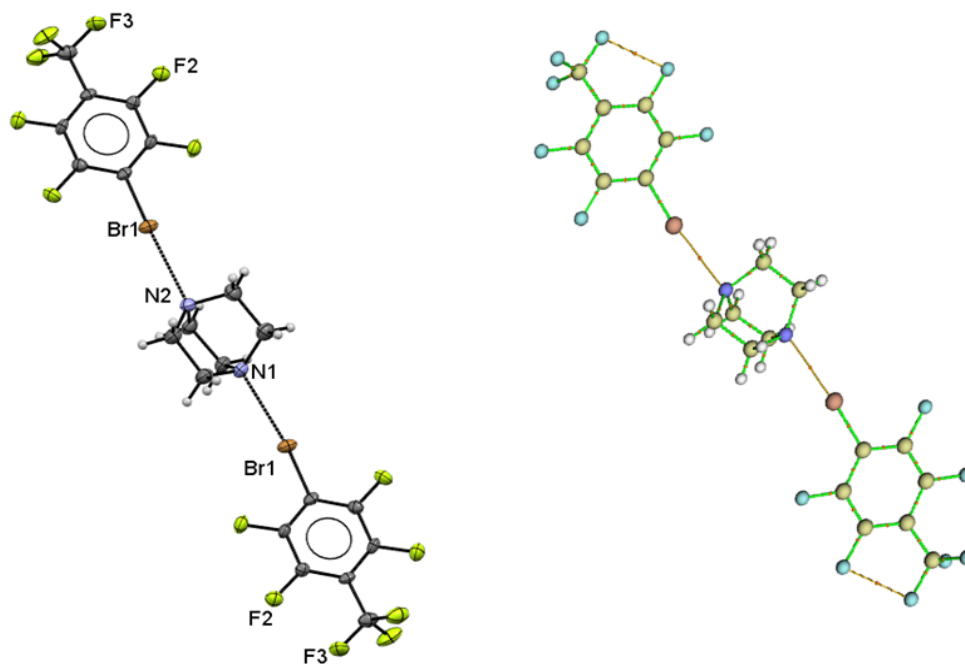


Figure 2.9 The determined X-ray structure (left) and molecular graph (right) for trimers from adducts **1a**

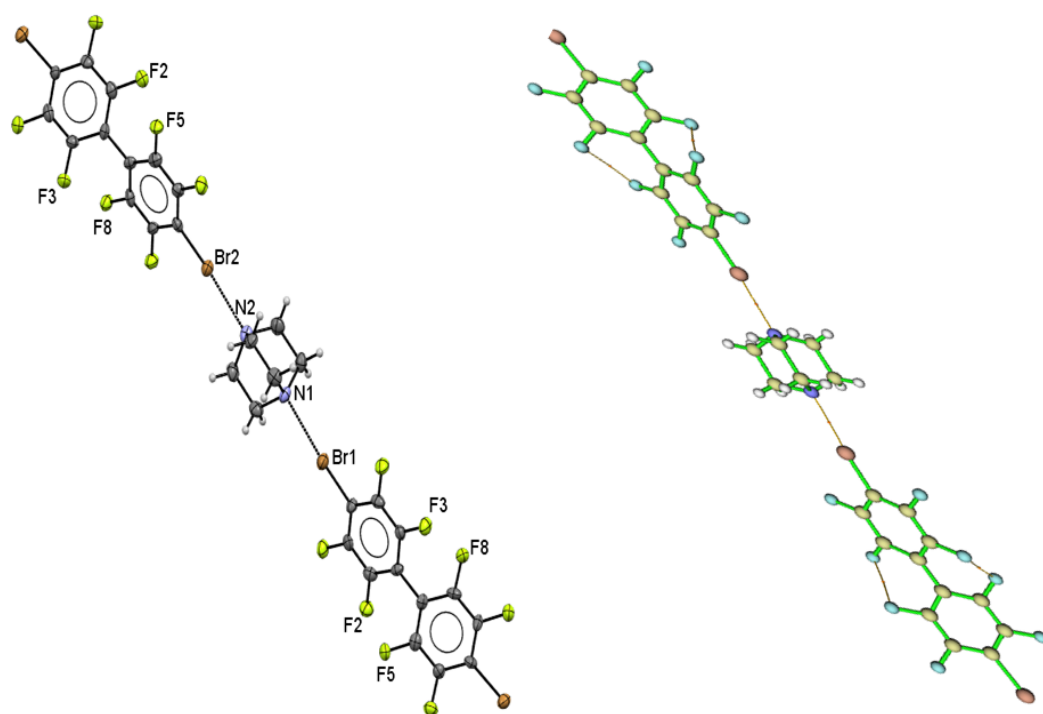


Figure 2.10 The determined X-ray structure (left) and molecular graph (right) for trimers from adducts **2a**

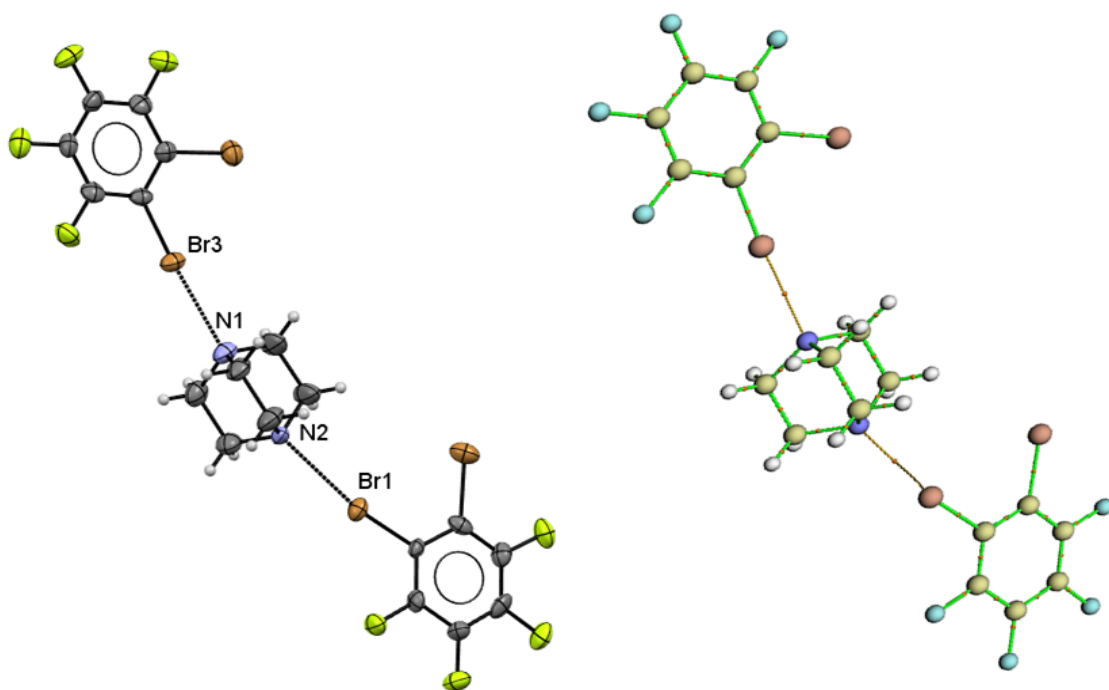


Figure 2.11 The determined X-ray structure (left) and molecular graph (right) for trimers from adducts **3a**

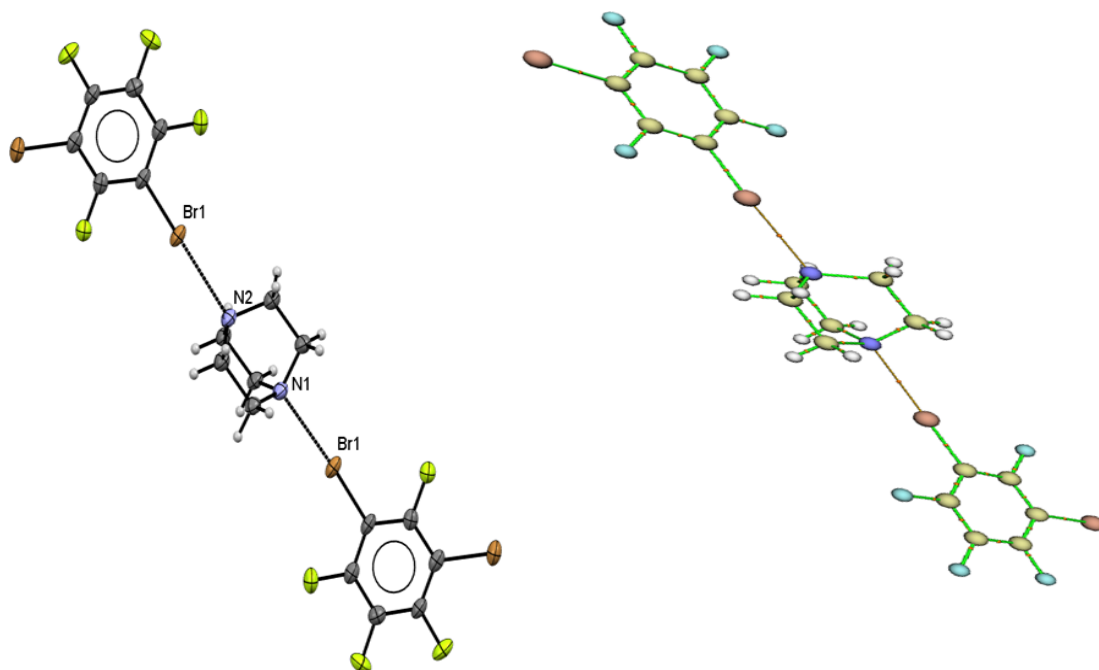


Figure 2.12 The determined X-ray structure (left) and molecular graph (right) for trimers from adducts **4a**

In conclusion a series of four halogen bonded adducts have been constructed from bromo-substituted fluoroaromatic compounds and DABCO. Directional and strong N...Br halogen bonds were observed and fully characterized via single crystal XRD. While it was found that in all cases IR spectroscopy confirmed the presence of halogen bonding in the solid state, NMR data suggests that the adducts do not remain in solution. The halogen bonds were also characterized via QTAIM theoretical calculations which shared a small value of the electron density, ρ_{BCP} , a positive value for the Laplacian, $\nabla^2\rho_{\text{BCP}}$, and a positive value for the total electron energy, H_r , for all of the bromine containing adducts. These values are in line with the N...Br distances which is shortest for adduct **4a** and has the highest value of electron density and Laplacian.

Acknowledgement

We thank the Ministry of Higher Education, Oman Government for support S.S Alkaabi. I acknowledge George Whitehead for help in solving structure **4a**.

References

- Alvarez, S. (2013). *Dalt. Trans.* **42**, 8617–8636.
- Auffinger, P., Hays, F. A., Westhof, E. & Ho, P. S. (2004). *Proc. Natl. Acad. Sci.* **101**, 16789–16794.
- Bader, R. F. W. (1994). *Atoms in Molecules: A Quantum Theory* Clarendon Press.
- Bondi, A. (1964). *J. Phys. Chem.* **68**, 441–451.
- Brinck, T., Murray, J. S. & Politzer, P. (1992). *Int. J. Quantum Chem.* **19**, 57–64.
- Brisdon, A. K., Muneer, A. M. T. & Pritchard, R. G. (2017). *Acta Crystallogr. Sect. C Struct. Chem.* **73**, 874–879.
- Cinčić, D., Friščić, T. & Jones, W. (2008). *Chem. Eur. J.* **14**, 747–753.
- Dolomanov, O. V, Bourhis, L. J., Gildea, R. J., Howard, J. A. K. & Puschmann, H. (2009). 2008–2010.
- Esfarili, M. D. (2012). *J. Mol. Model.* **18**, 5005–5016.
- Esfarili, M. D. & Ahmadi, B. (2012). *Comput. Theor. Chem.* **997**, 77–82.
- Jabłoński, M. & Palusiak, M. (2012). *J. Phys. Chem. A.* **116**, 2322–2332.
- Janiak, C. (2000). *J. Chem. Soc. Dalt. Trans.* 3885–3896.
- Jensen, J. H., Koseki, S., Matsunaga, N., Nguyen, K. A., Su, S., Windus, T. L., Dupuis, M., Jr, J. A. M., Schmidt, M. W., Baldrige, K. K., Boatz, J. A., Elbert, S. T. & Gordon, M. S. (1993). *J. Comput. Chem.* **14**, 1347–1363.
- Karlen, S. D., Reyes, H., Taylor, R. E., Khan, S. I., Frederick Hawthorne, M. & Garcia-Garibay, M. A. (2010). *Pnas.Org.* **107**, 14973–14977.
- Marquardt, R., Politzer, P., Resnati, G., Rissanen, K., Desiraju, G. R., Ho, P. S., Legon, A. C., Kloo, L. & Metrangolo, P. (2013). *Pure Appl. Chem.* **85**, 1711–1713.

- Metrangolo, P., Terraneo, G., Catalano, L., Pérez-Estrada, S., Resnati, G., Garcia-Garibay, M. A. & Pilati, T. (2015). *J. Am. Chem. Soc.* **137**, 15386–15389.
- Muneer, A. M. T. (2017). PhD thesis. The University of Manchester, Manchester, England.
- Navarrini, W., Metrangolo, P., Pilati, T. & Resnati, G. (2000). *New J. Chem.* **24**, 777–780.
- Nayak, S. K., Terraneo, G., Forni, A., Metrangolo, P. & Resnati, G. (2012). *CrystEngComm.* **14**, 4259–4261.
- Lu, T. & Chen, F. (2012). *J. Comput. Chem.* **33**, 580–592.
- Palusiak, M. (2010). *J. Mol. Struct. THEOCHEM.* **945**, 89–92.
- Pilati, T., Metrangolo, P. & Resnati, G. (2001). *Acta Crystallogr. Sect. C Cryst. Struct. Commun.* **57**, 113–114.
- Politzer, P., Murray, J. S. & Clark, T. (2010). *Phys. Chem. Chem. Phys.* **12**, 7748–7757.
- Rigaku, O. D. (2018). *Rigaku Oxford Diffraction Ltd, Yarnton, Oxfordshire, Engl.*
- Riley, K. E., Murray, J. S., Politzer, P., Concha, M. C. & Hobza, P. (2009). *J. Chem. Theory Comput.* **5**, 155–163.
- Rodríguez-Molina, B., Pérez-Estrada, S. & Garcia-Garibay, M. A. (2013). *J. Am. Chem. Soc.* **135**, 10388–10395.
- Rozas, I., Alkorta, I. & Elguero, J. (2000). *J. Am. Chem. Soc.* **122**, 11154–11161.
- Sauvajol, J. L. (1980). *J. Phys. C Solid State Phys.* **13**, L927–L934.
- Schmidt, M. W., Baldrige, K. K., Boatz, J. A., Elbert, S. T., Gordon, M. S., Jensen, J. H., Koseki, S., Matsunaga, N., Nguyen, K. A., Su, S., Windus, T. L., Dupuis, M. & Montgomery Jr, J. A. (1993). *J. Comput. Chem.* **14**, 1347–1363.

Sheldrick, G. M. (2015). *Acta Crystallogr. Sect. A Found. Crystallogr.* **71**, 3–8.

Chapter 3.

Manuscript 2: A Crystallographic and QTAIM study of halogen bonding in a series of iodofluorobenzenes and hexamethylenetetramine and 1,3,5-triaza-phosphaadamantane

Alan K. Brisdon* and Sultan Al kaabi

Department of Chemistry, The University of Manchester, Oxford Road, Manchester, M13 9PL, United Kingdom

Correspondence email: *alan.brisdon@manchester.ac.uk

3.1. Abstract

Six novel halogen-bonded adducts and their crystal structures are reported from the interaction of hexamethylenetetramine and 1,3,5-triaza-phosphaadamantane with a variety of iodofluorobenzenes. Each crystal structure shows N...I halogen bond interactions shorter than the sum of the van der Waals radii (3.53Å). Infrared analysis shows changes in C-H and C-F stretching frequencies, which support the existence of this interaction. This was further confirmed by QTAIM analysis of the bond critical points and the total electron density. However according to ¹⁹F NMR studies the halogen bonds do not remain intact in acetonitrile solution.

Key words:- Halogen bonds, Crystal structure, iodofluorobenzene, Hexamethylenetetramine, 1,3,5-Triaza-phosphaadamantane, QTAIM, infrared, ¹⁹F NMR, van der Waals radii.

3.2. Introduction

Halogen bonding is a field of rapidly expanding interest in science. It can be traced back following the preparation of the first known N...I interaction in the I₂...NH₃ adduct reported by Colin in 1814, (Colin., 1814) and subsequent further analysis to determine the exact composition of this system by F. Guthrie in 1863 (Guthrie, 1863). In 2009, The International Union of Applied Chemistry (IUPAC) launched a project (#2009-03221-1-100) to categorize the noncovalent interactions which

involving halogen atoms.(Marquardt *et al.*, 2013) This defined interactions which contain halogens as an electrophilic site, including halogen bonds. This directional interaction is represented by R-X...Y and arises from the electron deficient area known as the σ -hole, a positive region of X opposite the covalent R-X bond, which is attracted to the lone pair of a Lewis base Y, *i.e.* nitrogen.(Marquardt *et al.*, 2013)

The polarizability of X and the efficiency of the R group to reduce the electron density are key features in the formation of a strong XB halogen bond interaction. Incorporation of fluorine into R, because of its high electronegativity, which can act as an efficient withdrawing group means its compounds have been widely investigated and these have been shown to be efficient in producing strongly halogen-bonded adducts.(Mingos, 2008; Clark *et al.*, 2006) This interaction can compete with hydrogen bonds by its directionality, versatility and can be tuned using different donor and acceptor starting materials.(Primagi *et al.*, 2013)

The identification of interactions from X-ray studies can be complimented by QTAIM theoretical studies that support the recognition of interactions and determine the electron density, ρ , at the bond critical point (BCP) of the interaction. This along with the related Laplacian, $\nabla^2\rho_{\text{BCP}}$, and total electron energy density, H_{BCP} , can be used to describe the strength of the bond (Bader, 1994). Lu *et al.*, 2007; Esrafili, 2012 and Esrafili & Ahmadi, 2012 calculated the electron density for halogen-bonded containing compounds. Rozas *et al.*, 2000 proposed that medium strength interactions corresponded to $\nabla^2\rho_{\text{BCP}} > 0$ and $H_{\text{BCP}} < 0$. More recent work on one of the shortest N...I halogen bonds (2.6622(4) Å) was conducted by Wang and his group in 2018. This interaction between an iodine atom of 1,4-diodotetrafluorobenzene and 4-(dimethyleamine) was found to be associated with exceptionally high electron density 0.359(5) e.Å⁻³ calculated using the Gassian07 package using 6-311G(d,p) basis sets and AIM11 for topological analysis.(Wang *et al.*, 2018) This N...I halogen bond is also associated with a positive $\nabla^2\rho_{\text{BCP}}$ value of 1.95(5) e.Å⁻⁵, and a negative value of -0.0148 a.u for the H_{BCP} , which is consistent with this short distance.

Halogen bond participates in control self-assembly, helps designing specific usages co-crystal materials in crystal engineering, exploits in different areas include liquid crystal, drug design and biochemistry.

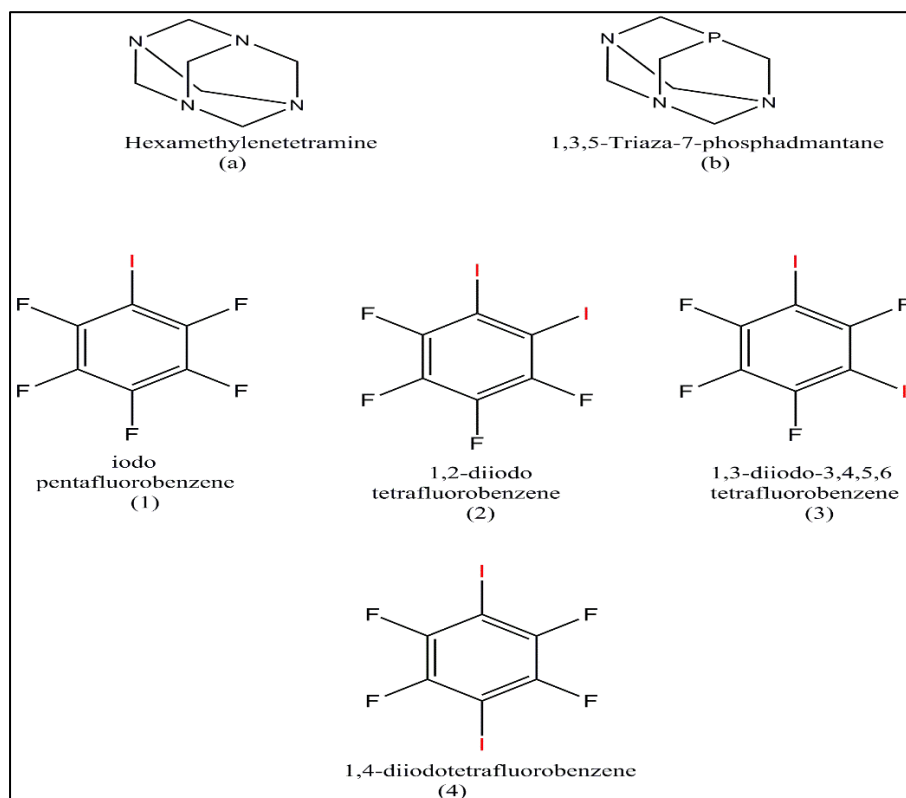
A search of the Cambridge Structure Database (CSD, Version 5.43, 22nd February 2022)(Groom *et al.*, 2016) was conducted using ConQuest (Bruno *et al.*, 2002) for N...I halogen bonded structures. It revealed that there are around 503 structures involving N...I halogen bonds based on fluorinated aromatic compounds and featuring close to linearity (150- 180°) N...I-C bond angles and N...I distances shorter than the sum of the van der Waals radii (3.53 Å). 35 of the structures contain tertiary amines however only five contain the heterocyclic polydentate hexamethylenetetramine (HTMA) compound.

The substitution of one nitrogen atom of HTMA with phosphorus results in the structural analogue 1,3,5-triaza-phosphaadamantane, which was first prepared in 1977 by Fluck and his group and has three nitrogen and one phosphorus atoms each possessing a pair of electrons which may act as halogen bond acceptors.(Ekkehard *et al.*, 1977)

Even though the phosphorus atom has a pair of electrons and can act as electron donor similar to nitrogen there is only one recently reported structure of phosphorus being involved in halogen bonding.(Xu *et al.*, 2018; Lisac *et al.*, 2019) Yijue Xu and his group used slow evaporation of diethyl ether solvent to prepare colourless needle-like crystals of (Ph₃P).(sym-C₆F₃I₃) in which the phosphine acts as a halogen bond acceptor (CSD ref code KIPCOE).(Xu *et al.*, 2018) Subsequently in 2019, Cinic and his group published the same structure (KIPCOE01-KIPCOE04) collected at a different temperature and two analogous structures involving arsenic (Ph₃As).(sym-C₆F₃I₃) and antimony (Ph₃Sb).(sym-C₆F₃I₃) centres as halogen bond acceptors.(Lisac *et al.*, 2019)

Herein we report the preparation of four new crystal structures involving hexamethylenetetramine HTMA and two containing 1,3,5-triaza-phosphaadamantane as halogen bond acceptors, **Scheme 3.1**. All of which were grown at ambient temperature and using simple laboratory apparatus. They are fully

characterised by single crystal and infrared spectroscopy as well as being the basis of a theoretical study using QTAIM. The main target of this study is to probe the ability of the phosphorus atom in 1,3,5-triaza-phosphaadamantane to form P...I halogen bond with a variety of iodofluorobenzenes, as it has a lone pair and similar structure to HTMA which is known to form halogen bond adducts.



Scheme 3.1 Compounds used in this study

3.3. Experimental

All materials were obtained from commercial suppliers (Aldrich, Apollo Scientific, Alfa Aesar, Fluorochem and Acros Organics), and used without further purification.

3.3.1. Synthesis and crystallization

Adducts **1a**, **2a**, **3a**, **4b** were grown by slow evaporation technique using dried acetonitrile as solvent, while crystals of **2a** and **4b** were also grown by vapour diffusion and are labelled as **2a.1** and **4b.1**

A 1:2 stoichiometric molar ratio was used to obtain adduct **1a** [0.08 ml (0.60 mmol) of **1** and 0.168 g (0.120 mmol) of **a**], **2a.1** [0.02 g (0.05 mmol) of **2** and 0.0292 g (0.1 mmol) of **a**], **3a** [0.285 g (0.71 mmol) of **3** and 0.020 g (1.42 mmol) of **a**] and **4b.1** [0.02 ml (0.05 mmol) of **4** and 0.142 g (0.10 mmol) of **b**]. For adduct **2a** [0.04 g (0.10 mmol) of **2** and 0.007 g (0.0249 mmol) of **a**] and **4b** [0.04 g (0.0996 mmol) of **4** and 0.003 g (0.0199 mmol) of **b**] excess amount were used, 4:1 and 5:1 ratio respectively.

Slow evaporation crystallization were carried out in a fume hood using two vials. Each starting material was weighed and placed in a separate vial. 5 ml of acetonitrile was added to dissolve each solid, and the solutions were added to each other.

Vapour diffusion crystallization was carried out using a sealed system consisting of 2 different sized vials. The arene was placed in the larger vial and the smaller vial container (used for XB acceptor) was then placed inside the big vial. The larger vial was then sealed until crystals appeared of a suitable size, which typically occurred within 5 days.

FTIR spectra were obtained using a Nicolet iS5-FT-IR spectrometer (ThermoFisher Scientific) and are shown in (S 3.1-S 3.6). IR $\nu(\text{cm}^{-1})$ data for adduct (**1a**): 2946 (C-H), 1135 (C-F); For adduct (**2a.1**): 2948 (C-H) 1106 (C-F); for adduct (**2a**): 2948 (C-H) 1106 (C-F); for adduct (**3a**): 2962 (C-H) 1068 (C-F); for adduct (**4b.1**): 2904 (C-H) 1452 (C-F); for adduct (**4b**): 2941 (C-H) 1430 (C-F).

^{19}F NMR spectra were recorded on a Bruker AMX 400 MHz instrument (see S 3.7-S 3.12), using CD_3CN as a solvent. No significant changes were detected in the spectra.

3.3.2. Refinement

A polarizing microscope was used to separate and chose a suitable crystal and fomblin oil was used to hold the crystal. Each single crystal was obtained and analyzed using a four-circle diffractometer (Supernova) utilizing Mo K α Radiation ($\lambda = 0.71073 \text{ \AA}$).

CrysAlis PRO 1.171.39.21 was used to collect the data. Structures were solved using direct methods and refined by full-matrix least-squares using SHELXL- 2015 (Sheldrick, 2015) and Olex2 software.(Dolomanov *et al.*, 2009) A CCDC check for all the structures was performed. ConQuest software was used to search for a similar structure and validate the new one.(Bruno *et al.*, 2002) Hydrogen atoms were introduced in geometrically calculated positions after final refinements. A summary of the crystallographic data are listed in Table 3.1 and 3.2.

Table 3.1 Experimental details of **1a-2a.1**

Crystal data	(1a)	(2a.1)	(2a)
Chemical formula	2(C ₆ F ₅ I)·C ₆ H ₁₂ N ₄	C ₆ F ₄ I ₂ ·C ₆ H ₁₂ N ₄	2(C ₆ F ₄ I ₂)·C ₆ H ₁₂ N ₄
M_r	728.12	542.06	943.92
Crystal system, space group	Monoclinic, $P2_1/c$	Monoclinic, $P2_1/c$	Triclinic, $P\bar{1}$
Temperature (K)	150	150	150
a, b, c (Å)	5.9745 (2), 14.6528 (7), 24.8061 (9)	9.3918 (6), 23.487 (1), 7.8101 (4)	10.5820 (8), 11.0427 (12), 11.1177 (12)
α, β, γ (°)	90, 91.036 (3), 90	90, 114.051 (7), 90	101.729 (9), 99.923 (8), 96.758 (8)
V (Å ³)	2171.25 (15)	1573.22 (16)	1237.2 (2)
Z	4	4	2
Radiation type	Mo $K\alpha$	Mo $K\alpha$	Mo $K\alpha$
μ (mm ⁻¹)	3.00	4.04	5.11
Crystal size (mm)	0.2 × 0.1 × 0.01	0.1 × 0.05 × 0.04	0.15 × 0.01 × 0.01
Data collection			
Diffractometer	SuperNova, Single source at offset/far, Eos	SuperNova, Single source at offset/far, Eos	SuperNova, Single source at offset/far, Eos
T_{\min}, T_{\max}	0.613, 1.000	0.351, 1.000	0.620, 1.000
No. of measured, independent and observed [$I > 2\sigma$ (I)] reflections	16755, 4276, 3543	12043, 3092, 2674	9105, 4856, 3560
R_{int}	0.058	0.065	0.068
$(\sin \theta/\lambda)_{\text{max}}$ (Å ⁻¹)	0.617	0.617	0.617

Refinement			
$R[F^2 > 2s(F^2)],$ $wR(F^2), S$	0.047, 0.092, 1.13	0.032, 0.076, 1.06	0.052, 0.096, 0.97
No. of reflections	4276	3092	4856
No. of parameters	308	199	307
H-atom treatment	H-atom parameters constrained	H-atom parameters constrained	H-atom parameters constrained
$\Delta)_{\max}, \Delta)_{\min}$ (e \AA^{-3})	1.22, -0.79	1.03, -0.94	1.09, -1.04

Computer programs: CrysAlis PRO 1.171.39.46(Rigaku, 2018) ShelXT (Sheldrick, 2015), SHELXL (Sheldrick, 2015), Olex2 (Dolomanov *et al.*, 2009)

Table 3.2 Experimental details of **3a-4b.1**

Crystal data	(3a)	(4b.1)	(4b)
Chemical formula	2(C ₆ F ₄ I ₂)·2(C ₃ H ₆ N ₂)	C ₆ F ₄ I ₂ ·C ₆ H ₁₂ N ₃ P	C ₃ F ₂ I·C ₆ H ₁₂ N ₃ OP
M_r	943.92	559.02	374.09
Crystal system, space group	Orthorhombic, <i>Pccn</i>	Monoclinic, <i>P12₁/m1</i>	Monoclinic, <i>P2₁/c</i>
Temperature (K)	150	150	150
a, b, c (\AA)	8.1827 (2), 33.0489 (7), 18.2069 (4)	5.9469 (4), 20.7380 (15), 6.8822 (5)	16.5224 (13), 6.1619 (3), 12.4580 (9)
α, β, γ ($^\circ$)	90, 90, 90	90, 104.719 (6), 90	90, 109.717 (8), 90
V (\AA^3)	4923.68 (19)	820.91 (10)	1193.98 (15)
Z	8	2	4
Radiation type	Mo $K\alpha$	Mo $K\alpha$	Mo $K\alpha$
μ (mm^{-1})	5.14	3.97	2.83
Crystal size (mm)	0.3 × 0.05 × 0.02	0.1 × 0.02 × 0.01	0.2 × 0.1 × 0.05
Data collection			
Diffractometer	SuperNova, Single source at offset/far, Eos	SuperNova, Single source at offset/far, Eos	SuperNova, Single source at offset/far, Eos
T_{\min}, T_{\max}	0.049, 1.000	0.772, 1.000	0.256, 1.000
No. of measured, independent and observed [$I > 2s(I)$] reflections	39545, 4839, 4181	4951, 1667, 1328	4529, 2349, 1865
R_{int}	0.069	0.058	0.047
$(\sin \theta/\lambda)_{\max}$ (\AA^{-1})	0.617	0.616	0.617
Refinement			
$R[F^2 > 2s(F^2)],$ $wR(F^2), S$	0.029, 0.062, 1.12	0.035, 0.055, 0.97	0.045, 0.089, 1.08
No. of reflections	4839	1667	2349
No. of parameters	309	106	154
H-atom treatment	H-atom parameters constrained	H-atom parameters constrained	H-atom parameters constrained
$\Delta)_{\max}, \Delta)_{\min}$ (e \AA^{-3})	0.74, -0.72	0.88, -0.77	1.12, -0.80

Computer programs: CrysAlis PRO 1.171.39.46(Rigaku, 2018) ShelXT (Sheldrick, 2015), SHELXL (Sheldrick, 2015), Olex2 (Dolomanov *et al.*, 2009)

3.3.3. QTAIM experimental

In this work, QTAIM analysis were performed using the atomic coordinates taken from the X-ray structures and the electron density was calculated through single - point calculations at the B3LYP/6-311G** level utilizing the GAMESS package. (Schmidt *et al.*, 1993) The Multiwfn programme was used to obtain the QTAIM parameters and obtain the displayed plots. (Lu & Chen, 2012)

3.4. Result and Discussion

There are three crystal structures involving hexamethylenetetramine (HTMA) in which N...I halogen bonds are present, while there are none with the analogue containing phosphorus that have been reported. The first of the HTMA adducts is with the widely used halogen bond donor 1,4-diiidotetrafluorobenzene which was prepared by Walsh and his group (Walsh *et al.*, 2001). They mixed a 1:1 molar equivalent of 1,4-diiidotetrafluorobenzene and hexamethylenetetramine (HTMA) in methylene chloride from which colourless crystals were obtained, resulting in a crystal structure (CSD ref code QIHCOZ) displaying an N...I halogen bond with a distance of 2.845(3) Å.(Walsh *et al.*, 2001) The second structure involving 1,4-diiidotetrafluorobenzene and hexamethylenetetramine (HTMA) (CSD ref code QIHCOZ01) came 3 years later as a private communication, in which the N...I distance is significantly (13 σ) shorter at 2.806(1) Å.(Bolte, 2004) Both structures have 2 symmetry equivalent nitrogen atoms involved in N...I halogen bonds. The latest and third structure (CSD ref code RORWEC) published in 2014 by Syssa-Magalé and his group involve 1,3,5 trifluoro-2,4,6-triiodobenzene with hexamethylenetetramine.(Syssa-Magalé *et al.*, 2014) It has the longest average bond distance, 2.872(5) Å, but the closest angle to linearity comparing with 1,4-diiidotetrafluorobenzene (CSD refcode QIHCOZ and QIHCOZ01).(Walsh *et al.*, 2001; Bolte, 2004)

Adduct **1a** was found to crystalize in the monoclinic space group with the asymmetric unit consisting of two molecules of iodotetrafluorobenzene and one molecule of hexamethylene-tetramine, in a 2:1 ratio, see Fig 3.1.

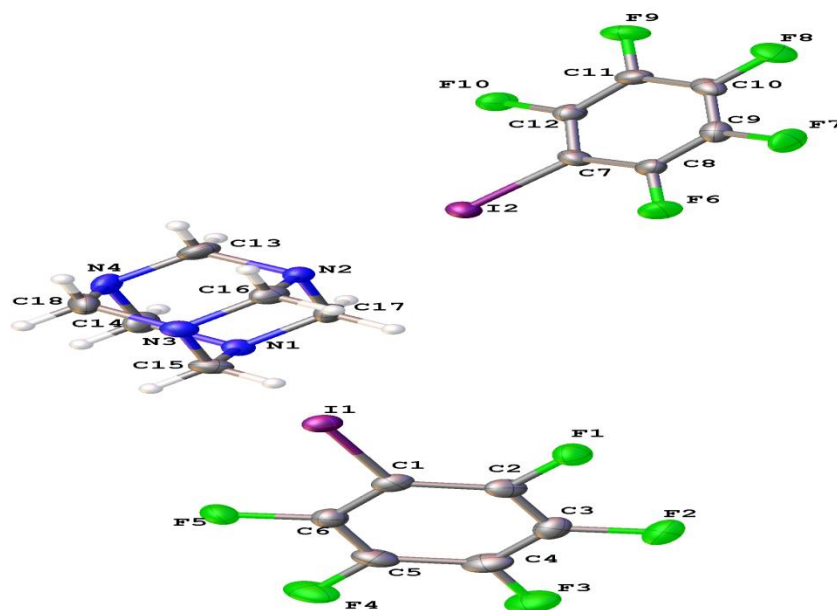


Figure 3.1 Views of the asymmetric unit of halogen-bonded adduct **1a**, showing the atom numbering, Ellipsoids are drawn at 50% probability level. The colour key is as follows: gray, carbon; purple, iodine; blue, nitrogen; green, fluorine; white, hydrogen.

Comparing some of the parameters of structure **1a** with previously reported structures, we find that the average C-I bond distance for **1a** is 2.112(5) Å which is significantly longer than the reported distance 2.077(4) Å for pure 1-iodopentafluorobenzene (CSD ref code ZAHGAQ) (Frohn *et al.*, 1995) by about 7σ , and close to the average C-I bond distance of 2.101(5) Å that is reported for the adduct of hexamethylenetetramine with 1,3,5-trifluoro-2,4,6-triodobenzene (CSD ref code RORWEC). (Syssa-Magalé *et al.*, 2014)

This extension in C-I distance may arise due to the formation of the directional N...I halogen bonds, which were observed with distances of 2.778(4) and 2.805(4) Å, with an average of 2.792(4) Å which is 20.9% shorter than the sum of the van der Waals radii (3.53 Å). This distance is the shortest of the 6 crystal structures in this report. This is expected and may be related to the highly electron-withdrawing ability of the 5 fluorine atoms on the ring which makes the σ hole on the iodine *p* orbital more positively charged than in other systems. The crystal structure of **1a**

displays near-linearity of the N...I-C halogen bond with angles of 174.6(2) and 170.9(2) °.

The extended structure of **1a** shows halogen bonds between 2 nitrogen atoms from hexamethylenetetramine to the only iodine atom on the ring of two different molecules, see Fig. 3.2.

A second interaction that appears in this structure is a set of weak non-conventional F...H bonds [F8...H18A, 2.59 and F2...H13B, 2.55 Å] with an average distance of 2.57 Å (3.7%), slightly shorter than the sum of the van der Waals radii (2.67 Å) of hydrogen and fluorine atoms, see Table 3.3. Similar to other halogen bonded structures (Bruce *et al.*, 2008) a trimeric complex is formed, which consists of one hexamethylenetetramine and two molecules of 1-iodopentafluorobenzene. Through weak F...F interactions each halogen bonded trimer is linked to another with an average F...F bond distance of 2.890(4) Å.

The remaining bond distances for structure **1a** are listed in Table 3.4.

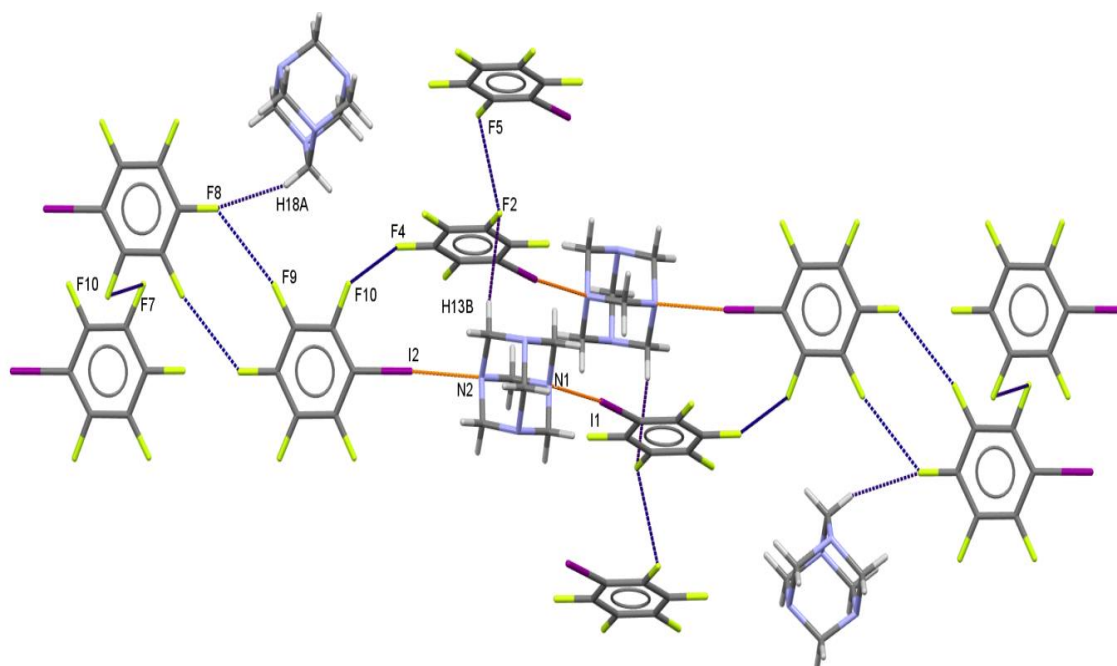


Figure 3.2 View of intermolecular halogen bonds (red lines) and the other non-covalent interactions (dark blue lines) in **1a**. The colour key is as follows: gray, carbon; purple, iodine; blue, nitrogen; green, fluorine; white, hydrogen.

Table 3.3 Hydrogen-bond geometry (Å, °) for **1a**

$D-H\cdots A$	$D-H$	$H\cdots A$	$D\cdots A$	$D-H\cdots A$
C13—H13B \cdots F2 ⁱ	0.97	2.55	3.493 (7)	164
C18—H18A \cdots F8 ⁱⁱ	0.97	2.59	3.514 (7)	159

Symmetry codes: (i) $-x+1, -y+1, -z+1$; (ii) $x+1, -y+3/2, z-1/2$.

Table 3.4 Selected bond distances (Å) in **1a**

I1—C1	2.112 (5)	C7—C8	1.392 (7)
F1—C2	1.343 (6)	C7—C12	1.373 (7)
F2—C3	1.357 (6)	C8—C9	1.382 (8)
F3—C4	1.341 (6)	C9—C10	1.376 (8)
F4—C5	1.340 (6)	C10—C11	1.378 (7)
F5—C6	1.346 (6)	C11—C12	1.374 (7)
C1—C2	1.386 (8)	N1—C14	1.476 (6)
C1—C6	1.370 (7)	N1—C15	1.474 (6)
C2—C3	1.376 (7)	N1—C17	1.476 (6)
C3—C4	1.372 (8)	N2—C13	1.491 (6)
C4—C5	1.371 (8)	N2—C16	1.461 (7)
C5—C6	1.385 (8)	N2—C17	1.483 (6)
I2—C7	2.109 (5)	N3—C15	1.471 (7)
F6—C8	1.328 (6)	N3—C16	1.466 (7)
F7—C9	1.345 (6)	N3—C18	1.473 (7)
F8—C10	1.347 (6)	N4—C13	1.467 (7)
F9—C11	1.345 (6)	N4—C14	1.474 (7)
F10—C12	1.358 (6)	N4—C18	1.464 (7)

Adduct **2a.1** was formed between 1,2-diiidotetrafluorobenzene (**2**) and hexamethylene-tetramine (**a**). This adduct crystallise in the $P2_1/c$ space group similar to adduct **1a** and the asymmetric unit consists of one molecule of 1,2-diiidotetrafluorobenzene and one molecule of hexamethylenetetramine (Fig 3.3). There are 4 of these units in the packing view of this structure.

The crystal structure shows N-C and C-C distances consistent with that observed in **1a** and the previously reported structures involving 1,3,5-trifluoro-2,4,6-triiodobenzene with hexamethylenetetramine (CSD refcode RORWEC). (Syssa-Magalé *et al.*, 2014) The average C-I bond distance in **2a.1** is 2.117(5) Å, longer than the C-I bond distance of pure 1,2-diiidotetrafluorobenzene (WISBOR), which has an average distance of 2.086(2) Å. (Xin Ding, 2012) A summary of the bond distances of **2a.1** are listed in Table 3.5.

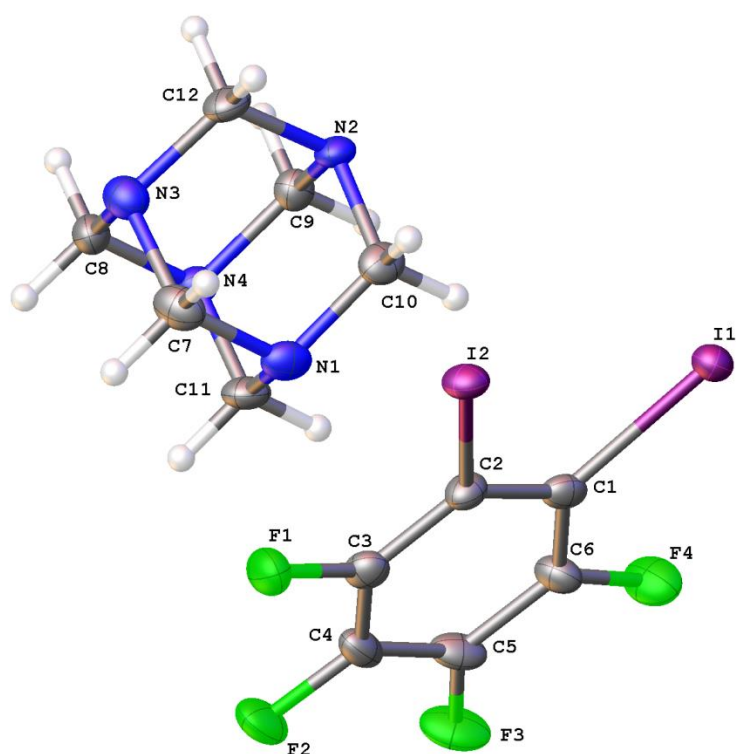


Figure 3.3 The asymmetric unit of **2a.1** showing the atom numbering, Ellipsoids are drawn at 50% probability level. The colour key is as follows: gray, carbon; purple, iodine; blue, nitrogen; green, fluorine; white, hydrogen.

The extended structure of **2a.1** shows N...I halogen bonds between both iodine atoms to different hexamethylenetetramine molecules. There are only 2 nitrogen atoms in the hexamethylenetetramine involved in halogen bond N...I, similar to adduct **1a**. The N...I distances are 2.830(4) and 2.879(3) Å which are 0.7 Å

(19.8%) and 0.65 Å (18.4 %) shorter than the sum of the van der Waals radii (3.53 Å). These distances are within the average distance of the published structures and slightly longer than the corresponding distance in QIHCOZ, 2.845(3) Å, and QIHCOZ01, 2.806(1) Å reported for adducts of 1,4-diiodotetrafluorobenzene with **a**. (Walsh *et al.*, 2001; Bolte, 2004)

The N...I-C halogen bond angles are near-linear, with an average of 171.4(1) °. In addition, to the halogen bonds there are other weak interactions that can be detected in this structure. There are a short contact between fluorine and hydrogen [F4...H10A, 2.45 Å and F3...H10B, 2.56 Å] with an average distance of 2.51 Å (see Table 3.6) and each arene is connected to the neighbour by weak F...F interactions with an average distance of 2.822(5) Å, Fig. 3.4.

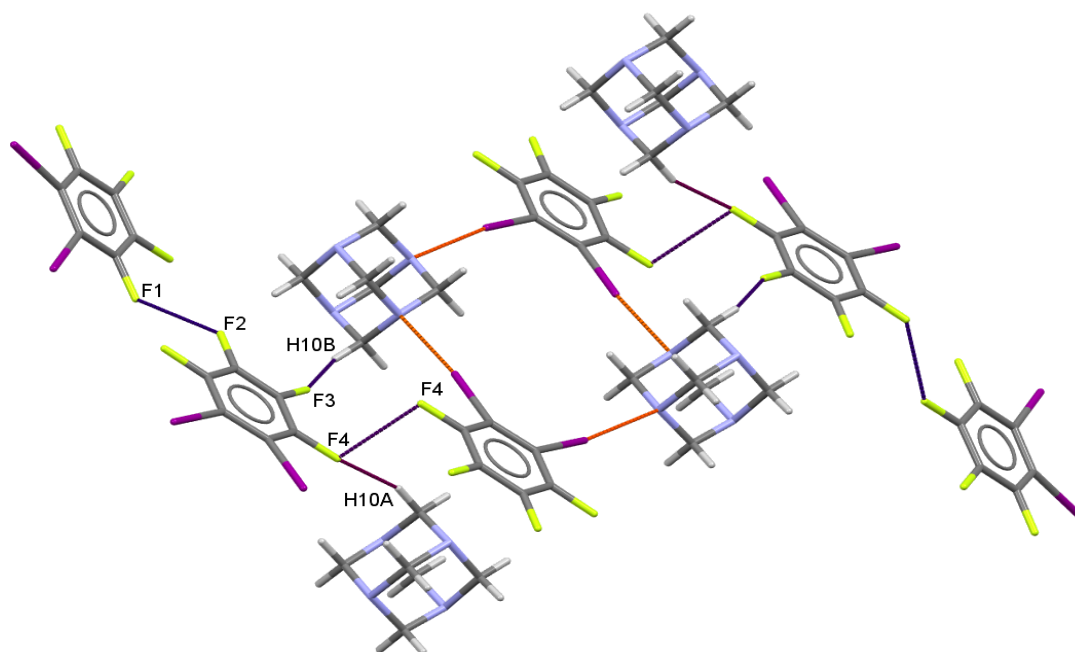


Figure 3.4 View of one halogen bonded (red lines) and other weak F...F and F...H interactions (dark blue lines) in **2a.1**. The colour key is as follows: gray, carbon; purple, iodine; blue, nitrogen; yellow, fluorine; white, hydrogen.

Table 3.5 Selected bond distances (Å) in **2a.1**

C1—C2	1.389 (6)	C7—N1	1.466 (6)
C1—C6	1.387 (6)	C7—N3	1.481 (6)
C1—I1	2.114 (5)	C8—N3	1.471 (6)
C2—C3	1.380 (6)	C8—N4	1.477 (6)
C2—I2	2.119 (4)	C9—N2	1.464 (5)
C3—C4	1.378 (6)	C9—N4	1.469 (6)
C3—F1	1.352 (5)	C10—N1	1.470 (6)
C4—C5	1.367 (7)	C10—N2	1.482 (5)
C4—F2	1.343 (5)	C11—N1	1.469 (5)
C5—C6	1.377 (6)	C11—N4	1.476 (6)
C5—F3	1.349 (5)	C12—N2	1.469 (6)
C6—F4	1.354 (5)	C12—N3	1.485 (6)

Table 3.6 Hydrogen-bond geometry (Å, °) for **2a.1**

<i>D</i> —H... <i>A</i>	<i>D</i> —H	H... <i>A</i>	<i>D</i> ... <i>A</i>	<i>D</i> —H... <i>A</i>
C10—H10A...F4 ⁱ	0.99	2.45	3.376 (5)	156
C10—H10B...F3 ⁱⁱ	0.99	2.56	3.449 (5)	150

Symmetry codes: (i) $-x, -y+1, -z$; (ii) $x, y, z-1$.

Increasing the molar stoichiometric ratio to 4:1 of 1,2-diodotetrafluorobenzene adduct (**2**) to hexamethylenetetramine (**a**) and using slow evaporation in acetonitrile resulted in a mixture of both **2a.1** and a new structure **2a**. The new structure belongs to the triclinic space group $P\bar{1}$ with 3 nitrogen atoms from hexamethylenetetramine involved in halogen bonds this time rather than 2 nitrogen atoms in structure **2a.1**.

The asymmetric unit of **2a** consists of two molecules of 1,2-diodotetrafluorobenzene and one molecule of hexamethylenetetramine in 2:1 ratio as shown in, Fig. 3.5, rather than the 1:1 ratio observed in **2a.1**.

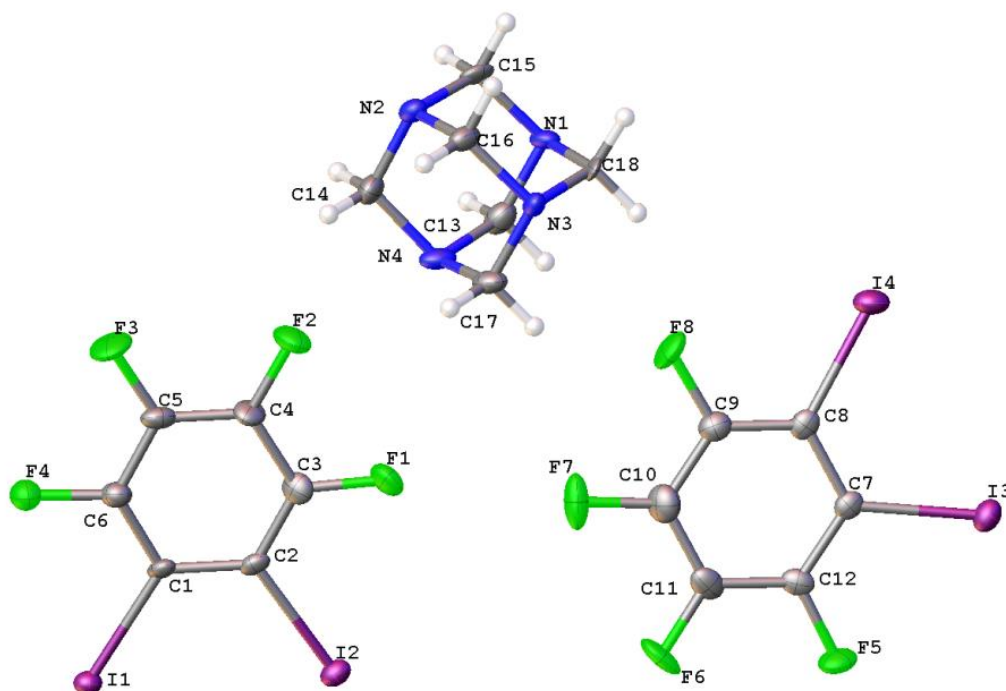


Figure 3.5 The asymmetric unit of **2a** and the atoms numbering. Ellipsoids are drawn at 50% probability level. The colour key is as follows: gray, carbon; purple, iodine; blue, nitrogen; green, fluorine; white, hydrogen.

The average C-I bond distance for structure **2a** is 2.105(9) Å which is shorter than the C-I distance of 2.086(2) Å for pure 1,2-diiodotetrafluorobenzene (WISBOR, [Xin Ding, 2012](#)) and close to the C-I distances in the other structures reported here. The rest of the bond distances for **2a** are listed in [Table 3.7](#).

The extended structure of **2a** shows three N...I halogen bonds. Two of them [N2...I2, 2.805(7) Å and N4...I1, 2.840(8) Å] are close to the distances observed in **1a** and **2a.1**, however the third one [N1...I4, 3.128 Å] is significantly longer, but still shorter than the sum of van der Waals radii of iodine and nitrogen atoms 3.53 Å. The N...I-C angles range from 177.7(3) ° corresponding to the shortest and more directional N2...I2 distance to 154.0(3) ° for the third and longest N1...I4 halogen bond.

In addition to the N...I halogen bonds, the two-dimensional extended structure shows other non-covalent interactions. Atom I1 which is involved in N...I halogen

bonding is simultaneously involved in I...I type II halogen-halogen interactions. The I1...I3 distance is 3.811(1) Å, slightly shorter than the sum of the van der Waals radii (3.96 Å) for two iodine atoms by 0.15 Å (3.8%) (Bondi, 1964; Alvarez, 2013). Once again there are F...F interactions 2.861(9) Å and F...H interactions [F8...H17B, 2.61 Å and F6...H18B, 2.61 Å] Table 3.8, beside this there is π - π stacking (Janiak, 2000) characterised by centroid-centroid distances of 3.749 and 3.789 Å, see Fig. 3.6.

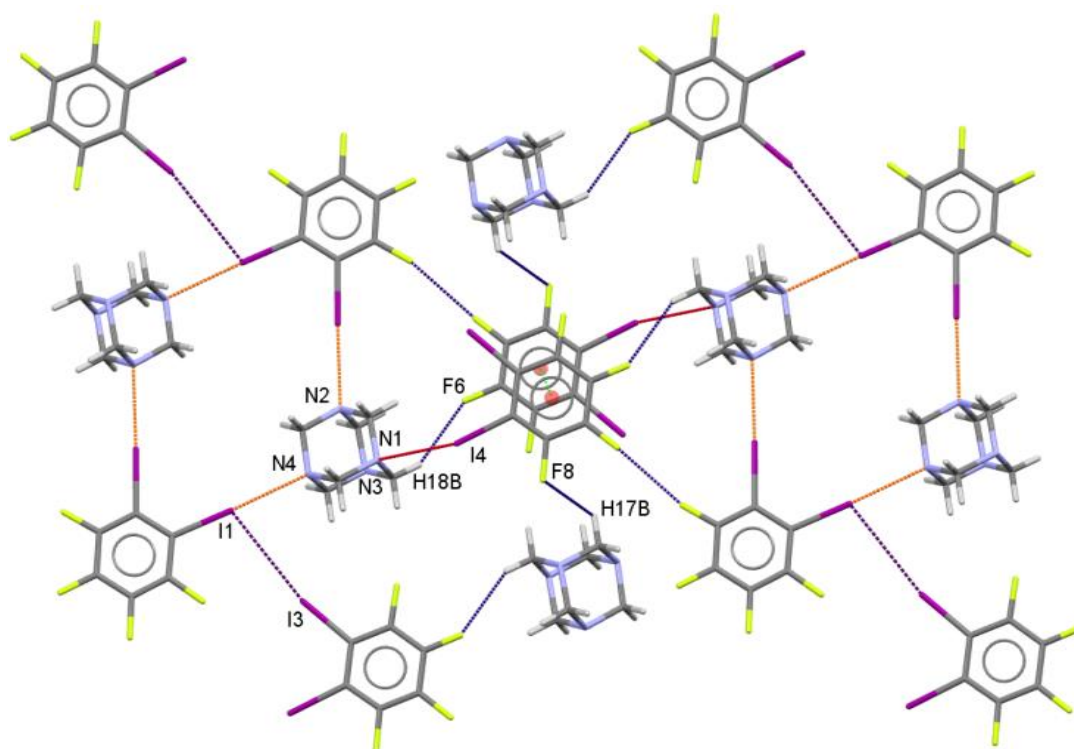


Figure 3.6 View of 2D halogen bonds (red lines), π - π stacking and other weak F...F and F...H interactions (dark blue lines) in **2a**. The colour key is as follows: gray, carbon; purple, iodine; blue, nitrogen; yellow, fluorine; white, hydrogen.

Table 3.7 Selected bond distances (Å) in **2a**

C1—C2	1.399 (12)	C8—I4	2.089 (10)
C1—C6	1.392 (10)	C9—C10	1.391 (14)
C1—I1	2.110 (9)	C9—F8	1.364 (9)
C2—C3	1.365 (13)	C10—C11	1.397 (12)
C2—I2	2.131 (8)	C10—F7	1.330 (11)
C3—C4	1.410 (11)	C11—C12	1.369 (13)
C3—F1	1.341 (11)	C11—F6	1.303 (11)
C4—C5	1.363 (13)	C12—F5	1.358 (9)
C4—F2	1.329 (10)	C13—N1	1.457 (12)
C5—C6	1.369 (13)	C13—N4	1.481 (12)
C5—F3	1.355 (9)	C14—N2	1.460 (11)
C6—F4	1.361 (11)	C14—N4	1.492 (10)
C7—C8	1.414 (11)	C15—N1	1.472 (10)
C7—C12	1.394 (12)	C15—N2	1.474 (11)
C7—I3	2.091 (9)	C16—N2	1.475 (10)
C8—C9	1.359 (12)	C16—N3	1.477 (10)

Table 3.8 Hydrogen-bond geometry (Å, °) for **2a**

<i>D</i> —H... <i>A</i>	<i>D</i> —H	H... <i>A</i>	<i>D</i> ... <i>A</i>	<i>D</i> —H... <i>A</i>
C17—H17 <i>B</i> ...F8	0.97	2.61	3.197 (11)	119
C18—H18 <i>B</i> ...F6 ⁱ	0.97	2.61	3.492 (10)	151

Symmetry code: (i) $x-1, y, z$.

Adduct **3a** was obtained from 1,3-diiodotetrafluorobenzene (**3**) and hexamethylenetetramine (**a**) forming two layers of crystals within 2 days, one set on the surface of the acetonitrile solvent and the second set as a precipitate. Both crystals were investigated and resulted in the same crystal structure, **3a**.

The asymmetric unit of **3a** consists of 2 molecules of 1,3-diiodotetrafluorobenzene and two separate halves of hexamethylenetetramine with 2-fold rotation axis passing through C14 and C16 in one molecule and C17 and C20 in the second (see

Fig. 3.7). This is the only orthorhombic structure (P_{ccn}) reported here, and has the biggest volume of 4923.68 Å³.

The geometric parameters in this structure are consistent with those observed in **1a**, **2a.1** and **2a**. The C-I bond distances are 2.113(4) and 2.107(4) Å (average 2.110 (4) Å) and there is no reported structure for pure 1,3-diiidotetrafluorobenzene to compare the resulted parameters, however these C-I distances are slightly longer than that recorded at different temperatures found in pure 1,4-diiidotetrafluorobenzene [CSD ref code QIHCOZ, 2.095(4) and QIHCOZ01, 2.104(2) Å]. (Walsh *et al.*, 2001) The remaining covalent bond distances of **3a** are listed in Table (3.9).

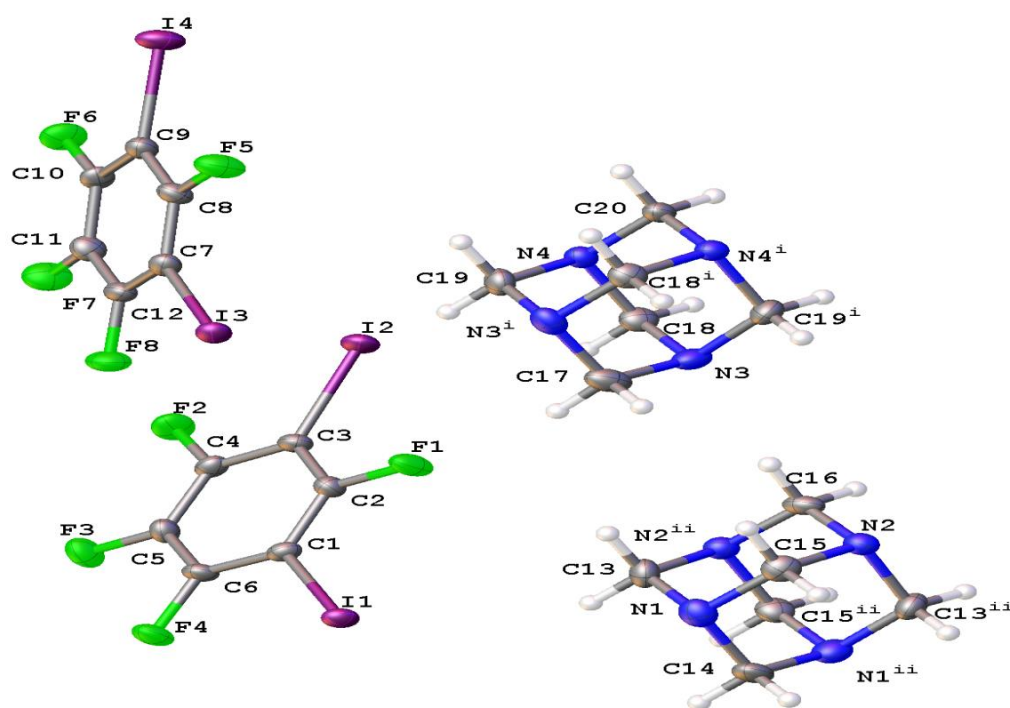


Figure 3.7 A view of the structure of halogen-bonded adduct **3a**, showing the atom numbering, Ellipsoids are drawn at 50% probability level, The colour key is as follows: gray, carbon; purple, iodine; blue, nitrogen; green, fluorine; white, hydrogen. [Symmetry codes: (i) $1/2-x, 3/2-y, +z$ (ii) $3/2-x, 3/2-y, +z$].

The expanded structure of **3a** shows two different layers containing two different 1,3-diiodotetrafluorobenzene and hexamethylenetetramine molecules, see **Fig. 3.8**. Two different nitrogen atoms of HTMA act as XB acceptors and only one iodine of each 1,3-triiodotetrafluorobenzene (I3 and I1) are involved in N...I halogen bonds. Simultaneously the same iodine atoms (I3 and I1) are involved in I...I interaction with another close arene through the electron density of the equatorial area perpendicular to the C-I axis along with the depletion of the charge (σ hole). *Metrangolo & Resnati, 2015a*

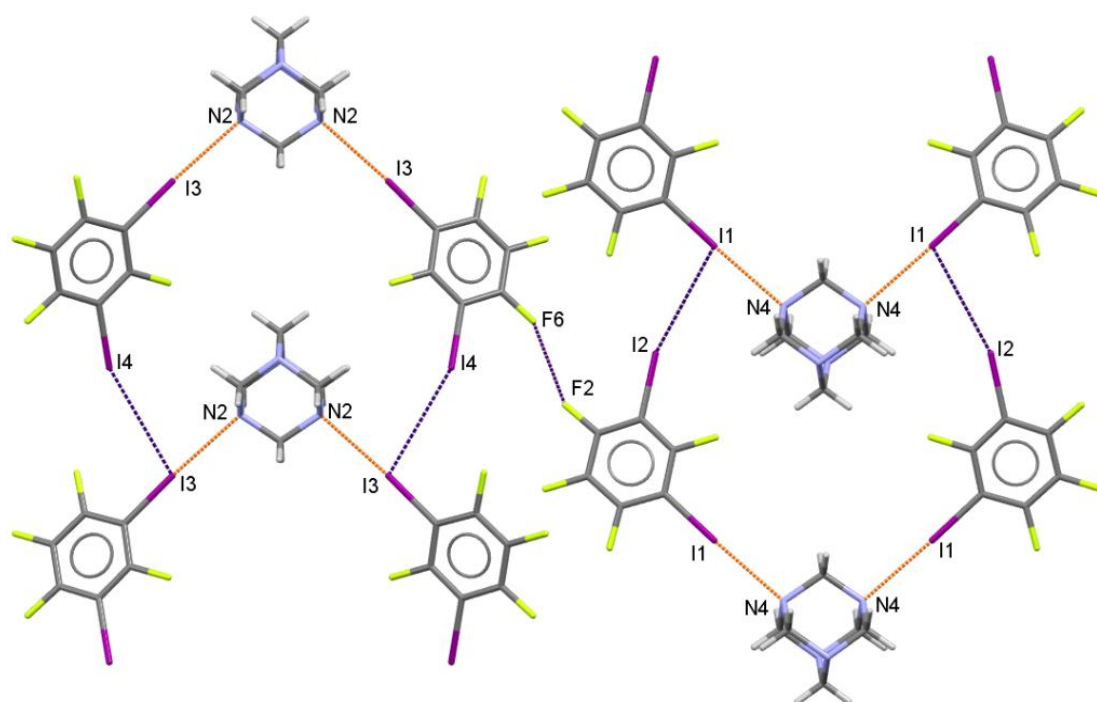


Figure 3.8 View of one halogen bonded (red lines) and I...I, F...F interactions (dark blue lines) in **3a**. The colour key is as follows: gray, carbon; purple, iodine; blue, nitrogen; yellow, fluorine; white, hydrogen.

Structure **3a** displays an average N...I bond distance of 2.824(4) Å which is 0.71 Å (20%) shorter than the sum of the van der Waal's radii (3.53 Å), and an approximately linear arrangement with an average N...I-C angle of 176.1(1) °, which is the closest angle to linearity reported here. The average orthogonal C-I...I angle is 106.0 ° suggesting type II halogen...halogen bonding, with an average I...I distance of 3.857(6) Å (0.103 Å, 2.6 %) just shorter than the sum of the van der

Waals radii of 3.96 Å of two iodine atoms. Beside the previous contacts there are F...F intermolecular interactions at distances of 2.868(3) and 2.810(4) Å between two opposite chains in structure **3a**. In addition to this, the structure displays two N...H weak interactions [N1...H20B, 2.51 Å and N1...H20B, 2.55 Å] (see Table 3.10).

Table 3.9 Selected bond distances (Å) in **3a**

C1—C2	1.388 (6)	C11—C12	1.376 (6)
C1—C6	1.381 (6)	C11—F7	1.351 (5)
C1—I1	2.108 (4)	C12—F8	1.342 (5)
C2—C3	1.380 (6)	C13—N1	1.458 (6)
C2—F1	1.347 (5)	C13—N2 ⁱ	1.474 (5)
C3—C4	1.386 (6)	C14—N1	1.471 (5)
C3—I2	2.085 (4)	C14—N1 ⁱ	1.471 (5)
C4—C5	1.374 (6)	C15—N1	1.468 (6)
C4—F2	1.340 (5)	C15—N2	1.478 (6)
C5—C6	1.384 (6)	C16—N2 ⁱ	1.464 (5)
C5—F3	1.344 (5)	C16—N2	1.464 (5)
C6—F4	1.343 (5)	N2—C13 ⁱ	1.474 (5)
C7—C8	1.378 (6)	C17—N3	1.465 (6)
C7—C12	1.385 (6)	C17—N3 ⁱⁱ	1.465 (6)
C7—I3	2.114 (4)	C18—N3	1.472 (5)
C8—C9	1.379 (6)	C18—N4	1.484 (5)
C8—F5	1.351 (5)	C19—N3 ⁱⁱ	1.470 (6)
C9—C10	1.393 (6)	C19—N4	1.476 (5)
C9—I4	2.087 (4)	C20—N4 ⁱⁱ	1.475 (5)
C10—C11	1.371 (6)	C20—N4	1.475 (5)
C10—F6	1.339 (5)	N3—C19 ⁱⁱ	1.470 (6)

Symmetry codes: (i) $-x+3/2, -y+3/2, z$; (ii) $-x+1/2, y, z-1/2$.

Table 3.10 Hydrogen-bond geometry (Å, °) for **3a**

<i>D</i> —H... <i>A</i>	<i>D</i> —H	H... <i>A</i>	<i>D</i> ... <i>A</i>	<i>D</i> —H... <i>A</i>
C16—H16A...N3 ⁱ	0.97	2.55	3.520 (5)	175
C20—H20A...N1 ⁱⁱ	0.97	2.51	3.478 (5)	174

Symmetry codes: (i) $-x+3/2, -y+3/2, z$; (ii) $-x+1/2, y, z-1/2$.

An attempt to prepare halogen-bonded adducts involving **1**, **2** and **3** with the monophosphorus-containing analogue of hexamethylenetetramine (1,3,5-triaza-

phosphaadamantane) using vapour diffusion and slow evaporation described previously was not successful. However, using **4** (1,4-diiidotetrafluorobenzene) resulted in adduct **4b.1**, that crystallised in the monoclinic $P2_1/m$ space group and the asymmetric unit consists of half a molecule of 1,4-diiidotetrafluorobenzene situated about an inversion centre and half a molecule of 1,3,5-triaza-phosphaadamantane laying on a crystallographic mirror plane **Fig. 9**.

This is the first structure involve 1,3,5-triaza-phosphaadamantane in N...I/Br halogen bonding and there are no reported structures with which to directly compare the structural parameters from **4b.1**. The formation of the N...I halogen bonds result in extension of the C-I bond distance to 2.107(6) Å, longer than the reported C-I bond distance for pure 1,4-diiidotetrafluorobenzene reported in structures ZZZAVM01 (2.0747(14) Å) and ZZZAVM02 (2.079 (4) Å). (*Chaplot et al.*, 1981; *Oh et al.*, 2012) The average C-N, C-P bond distances are listed in **Table 3.11** and are consistent with those reported for 1,3,5-triaza-phosphaadamantane at low temperature. (*Britvin & Lotnyk*, 2015)

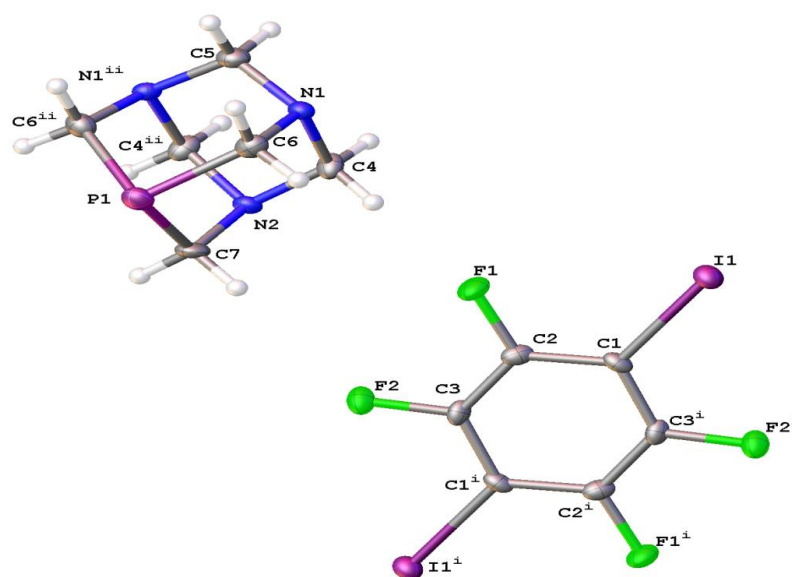


Figure 3.9 A view of halogen- bonded adduct **4b.1**, showing the atom numbering. Ellipsoids are drawn at 50% probability level, the colour key is as follows: gray, carbon; purple, iodine; blue, nitrogen; green, fluorine; white, hydrogen. [Symmetry codes: (i) $-x, 1-y, 2-z$ (ii) $+x, 3/2-y, +z$].

Table 3.11 Selected bond distances (Å) in **4b.1**

C1—C2	1.377 (7)	C5—N1	1.472 (5)
C1—C3 ⁱ	1.390 (6)	C5—N1 ⁱⁱ	1.472 (5)
C1—I1	2.107 (5)	C6—N1	1.481 (5)
C2—C3	1.376 (6)	C6—P1	1.851 (5)
C2—F1	1.359 (5)	C7—N2	1.473 (8)
C3—C1 ⁱ	1.390 (6)	C7—P1	1.858 (7)
C3—F2	1.351 (5)	N2—C4 ⁱⁱ	1.464 (5)
C4—N1	1.478 (6)	P1—C6 ⁱⁱ	1.851 (5)
C4—N2	1.464 (5)		

Symmetry codes: (i) $-x, -y+1, -z+2$; (ii) $x, -y+3/2, z$.

The extended structure of **4b.1** shows two symmetry-related N...I halogen bonds involving both equivalent iodine atoms of **4** with 2 equivalent nitrogen atoms from three available atoms, see Fig. 3.10. This results in a zigzag shape of donor-acceptor-donor-acceptor, similar to the reported hexamethylenetetramine analogue (Walsh *et al.*, 2001). The N...I distance is 2.838(4) Å, 0.692 Å (19.6%) shorter than the sum of the van der Waals radii (3.53 Å) and the N...I-C angle is near-linear 171.0(2) °. Unfortunately, the phosphorus atom did not participate in halogen bonding or other interactions in this structure.

In addition to the halogen bonds there is one F...H interaction, [F12...H4B, 2.62 Å, 1.9%] just less than the sum of the van der Waals radii of both fluorine and hydrogen atoms (2.67 Å) (Table 3.12).

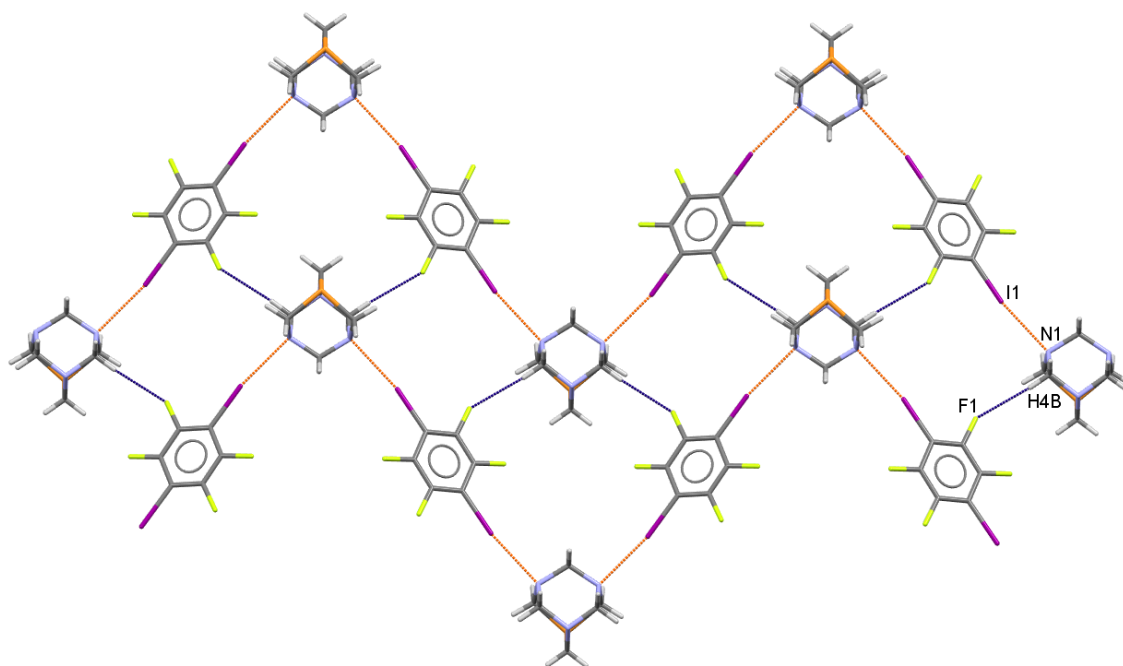


Figure 3.10 View of the zigzag halogen bonded shape (red lines) and F...H weak interactions (dark blue lines) in **4b.1**, the colour key is as follows: gray, carbon; purple, iodine; blue, nitrogen; yellow, fluorine; white, hydrogen.

Table 3.12 Hydrogen-bond geometry (Å, °) for **4b.1**

$D-H\cdots A$	$D-H$	$H\cdots A$	$D\cdots A$	$D-H\cdots A$
C4—H4B...F1	0.97	2.62	3.576 (6)	168

Increasing the molar stoichiometric ratio of 1,4-diodotetrafluorobenzene to 1,3,5-triaza-phosphaadamantane to 5:1, result in adduct **4b** which contained oxidized 1,3,5-triaza-phosphaadamantane (already known structure AZPADO) (Jogun *et al.*, 1978), bonded to 1,4-diodotetrafluorobenzene which is sitting on a crystallographic inversion centre, Fig. 3.11.

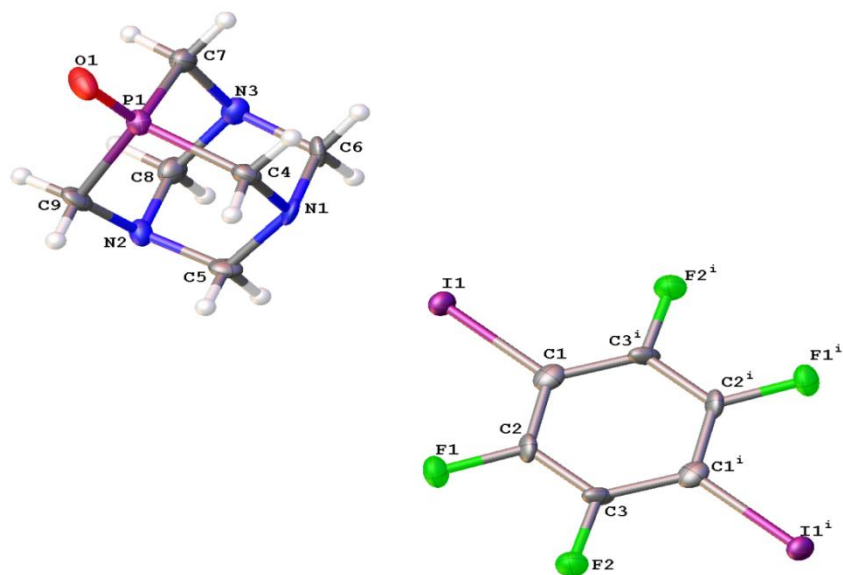


Figure 3.11 View of halogen- bonded adduct **4b**, showing the atom numbering. Ellipsoids are drawn at 50% probability level, The colour key is as follows: gray, carbon; purple, iodine; blue, nitrogen; green, fluorine; white, hydrogen. [Symmetry codes: (i) 1-x, 1-y, 1-z].

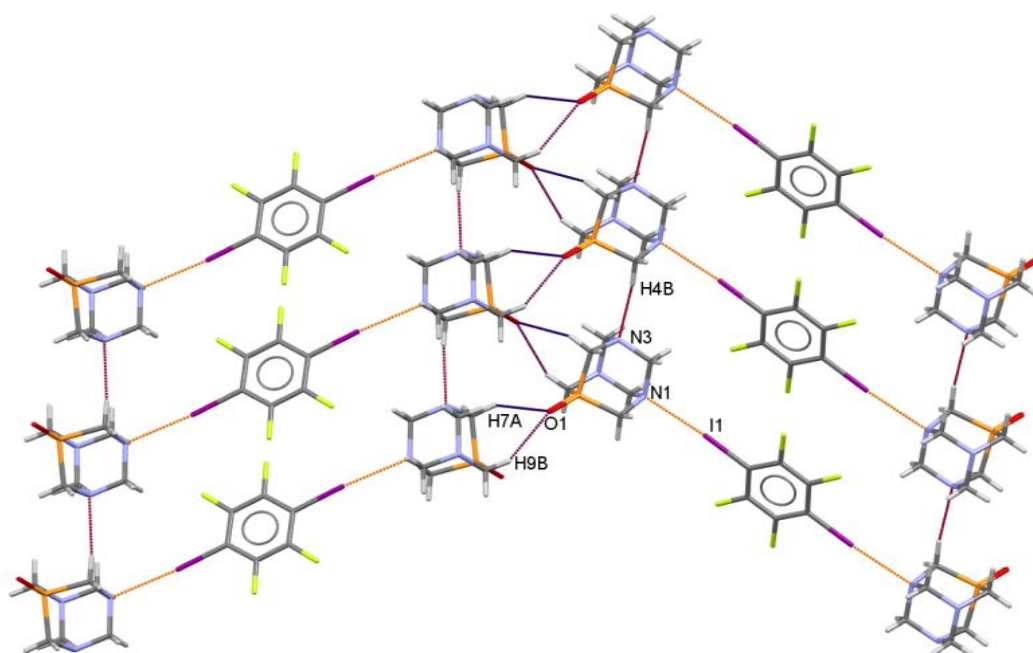


Figure 3.12 View of halogen bonds (red lines) and C-H...O interactions (dark blue lines) display in **4b**. The colour key is as follows: gray, carbon; purple, iodine; blue, nitrogen; yellow, fluorine; white, hydrogen; red, oxygen; orange, phosphorus.

This structure **4b** crystallises in the monoclinic space group ($P2_1/c$) and the asymmetric unit consists of half a molecule of 1,4-diiidotetrafluorobenzene situated about an inversion centre and one molecule of 1,3,5-triaza-phosphaadamantane-7-oxide.

On comparison of some of the parameters related to **4b** with the other structures reported here we noticed that the C-I covalent distance 2.109(7) Å is the same as 2.107(6) Å found in **4b.1**, but the corresponding N...I halogen bond (2.799(7) Å) is significantly shorter than 2.838(4) Å in **4b.1**.

However the average C-N bondlength in **4b** is consistent with the distances found in pure 1,3,5-triaza-phosphaadamantane-7-oxide, the P=O distance is 1.483(5) Å, which is longer than (CSD ref code AZPADO) 1.4763(13) Å and (CSD ref code AZPADO01) 1.476(3) Å. (Jogun *et al.*, 1978; Marsh *et al.*, 2002) The remaining covalent bond distances are listed in Table 3.13.

Even though, there are six reported structures in the CCDC of tertiary oxidized phosphines involved in O...I halogen bond interaction with 1,4-diiidotetrafluorobenzene, the only halogen bonds detected in **4b** are N...I. The extended structure still has a zig zag shape, but in (...DAADAA...) order, where D represent the donor and A is the acceptor, Fig. 13. Only one of the three nitrogen atoms are involved in N...I halogen bonding with a distance of 2.799(7) Å which is 0.731 Å (20.7%) shorter than the sum of the van der Waals radii (3.53 Å) and significantly (8σ) shorter than the distance in **4b.1**. This halogen bond possesses an angle of 176.0(2) °, close to linearity and even closer to linearity than **4b.1** (171.0(2) °). The structure of 1,3,5-triaza-phosphaadamantane-7-oxide, **4b**, displays C-H...N [N3...H14B 2.45 Å] and C-H...O non-conventional hydrogen bond interactions [O1...H4A 2.47 Å, O1...H7A 2.63 Å and O1...H9B 2.52 Å] with an average distance of 2.54 Å to the neighbour, see Table 3.14. These distances are almost 11% (N...H) and 6.6 % (O...H) shorter than their sum of van der Waals radii of 2.75 and 2.72 Å respectively for the N...H and O...H interactions.

Table 3.13 Selected bond distances (Å) in **4b**

C1—C2	1.381 (8)	C5—N2	1.463 (7)
C1—C3 ⁱ	1.384 (8)	C6—N1	1.489 (7)
C1—I1	2.110 (6)	C6—N3	1.474 (7)
C2—C3	1.381 (8)	C7—N3	1.490 (8)
C2—F1	1.354 (6)	C7—P1	1.824 (5)
C3—C1 ⁱ	1.384 (8)	C8—N2	1.478 (7)
C3—F2	1.343 (6)	C8—N3	1.463 (8)
C4—N1	1.480 (8)	C9—N2	1.474 (8)
C4—P1	1.810 (6)	C9—P1	1.828 (6)
C5—N1	1.466 (7)	O1—P1	1.483 (5)

Symmetry codes: (i) $-x+1, -y+1, -z+1$.

Table 3.14 Hydrogen-bond geometry (Å, °) for **4b**

$D-H\cdots A$	$D-H$	$H\cdots A$	$D\cdots A$	$D-H\cdots A$
C4—H4A \cdots O1 ⁱ	0.97	2.47	3.290 (8)	142
C4—H4B \cdots N3 ⁱⁱ	0.97	2.45	3.411 (7)	174
C7—H7A \cdots O1 ⁱⁱⁱ	0.97	2.63	3.446 (7)	142
C9—H9B \cdots O1 ⁱⁱⁱ	0.97	2.52	3.366 (7)	146

Symmetry codes: (i) $-x, -y, -z+1$; (ii) $x, y+1, z$; (iii) $-x, y-1/2, -z+3/2$.

All of the adducts reported here exhibit N...I halogen bonds shorter than the sum of the van der Waals radii, 3.53 Å and with N...I-C angles that are close to linearity. The shortest N...I bond distance is related to **1a**, which is probably due to the 5 fluorine atoms on the ring **Table 3.15**. Furthermore, there are other non-covalent interactions in each one of the distances listed in **Table 3.16**, but the only structure shows 3N...I halogen bonds and also the only one reported to contain π - π stacking within this chapter is structure **2a**.

Table 3.15 N...I halogen-bond distances (Å) and angles (°) in the current work and previously reported related structures.

Entry	Donor	Acceptor	N...I (Å)	N...I-C (°)	Reference
1	1-IPFB(1a)	C ₆ H ₁₂ N ₄ (a)	2.792(4) _(ave)	172.8(2) _(ave)	This work
2	1,2-DITFB(2a.1)	C ₆ H ₁₂ N ₄ (a)	2.855(4) _(ave)	171.4(1) _(ave)	This work
3	1,2-DITFB(2a)	C ₆ H ₁₂ N ₄ (a)	2.924(8) _(ave)	169.2(3) _(ave)	This work
4	1,3-DITFB(3a)	C ₆ H ₁₂ N ₄ (a)	2.824(4) _(ave)	176.1(1) _(ave)	This work
5	1,4DITFB(4b.1)	C ₆ H ₁₂ N ₃ P(b)	2.838(4)	171.0(2)	This work
6	1,4DITFB(4b)	C ₆ H ₁₂ N ₃ P(b)	2.799(7)	176.0(2)	This work
7	1,4DITFB(4) QIHCOZ	C ₆ H ₁₂ N ₄ (a)	2.845(3)	169.1(1)	(Walsh <i>et al.</i> , 2001)
8	1,4DITFB(4) QIHCOZ01	C ₆ H ₁₂ N ₄ (a)	2.806(1)	168.53(6)	(Bolte, 2004)
9	1,3,5-TF-2,4,6-TIB RORWEC	C ₆ H ₁₂ N ₄ (a)	2.872(5) _(ave)	171.1(2) _(ave)	(Syssa-Magalé <i>et al.</i> , 2014)

Table 3.16 Intermolecular interactions in (Å) shorter than the sum of the van der Waals radii

Entry	Donor	I...I (Å)	F...F (Å)	F...H-C (Å)	O...H-C (Å)	Reference
1	(1a)	-	2.923(4) 2.896(5) 2.863(4) 2.879(4)	2.557	-	This work
2	(2a.1)	-	2.849(5) 2.795(5)	2.550 2.592	-	This work
3	(2a)	3.811(1)	2.861(9)	2.610 2.615	-	This work
4	(3a)	3.8526(6) 3.8610(6)	2.868(3) 2.810(4)	2.512 2.553	-	This work
5	(4b.1)	-	-	2.621	-	This work
6	(4b)	-	-	2.646	2.633 2.468 2.522	This work
7	QIHCOZ	-	-	2.38(5)	-	(Walsh <i>et al.</i> , 2001)
8	QIHCOZ01	-	-	2.498	-	(Bolte, 2004)
9	RORWEC	-	-	-	-	(Syssa-Magalé <i>et al.</i> , 2014)

IR spectroscopy is one of the tools available to investigate the halogen bonds in the solid state (Metrangolo & Resnati, 2015a,b) and can be used to support the crystallographic evidence. All the spectra for the six adducts are reported in section S 3.1-S 3.6 of the supplementary information. Key arrangements are listed in Table 3.17. It is interesting to note that the hexamethylenetetramine-containing adducts give rise to shifts in C-F stretching modes in the order **1a** > **3a** > (**2a.1** + **2a**). It is interesting that the largest change is observed for adduct **1a** which was found to give rise to the shortest N...I halogen bond distance reported here, 2.778(4) Å.

Table 3.17 Summary of the C-H and C-F stretches found in adduct **1a-4b.1** compared with related amine and arene. Differences are given in brackets

	Adduct 1a	Adduct 2a.1	Adduct 2a	Adduct 3a	Adduct 4b.1	Adduct 4b
Structure						
C-H	2946 (7 cm ⁻¹)	2948 (5 cm ⁻¹)	2948 (5 cm ⁻¹)	2962 (9 cm ⁻¹)	2904 (6 cm ⁻¹)	2941 (43 cm ⁻¹)
C-F	1135 (13 cm ⁻¹)	1106 (2 cm ⁻¹)	1106 (2 cm ⁻¹)	1068 (3 cm ⁻¹)	1453 (5 cm ⁻¹)	1430 (1 cm ⁻¹)

A comparison of the crystal structures and the generated molecular graph from QTAIM analysis are shown in Fig 3.13 to Fig 3.18. While Table 3.18 lists the N...I halogen bond distances in Å, the total electron density ρ_{BCP} and Laplacian $\nabla^2\rho_{\text{BCP}}$.

An unambiguous trend between the shortening of the N...I halogen bonds distances compared with the non-halogen bonded starting material and the electron density ρ_{BCP} can be seen for all of the reported structures. The shortest N...I bond distance reported in this chapter 2.778(4) Å corresponds to the highest electron density ρ_{BCP} and Laplacian $\nabla^2\rho_{\text{BCP}}$.

Furthermore, the negative local electronic energy density $H(r)$ value for the N...I shorter distances indicate that this close-shell N...I interaction is strong (Angelina *et al.*, 2013; Wang *et al.*, 2018; Esrafilı & Ahmadi, 2012; Esrafilı, 2012; Rozas *et al.*, 2000).

Beside N...I halogen bonds there are some I...I, F...F, F...H, F...I and I...H weak contacts in **2a** and **3a** detected by QTAIM but related to long distances and correspond to negligible (ρ_{BCP} and $\nabla^2\rho_{\text{BCP}}$), see Fig 3.15 and 3.16. At the same time they have a positive $H(r)$ values which sorted them with the weak noncovalent contacts. (Esrafilı, 2012)

Table 3.18 Topological parameters calculated at B3LYP/6-311G** level of theory

Trimer	Interaction	X...B (Å)	ρ_{BCP} (a.u)	$\nabla^2\rho_{\text{BCP}}$ (a.u)	H(r)
1a	N1...I1	2.805(4)	0.0273	0.0748	-0.000279
	N2...I2	2.778(4)	0.0287	0.0788	-0.000462
2a.1	N1...I1	2.830(4)	0.0262	0.0719	-0.000123
	N4...I2	2.879(3)	0.0240	0.0663	0.000010
2a	N1...I4	3.128(8)	0.0159	0.0441	0.000581
	N2...I2	2.805(7)	0.0272	0.0755	-0.000224
	N4...I1	2.840(8)	0.0256	0.0710	-0.000008
3a	N2...I3	2.823(4)	0.0267	0.0716	-0.000290
	N4...I1	2.825(4)	0.0266	0.0712	-0.000302
4b.1	N1...I1	2.834(4)	0.0258	0.0705	-0.000143
4b	N1...I1	2.799(7)	0.0277	0.0759	-0.000367

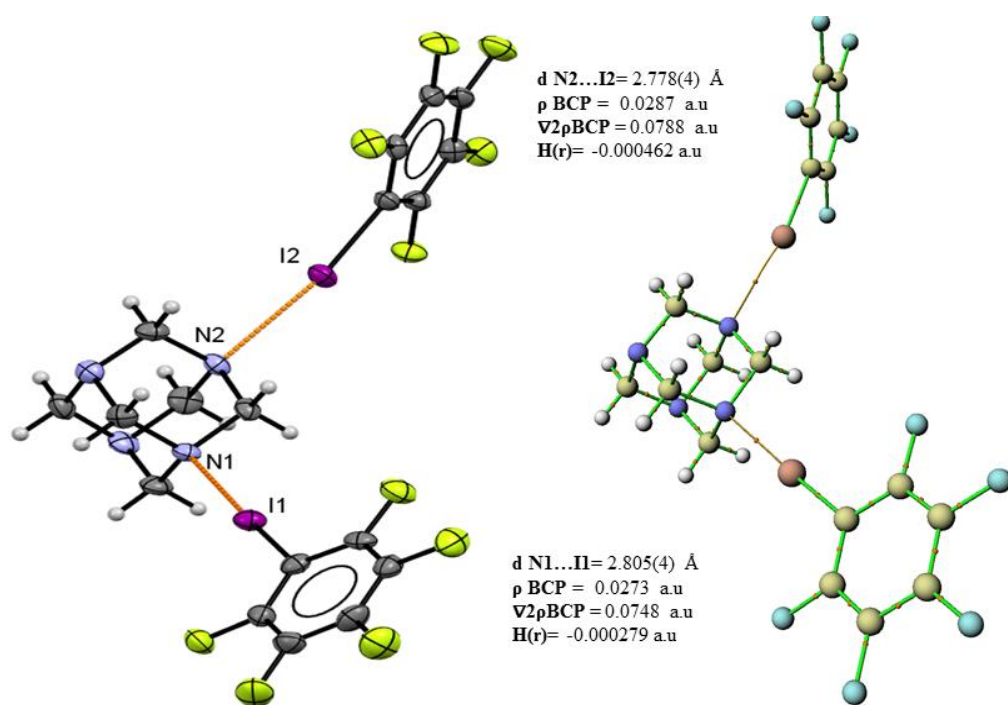


Figure 3.13 Showing determined X-ray structure (left) and molecular graph (right) of adducts **1a**

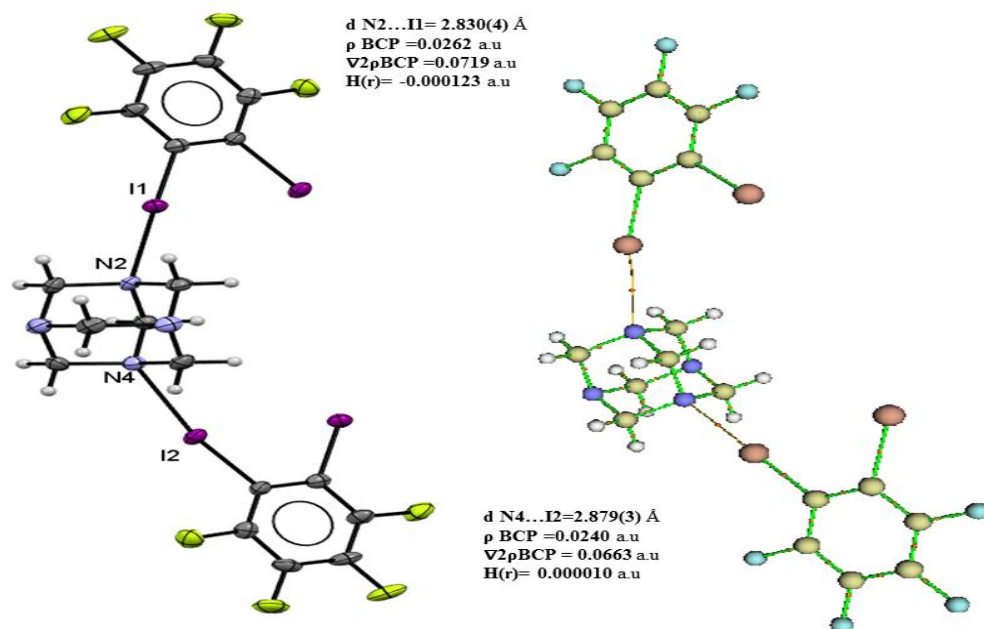


Figure 3.14 Showing determined X-ray structure (left) and molecular graph (right) of adducts **2a.1**

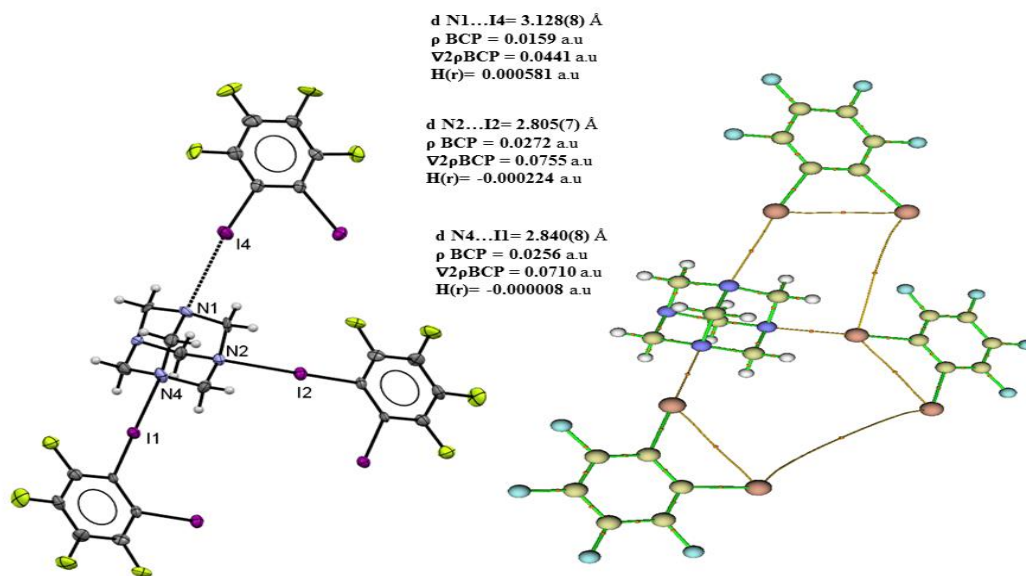


Figure 3.15 Showing determined X-ray structure (left) and molecular graph (right) of adducts **2a**

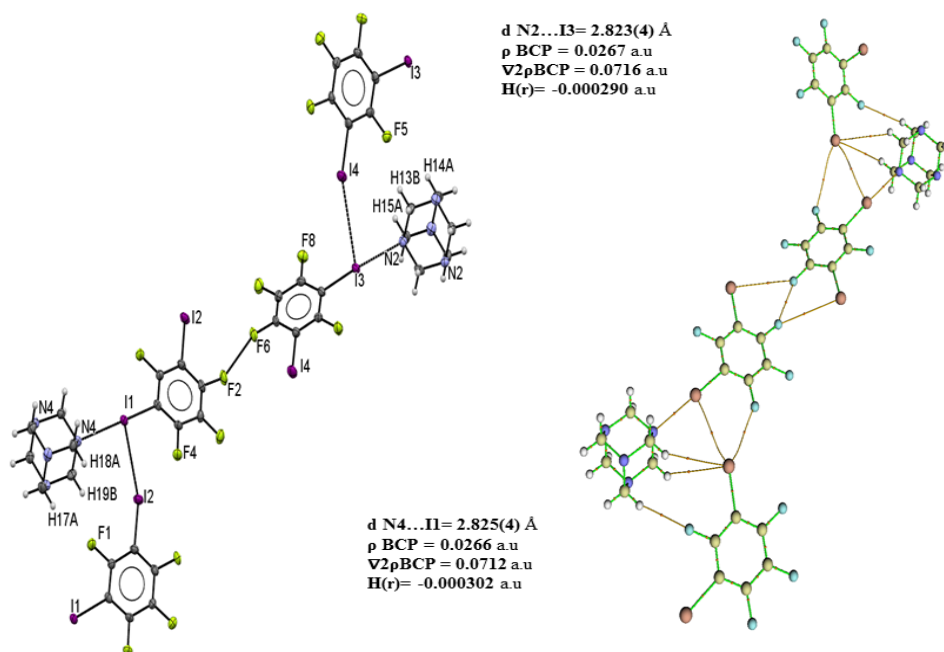


Figure 3.16 Showing determined X-ray structure (left) and molecular graph (right) of adducts **3a**

d N1...H1=2.834(4) Å
ρ BCP = 0.0258 a.u.
∇²ρ BCP = 0.0705 a.u.
H(r) = -0.000143 a.u.

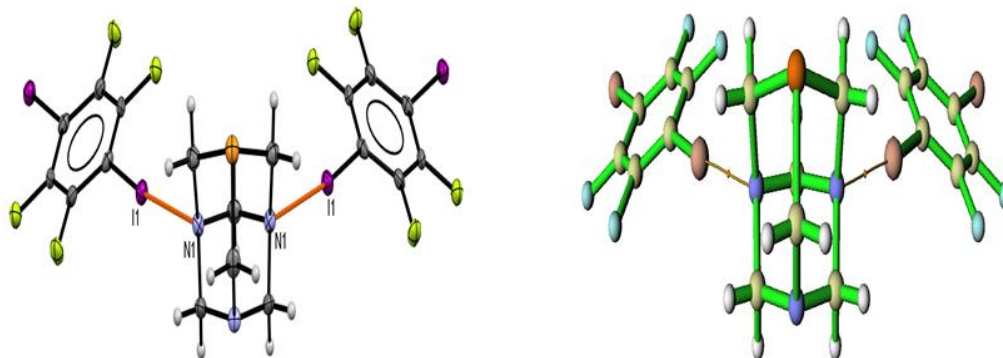


Figure 3.17 Showing determined X-ray structure (left) and molecular graph (right) for adducts **4b.1**

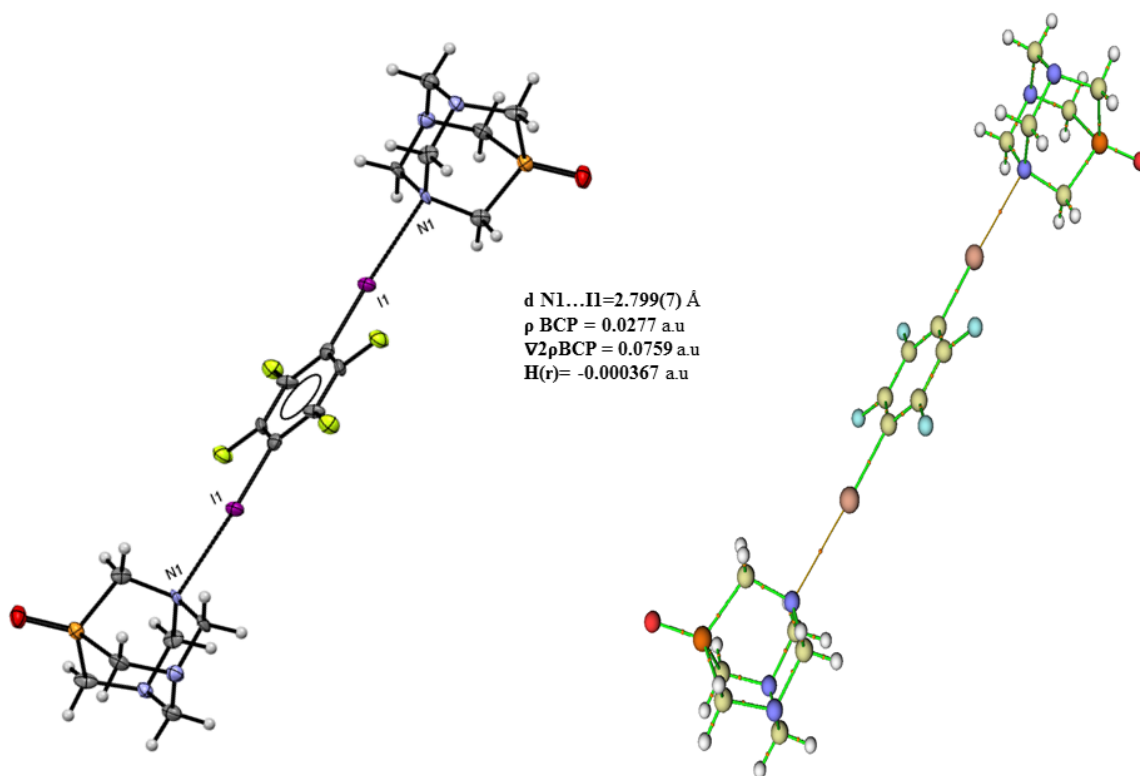


Figure 3.18 Showing determined X-ray structure (left) and molecular graph (right) of adducts **4b**

In summary, successful halogen bonded adducts have been prepared and characterized between four iodofluorobenzenes, acting as halogen bond donors, and hexamethylenetetramine, HTMA, all of which have been structurally characterised. N...I halogen bonds were observed in all cases, with the shortest distance, 2.778(4) Å being observed for adduct **1a**. QTAIM calculations reproduce the most significant interactions, but also suggest the presence of some additional weaker intra- and inter-molecular interactions between halogens, which are longer than the sum of the respective van der Waal's radii. Interestingly, in none of the adducts were all four of the nitrogen atoms involved in N...I halogen bond formation even when ratios of up to 5:1 donor:HTMA were utilised, instead two-dimensional extended arrangements were preferred.

When one of the nitrogen centres in HTMA is replaced with phosphorus to give 1,3,5-triaza-phosphaadamantane adduct formation was observed with 1,4-diodotetrafluorobenzene, however the phosphorus atom was found not to engage in halogen bond formation. In one further experiment oxidation occurred which resulted in the corresponding adduct containing 1,3,5-triaza-phosphaadamantane-7-oxide, this is the first such example to be reported.

References

- Alvarez, S. (2013). *Dalt. Trans.* **42**, 8617–8636.
- Angelina, E. L., Duarte, D. J. R. & Peruchena, N. M. (2013). *J. Mol. Model.* **19**, 2097–2106.
- Auffinger, P., Hays, F. A., Westhof, E. & Ho, P. S. (2004). *Proc. Natl. Acad. Sci.* **101**, 16789–16794.
- Bader, R. F. W. (1994). *Atoms in Molecules: A Quantum Theory* Clarendon Press.
- Bolte, M. (2004). CSD commun, deposited number CCDC 218129.
- Bondi, A. (1964). *J. Phys. Chem.* **68**, 441–451.
- Britvin, S. N. & Lotnyk, A. (2015). *J. Am. Chem. Soc.* **137**, 5526–5535.
- Bruce, D. W., Metrangolo, P., Meyer, F., Präsang, C., Resnati, G., Terraneo, G. & Whitwood, A. C. (2008). *New J. Chem.* **32**, 477–482.

- Bruno, I. J., Cole, J. C., Edgington, P. R., Macrae, C. F., Pearson, J. & Taylor, R. (2002). 389–397.
- Chaplot, S. L., McIntyre, G. J., Mierzejewski, A. & Pawley, G. S. (1981). *Acta Crystallogr. Sect. B.* **37**, 2210–2214.
- Clark, T., Hennemann, M., Murray, J. S. & Politzer, P. (2006). *J. Mol. Model.*
- Colin., J. (1814). *Ann Chim.* 252–272.
- Dolomanov, O. V, Bourhis, L. J., Gildea, R. J., Howard, J. A. K. & Puschmann, H. (2009). 2008–2010.
- Ekkehard, F., Juan-Enrique, F., Johann, W. & Erich, H. (1977). *Zeitschrift Für Naturforsch. B.* **32**, 499.
- Esfafili, M. D. (2012). *J. Mol. Model.* **18**, 5005–5016.
- Esfafili, M. D. & Ahmadi, B. (2012). *Comput. Theor. Chem.* **997**, 77–82.
- Frohn, H. J., Görg, S., Henkel, G. & Läge, M. (1995). *Zeitschrift Für Anorganische Und Allgemeine Chemie.* **621**, 1251–1256.
- Groom, C. R., Bruno, I. J., Lightfoot, M. P. & Ward, S. C. (2016). *Acta Crystallogr., Sec. B: Struct. Sci., Cryst. Eng. Mater.* 171–179.
- Guthrie, F. (1863). *J. Chem. Soc.* **16**, 239–244.
- Janiak, C. (2000). *J. Chem. Soc. Dalt. Trans.* 3885–3896.
- Jogun, K. H., Stezowski, J. J., Fluck, E. & Weidlein, J. (1978). *Phosphorus Sulfur Relat. Elem. Sulfur Relat. Elem.* **4**, 199–204.
- Lisac, K., Topić, F., Arhangeliskis, M., Cepić, S., Julien, P. A., Nickels, C. W., Morris, A. J., Frišćić, T. & Cinčić, D. (2019). *Nat. Commun.* **10**, 61.
- Lu, T. & Chen, F. (2012). *J. Comput. Chem.* **33**, 580–592.
- Lu, Y.-X., Zou, J.-W., Wang, Y.-H., Jiang, Y.-J. & Yu, Q.-S. (2007). *J. Phys. Chem. A.* **111**, 10781–10788.
- Marquardt, R., Politzer, P., Resnati, G., Rissanen, K., Desiraju, G. R., Ho, P. S., Legon, A. C., Kloo, L. & Metrangolo, P. (2013). *Pure Appl. Chem.* **85**, 1711–1713.
- Marsh, R. E., Kapon, M., Hu, S. & Herbstein, F. H. (2002). *Acta Crystallogr. Sect. B Struct. Sci.* **58**, 62–77.
- Metrangolo, P. & Resnati, G. (2015a). *Halogen Bonding I Impact on Materials Chemistry and Life Sciences* Springer International Publishing.

- Metrangolo, P. & Resnati, G. (2015*b*). Halogen Bonding II Impact on Materials Chemistry and Life Sciences Springer International Publishing.
- Mingos, D. M. P. (2008). Halogen bonding fundamental and applications New York: springer.com.
- Oh, S. Y., Nickels, C. W., Garcia, F., Jones, W. & Friščić, T. (2012). *CrystEngComm*. **14**, 6110–6114.
- Priimagi, A., Cavallo, G., Metrangolo, P. & Resnati, G. (2013). *Acc. Chem. Res.* **46**, 2686–2695.
- Rigaku, O. (2018). *Rigaku Oxford Diffraction Ltd, Yarnton, Oxfordshire, Engl.*
- Rozas, I., Alkorta, I. & Elguero, J. (2000). *J. Am. Chem. Soc.* **122**, 11154–11161.
- Schmidt, M. W., Baldrige, K. K., Boatz, J. A., Elbert, S. T., Gordon, M. S., Jensen, J. H., Koseki, S., Matsunaga, N., Nguyen, K. A., Su, S., Windus, T. L., Dupuis, M. & Montgomery Jr, J. A. (1993). *J. Comput. Chem.* **14**, 1347–1363.
- Sheldrick, G. M. (2015). *Acta Crystallogr. Sect. A Found. Crystallogr.* **71**, 3–8.
- Syssa-Magalé, J. L., Boubekour, K., Leroy, J., Chamoreau, L. M., Fave, C. & Schöllhorn, B. (2014). *CrystEngComm*. **16**, 10380–10384.
- Walsh, R. B., Padgett, C. W., Metrangolo, P., Resnati, G., Hanks, T. W. & Pennington, W. T. (2001). *Cryst. Growth Des.*
- Wang, R., Hartnick, D. & Englert, U. (2018). *Zeitschrift Für Kristallographie Crystalline Materials.* **233**, 733–744.
- Xin Ding, M. T. and M. H. A. (2012). *Intech*, Vol. 7, p. 143.
- Xu, Y., Huang, J., Gabidullin, B. & Bryce, D. L. (2018). *Chem. Commun.* **54**, 11041–11043.

Chapter 4.

Manuscript 3: Halogen bonds involving 1,4-diodotetrafluorobenzene with a variety of nitrogen-based aromatic halogen bond acceptors

Sultan Alkaabi, Alan K. Brisdon*

Department of Chemistry, University of Manchester, Oxford Road, Manchester M13 9PL, England.

Correspondence email: *alan.brisdon@manchester.ac.uk

4.1. Abstract

Four new halogen bonded adducts were prepared between 1,4-diodotetrafluorobenzene and four different nitrogen-containing halogen-bond acceptors: pyrimidine, 4,6-dimethyl pyrimidine and pyrimidine-5-amine and 1,3,5-triazine. Single crystal X-ray analysis revealed that all adducts contained N...I halogen bonds with distances that are shorter than the sum of the van der Waals radii (3.53 Å) and display different zig-zag architectures. QTAIM theoretical study confirm that each of the short N...I distances are interactions as they show high electron density, ρ_{BCP} , at each of these bond critical points. The combination of X-ray and QTAIM data allows us to rank the acceptors in the order pyrimidine > 4,6-dimethyl pyrimidine > pyrimidine-5-amine > 1,3,5-triazine. However, according to solution phase ^{19}F NMR data none of these halogen bonds remain in the solution phase.

4.2. Introduction

Following a large project set up between 2009 and 2013 by IUPAC to differentiate between different noncovalent interactions of halogens, the term halogen bonding was defined (Desiraju *et al.*, 2013), This is one of the possible intermolecular

interactions that can be used in self-assembly and to engineer aggregation in organic and inorganic chemistry based on the topicity of the donors and acceptors.

Halogen bonds arise from an area of positive charge that appears on the end of covalently bonded R-X axis called a σ hole. This electron deficiency area can interact electrostatically with a Lewis base Y and form what is defined as halogen bond. A variety of studies (Clark *et al.*, 2007; Politzer *et al.*, 2007) have shown that the positive charge of the σ hole of R-X increases as the electronegativity of X decreases (F>Cl>Br>I), the polarizability increases and as the withdrawing capability of the group R increase. A case in point are iodo- and bromo-aromatic compounds, which if fluorinated, such as 1,4-diiodotetrafluorobenzene have the ability to act as halogen bond donors in halogen bond adduct formation of the type RX...Y.(Riley *et al.*, 2011)

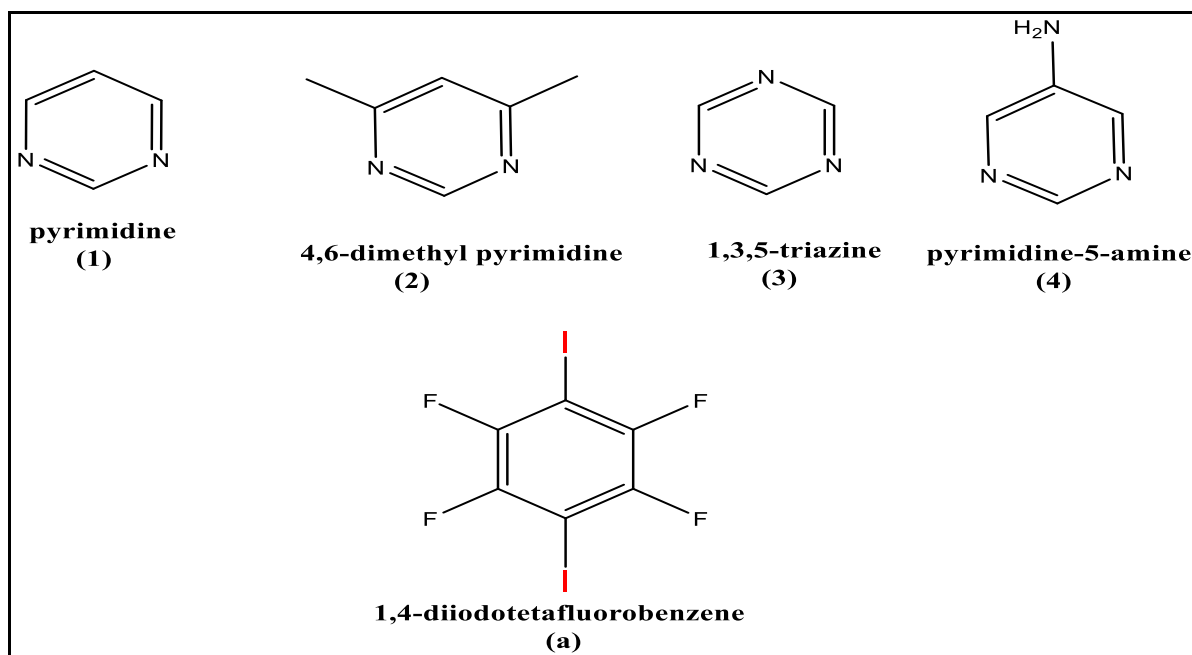
Thus 1,4-diodotetrafluorobenzene has been widely used as a halogen bond donor and considered as "an archetype of a halogen bond donor ".(Bedeković *et al.*, 2018) A search of the Cambridge Structure Database conducted on 22/02/2022 reveals that there are 294 neutral halogen bonded adducts containing nitrogen compounds.(Groom *et al.*, 2016) 238 of these involve basic aromatic rings. However, despite there being many reported halogen bonded structures involving nitrogen in an aromatic ring, there are no structures involving pyrimidine and only one halogen bonded structure containing 1,3,5-triazine.(Raatikainen & Rissanen, 2011) Therefore these two compounds were chosen as part of a series of nitrogen-containing Lewis bases for a study of how the ability of Y to act as a XB acceptor is related to the basicity of the lone pair of electrons on Y. It is known that Lewis bases form strong XB interaction with I₂ in the general order amine > pyridine> nitrile and this is related to the decrease in p-character of the Lewis base lone pair. (Gilday *et al.*, 2015; Laurence *et al.*, 2011)

While in the first instance XB interactions are usually identified from single-crystal X-ray structures in which distances are observed that are less than the sum of the van der Waals radii of the participating atoms, theoretical studies of XB systems are also possible, including using quantum theory of atoms in molecules, QTAIM, as a

technique to examine the topological analysis of the electron density. Bader found that electron density at the bond critical point ρ_{BCP} is positively charged and small for the close-shell interaction (Hydrogen bond, halogen bond and etc) and the related Laplacian $\nabla^2\rho_{\text{BCP}}$ have a positive value. (Bader, 1994) Thus QTAIM studies can be used to confirm and categorise observed interactions and to compare the strength of halogen bonds and other intermolecular forces. (Matta & Boyd, 2007; Angelina *et al.*, 2013; Wang *et al.*, 2018; Wzgarda-Raj *et al.*, 2020)

In a study of the structure derived from 1,4-diodotetrafluorobenzene and 4-(dimethylamine), Wang and his group found that the bond critical point related to the observed short N...I halogen bond had a relatively high electron density $0.359(5) \text{ e.}\text{\AA}^{-3}$ compared with other intermolecular contacts and their Laplacian $\nabla^2\rho_{\text{BCP}}$ have a positive value. (Wang *et al.*, 2018) Previously Rozas and his group used some of the QTAIM parameters to assign the strength of the interactions and the possible covalent character of medium-strength contacts when $\nabla^2\rho_{\text{BCP}} > 0$ and $H_{\text{BCP}} < 0$. Wang and his group reported a negative value of local electron density at the BCP related to this N...I halogen bond in this 2018 work and in their 2011 work on hydrogen bonds containing structures. (Rozas *et al.*, 2000; Wang *et al.*, 2018; Serb *et al.*, 2011) This is in line with many other studies of XB and HB using different software (GAMESS, GAUSSIAN) to calculate the energy using different basis sets and different software (Multiwfn and AIM) for the topology analysis. (Grabowski, 2013; Cremer & Kraka, 1984).

Herein, we aim to continue to explore the capability of 1,4-diodotetrafluorobenzene to form polymeric N...I halogen bonded structures with different nitrogen-based aromatic halogen bond acceptors, namely pyrimidine, 4,6-dimethyl pyrimidine, 1,3,5-Triazine and pyrimidine -5-amine, see **Scheme. 4.1**.



Scheme 4.1 Compounds used in crystallisation

4.3. Experimental

All chemicals and solvents were purchased from commercial suppliers (Aldrich Chemical, Acros organic, Fluorochem, Alfa) and used without further purification.

4.3.1. Synthesis and crystallization

2:1 molar stoichiometric ratios of 1,4-diiidotetrafluorobenzene and the selected nitrogen compounds 1-4 were combined as listed below:

1a [0.1g of **1** (0.025 mmol) and 0.001 ml of **a** (0.012 mmol)], **2a** [0.01g of **2** (0.025 mmol) and 0.0055 g of **a** (0.012 mmol)], **3a** [0.02 g of **3** (0.050 mmol) and 0.002 g of **a** (0.025 mmol)] and **4a** [0.02 g of **4** (0.050 mmol) and 0.0024 g of **a** (0.025 mmol)]

Adduct **2a** and **3a** were synthesized by vapour diffusion from the starting materials, however adducts **1a** and **4a** were prepared by slow evaporation of the solvent from a solution in dried acetonitrile.

FT-IR spectra were recorded of the adducts using a Nicolet iS5 FT-IR instrument. (See S 4.1- S 4.4). IR $\nu(\text{cm}^{-1})$ data for adduct (**1a**), formed between pyrimidine and 1,4-diodotetrafluorobenzene : 3037(w) (C-H), 1451, 1434, 1215(C-F); for adduct (**2a**) formed between 4,6-dimethylpyrimidine and 1,4-diodotetrafluorobenzene: shift from 3015 to low intensity (C-H), 1455, 1436, 1211 (C-F); for adduct (**3a**) formed between 1,3,5-Triazine and 1,4-diodotetrafluorobenzene: 3039 (C-H), 1457, 1357, 1209 (C-F); for adduct (**4a**) formed between pyrimidine-5-amine and 1,4-diodotetrafluorobenzene: 3026, 3167 (C-H), 1457, 1210 (C-F) cm^{-1} .

4.3.2. Refinement

Crystal data collection and structure refinement details are summarized in Table (4.1). Hydrogen atoms are visible from the difference Fourier map and were introduced in geometrically calculated position using the riding model, except for the 2 amine hydrogens in **4a**, which were located in the electron density map and treated independently.

Table 4.1 Experimental details.

Crystal data	1a	2a	3a	4a
Chemical formula	C ₄ H ₄ N ₂ ·2(C ₃ F ₂ I)	C ₆ F ₄ I ₂ ·C ₆ H ₈ N ₂	C ₆ F ₄ I ₂ ·C ₃ H ₃ N ₃	C ₆ F ₄ I ₂ ·C ₄ H ₅ N ₃
Mr	481.95	510.00	482.94	496.97
Crystal system, space group	Monoclinic, <i>P2₁/n</i>	Monoclinic, <i>P2₁/c</i>	Monoclinic, <i>I2/a</i>	Monoclinic, <i>P2₁/n</i>
Temperature (K)	150	150	150	150
<i>a</i>, <i>b</i>, <i>c</i> (Å)	13.7424 (5), 5.81858 (16), 16.5136 (6)	5.2138 (9), 20.304 (2), 14.2732 (16)	10.1820 (11), 6.2144 (6), 19.427 (2)	5.1974 (2), 21.7822 (8), 11.7303 (4)
β (°)	106.698 (4)	94.054 (12)	97.075 (10)	100.729 (4)
<i>V</i> (Å³)	1264.77 (7)	1507.2 (3)	1219.9 (2)	1304.78 (8)
<i>Z</i>	4	4	4	4
Radiation type	Mo Kα	Mo Kα	Mo Kα	Mo Kα
μ (mm⁻¹)	5.00	4.21	5.19	4.86
Crystal size (mm)	0.2 × 0.05 × 0.04	0.2 × 0.02 × 0.02	0.3 × 0.1 × 0.01	0.05 × 0.04 × 0.01
Data collection				
<i>T</i>_{min}, <i>T</i>_{max}	0.405, 1.000	0.062, 1.000	0.635, 1.000	0.452, 1.000
No. of measured, independent and observed [<i>I</i> > 2σ(<i>I</i>)] reflections	9509, 2483, 2033	10891, 2972, 1639	3977, 1205, 1032	6992, 2572, 2165
<i>R</i>_{int}	0.041	0.166	0.053	0.044
(sin θ/λ)_{max} (Å⁻¹)	0.617	0.617	0.617	0.617
Refinement				
R[F² > 2σ(F²)], wR(F²), S	0.027, 0.057, 1.06	0.079, 0.131, 1.00	0.032, 0.079, 1.09	0.032, 0.063, 1.02
No. of reflections	2483	2972	1205	2572
No. of parameters	163	171	83	180
H-atom treatment	H-atom parameters constrained	H-atom parameters constrained	H-atom parameters constrained	H atoms treated by a mixture of independent and constrained refinement
Δ_{max}, Δ_{min} (e Å⁻³)	0.405, 1.000	0.062, 1.000	0.635, 1.000	0.452, 1.000

Computer programs: CrysAlis PRO 1.171.39.4(Rigaku, 2018), ShelXT (Sheldrick, 2015), SHELXL (Sheldrick, 2015), Olex2 (Dolomanov *et al.*, 2009)

4.4. Result and Discussion

There are no reported halogen bonded structures involving pyrimidine as the halogen bond acceptor to date, hence adduct **1a** reported here is the first such example. Adduct **1a** crystallises in the monoclinic $P2_1/n$ space group and the asymmetric unit consists of two half-molecules of 1,4-diodotetrafluorobenzene situated about an inversion centre and one molecule of pyrimidine. Fig (4.1) shows the crystal structure of **1a** and the atom numbering scheme adopted.

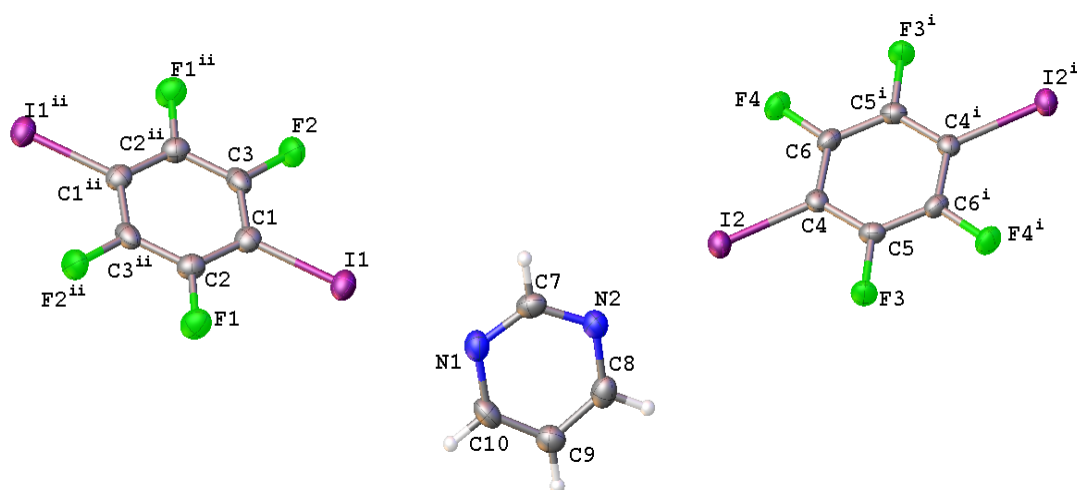


Figure 4.1 A view of the structure of halogen-bonded adduct **1a**, showing the atom numbering, Ellipsoids are drawn at 50% probability level, [Symmetry codes: (i) $-x, 1-y, -z$ (ii) $2-x, 1-y, 1-z$]. colour codes: Green, fluorine; blue, nitrogen; white, hydrogen and grey carbon.

The extended view of **1a** shows a polymeric zig-zag N...I halogen bonded structure in which the two iodine atoms are involved in N...I interactions, Fig .4.2. The N...I distances are N1...I1, 2.862(4) Å and N2...I2, 2.867(4) Å which are 0.663 Å (18.8%) and 0.668 Å (18.9%) shorter than the sum of van der Waals radii of nitrogen and iodine (3.53 Å). The two C-I...N bond angles are near to linear at 171.1(1) and 171.5(1) ° with an average of 171.3(1) °. The extended structure also shows a second interaction which is a non-conventional hydrogen bond C6-F4...H9 with distance of 2.64 Å, which is shorter than the sum of the van der Waals radii for both F and H atoms (2.67 Å), see Table 4.2.

Table 4.2 Hydrogen-bond geometry (Å, °) for **1a**

$D-H\cdots A$	$D-H$	$H\cdots A$	$D\cdots A$	$D-H\cdots A$
$C9-H9\cdots F4^i$	0.93	2.64	3.546 (6)	166

Symmetry code: (i) $-x+1/2, y-3/2, -z+1/2$.

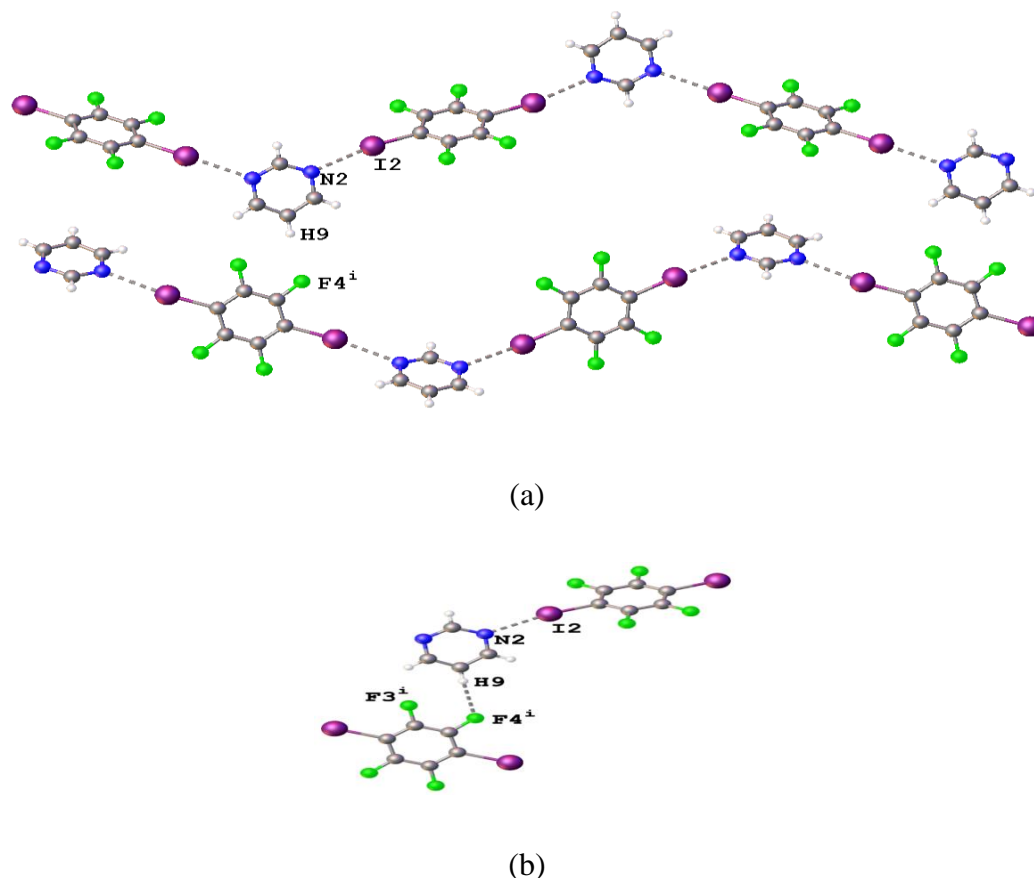


Figure 4.2 Main N...I halogen bonds (a) and secondary F...H interactions (b) in **1a** (stippled line), colour codes: purple, iodine; Green, fluorine; blue, nitrogen; white, hydrogen and grey carbon.

The average C-I bond distances in **1a** are 2.089(4) and 2.098(4) Å, both of which are longer than that found for pure 1,4-diiidotetrafluorobenzene in ZZZAVM01(2.075 Å) and ZZZAVM02(2.079 (4) Å). (Chaplot *et al.*, 1981; Oh *et al.*, 2012)

Moving to the dimethyl-substituted pyrimidine, 4,6-dimethyl pyrimidine, introduces a change in basicity and also steric encumbrance. As was the case for **1a** this is the first example of a N...I halogen bonded structure which involves 4,6-dimethyl pyrimidine as halogen-bond

acceptor. Adduct **2a** crystallises in the $P2_1/c$ monoclinic space group and the asymmetric unit cell consists of one molecule of 1,4-diiodotetrafluorobenzene and one molecule of 4,6-dimethylpyrimidine, Fig. 4.3. While Fig (4.4) shows the extended structure of **2a** with both iodine atoms involved in a zig zag polymeric XB motif.

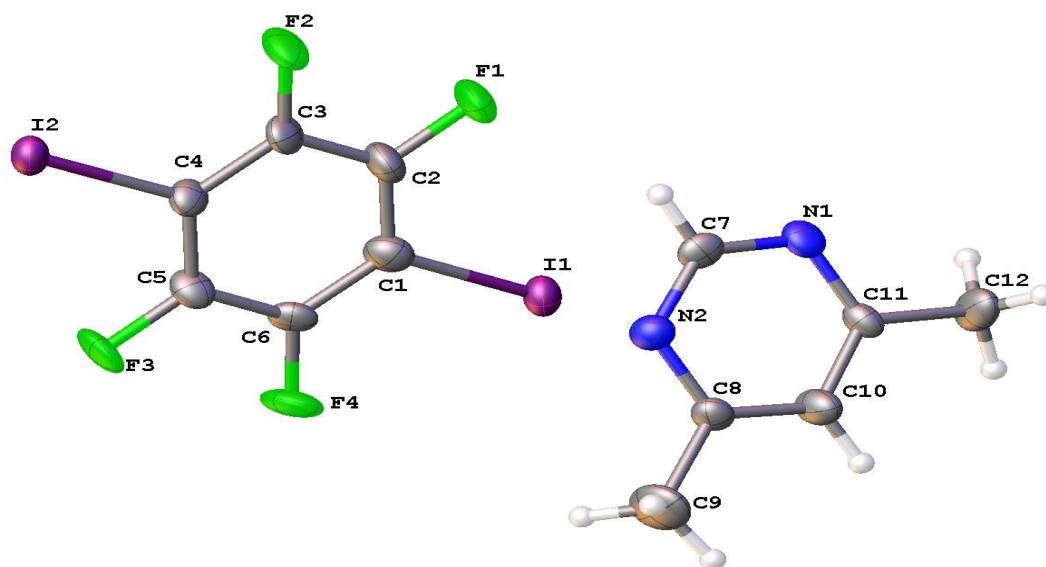
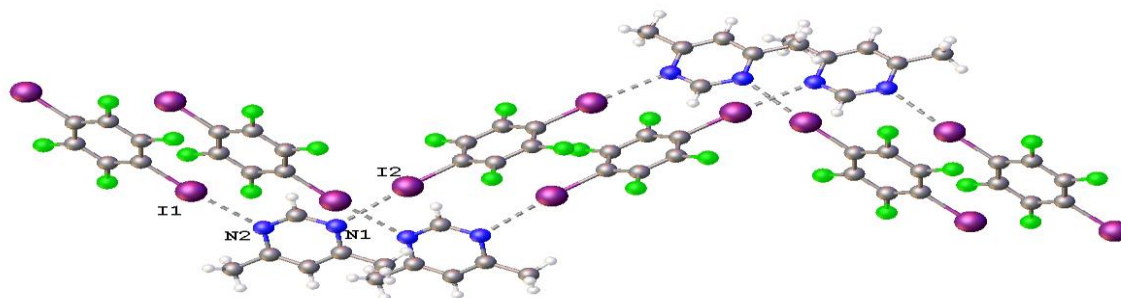


Figure 4.3 Views of the asymmetric unit of halogen-bonded adduct **2a**, showing the atom numbering, ellipsoids are drawn at 50% probability level, colour codes: purple, iodine; Green, fluorine; blue, nitrogen; white, hydrogen and grey carbon

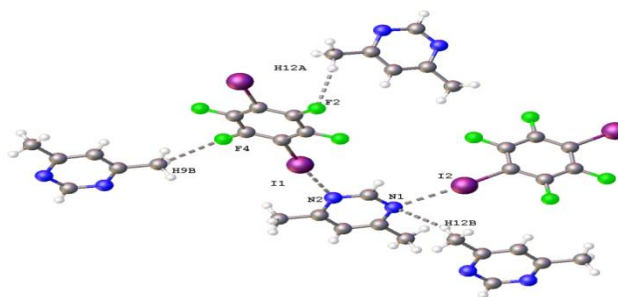
The extended view of **2a** shows a polymeric N...I halogen bonded structure with N...I distances of 2.96(1) and 2.87(1) Å the average of which is 2.92(1) Å, Fig 4.4a. These two distances are 0.57 Å (16%) and 0.66 Å (18.7%) shorter than the sum of the van der Waals radii (3.53 Å). (Bondi, 1964; Alvarez, 2013) The halogen bond angles C-N...I are close to linearity 168.2(3) and 173.0(3) °.

There are other non-covalent interactions in this structure (N...H and F...H), see Fig 4.4 b. The first non-conventional hydrogen bond is N1...H12B, which has a distance of 2.69 Å, although this is only 0.06 Å (2.18%) just shorter than the sum of the van der Waals radii of nitrogen and hydrogen atoms, 2.75 Å (Bondi, 1964; Alvarez, 2013), see Table 4.3. The second interaction is between two different pairs of fluorines and hydrogens, F4...H9B, 2.624 Å and F2...H12A, 2.464 Å. Both of which are shorter than the sum of van der Waals radii 2.67 Å, , 0.21 Å, 7.7 % with the second one slightly shorter than the first one.

The C-I bond distances in **2a** [2.123(8) and 2.127(8) Å, with an average of 2.125(8) Å] are slightly longer than that found in structure **1a**, and for pure 1,4-diiodotetrafluorobenzene, ZZZAVM01(2.075 Å) and ZZZAVM02(2.079(4) Å). (Chaplot *et al.*, 1981; Oh *et al.*, 2012)



(a)



(b)

Figure 4.4 Main N...I halogen bonds (a) and secondary interactions (b) in **2a**, (stippled line), colour codes: purple, iodine; Green, fluorine; blue, nitrogen; white, hydrogen and grey carbon

Table 4.3 Hydrogen-bond geometry (Å, °) for **2a**

$D-H\cdots A$	$D-H$	$H\cdots A$	$D\cdots A$	$D-H\cdots A$
$C9-H9B\cdots F4^i$	0.96	2.62	3.276 (17)	126
$C12-H12A\cdots F2^{ii}$	0.96	2.46	3.382 (17)	160
$C12-H12B\cdots N1^{iii}$	0.96	2.69	3.601 (17)	158

Symmetry codes: (i) $-x+1, -y, -z+1$; (ii) $-x+2, y-1/2, -z+3/2$; (iii) $-x+2, -y, -z+2$.

There is only one reported structure to date involving 1,3,5-triazine in an N...I halogen bond, in this case with N-iodosuccinimide [CSD ref code, IBIZEA, (Raatikainen & Rissanen,

2011)]. Thus, adduct **3a** is the second structure involving 1,3,5-triazine in halogen bonding, but this time with 1,4-diiodotetrafluorobenzene as the halogen bond donor.

Adduct **3a** crystallizes in the monoclinic $I2/a$ space group with half a molecule of 1,4-diiodotetrafluorobenzene situated about an inversion centre and half a molecule of 1,3,5-triazine with a 2-fold rotation axis passing through N2 and C5-H5 in the asymmetric unit. Fig (4.5) shows the structure.

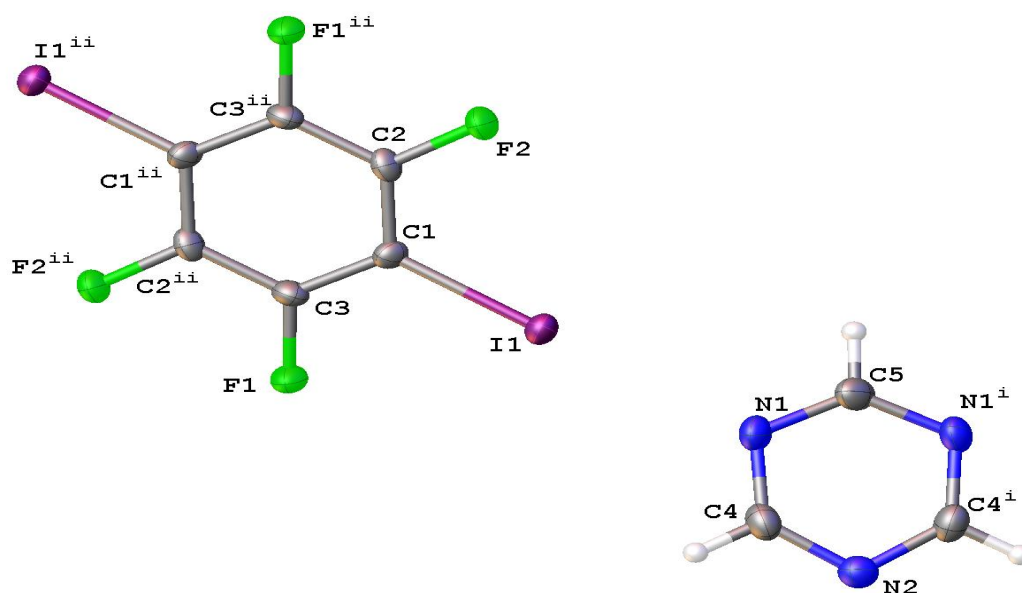


Figure 4.5 A view of the structure of halogen-bonded adduct **3a**, showing the atom numbering, Ellipsoids are drawn at 50% probability level, [Symmetry codes :(i) $3/2-x, +y, 1-z$ (ii) $1/2-x, 3/2-y, 1/2-z$], colour codes: purple, iodine; Green, fluorine; blue, nitrogen; white, hydrogen and grey carbon.

In the extended structure of **3a**, two of the three iodine atoms are involved in N...I halogen bonds, resulting in the formation of a polymeric 1D halogen bonded zig zag chain structure, see Fig. 4.6. The N...I distance is 2.973(4) Å corresponding to a 0.557 Å (15.8%) reduction in the sum of the van der Waals radii of I and N (3.53 Å). (Bondi, 1964; Alvarez, 2013) The halogen bond C-I...N angle is 176.1(2)° which is closer to linearity than **1a** and **2a**.

There are other interactions which are very weak compared with the N...I interaction. One of them is an F...F interaction at a distance of 2.822(5) Å which is 0.12 Å (4.0%) slightly shorter than double the van der Waals radius of fluorine (2.94 Å) (Bondi, 1964; Alvarez,

2013), see Fig. 4.6. In addition, there are no conventional hydrogen bonds but one non-conventional F...H interaction with a distance of 2.511 Å, (0.16 Å, 6%) slightly shorter than the sum of the van der Waals radii 2.67 Å. The remaining nitrogen atom is involved in an N...H interaction with a distance of 2.632 Å (0.12 Å, 4.3%), also slightly shorter than the sum of the van der Waal radii of N and H, 2.75 Å (Bondi, 1964; Alvarez, 2013), but longer than that found (2.475 Å) in IBIZEA (Raatikainen & Rissanen, 2011) which is the only other reported structure involving 1,3,5-triazine in a N...I halogen bond, see Table 4.4.

Due to the formation of N...I halogen bonds, the C-I covalent bond in **3a** becomes slightly elongated with a distance of 2.086(5) Å, longer than the distance in pure 1,4-diiodotetrafluorobenzene in ZZZAVM01(2.075 Å) and ZZZAVM02(2.079(4) Å) which support the existence of this N...I halogen bond interaction.(Chaplot *et al.*, 1981; Oh *et al.*, 2012)

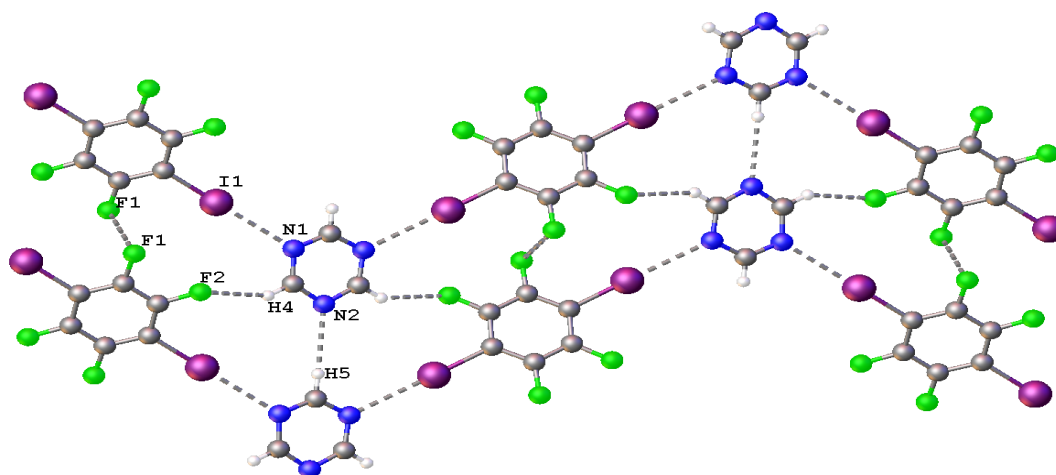


Figure 4.6 A view of intermolecular N...I halogen bonds and F...H and N...H non-conventional hydrogen bond (stippled line) in **3a**, colour codes: purple, iodine; Green, fluorine; blue, nitrogen; white, hydrogen and grey carbon.

Table 4.4 Hydrogen-bond geometry (Å, °) for **3a**

$D-H\cdots A$	$D-H$	$H\cdots A$	$D\cdots A$	$D-H\cdots A$
$C4-H4\cdots F2^i$	0.93	2.51	3.329 (6)	147
$C5-H5\cdots N2^{ii}$	0.93	2.63	3.562 (11)	180

Symmetry codes: (i) $x, y-1, z$; (ii) $x, y+1, z$.

The final adduct involving pyrimidine-5-amine (**4**) was chosen as an interesting pyrimidine derivative featuring a combination of aromatic and primary Lewis basic nitrogen atoms. For such compounds it is established that the basicity of the two nitrogen centres are quite different, with the aromatic nitrogen being the more basic. Co-crystallisation with 1,4-diiidotetrafluorobenzene results in adduct **4a** which crystallize in the $P2_1/n$ space group with 1 molecule of 1,4-diiidotetrafluorobenzene and 1 molecule of pyrimidine-5-amine in the asymmetric unit, see Fig (4.7).

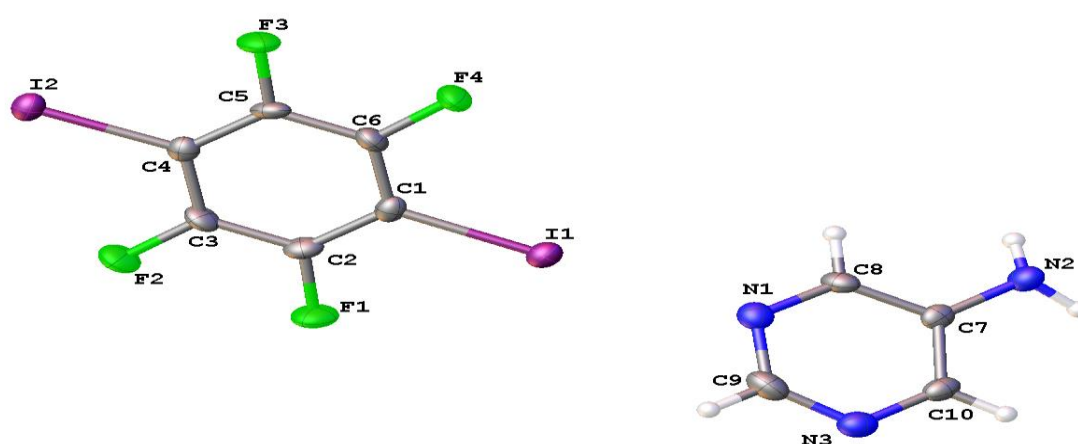


Figure 4.7 Views of the asymmetric unit of halogen-bonded adduct **4a**, showing the atom numbering, Ellipsoids are drawn at 50% probability level, colour codes: purple, iodine; Green, fluorine; blue, nitrogen; white, hydrogen and grey carbon.

In the extended structure of **4a**, we can clearly see the formation of two (N...I) halogen bond interactions, see Fig (4.8). One from the pyrimidine nitrogen with an N...I distance of 2.872 (4) Å (0.658, 18.6%) shorter than the sum of the van der Waals radii of nitrogen and iodine (3.53 Å) and the second from the primary amine nitrogen, which has a longer N...I halogen bond interaction distance of 3.083(4) Å, (only 0.447 Å, 12.7%) shorter than the sum of the van der Waals radii 3.53 Å. (Bondi, 1964; Alvarez, 2013) This distance is slightly longer than the only previously reported in the CCDC structure (JEHZUU) at room temperature with N...I distance of 3.044(3) Å, involving 1,4-diiidotetrafluorobenzene with 5-amino-2-methoxypyridine (Nemec & Cinčić, 2016).

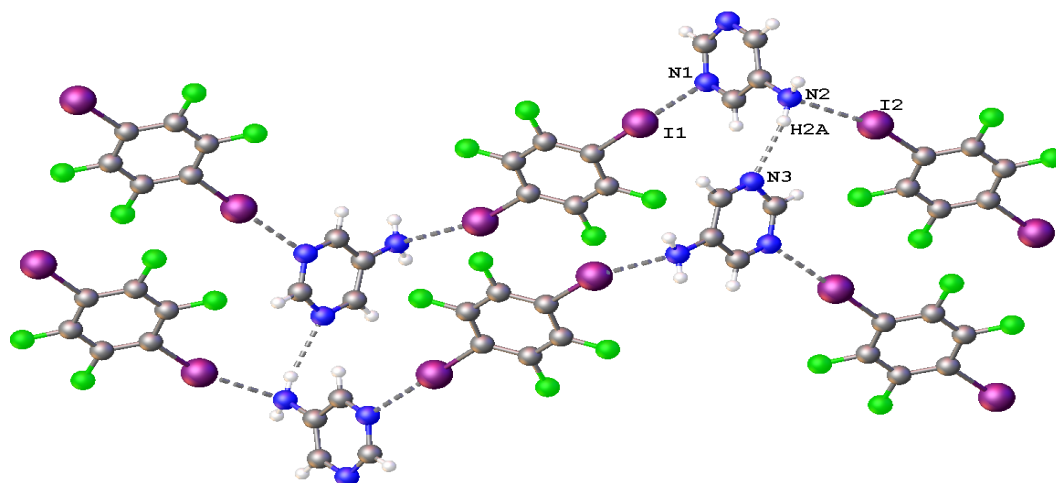


Figure 4.8 A view of intermolecular N...I halogen bonds and N...H-N traditional hydrogen bond interaction (stippled line) in **4a**, colour codes: purple, iodine; green, fluorine; blue, nitrogen; white, hydrogen and grey carbon.

The halogen bond C-I...N angle in **4a** is 179.2(1) ° for the halogen bond involving the pyrimidine nitrogen, however the C-I...N halogen bond angle related to the primary amine is much less linear than the first at 165.8(2) °.

We note that the second nitrogen in the ring preferentially is involved in a C-N...H conventional hydrogen bond with a distance of 2.29(5) Å, 0.46 Å (16.7%) shorter than the N...H traditional hydrogen bond in pure pyrimidine-5-amine (Schlueter *et al.*, 2006) and shorter than the sum of the van der Waals radii (2.75 Å) of N and H atoms (Bondi, 1964; Alvarez, 2013), see Table 4.5.

Table 4.5 Hydrogen-bond geometry (Å, °) for **4a**

$D-H\cdots A$	$D-H$	$H\cdots A$	$D\cdots A$	$D-H\cdots A$
$N2-H2A\cdots N3^i$	0.83 (4)	2.29 (5)	3.103 (6)	167 (4)

Symmetry code: (i) $x-1/2, -y+1/2, z-1/2$.

The C1-I1 covalent bond in **4a** elongates to 2.103(5) Å for the iodine involved in N...I halogen bonding with one of the 2 ring nitrogen atoms and 2.093(5) Å for C4-I2 involving with the amine nitrogen atom. Both C-I distances are within the C-I bond distance recorded in **1a**, **2a** and **3a**.

However, the average C-C and C-F bond lengths in the 1,4-diiidotetrafluorobenzene molecules in all the four adducts **1a-4a** are within 3σ of the related values reported at low temperature for pure 1,4-diiidotetrafluorobenzene, ZZZAVM01 and ZZZAVM02, (Chaplot *et al.*, 1981; Oh *et al.*, 2012) there are no such previously reported structures for all the halogen bond acceptors used in this study to compare the C-N bond distance.

Table 4.6 N...I halogen-bond distances (Å) and C-I...N angles (°) in this study.

Entry	code	Donor	Acceptor	N...I (Å)	N...I-C (°)	Reference
1	1a	1,4-DITFB	Pyrimidine	2.867(4) 2.862(4)	171.1(1) 171.5(1)	This work
2	2a	1,4-DITFB	4,6-dimethyl pyrimidine	2.96(1) 2.87(1)	168.2(3) 173.0(3)	This work
3	3a	1,4-DITFB	1,3,5-triazine	2.973(4)	176.1(2)	This work
4	4a	1,4-DITFB	Pyrimidine-5-amine	2.872(4) 3.083(4)	179.2(1) 165.8(2)	This work

Table 4.7 Intermolecular interactions in (Å) less than the sum of the van der Waals radii

Entry	code	Acceptor	C-I (Å)	N...H (Å)	F...H (Å)	F...F (Å)	References
1	1a	Pyrimidine	2.089(4) 2.098(4)	-	2.636	-	This work
2	2a	4,6-dimethyl pyrimidine	2.123(8) 2.127(8)	2.69	2.624 2.464	-	This work
3	3a	1,3,5-triazine	2.086(5)	2.632	2.511	2.822(5)	This work
4	4a	Pyrimidine- 5-amine	2.103(5) 2.093(5)	2.29(5)	-	-	This work

In general plotting all the 294 hits in the CCDC involving 1,4-diiidotetrafluorobenzene with nitrogen (ignoring ions, and requiring angles between 150-180 °) we notice that structures **1a-4a** have N...I bond distances that are amongst the shortest such distances reported to date, see Fig (4.9). The shortest bond distance reported here is 2.862(4) Å for one of the N...I distances in structure **1a**, see Table 4.6.

There is only one conventional hydrogen bond recorded within this chapter in structure **4a** which reflects that N...I halogen bonds are preferred over hydrogen bonds in these combinations of compounds, see [Table 4.7](#).

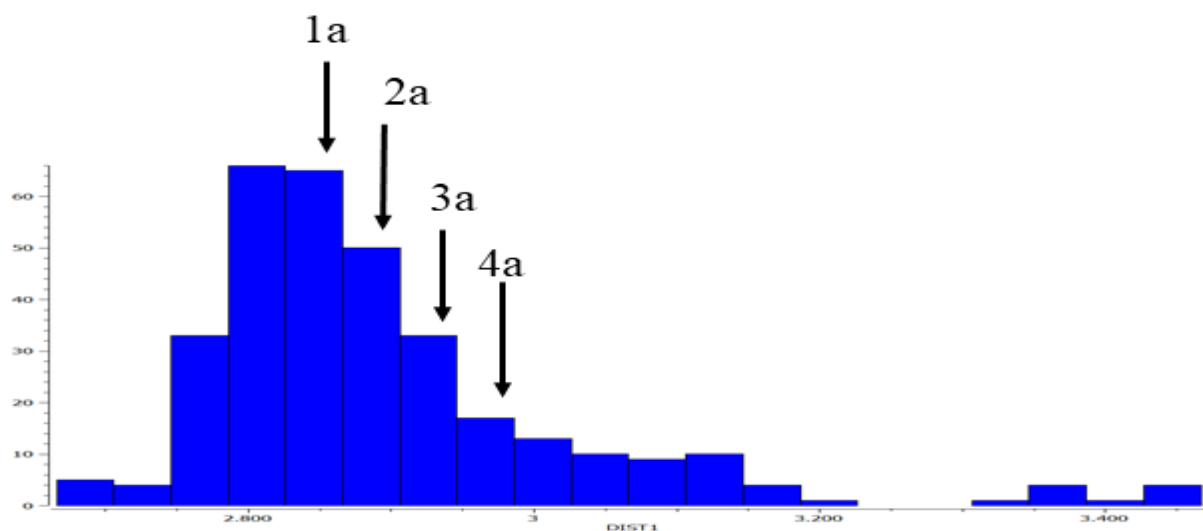


Figure 4.9 Histogram shows the average bond distances of the **1a-4a** and their position compared with the CSD reported structures for N...I containing structures reported until now.

QTAIM study

The X-ray experimental results for each structure was analysed and compared theoretically using the quantum theory of atoms in molecules (QTAIM). Initially electron density calculations were performed on the geometric coordinates determined in the X-ray studies at the B3LYP/6-311G** level of theory using the GAMESS package software ([Schmidt *et al.*, 1993](#)) followed by using the Multiwfn programme ([Lu & Chen, 2012](#)) to find the topological parameters, including the electron density σ_{BCP} distribution at the bond critical point, Laplacian $\nabla^2\rho_{\text{BCP}}$ and energy density, H_{BCP} .

The crystal structure derived from Mercury and the molecular graph generated using Multiwfn are shown for each of the systems in [Figs 4.10-4.13](#).

These N...I interactions have been examined in the light of QTAIM and the resulting values are presented in [Table \(4.8\)](#). From these data we find that as the N...I halogen bond distance decrease the value of the electron density increase as expected. The corresponding values of the Laplacian $\nabla^2\rho_{\text{BCP}}$ are all positive which support the existence of medium close shell

interactions. The local energy density, H_{BCP} , values are very small and confirm the existence of medium strength halogen bonds contacts. (Chapter 2; Angelina *et al.*, 2013; Wang *et al.*, 2018; Esrafilı & Ahmadi, 2012; Esrafilı, 2012; Rozas *et al.*, 2000).

Interestingly, an extra C12-H12C...I2 interaction is detected in structure **2a** which was not recognized as an interaction using Mercury as at a distance of 3.193 Å it is slightly longer than the sum of the van der Waals radii of hydrogen (1.20 Å) and iodine (1.98 Å) (Bondi, 1964; Alvarez, 2013).

Table 4.8 Topological parameters calculated at B3LYP/6-311G** level of theory

Trimer	Interaction	X...B (Å)	ρ_{BCP} (a.u)	H(r)	$\nabla^2\rho_{BCP}$ (a.u)
1a	N1...I1	2.862(4)	0.0227	0.000926	0.0705
	N2...I2	2.867(4)	0.0223	0.000956	0.0696
2a	N2...I1	2.87(1)	0.0227	0.000786	0.0694
	N1...I2	2.96(1)	0.0193	0.000935	0.0587
	I2...H12C	3.193	0.00594	0.000839	0.0190
3a	N1...I1	2.973(4)	0.0181	0.001200	0.0578
4a	N1...I1	2.872(4)	0.0221	0.000942	0.0684
	N2...I2	3.083(4)	0.0162	0.000682	0.0457

In conclusion and by maintaining a single halogen bond donor, in this case 1,4-diodotetrafluorobenzene, and varying the pyrimidine-based halogen bond acceptors we have been able to study the influence of basicity on XB formation. The consistent 1,3-dinitrogen substitution in the aromatic ring results in a consistent two-dimensional zig-zag arrangement being observed in all 4 crystal structures due to the formation of N...I halogen bonds. All of the N...I distances are shorter than the sum of the van der Waals radii of nitrogen and iodine (3.53 Å).

QTAIM analysis has been performed on all four adducts, and this shows an inverse relationship between N...I distance and electron density at the bond critical points. That is the shortest halogen-bonded distances correspond to the highest calculated electron density. According to both X-ray and QTAIM data adducts **1a** and **2a** have similar strength N...I interactions, suggesting that the inclusion of the two methyl groups on the aromatic ring has little effect. Both X-ray and QTAIM data suggests that adducts **3a** and **4a** have weaker

halogen-bonded interactions. In particular the N...I halogen bond involving the primary amine of **4a** is much weaker than those involving ring-nitrogens.

IR spectroscopy support the X-ray data and the existence of halogen bond formation in the solid state by showing changes similar to that previously reported in the literature (De Santis *et al.*, 2003) including changes in the ν_{C-F} bands from those recorded for 1,4-diodotetrafluorobenzene.

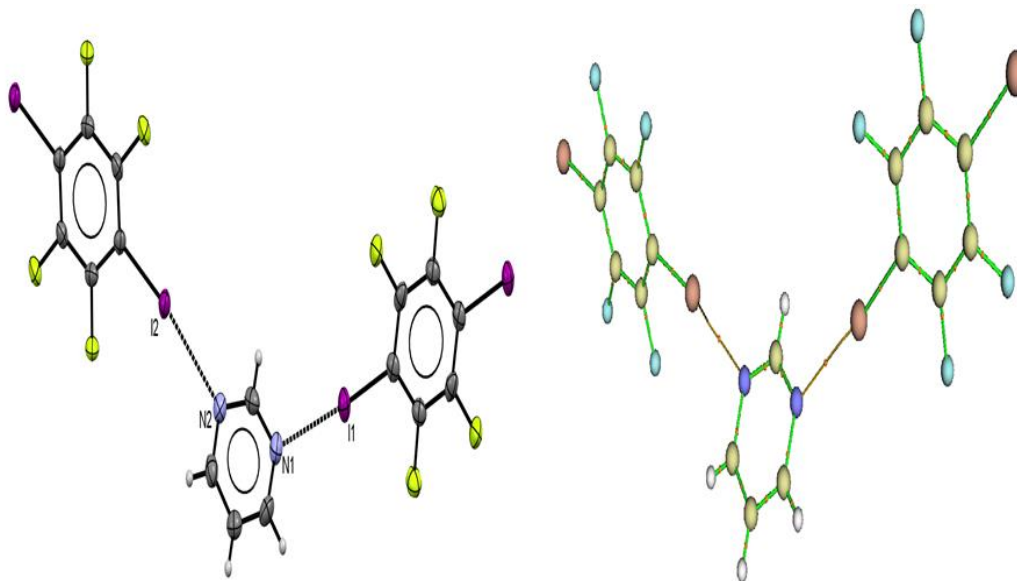


Figure 4.10 The determined X-ray structure (left) and molecular graph (right) for adduct **1a**

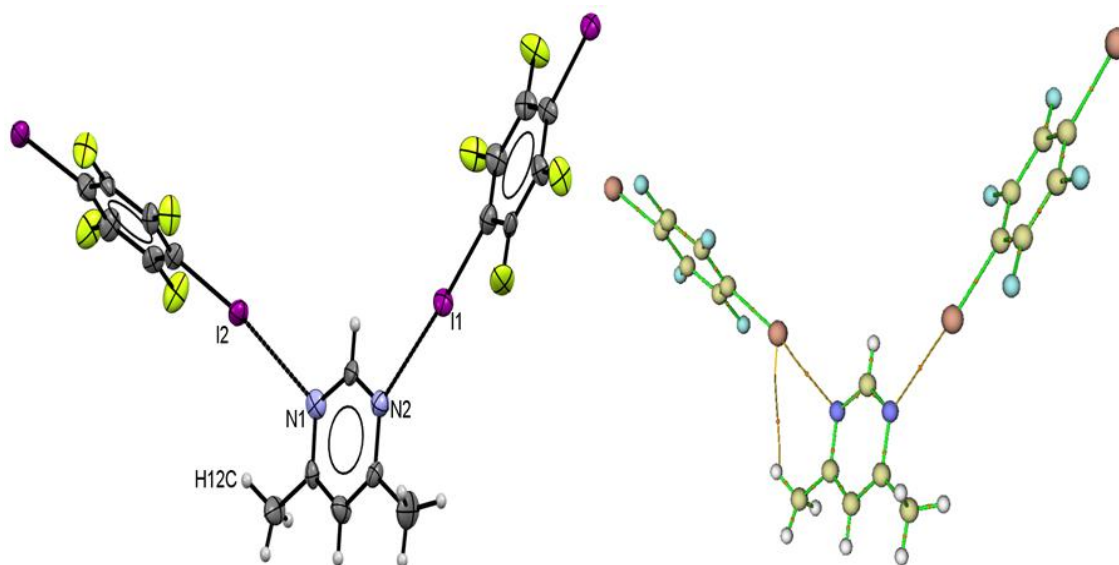


Figure 4.11 The determined X-ray structure (left) and molecular graph (right) for adduct **2a**

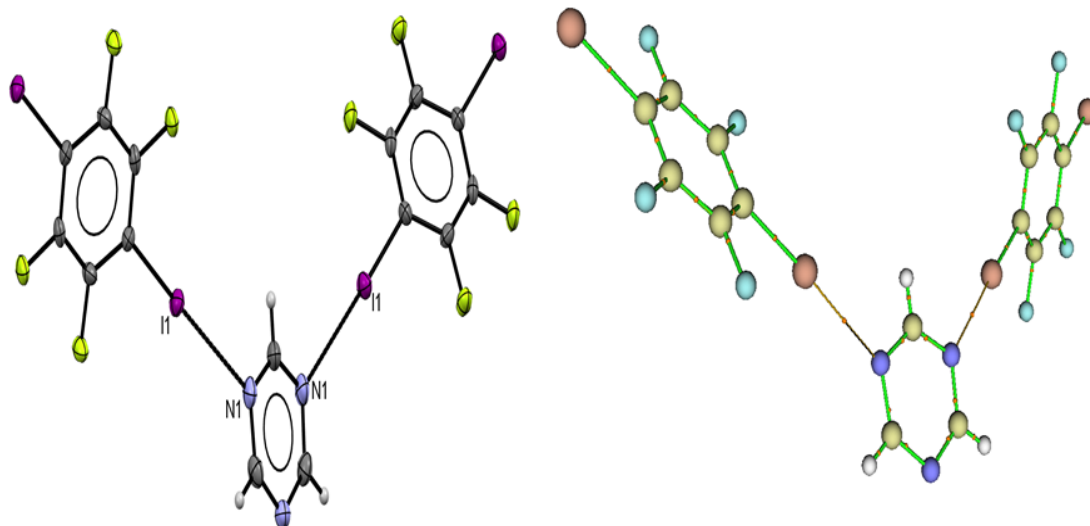


Figure 4.12 The determined X-ray structure (left) and molecular graph (right) for adduct **3a**

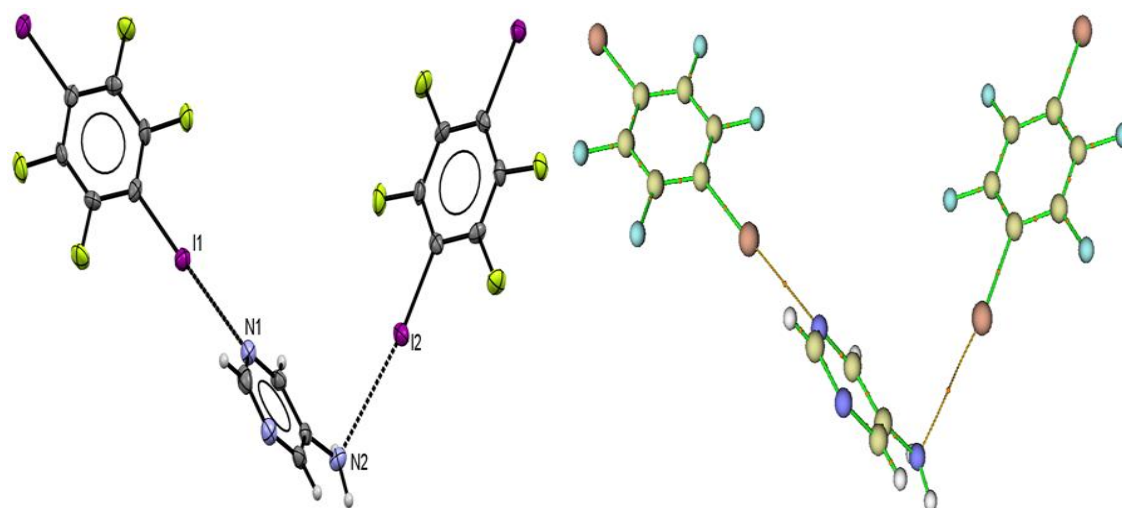


Figure 4.13 The determined X-ray structure (left) and molecular graph (right) for adduct **4a**

References

- Alvarez, S. (2013). *Dalt. Trans.* **42**, 8617–8636.
- Angelina, E. L., Duarte, D. J. R. & Peruchena, N. M. (2013). *J. Mol. Model.* **19**, 2097–2106.
- Bader, R. F. W. (1994). *Atoms in Molecules: A Quantum Theory* Oxford: Clarendon Press.
- Bedeković, N., Stilinović, V., Friščić, T. & Cinčić, D. (2018). *New J. Chem.* **42**, 10584–10591.
- Bondi, A. (1964). *J. Phys. Chem.* **68**, 441–451.
- Chaplot, S. L., McIntyre, G. J., Mierzejewski, A. & Pawley, G. S. (1981). *Acta Crystallogr. Sect. B.* **37**, 2210–2214.
- Clark, T., Hennemann, M., Murray, J. S. & Politzer, P. (2007). *J. Mol. Model.* **13**, 291–296.
- Cremer, D. & Kraka, E. (1984). *Croat. Chem. Acta.* **57**, 1259–1281.
- Desiraju, G. R., Ho, P. S., Kloo, L., Legon, A. C., Marquardt, R., Metrangolo, P., Politzer, P., Resnati, G. & Rissanen, K. (2013). *Pure Appl. Chem.* **85**, 1711–1713.
- Dolomanov, O. V, Bourhis, L. J., Gildea, R. J., Howard, J. A. K. & Puschmann, H. (2009). 2008–2010.
- Esfarili, M. D. (2012). *J. Mol. Model.* **18**, 5005–5016.
- Esfarili, M. D. & Ahmadi, B. (2012). *Comput. Theor. Chem.* **997**, 77–82.
- Gilday, L. C., Robinson, S. W., Barendt, T. A., Langton, M. J., Mullaney, B. R. & Beer, P. D. (2015). *Chem. Rev.* **115**, 7118–7195.
- Grabowski, S. J. (2013). *J. Mol. Model.* **19**, 4713–4721.
- Groom, C. R., Bruno, I. J., Lightfoot, M. P. & Ward, S. C. (2016). *Acta Crystallogr. Sect. B Struct. Sci. Cryst. Eng. Mater.* **72**, 171–179.
- Ji, B., Wang, W., Deng, D. & Zhang, Y. (2011). *Cryst. Growth Des.* **11**, 3622–3628.
- Laurence, C., Graton, J., Berthelot, M. & El Ghomari, M. J. (2011). *Chem. a Eur. Journal.* **17**, 10431–10444.
- Lu, T. & Chen, F. (2012). *J. Comput. Chem.* **33**, 580–592.
- Matta, C. F. & Boyd, R. J. (2007). *Quantum Theory Atoms Mol.* 1–34.
- Nemec, V. & Cinčić, D. (2016). *CrystEngComm.* **18**, 7425–7429.
- Oh, S. Y., Nickels, C. W., Garcia, F., Jones, W. & Friščić, T. (2012). *CrystEngComm.* **14**, 6110–6114.

- Politzer, P., Murray, J. S. & Concha, M. C. (2007). *J. Mol. Model.* **13**, 643–650.
- Raatikainen, K. & Rissanen, K. (2011). *CrystEngComm.* **13**, 6972–6977.
- Rigaku, O. (2018). *Rigaku Oxford Diffraction Ltd, Yarnton, Oxfordshire, Engl.*
- Riley, K. E., Murray, J. S., Fanfrlík, J., Řezáč, J., Solá, R. J., Concha, M. C., Ramos, F. M. & Politzer, P. (2011). *J. Mol. Model.* **17**, 3309–3318.
- Roselló, Y., Benito, M., Molins, E., Barceló-Oliver, M. & Frontera, A. (2019). *Cryst.* **9**, 224.
- Rozas, I., Alkorta, I. & Elguero, J. (2000). *J. Am. Chem. Soc.* **122**, 11154–11161.
- De Santis, A., Forni, A., Liantonio, R., Metrangolo, P., Pilati, T. & Resnati, G. (2003). *Chemistry-A European Journal.* **9**, 3974–3983.
- Schlueter, J. A., Funk, R. J. & Geiser, U. (2006). *Acta Crystallogr.* **62**, o339–o341.
- Schmidt, M. W., Baldrige, K. K., Boatz, J. A., Elbert, S. T., Gordon, M. S., Jensen, J. H., Koseki, S., Matsunaga, N., Nguyen, K. A., Su, S., Windus, T. L., Dupuis, M. & Montgomery Jr, J. A. (1993). *J. Comput. Chem.* **14**, 1347–1363.
- Serb, M.-D., Wang, R., Meven, M. & Englert, U. (2011). *Acta Crystallogr. Sect. B.* **67**, 552–559.
- Sheldrick, G. M. (2015). *Acta Crystallogr. Sect. A Found. Crystallogr.* **71**, 3–8.
- Wang, R., Hartnick, D. & Englert, U. (2018). *Zeitschrift Für Kristallographie - Crystalline Materials.* **233**, 733–744.
- Wzgarda-Raj, K., Rybarczyk-Pirek, A. J., Wojtulewski, S. & Palusiak, M. (2020). *Acta Crystallogr. Sect. C.* **76**, 170–176.

Chapter 5.

Manuscript 4: Variety of halogen bonded adducts containing compounds using pyrimidine derivatives

Sultan Alkaabi, Alan K. Brisdon,

Department of Chemistry, University of Manchester, Oxford Road, Manchester, M13 9PL, England.

Keywords: Halogen bonds, Crystal structure, iodofluorobenzene, pyrimidine, QTAIM, infrared, van der Waals radii

5.1. Abstract

Four halogen bonded adducts have been prepared involving ortho-, meta-diiidotetrafluorobenzene and 1,3,5-trifluoro-2,4,6-triiodobenzene, with pyrimidine and two derivatives (4,6-dimethyl-pyrimidine and pyrimidine-5-amine). All of the adducts display N...I halogen bonds with distances that are shorter than the sum of the van der Waals (3.53 Å) and near linear C-I...N angles typical of halogen bonds. QTAIM analysis of the structures gave topological parameters that support the interpretation of the crystallographic results.

5.2. Introduction

The ability of halogen atoms to interact with each other by utilizing different electron affinity sites have been analysed previously. Halogens can also interact with a Lewis base (R-X...B) to form a halogen bond, as defined by the International Union of Pure and Applied Chemistry, IUPAC, in 2013 following a comprehensive project (2009-032-1-100) conducted during 2009 and 2013 to classify different intermolecular interactions centred around halogen atoms (Marquardt *et al.*, 2013).

The halogen bond interactions are represented by R-X...Y (where X is a halogen and Y can be a lone pair containing atom, π system or anion) and defined as "a net attractive interaction between an electrophilic region associated with a halogen atom in one molecular entity and a nucleophilic region in another or the same entity" (Desiraju *et al.*, 2013).

These halogen bonds have been used in a variety of areas, such as crystal engineering, drug design and liquid crystal formation in order to assemble different geometries benefiting

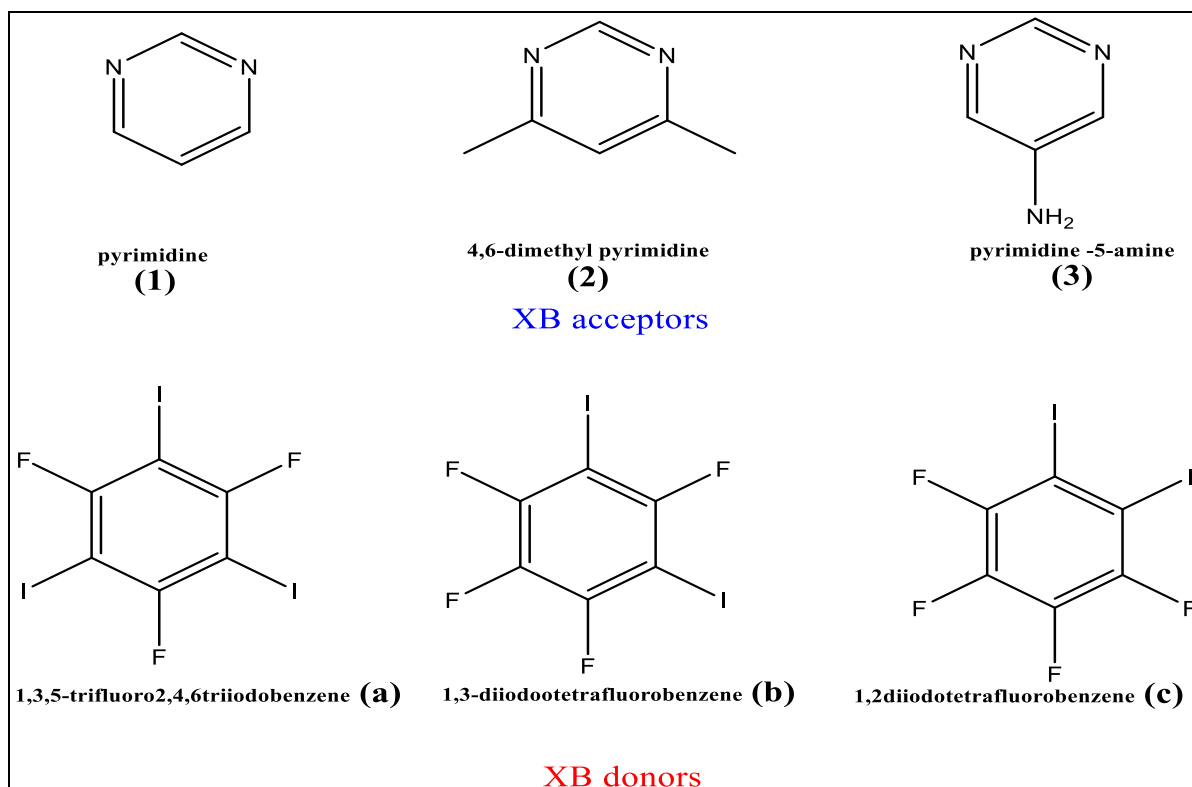
from the highly directional nature of halogen bonding related to the narrowly restricted positive area, or σ -hole, compared with hydrogen bonding where the range of angles associated with the hydrogen atom are spread out on the surface (Priimagi *et al.*, 2013).

According to the Cambridge Structure Database (CSD, search performed 22nd of February 2022) there are only 79 deposited structures containing C-X...N halogen bonds, where X = I or Br or Cl, and pyrimidine-based halogen bond acceptors with an interaction distance shorter than the sum of the van der Waals radii of N and X and C-X...N angles between 150 to 180°. Although iodine is known to be more polarizable than bromine and chlorine, only 21 of these structures involve iodine while 41 structures are based on chlorine (N...Cl-C) as the halogen bond donor atom.

Theoretical investigation of the non-covalent interactions has been applied widely. The quantum theory of atoms in molecules QTAIM theory has been used to study intermolecular interactions and halogen bonds. (Kumar *et al.*, 2016) The obtained bond critical point (BCP) parameters from QTAIM (electron density at the bond critical point, ρ_{BCP} , Laplacian, $\nabla^2\rho_{\text{BCP}}$, and the total electron energy density, H_{BCP}) have been used to describe the bond path and to compare the halogen bond strength in different systems (Wang *et al.*, 2018; Wzgarda-Raj *et al.*, 2020).

Based on these results, work has been conducted previously to investigate the possibility of halogen bonds (XB) formation in pyrimidine containing compounds (pyrimidine, 4,6-dimethylpyrimidine, pyrimidine-5-amine) beside 1,3,5-triazine with 1,4-diiodotetrafluorobenzene (chapter 4), but this has not extended to other iodotetrafluorobenzenes.

In this study, we aim to further explore growing crystals from different di and tri-iodofluorobenzenes and similar halogen bond acceptors used in chapter 4. We reported four structures involving 1,3,5-trifluoro-2,4,6-triodobenzene, 1,2-diiodotetrafluorobenzene and 1,3-diiodotetrafluorobenzene as halogen bond donors, Scheme (5.1). We investigated the structural characteristics of these adducts and compare them with those previously reported (Chapter 4) N...I distances and corresponding QTAIM parameters for 1,4-diiodotetrafluorobenzene with 4 different pyrimidines.



Scheme 5.1 Labelling notation of the compounds using in building XB halogen bonds adducts reported in this study

5.3. Experimental

Chemicals and solvents were purchased from commercial sources (FluoroChem, Sigma Aldrich) and were used without further purification.

5.3.1. Synthesis and crystallization

Adducts **1a**, **2a** and **3b** were grown using the slow evaporation technique by dissolving the starting materials separately in 3 ml of dried acetonitrile and adding to one single vial, while **2c** was grown using vapour diffusion technique using a sealed system of two different sized vials.

In each case a 1:1 molar ratio was used for all the experiments. Adduct **1a** [0.01 ml (0.014 mmol) of **1** and (0.056 g of **a** (0.014 mmol)], **2a** [0.00149 ml (0.014 mmol) of **2** and (0.006 g of **a** (0.014 mmol)], **3b** [0.012 g, (0.13 mmol) of **3** and (0.02 ml of **b** (0.13 mmol)] and **2c** [0.01 ml (0.099 mmol) of **2** and 0.04 g of **c** (0.099 mmol)]. Crystals suitable for X-ray single crystal investigation formed within 3 days and were sealed to avoid deterioration.

FT-IR spectra were recorded using a Nicolet iS5 FT-IR instrument (See S1- S4). IR $\nu(\text{cm}^{-1})$ data for adduct (**1a**) formed between pyrimidine and 1,3,5-trifluoro-2,4,6-triiodobenzene:- similar IR spectra to pure 1,3,5-trifluoro-2,4,6-triiodobenzene (**a**) (Lucassen *et al.*, 2007); For adduct (**2a**) formed between 4,6-dimethylpyrimidine and 1,3,5-trifluoro-2,4,6-triiodobenzene :- 2923 (C-H) 1041, 1054, 1397, 1561 (C-F); For adduct (**2c**) formed between 4,6-dimethylpyrimidine and 1,2-diiidotetrafluorobenzene:- 1009, 1020, 1104, 1434 (C-F); for adduct (**3b**) formed between pyrimidine-5-amine and 1,3-diiidotetrafluorobenzene:- 3401, 3494 primary amine (N-H), 1070, 1432, 1471 (C-F) cm^{-1} .

5.3.2. Refinement

After a suitable crystal was selected, collection of the crystallographic data for each of the single crystals was performed on a supernova diffractometer using graphite- monochromated Mo $K\alpha$ radiation ($\lambda = 0.71073 \text{ \AA}$) at 150 K. All structures were solved using direct method and SHELXL-2014/7 was used in the refinement process based on full-matrix least-squares methods. Hydrogen atoms were introduced at calculated positions (riding model) and a summary of each crystal dataset are listed in Table 5.1.

Table 5.1 Experimental details.

Crystal data	(1a)	(2a)	(2c)	(3b)
Chemical formula	C ₁₀ H ₅ F ₃ I ₃ N ₂ ·C ₆ F ₃ I ₃ ·C ₄ H ₅ N ₂	C ₆ F ₃ I ₃ ·2(C ₆ H ₈ N ₂)	2(C ₆ F ₄ I ₂)·2(C ₆ H ₈ N ₂)	4(C ₆ F ₄ I ₂)·2(C ₄ H ₅ N ₃)
Mr	1181.72	726.05	1020.01	1797.66
Crystal system, space group	Orthorhombic, <i>Pca</i> 2 ₁	Monoclinic, <i>P</i> 2 ₁ / <i>c</i>	Triclinic, <i>P</i> ⁻ <i>1</i>	Monoclinic, <i>Cc</i>
Temperature (K)	150	150	150	150
a, b, c (Å)	26.5221 (10), 4.7308 (2), 22.8651 (8)	7.4661 (3), 21.2636 (5), 14.1362 (7)	8.6005 (4), 13.5115 (7), 14.0306 (6)	12.8944 (5), 12.7987 (5), 27.0876 (13)
α, β, γ (°)	90°, 90°, 90°	90, 98.206 (4), 90°	77.609 (4), 89.057 (4), 71.743 (5)	90°, 100.731 (4), 90°
V (Å³)	2868.90 (19)	2221.23 (15)	1510.03 (13)	4392.1 (3)
Z	4	4	2	4
Radiation type	Mo Kα	Mo Kα	Mo Kα	Mo Kα
μ (mm⁻¹)	6.55	4.26	4.20	5.75
Crystal size (mm)	0.19 × 0.02 × 0.01	0.2 × 0.05 × 0.04	0.4 × 0.08 × 0.03	0.1 × 0.06 × 0.02
Data collection				
T_{min}, T_{max}	0.509, 1.000	0.445, 1.000	0.744, 1.000	0.654, 1.000
No. of measured, independent and observed [I > 2σ(I)] reflections	23779, 5599, 4807	19829, 4369, 3568	11244, 5954, 4438	17947, 7613, 6857
R_{int}	0.071	0.077	0.052	0.049
(sin θ/λ)_{max} (Å⁻¹)	0.617	0.617	0.617	0.617
Refinement				
R[F² > 2σ(F²)], wR(F²), S	0.038, 0.067, 1.05	0.034, 0.078, 1.10	0.044, 0.082, 0.99	0.038, 0.063, 1.03
No. of reflections	5599	4369	5954	7613
No. of parameters	302	257	365	549
H-atom treatment	H-atom parameters constrained	H-atom parameters constrained	H-atom parameters constrained	H-atom parameters constrained
Δ_{max}, Δ_{min} (e Å⁻³)	0.70, -0.70	0.95, -0.73	1.20, -0.89	0.79, -0.79

Computer programs: CrysAlis PRO 1.171.39.4(Rigaku, 2018), ShelXT (Sheldrick, 2015), SHELXL (Sheldrick,2015),Olex2(Dolomanovetal.,2009)

5.4. Result and discussion

After having successfully prepared and analysed the structure of a halogen-bonded adduct of 1,4-diiodotetrafluorobenzene and pyrimidine (Chapter 4), an attempt was made to crystallize pyrimidine with 1,3,5-trifluoro-2,4,6-triodobenzene, 1,2-diiodotetrafluorobenzene and 1,3-diiodotetrafluorobenzene using vapour diffusion and slow evaporation methods.

This first structure **1a** was solved in the orthorhombic $Pca2_1$ space group and the resulting asymmetric unit consists of 2 molecules of 1,3,5-trifluoro-2,4,6-triodobenzene and two molecules of pyrimidine in a 1:1 ratio, Fig (5.1).

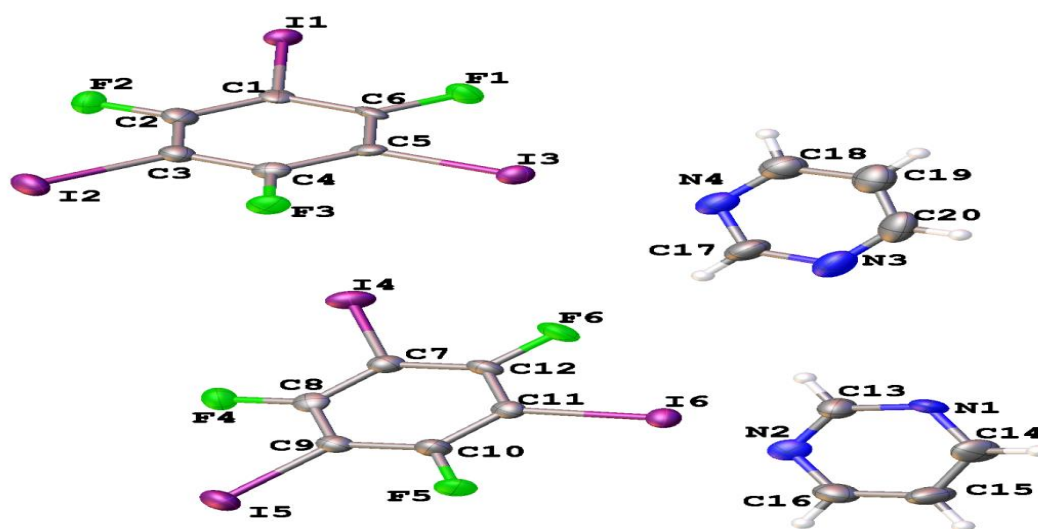


Figure 5.1 Views of the asymmetric unit of halogen-bonded adduct **1a**, showing the atom numbering. Ellipsoids are drawn at 50% probability level, colour codes: purple, iodine; green, fluorine; blue, nitrogen; white, hydrogen and grey carbon.

The three C-I bonds involved in N...I halogen bonds have bond lengths of 2.118(8), 2.128(7) and 2.127(7) Å, [average 2.124(7) Å] while the C-I bonds that are not involved in halogen bonding are: 2.089(8), 2.099(8) and 2.091(6) Å [average 2.093(8) Å]. This clearly shows an increase in C-I bond distances for the iodine atoms involved in halogen bonding compared with the average C-I distance, 2.090(4) Å, in pure 1,3,5-trifluoro-2,4,6-triodobenzene [UCEPEY01, (Lucassen *et al.*, 2007)] collected at 120 K. The three iodines (I1, I3 and I6) involved in N...I halogen bond with an average N...I distance of 2.87(1) Å are 0.66 Å

(18.7%) shorter than the sum of the van der Waals radii of iodine and nitrogen atoms, 3.53 Å (Bondi, 1964; Alvarez, 2013). This average distance is close to the average N...I distance 2.865(4) Å obtained by our group (Chapter 4) in the structure involved 1,4-DITFB and pyrimidine, the observed average C-I...N angles 177.0(3) ° is close to linearity than the reported one 171.3(1) ° (chapter 4).

The equatorial electron density belts associated with the anisotropic charge distribution of I3 and I6 were used to form I...I interaction (type II) halogen bonds with I4 and I2 respectively from neighbouring molecules, see Fig. 5.2. The I...I bond distances are 3.812(1) and 3.841(1) Å compared with the sum of van der Waals radii of iodine 3.96 Å respectively (Bondi, 1964; Alvarez, 2013). These distances are within the range of 3.9116(9) and 3.7360(8) Å, that previously observed in the structure related to pure 1,3,5-trifluoro-2,4,6-triiodobenzene [CSD ref code UCEPEY01, (Lucassen *et al.*, 2007)].

In this structure only two non-conventional hydrogen bonds can be detected N3...H13 (2.61 Å) and F4...H14 (2.440 Å). They are 0.14 Å, 5%, and 0.23 Å, 8.6%, shorter than the sum of the respective van der Waals radii 2.75 and 2.67 Å, see Table 5.2.

Table 5.2 Hydrogen-bond geometry (Å, °) for **1a**

$D-H\cdots A$	$D-H$	$H\cdots A$	$D\cdots A$	$D-H\cdots A$
C13—H13...N3 ⁱ	0.93	2.61	3.52 (2)	167
C14—H14...F4 ⁱⁱ	0.93	2.44	3.237 (17)	144

Symmetry codes: (i) $x, y+1, z$; (ii) $-x, -y-1, z-1/2$.

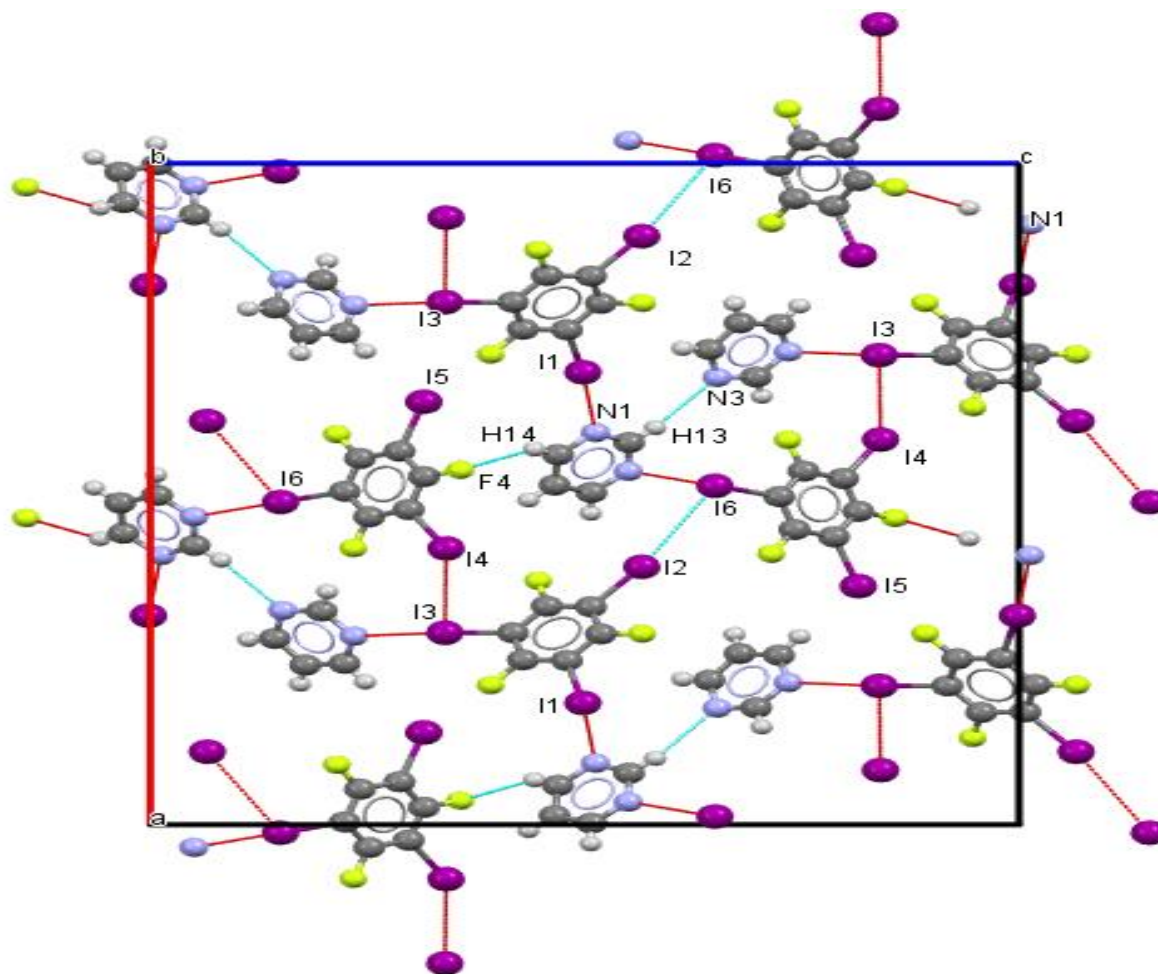


Figure 5.2 Crystal packing of **1a** down the a axis, showing N...I halogen bonds beside the other weak intermolecular interactions (H...F, H...N and π ... π stacking), The colour key is as follows: gray, carbon; purple, iodine; blue, nitrogen; yellow, fluorine; white, hydrogen.

Moving to structure **2a** which involves 4,6-dimethylpyrimidine (**2**) with 1,3,5-trifluoro-2,4,6-triodobenzene (**a**) which crystallises in the monoclinic crystal system and $P2_1/c$ space group similar to that previously reported when using 1,4-diiodotetrafluorobenzene as halogen bond donor (chapter 4).

However using a 1:1 molar stoichiometric resulted in crystals which gave rise to crystals with an asymmetric unit consisting of one unit of 1,3,5-trifluoro-2,4,6-triodobenzene and two units of 4,6-dimethylpyrimidine, i.e a 1:2 ratio, see **Fig 5.3**.

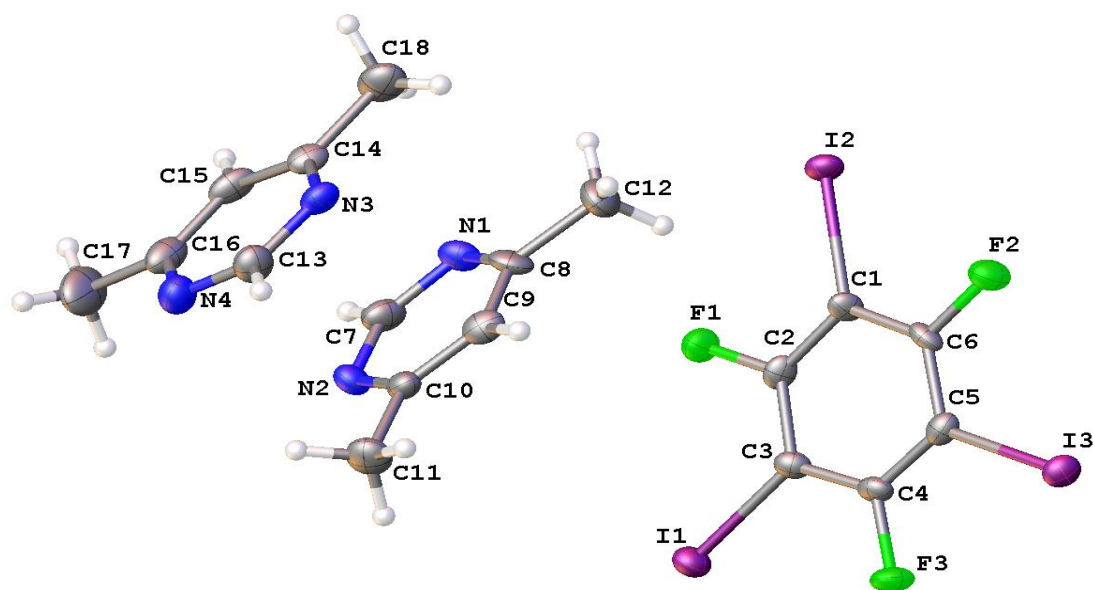


Figure 5.3 View of the asymmetric unit of halogen-bonded adduct **2a**, showing the atom numbering. Ellipsoids are drawn at 50% probability level. The colour key is as follows: grey, carbon; blue, nitrogen; green, fluorine; white, hydrogen.

All the 3 C-I bonds are now involved in halogen bonding with an average C-I bond distance, at 2.094(5) Å in **2a**, which is unchanged from 2.090(4) Å reported in pure 1,3,5-trifluoro-2,4,6-triiodobenzene [UCEPEY01, (Lucassen *et al.*, 2007)].

This lack of clear extension in C-I covalent bond can be contrasted with the average C-I distance recorded in **1a** 2.124(7) which is longer by 4σ . The reason behind this may be related to the formation of three N...I halogen bonds (two in one molecule but one in the other) rather than only two in **1a**.

The average N...I bond distance is 2.953(5) Å, which is 0.577 Å, 16.3% shorter than the sum of the van der Waals radii 3.53 Å (Bondi, 1964; Alvarez, 2013). The C-I...N halogen bond angles are close to linearity with an average of 175.1(2) °.

Beside the N...I halogen bonds there are two π ... π stacking (Janiak, 2000) interactions values found in this structure with two different centroid to centroid distances, 3.748 and 3.835 Å, see Fig 5.4. It is worth noting that the C-I bonds of one arene lie above the C-F bonds of the second one (Fig 4) which was not seen in our previous work (chapter 4) or in any CSD hits

reported halogen bonded structures involving 1,3,5-trifluoro-2,4,6-triodobenzene.

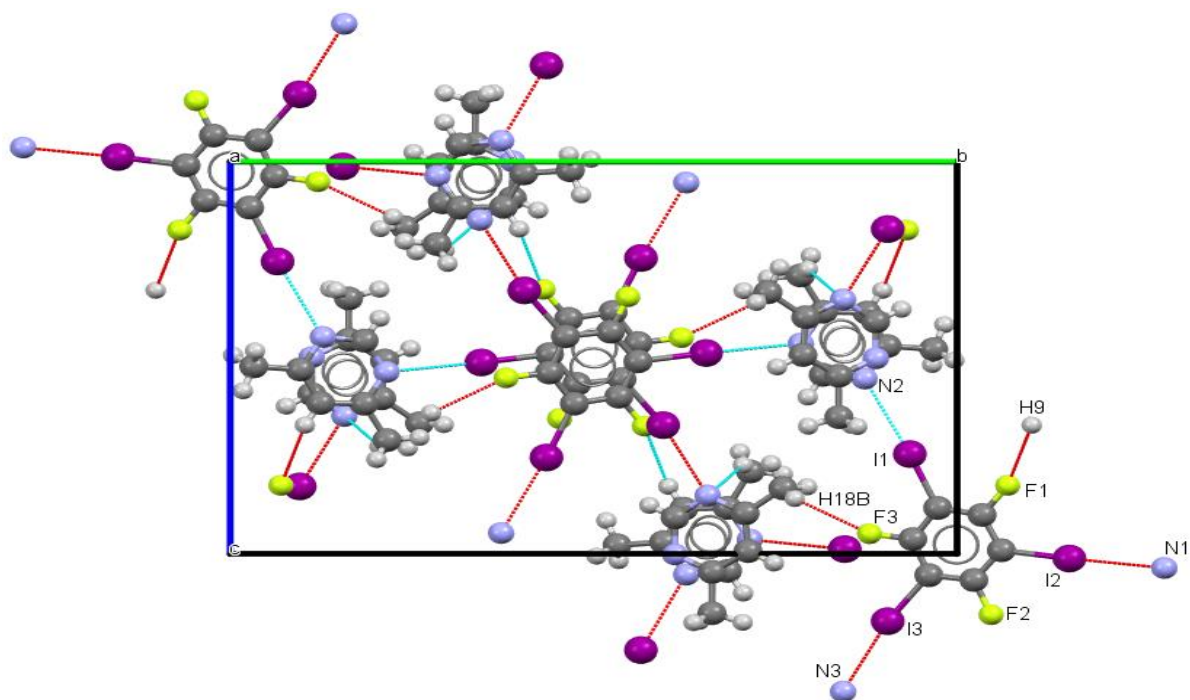


Figure 5.4 Crystal packing of **2a** down the b axis, showing N...I halogen bonds beside the other weak intermolecular interactions (H...F, H...N and π ... π stacking) colour codes: yellow, fluorine; blue, nitrogen; white, hydrogen and grey carbon; purple, iodine

There are three non-conventional hydrogen bonds that appear in **2a**, two F...H weak interactions with an average distance of 2.535 Å, 5% slightly shorter than the sum of van der Waals radii 2.67 Å, and one N...H interaction with a distance of 2.649 Å, shorter than the sum of van der Waals radii 2.75 Å by about 10% (see [Table 5.3](#)) ([Bondi, 1964](#); [Alvarez, 2013](#)).

Table 5.3 Hydrogen-bond geometry (Å, °) for **2a**

<i>D</i> —H... <i>A</i>	<i>D</i> —H	H... <i>A</i>	<i>D</i> ... <i>A</i>	<i>D</i> —H... <i>A</i>
C9—H9...F1	0.93	2.53	3.311 (7)	141
C12—H12 <i>B</i> ...N3 ⁱ	0.96	2.65	3.443 (7)	140
C18—H18 <i>B</i> ...F3 ⁱⁱ	0.96	2.53	3.078 (6)	116

Symmetry codes: (i) $x+1, y, z$; (ii) $-x+3, y+1/2, -z+3/2$

Adduct **2c** is the second adduct to contain 4,6-dimethylpyrimidine (**2**) as halogen bond acceptor successfully prepared with 1,2-diiodotetrafluorobenzene (**c**) in this work.

The 1:1 stoichiometric molar ratio of arene to 4,6-dimethylpyrimidine resulted in crystals with triclinic $P\bar{1}$ space group and an asymmetric unit consisting of two molecules of 1,2-diiodotetrafluorobenzene and two molecules of 4,6-dimethyl pyrimidine, Fig 5.5.

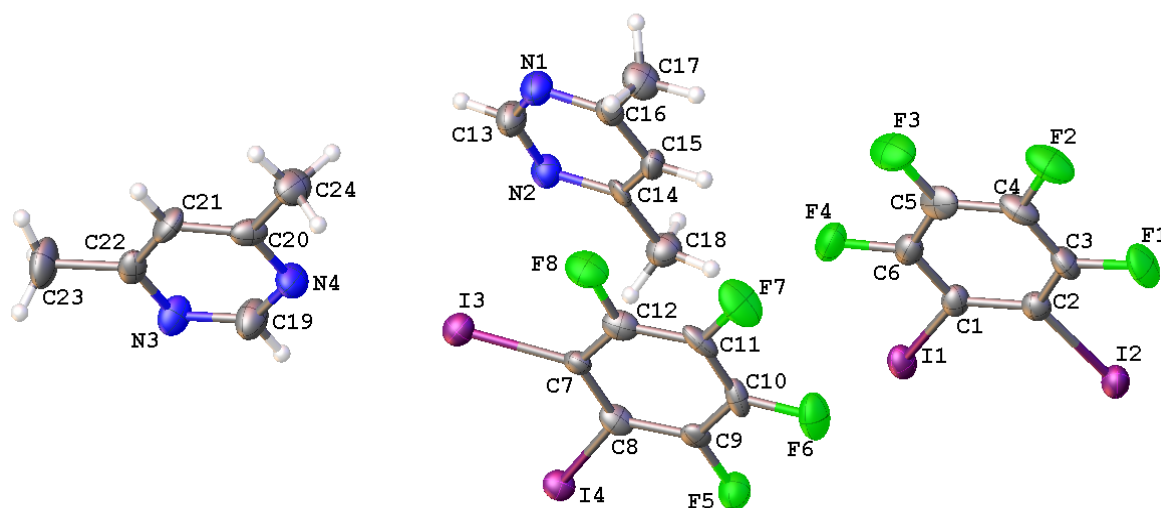


Figure 5.5 Views of the asymmetric unit of halogen-bonded adduct **2c**, showing the atom numbering. Ellipsoids are drawn at 50% probability level, colour codes: green, fluorine; blue, nitrogen; white, hydrogen and grey carbon, purple, iodine.

Comparing some of the parameters related to this structure **2c** we notice that the average C-I bond distance is 2.101(7) Å, similar to the average bond distance for the pure compound, 2.086(2) Å [CSD ref code WISBOR, (Drahansky *et al.*, 2016)].

The extended view of **2c** shows both iodine atoms involved in N...I halogen bonds forming a 3D ribbon-like shape, Fig.5.6.

The average N...I bond distance is 2.956(7) Å which is 0.574 Å (16.2%) shorter than the sum of the van der Waals radii 3.53 Å (Bondi, 1964; Alvarez, 2013). The related average N...I-C halogen bond angle is close to linearity 175.4(2) °.

The average C-F...H non-conventional hydrogen bond interactions is 0.678 Å (10%) slightly shorter than the sum of the van der Waals radii for fluorine and hydrogen, 2.67 Å, see [Table 5.4](#).

Table 5.4 Hydrogen-bond geometry (Å, °) for **2c**

<i>D</i> —H... <i>A</i>	<i>D</i> —H	H... <i>A</i>	<i>D</i> ... <i>A</i>	<i>D</i> —H... <i>A</i>
C15—H15...F4	0.93	2.42	3.342 (7)	170
C21—H21...F5 ⁱ	0.93	2.38	3.279 (7)	162

Symmetry code: (i) $-x, -y, -z+1$.

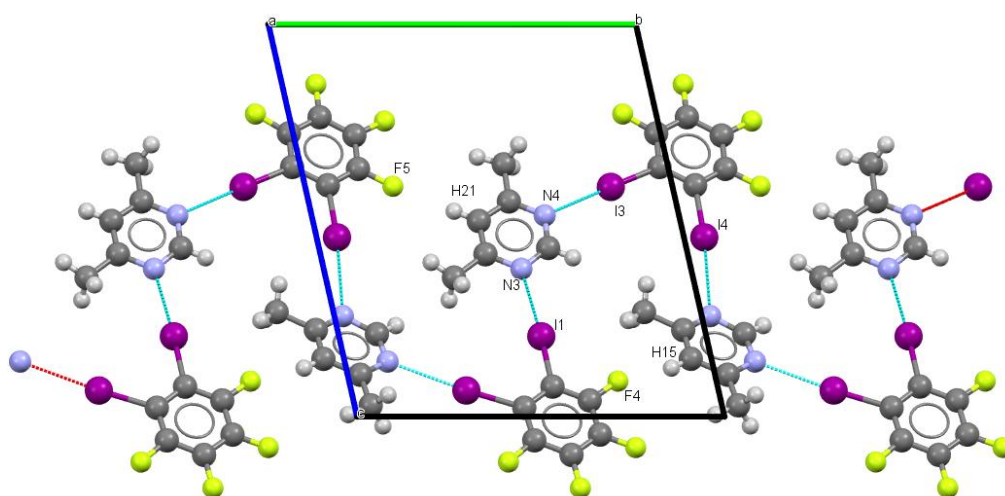


Figure 5.6 crystal packing of **2c** along a showing the N...I halogen bonds and the secondary interactions, colour codes: green, fluorine; blue, nitrogen; white, hydrogen and grey carbon, purple, iodine.

The last structure to be discussed is adduct **3b** which involves pyrimidine-5-amine (**3**) which features two different types of nitrogen centres (one aromatic and one a primary amine) and 1,3-diodotetrafluorobenzene (**b**). Adduct **3b** crystallises in the monoclinic *Cc* space group and it has a large unit cell volume (4392.1 Å³) consisting of four units of 1,3-diodotetrafluorobenzene and two units of pyrimidine-5-amine ([Fig 5.7](#)) in a 2:1 structure ratio respectively.

The 1:1 arene to pyrimidine-5-amine molar ratio used to prepare this adduct, result in 2:1 structure ratio and half of the C-I distances elongate (C1-I1, C13-I4, C23-I6 and C29-I8)

compared with the other C-I bonds (C3-I2, C11-I3, C27-I7 and C21-I5) which are not involved in N...I halogen bonding, but are involved in I...I interaction only, see [Table 5.5](#). Although there is no structural data available for 1,3-diiodotetrafluorobenzene with which to make a direct comparison, the average C-I distance is close to the average extension that occurs in previously discussed structures [1a](#), [2a](#), [2c](#).

Table 5.5 Different C-I bond distances detected in [3b](#)

C-I bond distances (involved in N...I and I...I interactions), Å		C-I bond distances (involved in I...I interactions only), Å	
C1-I1	2.11(1)	C3-I2	2.07(1)
C13-I4	2.11(1)	C11-I3	2.08(1)
C23-I6	2.11(1)	C27-I7	2.094(8)
C29-I8	2.108(6)	C21-I5	2.09(1)

One of two iodine atoms in each molecule is involved in forming N...I halogen bonds with average bond distance of 2.89(1) Å, which is 0.64 Å, 18% shorter than the sum of the van der Waals radii of nitrogen and iodine (3.53 Å) ([Bondi, 1964](#); [Alvarez, 2013](#)).

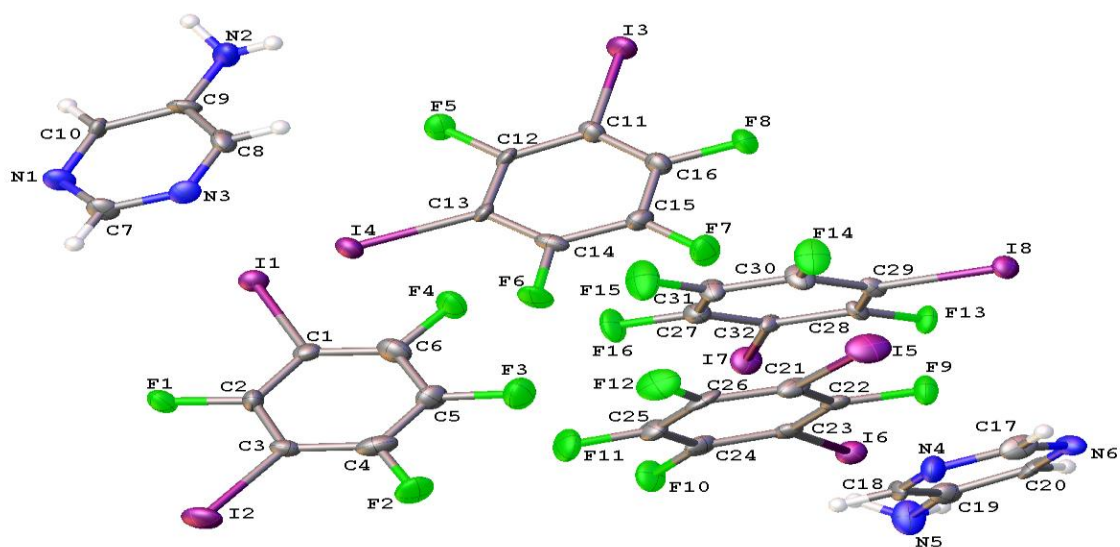


Figure 5.7 Views of the asymmetric unit of halogen-bonded adduct **3b**, showing the atom numbering. Ellipsoids are drawn at 50% probability level., colour codes: green, fluorine; blue, nitrogen; white, hydrogen and grey carbon, purple, iodine.

Possibly related to the reduced basicity(tertiary amine > secondary amine > primary amine) of the primary nitrogen in **3b** Fig (5.8), this nitrogen is not involved in N...I bonding, unlike when 1,4-diiodotetrafluorobenzene is used, as in chapter 4 when a weak halogen bond is formed, no N...I halogen bonds were formed from the primary amines of either of the two pyrimidine-5-amine molecules of **3b**, however a N2-H2B...F1 conventional hydrogen bond formed from one of the two riding hydrogens. The distance is 2.550 Å (0.12 Å, 4.49%) shorter than the sum of the hydrogen and fluorine atoms van der Waals radii, 2.67 Å (Bondi, 1964; Alvarez, 2013). The remaining F...H non-conventional hydrogen bond interactions in this structure are presented in Table (5.6).

Table 5.6 Hydrogen-bond geometry (Å, °) for **3b**

<i>D</i> —H... <i>A</i>	<i>D</i> —H	H... <i>A</i>	<i>D</i> ... <i>A</i>	<i>D</i> —H... <i>A</i>
C10—H10...F13 ⁱ	0.93	2.56	3.412 (15)	153
N2—H2B...F1 ⁱⁱ	0.87	2.55	3.347 (14)	153
C18—H18...F9 ⁱⁱⁱ	0.93	2.64	3.472 (14)	150

Symmetry codes: (i) $x+1/2, -y+1/2, z+1/2$; (ii) $x-1/2, y-1/2, z$; (iii) $x+1/2, y-1/2, z$.

The C-I...N halogen bond angles were close to linearity and range from 171.0 (3) ° to 174.6 (4) °. The negative electrostatic potential belt formed in the same halogen bonded atom was used to form type (II) I...I contacts to iodine from adjacent molecule. The average I...I bond distance is 3.829(1) Å, which is 0.131 Å (3.3%) just shorter than the sum of the van der Waals radii 3.96 Å.

In conclusion, the adducts generated in this study shows N...I halogen bonds as the shortest interaction between the detected intermolecular interactions. The obtained N...I halogen bonds are less than the sum of van der Waals radii of nitrogen (1.55Å) and iodine (1.98Å) atoms (Bondi, 1964; Alvarez, 2013), see Table 5.7. The shortest N...I bond distance recorded is 2.85(1) Å and belongs to the structure involving 1,3,5-trifluoro-2,4,6-triodobenzene and pyrimidine which support the reported result (chapter 4) using 1,4-diiidotetrafluorobenzene. Furthermore, this reflects the order of the number of reported neutral structures for each of the studied iodofluorobenzene with aromatic nitrogen base halogen bond acceptors to date [1,4-diidotetrafluorobenzene (238), 1,3,5-trifluoro-2,4,6-triidobenzene (54), 1,2-diidotetrafluorobenzene (33) and 1,3-diidotetrafluorobenzene (38)] according to the CSD [search conducted 22/02/2022. (Groom *et al.*, 2016)]

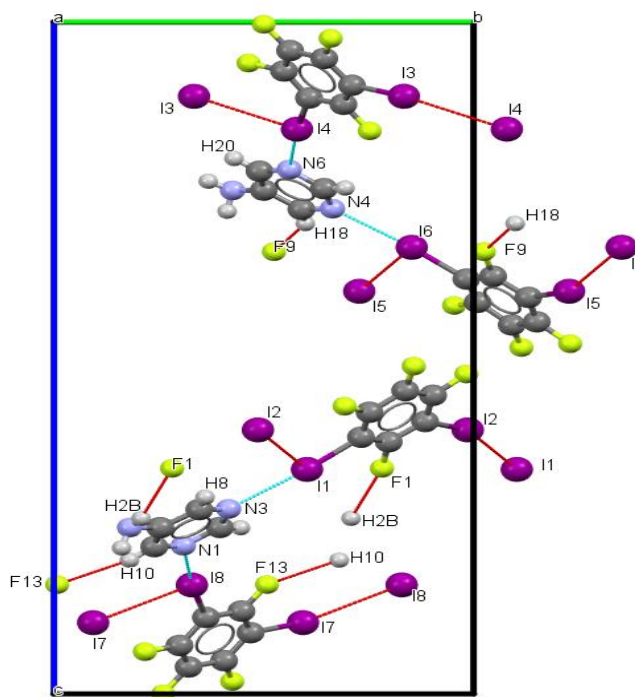


Figure 5.8 crystal packing of **3b** along a showing the N...I halogen bonds and the secondary interactions, colour codes: yellow, fluorine; blue, nitrogen; white, hydrogen and grey carbon, purple, iodine.

Table 5.7 C-I, N...I distances (Å) and C-I...N angles (°) related to the structures obtained in this study.

Entry	code	Donor	Acceptor	C-I (Å)	N...I (Å)	N...I-C (°)	Reference
1	1a	1,3,5-trifluoro-2,4,6-triodobenzene	pyrimidine	2.118(8) 2.127(7) 2.126(7)	2.85(1) 2.86(1) 2.90(1)	174.3(3) 179.8(3) 177.0(3)	This work
2	2a	"	4,6-dimethylpyrimidine	2.100(4) 2.091(5) 2.090(5)	2.955(4) 3.001(5) 2.904(5)	177.1(2) 176.8(2) 171.4(2)	This work
3	2c	1,2-diiidotetrafluoro benzene	4,6-dimethylpyrimidine	2.113(7) 2.099(7) 2.097(7) 2.093(7)	2.931(6) 2.993(6) 2.930(7) 2.968(7)	176.0(3) 172.6(2) 176.1(2) 176.5(2)	This work
4	3b	1,3-diiidotetrafluoro benzene	Pyrimidine-5-amine	2.108(6) 2.11(1) 2.11(1) 2.11(1)	2.92(1) 2.87(1) 2.91(1) 2.87(1)	171.0(3) 174.5(4) 173.9(4) 174.6(4)	This work

QTAIM analysis was carried out to analyse the crystal structures (Fig 9-12) following the procedures reported previously (Chapters 2+3+4) utilizing GAMESS (Schmidt *et al.*, 1993) and Multiwfn (Lu & Chen, 2012) software. The resulting parameters are presented in Table (5.8). Bond critical points related to N...I halogen bonds were detected and analysed. The obtained positive values for the electron density, ρ_{BCP} , and Laplacian, $\nabla^2\rho_{\text{BCP}}$, suggest that close shell interaction exist and their values increase as the halogen bond becomes shorter which supports the crystallographic data. The decrease of local energy density, H_{BCP} , values have been reported to possibly relate to the strength of the bond. (Angelina *et al.*, 2013; Wang *et al.*, 2018)

Table 5.8 Topological parameters calculated at B3LYP/6-311G** level of theory using GAMESS and Multiwfn programmes

Trimer	Interaction	X...B (Å)	ρ_{BCP} (a.u)	H(r) (a.u)	$\nabla^2\rho_{\text{BCP}}$ (a.u)
1a	N1...I1	2.85(1)	0.0229	0.000870	0.0709
	N2...I6	2.86(1)	0.0228	0.000864	0.0705
	N4...I3	2.90(1)	0.0214	0.000938	0.0657
2a	N2...I2	2.955(4)	0.0193	0.000995	0.0594
	N2...I1	3.001(5)	0.0177	0.001040	0.0545
	N3...I3	2.904(5)	0.0210	0.000939	0.0647
2c	N1...I2	2.931(6)	0.0202	0.000969	0.0624
	N2...I4	2.993(6)	0.0179	0.001060	0.0551
	N3...I1	2.930(7)	0.0202	0.000961	0.0618
	N4...I3	2.968(7)	0.0189	0.000983	0.0578
3b	N1...I8	2.92(1)	0.0207	0.000945	0.0638
	N3...I1	2.87(1)	0.0221	0.000932	0.0684
	N6...I4	2.91(1)	0.0207	0.001020	0.0647
	N4...I6	2.87(1)	0.0221	0.000973	0.0688

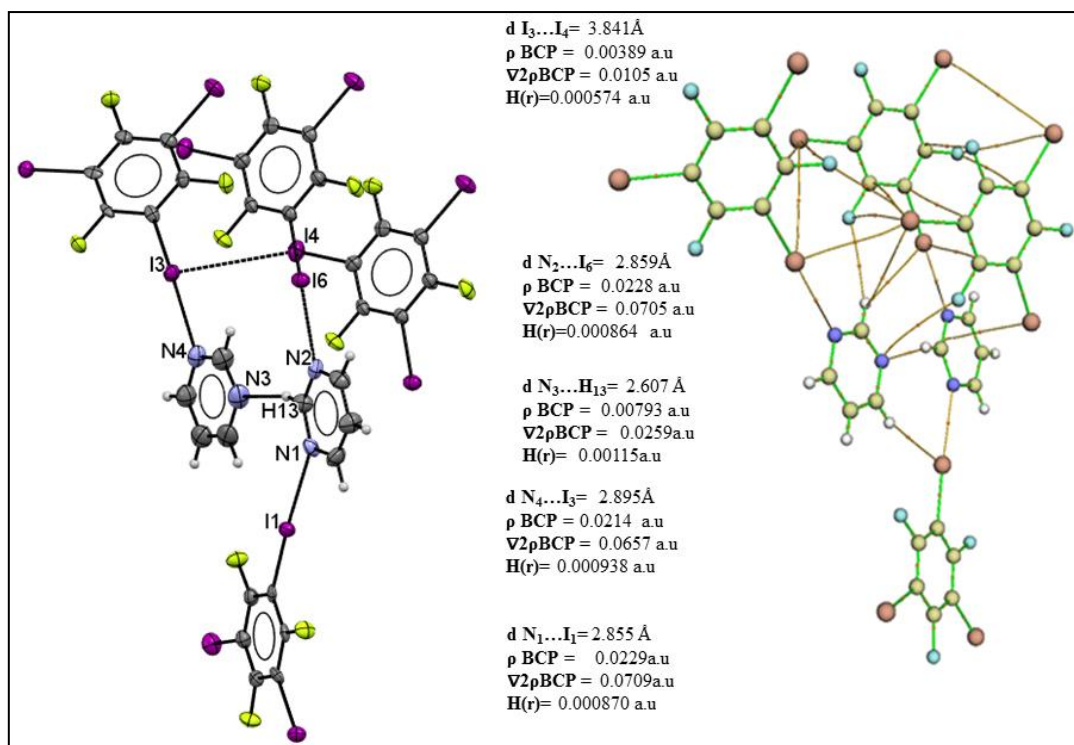


Figure 5.9 The determined X-ray structure (left) and molecular graph (right) for adduct **1a**

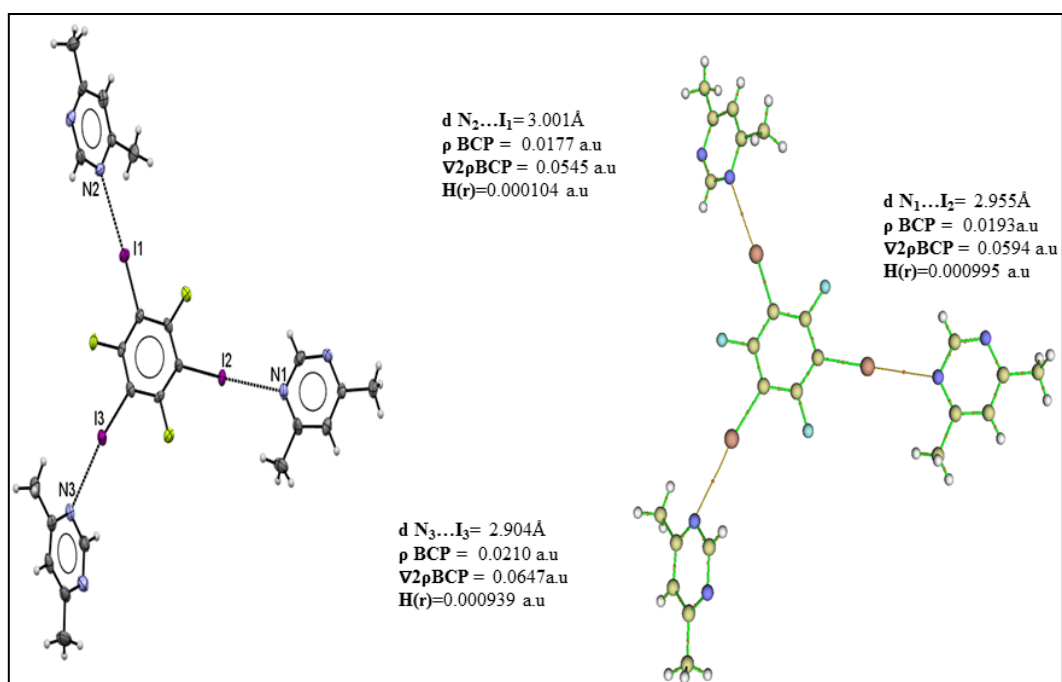


Figure 5.10 The determined X-ray structure (left) and molecular graph (right) for adduct **2a**

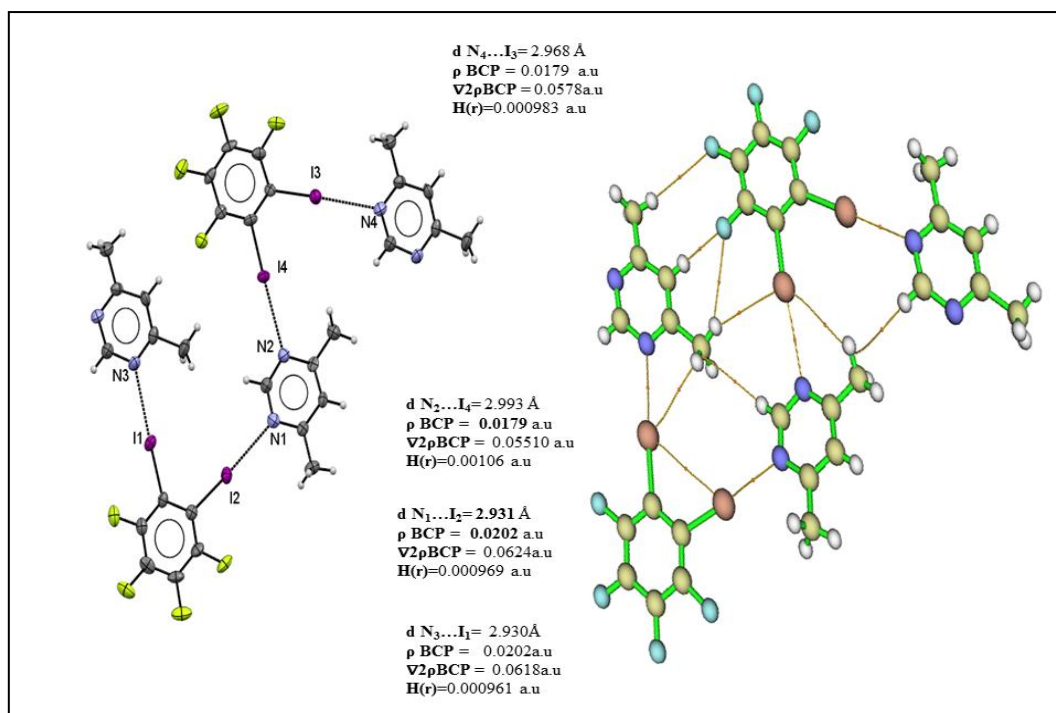


Figure 5.11 The determined X-ray structure (left) and molecular graph (right) for adduct **2c**

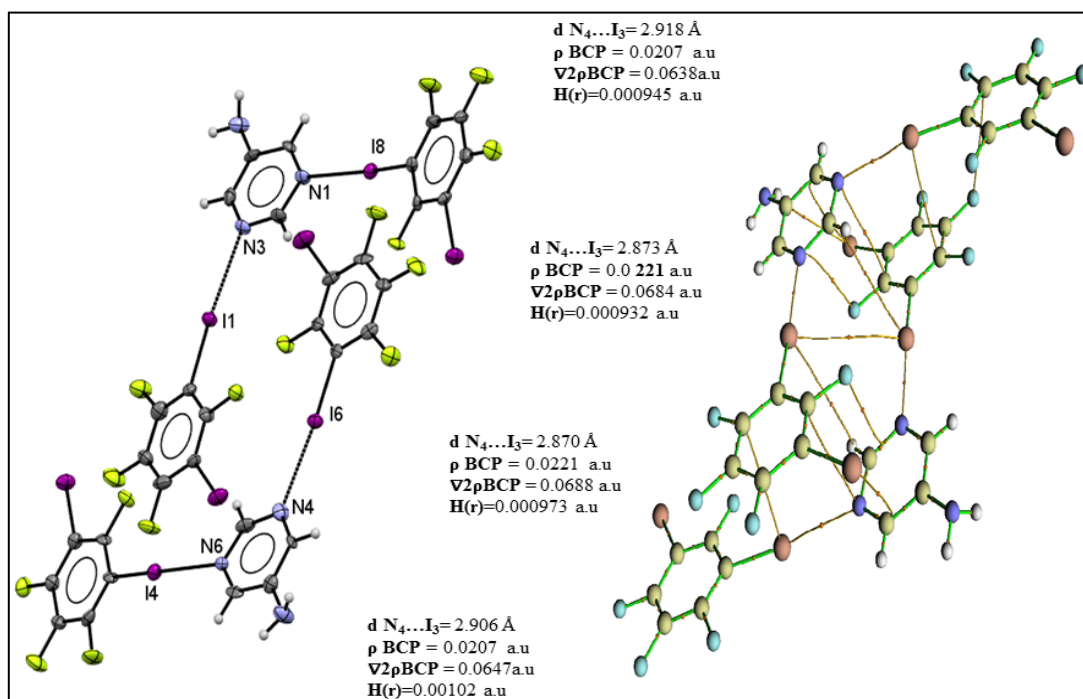


Figure 5.12 The determined X-ray structure (left) and molecular graph (right) for adduct **3b**

References

- Alvarez, S. (2013). *Dalt. Trans.* **42**, 8617–8636.
- Angelina, E. L., Duarte, D. J. R. & Peruchena, N. M. (2013). *J. Mol. Model.* **19**, 2097–2106.
- Bondi, A. (1964). *J. Phys. Chem.* **68**, 441–451.
- Desiraju, G. R., Ho, P. S., Kloo, L., Legon, A. C., Marquardt, R., Metrangolo, P., Politzer, P., Resnati, G. & Rissanen, K. (2013). *Pure Appl. Chem.* **85**, 1711–1713.
- Dolomanov, O. V., Bourhis, L. J., Gildea, R. J., Howard, J. A. K. & Puschmann, H. (2009). 2008–2010.
- Drahansky, M., Paridah, M. ., Moradbak, A., Mohamed, A. ., Owolabi, F. abdulwahab taiwo, Asniza, M. & Abdul Khalid, S. H. . (2016). *Intech*, 13.
- Groom, C. R., Bruno, I. J., Lightfoot, M. P. & Ward, S. C. (2016). *Acta Crystallogr. Sect. B Struct. Sci. Cryst. Eng. Mater.* **72**, 171–179.
- Janiak, C. (2000). *J. Chem. Soc. Dalt. Trans.* 3885–3896.
- Kumar, P. S. V., Raghavendra, V. & Subramanian, V. (2016). *J. Chem. Sci.* **128**, 1527–1536.
- Lu, T. & Chen, F. (2012). *J. Comput. Chem.* **33**, 580–592.
- Lucassen, A. C. B., Karton, A., Leitus, G., Shimon, L. J. W., Martin, J. M. L. & van der Boom, M. E. (2007). *Cryst. Growth Des.* **7**, 386–392.
- Marquardt, R., Politzer, P., Resnati, G., Rissanen, K., Desiraju, G. R., Ho, P. S., Legon, A. C., Kloo, L. & Metrangolo, P. (2013). *Pure Appl. Chem.* **85**, 1711–1713.
- Priimagi, A., Cavallo, G., Metrangolo, P. & Resnati, G. (2013). *Acc. Chem. Res.* **46**, 2686–2695.
- Richter, B. (2009). Essential of Hetrocyclic Chemistry-1.
<<http://www.scripps.edu/baran/heterocycles/Essentials1-2009.pdf> [cited 2021]
- Rigaku, O. (2018). *Rigaku Oxford Diffr. Ltd, Yarnton, Oxfordshire, Engl.*
- Schmidt, M. W., Baldrige, K. K., Boatz, J. A., Elbert, S. T., Gordon, M. S., Jensen, J. H., Koseki, S., Matsunaga, N., Nguyen, K. A. & Su, S. J. (1993). *J. Comput. Chem.* **14**, 1347.
- Sheldrick, G. M. (2015). *Acta Crystallogr. Sect. A Found. Crystallogr.* **71**, 3–8.
- Wang, R., Hartnick, D. & Englert, U. (2018). *Zeitschrift Für Kristallographie - Crystalline Materials.* **233**, 733–744.

Wzgarda-Raj, K., Rybarczyk-Pirek, A. J., Wojtulewski, S. & Palusiak, M. (2020). *Acta Crystallogr. Sect. C Struct. Chem.* **76**.

Chapter 6.

Manuscript 5: Crystallographic and QTAIM studies of variety of halogen bonded adducts containing compounds using piperazine

Sultan Alkaabi, Alan K. Brisdon*,

Department of Chemistry, University of Manchester, Oxford Road, Manchester M13 9PL, England.

Keywords: Halogen bonds, Crystal structure, bromofluorobenzene, piperazine, QTAIM, infrared, ^{19}F NMR, van der Waals radii

Correspondence email: *alan.brisdon@manchester.ac.uk

6.1. Abstract

A series of halogen bonded adducts formed between iodo- and bromofluorobenzenes with piperazine have been prepared. All of the adducts have been characterised by means of single crystal X-ray crystallography, revealing N...I and N...Br short-halogen bonds. Infrared spectroscopy confirmed the existence of the halogen bonds in the solid state, while solution phase NMR spectroscopy indicates that in all cases the XB interactions do not remain in solution. Theoretical studies based on Quantum Theory of Atoms in Molecules (QTAIM) was applied to the solid-state structures at B3LYP/6-311G** level of theory to compare the bond critical points features with the experimentally-determined halogen bond distances in their molecular structures in solid state. The calculated values of the electron density, ρ_{BCP} and Laplacian $\nabla^2\rho_{\text{BCP}}$ for the halogen bond critical points are compared with the crystallographic data.

6.2. Introduction

A halogen bond is one of the key directional noncovalent interactions in crystal engineering and there is a growing interest in the field of halogen bonding as it may be a possible alternate choice to hydrogen bond used to build networks of molecules.

A halogen bond is defined according to IUPAC as “occurs when there is evidence of a net attractive interaction between an electrophilic region associated with a halogen atom in a molecular entity and a nucleophilic region in another, or the same, molecular

entity”.(Marquardt *et al.*, 2013) This electrophilic region, generated on the halogen is called a σ hole and has been investigated experimentally and then theoretically and found to depend on both the electron acceptor (called a halogen bond donor) and the electron donor (halogen bond acceptor).

Haloarenes, especially those containing iodine or bromine are the most established typical halogen bond donors and have been investigated widely and shown to act as a positive σ hole at the halogen atoms when the aromatic system contains efficient withdrawing groups. (Poltzer & Murray, 2013)

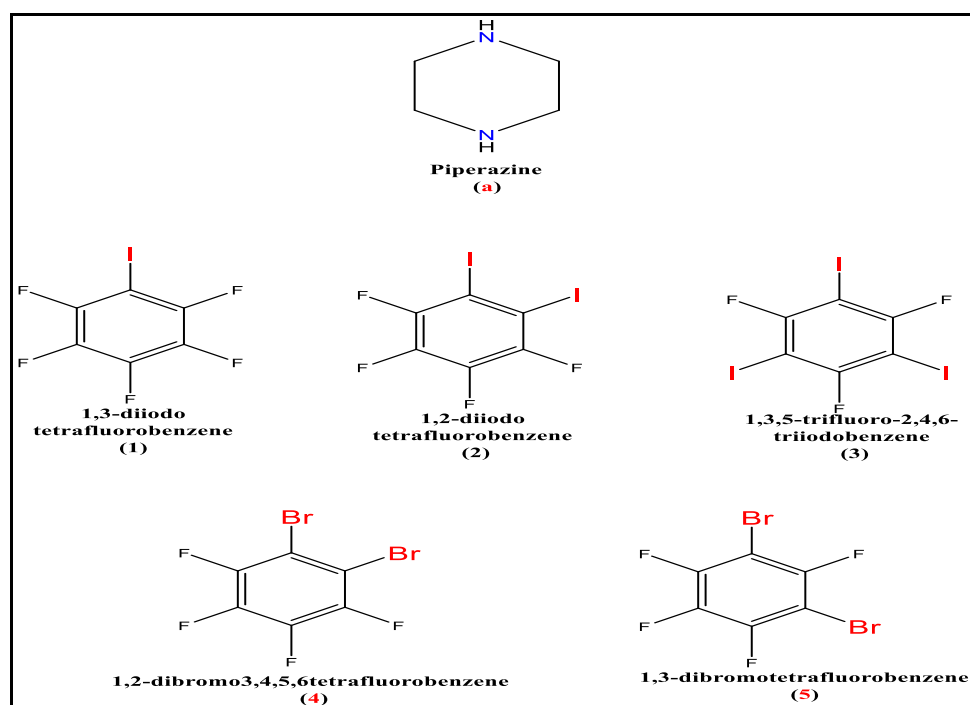
The high electronegativity, and poorly polarized characteristics of a fluorine atom makes it unsuitable as a halogen bond donor, but has been proven to be useful as an electron withdrawing atom within a halogen bond donor.(Clark *et al.*, 2007; Catalano *et al.*, 2015; Liantonio *et al.*, 2003) Iodine and bromine are the halogens that give rise to the most positive σ -hole (Poltzer & Murray, 2013) and this is related to their increased polarizability. Iodo- and bromofluorobenzene have proved to be good examples of halogen bond donors, because of presence the fluorine on the ring to withdraw the electron density. According to searches of the Cambridge Structure Database (CSD, performed 22nd February 2022) there are 428 hits for structures involving iodofluorobenzenes as halogen bond donors with nitrogen halogen bond acceptors, and especially 1,4-diiodotetrafluorobenzene (252 hits 59%). In comparison there are few halogen bonded structures involving bromofluorobenzenes (about 32 structures only). (Groom *et al.*, 2016)

The second component of any halogen bond is the electron donation site (halogen bond acceptor). Widely investigated among halogen bond acceptors are the tertiary amines, with a lesser number of articles reporting on secondary amines. For example, Piperazine has to date only 3 deposited halogen bonded structures in the CSD, and all of them with iodo or bromofluoroarenes_[CSD refcodes WIGTAK (Bedeković *et al.*, 2018), DIVDOC (Cinčić *et al.*, 2008), DIVCUH (Cinčić *et al.*, 2008)].

Theoretical studies have been used to describe and compare the closed-shell interactions including halogen bonds using the values of the electron density, ρ_{BCP} , and Laplacian, $\nabla^2\rho_{\text{BCP}}$, at the bond critical points (BCP).(Bader & Essén, 1984; Matta & Boyd, 2007) Different studies have analysed hydrogen and halogen bonds using QTAIM theory.(Tuikka *et al.*,

2011; Li *et al.*, 2019; Angelina *et al.*, 2013; Grabowski, 2012, 2013) Most of these studies agreed that the electron density ρ_{BCP} indicates the strength of the halogen bonds. (Matta & Boyd, 2007; Angelina *et al.*, 2013) While the Laplacian, $\nabla^2\rho_{\text{BCP}}$, for all closed-shell interactions is > 0 because it measures the depletion of the electron density in the region between the two atom contacts. (Matta & Boyd, 2007) Some authors report the sign of the local electron energy density, H_{BCP} , as an indication of the strength and expected nature of the interaction. With this being mainly electrostatic if $H_{\text{BCP}} > 0$, and may have partially covalent character if $H_{\text{BCP}} < 0$. (Cremer & Kraka, 1984; Jenkins & Morrison, 2000).

Herein we aim to examine the ability of piperazine to form halogen bonds with a variety of iodofluorobenzenes (1-iodofluorobenzene, 1,2-diiodotetrafluorobenzene and 1,3,5-trifluoro-2,4,6-triiodobenzene), see **Scheme 6.1**. We will also explore the ability of this secondary amine (pKa 9.8) to form halogen bonds with some bromofluorobenzenes and compare the resulting crystal structure data with those obtained using QTAIM.



Scheme 6.1 Compounds used in this study

6.3. Experimental

Piperazine (**a**), iodopentafluorobenzene (**1**), 1,2-diodotetrafluorobenzene (**2**), 1,3,5-trifluoro-2,4,6-triiodobenzene (**3**), 1,2-dibromotetrafluorobenzene (**4**) and 1,3-dibromotetrafluorobenzene (**5**) were obtained from commercial sources and used without further purification.

6.3.1. Synthesis and crystallization

Adducts **1a**, **2a**, **4a** and **5a** were grown by vapour diffusion techniques, however **3a** was grown by slow evaporation from an anhydrous acetonitrile solution.

The vapour diffusion technique used a sealed system consisting of a big vial (containing the arene) and inside this a small vial (containing piperazine) to grow adducts. Different ratios have been used to examine the possibility of having different number of nitrogen and halogens involving in halogen bonding. Adducts **2a** [prepared from 0.058 g (0.29 mmol) of **2** and 0.025 g (0.15 mmol) of **a**], **4a** [prepared from 0.02 ml (0.15 mmol) of **4** and 0.025 g (0.29 mmol) of **a**] and **5a** [prepared from 0.02 ml (0.15 mmol) of **5** and 0.025 g (0.29 mmol) of **a**] were grown using 1:2 stoichiometric ratios. In adduct **1a** [prepared from 0.02 ml (0.15 mmol) of **1** and 0.0123 g (0.15 mmol) of **a**] 1:1 ratio was used, whereas adduct **3a** [prepared from 0.049 ml (0.097 mmol) of **3** and 0.025 g (0.29 mmol) of **a**] in 1:3 ratio.

A Nicolet iS5 FT-IR instrument was used to measure changes in ν_{C-H} and ν_{C-F} absorption bands and results in IR $\nu(\text{cm}^{-1})$ data for all the adducts that shows demolished hydrogen bond broad peaks above 3000 cm^{-1} and other changes as follows :- Adduct (**1a**) : 2846 (C-H), 1506,1479, 1078 (C-F); for adduct (**2a**): (C-H), 1100, 1300 (C-F); for adduct (**3a**): 1042, 1559 (C-F); for adduct (**4a**): 1500, 1461, 1117 (C-F); for adduct (**5a**) : 2831 (C-H), 1482 (C-F).

^{19}F NMR spectra were recorded on a Bruker AMX 400 MHz spectrometer at ambient temperature using CD_3CN as solvent, except for **4a** when DMSO was used. The spectra (See S 6.6-S 6.10) showed no significant change from the starting materials that might indicate the ability of the halogen bonding interaction to remain in solution.

6.3.2. Refinement

All crystal data were collected at 150 K on a supernova Eos diffractometer, employing monochromated Mo K α radiation source ($\lambda = 0.71073 \text{ \AA}$). Structures were solved by direct methods using ShelXT(Sheldrick, 2015) except structure **4a** which solved with olex2 using Charge Flipping.(Bourhis *et al.*, 2015) All structures were refined using (SHELXL) by full-matrix least squares methods.(Sheldrick, 2015)

Hydrogen atoms were introduced at geometrically calculated positions and included in the final refinement using the "riding model". A summary of the crystallographic data reported for the structures are listed in Table (6.1).

Table 6.1 Experimental details of **1a- 5a** reported in this work.

Crystal data	(1a)	(2a)	(3a)	(4a)	(5a)
Chemical formula	C ₆ F ₅ I·C ₂ H ₅ N	C ₃ F ₂ I·C ₂ H ₅ N	C ₆ F ₃ I ₃ ·C ₂ H ₅ N	Br ₂ C ₆ F ₄ ·C ₂ H ₅ N	Br ₂ C ₆ F ₄ ·C ₂ H ₅ N
<i>M_r</i>	337.03	244.00	552.83	350.95	350.95
Crystal system, space group	Monoclinic, <i>P2₁/c</i>	Monoclinic, <i>P12₁/m1</i>	Triclinic, <i>P⁻1</i>	Triclinic, <i>P⁻1</i>	Triclinic, <i>P⁻1</i>
Temperature (K)	150	150	150	150	150
<i>a, b, c</i> (Å)	5.3154 (2), 10.5471 (4), 17.4651 (7)	5.2637 (6), 20.651 (3), 6.1156 (7)	8.6231 (9), 9.1223 (11), 9.3224 (9)	5.1117 (6), 5.9696 (9), 16.3344 (18)	5.1595 (5), 6.0243 (7), 16.7733 (14)
<i>α, β, γ</i> (°)	90,95.136 (4),90	90,101.244 (11),90	67.187 (10), 72.699 (9), 63.128 (11)	90.915 (10), 90.677 (9), 98.075 (11)	90.556 (8), 90.548 (7), 100.778 (9)
<i>V</i> (Å ³)	975.20 (6)	652.01 (14)	596.28 (13)	493.39 (11)	512.09 (9)
<i>Z</i>	4	4	2	2	2
Radiation type	Mo <i>Kα</i>	Mo <i>Kα</i>	Mo <i>Kα</i>	Mo <i>Kα</i>	Mo <i>Kα</i>
<i>μ</i> (mm ⁻¹)	3.32	4.86	7.87	8.24	7.94
Crystal size (mm)	0.08 × 0.06 × 0.01	0.28 × 0.02 × 0.01	0.05 × 0.03 × 0.01	0.1 × 0.05 × 0.02	0.2 × 0.1 × 0.02
Data collection					
<i>T_{min}, T_{max}</i>	0.746, 1.000	0.723, 1.000	0.883, 1.000	0.441, 1.000	0.336, 1.000
No. of measured, independent and observed [<i>I</i> > 2σ (<i>I</i>)] reflections	5525, 1918, 1575	2520, 1303, 1156	4283, 2342, 1952	3471, 1938, 1437	3358, 2018, 1476
<i>R_{int}</i>	0.050	0.031	0.047	0.069	0.043
<i>(sin θ/λ)_{max}</i> (Å ⁻¹)	0.617	0.617	0.616	0.617	0.617
Refinement					
<i>R</i> [<i>F</i> ² > 2 <i>s</i> (<i>F</i> ²)], <i>wR</i> (<i>F</i> ²), <i>S</i>	0.035, 1.03	0.061, 1.09	0.033, 0.092, 0.042, 0.078, 0.99	0.058, 0.110, 1.03	0.050, 0.123, 1.09
No. of reflections	1918	1303	2342	1938	2018
No. of parameters	139	85	139	127	216
H-atom treatment	H atoms treated by a mixture of independent and constrained refinement	H atoms treated by a mixture of independent and constrained refinement	H atoms treated by a mixture of independent and constrained refinement	H atoms treated by a mixture of independent and constrained refinement	H atoms treated by a mixture of independent and constrained refinement
<i>Δ_{max}, Δ_{min}</i> (e Å ⁻³)	0.63, -0.80	1.41, -0.69	0.97, -1.41	0.83, -0.73	0.67, -0.67

Computer programs: CrysAlis PRO 1.171.39.46(Rigaku, 2018) ShelXT (Sheldrick, 2015), SHELXL (Sheldrick, 2015), Olex2 (Dolomanov *et al.*, 2009)

6.4. Result and Discussion

Piperazine is known to have a solid-state structure that crystallizes in the $P2_1/n$ space group (ITIZOA) in which molecules are connected through N...H-N conventional hydrogen bonds with 2.318 Å separation distance and 170(1) ° N...H-N angle, see Fig 6.1. (Parkin *et al.*, 2004) Piperazine is very hygroscopic and a hexahydrate is formed when exposed to air.(Parkin *et al.*, 2004) The pKa of piperazine in aqueous solution at room temperature is 9.80 (Bedeković *et al.*, 2018) comparing with (pKa 8.82) for the more basic tertiary amine DABCO which has been used in previous work (Chapter 2). (Bedeković *et al.*, 2018; Kromann *et al.*, 2016)

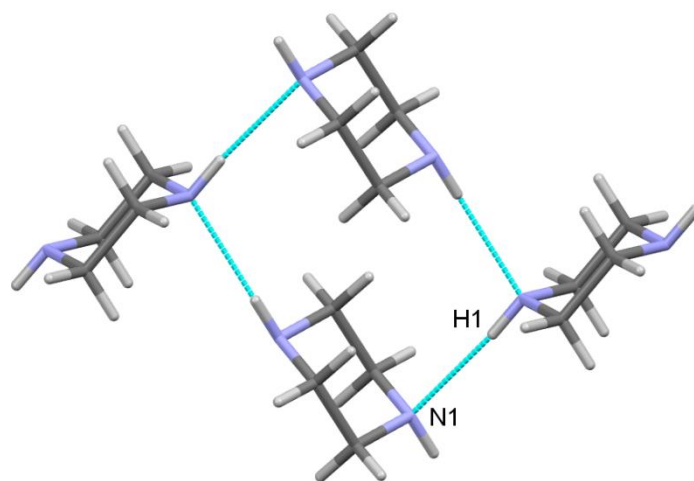


Figure 6.1 A view of intermolecular N...H hydrogen bonds (blue lines) in ITIZOA crystal structure reported by Parkin and his group, 2004. Generic atom labels without symmetry codes have been used.

We successfully prepared adduct **1a** from iodopentafluorobenzene and piperazine which resulted in clear, plate-like crystals that crystallized in a monoclinic crystal system ($P2_1/c$ space group) with one arene and half a piperazine molecule in the asymmetric unit, see Fig (6.2). The piperazine is situated on an inversion centre that resulted in four molecules related by symmetry in the unit cell, $Z=4$. The R factor was 3.54 %. The structure indicate the presence of XB between piperazine and two iodopentafluorobenzene molecules with a N...I bond distance of 2.791(4) Å, which is less than the sum of van der Waals radii, 3.53 Å, by 0.739 Å (20.9%).(Bondi, 1964; Alvarez, 2013) Comparing this distance with the one involving iodopentafluorobenzene and the tertiary amine, DABCO, (FUYFAI04 and

FUYFAI05) reported by Metrangolo and his group in 2015, which were collected at low temperature, 144 and 143 K respectively, we found that the latter have a shorter XB distances [2.699(2) and 2.709(5) Å] and more linear bond angles [177.84(9) and 178.1(2) °], compared with 174.4(2) ° in **1a**. This may related to the higher donor ability of DABCO compared with piperazine. (Metrangolo *et al.*, 2015)

The crystal packing diagram in Fig (6.3) shows an extended one-dimensional polymeric structure based on alternating N...I halogen bond and F...F interactions resulting in a zig-zag shape. The F2 atom is linked to the adjacent arene by F2...F3, 2.898(3) Å, only just shorter than twice the van der Waals radius of fluorine, 2.94 Å, by 0.042 Å, (1.4%).(Bondi, 1964; Alvarez, 2013)

There are no hydrogen bonds detected in **1a** and the formation of XB result in an elongation of the C-I covalent bond to 2.120(5) Å compared with 2.077(4) Å in pure iodopentafluorobenzene (CSD refcode ZAHGAQ). (Frohn *et al.*, 1995) This is similar to the average C-I distances that occurred in the halogen bonded adducts formed with DABCO (2.121 Å in FUYFAI04) and (2.121(6) Å in FUFAl05).(Catalano *et al.*, 2015)

The rest of the observed bond lengths in **1a** are given in Table (6.2), and the average C-N and C-C bond length 1.477(6) and 1.501(7) Å are comparable with the average values reported at 150 K for pure colourless plate crystal piperazine ITIZOA grown in ethanol (Parkin *et al.*, 2004) of 1.455(2) (5 σ) and 1.514(2) Å (6 σ). This change in C-N and C-C distance are consistent with the change in DIVCUH reported in 1,4-diiidotetrafluorobenzenewith piperazine [1.468(5), 1.511(5) Å respectively].(Cinčić *et al.*, 2008)

The average C-F bond distance in **1a**, at 1.346(5) Å, similar to the one reported 1.345(6) Å in pure iodopentafluorobenzene (CSD ref code ZAHGAQ) collected at low temperature 150 K. (Frohn *et al.*, 1995)

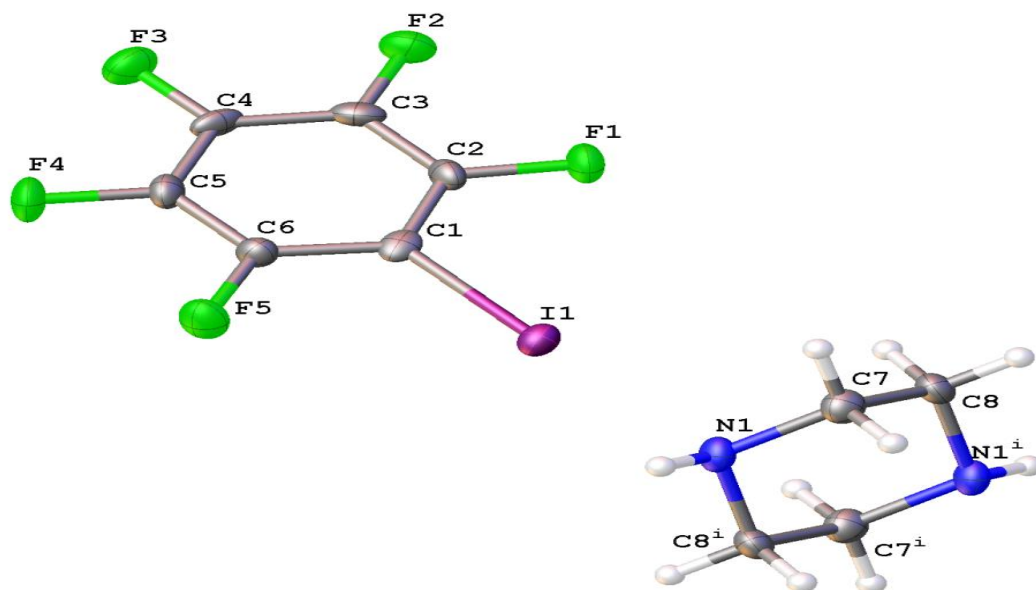


Figure 6.2 Views of the structure of halogen-bonded adduct **1a**, showing the atom numbering. Ellipsoids are drawn at 50% probability level. [Symmetry codes: (i) $-x+2, -y+2, -z+1$], colour codes: green, fluorine; blue, nitrogen; purple, iodine; white, hydrogen and grey carbon.

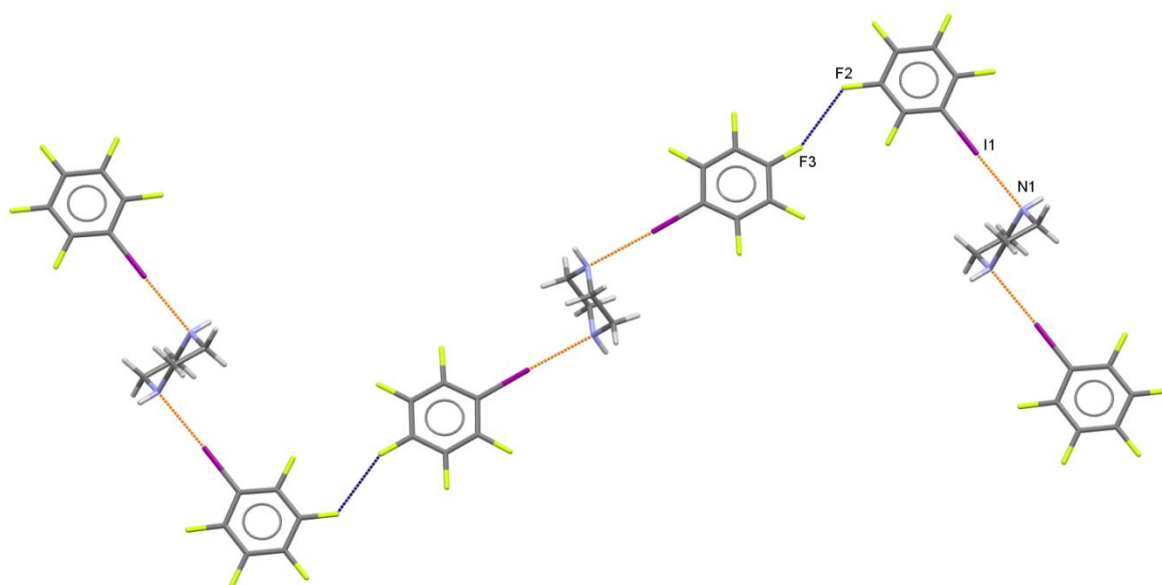


Figure 6.3 A view of intermolecular N...I halogen bonds (red lines), and F...F interactions in the crystal structure of **1a**. Generic atom labels without symmetry codes have been used. colour codes: Yellow, fluorine; blue, nitrogen; white, hydrogen, purple, iodine and grey carbon.

Table 6.2 Selected bond distances in Å for **1a**

I1—C1	2.120 (5)	C1—C2	1.373 (6)
F1—C2	1.350 (5)	C1—C6	1.391 (6)
F2—C3	1.343 (5)	C2—C3	1.383 (6)
F3—C4	1.335 (5)	C3—C4	1.378 (6)
F4—C5	1.352 (5)	C4—C5	1.364 (6)
F5—C6	1.348 (5)	C5—C6	1.374 (6)
N1—C7	1.462 (6)	C7—C8	1.501 (6)
N1—C8 ⁱ	1.491 (6)		

Symmetry code: (i) $-x+2, -y+2, -z+1$.

The second adduct is **2a** which involves 1,2-diiodotetrafluorobenzene with piperazine and revealed a structure in the $P2_1/m$ space group and an asymmetric unit consisting of half a molecule of piperazine and half a molecule of 1,2-diiodotetrafluorobenzene in a 1:1 ratio (Fig 6.4). The piperazine is situated on an inversion centre, whereas the 1,2-diiodotetrafluorobenzene is located on a mirror plane and there are 4 units related by symmetry in the unit cell.

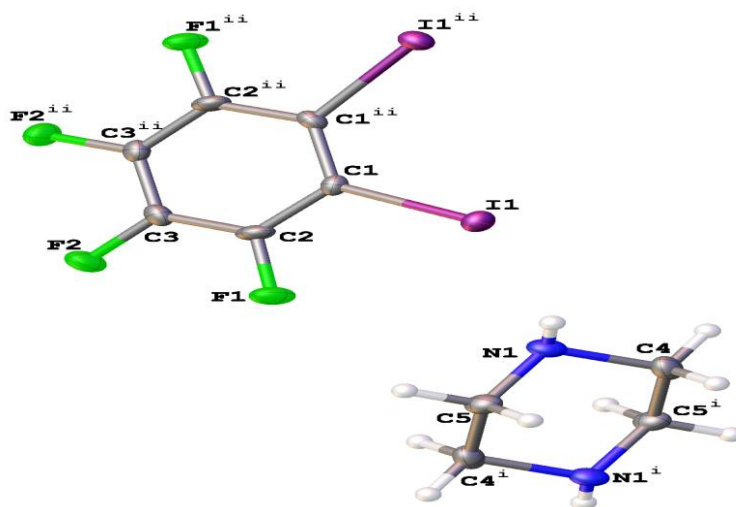


Figure 6.4 Views of the structure of halogen-bonded adduct **2a**, showing the atom numbering. Ellipsoids are drawn at 50% probability level. colour codes: green, fluorine; blue, nitrogen; purple, iodine; white, hydrogen and grey carbon. [Symmetry codes: (i) $1-x, 1-y, -1-z$ (ii) $+x, 3/2-y, +z$]

Both iodine atoms in **2a** are related by symmetry and only one N...I distance is detected, 2.937(5) Å, which is less than the sum of the van der Waals radii (3.53 Å) by 0.596 Å,

(16.9%).(Bondi, 1964; Alvarez, 2013) The extended structure displays a near linear C-I...N angle $169.5(2)^\circ$ and gives an infinite one dimensional halogen-bonded chain, (Fig. 5). Comparing the N...I halogen bond distances in **2a** with **1a**, shows that the distance in **1a** is significantly shorter than that in **2a**. This probably reflects how the greater number of fluorine atoms on the ring in **1** pulls the electron density from the single iodine centre forms a more positively charged σ hole, as has been discussed previously.(Riley *et al.*, 2009; Roper *et al.*, 2010; Riley & Merz, 2007)

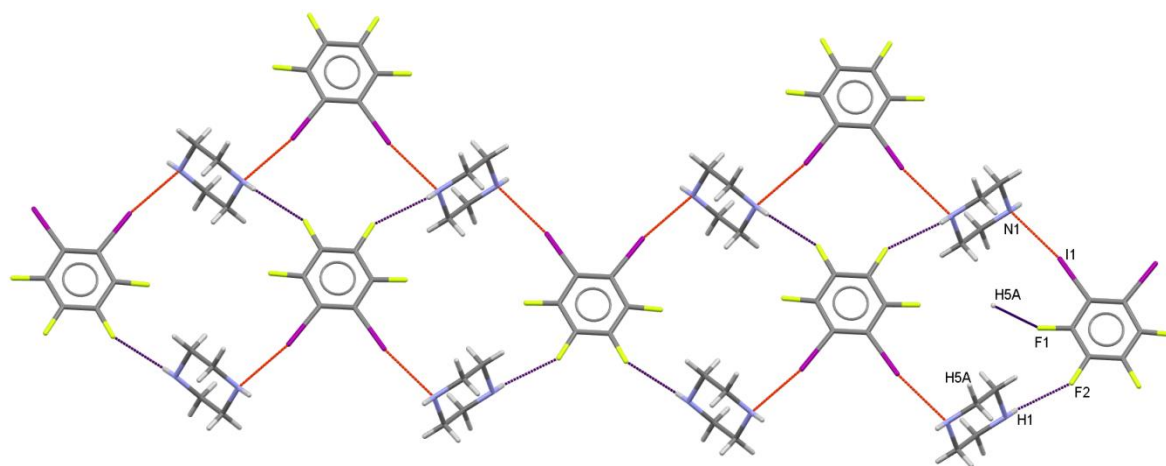


Figure 6.5 A view of intermolecular N...I halogen bonds (red lines), and F...H interactions in crystal structure **2a**, colour codes: Yellow, fluorine; blue, nitrogen; white, hydrogen; purple, iodine; and grey carbon.

Looking for any hydrogen bonds in structure **2a** revealed two weak conventional hydrogen bond [N1-H1...F2ⁱ (2.54 (6) Å) Symmetry code: (i) $x, y, z-1$] and C5-H5A...F1 2.55 Å. This is shorter than their sum of van der Waals radii 2.67 Å by 0.13 (4.9%), and 2.55 Å respectively see Table (6.3). (Bondi, 1964; Alvarez, 2013)

Table 6.3 Hydrogen-bond geometry (Å, °) for **2a**

$D-H\cdots A$	$D-H$	$H\cdots A$	$D\cdots A$	$D-H\cdots A$
$N1-H1\cdots F2^i$	0.71 (6)	2.54 (6)	2.980 (6)	123 (6)
$C5-H5A\cdots F1$	0.97	2.55	3.404 (7)	146

Symmetry code: (i) $x, y, z-1$.

As a result of N...I halogen bond formation in **2a**, an elongation in the C-I covalent bond to 2.115 (6) Å, can be detected compared with the average C-I distance of 2.086(2) Å reported for the crystal structure of pure 1,2-diiodotetrafluorobenzene (WISBOR). (Ding *et al.*, 2012)

The observed C-N and C-C bond length for **2a**, 1.472(7) and 1.508(8) Å are given in Table 6.4, and are comparable to the one observed in **1a** 1.477(6) and 1.501(7) and in DIVCUH, 1.468(5) and 1.511(5) Å reported at 180 K. (Cinčić *et al.*, 2008)

Unlike **1a** the average C-F bond distance are significantly difference 1.352(6) Å, (almost 3 σ longer), which may related to the use of F2 in short N-H...F hydrogen bond (see Table 6.3) resulted in extension in C-F bond distance from 1.345(6) to 1.352(6) Å, and F1 in C-H...F nonconventional hydrogen bond.

Table 6.4 Selected bond distances in Å for **2a**

I1—C1	2.114 (5)	C3—C3 ⁱ	1.364 (12)
F1—C2	1.332 (7)	N1—C4	1.471 (7)
F2—C3	1.352 (6)	N1—C5	1.474 (7)
C1—C1 ⁱ	1.386 (11)	C4—C5 ⁱⁱ	1.508 (8)
C1—C2	1.403 (8)	C5—C4 ⁱⁱ	1.508 (8)
C2—C3	1.377 (8)		

Symmetry codes: (i) $x, -y+3/2, z$; (ii) $-x+1, -y+1, -z-1$.

The third successfully prepared adduct in this work is **3a** and was achieved using 1,3,5-trifluoro-2,4,6-triiodobenzene (**3**) with piperazine (**a**). Interestingly, both 3:1 and 1:3 molar stoichiometric ratio mixtures of the two starting materials results in crystals with the same structure, which suggests that **3a** is the favoured structure for this combination.

Structure **3a** is found to crystallize in the triclinic $P\bar{1}$ space group, with one molecule of 1,3,4-trifluoro-2,4,6-triiodobenzene and half a molecule of piperazine in the asymmetric unit, which resulted in a 2:1 structure ratio respectively. The piperazine is located on an inversion centre and there are 2 units related by symmetry within the unit cell, see Fig (6.6).

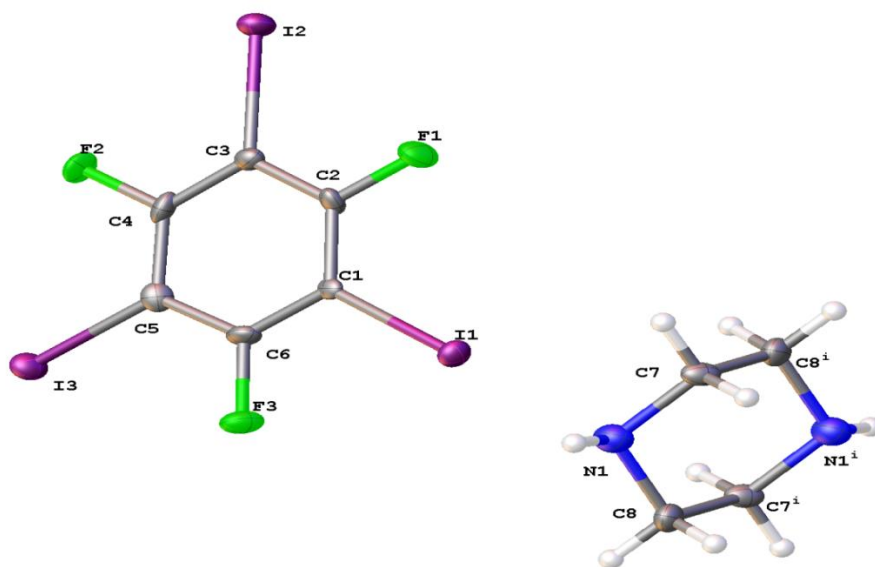


Figure 6.6 Views of the structure of halogen-bonded adduct **3a**, showing the atom numbering. Ellipsoids are drawn at 50% probability level. colour codes: green, fluorine; blue, nitrogen; purple, iodine; white, hydrogen and grey carbon. [Symmetry codes: (i)2-x, -y, 2-z]

Only one iodine atom from **3** is involved in N...I halogen bonding with a separation distance of 2.817(7) Å. This is notably short compared with the reported structures containing two iodine atoms on the ring, see Table (6.5). This interaction is characterized as a conventional halogen bond based on the near-linear C-I...N angle of 178.1(3) °. A second weak I1...I2 halogen...halogen interaction involving the negative electron density belt on I1 with I2 from a second molecule forms with a distance of 3.903(1) Å, although this is only 0.057 Å (1.4 %) and just shorter than the sum of van der Waals radii of two iodine atoms 3.96 Å. (Bondi, 1964; Alvarez, 2013) This I...I interaction cannot be detected in **1a**, **2a** nor in previously reported (CSD refcode WIGTAK and DIVCUH). (Bedekević *et al.*, 2018; Cinčić *et al.*, 2008)

Table 6.5 N...I halogen-bond distances (Å) and angles (°) in the current work and previously reported structures.

Entry	Donor	N...I/Br (Å)	Distance and % shorter than sum of vdW	N...I/Br-C (°)	C-I/Br (Å)	Reference
1	1-C ₆ I ₂ F ₅ (1a)	2.791(4)	0.739 20.9%	174.4(2)	2.120(5)	This work
2	1,2-C ₆ I ₂ F ₄ (2a)	2.937(5)	0.593 16.8%	169.5(2)	2.115(6)	This work
3	1,3-C ₆ I ₂ F ₄ WIGTAK	2.852(7) _{ave}	0.68 19.2%	177.5(2) _{ave}	2.112(7)	(Bedeković <i>et al.</i> , 2018)
4	1,4-C ₆ I ₂ F ₄ DIVCUH	2.842(3)	0.69 19.5%	176.9(1)	2.108(3)	(Cinčić <i>et al.</i> , 2008)
5	1,3,5-C ₆ I ₃ F ₃ (3a)	2.817(7)	0.713 20.2%	178.1(3)	2.131(7)	This work

The C1-I1 bond distance is found to increase from the average distance reported in (UCEPEY01), of 2.090(4) Å for pure **3** (reported at a lower temperature, 120K) (Lucassen *et al.*, 2007) to 2.131(7) Å in **3a**. This distance is slightly longer than the C1-I1, 2.111(4) in the DABCO analogue DATCIM. (Pfrunder *et al.*, 2012)

Offset $\pi \dots \pi$ stacking (Janiak, 2000) between the benzene rings is detected only in **3a** and is characterized by a centroid-centroid distance of 3.832 Å. This distance is slightly shorter than 3.872 Å reported by Pfrunder and his group for the DABCO analogue (DATCIM) at 173 K. (Pfrunder *et al.*, 2012)

Hydrogen bonds in this structure are formed from N1-H1...I2ⁱ [Symmetry codes: (i) $-x+2, -y+1, -z+1$] (3.07(8) Å, shorter than the sum of van der Waals of H=1.20 and I= 1.98 Å by 0.109 Å (3.43 %), see Fig (6.7). While a stronger non-conventional C7-H7A...F2ⁱⁱ interaction, [Symmetry codes: (ii) $x+1, y-1, z+1$] 2.42 Å, which is (9.5%) shorter than the sum of van der Waals of F =1.47 and H =1.20 Å, see Table (6.6), is also observed. (Bondi, 1964; Alvarez, 2013)

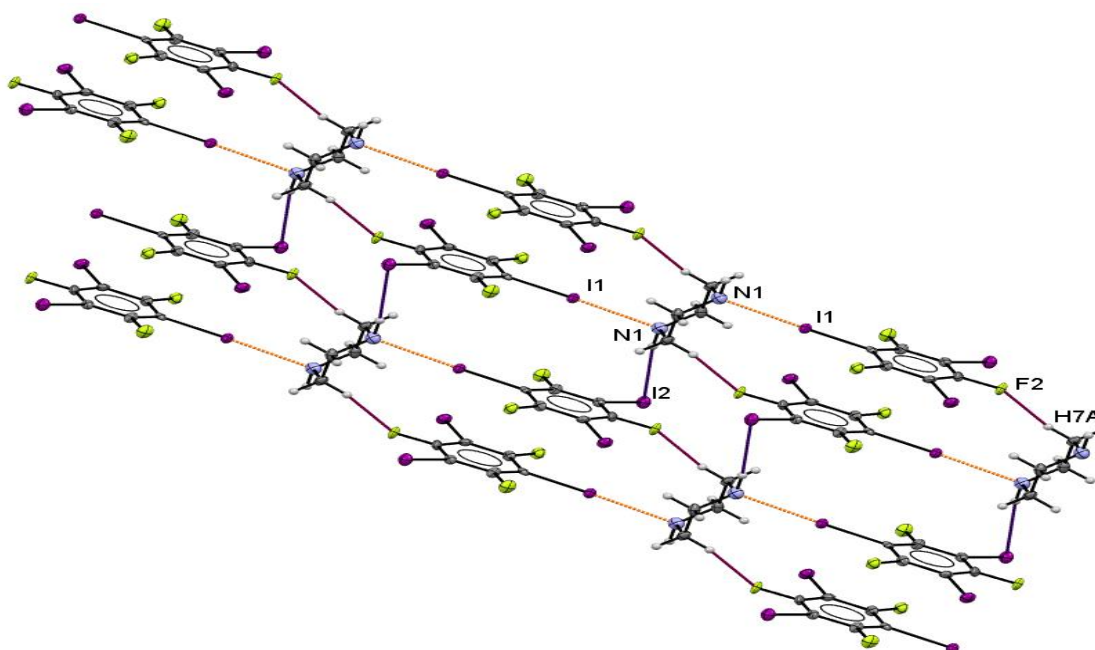


Figure 6.7 A view of intermolecular N...I halogen bonds (red lines), F...H and I...H interactions in crystal structure **3a**. Generic atom labels without symmetry codes have been used. colour codes: Yellow, fluorine; blue, nitrogen; white, hydrogen; purple, iodine; and grey carbon.

Table 6.6 Hydrogen-bond geometry (Å, °) for **3a**

$D-H\cdots A$	$D-H$	$H\cdots A$	$D\cdots A$	$D-H\cdots A$
N1—H1...I2 ⁱ	0.91 (8)	3.07 (8)	3.965 (8)	169 (7)
C7—H7A...F2 ⁱⁱ	0.97	2.42	3.297 (8)	151

Symmetry codes: (i) $-x+2, -y+1, -z+1$; (ii) $x+1, y-1, z+1$.

The observed C-N and C-C distances in **3a** are listed in Table 6.7, and are both significantly changed to 1.480(11) and 1.496(11) Å comparing with the pure piperazine, ITIZOA, [1.455(2) and 1.514(2) Å] (Parkin *et al.*, 2004) and consistent with **2a** and similar to **1a** values 1.477(6) and 1.501(7) Å respectively. The average C-F bond distance of 1.345(5) Å reported in pure 1,3,5-trifluoro-2,4,6-triiodobenzene (UCEPEY01) (Lucassen *et al.*, 2007) extend to average of 1.350(8) Å about 1σ longer than **3a**.

Table 6.7 Selected bond distances in Å for **3a**

I1—C1	2.131 (7)	C5—C6	1.395 (10)
I2—C3	2.108 (7)	N1—H1	0.91 (8)
I3—C5	2.062 (8)	N1—C7	1.484 (11)
F1—C2	1.348 (9)	N1—C8	1.475 (10)
F2—C4	1.356 (8)	C7—H7A	0.9700
F3—C6	1.347 (8)	C7—H7B	0.9700
C1—C2	1.372 (10)	C7—C8 ⁱ	1.496 (11)
C1—C6	1.387 (11)	C8—C7 ⁱ	1.496 (11)
C2—C3	1.375 (9)	C8—H8A	0.9700
C3—C4	1.370 (11)	C8—H8B	0.9700
C4—C5	1.391 (11)		

Symmetry code: (i) $-x+2, -y, -z+2$.

Table 6.8 Intermolecular interactions in (Å) less than the sum of the van der Waals radii observed in iodine containing adducts and related structures.

En try	Donor	F...F (Å)	N-H...F* N-H...I** (Å)	I...I Br...Br (Å)	π - π stacking (Å)	Reference
1	1-C ₆ I ₅ (1a)	2.898(3)	-	-	-	This work
2	1,2-C ₆ I ₂ F ₄ (2a)	-	2.53(6)*	-	-	This work
3	1,3-C ₆ I ₂ F ₄ WIGTAK	2.910(5)	2.36(6)*	-	-	(Bedeković <i>et al.</i> , 2018)
4	1,4-C ₆ I ₂ F ₄ DIVCUH	-	3.1265**	-	-	(Cinčić <i>et al.</i> , 2008)
5	1,3,5-C ₆ I ₃ F ₃ (3a)	-	3.07(8)**	3.903(1)	3.832	This work

Moving to the successfully prepared adducts involving bromofluorobenzenes with piperazine; the only reported adduct of this kind involves 1,4-dibromotetrafluorobenzene and piperazine (DIVDOC) prepared by Cinic and his group by grinding the starting materials with nitromethane followed by collecting X-ray single crystal data at 180K. (Cinčić *et al.*, 2008)

Adduct **4a** is the second structure to involve 1,2-dibromotetrafluorobenzene (**4**) with piperazine and results in light orange crystals from which a single crystal with dimensions of 0.1x0.05x0.02 mm was picked and subject to single crystal analysis at 150 K. The compound crystallized in the $P-1$ space group with one molecule of **4** and half a molecule of piperazine in the asymmetric unit, see Fig (6.8), and results in 2:1 structure ratio respectively. Similar to all the reported structures within this work, piperazine is located on an inversion centre and there are 2 units related by symmetry in the unit cell.

Unlike the iodine analogue, structure (**2a**), only one bromine atom is involved in halogen bonding with a N...Br separation of 2.875(7) Å, which is less than the sum of the van der Waals radii for nitrogen and bromine of 3.40 Å. (Bondi, 1964, Alvarez, 2013) This distance is slightly longer than that found for the adduct of 1,2-dibromotetrafluorobenzene and DABCO, 2.77(1) Å, obtained in our previous work. (Chapter 2) This is presumably related to DABCO being a better electron-donor.

The C-Br...N covalent bond angle of **4a** is 177.8(2) ° which is close to linear and consistent with the angles known for XB interactions.

The C1-Br1 covalent bond distance is found to be longer than the reported distance, 1.887(2) Å, for (DIVDOC) (Cinčić *et al.*, 2008) to 1.900(5) Å in **4a**, which is in line with the N...Br halogen bond short distance.

The same bromine atom uses the negative electron density belt that appears on Br1 to form a weak Br1...H1-N1 hydrogen bond, see Fig (6.9), with a distance of 2.90(6) Å, which is 0.15 Å (4.9 %) slightly shorter than the sum of van der Waals radii of bromine and hydrogen atoms of 3.05 Å, see Table (6.9). (Bondi, 1964; Alvarez, 2013) This distance is shorter than the Br...H-N distance (2.9414 Å) reported in (DIVDOC) of 1,4-diiidotetrafluorobenzene. (Cinčić *et al.*, 2008)

Similar to structure **1a**, F...F interactions appear to join the adjacent arenes, with distances F3...F4, 2.888(6) Å, and F4...F4, 2.812(6) Å. These are 0.05 Å (1.7%) and 0.12 Å (4.4%) just shorter than the sum of van der Waals radii of two fluorine atoms, 2.94 Å. (Bondi, 1964; Alvarez, 2013)

The remaining parameters in **4a** are listed in Table 6.10 and show increasing C-N distance 1.467(9) Å and decreasing the C-C distance to 1.511(10) in the piperazine fragment, similar to **1a**, **2a** and **3a** and the reported structure based on 1,4-dibromotetrafluorobenzene and piperazine (DIVDOC). (Cinčić *et al.*, 2008) However there are no reported structural data for 1,2-dibromotetrafluorobenzene systems with which to make a direct comparison of C-F distances.

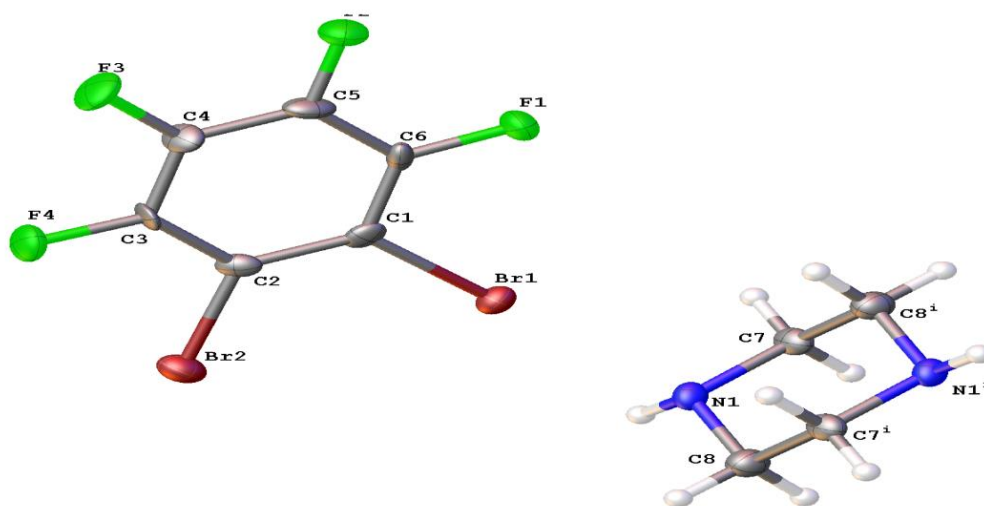


Figure 6.8 Views of the structure of halogen-bonded adduct **4a**, showing the atom numbering. Ellipsoids are drawn at 50% probability level. colour codes: brown, bromine; green, fluorine; blue, nitrogen; white, hydrogen and grey carbon. [Symmetry codes: (i) $-x, 2-y, 1-z$]

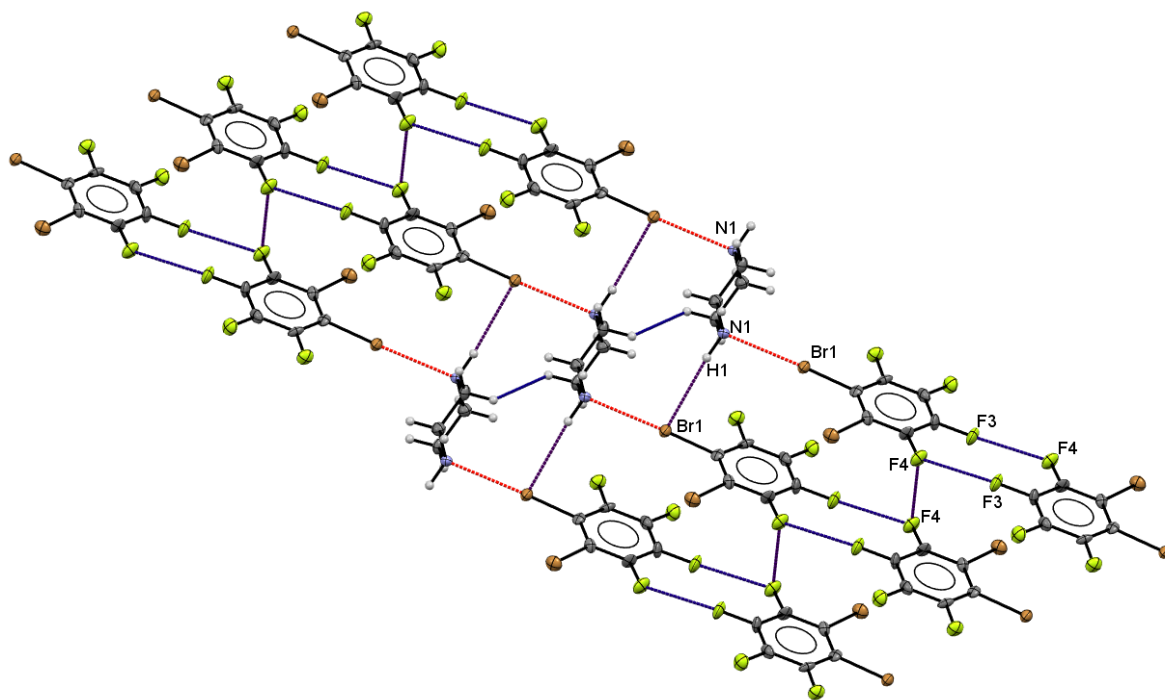


Figure 6.9 A view of intermolecular N...Br (red lines) halogen bonds, F...F and Br...H interactions in crystal structure **4a**. Generic atom labels without symmetry codes have been used. colour codes: brown, bromine; yellow, fluorine; blue, nitrogen; white, hydrogen and grey carbon.

Table 6.9 Hydrogen-bond geometry (Å, °) for **4a**.

$D-H\cdots A$	$D-H$	$H\cdots A$	$D\cdots A$	$D-H\cdots A$
$N1-H1\cdots Br1^i$	0.98 (7)	2.90 (7)	3.826 (6)	156 (5)

Symmetry code: (i) $x-1, y, z$.

Table 6.10 Selected bond distances in Å for **4a**

Br1—C1	1.900 (3)	C4—C3	1.3900
Br2—C2	1.864 (3)	N1—H1	0.98 (7)
F1—C6	1.327 (5)	N1—C7	1.473 (9)
F2—C5	1.329 (5)	N1—C8	1.461 (9)
F3—C4	1.331 (5)	C7—H7A	0.9700
F4—C3	1.315 (5)	C7—H7B	0.9700
C2—C1	1.3900	C7—C8 ⁱ	1.511 (10)
C2—C3	1.3900	C8—C7 ⁱ	1.511 (10)
C1—C6	1.3900	C8—H8A	0.9700
C6—C5	1.3900	C8—H8B	0.9700
C5—C4	1.3900		

Symmetry code: (i) $-x, -y+2, -z+1$.

The last reported structure in this work resulted from adduct **5a**, which involves 1,3-dibromotetrafluorobenzene and piperazine. A plate-shaped colourless single crystal (0.02x0.1x0.2 mm) was selected. The resulting compound is found to crystallise in the triclinic $P\bar{1}$ space group, similar to structures **3a**, **4a** and for that previously reported, DIVDOC, see Table (1). (Cinčić *et al.*, 2008)

One positionally disordered 1, 3-dibromotetrafluorobenzene molecule and half a piperazine molecule appeared in the asymmetric unit, Fig (6.10). Furthermore, the crystal packing also shows a 2:1 arene to piperazine ratio in the unit cell similar to **3a** and **4a** and similar to all of those structures the piperazine is located on an inversion centre.

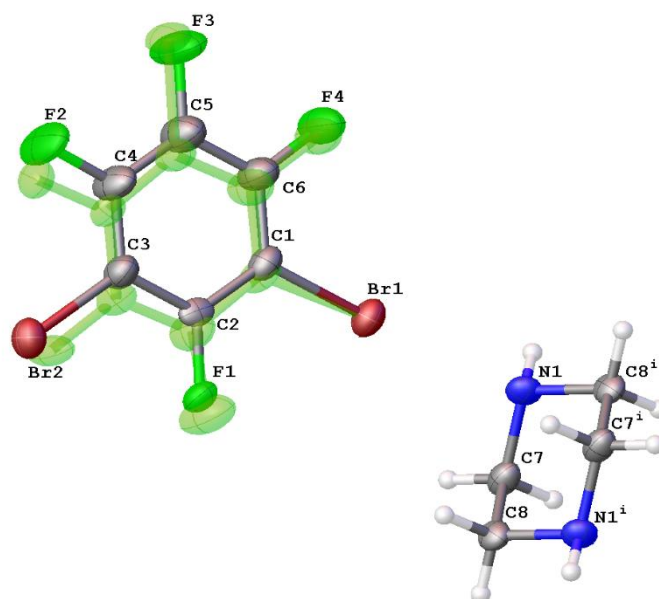


Figure 6.10 Views of the structure of halogen-bonded adduct **5a**, showing the atom numbering, the alternate disordered positions of atoms of the arene are shown shadowed. Ellipsoids are drawn at 50% probability level, colour codes: brown, bromine; green, fluorine; blue, nitrogen; white, hydrogen and grey carbon. [Symmetry codes: (i) $-x, 1-y, 1-z$].

Similar to structure **4a** only one bromine atom is involved in N...Br halogen bonding in **5a** with 2.876(6) Å distance. This distance is shorter than the sum of van der Waals radii (3.40 Å) and similar to the distance in DIVDOC, (Cinčić *et al.*, 2008) of 2.881(2) Å, see Table (6.11).

Table 6.11 N...Br halogen-bond distances (Å) and angles (°) in the current work and previously reported structures.

Entry	Donor	N...Br (Å)	Distance and % shorter than sum of vdW	N...Br-C (°)	C-Br (Å)	Reference
1	1,2-C ₆ Br ₂ F ₄ (4a)	2.875(7)	0.53 15.4%	177.8(2)	1.900(5)	This work
2	1,3-C ₆ Br ₂ F ₄ (5a)	2.876(6)	0.524 15.4%	175.9(4)	1.90(1)	This work
3	1,4-C ₆ Br ₂ F ₄ (DIVDOC)	2.881(2)	0.519 15.3%	177.72(7)	1.887(2)	(Cinčić <i>et al.</i> , 2008)

This interaction is characterized by a near-linear C-Br...N angle of 175.9(4) ° but less linear than that found for the **4a** structure which involves 1,2-dibromotetrafluorobenzene and piperazine. The second bromine atom used the negative electron density belt on Br1 to form a weak Br1...Br2, halogen...halogen interaction with a distance of 3.505(2) Å, only 0.20 Å (5.3 %) slightly shorter than the sum of the van der Waals radii of two bromine atoms of 3.7 Å. (Bondi, 1964; Alvarez, 2013)

Similar to **4a**, F...F interactions can be seen in the crystal packing between F3 of one molecule and F3 from a second one, Fig (6.11), with an F...F distance of 2.62(1) Å, less than twice the van der Waals radius of fluorine, 2.94 Å, by 0.3 Å. (Bondi, 1964; Alvarez, 2013)

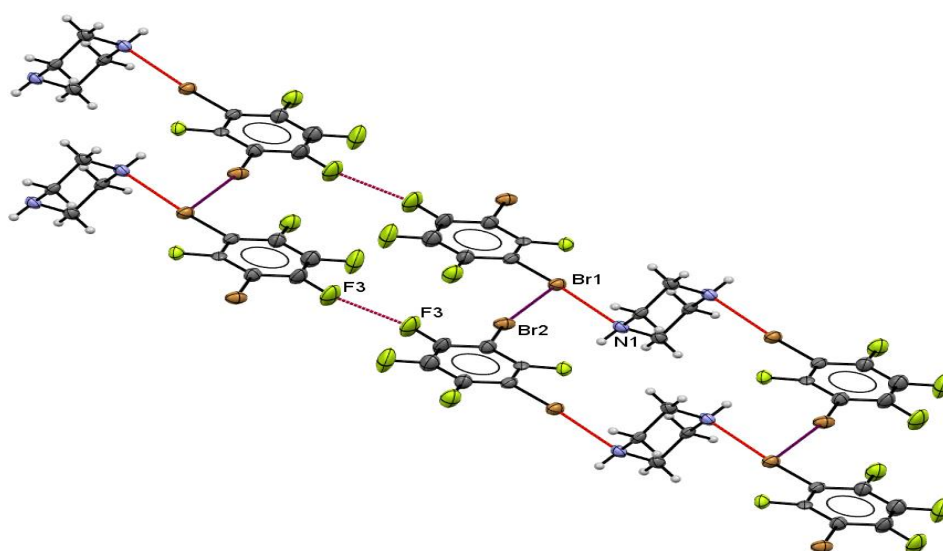


Figure 6.11 A view of intermolecular N...Br halogen bonds (red lines), Br...Br and F...H interactions in crystal structure **5a**. colour codes: brown, bromine; yellow, fluorine; blue, nitrogen; white, hydrogen and grey carbon.

The C1-Br1 bond distance in **5a** is found to extend to 1.91(1) Å, which is longer than that reported 1.887(2) Å in DIVDOC (Cinčić *et al.*, 2008) and similar to 1.900(5) Å found in **4a**.

There is a very weak hydrogen bond in **5a** formed by N1-H1...Br2 (3.04(6) Å, which is 0.01 Å (0.3 %) only just shorter than the sum of van der Waals radii of Br =1.85 and H =1.20 Å, Table 6.12. This distance is even weaker than the one in **4a** and DIVDOC, see Table (6.12).(Bondi, 1964; Alvarez, 2013)

The other bond distances in structure **5a** are listed in Table 6.13. Comparing the average C-N observed distance in **5a**, 1.471(8) Å are slightly longer than the one reported in DIVDOC (Cinčić *et al.*, 2008) 1.467(3) Å and the one observed in **4a**, 1.467(9) Å. However the C-C distance in **5a** and DIVDOC (Cinčić *et al.*, 2008) are slightly higher 1.523(8) (1 σ) and 1.520(3) Å (2 σ) and does not follow the expected lower distance similar to the reported in DIVCUH, **1a**, **2a**, **3a**, **4a**, and compared with the reported C-C distance for pure piperazine (CSD refcode ITIZOA) 1.514(2) Å. (Parkin *et al.*, 2004) Only C5-F3 covalent bond distance in **5a** elongated to 1.349(13) Å, comparing with the average C-F bond distances 1.342(3) Å detected in pure 1,3-diiodotetrafluorobenzene structure (CSD refcode PASKUR) (Nayak *et al.*, 2012).

Table 6.12 Hydrogen-bond geometry (Å, °) for **5a**

<i>D</i> —H··· <i>A</i>	<i>D</i> —H	H··· <i>A</i>	<i>D</i> ··· <i>A</i>	<i>D</i> —H··· <i>A</i>
N1—H1···Br2 ⁱ	0.86 (6)	3.04 (6)	3.572 (6)	122 (5)

Symmetry code: (i) $x-1, y+1, z$.

Table 6.13 Selected bond distances in Å for **5a**.

Br1—C1	1.909 (5)	C7—C8	1.523 (8)
Br1—C1A	1.886 (11)	N1—C8 ⁱ	1.468 (8)
F3—C5	1.349 (13)	C8—N1 ⁱ	1.468 (8)
F1—C2	1.322 (9)	F1A—C2A	1.333 (18)
F2—C4	1.333 (6)	F4A—C6A	1.322 (18)
C2—C1	1.3900	F3A—C5A	1.355 (19)
C2—C3	1.3900	Br2A—C3A	1.844 (14)
C1—C6	1.3900	F2A—C4A	1.332 (13)
C6—C5	1.3900	C6A—C1A	1.3900
C6—F4	1.326 (9)	C6A—C5A	1.3900
C5—C4	1.3900	C1A—C2A	1.3900
C4—C3	1.3900	C2A—C3A	1.3900
C3—Br2	1.868 (6)	C3A—C4A	1.3900
C7—N1	1.473 (8)	C4A—C5A	1.3900

Symmetry code: (i) $-x, -y+1, -z+1$.

Comparing the other weak interactions that appear in structures **4a** and **5a** with the only reported structure for a similar system (DIVDOC), Table (6.14), we can see that a Br...Br interaction is detected in **5a** which is not there in **4a** and DIVDOC. (Cinčić *et al.*, 2008) Furthermore, the F...F interaction in **5a** [2.62(1) Å] is significantly shorter than those detected in **4a**, 2.888(6) and 2.812(6) Å.

Table 6.14 Intermolecular interactions in (Å) less than the sum of the van der Waals radii observed.

Entry	Donor	F...F (Å)	N-H...F* N-H...Br** (Å)	Br...Br (Å)	π - π stackin g(Å)	Reference
1	1,2-C ₆ Br ₂ F ₄ (4a)	2.888(6) 2.812(6)	2.90(6)**	-	-	This work
2	1,3-C ₆ Br ₂ F ₄ (5a)	2.62(1)	3.04(6)**	3.505(2)	-	This work
3	1,4-C ₆ Br ₂ F ₄ (DIVDOC)	-	2.9414**	-	-	(Cinčić <i>et al.</i> , 2008)

To analyze the halogen bond interactions, especially in terms of their relative strength, QTAIM analysis of the bond critical points (BCPs) were undertaken using the GAMESS program (Schmidt *et al.*, 1993) to calculate electron densities for each structure and QTAIM analysis and visualization using Multiwfn software. (Lu & Chen, 2012)

Using this approach, the following parameters were determined: BCP electron densities, ρ_{BCP} , Laplacians, $\nabla^2\rho_{\text{BCP}}$, and total electronic energies, H_{BCP} . These are summarised for each structure in Table 13 and show medium-strength halogen bond interactions based on the proposal of Rozas *et al.* (Rozas *et al.*, 2000)

Figs 6.12 to 6.16 shows representations of the crystal structure and the corresponding molecular graph generated using the Multiwfn programme.

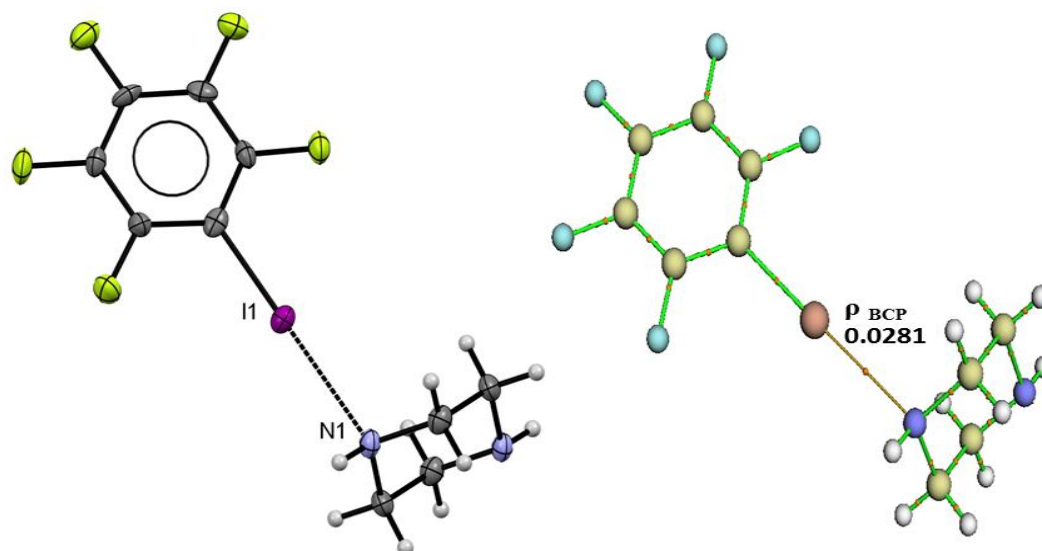


Figure 6.12 The determined X-ray structure (left) and molecular graph (right) with the related electron density ρ_{BCP} for adducts **1a**

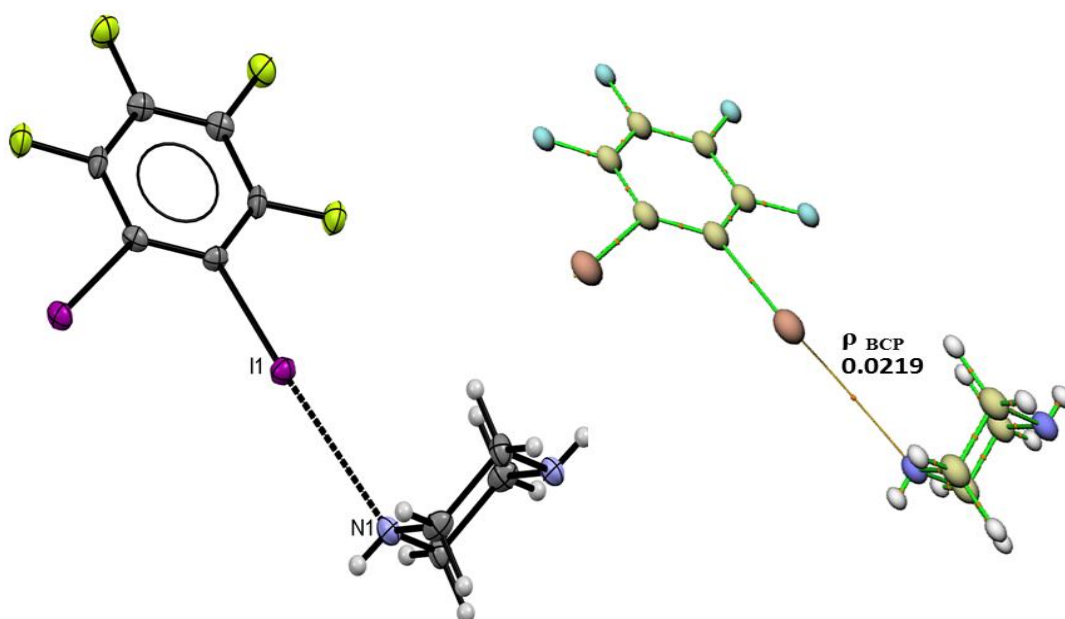


Figure 6.13 The determined X-ray structure (left) and molecular graph (right) with the related electron density ρ_{BCP} for adducts **2a**

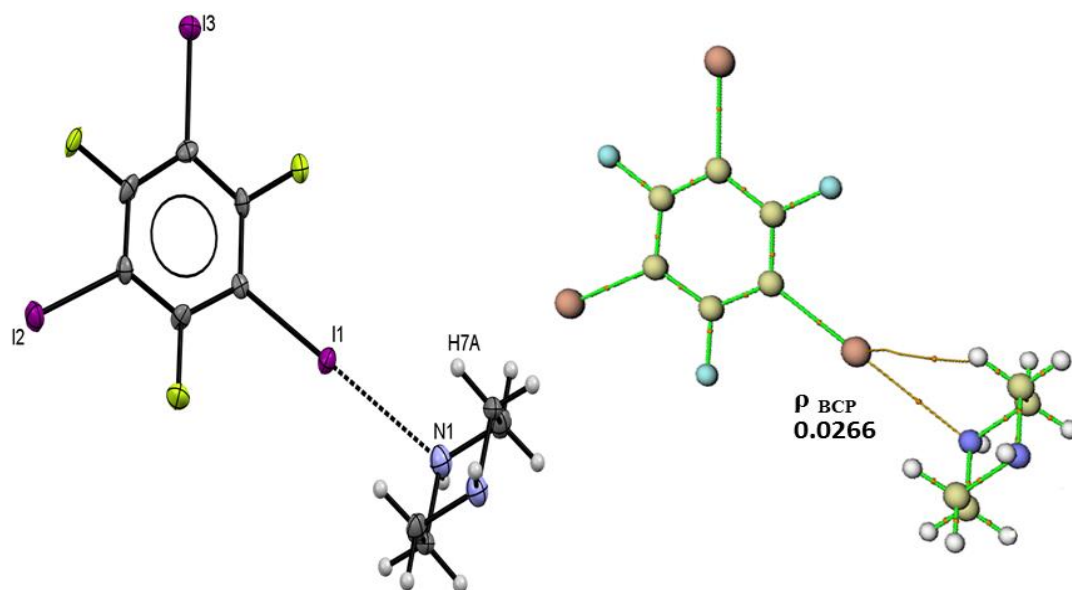


Figure 6.14 The determined X-ray structure (left) and molecular graph (right) with the related electron density ρ_{BCP} for adducts **3a**

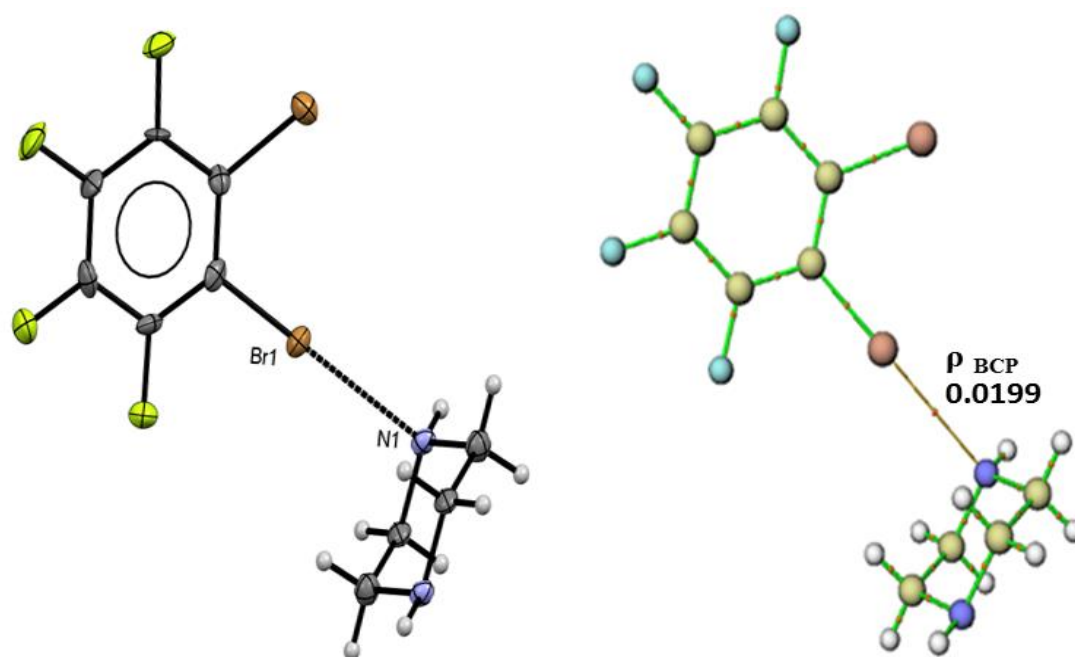


Figure 6.15 The determined X-ray structure (left) and molecular graph (right) with the related electron density ρ_{BCP} for adducts **4a**

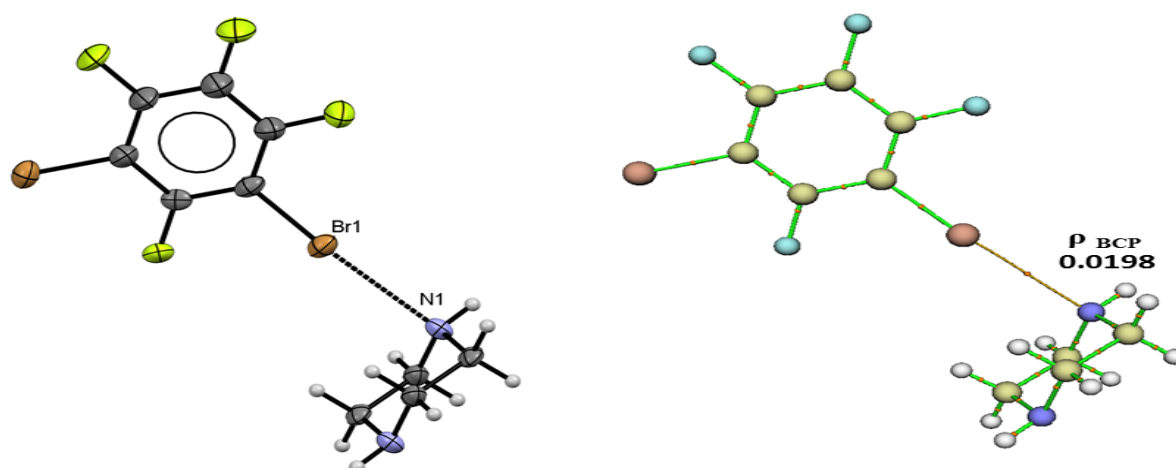


Figure 6.16 The determined X-ray structure (left) and molecular graph (right) with the related electron density ρ_{BCP} for adducts **5a**

A strong correlation was observed between the crystallographically-observed N...I distances and the QTAIM parameters. The shorter the distance the higher the electron density, ρ_{BCP} .

Comparing the structures reported in this study, we found that **1a** has the shortest N2...I1, halogen bond distance of 2.791(4) Å in X-ray crystal structure. The QTAIM results support this, by showing the highest electron density, ρ_{BCP} , positive Laplacian, $\nabla^2\rho_{\text{BCP}}$, and a negative value of the local electron energy density, H_{BCP} , for the corresponding (3, -1) bond critical point, see [Table \(6.15\)](#).

An interesting observation found in structure **3a**, [Fig \(6.14\)](#), that QTAIM found an I...H interaction that is not located in the crystallographic data and it is (3.463 Å) longer than the sum of van der Waals radii of iodine and hydrogen (3.18 Å) and gives significantly lower electron density ρ_{BCP} value 0.00455 a.u.

Table 6.15 Topological parameters calculated at B3LYP/6-311G** level of theory

Trimer	Interaction	X...B (Å)	ρ_{BCP} (a.u)	$\nabla^2\rho_{\text{BCP}}$ (a.u)	H(r) (a.u)
1a	N2...I1	2.791(4)	0.0281	0.0753	-0.0004640
2a	N1...I1	2.937(5)	0.0219	0.0593	0.0002274
3a	N1...I1	2.817(7)	0.0266	0.112	0.0025784
4a	N1...Br1	2.875(7)	0.0199	0.0627	0.0008580
5a	N2...Br1	2.876(6)	0.0198	0.0622	0.0008500

In conclusion we have obtained and described the crystal structure of 5 halogen bonded adducts from iodo and bromo-substituted fluoroaromatic compounds and piperazine. However 2:1 molar ratio of arene to piperazine starting materials were used in case of adduct **1a**, **2a**, **4a**, **5a** and 3:1 in **3a**, but 2:1 ratio were observed in their crystal structure. Even though adduct **3a** prepared using different molar ratio (3:1 and 1:3), but both of them ends with the same 2:1 stoichiometric structure of arene and piperazine. N...I/Br halogen bonds replace the previous N...H-N hydrogen bond in pure piperazine (Fig. 6.1).

Infrared spectroscopy indicate that the broad peak above 3000 cm^{-1} which represent the hydrogen bonds is no longer present in all adduct spectra. The IR data also supports the existence of the halogen bond in all the reported adducts in the solid state by showing changes in C-H and C-F absorption bands between the starting materials and their adducts spectra. However C-I stretches modes, usually appears less than 500 cm^{-1} , (Cavallo *et al.*, 2016) can provide a useful tool to support the existence of C-I...N halogen bond, but unfortunately it lies beyond the measurements range of our instrument ($500\text{-}4000\text{ cm}^{-1}$).

The strongest N...I halogen bond and shortest bond distance is detected in structure **1a** which has the highest number of fluorine atoms on the ring, and the strength of this interaction is supported theoretically by showing the highest electron density, ρ_{BCP} , positive Laplacian, $\nabla^2\rho_{\text{BCP}}$, and the only negative sign in total electron density energy, H_{BCP} .

Structure **2a** is the only structure that shows the formation of a polymeric long chain of strong N...I halogen bonds, however the rest shows a combination of traditional N...I and halogen...halogen interactions, when expanding the structure.

^{19}F NMR data shows no significant changes between the dissolved adduct and starting compounds which indicate the inability of the XB to remain in the solution phase.

References

- Alvarez, S. (2013). *Dalt. Trans.* **42**, 8617–8636.
- Angelina, E. L., Duarte, D. J. R. & Peruchena, N. M. (2013). *J. Mol. Model.* **19**, 2097–2106.
- Bader, R. F. W. & Essén, H. (1984). *J. Chem. Phys.* **80**, 1943–1960.
- Bedeković, N., Stilinović, V., Friščić, T. & Cinčić, D. (2018). *New J. Chem.* **42**, 10584–10591.
- Bondi, A. (1964). *J. Phys. Chem.* **68**, 441–451.
- Bourhis, L. J., Dolomanov, O. V, Gildea, R. J., Howard, J. A. K. & Puschmann, H. (2015). *Acta Crystallogr. Sect. A Found. Adv.* **71**, 59–75.
- Catalano, L., Pérez-Estrada, S., Terraneo, G., Pilati, T., Resnati, G., Metrangolo, P. & Garcia-Garibay, M. A. (2015). *J. Am. Chem. Soc.* **137**, 15386–15389.
- Cavallo, G., Metrangolo, P., Milani, R., Pilati, T., Priimagi, A., Resnati, G. & Terraneo, G. (2016). *Chem. Rev.* **116**,.
- Cinčić, D., Friščić, T. & Jones, W. (2008). *Chem. Eur. J.* **14**, 747–753.
- Clark, T., Hennemann, M., Murray, J. S. & Politzer, P. (2007). *J. Mol. Model.* **13**, 291–296.
- Cremer, D. & Kraka, E. (1984). *Croat. Chem. Acta.* **57**, 1259–1281.
- De Santis, A., Forni, A., Liantonio, R., Metrangolo, P., Pilati, T. & Resnati, G. (2003). *Chem. - A Eur. J.* **9**, 3974–3983.
- Ding, X., Tuikka, M. & Haukka, M. (2012). *Recent Adv. Crystallogr.* **262**, 143–168.
- Dolomanov, O. V, Bourhis, L. J., Gildea, R. J., Howard, J. A. K. & Puschmann, H. (2009). 2008–2010.
- Frohn, H. J., Görg, S., Henkel, G. & Läge, M. (1995). *Zeitschrift Für Anorganische Und Allgemeine Chemie.* **621**, 1251–1256.
- Grabowski, S. J. (2012). *J. Phys. Chem. A.* **116**, 1838–1845.
- Grabowski, S. J. (2013). *Phys. Chem. Chem. Phys.* **15**, 7249–7259.

- Groom, C. R., Bruno, I. J., Lightfoot, M. P. & Ward, S. C. (2016). *Acta Crystallogr. Sect. B Struct. Sci. Cryst. Eng. Mater.* **72**, 171–179.
- Janiak, C. (2000). *J. Chem. Soc. Dalt. Trans.* 3885–3896.
- Jenkins, S. & Morrison, I. (2000). *Chem. Phys. Lett.* **317**, 97–102.
- Jensen, J. H., Koseki, S., Matsunaga, N., Nguyen, K. A., Su, S., Windus, T. L., Dupuis, M., Jr, J. A. M., Schmidt, M. W., Baldridge, K. K., Boatz, J. A., Elbert, S. T. & Gordon, M. S. (1993). *J. Comput. Chem.* **14**, 1347–1363.
- Kromann, J. C., Larsen, F., Moustafa, H. & Jensen, J. H. (2016). *PeerJ.* **2016**,.
- Li, S., Xu, T., van Mourik, T., Früchtl, H., Kirk, S. R. & Jenkins, S. (2019). Halogen and Hydrogen Bonding in Halogenbenzene/NH₃ Complexes Compared Using Next-Generation QTAIM Multidisciplinary Digital Publishing Institute.
- Liantonio, R., Metrangolo, P., Pilati, T., Resnati, G. & Stevenazzi, A. (2003). *Cryst. Growth Des.* **3**, 799–803.
- Lu, T. & Chen, F. (2012). *J. Comput. Chem.* **33**, 580–592.
- Lucassen, A. C. B., Karton, A., Leitus, G., Shimon, L. J. W., Martin, J. M. L. & van der Boom, M. E. (2007). *Cryst. Growth Des.* **7**, 386–392.
- Marquardt, R., Politzer, P., Resnati, G., Rissanen, K., Desiraju, G. R., Ho, P. S., Legon, A. C., Kloo, L. & Metrangolo, P. (2013). *Pure Appl. Chem.* **85**, 1711–1713.
- Matta, C. F. & Boyd, R. J. (2007). *Quantum Theory Atoms Mol.* 1–34.
- Metrangolo, P., Terraneo, G., Catalano, L., Pérez-Estrada, S., Resnati, G., Garcia-Garibay, M. A. & Pilati, T. (2015). *J. Am. Chem. Soc.* **137**, 15386–15389.
- Parkin, A., Oswald, I. D. H. & Parsons, S. (2004). *Acta Crystallogr. Sect. B Struct. Sci.* **60**, 219–227.
- Pfrunder, M. C., Micalef, A. S., Rintoul, L., Arnold, D. P., Davy, K. J. P. & McMurtrie, J. (2012). *Cryst. Growth Des.* **12**, 714–724.
- Politzer, P. & Murray, J. S. (2013). *ChemPhysChem.* **14**, 278–294.

- Rigaku, O. (2018). *Rigaku Oxford Diffraction Ltd, Yarnton, Oxfordshire, Engl.*
- Riley, K. E. & Merz, K. M. (2007). *J. Phys. Chem. A* **111**, 1688–1694.
- Riley, K. E., Murray, J. S., Politzer, P., Concha, M. C. & Hobza, P. (2009). *J. Chem. Theory Comput.* **5**, 155–163.
- Roper, L. C., Präsang, C., Kozhevnikov, V. N., Whitwood, A. C., Karadakov, P. B. & Bruce, D. W. (2010). *Cryst. Growth Des.* **10**, 3710–3720.
- Rozas, I., Alkorta, I. & Elguero, J. (2000). *J. Am. Chem. Soc.* **122**, 11154–11161.
- Schmidt, M. W., Baldrige, K. K., Boatz, J. A., Elbert, S. T., Gordon, M. S., Jensen, J. H., Koseki, S., Matsunaga, N., Nguyen, K. A., Su, S., Windus, T. L., Dupuis, M. & Montgomery Jr, J. A. (1993). *J. Comput. Chem.* **14**, 1347–1363.
- Sheldrick, G. M. (2015). *Acta Crystallogr. Sect. A Found. Crystallogr.* **71**, 3–8.
- Tuikka, M., Niskanen, M., Hirva, P., Rissanen, K., Valkonen, A. & Haukka, M. (2011). *Chem. Commun.* **47**, 3427–3429.

Chapter 7.

Conclusions and Future work

Based on the halogen bond work previously done by our group ¹ using aliphatic and one aromatic fluorinated compound and DABCO, a further study was undertaken using a variety of iodo/bromofluorobenzenes as halogen bond donors and different nitrogen based XB acceptors to investigate the possibility and extent of halogen bond formation. In total over 300 experiments were conducted to study the possibility to form halogen bonds between 19 different bromo- and iodofluorobenzenes and eight nitrogen-containing Lewis bases with lone pairs of electrons. Two main techniques of growing crystals have been used (vapour diffusion and slow evaporation) and different molar ratios have been tested to see if this will result in different halogen bonded structures and motifs. A number of solid N...I and N...Br halogen bonded adducts have been achieved. Several characterisation techniques have been used to study these resulted adducts, however, X-ray single crystal diffraction studies have been the main technique used to collect crystallographic data related to the structures and to confirm the halogen-bond formation between the starting materials. This was followed by using infrared spectroscopy (IR), used to confirm the presence of the adducts in the bulk solid based on the expected shifts in C-H and C-F stretching bands. NMR spectroscopy has been used to study the possibility of the halogen bond persisting in the solution phase. Theoretical study using QTAIM were also conducted to confirm the existence of bond critical points between the N and I or Br atoms. By studying and compared the parameters (electron density, ρ_{BCP} , Laplacian, $\nabla^2\rho_{\text{BCP}}$, and total electron density, $H_{(r)}$) related to these BCP's a comparison of the relative strengths of the halogen bond interactions could be made.

Starting with DABCO as an example of a tertiary amine, interactions with a variety of bromo-substituted fluoroaromatic compounds (Chapter 2) resulted in 4 structures containing N...Br halogen bonds that were shorter than the sum of van der Waals radii, 3.40 Å. Previously only two reported structures^{1, 2} exist for this kind of system and this has now, therefore, increased to six. Interestingly, even though different stoichiometries were investigated, only one of the bromine atoms is involved in halogen bonding in the two di-bromo-containing adducts based on 1,2-dibromotetrafluorobenzene and 1,3-dibromotetrafluorobenzene. The halogen bond distances range from 2.84(2) to 2.667(15) Å, and the XB bond distance for the structure formed between 1,3-dibromotetrafluorobenzene

and DABCO, at 2.667(15) Å, is the shortest distance yet reported for this system. The bond angles range from 168.4(3) to 179.52(4) ° consistent with the strongly directional nature of halogen bonds. Infrared spectroscopy and QTAIM theoretical analysis confirm the existence of these N...Br short distances as interactions.

Chapter 3 describes the N...I halogen bonds formed between iodo-substituted fluoroaromatic compounds (as XB donors) and hexamethylenetetramine and 1,3,5-triaza-7-phosphaadamantane (as XB acceptors). The structure formed using 1-iodopentafluorobenzene and hexamethylenetetramine resulted in the shortest N...I distance, 2.805(4) Å, within this work and this is consistent with QTAIM calculations which show the highest electron density ρ_{BCP} , 0.0293 a.u and Laplacian 0.0788 a.u. for this interaction. The only XB structure formed using 1,3,5-triaza-7-phosphaadamantane was with 1,4-diiidotetrafluorobenzene. Unfortunately, the phosphorus atom was not involved in P...I halogen bond formation, or any other interactions even though it has the potential to do so. When an excess amount (4:1 and 5:1 molar ratio) of arene to 1,3,5-triaza-7-phosphaadamantane was used, the oxidised phosphorus compound formed which interacted with 1,4-diiidotetrafluorobenzene to form only one N...I halogen bond with the third shortest XB distance, 2.799(7) Å, reported in this study.

Chapter 4 is the only chapter to involve 1,4-diiidotetrafluorobenzene (exclusively) as a halogen bond donor. Although this donor has been extensively used before, its interactions with the nitrogen-based aromatic acceptors pyrimidine, 4,6-dimethyl pyrimidine, 1,3,5-triazine and pyrimidine-5-amine have not been previously reported. All of the structures were found to be similar, with adducts being found to crystallise in the monoclinic space group and possess a 1:1 ratio of the starting materials. The packing of the structures shows polymeric N...I halogen bonds, the shortest N...I distance within our structures was found when using pyrimidine, 2.862(4) Å, as halogen bond acceptor which may be related to the effectiveness of it as the electron donor (Lewis base).

Further related work is reported in chapter 5, using the same Lewis bases used in chapter 4, but with different iodofluorobenzene halogen bond donors (1,3,5-trifluoro-2,4,6-triiodobenzene, 1,2-diiidotetrafluorobenzene and 1,3-diiidotetrafluorobenzene). N...I halogen bonds were detected as the main interaction in the crystal structures. The only structure formed a N...I polymeric long chain is the one involving 4,6-dimethylpyrimidine with

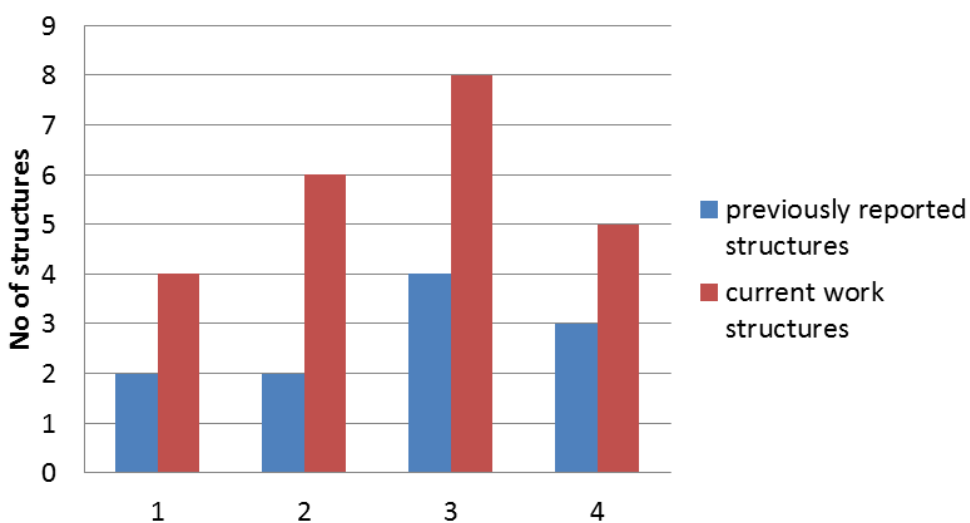
1,2-diiodotetrafluorobenzene formed in a 1:1 ratio, even though a 1:2 molar ratio of reactants was used to prepare the adduct.

Chapter 6 reports the structures of 5 different halogen bonded adducts involving the secondary amine piperazine with iodo-(3 structures) and bromo-(2 structures) fluorobenzenes. The resulting structures show that N...I and N...Br halogen bonds are preferred over N-H...N or N-H...F hydrogen bonds in these adducts. The shortest resulting N...I and N...Br distances are approximately 21% and 16% shorter than the sum of their van der Waals radii (3.53 Å) and (3.40 Å) respectively. Similar to what was found in chapter 3 the XB involving 1-iodopentafluorobenzene with piperazine results in the highest electron density ρ_{BCP} (0.0281 a.u) at the halogen bond bond critical point (BCP). This supports the crystallographic data which shows that this structure contains the shortest halogen bond distance of 2.791(4) Å. The very low total electron energy density $H_{(r)}$ at the PCB (-0.000464 a.u) compared with the other determined values, confirms the strength of this halogen bond.

In summary, **Figure 7.1** shows the significance of the number of structures related to the current work is compared with previously reported work for each system. In addition, the work described in chapters 4 and 5 suggest it is worth investigating interactions of 1,3,5-triaza-phosphaadamantane, pyrimidine, 4,6-dimethylpyrimidine, 1,3,5-triazine and pyrimidine-5-amine with other iodo- and bromo-fluorinated compounds. The combination of 1-iodopentafluorobenzene with hexamethylenetetramine gave the shortest N...I bond distances between these systems. Generally speaking, the current 23 structures resulting from this work indicate the effectiveness of using iodofluorobenzene rather than bromofluorobenzene to form halogen bonded adducts. This is presumably related to the higher polarizability of the iodine atom and the related larger σ hole formed.

QTAIM analysis has proven to be an effective tool in describing and comparing halogen bonds. The electron density and its Laplacian values increase as the halogen bond distances get shorter for all the studied structures, which is in line with the previous studies using different software and mathematical models^{3,4}. The total electron energy density (H_r) decreases as the N...I distance get shorter, in line with previous studies^{3,5} which can be used, along with the electron density ρ_{BCP} and the Laplacian $\nabla^2\rho_{\text{BCP}}$, as an indication of the strength of the halogen bonds that have been formed.

In future work, further improvement in experimental crystal growth may produce more crystals and help to better characterise the unique features associated with these halogen bond. This may include the use of X-ray powder diffraction to check the purity of our samples by comparing the original powder pattern with that generated from the single-crystal data using Mercury programme. Moreover, the use to different computational QTAIM basis set analysis with different halogen bonded structures will hopefully enable a better understanding of the halogen bond interactions.



1= DABCO + bromofluorobenzene (Chapter 2)

2=HTMA or 1,3,5-Triaza-7-phosphaadamantane + iodofluorobenzene (Chapter 3)

3=Aromatic pyrimidine + iodofluorobenzene (Chapter 4+5)

4=piperazine + iodo/bromo fluorobenzene (Chapter 6)

Figure 7.1 Current work structures comparing with the reported CSD structures up to date

References:-

- 1 A. M. T. Muneer, The University of Manchester, 2018.
- 2 D. Cinčić, T. Friščić and W. Jones, *Chem. - A Eur. J.*, 2008, **14**, 747–753.
- 3 R. Wang, D. Hartnick and U. Englert, *Zeitschrift für Krist. - Cryst. Mater.*, 2018, **233**, 733–744.
- 4 K. Wzgarda-Raj, A. J. Rybarczyk-Pirek, S. Wojtulewski and M. Palusiak, *Acta Crystallogr. Sect. C Struct. Chem.*
- 5 E. L. Angelina, D. J. R. Duarte and N. M. Peruchena, *J. Mol. Model.*, 2013, **19**, 2097–2106.

List of publication, conferences and presentations

- 1- Journal article: M. S. S. Jamil, S. Alkaabi, and A. K. Brisdon, “Simple NMR predictors of catalytic hydrogenation activity for [Rh(cod)Cl(NHC)] complexes featuring fluorinated NHC ligands,” *Dalton Trans.*, **48**, 9317–9327, 2019.
- 2- Poster presentation (Halogen bonds in Nitrogen acceptors) in 17th Annual RSC Fluorine subject Group Postgraduate Meeting held in University of Leicester (18/09/2017).
- 3- Postgraduate Research (PGR) Conference, 15/06/2018, title: Halogen bonding in nitrogen acceptors (poster)
- 4- Postgraduate Research (PGR) Conference, 12/06/2019, title: Halogen bonding in nitrogen compounds (Talk, Oral presentation)

Chapter 8. Appendices

Appendix 1

Crystallographic Information File (cif) related to each structure in each Chapter

Cif file code	chapter	structure
aab123	2	1a
aab113	2	2a
aab119	2	3a
aab124	2	4a
aab117	3	1a
aab155	3	2a.1
aab207	3	2a
aab157	3	3a
aab143	3	4b.1
aab228	3	4b
aab172	4	1a
aab164	4	2a
aab188	4	3a
aab128	4	4a
aab173	5	1a
aab176	5	2a
aab165	5	2c
aab62	5	3b
aab107	6	1a
aab14	6	2a
aab83	6	3a
EXP_2935	6	4a
aab38	6	5a

Appendix 2

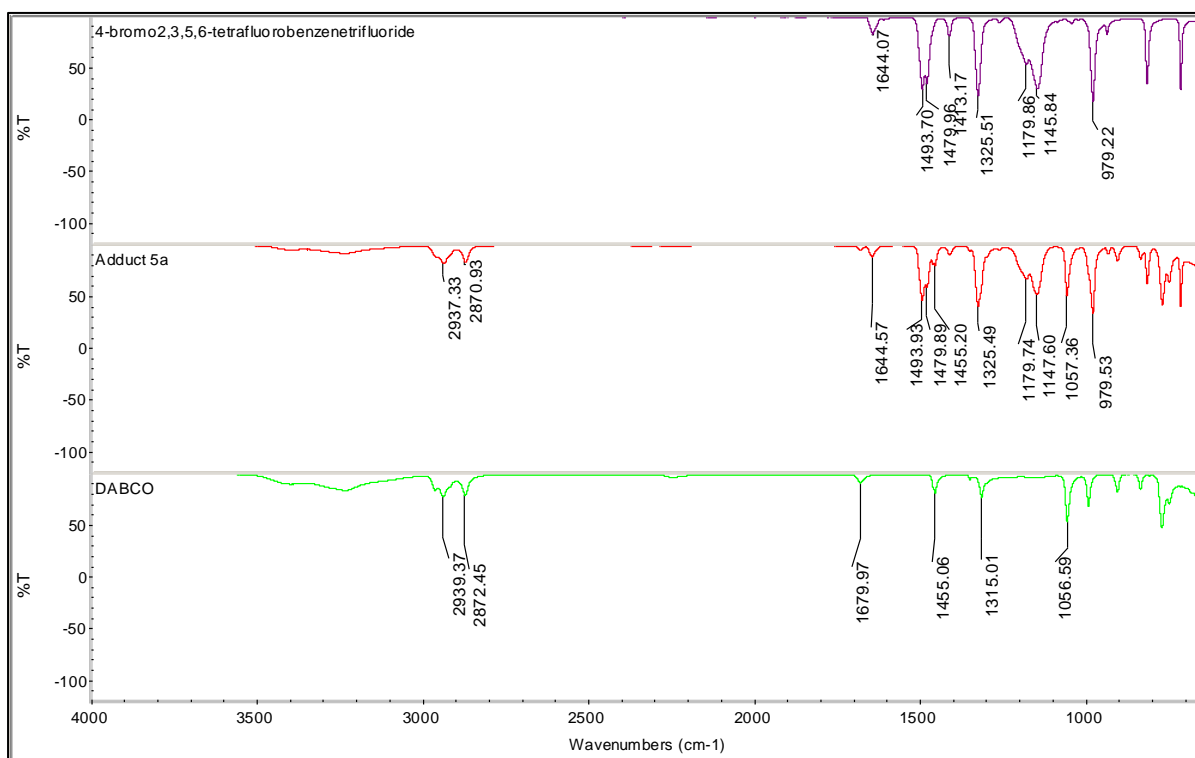
(Supplementary information)

Chapter 2 :- Halogen bonding in a series of bromofluorobenzene and 1,4-diazabicyclo[2.2.2]octane (DABCO)

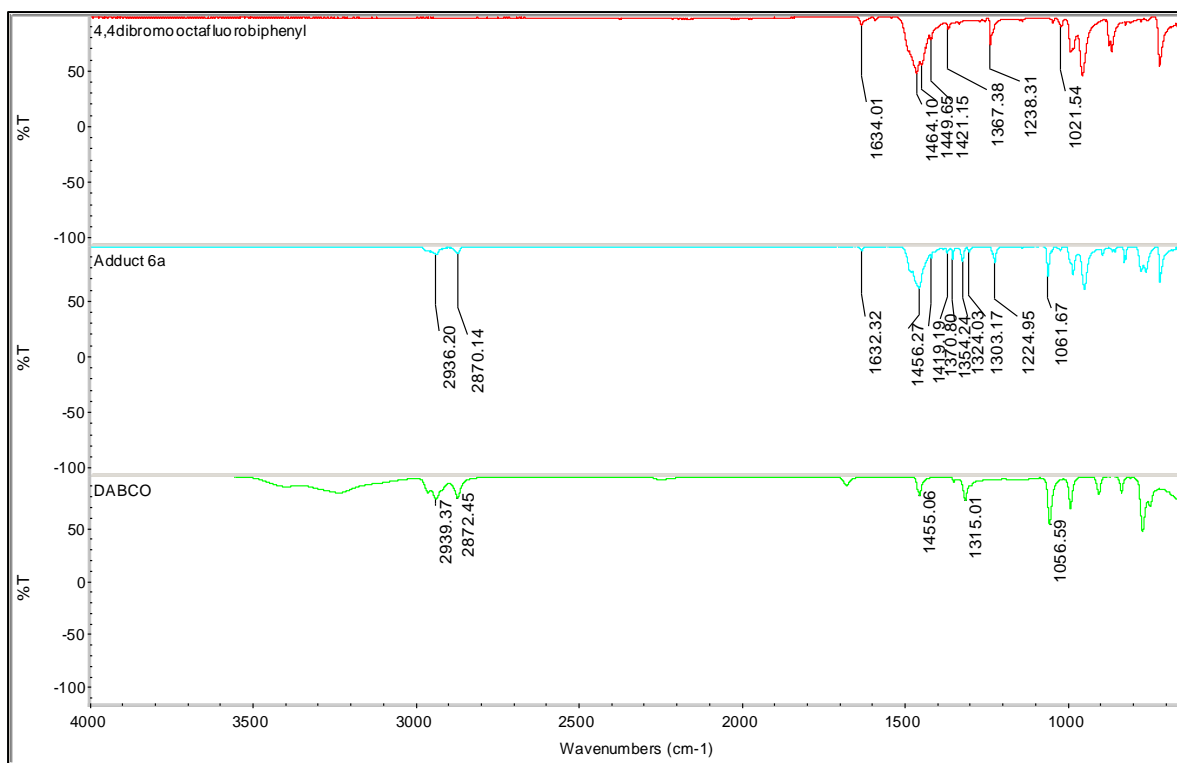
Alan K. Brisdon* and Sultan Alkaabi

Department of Chemistry, The University of Manchester, Oxford Road, Manchester, M13 9PL, United Kingdom

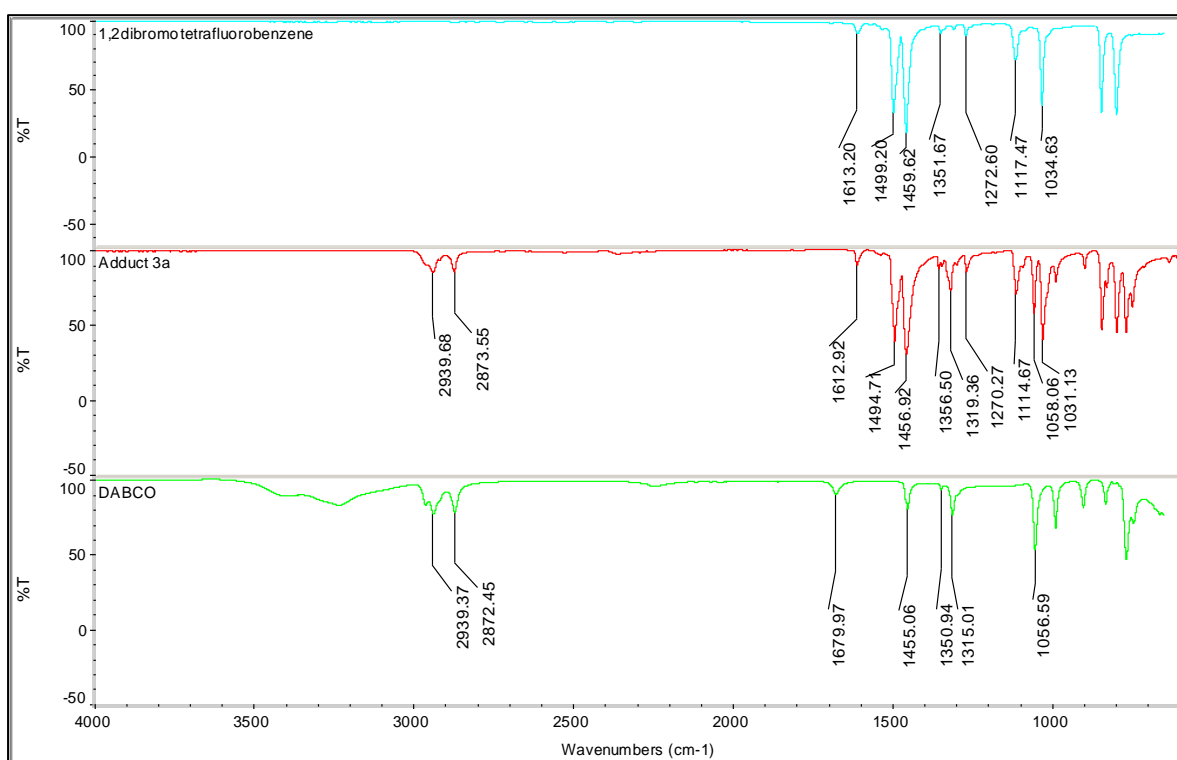
Correspondence email: *alan.brisdon@manchester.ac.uk



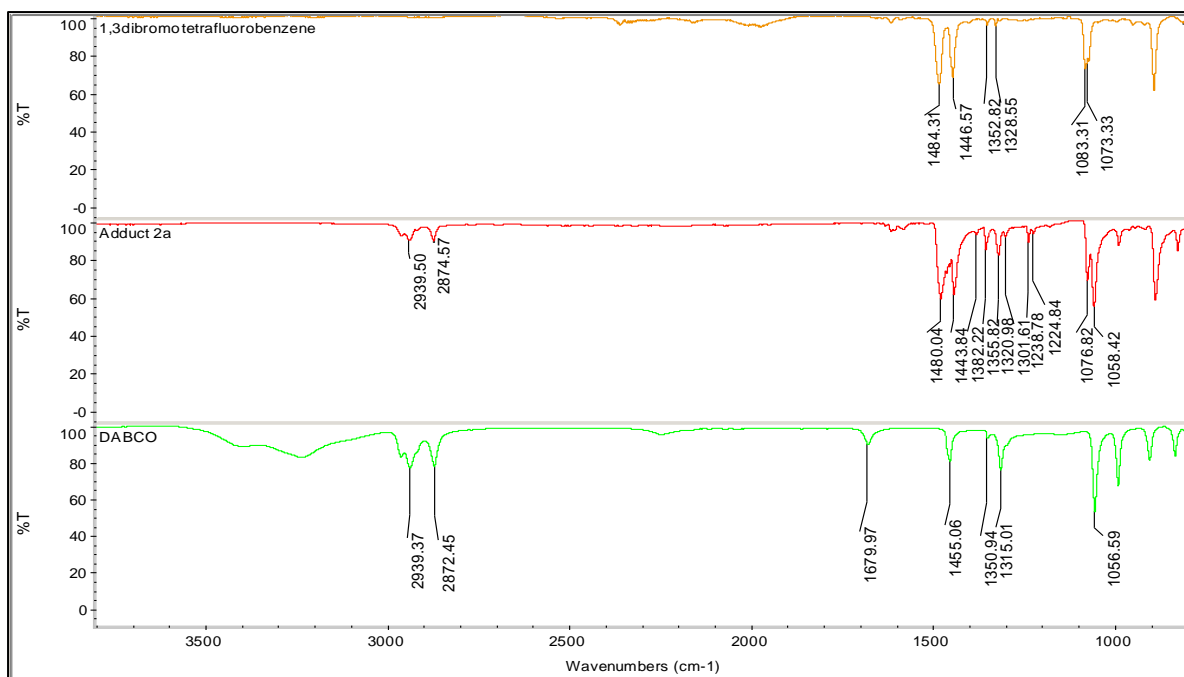
S2.1 IR spectra showing the two starting materials and adduct **1a**



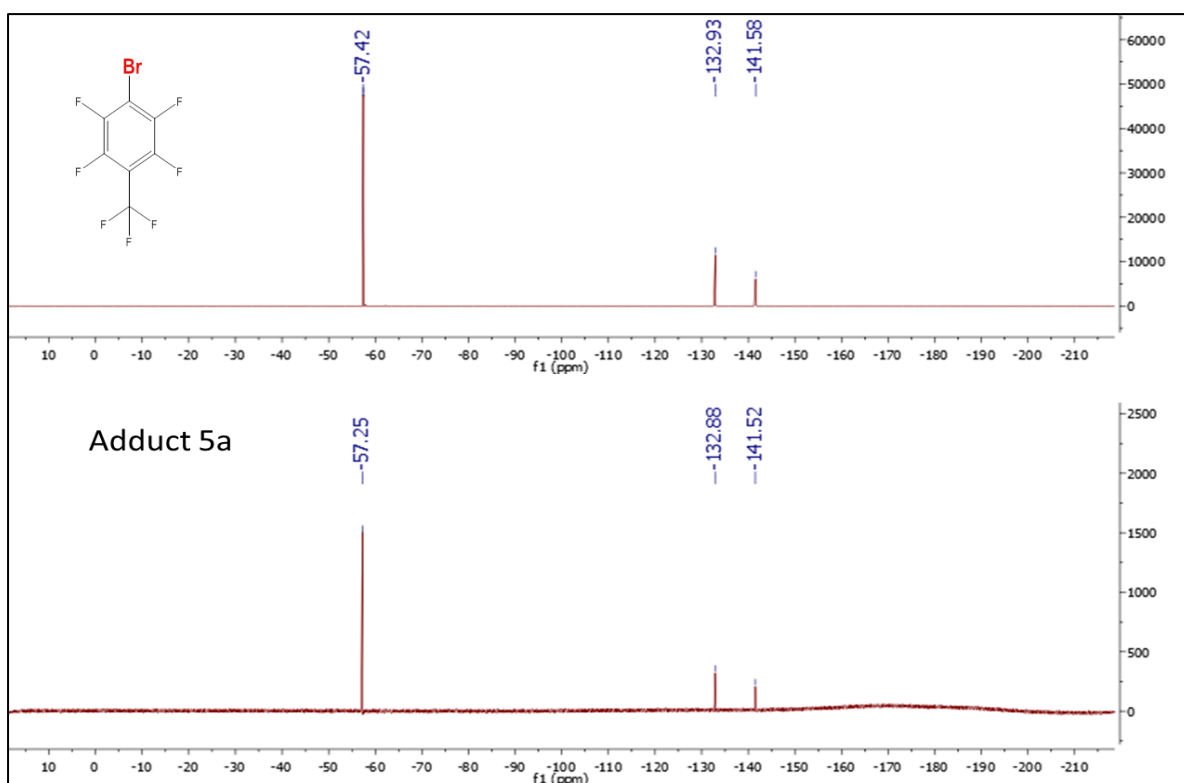
S2.2 IR spectra showing the two starting materials and adduct **2a**



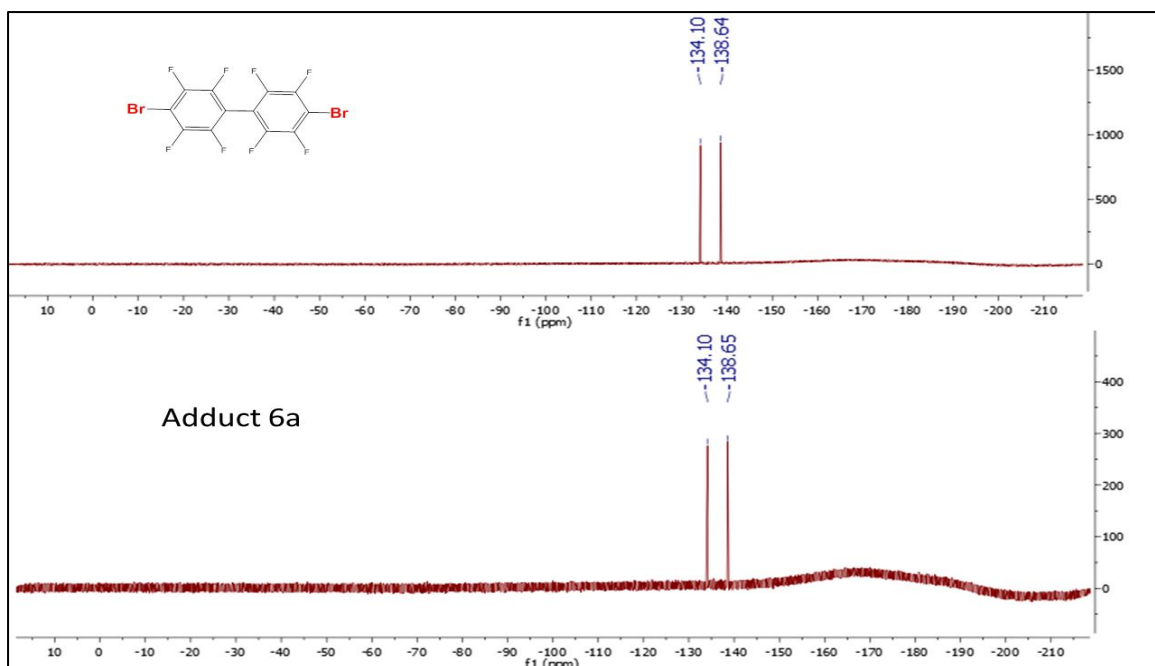
S2.3 IR spectra showing the two starting materials and adduct **3a**



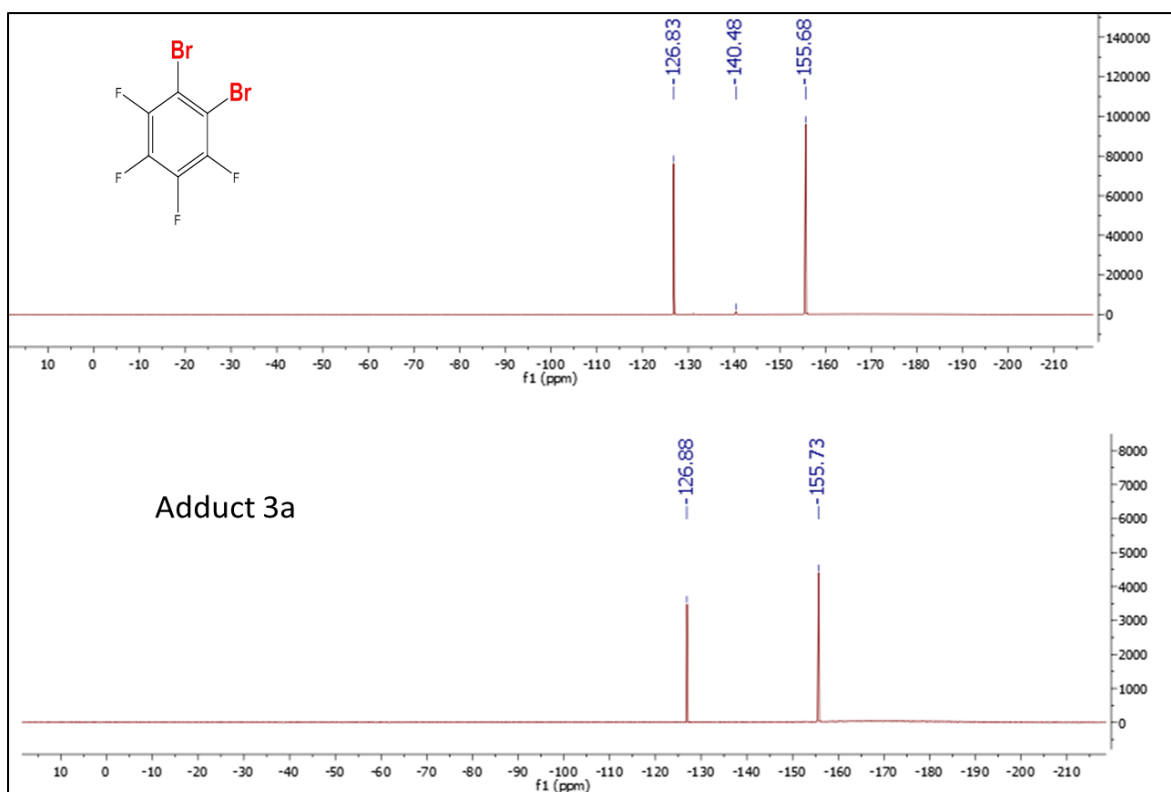
S2.4 IR spectra showing the two starting materials and adduct **4a**



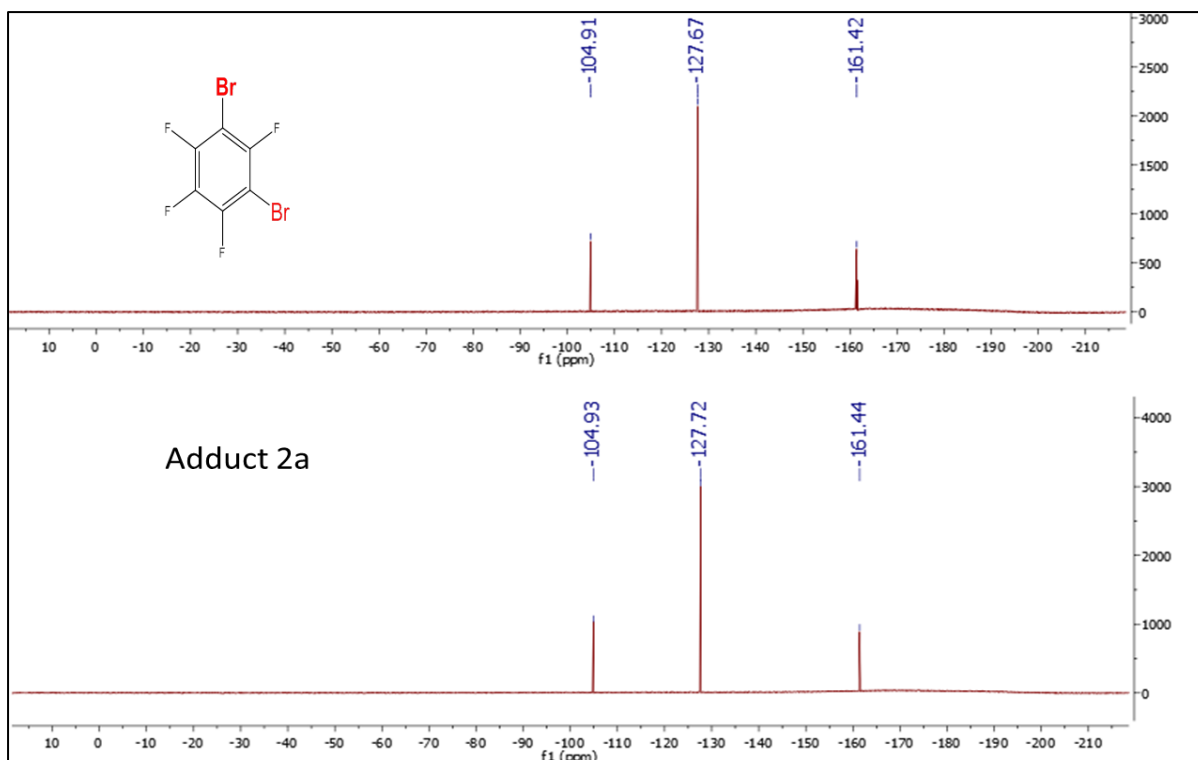
S2.5 ^{19}F NMR spectra for adduct **1a** and 4-bromo-2,3,5,6-tetrafluorobenzotrifluoride using acetonitrile- d_3



S2.6 ^{19}F NMR spectra for adduct **2a** and 4,4'-dibromooctafluorobiphenyl usinacetonitriled3



S2.7 ^{19}F NMR spectra for adduct **3a** and 1,2-dibromotetrafluorobenzene using acetonitrile-d3



S2.8 ^{19}F NMR spectra for adduct 4a and 1,3-dibromotetrafluorobenzene using acetonitrile- d_3

Computing details

Data collection: *CrysAlis PRO* 1.171.39.46 (Rigaku OD, 2018); cell refinement: *CrysAlis PRO* 1.171.39.46 (Rigaku OD, 2018); data reduction: *CrysAlis PRO* 1.171.39.46 (Rigaku OD, 2018); program(s) used to solve structure: ShelXT (Sheldrick, 2015); program(s) used to refine structure: *SHELXL* (Sheldrick, 2015); molecular graphics: Olex2 (Dolomanov *et al.*, 2009); software used to prepare material for publication: Olex2 (Dolomanov *et al.*, 2009).

4-bromo-2,3,5,6-tetrafluorobenzotrifluoride–1,4-diazabicyclo[2.2.2]octane (1a)

Crystal data

$2(\text{BrC}_7\text{F}_7) \cdot \text{C}_6\text{H}_{12}\text{N}_2$	$F(000) = 684$
$M_r = 706.14$	$D_x = 2.050 \text{ Mg m}^{-3}$
Monoclinic, $P2_1/c$	Mo $K\alpha$ radiation, $\lambda = 0.71073 \text{ \AA}$
$a = 9.4125 (12) \text{ \AA}$	Cell parameters from 1314 reflections
$b = 5.9434 (6) \text{ \AA}$	$\theta = 3.2\text{--}25.4^\circ$

$c = 20.7026 (19) \text{ \AA}$	$\mu = 3.67 \text{ mm}^{-1}$
$\beta = 99.010 (11)^\circ$	$T = 150 \text{ K}$
$V = 1143.9 (2) \text{ \AA}^3$	Needle, clear light colourless
$Z = 2$	$0.3 \times 0.03 \times 0.01 \text{ mm}$

Data collection

SuperNova, Single source at offset/far, Eos diffractometer	2469 independent reflections
Radiation source: micro-focus sealed X-ray tube, SuperNova (Mo) X-ray Source	1682 reflections with $I > 2\sigma(I)$
Mirror monochromator	$R_{\text{int}} = 0.073$
Detector resolution: $8.0714 \text{ pixels mm}^{-1}$	$\theta_{\text{max}} = 27.0^\circ$, $\theta_{\text{min}} = 3.2^\circ$
ω scans	$h = -11 \rightarrow 10$
Absorption correction: multi-scan <i>CrysAlis PRO</i> 1.171.39.46 (Rigaku Oxford Diffraction, 2018) Empirical absorption correction using spherical harmonics, implemented in SCALE3 ABSPACK scaling algorithm.	$k = -7 \rightarrow 6$
$T_{\text{min}} = 0.350$, $T_{\text{max}} = 1.000$	$l = -24 \rightarrow 26$
6217 measured reflections	

Refinement

Refinement on F^2	Primary atom site location: dual
Least-squares matrix: full	Hydrogen site location: inferred from neighbouring sites
$R[F^2 > 2\sigma(F^2)] = 0.057$	H-atom parameters constrained
$wR(F^2) = 0.084$	$w = 1/[\sigma^2(F_o^2) + (0.0084P)^2]$ where $P = (F_o^2 + 2F_c^2)/3$
$S = 1.02$	$(\Delta/\sigma)_{\text{max}} < 0.001$
2469 reflections	$\Delta_{\text{max}} = 0.62 \text{ e \AA}^{-3}$
208 parameters	$\Delta_{\text{min}} = -0.55 \text{ e \AA}^{-3}$
132 restraints	

Special details

Geometry. All esds (except the esd in the dihedral angle between two l.s. planes) are estimated using the full covariance matrix. The cell esds are taken into account individually in the estimation of esds in distances, angles and torsion angles; correlations between esds in cell parameters are only used when they are defined by crystal symmetry. An approximate (isotropic) treatment of cell esds is used for estimating esds involving l.s. planes.

*Fractional atomic coordinates and isotropic or equivalent isotropic displacement parameters
(Å²)*

	x	y	z	U_{iso}^*/U_{eq}	Occ. (<1)
Br1	0.31759 (6)	0.27949 (8)	0.32646 (3)	0.02805 (17)	
C1	0.2463 (5)	0.4585 (8)	0.2534 (2)	0.0201 (12)	
C2	0.3096 (5)	0.6615 (8)	0.2422 (2)	0.0227 (12)	
C3	0.2569 (5)	0.7925 (8)	0.1879 (2)	0.0191 (11)	
C4	0.1394 (5)	0.7250 (8)	0.1438 (2)	0.0199 (12)	
C5	0.0789 (6)	0.8563 (9)	0.0836 (3)	0.0292 (14)	
C6	0.0761 (5)	0.5210 (8)	0.1556 (2)	0.0209 (12)	
C7	0.1291 (6)	0.3906 (8)	0.2092 (2)	0.0214 (12)	
F1	0.4225 (3)	0.7379 (4)	0.28366 (13)	0.0303 (7)	
F2	0.3253 (3)	0.9874 (4)	0.18078 (13)	0.0296 (8)	
F3	0.1531 (3)	1.0428 (5)	0.07566 (14)	0.0433 (9)	
F4	0.0762 (3)	0.7352 (5)	0.02966 (14)	0.0454 (9)	
F5	-0.0560 (3)	0.9239 (5)	0.08570 (14)	0.0412 (9)	
F6	-0.0393 (3)	0.4485 (5)	0.11450 (14)	0.0335 (8)	
F7	0.0613 (3)	0.1959 (4)	0.21766 (13)	0.0323 (8)	
C8	0.5104 (12)	0.2559 (16)	0.4764 (5)	0.033 (3)	0.5
H8A	0.4327	0.3664	0.4786	0.040*	0.5
H8B	0.5826	0.3261	0.4527	0.040*	0.5
C9	0.5829 (13)	0.1892 (16)	0.5475 (5)	0.035 (3)	0.5
H9A	0.6847	0.2382	0.5546	0.043*	0.5
H9B	0.5333	0.2675	0.5798	0.043*	0.5
C10	0.6456 (11)	-0.1658 (18)	0.5070 (5)	0.031 (3)	0.5
H10A	0.6447	-0.3308	0.5136	0.037*	0.5
H10B	0.7471	-0.1166	0.5112	0.037*	0.5
C11	0.5662 (11)	-0.1080 (17)	0.4375 (5)	0.029 (2)	0.5
H11A	0.6353	-0.0435	0.4111	0.034*	0.5
H11B	0.5256	-0.2471	0.4156	0.034*	0.5
C12	0.3464 (12)	-0.052 (2)	0.4774 (5)	0.038 (3)	0.5
H12A	0.3050	-0.1881	0.4539	0.045*	0.5
H12B	0.2670	0.0539	0.4811	0.045*	0.5
C13	0.4248 (11)	-0.119 (2)	0.5476 (5)	0.035 (3)	0.5
H13A	0.3762	-0.0448	0.5809	0.043*	0.5
H13B	0.4175	-0.2838	0.5534	0.043*	0.5
N1	0.4507 (14)	0.053 (2)	0.4412 (9)	0.027 (3)	0.5
N2	0.5761 (14)	-0.054 (2)	0.5576 (9)	0.028 (3)	0.5

Atomic displacement parameters (\AA^2)

	U^{11}	U^{22}	U^{33}	U^{12}	U^{13}	U^{23}
Br1	0.0343 (3)	0.0309 (3)	0.0190 (3)	0.0063 (3)	0.0045 (2)	0.0066 (3)
C1	0.023 (3)	0.025 (3)	0.013 (3)	0.003 (2)	0.003 (2)	0.000 (2)
C2	0.018 (3)	0.031 (3)	0.017 (3)	0.000 (2)	-0.003 (2)	-0.001 (2)
C3	0.019 (3)	0.017 (3)	0.021 (3)	0.003 (2)	0.002 (2)	0.000 (2)
C4	0.023 (3)	0.024 (3)	0.013 (2)	0.006 (2)	0.005 (2)	0.003 (2)
C5	0.030 (4)	0.031 (3)	0.028 (3)	0.010 (3)	0.008 (3)	0.007 (3)
C6	0.016 (3)	0.027 (3)	0.017 (3)	0.004 (2)	-0.004 (2)	-0.003 (2)
C7	0.024 (3)	0.020 (3)	0.021 (3)	0.000 (2)	0.005 (3)	0.000 (2)
F1	0.0247 (18)	0.0340 (19)	0.0284 (17)	0.0001 (15)	-0.0072 (15)	0.0005 (14)
F2	0.033 (2)	0.0232 (17)	0.0316 (18)	-0.0013 (14)	0.0008 (16)	0.0046 (14)
F3	0.039 (2)	0.046 (2)	0.042 (2)	-0.0057 (17)	-0.0019 (18)	0.0256 (17)
F4	0.063 (3)	0.052 (2)	0.0188 (16)	0.0172 (19)	0.0007 (17)	0.0000 (16)
F5	0.032 (2)	0.056 (2)	0.037 (2)	0.0167 (17)	0.0076 (18)	0.0181 (17)
F6	0.027 (2)	0.0371 (19)	0.0333 (18)	-0.0046 (15)	-0.0061 (16)	0.0038 (15)
F7	0.0320 (19)	0.0282 (18)	0.0370 (19)	-0.0082 (15)	0.0070 (16)	0.0085 (15)
C8	0.040 (6)	0.032 (5)	0.025 (5)	-0.002 (4)	-0.003 (5)	0.004 (4)
C9	0.036 (6)	0.041 (5)	0.026 (5)	-0.005 (4)	-0.004 (5)	0.007 (4)
C10	0.025 (5)	0.040 (6)	0.025 (5)	0.004 (4)	-0.003 (4)	0.006 (4)
C11	0.026 (6)	0.035 (6)	0.023 (5)	-0.002 (4)	-0.003 (4)	0.004 (4)
C12	0.030 (6)	0.044 (7)	0.037 (6)	0.003 (5)	0.001 (4)	0.011 (5)
C13	0.027 (5)	0.046 (6)	0.035 (6)	-0.002 (4)	0.007 (4)	0.007 (5)
N1	0.024 (6)	0.033 (5)	0.022 (5)	-0.001 (4)	-0.003 (4)	0.006 (4)
N2	0.024 (6)	0.039 (5)	0.021 (5)	-0.001 (4)	0.003 (4)	0.008 (4)

Geometric parameters (\AA , $^\circ$)

Br1—C1	1.885 (5)	C8—N1	1.474 (12)
C1—C2	1.382 (6)	C9—H9A	0.9900
C1—C7	1.378 (6)	C9—H9B	0.9900
C2—C3	1.393 (6)	C9—N2	1.463 (12)
C2—F1	1.337 (5)	C10—H10A	0.9900
C3—C4	1.379 (6)	C10—H10B	0.9900
C3—F2	1.345 (5)	C10—C11	1.552 (12)
C4—C5	1.505 (6)	C10—N2	1.477 (12)
C4—C6	1.389 (6)	C11—H11A	0.9900
C5—F3	1.334 (6)	C11—H11B	0.9900
C5—F4	1.326 (6)	C11—N1	1.459 (11)

C5—F5	1.339 (5)	C12—H12A	0.9900
C6—C7	1.381 (6)	C12—H12B	0.9900
C6—F6	1.342 (5)	C12—C13	1.574 (13)
C7—F7	1.346 (5)	C12—N1	1.466 (11)
C8—H8A	0.9900	C13—H13A	0.9900
C8—H8B	0.9900	C13—H13B	0.9900
C8—C9	1.574 (13)	C13—N2	1.459 (11)
C2—C1—Br1	121.3 (4)	N2—C9—C8	111.1 (11)
C7—C1—Br1	121.0 (4)	N2—C9—H9A	109.4
C7—C1—C2	117.7 (5)	N2—C9—H9B	109.4
C1—C2—C3	121.0 (5)	H10A—C10—H10B	108.1
F1—C2—C1	120.6 (4)	C11—C10—H10A	109.5
F1—C2—C3	118.4 (5)	C11—C10—H10B	109.5
C4—C3—C2	121.3 (5)	N2—C10—H10A	109.5
F2—C3—C2	117.0 (5)	N2—C10—H10B	109.5
F2—C3—C4	121.8 (4)	N2—C10—C11	110.8 (11)
C3—C4—C5	123.9 (5)	C10—C11—H11A	109.5
C3—C4—C6	117.3 (5)	C10—C11—H11B	109.5
C6—C4—C5	118.8 (5)	H11A—C11—H11B	108.1
F3—C5—C4	113.3 (5)	N1—C11—C10	110.5 (11)
F3—C5—F5	105.8 (4)	N1—C11—H11A	109.5
F4—C5—C4	111.8 (4)	N1—C11—H11B	109.5
F4—C5—F3	106.8 (4)	H12A—C12—H12B	108.3
F4—C5—F5	107.3 (5)	C13—C12—H12A	109.9
F5—C5—C4	111.5 (4)	C13—C12—H12B	109.9
C7—C6—C4	121.3 (5)	N1—C12—H12A	109.9
F6—C6—C4	119.7 (4)	N1—C12—H12B	109.9
F6—C6—C7	119.0 (5)	N1—C12—C13	108.9 (11)
C1—C7—C6	121.3 (5)	C12—C13—H13A	109.3
F7—C7—C1	120.8 (4)	C12—C13—H13B	109.3
F7—C7—C6	117.9 (5)	H13A—C13—H13B	107.9
H8A—C8—H8B	108.2	N2—C13—C12	111.8 (11)
C9—C8—H8A	109.8	N2—C13—H13A	109.3
C9—C8—H8B	109.8	N2—C13—H13B	109.3
N1—C8—H8A	109.8	C11—N1—C8	109.5 (11)
N1—C8—H8B	109.8	C11—N1—C12	108.1 (11)
N1—C8—C9	109.4 (11)	C12—N1—C8	109.4 (11)
C8—C9—H9A	109.4	C9—N2—C10	108.0 (11)

C8—C9—H9B	109.4	C13—N2—C9	107.8 (11)
H9A—C9—H9B	108.0	C13—N2—C10	108.1 (11)

4,4-dibromooctafluorobiphenyl- 1,4-diazabicyclo[2.2.2]octane (2a)

Crystal data

Br ₂ C ₁₂ F ₈ ·C ₆ H ₁₂ N ₂	$F(000) = 1104$
$M_r = 568.12$	$D_x = 1.927 \text{ Mg m}^{-3}$
Monoclinic, $P2_1/n$	Mo $K\alpha$ radiation, $\lambda = 0.71073 \text{ \AA}$
$a = 13.1452 (7) \text{ \AA}$	Cell parameters from 1965 reflections
$b = 10.8897 (7) \text{ \AA}$	$\theta = 3.1\text{--}26.3^\circ$
$c = 14.3039 (7) \text{ \AA}$	$\mu = 4.22 \text{ mm}^{-1}$
$\beta = 107.025 (5)^\circ$	$T = 150 \text{ K}$
$V = 1957.8 (2) \text{ \AA}^3$	Plate, clear light colourless
$Z = 4$	$0.3 \times 0.1 \times 0.08 \text{ mm}$

Data collection

SuperNova, Single source at offset/far, Eos diffractometer	3841 independent reflections
Radiation source: micro-focus sealed X-ray tube, SuperNova (Mo) X-ray Source	2193 reflections with $I > 2\sigma(I)$
Mirror monochromator	$R_{\text{int}} = 0.078$
Detector resolution: $8.0714 \text{ pixels mm}^{-1}$	$\theta_{\text{max}} = 26.0^\circ$, $\theta_{\text{min}} = 3.1^\circ$
ω scans	$h = -16 \rightarrow 16$
Absorption correction: multi-scan <i>CrysAlis PRO</i> 1.171.39.46 (Rigaku Oxford Diffraction, 2018) Empirical absorption correction using spherical harmonics, implemented in SCALE3 ABSPACK scaling algorithm.	$k = -13 \rightarrow 12$
$T_{\text{min}} = 0.512$, $T_{\text{max}} = 1.000$	$l = -9 \rightarrow 17$
10318 measured reflections	

Refinement

Refinement on F^2	Primary atom site location: dual
Least-squares matrix: full	Hydrogen site location: inferred from neighbouring sites
$R[F^2 > 2\sigma(F^2)] = 0.058$	H-atom parameters constrained
$wR(F^2) = 0.090$	$w = 1/[\sigma^2(F_o^2) + (0.0053P)^2]$ where $P = (F_o^2 + 2F_c^2)/3$

$S = 0.98$	$(\Delta/\sigma)_{\max} = 0.001$
3841 reflections	$\Delta)_{\max} = 0.52 \text{ e } \text{\AA}^{-3}$
271 parameters	$\Delta)_{\min} = -0.58 \text{ e } \text{\AA}^{-3}$
0 restraints	

Special details

Geometry. All esds (except the esd in the dihedral angle between two l.s. planes) are estimated using the full covariance matrix. The cell esds are taken into account individually in the estimation of esds in distances, angles and torsion angles; correlations between esds in cell parameters are only used when they are defined by crystal symmetry. An approximate (isotropic) treatment of cell esds is used for estimating esds involving l.s. planes.

Fractional atomic coordinates and isotropic or equivalent isotropic displacement parameters (\AA^2)

	x	y	z	$U_{\text{iso}}^*/U_{\text{eq}}$
Br1	0.93418 (5)	0.71362 (6)	0.41057 (5)	0.0329 (2)
Br2	0.06741 (5)	0.70113 (6)	0.10164 (5)	0.03179 (19)
F1	0.7926 (3)	0.5014 (3)	0.2965 (2)	0.0357 (9)
F2	0.5802 (3)	0.4939 (3)	0.2206 (2)	0.0353 (9)
F3	0.5521 (3)	0.8880 (3)	0.3516 (2)	0.0361 (9)
F4	0.7640 (3)	0.8968 (3)	0.4271 (3)	0.0390 (10)
F5	0.4218 (3)	0.5045 (3)	0.3184 (2)	0.0319 (9)
F6	0.2097 (3)	0.5076 (3)	0.2392 (2)	0.0341 (9)
F7	0.2372 (3)	0.8744 (3)	0.0690 (2)	0.0332 (9)
F8	0.4492 (3)	0.8725 (3)	0.1507 (2)	0.0335 (9)
C1	0.7835 (5)	0.7011 (5)	0.3627 (4)	0.0238 (15)
C2	0.7345 (5)	0.5984 (5)	0.3115 (4)	0.0283 (16)
C3	0.6248 (5)	0.5924 (6)	0.2725 (4)	0.0292 (16)
C4	0.5593 (5)	0.6903 (5)	0.2834 (4)	0.0233 (15)
C5	0.6104 (5)	0.7916 (5)	0.3364 (4)	0.0263 (15)
C6	0.7196 (5)	0.7963 (6)	0.3753 (4)	0.0291 (16)
C7	0.4421 (5)	0.6882 (5)	0.2378 (4)	0.0224 (15)
C8	0.3769 (5)	0.5966 (6)	0.2563 (4)	0.0294 (16)
C9	0.2680 (5)	0.5984 (5)	0.2162 (4)	0.0262 (15)
C10	0.2182 (5)	0.6916 (5)	0.1525 (4)	0.0247 (15)
C11	0.2819 (5)	0.7829 (5)	0.1324 (4)	0.0252 (15)
C12	0.3910 (5)	0.7807 (5)	0.1726 (4)	0.0270 (16)
N1	-0.3517 (4)	0.7514 (5)	-0.0264 (4)	0.0275 (13)
N2	-0.1475 (4)	0.7324 (4)	0.0348 (3)	0.0272 (13)
C13	-0.3025 (5)	0.8722 (5)	-0.0336 (5)	0.0336 (17)

H13A	-0.3257	0.9322	0.0060	0.040*
H13B	-0.3245	0.9003	-0.1009	0.040*
C14	-0.1778 (5)	0.8593 (5)	0.0033 (5)	0.0356 (17)
H14A	-0.1480	0.8814	-0.0489	0.043*
H14B	-0.1491	0.9150	0.0576	0.043*
C15	-0.1929 (5)	0.7005 (6)	0.1134 (4)	0.0335 (17)
H15A	-0.1647	0.7552	0.1685	0.040*
H15B	-0.1729	0.6172	0.1350	0.040*
C16	-0.3164 (5)	0.7114 (5)	0.0774 (4)	0.0342 (17)
H16A	-0.3481	0.6325	0.0837	0.041*
H16B	-0.3399	0.7704	0.1174	0.041*
C17	-0.1918 (5)	0.6501 (6)	-0.0497 (5)	0.0378 (18)
H17A	-0.1717	0.5660	-0.0309	0.045*
H17B	-0.1627	0.6721	-0.1024	0.045*
C18	-0.3155 (5)	0.6606 (6)	-0.0859 (4)	0.0342 (17)
H18A	-0.3381	0.6856	-0.1540	0.041*
H18B	-0.3470	0.5813	-0.0809	0.041*

Atomic displacement parameters (\AA^2)

	U^{11}	U^{22}	U^{33}	U^{12}	U^{13}	U^{23}
Br1	0.0249 (4)	0.0382 (4)	0.0324 (4)	0.0019 (3)	0.0035 (3)	0.0039 (3)
Br2	0.0246 (4)	0.0344 (4)	0.0342 (4)	-0.0024 (3)	0.0050 (3)	-0.0034 (3)
F1	0.031 (2)	0.031 (2)	0.043 (2)	0.0096 (18)	0.0084 (19)	-0.0022 (18)
F2	0.035 (2)	0.031 (2)	0.039 (2)	-0.0010 (18)	0.0085 (19)	-0.0064 (18)
F3	0.029 (2)	0.032 (2)	0.046 (2)	0.0060 (18)	0.0082 (19)	-0.0093 (18)
F4	0.033 (3)	0.034 (2)	0.042 (2)	-0.0013 (18)	-0.0007 (19)	-0.0085 (19)
F5	0.030 (2)	0.028 (2)	0.034 (2)	0.0039 (17)	0.0038 (18)	0.0069 (17)
F6	0.035 (2)	0.031 (2)	0.037 (2)	-0.0071 (18)	0.0120 (19)	0.0032 (18)
F7	0.029 (2)	0.033 (2)	0.035 (2)	0.0031 (17)	0.0049 (18)	0.0062 (18)
F8	0.025 (2)	0.032 (2)	0.040 (2)	-0.0032 (18)	0.0056 (18)	0.0053 (18)
C1	0.021 (4)	0.026 (4)	0.022 (3)	0.002 (3)	0.003 (3)	-0.005 (3)
C2	0.030 (4)	0.024 (4)	0.029 (4)	0.004 (3)	0.006 (3)	0.008 (3)
C3	0.034 (5)	0.027 (4)	0.029 (4)	-0.005 (3)	0.013 (3)	-0.002 (3)
C4	0.021 (4)	0.029 (4)	0.019 (3)	-0.006 (3)	0.004 (3)	-0.002 (3)
C5	0.027 (4)	0.021 (4)	0.032 (4)	0.004 (3)	0.010 (3)	0.004 (3)
C6	0.037 (5)	0.025 (4)	0.024 (3)	-0.008 (3)	0.007 (3)	-0.003 (3)
C7	0.022 (4)	0.028 (4)	0.020 (3)	0.004 (3)	0.011 (3)	0.000 (3)
C8	0.030 (4)	0.035 (4)	0.024 (4)	0.005 (3)	0.009 (3)	0.000 (3)
C9	0.026 (4)	0.027 (4)	0.029 (4)	0.001 (3)	0.013 (3)	0.001 (3)

C10	0.029 (4)	0.017 (3)	0.029 (4)	-0.004 (3)	0.012 (3)	-0.003 (3)
C11	0.022 (4)	0.028 (4)	0.022 (3)	0.007 (3)	0.000 (3)	-0.005 (3)
C12	0.033 (4)	0.023 (4)	0.028 (4)	-0.012 (3)	0.012 (3)	-0.005 (3)
N1	0.019 (3)	0.033 (3)	0.029 (3)	-0.005 (3)	0.005 (3)	0.005 (3)
N2	0.029 (4)	0.032 (3)	0.020 (3)	-0.004 (3)	0.007 (3)	0.005 (2)
C13	0.040 (5)	0.028 (4)	0.033 (4)	0.002 (3)	0.010 (4)	0.006 (3)
C14	0.038 (5)	0.028 (4)	0.040 (4)	-0.011 (3)	0.010 (4)	0.004 (3)
C15	0.027 (4)	0.038 (4)	0.031 (4)	0.002 (3)	0.001 (3)	0.002 (3)
C16	0.041 (5)	0.038 (4)	0.027 (4)	0.000 (4)	0.016 (3)	0.002 (3)
C17	0.037 (5)	0.041 (4)	0.039 (4)	-0.001 (4)	0.016 (4)	-0.009 (4)
C18	0.035 (5)	0.040 (4)	0.027 (4)	-0.008 (3)	0.009 (3)	-0.008 (3)

Geometric parameters (Å, °)

Br1—C1	1.902 (6)	C5—C6	1.380 (8)
Br2—C10	1.904 (6)	C7—C8	1.389 (8)
F1—C2	1.356 (6)	C7—C12	1.403 (8)
F2—C3	1.337 (6)	C8—C9	1.378 (8)
F3—C5	1.355 (6)	C9—C10	1.392 (8)
F4—C6	1.355 (6)	C10—C11	1.384 (7)
F5—C8	1.356 (6)	C11—C12	1.380 (8)
F6—C9	1.349 (6)	N1—C13	1.482 (7)
F7—C11	1.359 (6)	N1—C16	1.485 (7)
F8—C12	1.350 (6)	N1—C18	1.472 (7)
C1—C2	1.387 (8)	N2—C14	1.472 (7)
C1—C6	1.379 (8)	N2—C15	1.461 (6)
C2—C3	1.387 (8)	N2—C17	1.480 (7)
C3—C4	1.407 (8)	C13—C14	1.575 (8)
C4—C5	1.394 (8)	C15—C16	1.558 (7)
C4—C7	1.488 (7)	C17—C18	1.559 (8)
C2—C1—Br1	121.4 (5)	F6—C9—C8	118.9 (6)
C6—C1—Br1	120.6 (5)	F6—C9—C10	120.2 (6)
C6—C1—C2	118.0 (6)	C8—C9—C10	120.9 (6)
F1—C2—C1	121.0 (6)	C9—C10—Br2	121.8 (5)
F1—C2—C3	117.9 (6)	C11—C10—Br2	120.5 (5)
C1—C2—C3	121.1 (6)	C11—C10—C9	117.6 (6)
F2—C3—C2	119.7 (6)	F7—C11—C10	119.7 (6)
F2—C3—C4	119.1 (6)	F7—C11—C12	119.0 (6)
C2—C3—C4	121.2 (6)	C12—C11—C10	121.2 (6)

C3—C4—C7	121.9 (6)	F8—C12—C7	119.5 (6)
C5—C4—C3	116.5 (6)	F8—C12—C11	118.6 (6)
C5—C4—C7	121.5 (6)	C11—C12—C7	121.8 (6)
F3—C5—C4	119.7 (6)	C13—N1—C16	108.3 (5)
F3—C5—C6	118.5 (6)	C18—N1—C13	109.5 (5)
C6—C5—C4	121.8 (6)	C18—N1—C16	108.8 (5)
F4—C6—C1	119.9 (6)	C14—N2—C17	108.2 (5)
F4—C6—C5	118.8 (6)	C15—N2—C14	108.9 (5)
C1—C6—C5	121.4 (6)	C15—N2—C17	109.5 (5)
C8—C7—C4	123.0 (6)	N1—C13—C14	109.3 (5)
C8—C7—C12	116.1 (6)	N2—C14—C13	110.4 (5)
C12—C7—C4	120.9 (6)	N2—C15—C16	110.4 (5)
F5—C8—C7	118.8 (6)	N1—C16—C15	110.1 (5)
F5—C8—C9	118.8 (6)	N2—C17—C18	110.5 (5)
C9—C8—C7	122.3 (6)	N1—C18—C17	109.9 (5)

1,2-dibromotetrafluorobenzene-1,4-diazabicyclo[2.2.2]octane (3a)

Crystal data

2(Br ₂ C ₆ F ₄)·C ₆ H ₁₂ N ₂	$F(000) = 1384$
$M_r = 727.94$	$D_x = 2.164 \text{ Mg m}^{-3}$
Monoclinic, $P2_1/n$	Mo $K\alpha$ radiation, $\lambda = 0.71073 \text{ \AA}$
$a = 7.0217 (6) \text{ \AA}$	Cell parameters from 1794 reflections
$b = 25.4798 (17) \text{ \AA}$	$\theta = 3.1\text{--}24.2^\circ$
$c = 12.7701 (9) \text{ \AA}$	$\mu = 7.28 \text{ mm}^{-1}$
$\beta = 102.039 (8)^\circ$	$T = 150 \text{ K}$
$V = 2234.5 (3) \text{ \AA}^3$	Needle, clear light colourless
$Z = 4$	$0.1 \times 0.05 \times 0.02 \text{ mm}$

Data collection

SuperNova, Single source at offset/far, Eos diffractometer	4373 independent reflections
Radiation source: micro-focus sealed X-ray tube, SuperNova (Mo) X-ray Source	2763 reflections with $I > 2\sigma(I)$
Mirror monochromator	$R_{\text{int}} = 0.073$
Detector resolution: $8.0714 \text{ pixels mm}^{-1}$	$\theta_{\text{max}} = 26.0^\circ$, $\theta_{\text{min}} = 3.1^\circ$
ω scans	$h = -8 \rightarrow 4$
Absorption correction: multi-scan	$k = -31 \rightarrow 27$

CrysAlis PRO 1.171.39.46 (Rigaku Oxford Diffraction, 2018) Empirical absorption correction using spherical harmonics, implemented in SCALE3 ABSPACK scaling algorithm.	
$T_{\min} = 0.353$, $T_{\max} = 1.000$	$l = -14 \rightarrow 15$
10422 measured reflections	

Refinement

Refinement on F^2	Primary atom site location: dual
Least-squares matrix: full	Hydrogen site location: inferred from neighbouring sites
$R[F^2 > 2\sigma(F^2)] = 0.072$	H-atom parameters constrained
$wR(F^2) = 0.138$	$w = 1/[\sigma^2(F_o^2) + (0.0365P)^2]$ where $P = (F_o^2 + 2F_c^2)/3$
$S = 1.04$	$(\Delta/\sigma)_{\max} = 0.001$
4373 reflections	$\Delta_{\max} = 0.99 \text{ e } \text{\AA}^{-3}$
289 parameters	$\Delta_{\min} = -0.63 \text{ e } \text{\AA}^{-3}$
0 restraints	

Special details

Geometry. All esds (except the esd in the dihedral angle between two l.s. planes) are estimated using the full covariance matrix. The cell esds are taken into account individually in the estimation of esds in distances, angles and torsion angles; correlations between esds in cell parameters are only used when they are defined by crystal symmetry. An approximate (isotropic) treatment of cell esds is used for estimating esds involving l.s. planes.

Fractional atomic coordinates and isotropic or equivalent isotropic displacement parameters (\AA^2)

	x	y	z	$U_{\text{iso}}^*/U_{\text{eq}}$
Br1	0.59458 (13)	0.59760 (4)	-0.32811 (7)	0.0334 (3)
Br2	0.62583 (15)	0.72766 (4)	-0.27164 (8)	0.0447 (3)
C1	0.6782 (12)	0.6229 (3)	-0.1863 (6)	0.025 (2)
C2	0.6928 (12)	0.6765 (3)	-0.1627 (7)	0.032 (2)
C3	0.7523 (13)	0.6925 (4)	-0.0597 (7)	0.033 (2)
C4	0.7992 (13)	0.6577 (4)	0.0216 (7)	0.036 (2)
C5	0.7892 (13)	0.6046 (4)	0.0029 (7)	0.032 (2)
C6	0.7294 (13)	0.5877 (3)	-0.1029 (7)	0.030 (2)
F1	0.7688 (8)	0.74424 (19)	-0.0345 (4)	0.0478 (15)
F2	0.8640 (8)	0.6733 (2)	0.1242 (4)	0.0474 (15)
F3	0.8364 (8)	0.5697 (2)	0.0809 (4)	0.0449 (14)

F4	0.7161 (8)	0.53629 (18)	-0.1210 (4)	0.0427 (14)
Br3	0.29782 (13)	0.61058 (4)	1.02883 (7)	0.0360 (3)
Br4	0.25741 (15)	0.73607 (4)	0.93725 (8)	0.0425 (3)
C13	0.2153 (12)	0.6268 (4)	0.8818 (6)	0.028 (2)
C14	0.1948 (12)	0.6784 (3)	0.8445 (7)	0.030 (2)
C15	0.1283 (13)	0.6877 (4)	0.7349 (7)	0.036 (2)
C16	0.0829 (14)	0.6485 (4)	0.6642 (7)	0.038 (2)
C17	0.1012 (13)	0.5971 (4)	0.7001 (7)	0.033 (2)
C18	0.1666 (13)	0.5872 (4)	0.8083 (7)	0.034 (2)
F5	0.1145 (8)	0.7375 (2)	0.6977 (4)	0.0452 (14)
F6	0.0251 (8)	0.6575 (2)	0.5595 (4)	0.0525 (16)
F7	0.0609 (8)	0.5566 (2)	0.6306 (4)	0.0523 (16)
F8	0.1798 (8)	0.53636 (19)	0.8413 (4)	0.0468 (15)
C7	0.5703 (14)	0.5582 (4)	0.2770 (7)	0.044 (3)
H7A	0.6844	0.5727	0.2559	0.053*
H7B	0.5414	0.5247	0.2413	0.053*
C8	0.6143 (14)	0.5498 (4)	0.3997 (7)	0.046 (3)
H8A	0.6002	0.5130	0.4154	0.055*
H8B	0.7475	0.5601	0.4297	0.055*
C9	0.2808 (15)	0.5639 (4)	0.4006 (7)	0.052 (3)
H9A	0.1882	0.5835	0.4319	0.063*
H9B	0.2665	0.5270	0.4159	0.063*
C10	0.2381 (14)	0.5725 (4)	0.2789 (7)	0.046 (3)
H10A	0.2005	0.5394	0.2430	0.055*
H10B	0.1300	0.5967	0.2592	0.055*
C11	0.4599 (19)	0.6442 (4)	0.2979 (7)	0.065 (4)
H11A	0.3539	0.6690	0.2769	0.078*
H11B	0.5742	0.6584	0.2765	0.078*
C12	0.5024 (19)	0.6364 (4)	0.4211 (7)	0.062 (4)
H12A	0.6341	0.6478	0.4515	0.075*
H12B	0.4135	0.6577	0.4517	0.075*
N1	0.4070 (11)	0.5934 (3)	0.2437 (5)	0.039 (2)
N2	0.4803 (12)	0.5812 (3)	0.4485 (5)	0.0341 (19)

Atomic displacement parameters (\AA^2)

	U^{11}	U^{22}	U^{33}	U^{12}	U^{13}	U^{23}
Br1	0.0314 (5)	0.0414 (6)	0.0270 (5)	-0.0027 (5)	0.0049 (4)	-0.0066 (4)
Br2	0.0418 (6)	0.0375 (6)	0.0528 (7)	0.0011 (5)	0.0055 (5)	0.0143 (5)
C1	0.022 (5)	0.034 (5)	0.019 (4)	0.007 (4)	0.006 (4)	-0.004 (4)
C2	0.023 (5)	0.027 (5)	0.045 (6)	0.003 (4)	0.007 (4)	0.008 (5)
C3	0.026 (5)	0.037 (6)	0.036 (6)	-0.002 (5)	0.002 (4)	-0.010 (5)
C4	0.028 (5)	0.060 (7)	0.023 (5)	-0.002 (5)	0.013 (4)	-0.005 (5)
C5	0.035 (6)	0.033 (6)	0.027 (5)	0.000 (5)	0.006 (4)	0.005 (4)
C6	0.034 (5)	0.025 (5)	0.030 (5)	-0.006 (5)	0.002 (4)	-0.010 (4)
F1	0.055 (4)	0.029 (3)	0.061 (4)	-0.004 (3)	0.014 (3)	-0.014 (3)
F2	0.053 (4)	0.054 (4)	0.032 (3)	-0.009 (3)	0.002 (3)	-0.015 (3)
F3	0.054 (4)	0.048 (4)	0.030 (3)	-0.005 (3)	0.002 (3)	0.010 (3)
F4	0.065 (4)	0.023 (3)	0.036 (3)	-0.003 (3)	0.002 (3)	-0.002 (2)
Br3	0.0312 (5)	0.0476 (7)	0.0282 (5)	0.0040 (5)	0.0042 (4)	0.0086 (5)
Br4	0.0448 (6)	0.0360 (6)	0.0458 (6)	0.0007 (5)	0.0075 (5)	-0.0082 (5)
C13	0.020 (5)	0.033 (6)	0.029 (5)	0.002 (4)	0.002 (4)	0.007 (4)
C14	0.023 (5)	0.036 (6)	0.032 (5)	0.000 (4)	0.010 (4)	0.003 (4)
C15	0.026 (5)	0.042 (6)	0.037 (6)	0.011 (5)	0.004 (4)	0.004 (5)
C16	0.039 (6)	0.051 (7)	0.026 (5)	0.011 (5)	0.012 (5)	0.002 (5)
C17	0.029 (5)	0.036 (6)	0.034 (5)	0.001 (5)	0.005 (4)	-0.011 (5)
C18	0.024 (5)	0.038 (6)	0.040 (6)	0.007 (5)	0.004 (4)	0.004 (5)
F5	0.042 (3)	0.044 (4)	0.049 (3)	0.005 (3)	0.009 (3)	0.015 (3)
F6	0.053 (4)	0.077 (4)	0.024 (3)	0.001 (3)	0.001 (3)	0.006 (3)
F7	0.055 (4)	0.055 (4)	0.048 (4)	0.001 (3)	0.013 (3)	-0.018 (3)
F8	0.056 (4)	0.029 (3)	0.058 (4)	0.005 (3)	0.018 (3)	0.007 (3)
C7	0.037 (6)	0.058 (7)	0.039 (6)	0.007 (6)	0.014 (5)	-0.003 (5)
C8	0.046 (6)	0.054 (7)	0.033 (6)	0.009 (6)	0.000 (5)	0.002 (5)
C9	0.057 (7)	0.070 (8)	0.028 (6)	0.001 (6)	0.004 (5)	0.000 (5)
C10	0.045 (6)	0.060 (7)	0.027 (5)	0.005 (6)	-0.001 (5)	-0.003 (5)
C11	0.120 (11)	0.023 (6)	0.045 (7)	-0.008 (7)	0.004 (7)	0.003 (5)
C12	0.109 (10)	0.029 (6)	0.039 (6)	-0.004 (7)	-0.007 (6)	0.001 (5)
N1	0.040 (5)	0.049 (6)	0.026 (4)	0.001 (4)	0.002 (4)	0.002 (4)
N2	0.061 (5)	0.021 (4)	0.019 (4)	-0.001 (4)	0.006 (4)	-0.001 (3)

Geometric parameters (Å, °)

Br1—C1	1.896 (8)	C18—F8	1.359 (10)
Br2—C2	1.892 (8)	C7—H7A	0.9700
C1—C2	1.398 (11)	C7—H7B	0.9700
C1—C6	1.381 (11)	C7—C8	1.547 (12)
C2—C3	1.357 (11)	C7—N1	1.448 (11)
C3—C4	1.352 (12)	C8—H8A	0.9700
C3—F1	1.357 (9)	C8—H8B	0.9700
C4—C5	1.372 (12)	C8—N2	1.468 (11)
C4—F2	1.354 (9)	C9—H9A	0.9700
C5—C6	1.397 (11)	C9—H9B	0.9700
C5—F3	1.325 (9)	C9—C10	1.536 (11)
C6—F4	1.330 (9)	C9—N2	1.474 (11)
Br3—C13	1.892 (8)	C10—H10A	0.9700
Br4—C14	1.881 (9)	C10—H10B	0.9700
C13—C14	1.395 (11)	C10—N1	1.454 (11)
C13—C18	1.372 (12)	C11—H11A	0.9700
C14—C15	1.400 (11)	C11—H11B	0.9700
C15—C16	1.339 (12)	C11—C12	1.552 (12)
C15—F5	1.352 (10)	C11—N1	1.479 (11)
C16—C17	1.386 (12)	C12—H12A	0.9700
C16—F6	1.333 (9)	C12—H12B	0.9700
C17—C18	1.385 (12)	C12—N2	1.466 (11)
C17—F7	1.351 (9)		
C2—C1—Br1	122.2 (6)	N1—C7—H7A	109.4
C6—C1—Br1	119.6 (6)	N1—C7—H7B	109.4
C6—C1—C2	118.2 (7)	N1—C7—C8	111.2 (7)
C1—C2—Br2	121.2 (7)	C7—C8—H8A	109.6
C3—C2—Br2	119.0 (7)	C7—C8—H8B	109.6
C3—C2—C1	119.7 (8)	H8A—C8—H8B	108.1
C4—C3—C2	121.6 (9)	N2—C8—C7	110.2 (7)
C4—C3—F1	117.4 (8)	N2—C8—H8A	109.6
F1—C3—C2	121.0 (8)	N2—C8—H8B	109.6
C3—C4—C5	121.1 (8)	H9A—C9—H9B	108.1
C3—C4—F2	122.0 (9)	C10—C9—H9A	109.6
F2—C4—C5	116.8 (8)	C10—C9—H9B	109.6
C4—C5—C6	117.8 (8)	N2—C9—H9A	109.6
F3—C5—C4	122.4 (8)	N2—C9—H9B	109.6

F3—C5—C6	119.8 (8)	N2—C9—C10	110.2 (8)
C1—C6—C5	121.5 (8)	C9—C10—H10A	109.3
F4—C6—C1	120.5 (7)	C9—C10—H10B	109.3
F4—C6—C5	117.9 (8)	H10A—C10—H10B	108.0
C14—C13—Br3	122.2 (7)	N1—C10—C9	111.5 (8)
C18—C13—Br3	119.9 (7)	N1—C10—H10A	109.3
C18—C13—C14	117.8 (8)	N1—C10—H10B	109.3
C13—C14—Br4	121.8 (6)	H11A—C11—H11B	108.2
C13—C14—C15	119.3 (8)	C12—C11—H11A	109.7
C15—C14—Br4	118.9 (7)	C12—C11—H11B	109.7
C16—C15—C14	122.1 (9)	N1—C11—H11A	109.7
C16—C15—F5	118.2 (8)	N1—C11—H11B	109.7
F5—C15—C14	119.6 (8)	N1—C11—C12	109.8 (7)
C15—C16—C17	119.2 (8)	C11—C12—H12A	109.4
F6—C16—C15	121.9 (9)	C11—C12—H12B	109.4
F6—C16—C17	118.9 (8)	H12A—C12—H12B	108.0
C18—C17—C16	119.4 (8)	N2—C12—C11	111.0 (7)
F7—C17—C16	120.8 (8)	N2—C12—H12A	109.4
F7—C17—C18	119.8 (9)	N2—C12—H12B	109.4
C13—C18—C17	122.1 (9)	C7—N1—C10	109.2 (8)
F8—C18—C13	119.9 (8)	C7—N1—C11	107.3 (8)
F8—C18—C17	118.0 (8)	C10—N1—C11	108.5 (8)
H7A—C7—H7B	108.0	C8—N2—C9	107.4 (7)
C8—C7—H7A	109.4	C12—N2—C8	108.1 (8)
C8—C7—H7B	109.4	C12—N2—C9	109.1 (8)

1,3-dibromotetrafluorobenzene–1,4-diazabicyclo[2.2.2]octane (4a)

Crystal data

Br ₂ C ₆ F ₄ ·0.5(C ₆ H ₁₂ N ₂)	$F(000) = 692$
$M_r = 363.97$	$D_x = 2.136 \text{ Mg m}^{-3}$
Monoclinic, $C2/m$	Mo $K\alpha$ radiation, $\lambda = 0.71073 \text{ \AA}$
$a = 18.8934 (9) \text{ \AA}$	Cell parameters from 2296 reflections
$b = 6.8201 (3) \text{ \AA}$	$\theta = 3.2\text{--}28.4^\circ$
$c = 8.7971 (4) \text{ \AA}$	$\mu = 7.19 \text{ mm}^{-1}$
$\beta = 93.395 (4)^\circ$	$T = 150 \text{ K}$
$V = 1131.56 (9) \text{ \AA}^3$	Irregular, clear light colourless
$Z = 4$	$0.25 \times 0.05 \times 0.01 \text{ mm}$

Data collection

SuperNova, Single source at offset/far, Eos diffractometer	1445 independent reflections
Radiation source: micro-focus sealed X-ray tube, SuperNova (Mo) X-ray Source	1264 reflections with $I > 2\sigma(I)$
Mirror monochromator	$R_{\text{int}} = 0.028$
Detector resolution: 8.0714 pixels mm^{-1}	$\theta_{\text{max}} = 28.9^\circ$, $\theta_{\text{min}} = 3.1^\circ$
ω scans	$h = -24 \rightarrow 25$
Absorption correction: multi-scan <i>CrysAlis PRO</i> 1.171.39.46 (Rigaku Oxford Diffraction, 2018) Empirical absorption correction using spherical harmonics, implemented in SCALE3 ABSPACK scaling algorithm.	$k = -9 \rightarrow 8$
$T_{\text{min}} = 0.693$, $T_{\text{max}} = 1.000$	$l = -11 \rightarrow 11$
4623 measured reflections	

Refinement

Refinement on F^2	153 restraints
Least-squares matrix: full	Hydrogen site location: inferred from neighbouring sites
$R[F^2 > 2\sigma(F^2)] = 0.036$	H-atom parameters constrained
$wR(F^2) = 0.081$	$w = 1/[\sigma^2(F_o^2) + (0.0215P)^2 + 8.1636P]$ where $P = (F_o^2 + 2F_c^2)/3$
$S = 1.08$	$(\Delta/\sigma)_{\text{max}} < 0.001$
1445 reflections	$\Delta_{\text{max}} = 1.41 \text{ e } \text{\AA}^{-3}$
145 parameters	$\Delta_{\text{min}} = -0.60 \text{ e } \text{\AA}^{-3}$

Special details

Geometry. All esds (except the esd in the dihedral angle between two l.s. planes) are estimated using the full covariance matrix. The cell esds are taken into account individually in the estimation of esds in distances, angles and torsion angles; correlations between esds in cell parameters are only used when they are defined by crystal symmetry. An approximate (isotropic) treatment of cell esds is used for estimating esds involving l.s. planes.

*Fractional atomic coordinates and isotropic or equivalent isotropic displacement parameters
(\AA^2)*

	x	y	z	$U_{\text{iso}}^*/U_{\text{eq}}$	Occ. (<1)
Br1	0.34257 (3)	0.5000	0.28238 (6)	0.02737 (16)	
Br2	0.23154 (3)	0.5000	0.87155 (6)	0.03658 (18)	
F1	0.34032 (18)	0.5000	0.6296 (4)	0.0338 (8)	
F2	0.09360 (18)	0.5000	0.6790 (4)	0.0397 (9)	
F3	0.06985 (19)	0.5000	0.3768 (4)	0.0437 (9)	
F4	0.1826 (2)	0.5000	0.1955 (4)	0.0426 (9)	
C1	0.2645 (3)	0.5000	0.4092 (6)	0.0241 (11)	
C2	0.2737 (3)	0.5000	0.5655 (6)	0.0252 (11)	
C3	0.2173 (3)	0.5000	0.6598 (6)	0.0256 (11)	
C4	0.1501 (3)	0.5000	0.5935 (6)	0.0266 (12)	
C5	0.1379 (3)	0.5000	0.4382 (7)	0.0300 (12)	
C6	0.1955 (3)	0.5000	0.3462 (6)	0.0275 (12)	
N1	0.4549 (8)	0.503 (3)	0.0983 (17)	0.028 (2)	0.25
N2	0.5539 (8)	0.504 (3)	-0.0891 (17)	0.027 (2)	0.25
C7	0.5054 (9)	0.662 (3)	0.135 (2)	0.030 (3)	0.25
H7A	0.5255	0.6461	0.2378	0.036*	0.25
H7B	0.4806	0.7869	0.1288	0.036*	0.25
C8	0.5656 (10)	0.663 (3)	0.0224 (19)	0.027 (3)	0.25
H8A	0.5665	0.7881	-0.0298	0.033*	0.25
H8B	0.6110	0.6447	0.0782	0.033*	0.25
C9	0.4851 (6)	0.533 (2)	-0.1721 (13)	0.030 (3)	0.25
H9A	0.4772	0.4304	-0.2472	0.036*	0.25
H9B	0.4848	0.6582	-0.2251	0.036*	0.25
C10	0.4252 (6)	0.530 (3)	-0.0597 (12)	0.031 (3)	0.25
H10A	0.3991	0.6524	-0.0670	0.037*	0.25
H10B	0.3926	0.4242	-0.0864	0.037*	0.25
C11	0.4930 (9)	0.315 (3)	0.1059 (19)	0.029 (3)	0.25
H11A	0.4601	0.2083	0.0813	0.034*	0.25
H11B	0.5134	0.2937	0.2084	0.034*	0.25
C12	0.5527 (9)	0.316 (3)	-0.0086 (19)	0.028 (3)	0.25
H12A	0.5981	0.2937	0.0458	0.033*	0.25
H12B	0.5447	0.2105	-0.0817	0.033*	0.25

Atomic displacement parameters (\AA^2)

	U^{11}	U^{22}	U^{33}	U^{12}	U^{13}	U^{23}
Br1	0.0343 (3)	0.0226 (3)	0.0268 (3)	0.000	0.0154 (2)	0.000
Br2	0.0461 (4)	0.0415 (4)	0.0229 (3)	0.000	0.0084 (3)	0.000
F1	0.0330 (18)	0.043 (2)	0.0259 (17)	0.000	0.0027 (14)	0.000
F2	0.0346 (19)	0.042 (2)	0.045 (2)	0.000	0.0225 (16)	0.000
F3	0.0278 (18)	0.057 (2)	0.045 (2)	0.000	-0.0133 (15)	0.000
F4	0.047 (2)	0.058 (2)	0.0223 (17)	0.000	0.0024 (15)	0.000
C1	0.032 (3)	0.018 (2)	0.024 (3)	0.000	0.014 (2)	0.000
C2	0.033 (3)	0.020 (2)	0.023 (3)	0.000	0.004 (2)	0.000
C3	0.036 (3)	0.014 (2)	0.027 (3)	0.000	0.012 (2)	0.000
C4	0.031 (3)	0.024 (3)	0.026 (3)	0.000	0.013 (2)	0.000
C5	0.027 (3)	0.030 (3)	0.033 (3)	0.000	0.005 (2)	0.000
C6	0.034 (3)	0.024 (3)	0.025 (3)	0.000	0.010 (2)	0.000
N1	0.025 (4)	0.035 (4)	0.026 (4)	0.000 (5)	0.009 (3)	-0.002 (4)
N2	0.023 (4)	0.032 (4)	0.027 (4)	-0.001 (4)	0.008 (3)	-0.001 (5)
C7	0.027 (5)	0.035 (5)	0.029 (5)	0.000 (5)	0.006 (4)	-0.002 (5)
C8	0.024 (5)	0.030 (5)	0.029 (5)	0.001 (4)	0.005 (4)	-0.001 (5)
C9	0.025 (4)	0.035 (8)	0.030 (4)	-0.001 (4)	0.005 (3)	-0.001 (4)
C10	0.026 (4)	0.038 (8)	0.029 (4)	-0.001 (4)	0.006 (3)	0.000 (4)
C11	0.025 (6)	0.035 (4)	0.027 (6)	-0.001 (4)	0.008 (4)	-0.002 (4)
C12	0.025 (6)	0.031 (4)	0.027 (6)	0.000 (4)	0.009 (4)	-0.001 (4)

Geometric parameters (\AA , $^\circ$)

Br1—C1	1.901 (5)	N2—C12	1.470 (14)
Br2—C3	1.866 (6)	C7—H7A	0.9700
F1—C2	1.348 (6)	C7—H7B	0.9700
F2—C4	1.342 (6)	C7—C8	1.550 (13)
F3—C5	1.365 (7)	C8—H8A	0.9700
F4—C6	1.334 (6)	C8—H8B	0.9700
C1—C2	1.375 (7)	C9—H9A	0.9700
C1—C6	1.387 (8)	C9—H9B	0.9700
C2—C3	1.389 (7)	C9—C10	1.546 (12)
C3—C4	1.366 (8)	C10—H10A	0.9700
C4—C5	1.372 (8)	C10—H10B	0.9700
C5—C6	1.393 (7)	C11—H11A	0.9700
N1—C7	1.469 (13)	C11—H11B	0.9700
N1—C10	1.479 (13)	C11—C12	1.556 (13)

N1—C11	1.470 (14)	C12—H12A	0.9700
N2—C8	1.468 (13)	C12—H12B	0.9700
N2—C9	1.467 (13)		
C2—C1—Br1	122.0 (4)	N2—C8—C7	109.7 (12)
C2—C1—C6	117.3 (5)	N2—C8—H8A	109.7
C6—C1—Br1	120.6 (4)	N2—C8—H8B	109.7
F1—C2—C1	118.5 (5)	C7—C8—H8A	109.7
F1—C2—C3	118.7 (5)	C7—C8—H8B	109.7
C1—C2—C3	122.8 (5)	H8A—C8—H8B	108.2
C2—C3—Br2	121.8 (4)	N2—C9—H9A	109.7
C4—C3—Br2	120.1 (4)	N2—C9—H9B	109.7
C4—C3—C2	118.1 (5)	N2—C9—C10	109.9 (10)
F2—C4—C3	120.7 (5)	H9A—C9—H9B	108.2
F2—C4—C5	117.8 (5)	C10—C9—H9A	109.7
C3—C4—C5	121.5 (5)	C10—C9—H9B	109.7
F3—C5—C4	119.5 (5)	N1—C10—C9	110.6 (10)
F3—C5—C6	121.3 (5)	N1—C10—H10A	109.5
C4—C5—C6	119.2 (5)	N1—C10—H10B	109.5
F4—C6—C1	120.6 (5)	C9—C10—H10A	109.5
F4—C6—C5	118.3 (5)	C9—C10—H10B	109.5
C1—C6—C5	121.1 (5)	H10A—C10—H10B	108.1
C7—N1—C10	108.4 (11)	N1—C11—H11A	109.7
C7—N1—C11	109.1 (10)	N1—C11—H11B	109.7
C11—N1—C10	108.1 (11)	N1—C11—C12	109.7 (14)
C8—N2—C12	109.2 (10)	H11A—C11—H11B	108.2
C9—N2—C8	109.1 (11)	C12—C11—H11A	109.7
C9—N2—C12	108.6 (11)	C12—C11—H11B	109.7
N1—C7—H7A	109.5	N2—C12—C11	110.5 (14)
N1—C7—H7B	109.5	N2—C12—H12A	109.6
N1—C7—C8	110.8 (13)	N2—C12—H12B	109.6
H7A—C7—H7B	108.1	C11—C12—H12A	109.6
C8—C7—H7A	109.5	C11—C12—H12B	109.6
C8—C7—H7B	109.5	H12A—C12—H12B	108.1

Appendix 3

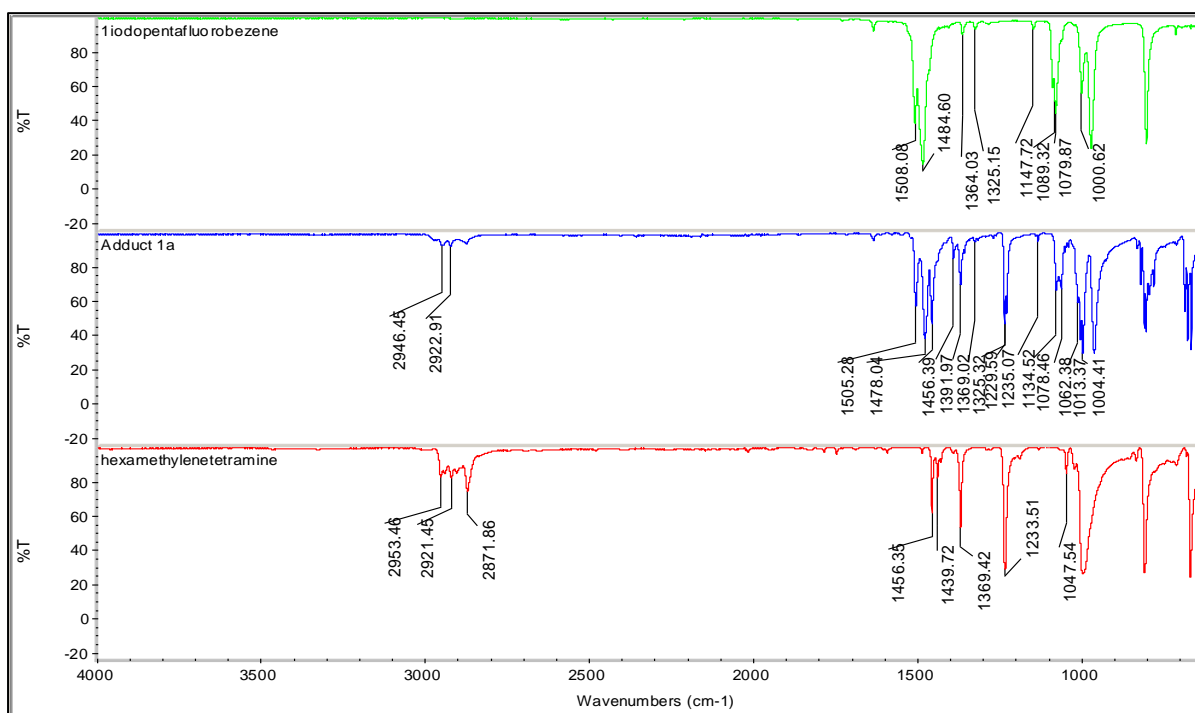
(Supplementary information)

Chapter 3:- A Crystallographic and QTAIM study of halogen bonding in a series of iodofluorobenzenes and hexamethylenetetramine and 1,3,5-triazaphosphaadamantane

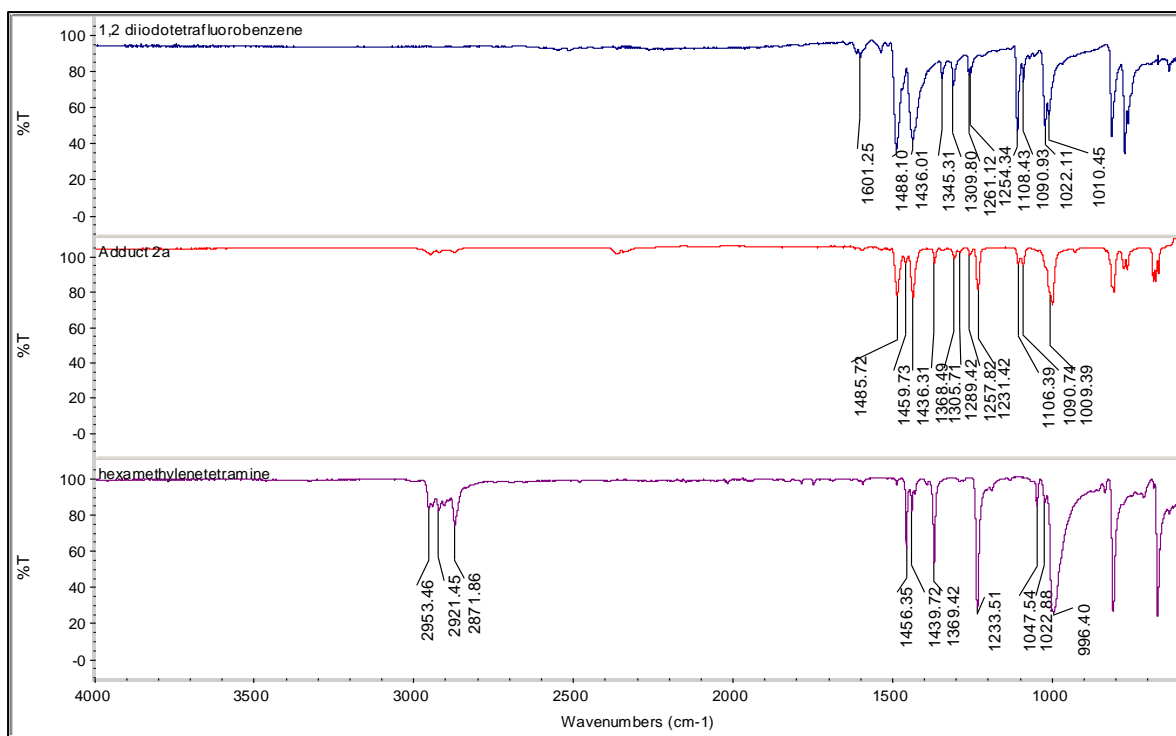
Alan K. Brisdon* and Sultan Al kaabi

Department of Chemistry, The University of Manchester, Oxford Road, Manchester, M13 9PL, United Kingdom

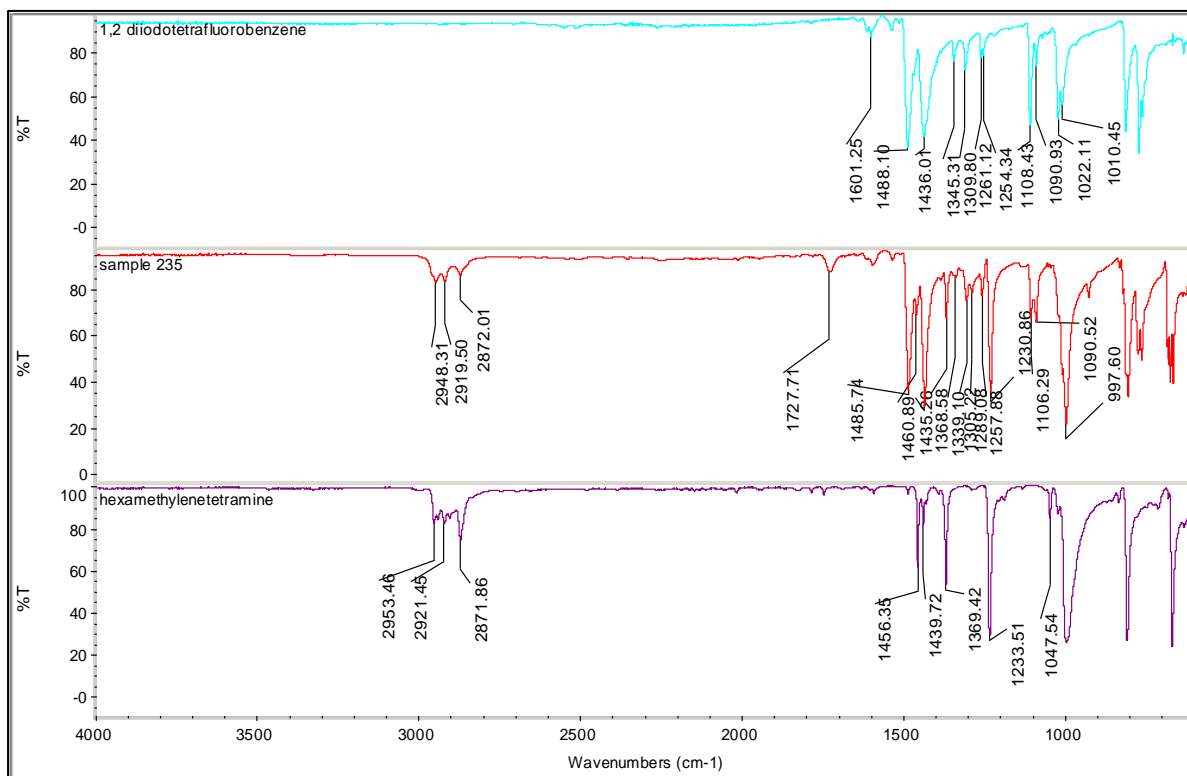
Correspondence email: *alan.brisdon@manchester.ac.uk



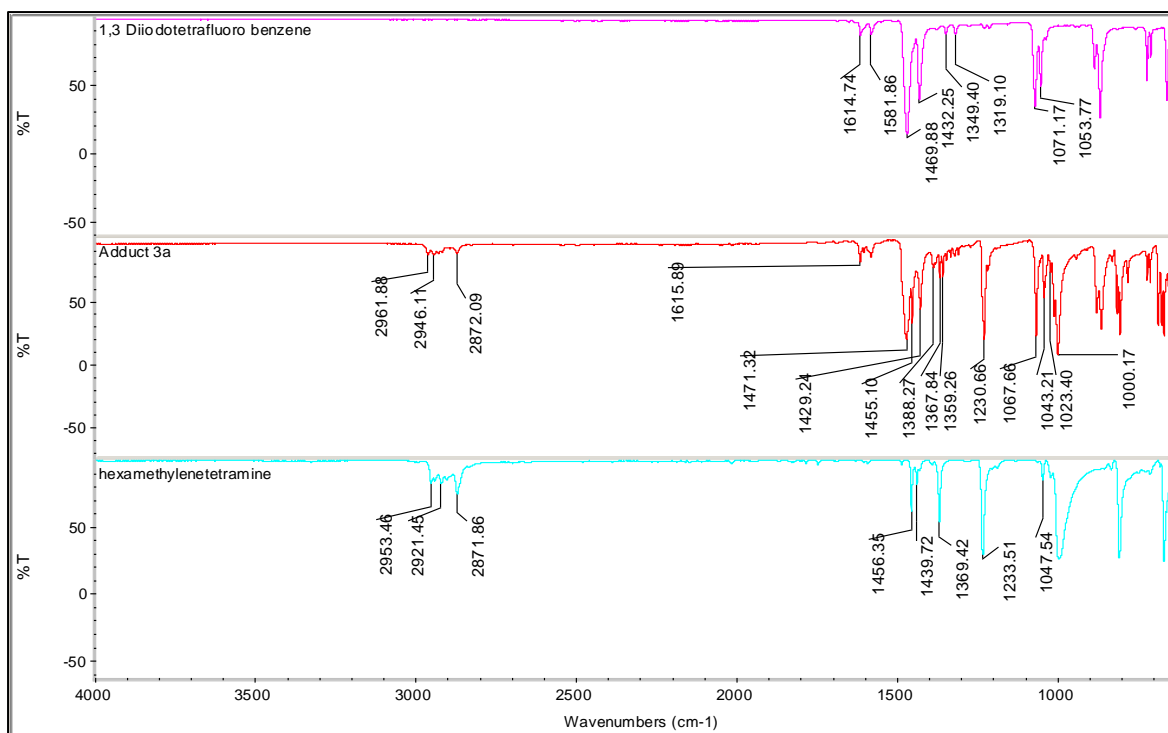
S 3.1 IR spectra showing the two starting materials and adduct **1a**



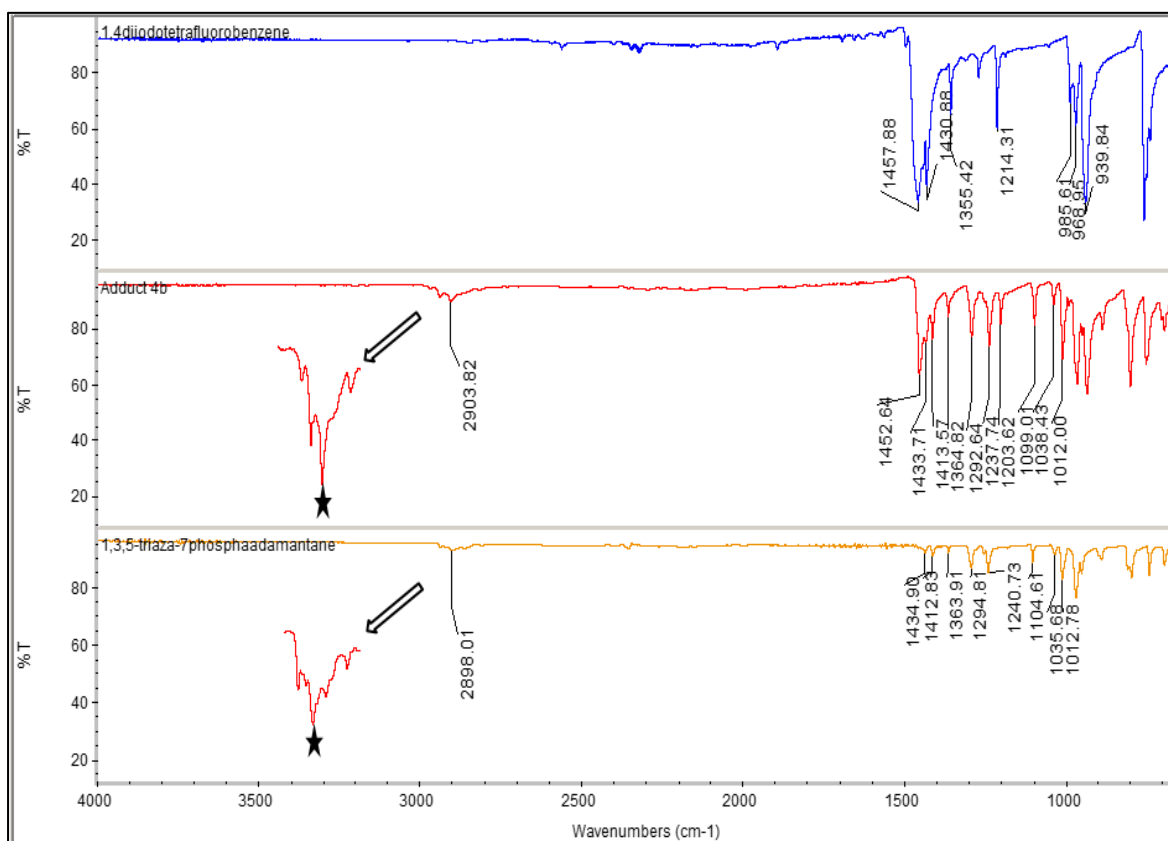
S 3.2 IR spectra showing the two starting materials and adduct **2a.1**



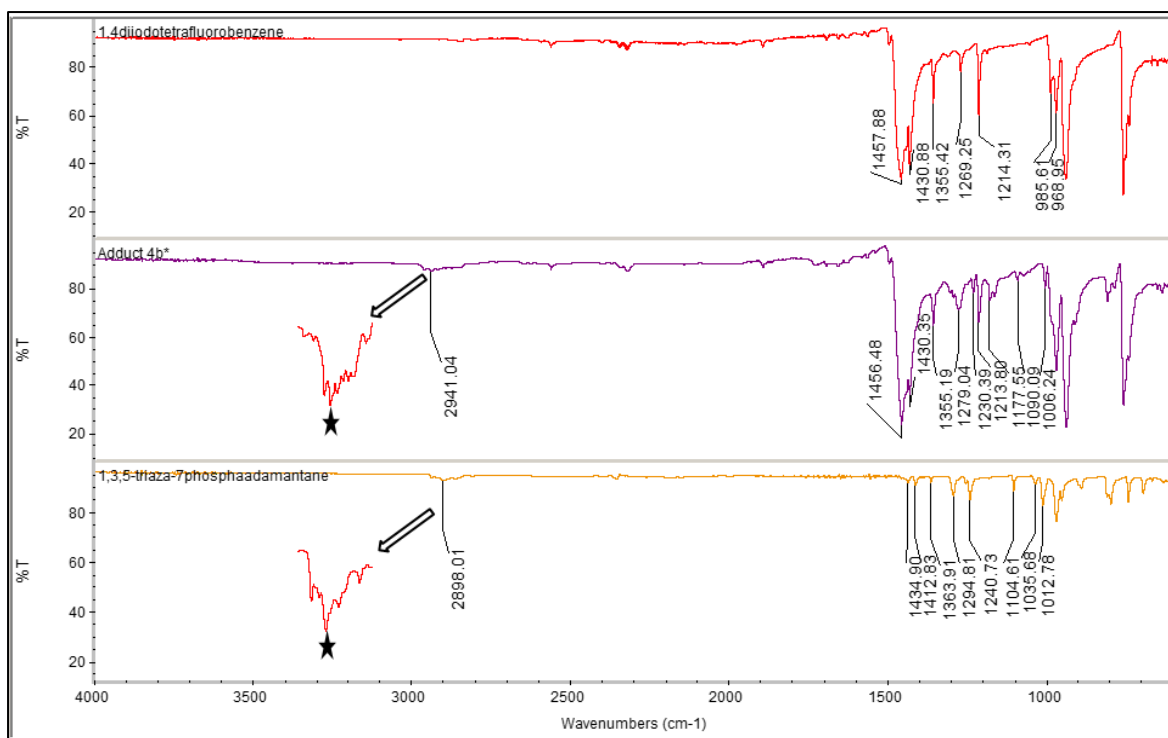
S3.3 IR spectra showing the two starting materials and adduct **2a**



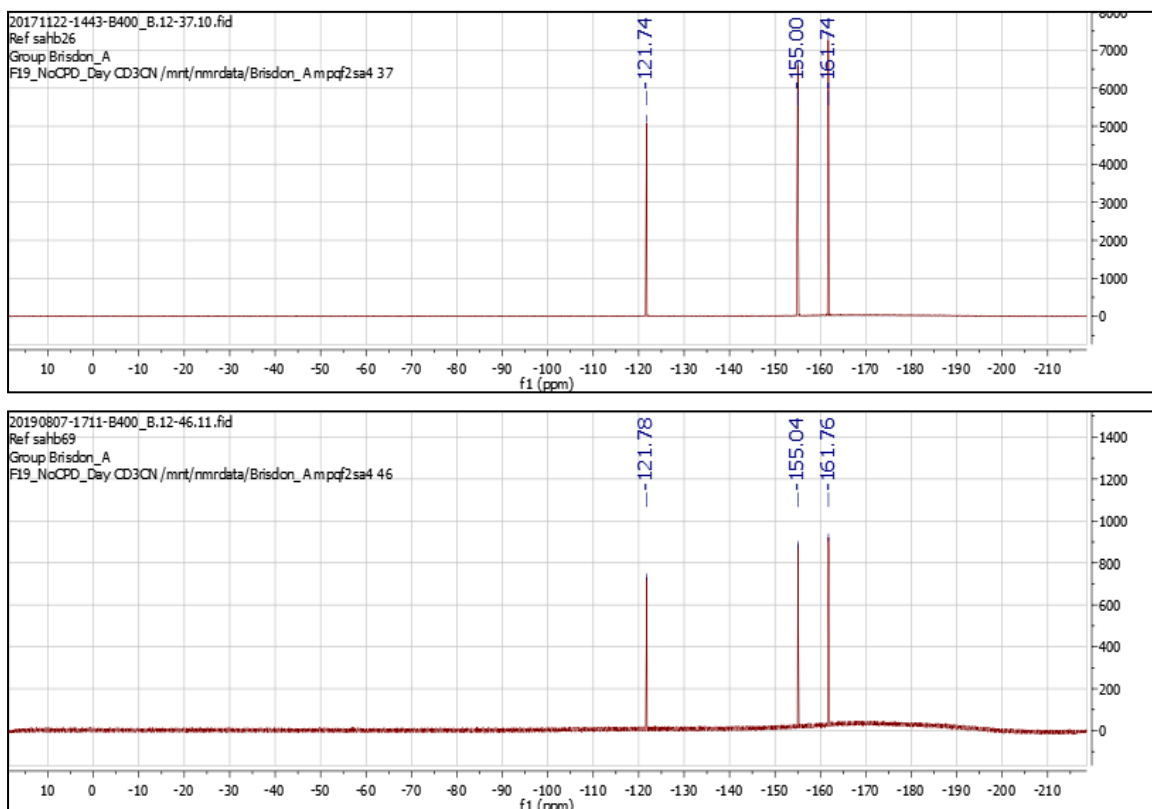
S 3.4 IR spectra showing the two starting materials and adduct **3a**



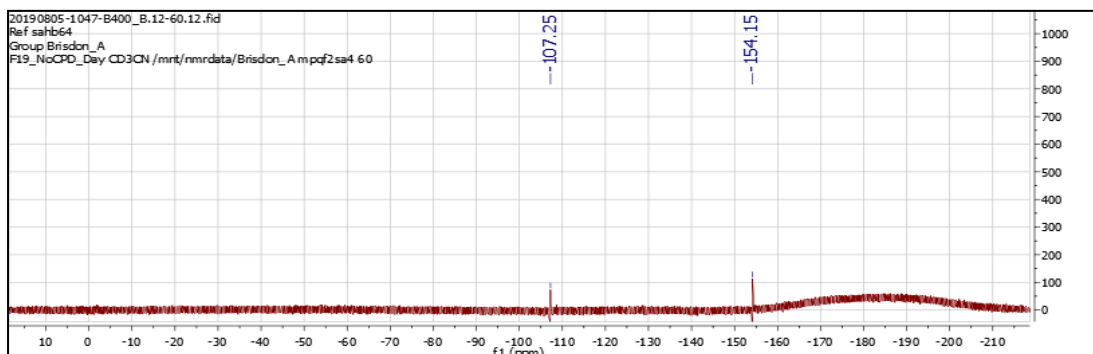
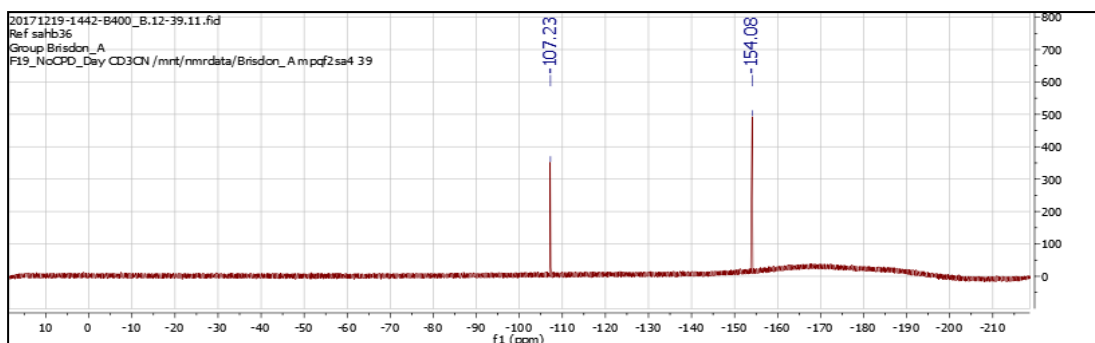
S 3.5 IR spectra showing the two starting materials and adduct **4b.1**



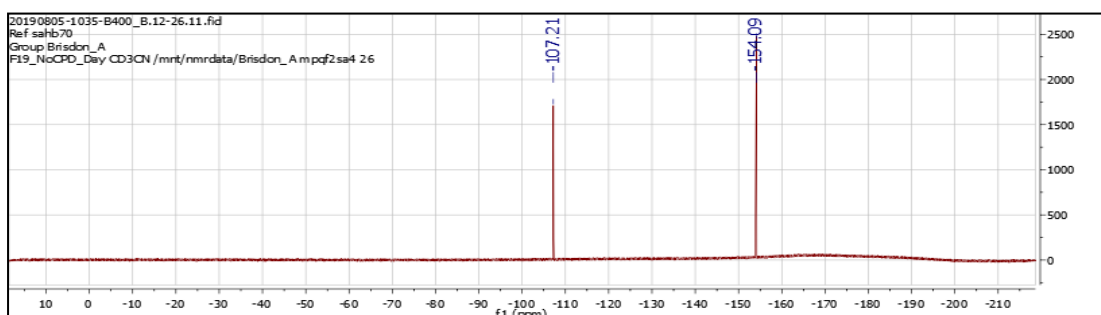
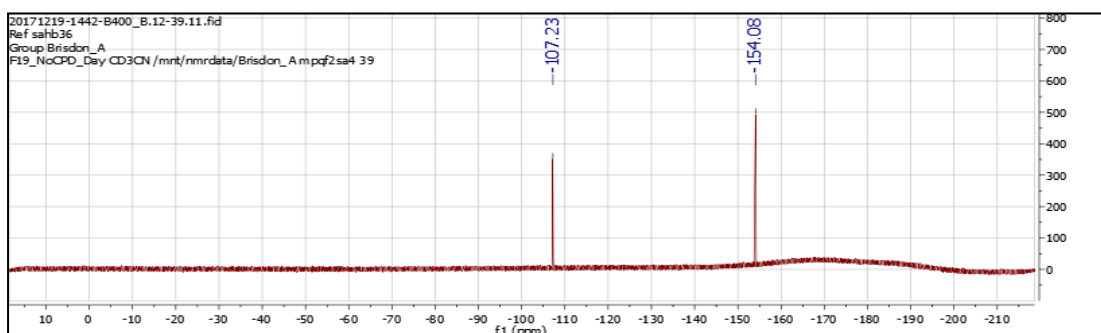
S 3.6 IR spectra showing the two starting materials and adduct **4b**



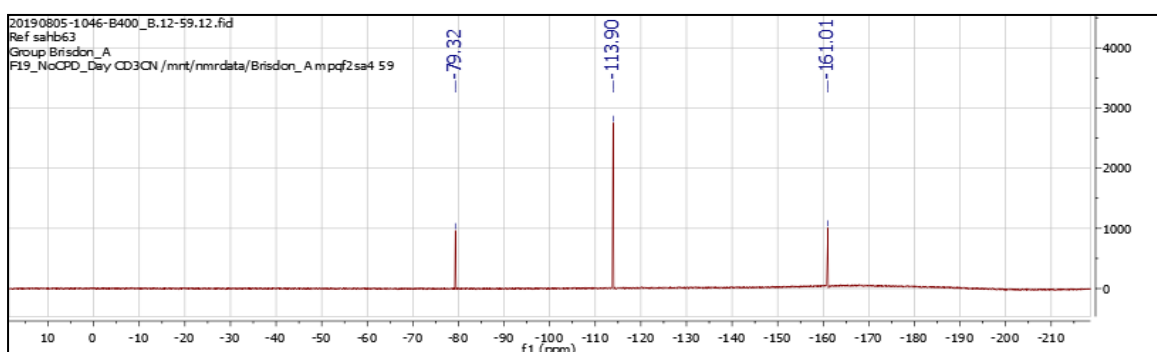
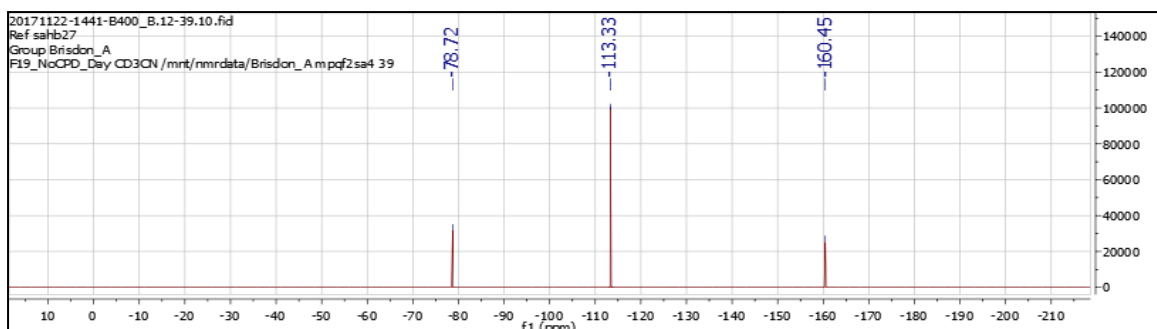
S 3.7 ¹⁹F NMR spectra for adduct **1a** and iodopentafluorobenzene using acetonitrile-d₃



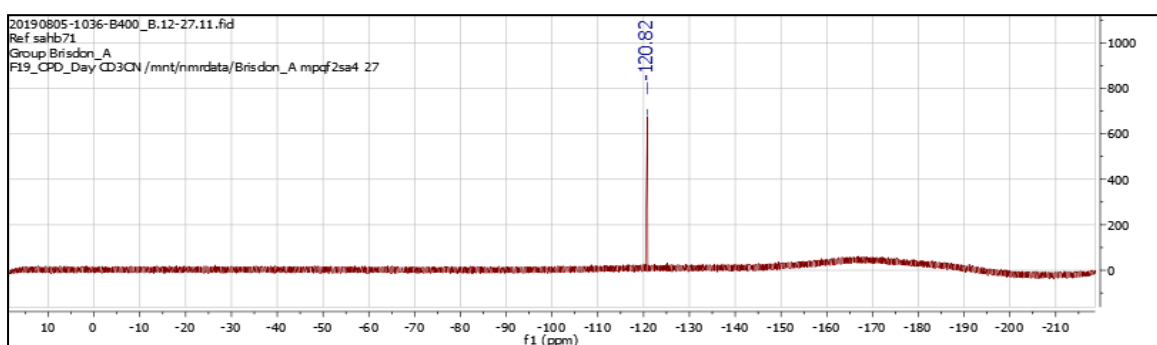
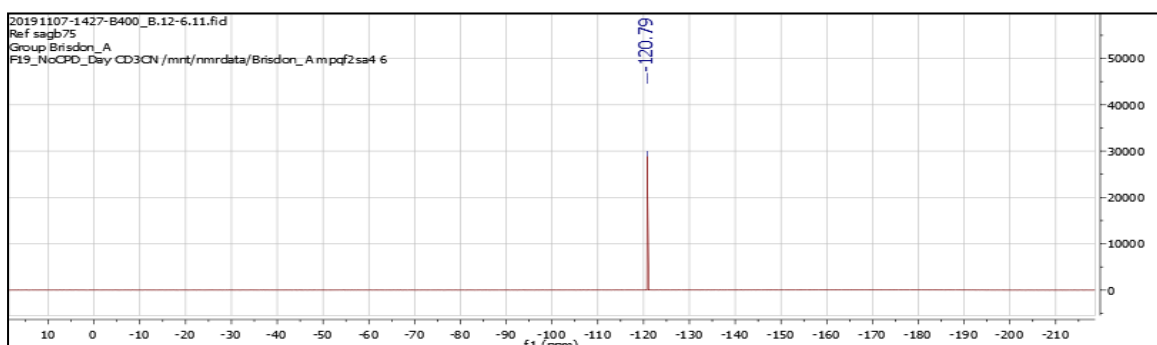
S3.8 ¹⁹F NMR spectra for adduct **2a.1** and 1,2-diiodotetrafluorobenzene using acetonitrile-d₃



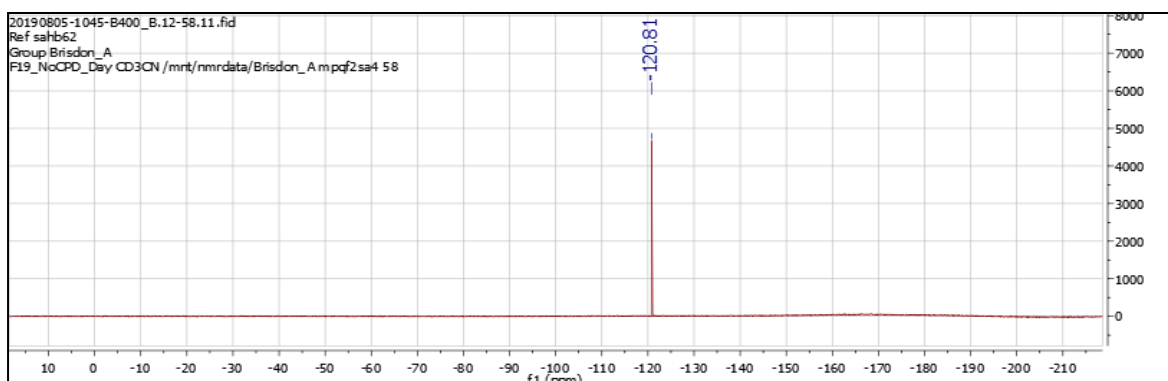
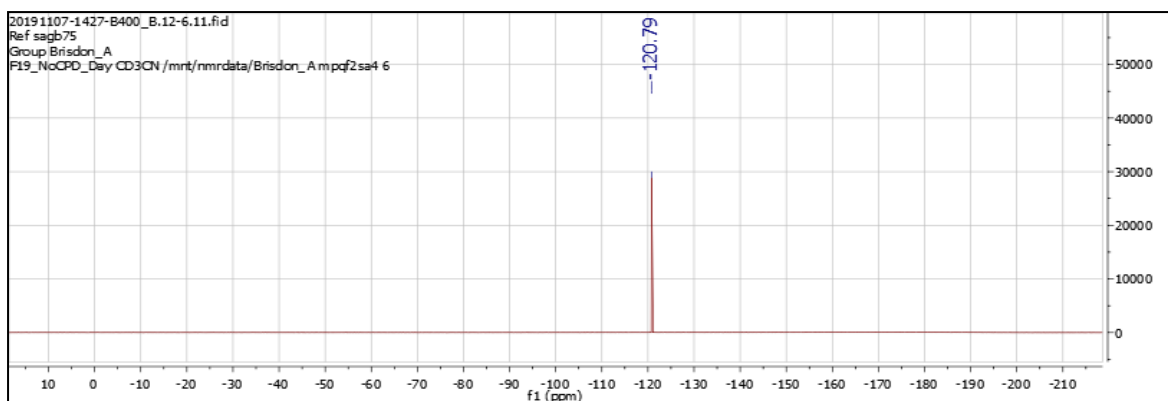
S3.9 ¹⁹F NMR spectra for adduct **2a** and 1,2-diiodotetrafluorobenzene using



S 3.10 ^{19}F NMR spectra for adduct **3a** and 1,3-diiodotetrafluorobenzene using acetonitrile-



S 3.11 ^{19}F NMR spectra for adduct **4b.1** and 1,4-diiodotetrafluorobenzene using acetonitrile- d_3



S 3.12 ^{19}F NMR spectra for adduct **4b** and 1,4-diiodotetrafluorobenzene using acetonitrile- d_3

Computing details

Data collection: *CrysAlis PRO* 1.171.39.46 (Rigaku OD, 2018); cell refinement: *CrysAlis PRO* 1.171.39.46 (Rigaku OD, 2018); data reduction: *CrysAlis PRO* 1.171.39.46 (Rigaku OD, 2018); program(s) used to solve structure: ShelXT (Sheldrick, 2015); program(s) used to refine structure: *SHELXL* (Sheldrick, 2015); molecular graphics: Olex2 (Dolomanov *et al.*, 2009); software used to prepare material for publication: Olex2 (Dolomanov *et al.*, 2009).

iodotetrafluorobenzene– hexamethylene-tetramine(**1a**)

Crystal data

$2(\text{C}_6\text{F}_5\text{I}) \cdot \text{C}_6\text{H}_{12}\text{N}_4$	$F(000) = 1376$
$M_r = 728.12$	$D_x = 2.227 \text{ Mg m}^{-3}$
Monoclinic, $P2_1/c$	Mo $K\alpha$ radiation, $\lambda = 0.71073 \text{ \AA}$
$a = 5.9745 (2) \text{ \AA}$	Cell parameters from 5205 reflections
$b = 14.6528 (7) \text{ \AA}$	$\theta = 3.3\text{--}27.4^\circ$
$c = 24.8061 (9) \text{ \AA}$	$\mu = 3.00 \text{ mm}^{-1}$
$\beta = 91.036 (3)^\circ$	$T = 150 \text{ K}$
$V = 2171.25 (15) \text{ \AA}^3$	Needle, clear light colourless
$Z = 4$	$0.2 \times 0.1 \times 0.01 \text{ mm}$

Data collection

SuperNova, Single source at offset/far, Eos diffractometer	4276 independent reflections
Radiation source: micro-focus sealed X-ray tube, SuperNova (Mo) X-ray Source	3543 reflections with $I > 2\sigma(I)$
Mirror monochromator	$R_{\text{int}} = 0.058$
Detector resolution: 8.0714 pixels mm^{-1}	$\theta_{\text{max}} = 26.0^\circ$, $\theta_{\text{min}} = 3.2^\circ$
ω scans	$h = -7 \rightarrow 7$
Absorption correction: multi-scan <i>CrysAlis PRO</i> 1.171.39.46 (Rigaku Oxford Diffraction, 2018) Empirical absorption correction using spherical harmonics, implemented in SCALE3 ABSPACK scaling algorithm.	$k = -11 \rightarrow 18$
$T_{\text{min}} = 0.613$, $T_{\text{max}} = 1.000$	$l = -30 \rightarrow 30$
16755 measured reflections	

Refinement

Refinement on F^2	Primary atom site location: dual
Least-squares matrix: full	Hydrogen site location: inferred from neighbouring sites
$R[F^2 > 2\sigma(F^2)] = 0.047$	H-atom parameters constrained
$wR(F^2) = 0.092$	$w = 1/[\sigma^2(F_o^2) + (0.029P)^2 + 0.9877P]$ where $P = (F_o^2 + 2F_c^2)/3$
$S = 1.13$	$(\Delta/\sigma)_{\text{max}} = 0.001$
4276 reflections	$\Delta_{\text{max}} = 1.22 \text{ e } \text{\AA}^{-3}$
308 parameters	$\Delta_{\text{min}} = -0.79 \text{ e } \text{\AA}^{-3}$
0 restraints	

Special details

<p><i>Geometry.</i> All esds (except the esd in the dihedral angle between two l.s. planes) are estimated using the full covariance matrix. The cell esds are taken into account individually in the estimation of esds in distances, angles and torsion angles; correlations between esds in cell parameters are only used when they are defined by crystal symmetry. An approximate (isotropic) treatment of cell esds is used for estimating esds involving l.s. planes.</p>
<p><i>Refinement.</i> Refined as a 2-component twin.</p>

Fractional atomic coordinates and isotropic or equivalent isotropic displacement parameters
(\AA^2)

	<i>x</i>	<i>y</i>	<i>z</i>	$U_{\text{iso}}^*/U_{\text{eq}}$
I1	0.50215 (6)	0.65268 (3)	0.45467 (2)	0.02704 (12)
F1	0.0364 (5)	0.5429 (2)	0.44699 (13)	0.0381 (9)
F2	-0.2231 (5)	0.4887 (2)	0.36341 (14)	0.0420 (9)
F3	-0.0877 (6)	0.5180 (3)	0.26048 (14)	0.0511 (10)
F4	0.3113 (7)	0.5997 (3)	0.24250 (13)	0.0489 (10)
F5	0.5715 (5)	0.6554 (2)	0.32605 (13)	0.0342 (8)
C1	0.3091 (9)	0.6032 (4)	0.3887 (2)	0.0251 (13)
C2	0.1070 (9)	0.5594 (4)	0.3968 (2)	0.0272 (13)
C3	-0.0262 (9)	0.5316 (4)	0.3541 (2)	0.0302 (14)
C4	0.0424 (11)	0.5447 (4)	0.3022 (2)	0.0357 (15)
C5	0.2437 (10)	0.5865 (4)	0.2931 (2)	0.0323 (14)
C6	0.3745 (9)	0.6152 (4)	0.3365 (2)	0.0267 (13)
I2	0.53377 (6)	0.66130 (3)	0.73739 (2)	0.02674 (12)
F6	0.0785 (5)	0.7115 (2)	0.79906 (13)	0.0349 (8)
F7	-0.0518 (5)	0.6837 (2)	0.90151 (13)	0.0380 (9)
F8	0.2066 (6)	0.5834 (2)	0.96999 (13)	0.0406 (9)
F9	0.6079 (5)	0.5172 (2)	0.93780 (12)	0.0342 (8)
F10	0.7420 (5)	0.5452 (2)	0.83611 (12)	0.0308 (8)
C7	0.4141 (9)	0.6291 (4)	0.8146 (2)	0.0231 (13)
C8	0.2099 (9)	0.6629 (4)	0.8319 (2)	0.0232 (12)
C9	0.1427 (9)	0.6489 (4)	0.8843 (2)	0.0277 (13)
C10	0.2748 (9)	0.5987 (4)	0.9193 (2)	0.0261 (13)
C11	0.4775 (9)	0.5645 (4)	0.9030 (2)	0.0249 (13)
C12	0.5407 (9)	0.5793 (4)	0.8507 (2)	0.0231 (12)
N1	0.7244 (7)	0.7290 (3)	0.54446 (17)	0.0220 (10)
N2	0.7122 (7)	0.7297 (3)	0.64298 (17)	0.0230 (10)
N3	0.7412 (7)	0.8731 (3)	0.59361 (18)	0.0259 (11)
N4	1.0599 (7)	0.7686 (3)	0.59731 (19)	0.0299 (12)
C13	0.9614 (9)	0.7240 (4)	0.6442 (2)	0.0317 (14)
H13A	1.0186	0.7527	0.6769	0.038*
H13B	1.0063	0.6604	0.6450	0.038*
C14	0.9708 (8)	0.7232 (4)	0.5484 (2)	0.0298 (14)
H14A	1.0154	0.6596	0.5489	0.036*
H14B	1.0349	0.7515	0.5169	0.036*
C15	0.6612 (10)	0.8262 (4)	0.5445 (2)	0.0277 (14)

H15A	0.7238	0.8559	0.5132	0.033*
H15B	0.4995	0.8313	0.5418	0.033*
C16	0.6516 (9)	0.8262 (4)	0.6408 (2)	0.0279 (14)
H16A	0.7073	0.8561	0.6732	0.033*
H16B	0.4898	0.8316	0.6401	0.033*
C17	0.6314 (9)	0.6849 (4)	0.5927 (2)	0.0246 (13)
H17A	0.6745	0.6211	0.5933	0.029*
H17B	0.4693	0.6879	0.5907	0.029*
C18	0.9867 (9)	0.8639 (4)	0.5967 (2)	0.0312 (15)
H18A	1.0513	0.8946	0.5660	0.037*
H18B	1.0422	0.8940	0.6291	0.037*

Atomic displacement parameters (\AA^2)

	U^{11}	U^{22}	U^{33}	U^{12}	U^{13}	U^{23}
I1	0.0222 (2)	0.0333 (2)	0.0256 (2)	0.00361 (17)	0.00123 (16)	-0.00220 (17)
F1	0.0288 (19)	0.050 (2)	0.036 (2)	-0.0050 (17)	0.0083 (16)	-0.0019 (17)
F2	0.0258 (19)	0.043 (2)	0.057 (2)	-0.0052 (17)	0.0007 (17)	-0.0091 (18)
F3	0.050 (2)	0.059 (3)	0.044 (2)	-0.010 (2)	-0.0101 (19)	-0.0108 (19)
F4	0.069 (3)	0.051 (3)	0.0266 (19)	-0.014 (2)	0.0035 (18)	-0.0045 (17)
F5	0.034 (2)	0.038 (2)	0.0305 (19)	-0.0074 (17)	0.0067 (15)	0.0026 (15)
C1	0.023 (3)	0.023 (3)	0.030 (3)	0.006 (3)	-0.001 (2)	-0.005 (3)
C2	0.025 (3)	0.030 (3)	0.026 (3)	0.007 (3)	0.006 (3)	-0.004 (3)
C3	0.023 (3)	0.026 (3)	0.042 (4)	0.000 (3)	0.004 (3)	-0.007 (3)
C4	0.042 (4)	0.031 (4)	0.034 (4)	-0.001 (3)	-0.008 (3)	-0.009 (3)
C5	0.042 (4)	0.032 (4)	0.023 (3)	0.003 (3)	0.005 (3)	0.000 (3)
C6	0.024 (3)	0.025 (3)	0.031 (3)	0.000 (3)	0.003 (3)	-0.001 (3)
I2	0.0249 (2)	0.0341 (2)	0.0212 (2)	-0.00385 (17)	0.00230 (16)	0.00204 (16)
F6	0.0242 (18)	0.039 (2)	0.041 (2)	0.0054 (16)	-0.0042 (15)	0.0085 (16)
F7	0.0168 (17)	0.054 (2)	0.044 (2)	0.0019 (16)	0.0107 (15)	-0.0071 (17)
F8	0.043 (2)	0.056 (3)	0.0229 (18)	-0.0061 (19)	0.0083 (16)	0.0003 (16)
F9	0.038 (2)	0.036 (2)	0.0282 (18)	0.0040 (17)	-0.0066 (15)	0.0063 (15)
F10	0.0223 (17)	0.040 (2)	0.0302 (18)	0.0060 (15)	0.0035 (14)	0.0001 (15)
C7	0.025 (3)	0.025 (3)	0.019 (3)	-0.003 (3)	0.004 (2)	0.001 (2)
C8	0.019 (3)	0.022 (3)	0.028 (3)	-0.004 (2)	-0.002 (2)	0.004 (2)
C9	0.022 (3)	0.027 (3)	0.035 (3)	-0.005 (3)	0.007 (3)	-0.004 (3)
C10	0.033 (3)	0.027 (3)	0.019 (3)	-0.010 (3)	0.004 (3)	-0.003 (2)
C11	0.024 (3)	0.026 (3)	0.024 (3)	-0.002 (3)	-0.005 (2)	0.002 (2)

C12	0.019 (3)	0.027 (3)	0.024 (3)	-0.001 (2)	0.003 (2)	-0.003 (2)
N1	0.018 (2)	0.027 (3)	0.021 (2)	0.001 (2)	0.0047 (19)	-0.001 (2)
N2	0.017 (2)	0.029 (3)	0.023 (2)	-0.002 (2)	0.0011 (19)	0.003 (2)
N3	0.024 (3)	0.027 (3)	0.026 (3)	0.002 (2)	0.001 (2)	0.003 (2)
N4	0.015 (2)	0.038 (3)	0.036 (3)	-0.003 (2)	0.006 (2)	-0.003 (2)
C13	0.020 (3)	0.040 (4)	0.035 (4)	0.003 (3)	-0.008 (3)	0.001 (3)
C14	0.020 (3)	0.037 (4)	0.033 (3)	0.001 (3)	0.009 (3)	-0.007 (3)
C15	0.031 (3)	0.030 (4)	0.022 (3)	0.005 (3)	-0.002 (3)	0.004 (2)
C16	0.021 (3)	0.036 (4)	0.027 (3)	0.004 (3)	0.004 (2)	-0.005 (3)
C17	0.015 (3)	0.025 (3)	0.034 (3)	-0.001 (2)	0.004 (2)	0.002 (3)
C18	0.026 (3)	0.034 (4)	0.034 (3)	-0.011 (3)	0.005 (3)	0.001 (3)

Geometric parameters (Å, °)

I1—C1	2.112 (5)	N1—C14	1.476 (6)
F1—C2	1.343 (6)	N1—C15	1.474 (6)
F2—C3	1.357 (6)	N1—C17	1.476 (6)
F3—C4	1.341 (6)	N2—C13	1.491 (6)
F4—C5	1.340 (6)	N2—C16	1.461 (7)
F5—C6	1.346 (6)	N2—C17	1.483 (6)
C1—C2	1.386 (8)	N3—C15	1.471 (7)
C1—C6	1.370 (7)	N3—C16	1.466 (7)
C2—C3	1.376 (7)	N3—C18	1.473 (7)
C3—C4	1.372 (8)	N4—C13	1.467 (7)
C4—C5	1.371 (8)	N4—C14	1.474 (7)
C5—C6	1.385 (8)	N4—C18	1.464 (7)
I2—C7	2.109 (5)	C13—H13A	0.9700
F6—C8	1.328 (6)	C13—H13B	0.9700
F7—C9	1.345 (6)	C14—H14A	0.9700
F8—C10	1.347 (6)	C14—H14B	0.9700
F9—C11	1.345 (6)	C15—H15A	0.9700
F10—C12	1.358 (6)	C15—H15B	0.9700
C7—C8	1.392 (7)	C16—H16A	0.9700
C7—C12	1.373 (7)	C16—H16B	0.9700
C8—C9	1.382 (8)	C17—H17A	0.9700
C9—C10	1.376 (8)	C17—H17B	0.9700
C10—C11	1.378 (7)	C18—H18A	0.9700
C11—C12	1.374 (7)	C18—H18B	0.9700
C2—C1—I1	120.8 (4)	C15—N3—C18	108.0 (4)

C6—C1—I1	121.8 (4)	C16—N3—C15	108.9 (4)
C6—C1—C2	117.4 (5)	C16—N3—C18	107.0 (4)
F1—C2—C1	120.4 (5)	C13—N4—C14	107.9 (5)
F1—C2—C3	118.3 (5)	C18—N4—C13	108.0 (4)
C3—C2—C1	121.3 (5)	C18—N4—C14	108.6 (5)
F2—C3—C2	119.8 (5)	N2—C13—H13A	109.2
F2—C3—C4	120.0 (5)	N2—C13—H13B	109.2
C4—C3—C2	120.2 (5)	N4—C13—N2	111.9 (4)
F3—C4—C3	120.3 (6)	N4—C13—H13A	109.2
F3—C4—C5	120.1 (6)	N4—C13—H13B	109.2
C5—C4—C3	119.6 (5)	H13A—C13—H13B	107.9
F4—C5—C4	119.9 (5)	N1—C14—H14A	109.2
F4—C5—C6	120.6 (6)	N1—C14—H14B	109.2
C4—C5—C6	119.5 (6)	N4—C14—N1	112.0 (4)
F5—C6—C1	120.3 (5)	N4—C14—H14A	109.2
F5—C6—C5	117.8 (5)	N4—C14—H14B	109.2
C1—C6—C5	122.0 (5)	H14A—C14—H14B	107.9
C8—C7—I2	120.9 (4)	N1—C15—H15A	109.2
C12—C7—I2	121.3 (4)	N1—C15—H15B	109.2
C12—C7—C8	117.6 (5)	N3—C15—N1	111.9 (4)
F6—C8—C7	120.9 (5)	N3—C15—H15A	109.2
F6—C8—C9	118.6 (5)	N3—C15—H15B	109.2
C9—C8—C7	120.5 (5)	H15A—C15—H15B	107.9
F7—C9—C8	120.6 (5)	N2—C16—N3	112.9 (4)
F7—C9—C10	119.4 (5)	N2—C16—H16A	109.0
C10—C9—C8	120.0 (5)	N2—C16—H16B	109.0
F8—C10—C9	119.9 (5)	N3—C16—H16A	109.0
F8—C10—C11	119.7 (5)	N3—C16—H16B	109.0
C9—C10—C11	120.4 (5)	H16A—C16—H16B	107.8
F9—C11—C10	120.1 (5)	N1—C17—N2	111.5 (4)
F9—C11—C12	121.4 (5)	N1—C17—H17A	109.3
C12—C11—C10	118.6 (5)	N1—C17—H17B	109.3
F10—C12—C7	120.1 (5)	N2—C17—H17A	109.3
F10—C12—C11	117.0 (5)	N2—C17—H17B	109.3
C7—C12—C11	122.8 (5)	H17A—C17—H17B	108.0
C14—N1—C17	108.1 (4)	N3—C18—H18A	109.1
C15—N1—C14	108.1 (4)	N3—C18—H18B	109.1
C15—N1—C17	108.8 (4)	N4—C18—N3	112.6 (5)
C16—N2—C13	107.5 (4)	N4—C18—H18A	109.1

C16—N2—C17	108.7 (4)	N4—C18—H18B	109.1
C17—N2—C13	107.6 (4)	H18A—C18—H18B	107.8

1,2-diiodotetrafluorobenzene –hexamethylene-tetramine (2a.1)

Crystal data

C ₆ F ₄ I ₂ ·C ₆ H ₁₂ N ₄	$F(000) = 1016$
$M_r = 542.06$	$D_x = 2.289 \text{ Mg m}^{-3}$
Monoclinic, $P2_1/c$	Mo $K\alpha$ radiation, $\lambda = 0.71073 \text{ \AA}$
$a = 9.3918 (6) \text{ \AA}$	Cell parameters from 4847 reflections
$b = 23.487 (1) \text{ \AA}$	$\theta = 2.9\text{--}28.9^\circ$
$c = 7.8101 (4) \text{ \AA}$	$\mu = 4.04 \text{ mm}^{-1}$
$\beta = 114.051 (7)^\circ$	$T = 150 \text{ K}$
$V = 1573.22 (16) \text{ \AA}^3$	Needle, clear light colourless
$Z = 4$	$0.1 \times 0.05 \times 0.04 \text{ mm}$

Data collection

SuperNova, Single source at offset/far, Eos diffractometer	3092 independent reflections
Radiation source: micro-focus sealed X-ray tube, SuperNova (Mo) X-ray Source	2674 reflections with $I > 2\sigma(I)$
Mirror monochromator	$R_{\text{int}} = 0.065$
Detector resolution: $16.1428 \text{ pixels mm}^{-1}$	$\theta_{\text{max}} = 26.0^\circ$, $\theta_{\text{min}} = 2.9^\circ$
ω scans	$h = -11 \rightarrow 11$
Absorption correction: multi-scan <i>CrysAlis PRO</i> 1.171.39.46 (Rigaku Oxford Diffraction, 2018) Empirical absorption correction using spherical harmonics, implemented in SCALE3 ABSPACK scaling algorithm.	$k = -28 \rightarrow 28$
$T_{\text{min}} = 0.351$, $T_{\text{max}} = 1.000$	$l = -9 \rightarrow 9$
12043 measured reflections	

Refinement

Refinement on F^2	Primary atom site location: dual
Least-squares matrix: full	Hydrogen site location: inferred from neighbouring sites
$R[F^2 > 2\sigma(F^2)] = 0.032$	H-atom parameters constrained
$wR(F^2) = 0.076$	$w = 1/[\sigma^2(F_o^2) + (0.0303P)^2]$ where $P = (F_o^2 + 2F_c^2)/3$

$S = 1.06$	$(\Delta/\sigma)_{\max} = 0.002$
3092 reflections	$\Delta)_{\max} = 1.03 \text{ e } \text{\AA}^{-3}$
199 parameters	$\Delta)_{\min} = -0.94 \text{ e } \text{\AA}^{-3}$
0 restraints	

Special details

Geometry. All esds (except the esd in the dihedral angle between two l.s. planes) are estimated using the full covariance matrix. The cell esds are taken into account individually in the estimation of esds in distances, angles and torsion angles; correlations between esds in cell parameters are only used when they are defined by crystal symmetry. An approximate (isotropic) treatment of cell esds is used for estimating esds involving l.s. planes.

Fractional atomic coordinates and isotropic or equivalent isotropic displacement parameters (\AA^2)

	x	y	z	$U_{\text{iso}}^*/U_{\text{eq}}$
C1	-0.2594 (5)	0.4383 (2)	-0.2875 (6)	0.0212 (10)
C2	-0.3021 (5)	0.3834 (2)	-0.3546 (6)	0.0213 (10)
C3	-0.2753 (5)	0.3392 (2)	-0.2286 (6)	0.0225 (10)
C4	-0.2056 (5)	0.3479 (2)	-0.0377 (6)	0.0257 (11)
C5	-0.1674 (5)	0.4021 (2)	0.0296 (6)	0.0265 (11)
C6	-0.1952 (5)	0.4465 (2)	-0.0949 (6)	0.0235 (10)
F1	-0.3135 (3)	0.28502 (12)	-0.2878 (4)	0.0344 (7)
F2	-0.1770 (3)	0.30420 (13)	0.0825 (4)	0.0384 (8)
F3	-0.1007 (3)	0.41178 (13)	0.2160 (3)	0.0391 (8)
F4	-0.1552 (4)	0.49932 (12)	-0.0215 (4)	0.0354 (7)
I1	-0.26531 (3)	0.50919 (2)	-0.45702 (4)	0.02193 (10)
I2	-0.41834 (3)	0.36403 (2)	-0.64383 (4)	0.02326 (11)
C7	0.0891 (6)	0.2978 (2)	-0.2894 (6)	0.0287 (11)
H7A	0.0001	0.2971	-0.4137	0.034*
H7B	0.0784	0.2648	-0.2168	0.034*
C8	0.3672 (6)	0.2952 (2)	-0.1301 (6)	0.0253 (11)
H8A	0.4663	0.2925	-0.1460	0.030*
H8B	0.3619	0.2622	-0.0540	0.030*
C9	0.3738 (5)	0.3962 (2)	-0.1456 (6)	0.0228 (10)
H9A	0.3728	0.4323	-0.0807	0.027*
H9B	0.4731	0.3944	-0.1614	0.027*
C10	0.0960 (5)	0.3985 (2)	-0.3045 (6)	0.0245 (11)
H10A	0.0917	0.4347	-0.2415	0.029*
H10B	0.0069	0.3980	-0.4287	0.029*
C11	0.2171 (5)	0.3515 (2)	-0.0102 (6)	0.0258 (11)

H11A	0.2095	0.3190	0.0666	0.031*
H11B	0.2144	0.3870	0.0565	0.031*
C12	0.2470 (6)	0.3424 (2)	-0.4248 (6)	0.0257 (11)
H12A	0.3452	0.3402	-0.4432	0.031*
H12B	0.1591	0.3417	-0.5500	0.031*
N1	0.0820 (4)	0.35044 (18)	-0.1920 (5)	0.0247 (9)
N2	0.2436 (4)	0.39619 (16)	-0.3306 (5)	0.0194 (8)
N3	0.2360 (5)	0.29210 (17)	-0.3155 (5)	0.0259 (9)
N4	0.3672 (4)	0.34818 (16)	-0.0285 (5)	0.0207 (8)

Atomic displacement parameters (\AA^2)

	U^{11}	U^{22}	U^{33}	U^{12}	U^{13}	U^{23}
C1	0.016 (2)	0.030 (3)	0.020 (2)	0.002 (2)	0.0090 (18)	0.0025 (19)
C2	0.023 (2)	0.025 (3)	0.016 (2)	0.003 (2)	0.0088 (18)	-0.0014 (19)
C3	0.020 (2)	0.025 (3)	0.026 (2)	-0.003 (2)	0.0127 (19)	-0.002 (2)
C4	0.023 (3)	0.029 (3)	0.027 (3)	0.005 (2)	0.013 (2)	0.012 (2)
C5	0.021 (3)	0.043 (3)	0.014 (2)	-0.003 (2)	0.0051 (18)	0.005 (2)
C6	0.027 (3)	0.024 (3)	0.021 (2)	-0.006 (2)	0.012 (2)	0.0003 (19)
F1	0.0493 (19)	0.0218 (16)	0.0403 (16)	0.0007 (13)	0.0266 (14)	0.0023 (12)
F2	0.0448 (19)	0.0417 (19)	0.0330 (16)	0.0103 (15)	0.0201 (14)	0.0202 (14)
F3	0.0425 (18)	0.058 (2)	0.0140 (13)	-0.0107 (15)	0.0088 (12)	0.0012 (13)
F4	0.049 (2)	0.0339 (18)	0.0243 (15)	-0.0103 (14)	0.0163 (14)	-0.0091 (12)
I1	0.02536 (19)	0.02173 (18)	0.02136 (17)	0.00009 (13)	0.01226 (13)	0.00261 (11)
I2	0.0284 (2)	0.02646 (19)	0.01861 (17)	-0.00278 (13)	0.01332 (13)	-0.00285 (12)
C7	0.033 (3)	0.027 (3)	0.025 (3)	-0.009 (2)	0.012 (2)	-0.002 (2)
C8	0.032 (3)	0.021 (3)	0.027 (3)	0.007 (2)	0.017 (2)	0.006 (2)
C9	0.023 (3)	0.022 (3)	0.024 (2)	0.002 (2)	0.0102 (19)	0.0013 (19)
C10	0.023 (3)	0.032 (3)	0.017 (2)	0.004 (2)	0.0058 (19)	0.0015 (19)
C11	0.030 (3)	0.032 (3)	0.022 (2)	0.001 (2)	0.017 (2)	0.002 (2)
C12	0.031 (3)	0.031 (3)	0.021 (2)	0.003 (2)	0.016 (2)	-0.003 (2)
N1	0.017 (2)	0.035 (2)	0.023 (2)	-0.0002 (18)	0.0087 (16)	0.0019 (18)
N2	0.023 (2)	0.023 (2)	0.0167 (18)	0.0014 (17)	0.0120 (16)	-0.0005 (15)
N3	0.031 (2)	0.025 (2)	0.023 (2)	-0.0024 (18)	0.0117 (17)	-0.0006 (16)
N4	0.019 (2)	0.024 (2)	0.0198 (19)	0.0010 (17)	0.0084 (16)	0.0013 (16)

Geometric parameters (Å, °)

C1—C2	1.389 (6)	C8—N3	1.471 (6)
C1—C6	1.387 (6)	C8—N4	1.477 (6)
C1—I1	2.114 (5)	C9—H9A	0.9900
C2—C3	1.380 (6)	C9—H9B	0.9900
C2—I2	2.119 (4)	C9—N2	1.464 (5)
C3—C4	1.378 (6)	C9—N4	1.469 (6)
C3—F1	1.352 (5)	C10—H10A	0.9900
C4—C5	1.367 (7)	C10—H10B	0.9900
C4—F2	1.343 (5)	C10—N1	1.470 (6)
C5—C6	1.377 (6)	C10—N2	1.482 (5)
C5—F3	1.349 (5)	C11—H11A	0.9900
C6—F4	1.354 (5)	C11—H11B	0.9900
C7—H7A	0.9900	C11—N1	1.469 (5)
C7—H7B	0.9900	C11—N4	1.476 (6)
C7—N1	1.466 (6)	C12—H12A	0.9900
C7—N3	1.481 (6)	C12—H12B	0.9900
C8—H8A	0.9900	C12—N2	1.469 (6)
C8—H8B	0.9900	C12—N3	1.485 (6)
C2—C1—I1	124.4 (3)	N2—C9—N4	112.6 (4)
C6—C1—C2	118.0 (4)	N4—C9—H9A	109.1
C6—C1—I1	117.3 (3)	N4—C9—H9B	109.1
C1—C2—I2	123.1 (3)	H10A—C10—H10B	107.9
C3—C2—C1	119.2 (4)	N1—C10—H10A	109.3
C3—C2—I2	117.7 (3)	N1—C10—H10B	109.3
C4—C3—C2	121.9 (4)	N1—C10—N2	111.8 (4)
F1—C3—C2	121.2 (4)	N2—C10—H10A	109.3
F1—C3—C4	116.9 (4)	N2—C10—H10B	109.3
C5—C4—C3	119.3 (4)	H11A—C11—H11B	107.8
F2—C4—C3	120.9 (5)	N1—C11—H11A	109.0
F2—C4—C5	119.8 (4)	N1—C11—H11B	109.0
C4—C5—C6	119.3 (4)	N1—C11—N4	112.9 (4)
F3—C5—C4	120.4 (4)	N4—C11—H11A	109.0
F3—C5—C6	120.3 (5)	N4—C11—H11B	109.0
C5—C6—C1	122.3 (4)	H12A—C12—H12B	107.9
F4—C6—C1	120.6 (4)	N2—C12—H12A	109.2
F4—C6—C5	117.1 (4)	N2—C12—H12B	109.2
H7A—C7—H7B	107.8	N2—C12—N3	112.0 (4)

N1—C7—H7A	109.0	N3—C12—H12A	109.2
N1—C7—H7B	109.0	N3—C12—H12B	109.2
N1—C7—N3	112.9 (4)	C7—N1—C10	107.6 (4)
N3—C7—H7A	109.0	C7—N1—C11	108.2 (4)
N3—C7—H7B	109.0	C11—N1—C10	108.2 (4)
H8A—C8—H8B	107.8	C9—N2—C10	108.4 (3)
N3—C8—H8A	109.0	C9—N2—C12	108.3 (3)
N3—C8—H8B	109.0	C12—N2—C10	108.3 (3)
N3—C8—N4	112.8 (4)	C7—N3—C12	107.1 (4)
N4—C8—H8A	109.0	C8—N3—C7	108.3 (4)
N4—C8—H8B	109.0	C8—N3—C12	107.5 (4)
H9A—C9—H9B	107.8	C9—N4—C8	107.7 (3)
N2—C9—H9A	109.1	C9—N4—C11	107.7 (3)
N2—C9—H9B	109.1	C11—N4—C8	107.8 (4)

1,2-diiodotetrafluorobenzene–hexamethylene-tetramine (2a)

Crystal data

$2(\text{C}_6\text{F}_4\text{I}_2) \cdot \text{C}_6\text{H}_{12}\text{N}_4$	$Z = 2$
$M_r = 943.92$	$F(000) = 864$
Triclinic, $P\bar{1}$	$D_x = 2.534 \text{ Mg m}^{-3}$
$a = 10.5820 (8) \text{ \AA}$	Mo $K\alpha$ radiation, $\lambda = 0.71073 \text{ \AA}$
$b = 11.0427 (12) \text{ \AA}$	Cell parameters from 2816 reflections
$c = 11.1177 (12) \text{ \AA}$	$\theta = 3.1\text{--}28.1^\circ$
$\alpha = 101.729 (9)^\circ$	$\mu = 5.11 \text{ mm}^{-1}$
$\beta = 99.923 (8)^\circ$	$T = 150 \text{ K}$
$\gamma = 96.758 (8)^\circ$	Needle, clear light colourless
$V = 1237.2 (2) \text{ \AA}^3$	$0.15 \times 0.01 \times 0.01 \text{ mm}$

Data collection

SuperNova, Single source at offset/far, Eos diffractometer	4856 independent reflections
Radiation source: micro-focus sealed X-ray tube, SuperNova (Mo) X-ray Source	3560 reflections with $I > 2\sigma(I)$
Mirror monochromator	$R_{\text{int}} = 0.068$
Detector resolution: $8.0714 \text{ pixels mm}^{-1}$	$\theta_{\text{max}} = 26.0^\circ$, $\theta_{\text{min}} = 3.0^\circ$
ω scans	$h = -13 \rightarrow 13$

Absorption correction: multi-scan <i>CrysAlis PRO</i> 1.171.39.46 (Rigaku Oxford Diffraction, 2018) Empirical absorption correction using spherical harmonics, implemented in SCALE3 ABSPACK scaling algorithm.	$k = -13 \rightarrow 13$
$T_{\min} = 0.620$, $T_{\max} = 1.000$	$l = -13 \rightarrow 13$
9105 measured reflections	

Refinement

Refinement on F^2	Primary atom site location: dual
Least-squares matrix: full	Hydrogen site location: inferred from neighbouring sites
$R[F^2 > 2\sigma(F^2)] = 0.052$	H-atom parameters constrained
$wR(F^2) = 0.096$	$w = 1/[\sigma^2(F_o^2)]$ where $P = (F_o^2 + 2F_c^2)/3$
$S = 0.97$	$(\Delta/\sigma)_{\max} = 0.001$
4856 reflections	$\Delta_{\max} = 1.09 \text{ e } \text{\AA}^{-3}$
307 parameters	$\Delta_{\min} = -1.04 \text{ e } \text{\AA}^{-3}$
72 restraints	

Special details

<i>Geometry.</i> All esds (except the esd in the dihedral angle between two l.s. planes) are estimated using the full covariance matrix. The cell esds are taken into account individually in the estimation of esds in distances, angles and torsion angles; correlations between esds in cell parameters are only used when they are defined by crystal symmetry. An approximate (isotropic) treatment of cell esds is used for estimating esds involving l.s. planes.
--

Fractional atomic coordinates and isotropic or equivalent isotropic displacement parameters (\AA^2)

	x	y	z	$U_{\text{iso}}^*/U_{\text{eq}}$
C1	1.4805 (8)	0.9172 (8)	-0.6837 (7)	0.0165 (18)
C2	1.4847 (8)	0.8363 (8)	-0.6018 (7)	0.0168 (18)
C3	1.3734 (9)	0.7677 (8)	-0.5900 (8)	0.021 (2)
C4	1.2515 (8)	0.7777 (8)	-0.6588 (9)	0.023 (2)
C5	1.2467 (8)	0.8549 (8)	-0.7403 (8)	0.022 (2)
C6	1.3592 (8)	0.9210 (8)	-0.7538 (8)	0.021 (2)
F1	1.3715 (5)	0.6891 (5)	-0.5127 (5)	0.0306 (14)
F2	1.1438 (5)	0.7111 (5)	-0.6457 (5)	0.0343 (14)
F3	1.1309 (5)	0.8660 (5)	-0.8079 (5)	0.0393 (16)
F4	1.3481 (5)	0.9978 (5)	-0.8353 (5)	0.0273 (13)
I1	1.64602 (5)	1.02603 (5)	-0.71170 (5)	0.01787 (15)

I2	1.66253 (5)	0.81224 (5)	-0.49273 (5)	0.01956 (16)
C7	1.4758 (8)	0.3271 (8)	-0.0699 (7)	0.0172 (18)
C8	1.3496 (8)	0.3423 (8)	-0.1252 (7)	0.0181 (19)
C9	1.3386 (8)	0.4107 (8)	-0.2142 (8)	0.0217 (19)
C10	1.4438 (10)	0.4651 (9)	-0.2550 (8)	0.029 (2)
C11	1.5685 (9)	0.4510 (8)	-0.1997 (8)	0.023 (2)
C12	1.5816 (8)	0.3844 (8)	-0.1083 (7)	0.0184 (19)
F5	1.7041 (5)	0.3713 (5)	-0.0575 (5)	0.0286 (14)
F6	1.6684 (5)	0.5008 (5)	-0.2370 (5)	0.0349 (14)
F7	1.4259 (6)	0.5279 (5)	-0.3452 (5)	0.0397 (16)
F8	1.2187 (5)	0.4272 (5)	-0.2703 (4)	0.0326 (15)
I3	1.51116 (6)	0.21943 (6)	0.06315 (5)	0.02277 (17)
I4	1.18362 (6)	0.27684 (6)	-0.06491 (6)	0.02681 (18)
C13	1.1003 (9)	0.8333 (9)	-0.1411 (8)	0.028 (2)
H13A	1.1729	0.8126	-0.0872	0.033*
H13B	1.0928	0.9199	-0.1080	0.033*
C14	1.0130 (8)	0.8515 (8)	-0.3492 (9)	0.025 (2)
H14A	1.0039	0.9379	-0.3171	0.031*
H14B	1.0278	0.8435	-0.4339	0.031*
C15	0.8726 (8)	0.7834 (8)	-0.2223 (8)	0.023 (2)
H15A	0.8605	0.8688	-0.1901	0.027*
H15B	0.7938	0.7285	-0.2227	0.027*
C16	0.9088 (8)	0.6388 (8)	-0.3980 (8)	0.023 (2)
H16A	0.9237	0.6276	-0.4829	0.028*
H16B	0.8291	0.5842	-0.4003	0.028*
C17	1.1358 (8)	0.6855 (9)	-0.3175 (9)	0.025 (2)
H17A	1.1519	0.6740	-0.4020	0.031*
H17B	1.2089	0.6632	-0.2654	0.031*
C18	0.9977 (8)	0.6224 (8)	-0.1897 (8)	0.022 (2)
H18A	1.0713	0.6016	-0.1372	0.026*
H18B	0.9208	0.5664	-0.1872	0.026*
N1	0.9817 (7)	0.7533 (7)	-0.1379 (6)	0.0205 (18)
N2	0.8930 (7)	0.7700 (7)	-0.3519 (6)	0.0209 (18)
N3	1.0178 (7)	0.6020 (7)	-0.3184 (6)	0.0200 (18)
N4	1.1271 (7)	0.8199 (7)	-0.2692 (7)	0.0232 (19)

Atomic displacement parameters (\AA^2)

	U^{11}	U^{22}	U^{33}	U^{12}	U^{13}	U^{23}
C1	0.011 (4)	0.024 (5)	0.016 (4)	0.009 (3)	0.005 (3)	0.005 (3)
C2	0.014 (4)	0.020 (4)	0.016 (4)	0.008 (3)	0.003 (3)	0.001 (3)
C3	0.025 (4)	0.024 (5)	0.012 (4)	0.002 (3)	0.003 (3)	0.000 (3)
C4	0.014 (4)	0.021 (5)	0.031 (5)	-0.005 (3)	0.001 (3)	0.007 (4)
C5	0.013 (4)	0.023 (5)	0.030 (4)	0.004 (3)	0.006 (3)	0.001 (4)
C6	0.017 (4)	0.026 (5)	0.022 (4)	0.004 (3)	0.005 (3)	0.005 (4)
F1	0.030 (3)	0.039 (3)	0.030 (3)	0.005 (3)	0.018 (3)	0.015 (3)
F2	0.018 (3)	0.046 (4)	0.041 (3)	-0.005 (3)	0.008 (3)	0.017 (3)
F3	0.013 (3)	0.052 (4)	0.048 (4)	0.002 (3)	-0.009 (3)	0.016 (3)
F4	0.023 (3)	0.032 (3)	0.029 (3)	0.004 (2)	0.005 (2)	0.012 (3)
I1	0.0135 (3)	0.0202 (3)	0.0202 (3)	0.0025 (2)	0.0038 (2)	0.0048 (2)
I2	0.0173 (3)	0.0217 (3)	0.0186 (3)	0.0060 (3)	0.0009 (2)	0.0027 (2)
C7	0.020 (4)	0.014 (4)	0.015 (4)	0.005 (3)	0.002 (3)	-0.002 (3)
C8	0.023 (4)	0.015 (4)	0.015 (4)	0.006 (3)	0.002 (3)	-0.002 (3)
C9	0.021 (4)	0.022 (5)	0.019 (4)	0.004 (3)	0.002 (3)	0.000 (3)
C10	0.037 (4)	0.032 (5)	0.018 (4)	0.005 (4)	0.006 (3)	0.004 (4)
C11	0.030 (4)	0.016 (5)	0.026 (4)	0.005 (4)	0.015 (3)	0.000 (3)
C12	0.018 (4)	0.018 (4)	0.015 (4)	0.001 (3)	0.005 (3)	-0.005 (3)
F5	0.012 (3)	0.031 (3)	0.038 (3)	0.000 (2)	-0.002 (2)	0.006 (3)
F6	0.036 (3)	0.032 (3)	0.039 (3)	-0.010 (3)	0.024 (3)	0.009 (3)
F7	0.075 (5)	0.023 (3)	0.021 (3)	0.006 (3)	0.006 (3)	0.011 (2)
F8	0.031 (3)	0.042 (4)	0.026 (3)	0.017 (3)	-0.005 (3)	0.014 (3)
I3	0.0243 (3)	0.0226 (4)	0.0209 (3)	0.0062 (3)	0.0002 (3)	0.0062 (3)
I4	0.0156 (3)	0.0319 (4)	0.0338 (4)	0.0037 (3)	0.0071 (3)	0.0078 (3)
C13	0.028 (6)	0.032 (6)	0.026 (5)	0.014 (5)	0.005 (4)	0.009 (5)
C14	0.022 (5)	0.026 (6)	0.033 (5)	0.009 (4)	0.004 (4)	0.016 (5)
C15	0.013 (5)	0.021 (5)	0.035 (5)	0.011 (4)	0.006 (4)	0.004 (4)
C16	0.016 (5)	0.020 (5)	0.036 (5)	0.005 (4)	0.004 (4)	0.009 (4)
C17	0.014 (5)	0.038 (6)	0.026 (5)	0.006 (4)	0.005 (4)	0.008 (4)
C18	0.015 (5)	0.032 (6)	0.026 (5)	0.009 (4)	0.001 (4)	0.023 (4)
N1	0.010 (4)	0.033 (5)	0.021 (4)	0.005 (3)	0.006 (3)	0.009 (4)
N2	0.016 (4)	0.029 (5)	0.022 (4)	0.010 (3)	0.006 (3)	0.010 (4)
N3	0.018 (4)	0.028 (5)	0.021 (4)	0.011 (3)	0.007 (3)	0.015 (3)
N4	0.011 (4)	0.025 (5)	0.031 (4)	0.003 (3)	0.004 (3)	0.002 (4)

Geometric parameters (Å, °)

C1—C2	1.399 (12)	C13—H13A	0.9700
C1—C6	1.392 (10)	C13—H13B	0.9700
C1—I1	2.110 (9)	C13—N1	1.457 (12)
C2—C3	1.365 (13)	C13—N4	1.481 (12)
C2—I2	2.131 (8)	C14—H14A	0.9700
C3—C4	1.410 (11)	C14—H14B	0.9700
C3—F1	1.341 (11)	C14—N2	1.460 (11)
C4—C5	1.363 (13)	C14—N4	1.492 (10)
C4—F2	1.329 (10)	C15—H15A	0.9700
C5—C6	1.369 (13)	C15—H15B	0.9700
C5—F3	1.355 (9)	C15—N1	1.472 (10)
C6—F4	1.361 (11)	C15—N2	1.474 (11)
C7—C8	1.414 (11)	C16—H16A	0.9700
C7—C12	1.394 (12)	C16—H16B	0.9700
C7—I3	2.091 (9)	C16—N2	1.475 (10)
C8—C9	1.359 (12)	C16—N3	1.477 (10)
C8—I4	2.089 (10)	C17—H17A	0.9700
C9—C10	1.391 (14)	C17—H17B	0.9700
C9—F8	1.364 (9)	C17—N3	1.459 (11)
C10—C11	1.397 (12)	C17—N4	1.491 (11)
C10—F7	1.330 (11)	C18—H18A	0.9700
C11—C12	1.369 (13)	C18—H18B	0.9700
C11—F6	1.303 (11)	C18—N1	1.484 (10)
C12—F5	1.358 (9)	C18—N3	1.459 (11)
C2—C1—I1	124.0 (6)	H14A—C14—H14B	107.9
C6—C1—C2	116.9 (8)	N2—C14—H14A	109.3
C6—C1—I1	119.0 (7)	N2—C14—H14B	109.3
C1—C2—I2	122.2 (6)	N2—C14—N4	111.8 (8)
C3—C2—C1	120.6 (8)	N4—C14—H14A	109.3
C3—C2—I2	117.2 (7)	N4—C14—H14B	109.3
C2—C3—C4	120.9 (9)	H15A—C15—H15B	107.8
F1—C3—C2	123.2 (8)	N1—C15—H15A	109.0
F1—C3—C4	115.9 (9)	N1—C15—H15B	109.0
C5—C4—C3	118.9 (9)	N1—C15—N2	112.8 (7)
F2—C4—C3	120.2 (9)	N2—C15—H15A	109.0
F2—C4—C5	120.9 (8)	N2—C15—H15B	109.0
C4—C5—C6	119.8 (8)	H16A—C16—H16B	107.9

F3—C5—C4	120.1 (9)	N2—C16—H16A	109.1
F3—C5—C6	120.1 (9)	N2—C16—H16B	109.1
C5—C6—C1	122.8 (9)	N2—C16—N3	112.3 (6)
F4—C6—C1	120.0 (8)	N3—C16—H16A	109.1
F4—C6—C5	117.1 (7)	N3—C16—H16B	109.1
C8—C7—I3	123.2 (7)	H17A—C17—H17B	107.8
C12—C7—C8	118.3 (8)	N3—C17—H17A	109.1
C12—C7—I3	118.4 (6)	N3—C17—H17B	109.1
C7—C8—I4	122.5 (7)	N3—C17—N4	112.5 (7)
C9—C8—C7	117.9 (9)	N4—C17—H17A	109.1
C9—C8—I4	119.4 (6)	N4—C17—H17B	109.1
C8—C9—C10	123.9 (8)	H18A—C18—H18B	107.8
C8—C9—F8	119.8 (9)	N1—C18—H18A	109.0
F8—C9—C10	116.3 (9)	N1—C18—H18B	109.0
C9—C10—C11	118.3 (9)	N3—C18—H18A	109.0
F7—C10—C9	120.8 (9)	N3—C18—H18B	109.0
F7—C10—C11	120.9 (10)	N3—C18—N1	112.9 (7)
C12—C11—C10	118.7 (10)	C13—N1—C15	108.6 (8)
F6—C11—C10	119.2 (9)	C13—N1—C18	107.0 (7)
F6—C11—C12	122.1 (8)	C15—N1—C18	107.6 (6)
C11—C12—C7	122.9 (8)	C14—N2—C15	108.3 (7)
F5—C12—C7	119.9 (8)	C14—N2—C16	108.8 (7)
F5—C12—C11	117.1 (8)	C15—N2—C16	107.4 (7)
H13A—C13—H13B	107.8	C17—N3—C16	107.6 (7)
N1—C13—H13A	109.1	C17—N3—C18	107.2 (7)
N1—C13—H13B	109.1	C18—N3—C16	109.3 (7)
N1—C13—N4	112.7 (7)	C13—N4—C14	107.4 (7)
N4—C13—H13A	109.1	C13—N4—C17	107.5 (7)
N4—C13—H13B	109.1	C17—N4—C14	108.2 (6)

1,3-diiodotetrafluorobenzene –hexamethylene-tetramine (3a)

Crystal data

$2(\text{C}_6\text{F}_4\text{I}_2) \cdot 2(\text{C}_3\text{H}_6\text{N}_2)$	$D_x = 2.547 \text{ Mg m}^{-3}$
$M_r = 943.92$	Mo $K\alpha$ radiation, $\lambda = 0.71073 \text{ \AA}$
Orthorhombic, <i>Pccn</i>	Cell parameters from 14480 reflections
$a = 8.1827 (2) \text{ \AA}$	$\theta = 2.8\text{--}28.6^\circ$
$b = 33.0489 (7) \text{ \AA}$	$\mu = 5.14 \text{ mm}^{-1}$

$c = 18.2069 (4) \text{ \AA}$	$T = 150 \text{ K}$
$V = 4923.68 (19) \text{ \AA}^3$	Needle, clear light colourless
$Z = 8$	$0.3 \times 0.05 \times 0.02 \text{ mm}$
$F(000) = 3456$	

Data collection

SuperNova, Single source at offset/far, Eos diffractometer	4839 independent reflections
Radiation source: micro-focus sealed X-ray tube, SuperNova (Mo) X-ray Source	4181 reflections with $I > 2\sigma(I)$
Mirror monochromator	$R_{\text{int}} = 0.069$
Detector resolution: $16.1428 \text{ pixels mm}^{-1}$	$\theta_{\text{max}} = 26.0^\circ$, $\theta_{\text{min}} = 3.0^\circ$
ω scans	$h = -9 \rightarrow 10$
Absorption correction: multi-scan CrysAlis PRO 1.171.39.46 (Rigaku Oxford Diffraction, 2018) Empirical absorption correction using spherical harmonics, implemented in SCALE3 ABSPACK scaling algorithm.	$k = -40 \rightarrow 26$
$T_{\text{min}} = 0.049$, $T_{\text{max}} = 1.000$	$l = -22 \rightarrow 22$
39545 measured reflections	

Refinement

Refinement on F^2	Primary atom site location: dual
Least-squares matrix: full	Hydrogen site location: inferred from neighbouring sites
$R[F^2 > 2\sigma(F^2)] = 0.029$	H-atom parameters constrained
$wR(F^2) = 0.062$	$w = 1/[\sigma^2(F_o^2) + (0.0161P)^2 + 7.6918P]$ where $P = (F_o^2 + 2F_c^2)/3$
$S = 1.12$	$(\Delta/\sigma)_{\text{max}} = 0.003$
4839 reflections	$\Delta_{\text{max}} = 0.74 \text{ e \AA}^{-3}$
309 parameters	$\Delta_{\text{min}} = -0.72 \text{ e \AA}^{-3}$
75 restraints	

Special details

Geometry. All esds (except the esd in the dihedral angle between two l.s. planes) are estimated using the full covariance matrix. The cell esds are taken into account individually in the estimation of esds in distances, angles and torsion angles; correlations between esds in cell parameters are only used when they are defined by crystal symmetry. An approximate (isotropic) treatment of cell esds is used for estimating esds involving l.s. planes.

*Fractional atomic coordinates and isotropic or equivalent isotropic displacement parameters
(Å²)*

	x	y	z	U_{iso}^*/U_{eq}	Occ. (<1)
C1	0.2825 (5)	0.60368 (13)	0.6004 (2)	0.0190 (9)	
C2	0.3025 (5)	0.61205 (13)	0.5262 (2)	0.0201 (9)	
C3	0.3248 (5)	0.58244 (13)	0.4737 (2)	0.0205 (9)	
C4	0.3283 (5)	0.54263 (13)	0.4975 (2)	0.0204 (9)	
C5	0.3097 (5)	0.53298 (12)	0.5705 (2)	0.0206 (9)	
C6	0.2853 (5)	0.56352 (13)	0.6213 (2)	0.0199 (9)	
F1	0.2986 (3)	0.65097 (7)	0.50435 (14)	0.0304 (6)	
F2	0.3472 (3)	0.51221 (7)	0.44958 (14)	0.0305 (6)	
F3	0.3158 (3)	0.49416 (7)	0.59223 (15)	0.0311 (6)	
F4	0.2671 (3)	0.55324 (8)	0.69214 (14)	0.0280 (6)	
I1	0.25254 (3)	0.64964 (2)	0.67950 (2)	0.02045 (8)	
I2	0.34323 (4)	0.59567 (2)	0.36205 (2)	0.02659 (9)	
C7	-0.1695 (5)	0.60611 (13)	0.3484 (2)	0.0210 (9)	
C8	-0.2172 (5)	0.61153 (13)	0.2764 (2)	0.0216 (9)	
C9	-0.1968 (5)	0.58270 (13)	0.2225 (2)	0.0218 (9)	
C10	-0.1213 (5)	0.54659 (12)	0.2427 (2)	0.0208 (9)	
C11	-0.0695 (5)	0.54058 (13)	0.3135 (2)	0.0233 (9)	
C12	-0.0947 (5)	0.56982 (13)	0.3661 (2)	0.0218 (9)	
F5	-0.2883 (3)	0.64698 (8)	0.25787 (15)	0.0317 (6)	
F6	-0.0976 (3)	0.51729 (7)	0.19302 (14)	0.0312 (6)	
F7	0.0069 (3)	0.50581 (8)	0.33204 (15)	0.0345 (7)	
F8	-0.0448 (3)	0.56249 (8)	0.43502 (14)	0.0294 (6)	
I3	-0.20753 (4)	0.65050 (2)	0.43019 (2)	0.02233 (8)	
I4	-0.26828 (4)	0.59245 (2)	0.11390 (2)	0.03086 (9)	
C13	0.6107 (5)	0.71265 (13)	0.5821 (3)	0.0258 (10)	
H13A	0.5129	0.7109	0.5522	0.031*	
H13B	0.6150	0.6887	0.6130	0.031*	
C14	0.7500	0.7500	0.6735 (4)	0.0293 (16)	
H14A	0.7461	0.7737	0.7049	0.035*	0.5
H14B	0.7539	0.7263	0.7049	0.035*	0.5
C15	0.5987 (5)	0.78451 (13)	0.5815 (3)	0.0252 (10)	
H15A	0.5939	0.8085	0.6121	0.030*	
H15B	0.5013	0.7840	0.5511	0.030*	
C16	0.7500	0.7500	0.4889 (3)	0.0242 (14)	
H16A	0.8458	0.7509	0.4575	0.029*	0.5

H16B	0.6542	0.7491	0.4575	0.029*	0.5
N1	0.6005 (5)	0.74849 (11)	0.6287 (2)	0.0276 (9)	
N2	0.7446 (4)	0.78668 (11)	0.5339 (2)	0.0213 (8)	
C17	0.2500	0.7500	0.4219 (4)	0.0298 (16)	
H17A	0.2398	0.7736	0.4533	0.036*	0.5
H17B	0.2602	0.7264	0.4533	0.036*	0.5
C18	0.4111 (5)	0.71776 (13)	0.3308 (3)	0.0245 (10)	
H18A	0.4212	0.6939	0.3615	0.029*	
H18B	0.5088	0.7197	0.3007	0.029*	
C19	0.1209 (5)	0.71033 (13)	0.3302 (3)	0.0250 (10)	
H19A	0.0242	0.7073	0.2999	0.030*	
H19B	0.1304	0.6864	0.3607	0.030*	
C20	0.2500	0.7500	0.2367 (3)	0.0212 (14)	
H20A	0.1546	0.7474	0.2054	0.025*	0.5
H20B	0.3454	0.7526	0.2054	0.025*	0.5
N3	0.3985 (5)	0.75395 (11)	0.3776 (2)	0.0261 (9)	
N4	0.2661 (4)	0.71342 (10)	0.2825 (2)	0.0195 (8)	

Atomic displacement parameters (\AA^2)

	U^{11}	U^{22}	U^{33}	U^{12}	U^{13}	U^{23}
C1	0.020 (2)	0.022 (2)	0.015 (2)	-0.0011 (17)	-0.0011 (16)	-0.0043 (16)
C2	0.024 (2)	0.019 (2)	0.017 (2)	-0.0025 (17)	0.0006 (17)	0.0015 (17)
C3	0.024 (2)	0.025 (2)	0.012 (2)	-0.0029 (17)	0.0003 (16)	-0.0005 (17)
C4	0.021 (2)	0.023 (2)	0.018 (2)	-0.0032 (17)	0.0018 (16)	-0.0064 (17)
C5	0.024 (2)	0.017 (2)	0.021 (2)	-0.0035 (17)	0.0038 (17)	-0.0006 (17)
C6	0.025 (2)	0.024 (2)	0.011 (2)	-0.0002 (17)	0.0004 (16)	0.0001 (16)
F1	0.0530 (18)	0.0206 (14)	0.0176 (15)	-0.0008 (12)	-0.0011 (12)	0.0018 (11)
F2	0.0453 (17)	0.0239 (14)	0.0222 (15)	-0.0023 (12)	0.0055 (12)	-0.0102 (11)
F3	0.0435 (17)	0.0202 (14)	0.0296 (16)	-0.0023 (12)	0.0071 (12)	0.0031 (12)
F4	0.0428 (16)	0.0271 (14)	0.0141 (14)	-0.0022 (12)	0.0036 (11)	0.0021 (11)
I1	0.02683 (16)	0.02090 (16)	0.01362 (16)	0.00056 (11)	0.00008 (10)	-0.00272 (11)
I2	0.03449 (18)	0.03326 (18)	0.01202 (15)	-0.00739 (13)	0.00084 (12)	-0.00053 (12)
C7	0.024 (2)	0.023 (2)	0.016 (2)	-0.0040 (17)	0.0051 (16)	-0.0034 (17)
C8	0.027 (2)	0.021 (2)	0.016 (2)	0.0003 (18)	0.0023 (17)	0.0023 (17)
C9	0.027 (2)	0.022 (2)	0.016 (2)	-0.0045 (17)	0.0026 (17)	-0.0012 (17)
C10	0.026 (2)	0.019 (2)	0.017 (2)	-0.0020 (17)	0.0039 (17)	-0.0063 (17)
C11	0.026 (2)	0.019 (2)	0.024 (2)	0.0016 (18)	0.0021 (17)	0.0012 (17)

C12	0.023 (2)	0.027 (2)	0.015 (2)	-0.0055 (17)	-0.0002 (17)	0.0018 (17)
F5	0.0470 (17)	0.0275 (15)	0.0207 (16)	0.0093 (12)	-0.0013 (12)	0.0003 (12)
F6	0.0424 (17)	0.0257 (14)	0.0255 (16)	0.0035 (12)	0.0022 (12)	-0.0104 (11)
F7	0.0407 (17)	0.0291 (15)	0.0337 (17)	0.0089 (12)	-0.0044 (13)	0.0010 (12)
F8	0.0335 (15)	0.0359 (15)	0.0189 (15)	0.0008 (12)	-0.0060 (11)	0.0022 (11)
I3	0.02787 (17)	0.02417 (16)	0.01495 (16)	-0.00344 (12)	0.00261 (11)	-0.00325 (12)
I4	0.0433 (2)	0.03425 (19)	0.01498 (17)	0.00429 (14)	-0.00282 (13)	-0.00186 (13)
C13	0.024 (2)	0.022 (2)	0.031 (3)	-0.0064 (19)	0.0040 (19)	0.001 (2)
C14	0.043 (4)	0.032 (4)	0.013 (4)	-0.006 (3)	0.000	0.000
C15	0.026 (2)	0.024 (2)	0.026 (3)	0.0032 (19)	0.0024 (19)	-0.004 (2)
C16	0.024 (3)	0.035 (4)	0.014 (3)	0.001 (3)	0.000	0.000
N1	0.028 (2)	0.028 (2)	0.027 (2)	-0.0004 (16)	0.0075 (17)	-0.0011 (17)
N2	0.023 (2)	0.022 (2)	0.019 (2)	0.0003 (15)	-0.0001 (15)	0.0012 (16)
C17	0.045 (4)	0.026 (4)	0.019 (4)	0.005 (3)	0.000	0.000
C18	0.028 (2)	0.021 (2)	0.025 (3)	0.0030 (19)	-0.0018 (19)	0.0012 (19)
C19	0.023 (2)	0.025 (2)	0.027 (3)	-0.0059 (19)	0.0040 (19)	0.001 (2)
C20	0.028 (3)	0.021 (3)	0.015 (3)	-0.004 (3)	0.000	0.000
N3	0.031 (2)	0.024 (2)	0.023 (2)	-0.0013 (16)	-0.0096 (17)	-0.0002 (16)
N4	0.0223 (19)	0.0195 (19)	0.017 (2)	-0.0006 (15)	0.0016 (14)	-0.0007 (15)

Geometric parameters (Å, °)

C1—C2	1.388 (6)	C14—H14B	0.9700
C1—C6	1.381 (6)	C14—N1 ⁱ	1.471 (5)
C1—I1	2.108 (4)	C14—N1	1.471 (5)
C2—C3	1.380 (6)	C15—H15A	0.9700
C2—F1	1.347 (5)	C15—H15B	0.9700
C3—C4	1.386 (6)	C15—N1	1.468 (6)
C3—I2	2.085 (4)	C15—N2	1.478 (6)
C4—C5	1.374 (6)	C16—H16A	0.9700
C4—F2	1.340 (5)	C16—H16B	0.9700
C5—C6	1.384 (6)	C16—N2	1.464 (5)
C5—F3	1.344 (5)	C16—N2 ⁱ	1.464 (5)
C6—F4	1.343 (5)	N2—C13 ⁱ	1.474 (6)
C7—C8	1.378 (6)	C17—H17A	0.9700
C7—C12	1.385 (6)	C17—H17B	0.9700
C7—I3	2.114 (4)	C17—N3 ⁱⁱ	1.465 (6)
C8—C9	1.379 (6)	C17—N3	1.465 (6)

C8—F5	1.351 (5)	C18—H18A	0.9700
C9—C10	1.393 (6)	C18—H18B	0.9700
C9—I4	2.087 (4)	C18—N3	1.472 (5)
C10—C11	1.371 (6)	C18—N4	1.484 (5)
C10—F6	1.339 (5)	C19—H19A	0.9700
C11—C12	1.376 (6)	C19—H19B	0.9700
C11—F7	1.351 (5)	C19—N3 ⁱⁱ	1.470 (6)
C12—F8	1.342 (5)	C19—N4	1.476 (5)
C13—H13A	0.9700	C20—H20A	0.9700
C13—H13B	0.9700	C20—H20B	0.9700
C13—N1	1.458 (6)	C20—N4 ⁱⁱ	1.475 (5)
C13—N2 ⁱ	1.474 (5)	C20—N4	1.475 (5)
C14—H14A	0.9700	N3—C19 ⁱⁱ	1.470 (6)
C2—C1—I1	122.3 (3)	H15A—C15—H15B	107.9
C6—C1—C2	117.2 (4)	N1—C15—H15A	109.2
C6—C1—I1	120.4 (3)	N1—C15—H15B	109.2
C3—C2—C1	123.2 (4)	N1—C15—N2	112.0 (3)
F1—C2—C1	118.4 (4)	N2—C15—H15A	109.2
F1—C2—C3	118.4 (4)	N2—C15—H15B	109.2
C2—C3—C4	117.4 (4)	H16A—C16—H16B	107.9
C2—C3—I2	122.4 (3)	N2—C16—H16A	109.2
C4—C3—I2	120.2 (3)	N2 ⁱ —C16—H16A	109.2
C5—C4—C3	121.4 (4)	N2 ⁱ —C16—H16B	109.2
F2—C4—C3	120.7 (4)	N2—C16—H16B	109.2
F2—C4—C5	117.9 (4)	N2—C16—N2 ⁱ	111.9 (5)
C4—C5—C6	119.5 (4)	C13—N1—C14	107.6 (3)
F3—C5—C4	120.2 (4)	C13—N1—C15	108.7 (4)
F3—C5—C6	120.3 (4)	C15—N1—C14	107.8 (3)
C1—C6—C5	121.3 (4)	C13 ⁱ —N2—C15	107.4 (4)
F4—C6—C1	120.4 (4)	C16—N2—C13 ⁱ	108.8 (3)
F4—C6—C5	118.3 (4)	C16—N2—C15	108.2 (3)
C8—C7—C12	117.3 (4)	H17A—C17—H17B	107.8
C8—C7—I3	122.5 (3)	N3—C17—H17A	109.0
C12—C7—I3	120.1 (3)	N3 ⁱⁱ —C17—H17A	109.0
C7—C8—C9	123.6 (4)	N3 ⁱⁱ —C17—H17B	109.0
F5—C8—C7	118.2 (4)	N3—C17—H17B	109.0
F5—C8—C9	118.2 (4)	N3—C17—N3 ⁱⁱ	113.1 (6)
C8—C9—C10	117.2 (4)	H18A—C18—H18B	108.0

C8—C9—I4	122.3 (3)	N3—C18—H18A	109.3
C10—C9—I4	120.5 (3)	N3—C18—H18B	109.3
C11—C10—C9	120.6 (4)	N3—C18—N4	111.4 (3)
F6—C10—C9	120.3 (4)	N4—C18—H18A	109.3
F6—C10—C11	119.0 (4)	N4—C18—H18B	109.3
C10—C11—C12	120.4 (4)	H19A—C19—H19B	107.9
F7—C11—C10	120.1 (4)	N3 ⁱⁱ —C19—H19A	109.2
F7—C11—C12	119.5 (4)	N3 ⁱⁱ —C19—H19B	109.2
C11—C12—C7	120.8 (4)	N3 ⁱⁱ —C19—N4	112.1 (3)
F8—C12—C7	120.6 (4)	N4—C19—H19A	109.2
F8—C12—C11	118.6 (4)	N4—C19—H19B	109.2
H13A—C13—H13B	107.9	H20A—C20—H20B	108.0
N1—C13—H13A	109.1	N4 ⁱⁱ —C20—H20A	109.4
N1—C13—H13B	109.1	N4—C20—H20A	109.4
N1—C13—N2 ⁱ	112.3 (3)	N4 ⁱⁱ —C20—H20B	109.4
N2 ⁱ —C13—H13A	109.1	N4—C20—H20B	109.4
N2 ⁱ —C13—H13B	109.1	N4—C20—N4 ⁱⁱ	111.1 (5)
H14A—C14—H14B	107.8	C17—N3—C18	107.7 (3)
N1 ⁱ —C14—H14A	109.1	C17—N3—C19 ⁱⁱ	107.8 (3)
N1—C14—H14A	109.1	C19 ⁱⁱ —N3—C18	108.7 (4)
N1 ⁱ —C14—H14B	109.1	C19—N4—C18	107.6 (4)
N1—C14—H14B	109.1	C20—N4—C18	109.1 (3)
N1 ⁱ —C14—N1	112.6 (5)	C20—N4—C19	108.5 (3)

Symmetry codes: (i) $-x+3/2, -y+3/2, z$; (ii) $-x+1/2, -y+3/2, z$.

1,4-diiodotetrafluorobenzene-1,3,5-triaza-phosphaadamantane (4b.1)

Crystal data

C ₆ F ₄ I ₂ ·C ₆ H ₁₂ N ₃ P	$F(000) = 524$
$M_r = 559.02$	$D_x = 2.262 \text{ Mg m}^{-3}$
Monoclinic, $P12_1/m1$	Mo $K\alpha$ radiation, $\lambda = 0.71073 \text{ \AA}$
$a = 5.9469 (4) \text{ \AA}$	Cell parameters from 1876 reflections
$b = 20.7380 (15) \text{ \AA}$	$\theta = 3.1\text{--}28.3^\circ$
$c = 6.8822 (5) \text{ \AA}$	$\mu = 3.97 \text{ mm}^{-1}$
$\beta = 104.719 (6)^\circ$	$T = 150 \text{ K}$
$V = 820.91 (10) \text{ \AA}^3$	Needle, clear light colourless
$Z = 2$	$0.1 \times 0.02 \times 0.01 \text{ mm}$

Data collection

SuperNova, Single source at offset/far, Eos diffractometer	1667 independent reflections
Radiation source: micro-focus sealed X-ray tube, SuperNova (Mo) X-ray Source	1328 reflections with $I > 2\sigma(I)$
Mirror monochromator	$R_{\text{int}} = 0.058$
Detector resolution: 8.0714 pixels mm^{-1}	$\theta_{\text{max}} = 26.0^\circ$, $\theta_{\text{min}} = 3.1^\circ$
ω scans	$h = -7 \rightarrow 4$
Absorption correction: multi-scan <i>CrysAlis PRO</i> 1.171.39.46 (Rigaku Oxford Diffraction, 2018) Empirical absorption correction using spherical harmonics, implemented in SCALE3 ABSPACK scaling algorithm.	$k = -25 \rightarrow 25$
$T_{\text{min}} = 0.772$, $T_{\text{max}} = 1.000$	$l = -6 \rightarrow 8$
4951 measured reflections	

Refinement

Refinement on F^2	Primary atom site location: dual
Least-squares matrix: full	Hydrogen site location: inferred from neighbouring sites
$R[F^2 > 2\sigma(F^2)] = 0.035$	H-atom parameters constrained
$wR(F^2) = 0.055$	$w = 1/[\sigma^2(F_o^2) + (0.0063P)^2]$ where $P = (F_o^2 + 2F_c^2)/3$
$S = 0.97$	$(\Delta/\sigma)_{\text{max}} = 0.001$
1667 reflections	$\Delta_{\text{max}} = 0.88 \text{ e } \text{\AA}^{-3}$
106 parameters	$\Delta_{\text{min}} = -0.77 \text{ e } \text{\AA}^{-3}$
0 restraints	

Special details

Geometry. All esds (except the esd in the dihedral angle between two l.s. planes) are estimated using the full covariance matrix. The cell esds are taken into account individually in the estimation of esds in distances, angles and torsion angles; correlations between esds in cell parameters are only used when they are defined by crystal symmetry. An approximate (isotropic) treatment of cell esds is used for estimating esds involving l.s. planes.

Fractional atomic coordinates and isotropic or equivalent isotropic displacement parameters (\AA^2)

	x	y	z	$U_{\text{iso}}^*/U_{\text{eq}}$	Occ. (<1)
C1	0.0868 (8)	0.4632 (3)	0.8610 (7)	0.0143 (12)	
C2	0.1714 (8)	0.5237 (3)	0.9216 (7)	0.0159 (12)	
C3	0.0883 (8)	0.5597 (2)	1.0564 (8)	0.0147 (13)	
F1	0.3454 (5)	0.54869 (15)	0.8494 (4)	0.0229 (8)	
F2	0.1809 (5)	0.61861 (14)	1.1078 (4)	0.0218 (7)	
I1	0.22156 (6)	0.40491 (2)	0.66658 (5)	0.01901 (11)	
C4	0.3815 (8)	0.6933 (2)	0.5761 (8)	0.0189 (13)	
H4A	0.2843	0.6928	0.4395	0.023*	
H4B	0.3455	0.6549	0.6429	0.023*	
C5	0.6801 (12)	0.7500	0.4745 (11)	0.0198 (19)	
H5A	0.5927	0.7500	0.3348	0.024*	
H5B	0.8439	0.7500	0.4771	0.024*	
C6	0.7835 (8)	0.6837 (3)	0.7733 (7)	0.0200 (13)	
H6A	0.9424	0.6808	0.7617	0.024*	
H6B	0.7478	0.6435	0.8311	0.024*	
C7	0.4441 (11)	0.7500	0.8937 (10)	0.0204 (19)	
H7A	0.3957	0.7123	0.9560	0.024*	0.5
H7B	0.3957	0.7877	0.9560	0.024*	0.5
N1	0.6275 (7)	0.6901 (2)	0.5689 (6)	0.0145 (10)	
N2	0.3210 (9)	0.7500	0.6790 (8)	0.0154 (14)	
P1	0.7666 (3)	0.7500	0.9492 (3)	0.0206 (5)	

Atomic displacement parameters (\AA^2)

	U^{11}	U^{22}	U^{33}	U^{12}	U^{13}	U^{23}
C1	0.014 (3)	0.017 (3)	0.012 (3)	0.006 (2)	0.003 (2)	-0.001 (3)
C2	0.012 (3)	0.017 (3)	0.019 (3)	0.004 (2)	0.005 (2)	0.005 (3)
C3	0.012 (3)	0.009 (3)	0.020 (3)	0.001 (2)	0.000 (2)	0.001 (3)
F1	0.0175 (16)	0.0210 (19)	0.0339 (19)	-0.0041 (14)	0.0135 (14)	-0.0020 (16)
F2	0.0180 (16)	0.0176 (18)	0.0296 (19)	-0.0003 (14)	0.0056 (14)	-0.0057 (16)
I1	0.01697 (19)	0.0200 (2)	0.0203 (2)	0.00185 (18)	0.00529 (14)	-0.0040 (2)
C4	0.012 (3)	0.018 (3)	0.026 (3)	-0.001 (2)	0.003 (2)	-0.004 (3)
C5	0.017 (4)	0.026 (5)	0.019 (4)	0.000	0.008 (3)	0.000
C6	0.018 (3)	0.023 (3)	0.018 (3)	-0.001 (3)	0.003 (2)	0.003 (3)
C7	0.022 (4)	0.026 (5)	0.018 (4)	0.000	0.013 (3)	0.000
N1	0.015 (2)	0.016 (3)	0.013 (2)	-0.001 (2)	0.0054 (19)	-0.002 (2)

N2	0.017 (3)	0.020 (4)	0.010 (3)	0.000	0.005 (3)	0.000
P1	0.0236 (12)	0.0226 (13)	0.0155 (11)	0.000	0.0049 (9)	0.000

Geometric parameters (Å, °)

C1—C2	1.377 (7)	C5—N1	1.472 (5)
C1—C3 ⁱ	1.390 (6)	C5—N1 ⁱⁱ	1.472 (5)
C1—I1	2.107 (5)	C6—H6A	0.9700
C2—C3	1.376 (6)	C6—H6B	0.9700
C2—F1	1.359 (5)	C6—N1	1.481 (5)
C3—C1 ⁱ	1.390 (6)	C6—P1	1.851 (5)
C3—F2	1.351 (5)	C7—H7A	0.9700
C4—H4A	0.9700	C7—H7B	0.9700
C4—H4B	0.9700	C7—N2	1.473 (8)
C4—N1	1.478 (6)	C7—P1	1.858 (7)
C4—N2	1.464 (5)	N2—C4 ⁱⁱ	1.464 (5)
C5—H5A	0.9700	P1—C6 ⁱⁱ	1.851 (5)
C5—H5B	0.9700		
C2—C1—C3 ⁱ	116.1 (5)	H6A—C6—H6B	107.5
C2—C1—I1	123.1 (4)	N1—C6—H6A	108.4
C3 ⁱ —C1—I1	120.7 (4)	N1—C6—H6B	108.4
C3—C2—C1	122.2 (5)	N1—C6—P1	115.5 (4)
F1—C2—C1	119.4 (5)	P1—C6—H6A	108.4
F1—C2—C3	118.5 (5)	P1—C6—H6B	108.4
C2—C3—C1 ⁱ	121.7 (5)	H7A—C7—H7B	107.5
F2—C3—C1 ⁱ	119.9 (5)	N2—C7—H7A	108.4
F2—C3—C2	118.4 (5)	N2—C7—H7B	108.4
H4A—C4—H4B	107.5	N2—C7—P1	115.5 (4)
N1—C4—H4A	108.6	P1—C7—H7A	108.4
N1—C4—H4B	108.6	P1—C7—H7B	108.4
N2—C4—H4A	108.6	C4—N1—C6	111.0 (4)
N2—C4—H4B	108.6	C5—N1—C4	107.4 (4)
N2—C4—N1	114.8 (4)	C5—N1—C6	110.0 (4)
H5A—C5—H5B	107.5	C4—N2—C4 ⁱⁱ	106.9 (5)
N1—C5—H5A	108.5	C4 ⁱⁱ —N2—C7	111.4 (3)
N1 ⁱⁱ —C5—H5A	108.5	C4—N2—C7	111.4 (3)
N1 ⁱⁱ —C5—H5B	108.5	C6—P1—C6 ⁱⁱ	95.9 (3)
N1—C5—H5B	108.5	C6 ⁱⁱ —P1—C7	95.2 (2)
N1—C5—N1 ⁱⁱ	115.2 (5)	C6—P1—C7	95.2 (2)

Symmetry codes: (i) $-x, -y+1, -z+2$; (ii) $x, -y+3/2, z$.

1,4-diiodotetrafluorobenzene-1,3,5-triaza-phoshaadamantane-7-oxide (4b)

Crystal data

$C_3F_2I \cdot C_6H_{12}N_3OP$	$F(000) = 724$
$M_r = 374.09$	$D_x = 2.081 \text{ Mg m}^{-3}$
Monoclinic, $P2_1/c$	Mo $K\alpha$ radiation, $\lambda = 0.71073 \text{ \AA}$
$a = 16.5224 (13) \text{ \AA}$	Cell parameters from 1738 reflections
$b = 6.1619 (3) \text{ \AA}$	$\theta = 3.3\text{--}26.9^\circ$
$c = 12.4580 (9) \text{ \AA}$	$\mu = 2.83 \text{ mm}^{-1}$
$\beta = 109.717 (8)^\circ$	$T = 150 \text{ K}$
$V = 1193.98 (15) \text{ \AA}^3$	Block, clear light colourless
$Z = 4$	$0.2 \times 0.1 \times 0.05 \text{ mm}$

Data collection

SuperNova, Single source at offset/far, Eos diffractometer	2349 independent reflections
Radiation source: micro-focus sealed X-ray tube, SuperNova (Mo) X-ray Source	1865 reflections with $I > 2\sigma(I)$
Mirror monochromator	$R_{\text{int}} = 0.047$
Detector resolution: $8.0714 \text{ pixels mm}^{-1}$	$\theta_{\text{max}} = 26.0^\circ, \theta_{\text{min}} = 3.3^\circ$
ω scans	$h = -20 \rightarrow 14$
Absorption correction: multi-scan <i>CrysAlis PRO</i> 1.171.39.46 (Rigaku Oxford Diffraction, 2018) Empirical absorption correction using spherical harmonics, implemented in SCALE3 ABSPACK scaling algorithm.	$k = -7 \rightarrow 4$
$T_{\text{min}} = 0.256, T_{\text{max}} = 1.000$	$l = -10 \rightarrow 15$
4529 measured reflections	

Refinement

Refinement on F^2	Primary atom site location: dual
Least-squares matrix: full	Hydrogen site location: inferred from neighbouring sites
$R[F^2 > 2\sigma(F^2)] = 0.045$	H-atom parameters constrained
$wR(F^2) = 0.089$	$w = 1/[\sigma^2(F_o^2) + (0.0194P)^2]$ where $P = (F_o^2 + 2F_c^2)/3$
$S = 1.08$	$(\Delta/\sigma)_{\text{max}} < 0.001$

2349 reflections	$\Delta_{\max} = 1.12 \text{ e } \text{\AA}^{-3}$
154 parameters	$\Delta_{\min} = -0.80 \text{ e } \text{\AA}^{-3}$
0 restraints	

Special details

Geometry. All esds (except the esd in the dihedral angle between two l.s. planes) are estimated using the full covariance matrix. The cell esds are taken into account individually in the estimation of esds in distances, angles and torsion angles; correlations between esds in cell parameters are only used when they are defined by crystal symmetry. An approximate (isotropic) treatment of cell esds is used for estimating esds involving l.s. planes.

Fractional atomic coordinates and isotropic or equivalent isotropic displacement parameters (\AA^2)

	<i>x</i>	<i>y</i>	<i>z</i>	$U_{\text{iso}}^*/U_{\text{eq}}$
C1	0.4421 (4)	0.3755 (9)	0.5358 (6)	0.0198 (15)
C2	0.4724 (4)	0.5736 (8)	0.5850 (5)	0.0175 (14)
C3	0.5295 (4)	0.6951 (8)	0.5508 (5)	0.0175 (15)
C4	0.1530 (4)	0.0846 (9)	0.6131 (5)	0.0186 (15)
H4A	0.1331	0.0675	0.5309	0.022*
H4B	0.1610	0.2383	0.6302	0.022*
C5	0.2691 (4)	-0.0095 (9)	0.7884 (5)	0.0198 (15)
H5A	0.3268	-0.0691	0.8163	0.024*
H5B	0.2732	0.1435	0.8080	0.024*
C6	0.2277 (5)	-0.2657 (8)	0.6359 (6)	0.0195 (15)
H6A	0.2039	-0.2829	0.5538	0.023*
H6B	0.2844	-0.3311	0.6616	0.023*
C7	0.0809 (4)	-0.3114 (8)	0.6420 (6)	0.0201 (15)
H7A	0.0470	-0.3937	0.6779	0.024*
H7B	0.0584	-0.3393	0.5606	0.024*
C8	0.2076 (5)	-0.3477 (9)	0.8121 (6)	0.0224 (16)
H8A	0.2634	-0.4175	0.8412	0.027*
H8B	0.1701	-0.4184	0.8469	0.027*
C9	0.1325 (5)	-0.0134 (9)	0.8219 (5)	0.0219 (16)
H9A	0.1401	0.1364	0.8474	0.026*
H9B	0.1001	-0.0878	0.8628	0.026*
F1	0.4464 (3)	0.6504 (5)	0.6699 (3)	0.0240 (9)
F2	0.5564 (2)	0.8857 (5)	0.6029 (3)	0.0237 (9)
I1	0.35447 (3)	0.18996 (5)	0.58756 (4)	0.01791 (15)

N1	0.2359 (4)	-0.0300 (7)	0.6639 (5)	0.0164 (12)
N2	0.2173 (4)	-0.1174 (7)	0.8474 (4)	0.0182 (12)
N3	0.1725 (4)	-0.3810 (7)	0.6887 (5)	0.0204 (13)
O1	-0.0133 (3)	0.0790 (6)	0.6305 (4)	0.0275 (12)
P1	0.07314 (12)	-0.0225 (2)	0.66879 (15)	0.0188 (4)

Atomic displacement parameters (\AA^2)

	U^{11}	U^{22}	U^{33}	U^{12}	U^{13}	U^{23}
C1	0.013 (4)	0.022 (3)	0.022 (4)	0.004 (3)	0.004 (3)	0.006 (3)
C2	0.016 (4)	0.023 (3)	0.018 (4)	0.007 (3)	0.011 (3)	0.001 (3)
C3	0.021 (4)	0.016 (3)	0.013 (4)	-0.009 (3)	0.003 (3)	0.000 (3)
C4	0.022 (4)	0.018 (3)	0.014 (3)	-0.004 (3)	0.004 (3)	-0.003 (3)
C5	0.017 (4)	0.024 (3)	0.013 (3)	-0.003 (3)	-0.002 (3)	-0.002 (3)
C6	0.024 (4)	0.022 (3)	0.019 (4)	0.004 (3)	0.017 (3)	-0.001 (3)
C7	0.021 (4)	0.023 (3)	0.017 (4)	-0.006 (3)	0.009 (3)	-0.001 (3)
C8	0.022 (4)	0.028 (3)	0.018 (4)	-0.003 (3)	0.008 (3)	0.003 (3)
C9	0.031 (5)	0.024 (3)	0.009 (3)	-0.006 (3)	0.005 (3)	-0.003 (3)
F1	0.031 (3)	0.0268 (17)	0.020 (2)	0.0007 (18)	0.015 (2)	0.0002 (16)
F2	0.025 (3)	0.0221 (16)	0.025 (2)	-0.0054 (17)	0.010 (2)	-0.0035 (16)
I1	0.0187 (3)	0.0195 (2)	0.0170 (3)	-0.00287 (18)	0.0078 (2)	0.00200 (17)
N1	0.012 (3)	0.020 (2)	0.022 (3)	0.001 (2)	0.013 (3)	0.001 (2)
N2	0.019 (3)	0.022 (2)	0.015 (3)	0.003 (2)	0.009 (3)	0.000 (2)
N3	0.022 (4)	0.019 (2)	0.023 (3)	-0.001 (3)	0.011 (3)	0.001 (2)
O1	0.026 (3)	0.037 (2)	0.019 (3)	0.011 (2)	0.008 (2)	-0.004 (2)
P1	0.0199 (11)	0.0205 (8)	0.0182 (10)	0.0008 (8)	0.0092 (8)	-0.0018 (7)

Geometric parameters (\AA , $^\circ$)

C1—C2	1.381 (8)	C6—H6B	0.9700
C1—C3 ⁱ	1.384 (8)	C6—N1	1.489 (7)
C1—I1	2.110 (6)	C6—N3	1.474 (7)
C2—C3	1.381 (8)	C7—H7A	0.9700
C2—F1	1.354 (6)	C7—H7B	0.9700
C3—C1 ⁱ	1.384 (8)	C7—N3	1.490 (8)
C3—F2	1.343 (6)	C7—P1	1.824 (5)
C4—H4A	0.9700	C8—H8A	0.9700
C4—H4B	0.9700	C8—H8B	0.9700
C4—N1	1.480 (8)	C8—N2	1.478 (7)
C4—P1	1.810 (6)	C8—N3	1.463 (8)

C5—H5A	0.9700	C9—H9A	0.9700
C5—H5B	0.9700	C9—H9B	0.9700
C5—N1	1.466 (7)	C9—N2	1.474 (8)
C5—N2	1.463 (7)	C9—P1	1.828 (6)
C6—H6A	0.9700	O1—P1	1.483 (5)
C2—C1—C3 ⁱ	117.2 (6)	N3—C7—P1	109.5 (4)
C2—C1—I1	121.7 (5)	P1—C7—H7A	109.8
C3 ⁱ —C1—I1	121.0 (4)	P1—C7—H7B	109.8
C3—C2—C1	121.7 (5)	H8A—C8—H8B	107.6
F1—C2—C1	119.5 (5)	N2—C8—H8A	108.7
F1—C2—C3	118.8 (5)	N2—C8—H8B	108.7
C2—C3—C1 ⁱ	121.1 (5)	N3—C8—H8A	108.7
F2—C3—C1 ⁱ	120.5 (5)	N3—C8—H8B	108.7
F2—C3—C2	118.4 (5)	N3—C8—N2	114.3 (5)
H4A—C4—H4B	108.1	H9A—C9—H9B	108.1
N1—C4—H4A	109.5	N2—C9—H9A	109.6
N1—C4—H4B	109.5	N2—C9—H9B	109.6
N1—C4—P1	110.5 (4)	N2—C9—P1	110.3 (4)
P1—C4—H4A	109.5	P1—C9—H9A	109.6
P1—C4—H4B	109.5	P1—C9—H9B	109.6
H5A—C5—H5B	107.6	C4—N1—C6	111.5 (5)
N1—C5—H5A	108.6	C5—N1—C4	112.0 (4)
N1—C5—H5B	108.6	C5—N1—C6	107.7 (5)
N2—C5—H5A	108.6	C5—N2—C8	108.1 (4)
N2—C5—H5B	108.6	C5—N2—C9	111.6 (5)
N2—C5—N1	114.7 (5)	C9—N2—C8	110.7 (5)
H6A—C6—H6B	107.8	C6—N3—C7	112.8 (5)
N1—C6—H6A	109.0	C8—N3—C6	108.4 (5)
N1—C6—H6B	109.0	C8—N3—C7	111.1 (5)
N3—C6—H6A	109.0	C4—P1—C7	100.4 (3)
N3—C6—H6B	109.0	C4—P1—C9	100.7 (3)
N3—C6—N1	112.7 (4)	C7—P1—C9	100.1 (3)
H7A—C7—H7B	108.2	O1—P1—C4	118.0 (3)
N3—C7—H7A	109.8	O1—P1—C7	118.2 (3)
N3—C7—H7B	109.8	O1—P1—C9	116.3 (3)

Symmetry code: (i) $-x+1, -y+1, -z+1$.

Appendix 4

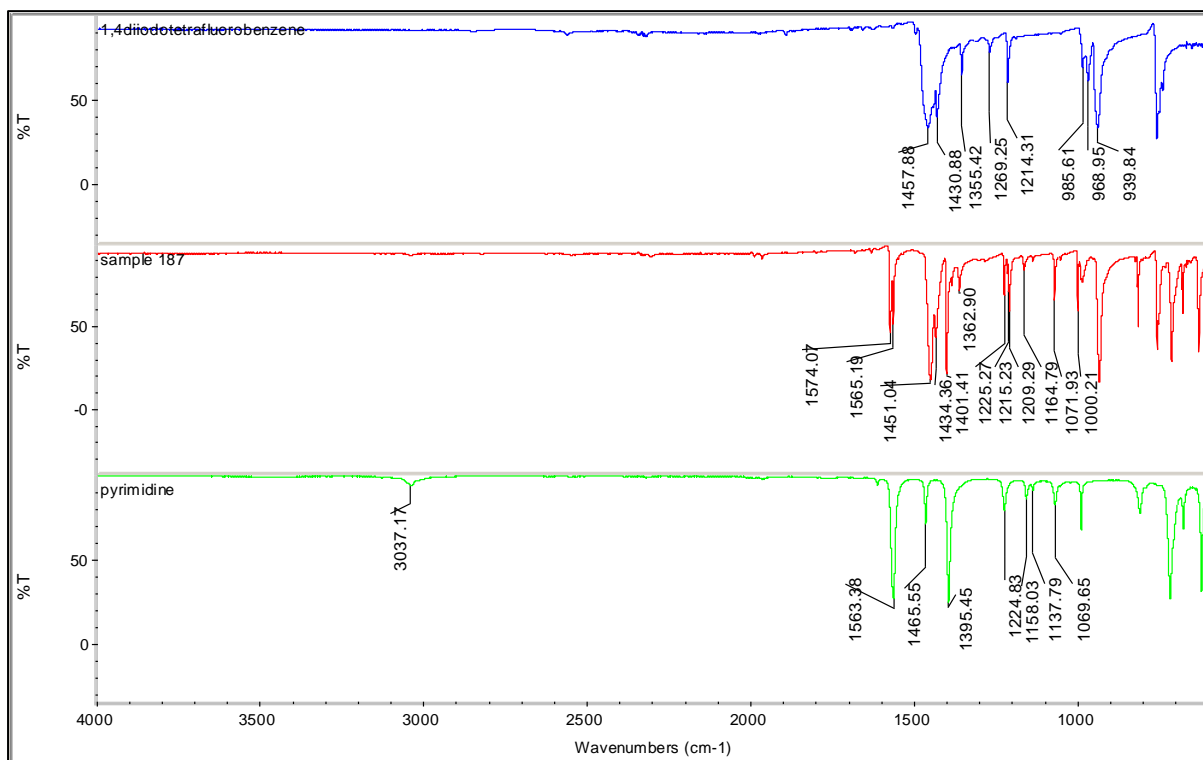
(Supplementary information)

Chapter 4:- Halogen bonds involving 1,4-diiodotetrafluorobenzene with a variety of nitrogen-based aromatic halogen bonds acceptors

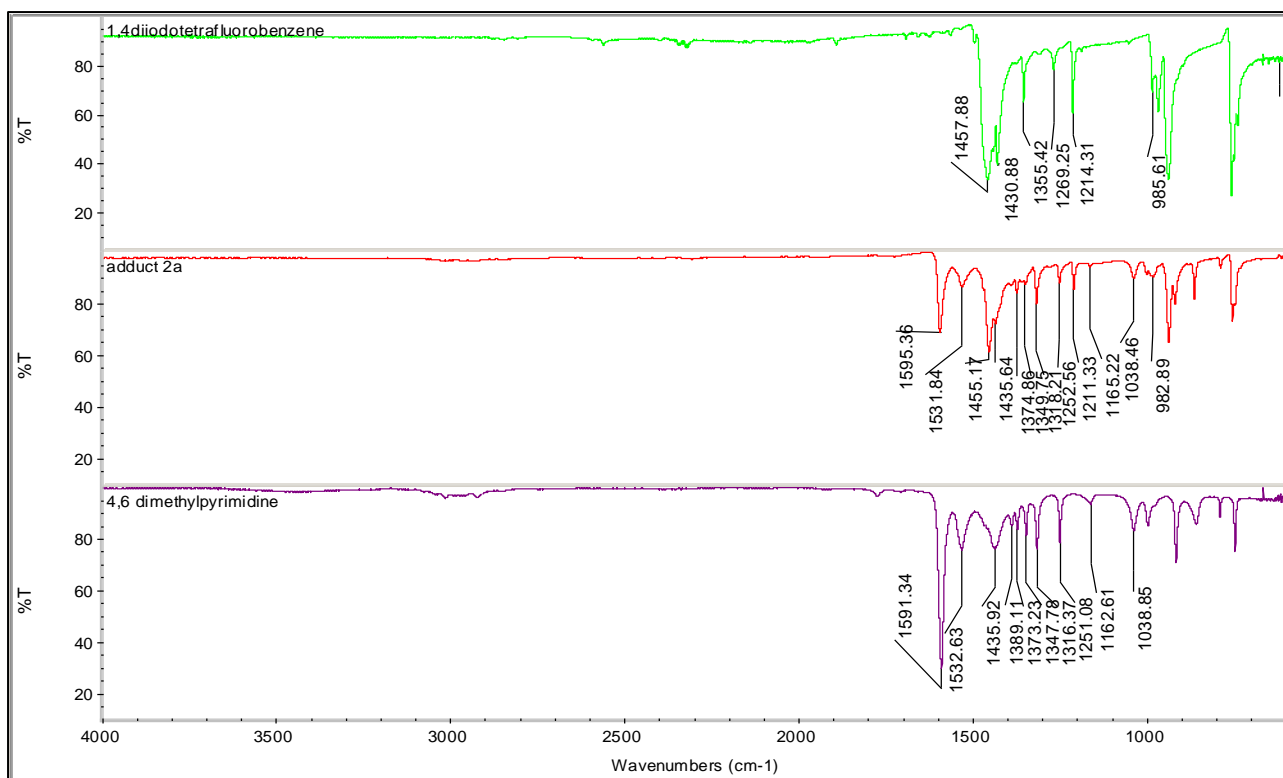
Sultan Alkaabi, Alan K. Brisdon

Department of Chemistry, University of Manchester, Oxford Road, Manchester M13 9PL, England.

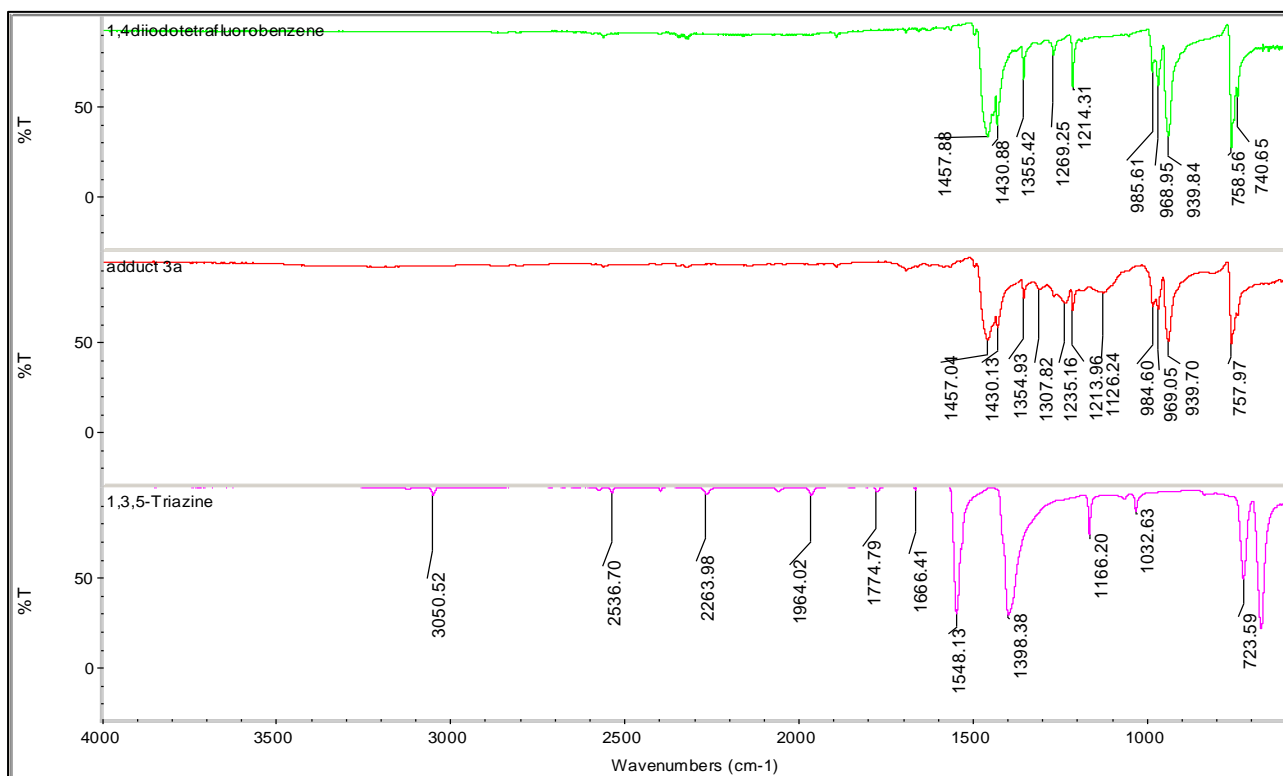
Keywords: Halogen bonds, Crystal structure, 1,4-diiodotetrafluorobenzene, QTAIM, infrared, ^{19}F NMR, van der Waals radii, Pyrimidine, 4,6-dimethyl pyrimidine, 1,3,5-triazine, Pyrimidine -5-amine.



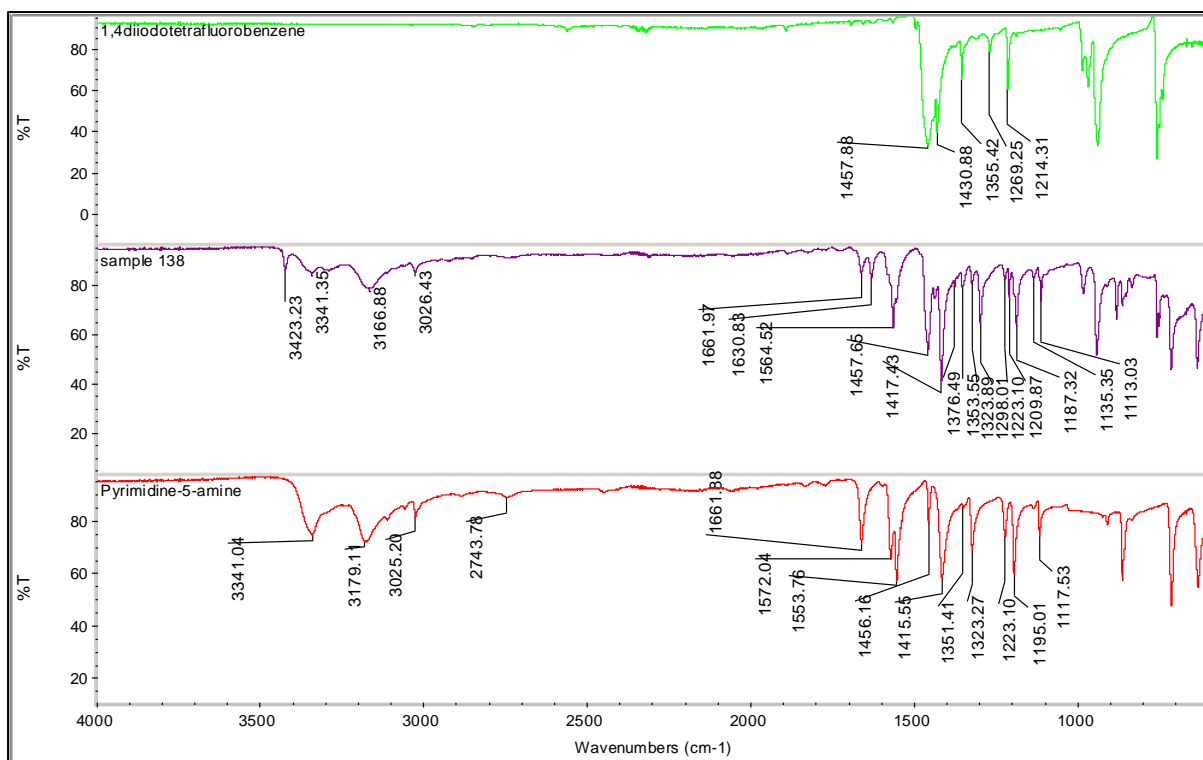
S4.1 IR spectra showing the two starting materials and adduct adduct **1a**



S 4.2 IR spectra showing the two starting materials and adduct **2a**



S4.3 IR spectra showing the two starting materials and adduct **3a**



S4.4 A IR spectra showing the two starting materials and adduct dduct **4a**

Computing details

Data collection: *CrysAlis PRO* 1.171.39.46 (Rigaku OD, 2018); cell refinement: *CrysAlis PRO* 1.171.39.46 (Rigaku OD, 2018); data reduction: *CrysAlis PRO* 1.171.39.46 (Rigaku OD, 2018); program(s) used to solve structure: *SHELXS* (Sheldrick, 2008) for (1a and 2a); *ShelXT* (Sheldrick, 2015) for (3a and 4a); program(s) used to refine structure: *SHELXL* (Sheldrick, 2015); molecular graphics: *Olex2* (Dolomanov *et al.*, 2009); software used to prepare material for publication: *Olex2* (Dolomanov *et al.*, 2009).

1,4-diiodotetrafluorobenzene– pyrimidine(1a)

Crystal data

$C_4H_4N_2 \cdot 2(C_3F_2I)$	$F(000) = 880$
$M_r = 481.95$	$D_x = 2.531 \text{ Mg m}^{-3}$
Monoclinic, $P2_1/n$	Mo $K\alpha$ radiation, $\lambda = 0.71073 \text{ \AA}$
$a = 13.7424 (5) \text{ \AA}$	Cell parameters from 3179 reflections
$b = 5.81858 (16) \text{ \AA}$	$\theta = 3.4\text{--}28.1^\circ$
$c = 16.5136 (6) \text{ \AA}$	$\mu = 5.00 \text{ mm}^{-1}$
$\beta = 106.698 (4)^\circ$	$T = 150 \text{ K}$
$V = 1264.77 (7) \text{ \AA}^3$	Needle, clear light colourless
$Z = 4$	$0.2 \times 0.05 \times 0.04 \text{ mm}$

Data collection

SuperNova, Single source at offset/far, Eos diffractometer	2483 independent reflections
Radiation source: micro-focus sealed X-ray tube, SuperNova (Mo) X-ray Source	2033 reflections with $I > 2\sigma(I)$
Mirror monochromator	$R_{\text{int}} = 0.041$
Detector resolution: $16.1428 \text{ pixels mm}^{-1}$	$\theta_{\text{max}} = 26.0^\circ$, $\theta_{\text{min}} = 3.1^\circ$
ω scans	$h = -16 \rightarrow 16$
Absorption correction: multi-scan <i>CrysAlis PRO</i> 1.171.39.46 (Rigaku Oxford Diffraction, 2018) Empirical absorption correction using spherical harmonics, implemented in SCALE3 ABSPACK scaling algorithm.	$k = -6 \rightarrow 7$
$T_{\text{min}} = 0.405$, $T_{\text{max}} = 1.000$	$l = -20 \rightarrow 18$
9509 measured reflections	

Refinement

Refinement on F^2	Primary atom site location: structure-invariant direct methods
Least-squares matrix: full	Hydrogen site location: inferred from neighbouring sites
$R[F^2 > 2\sigma(F^2)] = 0.027$	H-atom parameters constrained
$wR(F^2) = 0.057$	$w = 1/[\sigma^2(F_o^2) + (0.0167P)^2]$ where $P = (F_o^2 + 2F_c^2)/3$
$S = 1.06$	$(\Delta/\sigma)_{\text{max}} < 0.001$
2483 reflections	$\Delta_{\text{max}} = 0.64 \text{ e \AA}^{-3}$
163 parameters	$\Delta_{\text{min}} = -0.58 \text{ e \AA}^{-3}$

0 restraints	
--------------	--

Special details

Geometry. All esds (except the esd in the dihedral angle between two l.s. planes) are estimated using the full covariance matrix. The cell esds are taken into account individually in the estimation of esds in distances, angles and torsion angles; correlations between esds in cell parameters are only used when they are defined by crystal symmetry. An approximate (isotropic) treatment of cell esds is used for estimating esds involving l.s. planes.

Fractional atomic coordinates and isotropic or equivalent isotropic displacement parameters (\AA^2)

	x	y	z	$U_{\text{iso}}^*/U_{\text{eq}}$
C7	0.5228 (4)	0.1273 (8)	0.2272 (3)	0.0310 (11)
H7	0.5406	0.2664	0.2077	0.037*
C10	0.5699 (4)	-0.1873 (8)	0.3084 (3)	0.0338 (12)
H10	0.6196	-0.2734	0.3465	0.041*
C9	0.4733 (4)	-0.2721 (8)	0.2818 (3)	0.0330 (12)
H9	0.4562	-0.4127	0.3007	0.040*
C8	0.4025 (4)	-0.1386 (8)	0.2254 (3)	0.0328 (12)
H8	0.3358	-0.1909	0.2064	0.039*
N1	0.5961 (3)	0.0142 (7)	0.2820 (2)	0.0329 (10)
N2	0.4257 (3)	0.0631 (6)	0.1969 (2)	0.0303 (10)
I1	0.78549 (2)	0.22473 (5)	0.36918 (2)	0.03093 (11)
C1	0.9137 (3)	0.3885 (8)	0.4470 (3)	0.0271 (11)
C2	1.0099 (4)	0.3001 (7)	0.4596 (3)	0.0286 (11)
C3	0.9057 (3)	0.5899 (8)	0.4886 (3)	0.0292 (11)
F1	1.02397 (19)	0.1038 (4)	0.42165 (16)	0.0373 (7)
F2	0.8137 (2)	0.6838 (4)	0.48006 (17)	0.0368 (7)
I2	0.24331 (2)	0.29678 (5)	0.10609 (2)	0.02686 (10)
C5	0.0348 (3)	0.2996 (7)	-0.0241 (3)	0.0241 (10)
C4	0.0982 (3)	0.4202 (7)	0.0419 (2)	0.0220 (10)
C6	0.0615 (3)	0.6227 (7)	0.0641 (3)	0.0242 (10)
F3	0.06565 (19)	0.0981 (4)	-0.04934 (15)	0.0302 (6)
F4	0.1196 (2)	0.7510 (4)	0.12916 (15)	0.0316 (7)

Atomic displacement parameters (\AA^2)

	U^{11}	U^{22}	U^{33}	U^{12}	U^{13}	U^{23}
C7	0.037 (3)	0.023 (3)	0.037 (3)	-0.001 (2)	0.016 (2)	-0.003 (2)
C10	0.034 (3)	0.034 (3)	0.031 (3)	0.011 (2)	0.007 (2)	0.007 (2)
C9	0.037 (3)	0.028 (3)	0.035 (3)	0.003 (2)	0.013 (2)	0.000 (2)
C8	0.028 (3)	0.036 (3)	0.034 (3)	-0.002 (2)	0.009 (2)	-0.008 (2)
N1	0.026 (2)	0.035 (2)	0.036 (2)	0.0007 (19)	0.0058 (18)	-0.0011 (19)
N2	0.028 (2)	0.029 (2)	0.033 (2)	0.0023 (18)	0.0069 (18)	-0.0001 (18)
I1	0.0283 (2)	0.0350 (2)	0.02916 (19)	-0.00535 (14)	0.00763 (14)	0.00101 (13)
C1	0.029 (3)	0.027 (3)	0.027 (3)	-0.003 (2)	0.012 (2)	0.004 (2)
C2	0.035 (3)	0.025 (3)	0.029 (3)	-0.001 (2)	0.013 (2)	0.001 (2)
C3	0.025 (3)	0.029 (3)	0.035 (3)	0.004 (2)	0.011 (2)	0.013 (2)
F1	0.0372 (17)	0.0314 (16)	0.0466 (17)	-0.0003 (13)	0.0174 (13)	-0.0085 (13)
F2	0.0255 (16)	0.0329 (16)	0.0519 (18)	0.0024 (12)	0.0113 (13)	-0.0024 (13)
I2	0.02280 (18)	0.02866 (18)	0.02812 (19)	0.00088 (13)	0.00573 (13)	0.00153 (13)
C5	0.029 (3)	0.018 (2)	0.029 (3)	0.0001 (19)	0.013 (2)	0.0006 (19)
C4	0.024 (3)	0.021 (2)	0.022 (2)	-0.0004 (19)	0.0067 (19)	0.0049 (19)
C6	0.028 (3)	0.021 (2)	0.023 (2)	-0.006 (2)	0.006 (2)	-0.001 (2)
F3	0.0301 (16)	0.0216 (14)	0.0374 (15)	0.0034 (11)	0.0073 (12)	-0.0065 (12)
F4	0.0317 (16)	0.0278 (15)	0.0325 (16)	-0.0056 (12)	0.0046 (12)	-0.0090 (11)

Geometric parameters (\AA , $^\circ$)

C7—N1	1.320 (5)	C2—F1	1.344 (5)
C7—N2	1.337 (5)	C3—C2 ⁱ	1.385 (6)
C10—C9	1.365 (6)	C3—F2	1.347 (5)
C10—N1	1.335 (6)	I2—C4	2.097 (4)
C9—C8	1.377 (6)	C5—C4	1.376 (5)
C8—N2	1.337 (6)	C5—C6 ⁱⁱ	1.375 (6)
I1—C1	2.089 (4)	C5—F3	1.353 (5)
C1—C2	1.377 (6)	C4—C6	1.373 (6)
C1—C3	1.379 (6)	C6—C5 ⁱⁱ	1.375 (6)
C2—C3 ⁱ	1.385 (6)	C6—F4	1.362 (4)
N1—C7—N2	126.9 (4)	C1—C3—C2 ⁱ	121.8 (4)
N1—C10—C9	122.7 (4)	F2—C3—C1	120.0 (4)
C10—C9—C8	116.6 (5)	F2—C3—C2 ⁱ	118.1 (4)
N2—C8—C9	122.6 (5)	C6 ⁱⁱ —C5—C4	121.1 (4)
C7—N1—C10	116.0 (4)	F3—C5—C4	120.2 (4)

C7—N2—C8	115.3 (4)	F3—C5—C6 ⁱⁱ	118.7 (4)
C2—C1—I1	121.7 (3)	C5—C4—I2	121.3 (3)
C2—C1—C3	117.0 (4)	C6—C4—I2	121.9 (3)
C3—C1—I1	121.3 (4)	C6—C4—C5	116.8 (4)
C1—C2—C3 ⁱ	121.2 (4)	C4—C6—C5 ⁱⁱ	122.1 (4)
F1—C2—C1	120.5 (4)	F4—C6—C5 ⁱⁱ	117.6 (4)
F1—C2—C3 ⁱ	118.3 (4)	F4—C6—C4	120.3 (4)

Symmetry codes: (i) $-x+2, -y+1, -z+1$; (ii) $-x, -y+1, -z$.

1,4-diiodotetrafluorobenzene– 4,6-dimethylpyrimidine(2a)

Crystal data

$C_6F_4I_2 \cdot C_6H_8N_2$	$F(000) = 944$
$M_r = 510.00$	$D_x = 2.248 \text{ Mg m}^{-3}$
Monoclinic, $P2_1/c$	Mo $K\alpha$ radiation, $\lambda = 0.71073 \text{ \AA}$
$a = 5.2138 (9) \text{ \AA}$	Cell parameters from 1063 reflections
$b = 20.304 (2) \text{ \AA}$	$\theta = 3.0\text{--}26.0^\circ$
$c = 14.2732 (16) \text{ \AA}$	$\mu = 4.21 \text{ mm}^{-1}$
$\beta = 94.054 (12)^\circ$	$T = 150 \text{ K}$
$V = 1507.2 (3) \text{ \AA}^3$	Needle, clear light colourless
$Z = 4$	$0.2 \times 0.02 \times 0.02 \text{ mm}$

Data collection

SuperNova, Single source at offset/far, Eos diffractometer	2972 independent reflections
Radiation source: micro-focus sealed X-ray tube, SuperNova (Mo) X-ray Source	1639 reflections with $I > 2\sigma(I)$
Mirror monochromator	$R_{\text{int}} = 0.166$
Detector resolution: $8.0714 \text{ pixels mm}^{-1}$	$\theta_{\text{max}} = 26.0^\circ, \theta_{\text{min}} = 3.0^\circ$
ω scans	$h = -6 \rightarrow 5$
Absorption correction: multi-scan <i>CrysAlis PRO</i> 1.171.39.46 (Rigaku Oxford Diffraction, 2018) Empirical absorption correction using spherical harmonics, implemented in SCALE3 ABSPACK scaling algorithm.	$k = -25 \rightarrow 24$
$T_{\text{min}} = 0.062, T_{\text{max}} = 1.000$	$l = -17 \rightarrow 17$
10891 measured reflections	

Refinement

Refinement on F^2	Primary atom site location: structure-invariant direct methods
Least-squares matrix: full	Hydrogen site location: inferred from neighbouring sites
$R[F^2 > 2\sigma(F^2)] = 0.079$	H-atom parameters constrained
$wR(F^2) = 0.131$	$w = 1/[\sigma^2(F_o^2) + (0.0133P)^2]$ where $P = (F_o^2 + 2F_c^2)/3$
$S = 1.00$	$(\Delta/\sigma)_{\max} < 0.001$
2972 reflections	$\Delta_{\max} = 1.06 \text{ e } \text{\AA}^{-3}$
171 parameters	$\Delta_{\min} = -1.35 \text{ e } \text{\AA}^{-3}$
72 restraints	

Special details

Geometry. All esds (except the esd in the dihedral angle between two l.s. planes) are estimated using the full covariance matrix. The cell esds are taken into account individually in the estimation of esds in distances, angles and torsion angles; correlations between esds in cell parameters are only used when they are defined by crystal symmetry. An approximate (isotropic) treatment of cell esds is used for estimating esds involving l.s. planes.

Fractional atomic coordinates and isotropic or equivalent isotropic displacement parameters

(\AA^2)

	x	y	z	$U_{\text{iso}}^*/U_{\text{eq}}$
I1	1.2212 (2)	0.12636 (5)	0.63678 (6)	0.0289 (3)
I2	0.2546 (2)	0.34471 (5)	0.46388 (6)	0.0289 (3)
F4	0.9204 (16)	0.1451 (4)	0.4330 (5)	0.041 (2)
F3	0.5435 (16)	0.2260 (4)	0.3696 (5)	0.039 (2)
F2	0.5388 (17)	0.3233 (4)	0.6717 (5)	0.043 (3)
F1	0.9274 (18)	0.2432 (4)	0.7335 (5)	0.047 (3)
N2	0.620 (2)	0.0468 (6)	0.7269 (7)	0.029 (3)
C10	0.904 (3)	-0.0407 (8)	0.7675 (9)	0.033 (4)
H10	0.9609	-0.0832	0.7565	0.039*
C11	1.017 (3)	-0.0056 (7)	0.8407 (9)	0.022 (3)
C7	0.737 (3)	0.0780 (7)	0.7994 (9)	0.024 (3)
H7	0.6762	0.1199	0.8120	0.029*
N1	0.938 (2)	0.0557 (6)	0.8579 (7)	0.028 (3)
C1	0.9247 (16)	0.1917 (4)	0.5857 (6)	0.032 (4)
C6	0.8262 (17)	0.1877 (4)	0.4928 (6)	0.024 (3)
C5	0.6324 (17)	0.2305 (5)	0.4595 (4)	0.028 (3)
C4	0.5371 (16)	0.2772 (4)	0.5192 (6)	0.026 (3)

C3	0.6356 (18)	0.2812 (4)	0.6121 (5)	0.029 (4)
C2	0.8294 (18)	0.2384 (5)	0.6453 (4)	0.033 (4)
C8	0.708 (3)	-0.0147 (7)	0.7094 (9)	0.024 (3)
C9	0.574 (3)	-0.0511 (8)	0.6286 (10)	0.052 (5)
H9A	0.5983	-0.0281	0.5712	0.079*
H9B	0.3933	-0.0539	0.6376	0.079*
H9C	0.6441	-0.0947	0.6254	0.079*
C12	1.234 (3)	-0.0317 (7)	0.9045 (9)	0.040 (4)
H12A	1.3209	-0.0659	0.8730	0.060*
H12B	1.1666	-0.0492	0.9603	0.060*
H12C	1.3521	0.0033	0.9212	0.060*

Atomic displacement parameters (\AA^2)

	U^{11}	U^{22}	U^{33}	U^{12}	U^{13}	U^{23}
I1	0.0312 (7)	0.0297 (6)	0.0254 (6)	0.0002 (5)	-0.0021 (5)	0.0068 (5)
I2	0.0329 (7)	0.0271 (6)	0.0260 (6)	-0.0003 (5)	-0.0025 (5)	0.0064 (4)
F4	0.047 (7)	0.043 (6)	0.032 (5)	0.003 (5)	-0.007 (4)	-0.023 (4)
F3	0.041 (6)	0.060 (7)	0.014 (4)	0.004 (5)	-0.011 (4)	-0.002 (4)
F2	0.060 (7)	0.053 (7)	0.017 (5)	0.020 (5)	0.004 (4)	-0.002 (4)
F1	0.069 (8)	0.051 (7)	0.019 (5)	0.014 (5)	-0.011 (5)	0.001 (4)
N2	0.029 (7)	0.026 (6)	0.030 (6)	0.000 (5)	-0.002 (5)	-0.001 (4)
C10	0.032 (8)	0.033 (7)	0.031 (7)	0.007 (5)	-0.010 (6)	-0.005 (5)
C11	0.017 (7)	0.032 (6)	0.018 (6)	-0.001 (5)	-0.001 (5)	-0.001 (5)
C7	0.021 (7)	0.021 (7)	0.032 (6)	-0.006 (5)	0.006 (5)	0.002 (5)
N1	0.031 (7)	0.034 (6)	0.019 (5)	0.001 (5)	0.006 (5)	0.001 (4)
C1	0.030 (8)	0.033 (8)	0.031 (6)	-0.005 (6)	-0.002 (5)	-0.004 (5)
C6	0.019 (7)	0.026 (7)	0.027 (6)	-0.007 (5)	-0.001 (5)	-0.008 (5)
C5	0.025 (8)	0.038 (8)	0.022 (6)	0.002 (6)	0.006 (5)	0.001 (5)
C4	0.029 (8)	0.028 (8)	0.021 (5)	0.003 (6)	0.008 (5)	0.005 (5)
C3	0.038 (9)	0.031 (8)	0.018 (6)	0.000 (6)	0.007 (5)	0.007 (5)
C2	0.040 (9)	0.041 (8)	0.019 (6)	0.003 (6)	-0.005 (5)	0.002 (5)
C8	0.025 (7)	0.024 (6)	0.024 (6)	-0.006 (5)	-0.002 (5)	-0.001 (5)
C9	0.048 (13)	0.054 (13)	0.051 (11)	-0.002 (10)	-0.030 (10)	-0.010 (9)
C12	0.040 (12)	0.032 (11)	0.045 (10)	0.004 (8)	-0.023 (8)	0.002 (8)

Geometric parameters (Å, °)

I1—C1	2.126 (7)	C11—N1	1.338 (16)
I2—C4	2.123 (7)	C11—C12	1.495 (18)
F4—C6	1.333 (9)	C7—N1	1.371 (17)
F3—C5	1.337 (8)	C1—C6	1.3900
F2—C3	1.331 (9)	C1—C2	1.3900
F1—C2	1.328 (9)	C6—C5	1.3900
N2—C7	1.325 (16)	C5—C4	1.3900
N2—C8	1.360 (17)	C4—C3	1.3900
C10—C11	1.364 (17)	C3—C2	1.3900
C10—C8	1.376 (18)	C8—C9	1.500 (17)
C7—N2—C8	116.1 (13)	F3—C5—C4	121.3 (7)
C11—C10—C8	121.7 (15)	C6—C5—C4	120.0
C10—C11—C12	123.3 (14)	C5—C4—I2	118.8 (5)
N1—C11—C10	120.2 (13)	C3—C4—I2	121.1 (5)
N1—C11—C12	116.5 (12)	C3—C4—C5	120.0
N2—C7—N1	127.5 (14)	F2—C3—C4	121.1 (7)
C11—N1—C7	115.4 (12)	F2—C3—C2	118.9 (7)
C6—C1—I1	120.1 (5)	C2—C3—C4	120.0
C6—C1—C2	120.0	F1—C2—C1	120.0 (7)
C2—C1—I1	119.9 (5)	F1—C2—C3	120.0 (7)
F4—C6—C1	121.3 (7)	C3—C2—C1	120.0
F4—C6—C5	118.6 (7)	N2—C8—C10	119.1 (13)
C1—C6—C5	120.0	N2—C8—C9	116.8 (13)
F3—C5—C6	118.7 (7)	C10—C8—C9	124.1 (14)

1,4-diiodotetrafluorobenzene– 1,3,5-triazine(3a)

Crystal data

$C_6F_4I_2 \cdot C_3H_3N_3$	$F(000) = 880$
$M_r = 482.94$	$D_x = 2.630 \text{ Mg m}^{-3}$
Monoclinic, $I2/a$	Mo $K\alpha$ radiation, $\lambda = 0.71073 \text{ \AA}$
$a = 10.1820 (11) \text{ \AA}$	Cell parameters from 1613 reflections
$b = 6.2144 (6) \text{ \AA}$	$\theta = 3.4\text{--}28.6^\circ$
$c = 19.427 (2) \text{ \AA}$	$\mu = 5.19 \text{ mm}^{-1}$
$\beta = 97.075 (10)^\circ$	$T = 150 \text{ K}$
$V = 1219.9 (2) \text{ \AA}^3$	Plate, clear light colourless
$Z = 4$	$0.3 \times 0.1 \times 0.01 \text{ mm}$

Data collection

SuperNova, Single source at offset/far, Eos diffractometer	1205 independent reflections
Radiation source: micro-focus sealed X-ray tube, SuperNova (Mo) X-ray Source	1032 reflections with $I > 2\sigma(I)$
Mirror monochromator	$R_{\text{int}} = 0.053$
Detector resolution: 16.1428 pixels mm^{-1}	$\theta_{\text{max}} = 26.0^\circ$, $\theta_{\text{min}} = 3.4^\circ$
ω scans	$h = -12 \rightarrow 12$
Absorption correction: multi-scan <i>CrysAlis PRO</i> 1.171.39.46 (Rigaku Oxford Diffraction, 2018) Empirical absorption correction using spherical harmonics, implemented in SCALE3 ABSPACK scaling algorithm.	$k = -7 \rightarrow 6$
$T_{\text{min}} = 0.635$, $T_{\text{max}} = 1.000$	$l = -20 \rightarrow 23$
3977 measured reflections	

Refinement

Refinement on F^2	Primary atom site location: dual
Least-squares matrix: full	Hydrogen site location: inferred from neighbouring sites
$R[F^2 > 2\sigma(F^2)] = 0.032$	H-atom parameters constrained
$wR(F^2) = 0.079$	$w = 1/[\sigma^2(F_o^2) + (0.037P)^2 + 0.3023P]$ where $P = (F_o^2 + 2F_c^2)/3$
$S = 1.09$	$(\Delta/\sigma)_{\text{max}} = 0.001$
1205 reflections	$\Delta_{\text{max}} = 0.91 \text{ e } \text{\AA}^{-3}$
83 parameters	$\Delta_{\text{min}} = -0.89 \text{ e } \text{\AA}^{-3}$
0 restraints	

Special details

Geometry. All esds (except the esd in the dihedral angle between two l.s. planes) are estimated using the full covariance matrix. The cell esds are taken into account individually in the estimation of esds in distances, angles and torsion angles; correlations between esds in cell parameters are only used when they are defined by crystal symmetry. An approximate (isotropic) treatment of cell esds is used for estimating esds involving l.s. planes.

Fractional atomic coordinates and isotropic or equivalent isotropic displacement parameters (\AA^2)

	<i>x</i>	<i>y</i>	<i>z</i>	$U_{\text{iso}}^*/U_{\text{eq}}$
I1	0.47632 (3)	0.44611 (6)	0.35963 (2)	0.02420 (16)
F2	0.3595 (3)	0.9159 (5)	0.37265 (16)	0.0270 (7)
F1	0.3262 (3)	0.3617 (5)	0.20564 (16)	0.0277 (7)
N2	0.7500	-0.1461 (11)	0.5000	0.0267 (14)
N1	0.6497 (4)	0.1850 (8)	0.4620 (2)	0.0282 (11)
C2	0.3062 (5)	0.8306 (9)	0.3118 (2)	0.0204 (11)
C3	0.2888 (5)	0.5525 (8)	0.2291 (3)	0.0211 (11)
C1	0.3451 (5)	0.6293 (9)	0.2925 (3)	0.0199 (11)
C5	0.7500	0.2807 (13)	0.5000	0.0281 (18)
H5	0.7500	0.4303	0.5000	0.034*
C4	0.6558 (6)	-0.0276 (9)	0.4644 (3)	0.0282 (13)
H4	0.5873	-0.1020	0.4387	0.034*

Atomic displacement parameters (\AA^2)

	U^{11}	U^{22}	U^{33}	U^{12}	U^{13}	U^{23}
I1	0.0238 (2)	0.0220 (2)	0.0247 (2)	0.00201 (13)	-0.00543 (15)	0.00249 (14)
F2	0.0310 (17)	0.0271 (17)	0.0202 (16)	0.0015 (13)	-0.0074 (13)	-0.0042 (13)
F1	0.0323 (17)	0.0214 (16)	0.0270 (17)	0.0077 (14)	-0.0062 (13)	-0.0054 (14)
N2	0.030 (4)	0.024 (4)	0.025 (3)	0.000	0.000 (3)	0.000
N1	0.030 (3)	0.030 (3)	0.022 (2)	0.003 (2)	-0.0080 (18)	0.000 (2)
C2	0.020 (3)	0.027 (3)	0.013 (2)	-0.003 (2)	0.0004 (18)	-0.002 (2)
C3	0.023 (3)	0.017 (3)	0.023 (3)	0.000 (2)	0.001 (2)	-0.005 (2)
C1	0.024 (3)	0.018 (3)	0.017 (2)	0.002 (2)	0.0009 (19)	0.003 (2)
C5	0.039 (5)	0.025 (4)	0.019 (4)	0.000	-0.003 (3)	0.000
C4	0.024 (3)	0.033 (3)	0.026 (3)	-0.002 (2)	-0.003 (2)	-0.005 (3)

Geometric parameters (\AA , $^\circ$)

I1—C1	2.087 (5)	C2—C3 ⁱⁱ	1.381 (7)
F2—C2	1.347 (5)	C2—C1	1.378 (7)
F1—C3	1.342 (6)	C3—C2 ⁱⁱ	1.381 (7)
N2—C4 ⁱ	1.333 (7)	C3—C1	1.377 (7)
N2—C4	1.333 (7)	C5—N1 ⁱ	1.325 (5)
N1—C5	1.325 (5)	C5—H5	0.9300
N1—C4	1.323 (8)	C4—H4	0.9300

C4 ⁱ —N2—C4	112.9 (7)	C3—C1—I1	122.2 (4)
C4—N1—C5	113.5 (5)	C3—C1—C2	117.1 (5)
F2—C2—C3 ⁱⁱ	118.4 (5)	N1 ⁱ —C5—N1	126.7 (7)
F2—C2—C1	119.9 (4)	N1 ⁱ —C5—H5	116.7
C1—C2—C3 ⁱⁱ	121.7 (4)	N1—C5—H5	116.7
F1—C3—C2 ⁱⁱ	118.5 (5)	N2—C4—H4	116.6
F1—C3—C1	120.4 (5)	N1—C4—N2	126.7 (5)
C1—C3—C2 ⁱⁱ	121.1 (5)	N1—C4—H4	116.6
C2—C1—I1	120.5 (4)		

Symmetry codes: (i) $-x+3/2, y, -z+1$; (ii) $-x+1/2, -y+3/2, -z+1/2$.

1,4-diiodotetrafluorobenzene– pyrimidine-5-amine (4a)

Crystal data

$C_6F_4I_2 \cdot C_4H_5N_3$	$F(000) = 912$
$M_r = 496.97$	$D_x = 2.530 \text{ Mg m}^{-3}$
Monoclinic, $P2_1/n$	Mo $K\alpha$ radiation, $\lambda = 0.71073 \text{ \AA}$
$a = 5.1974 (2) \text{ \AA}$	Cell parameters from 3050 reflections
$b = 21.7822 (8) \text{ \AA}$	$\theta = 3.3\text{--}28.1^\circ$
$c = 11.7303 (4) \text{ \AA}$	$\mu = 4.86 \text{ mm}^{-1}$
$\beta = 100.729 (4)^\circ$	$T = 150 \text{ K}$
$V = 1304.78 (8) \text{ \AA}^3$	Irregular, clear light colourless
$Z = 4$	$0.05 \times 0.04 \times 0.01 \text{ mm}$

Data collection

SuperNova, Single source at offset/far, Eos diffractometer	2572 independent reflections
Radiation source: micro-focus sealed X-ray tube, SuperNova (Mo) X-ray Source	2165 reflections with $I > 2\sigma(I)$
Mirror monochromator	$R_{\text{int}} = 0.044$
Detector resolution: $8.0714 \text{ pixels mm}^{-1}$	$\theta_{\text{max}} = 26.0^\circ, \theta_{\text{min}} = 3.3^\circ$
ω scans	$h = -6 \rightarrow 3$
Absorption correction: multi-scan <i>CrysAlis PRO</i> 1.171.39.46 (Rigaku Oxford Diffraction, 2018) Empirical absorption correction using spherical harmonics, implemented in SCALE3 ABSPACK scaling algorithm.	$k = -26 \rightarrow 25$
$T_{\text{min}} = 0.452, T_{\text{max}} = 1.000$	$l = -14 \rightarrow 14$
6992 measured reflections	

Refinement

Refinement on F^2	Primary atom site location: dual
Least-squares matrix: full	Hydrogen site location: mixed
$R[F^2 > 2\sigma(F^2)] = 0.032$	H atoms treated by a mixture of independent and constrained refinement
$wR(F^2) = 0.063$	$w = 1/[\sigma^2(F_o^2) + (0.0159P)^2]$ where $P = (F_o^2 + 2F_c^2)/3$
$S = 1.02$	$(\Delta/\sigma)_{\max} = 0.001$
2572 reflections	$\Delta_{\max} = 0.56 \text{ e } \text{\AA}^{-3}$
180 parameters	$\Delta_{\min} = -0.71 \text{ e } \text{\AA}^{-3}$
0 restraints	

Special details

Geometry. All esds (except the esd in the dihedral angle between two l.s. planes) are estimated using the full covariance matrix. The cell esds are taken into account individually in the estimation of esds in distances, angles and torsion angles; correlations between esds in cell parameters are only used when they are defined by crystal symmetry. An approximate (isotropic) treatment of cell esds is used for estimating esds involving l.s. planes.

Fractional atomic coordinates and isotropic or equivalent isotropic displacement parameters (\AA^2)

	<i>x</i>	<i>y</i>	<i>z</i>	$U_{\text{iso}}^*/U_{\text{eq}}$
C1	0.8374 (9)	0.4396 (2)	0.3049 (4)	0.0204 (11)
C2	0.8697 (9)	0.5002 (2)	0.3379 (4)	0.0217 (11)
C3	1.0213 (9)	0.5394 (2)	0.2860 (4)	0.0223 (11)
C4	1.1454 (9)	0.5200 (2)	0.1981 (4)	0.0197 (11)
C5	1.1142 (9)	0.4595 (2)	0.1653 (4)	0.0211 (11)
C6	0.9615 (10)	0.4205 (2)	0.2169 (4)	0.0221 (11)
F1	0.7523 (6)	0.52306 (13)	0.4223 (2)	0.0331 (7)
F2	1.0430 (6)	0.59867 (13)	0.3202 (3)	0.0331 (7)
F3	1.2354 (6)	0.43661 (13)	0.0820 (2)	0.0319 (7)
F4	0.9424 (5)	0.36077 (13)	0.1812 (2)	0.0298 (7)
I1	0.61375 (6)	0.37946 (2)	0.38740 (3)	0.02318 (10)
I2	1.37713 (6)	0.58063 (2)	0.12237 (3)	0.02399 (11)
C7	-0.0473 (9)	0.2267 (2)	0.4941 (4)	0.0193 (11)
C8	0.1278 (8)	0.2591 (2)	0.4410 (4)	0.0214 (11)
H8	0.1163	0.2548	0.3614	0.026*
C9	0.3208 (10)	0.3007 (2)	0.6130 (4)	0.0292 (13)
H9	0.4485	0.3264	0.6540	0.035*
C10	-0.0168 (9)	0.2348 (2)	0.6137 (4)	0.0223 (11)

H10	-0.1268	0.2132	0.6535	0.027*
N1	0.3112 (8)	0.29586 (19)	0.4985 (3)	0.0252 (10)
N2	-0.2288 (8)	0.1867 (2)	0.4313 (4)	0.0245 (10)
H2A	-0.264 (9)	0.192 (2)	0.360 (4)	0.017 (14)*
H2B	-0.353 (9)	0.176 (2)	0.472 (4)	0.030 (15)*
N3	0.1625 (8)	0.27194 (19)	0.6737 (3)	0.0268 (10)

Atomic displacement parameters (Å²)

	U^{11}	U^{22}	U^{33}	U^{12}	U^{13}	U^{23}
C1	0.018 (2)	0.022 (3)	0.020 (3)	-0.002 (2)	0.001 (2)	0.005 (2)
C2	0.018 (2)	0.027 (3)	0.021 (2)	0.005 (2)	0.007 (2)	-0.001 (2)
C3	0.024 (3)	0.014 (3)	0.029 (3)	0.003 (2)	0.004 (2)	-0.005 (2)
C4	0.017 (2)	0.021 (3)	0.020 (2)	-0.001 (2)	0.000 (2)	0.002 (2)
C5	0.018 (3)	0.031 (3)	0.014 (2)	0.001 (2)	0.004 (2)	-0.006 (2)
C6	0.026 (3)	0.016 (3)	0.024 (3)	-0.002 (2)	0.003 (2)	-0.004 (2)
F1	0.0403 (18)	0.0314 (18)	0.0328 (17)	0.0064 (15)	0.0200 (15)	-0.0063 (14)
F2	0.0431 (19)	0.0191 (17)	0.0387 (18)	0.0021 (14)	0.0116 (15)	-0.0079 (14)
F3	0.0360 (18)	0.0350 (19)	0.0293 (16)	-0.0031 (15)	0.0181 (14)	-0.0118 (14)
F4	0.0366 (17)	0.0198 (16)	0.0358 (17)	-0.0054 (14)	0.0140 (14)	-0.0083 (14)
I1	0.02137 (18)	0.0256 (2)	0.02303 (18)	0.00034 (14)	0.00537 (14)	0.00320 (14)
I2	0.02110 (18)	0.0253 (2)	0.02488 (18)	-0.00238 (14)	0.00261 (14)	0.00455 (14)
C7	0.021 (3)	0.015 (3)	0.022 (2)	0.005 (2)	0.005 (2)	0.005 (2)
C8	0.019 (3)	0.025 (3)	0.020 (2)	0.002 (2)	0.004 (2)	-0.006 (2)
C9	0.027 (3)	0.025 (3)	0.033 (3)	0.001 (2)	-0.002 (2)	-0.008 (2)
C10	0.026 (3)	0.020 (3)	0.022 (2)	0.006 (2)	0.010 (2)	0.005 (2)
N1	0.024 (2)	0.022 (3)	0.030 (2)	0.0007 (19)	0.0065 (19)	-0.0013 (19)
N2	0.022 (2)	0.029 (3)	0.023 (2)	-0.002 (2)	0.006 (2)	0.001 (2)
N3	0.030 (2)	0.025 (3)	0.025 (2)	0.003 (2)	0.006 (2)	0.0002 (19)

Geometric parameters (Å, °)

C1—C2	1.376 (7)	C7—C8	1.387 (6)
C1—C6	1.379 (6)	C7—C10	1.392 (6)
C1—I1	2.103 (4)	C7—N2	1.391 (6)
C2—C3	1.379 (6)	C8—H8	0.9300
C2—F1	1.352 (5)	C8—N1	1.329 (6)
C3—C4	1.381 (6)	C9—H9	0.9300
C3—F2	1.350 (5)	C9—N1	1.339 (6)
C4—C5	1.374 (7)	C9—N3	1.340 (6)

C4—I2	2.094 (5)	C10—H10	0.9300
C5—C6	1.377 (6)	C10—N3	1.332 (6)
C5—F3	1.353 (5)	N2—H2A	0.83 (4)
C6—F4	1.365 (5)	N2—H2B	0.90 (5)
C2—C1—C6	116.8 (4)	C8—C7—C10	115.3 (5)
C2—C1—I1	121.1 (4)	C8—C7—N2	121.1 (4)
C6—C1—I1	122.1 (4)	N2—C7—C10	123.5 (4)
C1—C2—C3	121.4 (4)	C7—C8—H8	118.4
F1—C2—C1	120.8 (4)	N1—C8—C7	123.2 (4)
F1—C2—C3	117.8 (4)	N1—C8—H8	118.4
C2—C3—C4	121.6 (5)	N1—C9—H9	117.1
F2—C3—C2	119.0 (4)	N1—C9—N3	125.7 (5)
F2—C3—C4	119.4 (4)	N3—C9—H9	117.1
C3—C4—I2	120.6 (4)	C7—C10—H10	118.5
C5—C4—C3	117.2 (4)	N3—C10—C7	123.1 (5)
C5—C4—I2	122.2 (3)	N3—C10—H10	118.5
C4—C5—C6	121.1 (4)	C8—N1—C9	116.5 (4)
F3—C5—C4	120.6 (4)	C7—N2—H2A	117 (3)
F3—C5—C6	118.3 (4)	C7—N2—H2B	112 (3)
C5—C6—C1	122.0 (5)	H2A—N2—H2B	121 (5)
F4—C6—C1	120.0 (4)	C10—N3—C9	116.2 (4)
F4—C6—C5	117.9 (4)		

Appendix 5

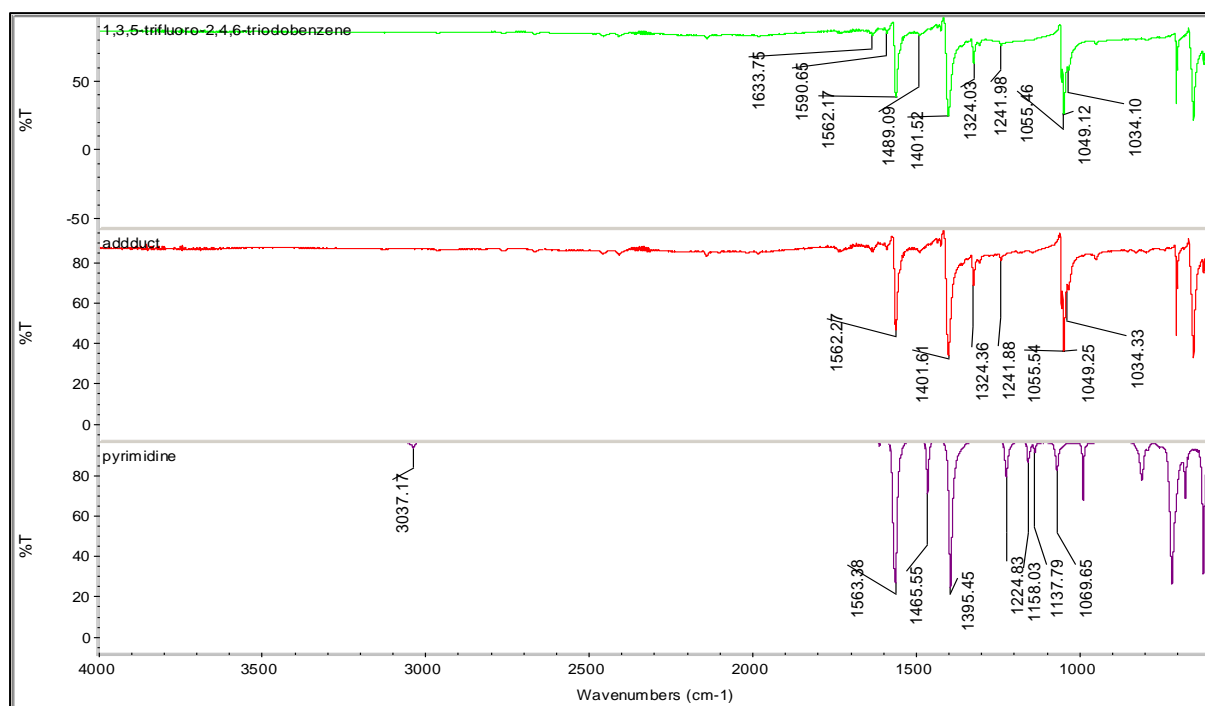
(Supplementary information)

Chapter 5:- Variety of halogen bonds containing compounds using pyrimidine derivatives

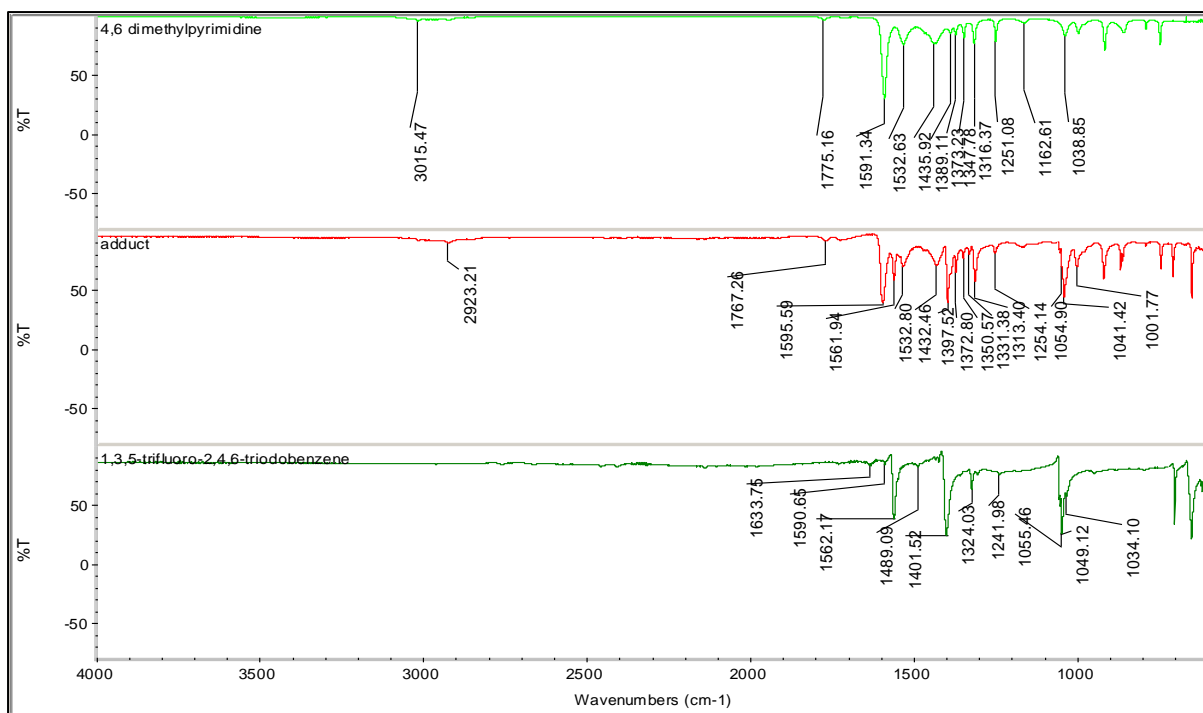
Sultan Alkaabi, Alan K. Brisdon,

Department of Chemistry, University of Manchester, Oxford Road, Manchester, M13 9PL, England.

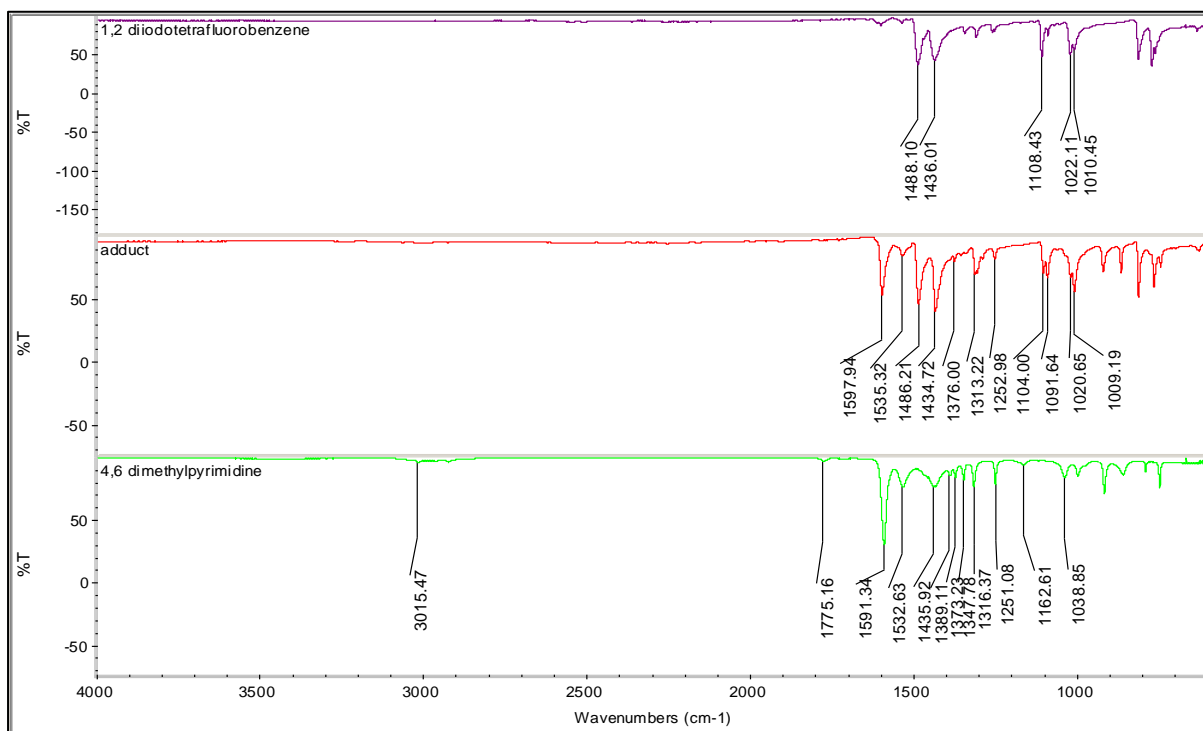
Correspondence email: *alan.brisdon@manchester.ac.uk



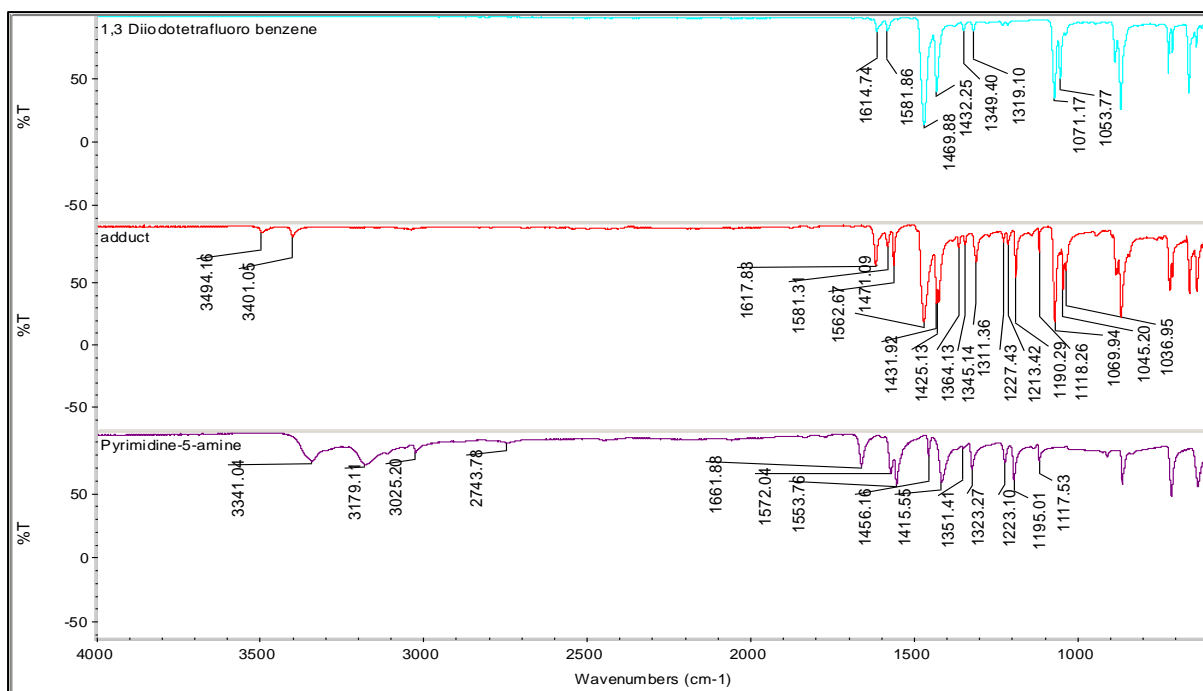
S 5.1 IR spectra showing the two starting materials and adduct **1a**



S 5.2 IR spectra showing the two starting materials and adduct **2a**



S 5.3 IR spectra showing the two starting materials and adduct **2c**



S 5.4 IR spectra showing the two starting materials and adduct adduct **3b**

Computing details

Data collection: *CrysAlis PRO* 1.171.38.46 (Rigaku OD, 2015) for (3b); *CrysAlis PRO* 1.171.39.46 (Rigaku OD, 2018) for (1a,2a and 2c); cell refinement: *CrysAlis PRO* 1.171.38.46 (Rigaku OD, 2015) for (3b); *CrysAlis PRO* 1.171.39.46 (Rigaku OD, 2018) for (1a,2a and 2c); data reduction: *CrysAlis PRO* 1.171.38.46 (Rigaku OD, 2015) for (1b); *CrysAlis PRO* 1.171.39.46 (Rigaku OD, 2018) for (1a,2a and 2c); program(s) used to solve structure: ShelXT (Sheldrick, 2015); program(s) used to refine structure: *SHELXL* (Sheldrick, 2015); molecular graphics: Olex2 (Dolomanov *et al.*, 2009); software used to prepare material for publication: Olex2 (Dolomanov *et al.*, 2009).

1, 3, 5-trifluoro-2, 4, 6-triodobenzene– pyrimidine (1a)

Crystal data

$2(\text{C}_6\text{F}_3\text{I}_3) \cdot 2(\text{C}_4\text{H}_4\text{N}_2)$	$D_x = 2.731 \text{ Mg m}^{-3}$
$M_r = 1179.70$	Mo $K\alpha$ radiation, $\lambda = 0.71073 \text{ \AA}$
Orthorhombic, $Pca2_1$	Cell parameters from 5667 reflections
$a = 26.5221 (10) \text{ \AA}$	$\theta = 3.1\text{--}26.8^\circ$
$b = 4.7308 (2) \text{ \AA}$	$\mu = 6.55 \text{ mm}^{-1}$
$c = 22.8651 (8) \text{ \AA}$	$T = 150 \text{ K}$
$V = 2868.90 (19) \text{ \AA}^3$	Needle, clear light colourless
$Z = 4$	$0.19 \times 0.02 \times 0.01 \text{ mm}$
$F(000) = 2112$	

Data collection

SuperNova, Single source at offset/far, Eos diffractometer	5599 independent reflections
Radiation source: micro-focus sealed X-ray tube, SuperNova (Mo) X-ray Source	4807 reflections with $I > 2\sigma(I)$
Mirror monochromator	$R_{\text{int}} = 0.071$
Detector resolution: 16.1428 pixels mm^{-1}	$\theta_{\text{max}} = 26.0^\circ$, $\theta_{\text{min}} = 3.1^\circ$
ω scans	$h = -32 \rightarrow 30$
Absorption correction: multi-scan <i>CrysAlis PRO</i> 1.171.39.46 (Rigaku Oxford Diffraction, 2018) Empirical absorption correction using spherical harmonics, implemented in SCALE3 ABSPACK scaling algorithm.	$k = -5 \rightarrow 5$
$T_{\text{min}} = 0.509$, $T_{\text{max}} = 1.000$	$l = -28 \rightarrow 28$
23779 measured reflections	

Refinement

Refinement on F^2	Hydrogen site location: inferred from neighbouring sites
Least-squares matrix: full	H-atom parameters constrained
$R[F^2 > 2\sigma(F^2)] = 0.038$	$w = 1/[\sigma^2(F_o^2) + (0.0127P)^2]$ where $P = (F_o^2 + 2F_c^2)/3$
$wR(F^2) = 0.066$	$(\Delta/\sigma)_{\text{max}} < 0.001$
$S = 1.06$	$\Delta_{\text{max}} = 0.70 \text{ e } \text{\AA}^{-3}$
5599 reflections	$\Delta_{\text{min}} = -0.70 \text{ e } \text{\AA}^{-3}$
302 parameters	Absolute structure: Refined as an inversion twin.
109 restraints	Absolute structure parameter: 0.00 (5)
Primary atom site location: dual	

Special details

<i>Geometry.</i> All esds (except the esd in the dihedral angle between two l.s. planes) are estimated using the full covariance matrix. The cell esds are taken into account individually in the estimation of esds in distances, angles and torsion angles; correlations between esds in cell parameters are only used when they are defined by crystal symmetry. An approximate (isotropic) treatment of cell esds is used for estimating esds involving l.s. planes.
<i>Refinement.</i> Refined as a 2-component inversion twin.

Fractional atomic coordinates and isotropic or equivalent isotropic displacement parameters
(\AA^2)

	<i>x</i>	<i>y</i>	<i>z</i>	$U_{\text{iso}}^*/U_{\text{eq}}$
I3	0.20991 (3)	-0.65443 (17)	0.33908 (4)	0.0268 (2)
I6	0.01228 (3)	-0.83642 (18)	0.14988 (4)	0.0267 (2)
I1	0.31600 (3)	0.17536 (18)	0.49792 (4)	0.0257 (2)
I4	0.08231 (3)	-0.03844 (18)	0.34052 (5)	0.0337 (2)
I2	0.11015 (4)	-0.2741 (2)	0.56562 (5)	0.0358 (2)
I5	-0.13936 (4)	-0.3065 (2)	0.31485 (5)	0.0370 (3)
F1	0.2890 (3)	-0.2289 (15)	0.3917 (4)	0.032 (2)
F3	0.1312 (3)	-0.5992 (16)	0.4465 (3)	0.031 (2)
F6	0.0819 (3)	-0.4684 (16)	0.2337 (4)	0.034 (2)
F5	-0.0905 (3)	-0.6799 (16)	0.2148 (4)	0.034 (2)
F2	0.2112 (3)	0.0781 (15)	0.5661 (3)	0.0315 (19)
F4	-0.0364 (3)	-0.0283 (16)	0.3569 (3)	0.034 (2)
N2	0.0343 (4)	-0.180 (2)	0.0502 (5)	0.029 (3)
N1	0.0930 (4)	-0.510 (2)	0.0124 (5)	0.029 (3)
N3	0.1763 (5)	-1.220 (3)	0.1523 (6)	0.048 (3)
C1	0.2517 (3)	-0.0746 (15)	0.4795 (4)	0.021 (3)
C6	0.2508 (3)	-0.2377 (17)	0.4290 (3)	0.018 (3)
C5	0.2099 (3)	-0.4123 (16)	0.4174 (3)	0.020 (3)
C4	0.1697 (3)	-0.4238 (17)	0.4565 (4)	0.022 (3)
C3	0.1706 (3)	-0.2607 (18)	0.5071 (3)	0.025 (3)
C2	0.2116 (3)	-0.0861 (16)	0.5186 (3)	0.026 (3)
C7	0.0235 (3)	-0.2499 (17)	0.2974 (4)	0.024 (3)
C12	0.0346 (2)	-0.4344 (18)	0.2519 (4)	0.022 (3)
C11	-0.0040 (3)	-0.5798 (17)	0.2239 (3)	0.022 (3)
C10	-0.0537 (3)	-0.5407 (18)	0.2414 (4)	0.027 (3)
C9	-0.0648 (2)	-0.3562 (18)	0.2869 (4)	0.023 (3)
C8	-0.0262 (3)	-0.2108 (15)	0.3149 (3)	0.023 (3)
C13	0.0778 (6)	-0.314 (3)	0.0510 (7)	0.033 (4)
H13	0.1001	-0.2692	0.0810	0.040*
N4	0.2149 (5)	-0.997 (3)	0.2343 (5)	0.035 (3)
C16	0.0023 (6)	-0.249 (3)	0.0077 (7)	0.037 (4)
H16	-0.0291	-0.1607	0.0068	0.045*
C17	0.1769 (6)	-1.042 (3)	0.1973 (7)	0.041 (4)
H17	0.1477	-0.9373	0.2036	0.049*
C14	0.0593 (6)	-0.575 (3)	-0.0308 (7)	0.039 (4)

H14	0.0677	-0.7131	-0.0582	0.046*
C18	0.2561 (7)	-1.146 (3)	0.2236 (7)	0.042 (4)
H18	0.2843	-1.1210	0.2473	0.051*
C20	0.2185 (7)	-1.368 (4)	0.1435 (8)	0.050 (4)
H20	0.2200	-1.4950	0.1125	0.060*
C15	0.0134 (6)	-0.442 (3)	-0.0346 (7)	0.041 (4)
H15	-0.0091	-0.4818	-0.0648	0.049*
C19	0.2586 (7)	-1.337 (3)	0.1785 (7)	0.047 (4)
H19	0.2876	-1.4436	0.1723	0.056*

Atomic displacement parameters (\AA^2)

	U^{11}	U^{22}	U^{33}	U^{12}	U^{13}	U^{23}
I3	0.0281 (5)	0.0276 (5)	0.0248 (5)	-0.0036 (4)	-0.0010 (4)	-0.0019 (5)
I6	0.0297 (5)	0.0276 (5)	0.0227 (5)	0.0033 (4)	0.0021 (4)	0.0005 (5)
I1	0.0237 (5)	0.0279 (5)	0.0254 (5)	-0.0013 (4)	-0.0023 (4)	-0.0024 (5)
I4	0.0295 (5)	0.0338 (5)	0.0377 (6)	-0.0053 (4)	-0.0091 (5)	0.0000 (5)
I2	0.0276 (5)	0.0454 (6)	0.0343 (6)	0.0009 (4)	0.0108 (5)	0.0026 (5)
I5	0.0232 (6)	0.0513 (6)	0.0366 (6)	0.0023 (4)	0.0083 (5)	-0.0004 (5)
F1	0.022 (5)	0.040 (5)	0.034 (5)	-0.006 (4)	0.008 (4)	-0.006 (4)
F3	0.026 (5)	0.036 (5)	0.032 (5)	-0.012 (4)	-0.001 (4)	0.001 (4)
F6	0.018 (5)	0.044 (5)	0.042 (5)	0.004 (4)	0.008 (4)	-0.001 (4)
F5	0.018 (5)	0.050 (5)	0.033 (5)	-0.009 (4)	-0.001 (4)	-0.004 (4)
F2	0.037 (5)	0.033 (4)	0.025 (5)	-0.005 (3)	0.005 (4)	-0.007 (4)
F4	0.033 (5)	0.039 (5)	0.029 (5)	-0.001 (4)	0.007 (4)	-0.006 (4)
N2	0.033 (8)	0.024 (7)	0.031 (8)	-0.009 (6)	-0.001 (6)	0.003 (6)
N1	0.018 (7)	0.043 (7)	0.025 (7)	-0.004 (6)	-0.001 (5)	-0.004 (6)
N3	0.055 (8)	0.061 (8)	0.029 (7)	-0.017 (6)	-0.001 (6)	-0.007 (6)
C1	0.020 (6)	0.022 (6)	0.022 (6)	0.012 (5)	-0.002 (5)	0.004 (5)
C6	0.010 (6)	0.022 (6)	0.023 (6)	0.006 (5)	0.004 (5)	0.008 (5)
C5	0.014 (6)	0.028 (7)	0.019 (6)	0.001 (5)	-0.004 (5)	0.008 (5)
C4	0.023 (6)	0.020 (7)	0.023 (6)	-0.002 (5)	-0.001 (5)	0.007 (5)
C3	0.022 (6)	0.030 (7)	0.025 (7)	0.004 (5)	0.001 (5)	0.002 (5)
C2	0.022 (6)	0.028 (7)	0.028 (7)	0.006 (5)	0.001 (5)	-0.001 (6)
C7	0.026 (6)	0.023 (7)	0.024 (7)	0.001 (5)	-0.002 (5)	0.001 (5)
C12	0.015 (6)	0.025 (6)	0.027 (7)	0.000 (5)	0.003 (5)	0.005 (5)
C11	0.023 (6)	0.023 (6)	0.020 (7)	0.000 (5)	0.003 (5)	0.005 (5)
C10	0.020 (6)	0.034 (7)	0.026 (7)	-0.003 (5)	0.002 (5)	-0.002 (6)
C9	0.022 (6)	0.024 (7)	0.024 (7)	0.001 (5)	0.001 (5)	0.005 (5)
C8	0.030 (6)	0.020 (6)	0.020 (6)	0.002 (5)	0.001 (5)	0.008 (5)

C13	0.033 (9)	0.037 (9)	0.029 (9)	0.005 (7)	-0.002 (7)	0.000 (7)
N4	0.041 (7)	0.039 (7)	0.026 (6)	-0.010 (5)	-0.004 (5)	0.001 (5)
C16	0.029 (9)	0.042 (10)	0.040 (11)	0.008 (7)	-0.001 (8)	0.004 (8)
C17	0.043 (8)	0.053 (9)	0.028 (7)	-0.005 (6)	-0.009 (6)	-0.002 (7)
C14	0.042 (10)	0.031 (9)	0.043 (10)	-0.004 (7)	-0.004 (8)	-0.012 (8)
C18	0.043 (8)	0.047 (8)	0.036 (8)	-0.007 (6)	-0.003 (6)	-0.001 (7)
C20	0.065 (9)	0.056 (9)	0.029 (8)	-0.016 (7)	0.014 (6)	-0.003 (7)
C15	0.039 (11)	0.045 (10)	0.037 (10)	0.006 (8)	-0.015 (8)	-0.009 (8)
C19	0.058 (9)	0.049 (9)	0.034 (8)	-0.008 (7)	0.009 (6)	0.003 (7)

Geometric parameters (Å, °)

I3—C5	2.127 (6)	C4—C3	1.3900
I6—C11	2.127 (6)	C3—C2	1.3900
I1—C1	2.118 (6)	C7—C12	1.3900
I4—C7	2.099 (6)	C7—C8	1.3900
I2—C3	2.090 (6)	C12—C11	1.3900
I5—C9	2.091 (6)	C11—C10	1.3900
F1—C6	1.324 (9)	C10—C9	1.3900
F3—C4	1.335 (9)	C9—C8	1.3900
F6—C12	1.332 (9)	C13—H13	0.9300
F5—C10	1.324 (9)	N4—C17	1.332 (18)
F2—C2	1.335 (9)	N4—C18	1.325 (19)
F4—C8	1.319 (9)	C16—H16	0.9300
N2—C13	1.318 (17)	C16—C15	1.36 (2)
N2—C16	1.332 (18)	C17—H17	0.9300
N1—C13	1.341 (17)	C14—H14	0.9300
N1—C14	1.368 (17)	C14—C15	1.37 (2)
N3—C17	1.33 (2)	C18—H18	0.9300
N3—C20	1.33 (2)	C18—C19	1.37 (2)
C1—C6	1.3900	C20—H20	0.9300
C1—C2	1.3900	C20—C19	1.34 (2)
C6—C5	1.3900	C15—H15	0.9300
C5—C4	1.3900	C19—H19	0.9300
C13—N2—C16	116.9 (13)	C9—C10—C11	120.0
C13—N1—C14	115.7 (13)	C10—C9—I5	120.0 (5)
C17—N3—C20	116.0 (15)	C8—C9—I5	120.0 (5)
C6—C1—I1	119.2 (4)	C8—C9—C10	120.0
C6—C1—C2	120.0	F4—C8—C7	119.4 (7)

C2—C1—I1	120.7 (4)	F4—C8—C9	120.6 (7)
F1—C6—C1	120.3 (6)	C9—C8—C7	120.0
F1—C6—C5	119.7 (6)	N2—C13—N1	126.0 (14)
C1—C6—C5	120.0	N2—C13—H13	117.0
C6—C5—I3	118.6 (4)	N1—C13—H13	117.0
C4—C5—I3	121.4 (4)	C18—N4—C17	115.0 (14)
C4—C5—C6	120.0	N2—C16—H16	118.6
F3—C4—C5	120.0 (7)	N2—C16—C15	122.9 (14)
F3—C4—C3	119.9 (7)	C15—C16—H16	118.6
C5—C4—C3	120.0	N3—C17—H17	116.5
C4—C3—I2	120.2 (4)	N4—C17—N3	126.9 (16)
C2—C3—I2	119.8 (4)	N4—C17—H17	116.5
C2—C3—C4	120.0	N1—C14—H14	119.3
F2—C2—C1	120.3 (7)	N1—C14—C15	121.4 (14)
F2—C2—C3	119.6 (7)	C15—C14—H14	119.3
C3—C2—C1	120.0	N4—C18—H18	119.0
C12—C7—I4	119.6 (4)	N4—C18—C19	121.9 (16)
C12—C7—C8	120.0	C19—C18—H18	119.0
C8—C7—I4	120.4 (4)	N3—C20—H20	119.4
F6—C12—C7	120.6 (7)	N3—C20—C19	121.3 (17)
F6—C12—C11	119.4 (7)	C19—C20—H20	119.4
C11—C12—C7	120.0	C16—C15—C14	117.1 (14)
C12—C11—I6	120.0 (4)	C16—C15—H15	121.5
C12—C11—C10	120.0	C14—C15—H15	121.5
C10—C11—I6	119.9 (4)	C18—C19—H19	120.6
F5—C10—C11	120.0 (7)	C20—C19—C18	118.9 (18)
F5—C10—C9	120.0 (7)	C20—C19—H19	120.6

1,3,5-trifluoro-2,4,6-triiodobenzene– 4,6-dimethylpyrimidine (2a)*Crystal data*

$C_6F_3I_3 \cdot 2(C_6H_8N_2)$	$F(000) = 1352$
$M_r = 726.05$	$D_x = 2.171 \text{ Mg m}^{-3}$
Monoclinic, $P2_1/c$	Mo $K\alpha$ radiation, $\lambda = 0.71073 \text{ \AA}$
$a = 7.4661 (3) \text{ \AA}$	Cell parameters from 6447 reflections
$b = 21.2636 (5) \text{ \AA}$	$\theta = 2.9\text{--}28.9^\circ$
$c = 14.1362 (7) \text{ \AA}$	$\mu = 4.26 \text{ mm}^{-1}$
$\beta = 98.206 (4)^\circ$	$T = 150 \text{ K}$
$V = 2221.23 (15) \text{ \AA}^3$	Needle, clear light colourless
$Z = 4$	$0.2 \times 0.05 \times 0.04 \text{ mm}$

Data collection

SuperNova, Single source at offset/far, Eos diffractometer	4369 independent reflections
Radiation source: micro-focus sealed X-ray tube, SuperNova (Mo) X-ray Source	3568 reflections with $I > 2\sigma(I)$
Mirror monochromator	$R_{\text{int}} = 0.077$
Detector resolution: $16.1428 \text{ pixels mm}^{-1}$	$\theta_{\text{max}} = 26.0^\circ$, $\theta_{\text{min}} = 2.9^\circ$
ω scans	$h = -8 \rightarrow 9$
Absorption correction: multi-scan <i>CrysAlis PRO</i> 1.171.39.46 (Rigaku Oxford Diffraction, 2018) Empirical absorption correction using spherical harmonics, implemented in SCALE3 ABSPACK scaling algorithm.	$k = -26 \rightarrow 26$
$T_{\text{min}} = 0.445$, $T_{\text{max}} = 1.000$	$l = -17 \rightarrow 12$
19829 measured reflections	

Refinement

Refinement on F^2	Primary atom site location: dual
Least-squares matrix: full	Hydrogen site location: inferred from neighbouring sites
$R[F^2 > 2\sigma(F^2)] = 0.034$	H-atom parameters constrained
$wR(F^2) = 0.078$	$w = 1/[\sigma^2(F_o^2) + (0.0225P)^2 + 0.5296P]$ where $P = (F_o^2 + 2F_c^2)/3$
$S = 1.10$	$(\Delta/\sigma)_{\text{max}} = 0.002$
4369 reflections	$\Delta_{\text{max}} = 0.95 \text{ e \AA}^{-3}$
257 parameters	$\Delta_{\text{min}} = -0.73 \text{ e \AA}^{-3}$
0 restraints	

Special details

Geometry. All esds (except the esd in the dihedral angle between two l.s. planes) are estimated using the full covariance matrix. The cell esds are taken into account individually in the estimation of esds in distances, angles and torsion angles; correlations between esds in cell parameters are only used when they are defined by crystal symmetry. An approximate (isotropic) treatment of cell esds is used for estimating esds involving l.s. planes.

Fractional atomic coordinates and isotropic or equivalent isotropic displacement parameters

(\AA^2)

	x	y	z	$U_{\text{iso}}^*/U_{\text{eq}}$
C1	1.6899 (6)	0.06091 (19)	0.9909 (4)	0.0194 (12)
C2	1.6700 (6)	0.0344 (2)	0.9008 (4)	0.0204 (12)
C3	1.7208 (6)	-0.0266 (2)	0.8831 (4)	0.0202 (12)
C4	1.7921 (6)	-0.06100 (19)	0.9624 (4)	0.0199 (13)
C5	1.8119 (6)	-0.0389 (2)	1.0546 (4)	0.0211 (13)
C6	1.7595 (6)	0.0231 (2)	1.0667 (4)	0.0185 (12)
F1	1.6002 (4)	0.06968 (12)	0.8255 (3)	0.0289 (8)
F2	1.7765 (4)	0.04685 (12)	1.1553 (3)	0.0295 (8)
F3	1.8477 (4)	-0.12050 (11)	0.9488 (2)	0.0277 (8)
I1	1.68891 (5)	-0.06503 (2)	0.74556 (3)	0.02631 (11)
I2	1.61601 (4)	0.15458 (2)	1.01205 (3)	0.02336 (11)
I3	1.90838 (4)	-0.09545 (2)	1.17182 (3)	0.02340 (11)
C7	1.4311 (7)	0.1841 (2)	0.4564 (5)	0.0303 (14)
H7	1.4383	0.2055	0.3997	0.036*
C8	1.4856 (7)	0.1840 (2)	0.6172 (5)	0.0264 (14)
C9	1.4120 (6)	0.1240 (2)	0.6151 (5)	0.0269 (14)
H9	1.4052	0.1027	0.6719	0.032*
C10	1.3497 (6)	0.0962 (2)	0.5298 (5)	0.0226 (13)
C11	1.2669 (7)	0.0322 (2)	0.5220 (5)	0.0349 (16)
H11A	1.3446	0.0039	0.4939	0.052*
H11B	1.1512	0.0342	0.4826	0.052*
H11C	1.2516	0.0174	0.5845	0.052*
C12	1.5600 (8)	0.2155 (3)	0.7100 (5)	0.0391 (16)
H12A	1.5467	0.2603	0.7031	0.059*
H12B	1.6858	0.2053	0.7262	0.059*
H12C	1.4948	0.2012	0.7597	0.059*
N1	1.4942 (6)	0.21490 (18)	0.5361 (4)	0.0260 (12)
N2	1.3596 (5)	0.12733 (18)	0.4469 (4)	0.0241 (11)
C13	0.8767 (7)	0.1120 (2)	0.5928 (5)	0.0302 (15)

H13	0.8406	0.0766	0.6236	0.036*
C14	1.0080 (6)	0.2082 (2)	0.6035 (4)	0.0231 (13)
C15	0.9777 (7)	0.2122 (2)	0.5071 (5)	0.0295 (15)
H15	1.0133	0.2478	0.4765	0.035*
C16	0.8936 (8)	0.1631 (3)	0.4540 (5)	0.0326 (15)
C17	0.8590 (9)	0.1627 (3)	0.3487 (5)	0.0526 (19)
H17A	0.9487	0.1374	0.3244	0.079*
H17B	0.8648	0.2049	0.3253	0.079*
H17C	0.7411	0.1455	0.3278	0.079*
C18	1.0964 (8)	0.2603 (2)	0.6671 (5)	0.0397 (17)
H18A	1.0107	0.2936	0.6707	0.060*
H18B	1.1990	0.2763	0.6409	0.060*
H18C	1.1353	0.2440	0.7300	0.060*
N3	0.9575 (6)	0.15684 (17)	0.6485 (4)	0.0257 (12)
N4	0.8416 (6)	0.1119 (2)	0.4986 (4)	0.0348 (13)

Atomic displacement parameters (Å²)

	U^{11}	U^{22}	U^{33}	U^{12}	U^{13}	U^{23}
C1	0.027 (3)	0.013 (2)	0.019 (4)	-0.0033 (19)	0.004 (2)	0.004 (2)
C2	0.020 (3)	0.018 (2)	0.023 (4)	-0.0030 (19)	0.004 (2)	0.009 (2)
C3	0.023 (3)	0.016 (2)	0.022 (4)	-0.0033 (19)	0.007 (2)	-0.001 (2)
C4	0.019 (3)	0.014 (2)	0.027 (4)	-0.0037 (18)	0.005 (2)	-0.004 (2)
C5	0.017 (2)	0.020 (2)	0.026 (4)	-0.0008 (19)	0.003 (2)	0.006 (2)
C6	0.020 (3)	0.022 (2)	0.015 (4)	-0.0075 (19)	0.006 (2)	-0.007 (2)
F1	0.0357 (17)	0.0245 (15)	0.025 (3)	0.0041 (12)	-0.0004 (16)	0.0035 (13)
F2	0.0392 (18)	0.0249 (15)	0.024 (3)	0.0025 (13)	0.0047 (16)	-0.0032 (13)
F3	0.0372 (17)	0.0169 (14)	0.030 (3)	0.0063 (12)	0.0082 (16)	-0.0025 (12)
I1	0.0318 (2)	0.02498 (19)	0.0221 (3)	0.00048 (13)	0.00371 (17)	-0.00432 (14)
I2	0.02635 (19)	0.01432 (16)	0.0297 (3)	0.00022 (12)	0.00496 (16)	-0.00064 (13)
I3	0.02602 (19)	0.01991 (17)	0.0249 (3)	0.00074 (12)	0.00590 (16)	0.00554 (13)
C7	0.039 (3)	0.023 (3)	0.029 (5)	0.007 (2)	0.008 (3)	0.006 (2)
C8	0.034 (3)	0.021 (3)	0.026 (4)	-0.001 (2)	0.012 (3)	-0.010 (2)
C9	0.022 (3)	0.025 (3)	0.035 (5)	0.000 (2)	0.011 (3)	0.005 (2)
C10	0.020 (3)	0.018 (2)	0.029 (4)	0.0021 (19)	0.001 (3)	-0.001 (2)
C11	0.040 (3)	0.022 (3)	0.042 (5)	-0.008 (2)	0.004 (3)	0.000 (3)
C12	0.044 (4)	0.045 (3)	0.026 (5)	0.004 (3)	-0.002 (3)	-0.010 (3)
N1	0.030 (2)	0.019 (2)	0.030 (4)	-0.0063 (17)	0.009 (2)	-0.003 (2)

N2	0.029 (2)	0.023 (2)	0.020 (3)	-0.0027 (18)	0.003 (2)	-0.0041 (19)
C13	0.034 (3)	0.026 (3)	0.030 (5)	-0.001 (2)	0.002 (3)	0.007 (2)
C14	0.023 (3)	0.024 (3)	0.025 (4)	0.004 (2)	0.013 (3)	0.004 (2)
C15	0.031 (3)	0.025 (3)	0.036 (5)	0.008 (2)	0.015 (3)	0.015 (2)
C16	0.037 (3)	0.040 (3)	0.022 (5)	0.015 (3)	0.009 (3)	0.007 (3)
C17	0.066 (5)	0.069 (5)	0.021 (5)	0.017 (4)	0.001 (4)	0.004 (3)
C18	0.041 (4)	0.022 (3)	0.055 (6)	-0.004 (2)	0.004 (3)	0.005 (3)
N3	0.026 (2)	0.020 (2)	0.031 (4)	0.0041 (17)	0.004 (2)	0.0065 (19)
N4	0.036 (3)	0.031 (3)	0.034 (4)	0.002 (2)	-0.004 (3)	0.003 (2)

Geometric parameters (Å, °)

C1—C2	1.381 (8)	C11—H11A	0.9600
C1—C6	1.381 (7)	C11—H11B	0.9600
C1—I2	2.099 (4)	C11—H11C	0.9600
C2—C3	1.384 (6)	C12—H12A	0.9600
C2—F1	1.345 (6)	C12—H12B	0.9600
C3—C4	1.381 (8)	C12—H12C	0.9600
C3—I1	2.091 (6)	C13—H13	0.9300
C4—C5	1.373 (8)	C13—N3	1.325 (7)
C4—F3	1.354 (5)	C13—N4	1.319 (8)
C5—C6	1.391 (6)	C14—C15	1.352 (8)
C5—I3	2.091 (5)	C14—C18	1.517 (8)
C6—F2	1.340 (6)	C14—N3	1.345 (6)
C7—H7	0.9300	C15—H15	0.9300
C7—N1	1.329 (8)	C15—C16	1.383 (8)
C7—N2	1.320 (6)	C16—C17	1.475 (9)
C8—C9	1.388 (7)	C16—N4	1.343 (7)
C8—C12	1.507 (8)	C17—H17A	0.9600
C8—N1	1.331 (7)	C17—H17B	0.9600
C9—H9	0.9300	C17—H17C	0.9600
C9—C10	1.363 (8)	C18—H18A	0.9600
C10—C11	1.491 (6)	C18—H18B	0.9600
C10—N2	1.358 (7)	C18—H18C	0.9600
C2—C1—C6	117.1 (4)	H11B—C11—H11C	109.5
C2—C1—I2	121.5 (4)	C8—C12—H12A	109.5
C6—C1—I2	121.3 (4)	C8—C12—H12B	109.5
C1—C2—C3	123.6 (5)	C8—C12—H12C	109.5
F1—C2—C1	118.7 (4)	H12A—C12—H12B	109.5

F1—C2—C3	117.7 (5)	H12A—C12—H12C	109.5
C2—C3—I1	122.5 (4)	H12B—C12—H12C	109.5
C4—C3—C2	115.7 (5)	C7—N1—C8	115.6 (4)
C4—C3—I1	121.8 (3)	C7—N2—C10	115.4 (5)
C5—C4—C3	124.5 (4)	N3—C13—H13	116.2
F3—C4—C3	118.1 (5)	N4—C13—H13	116.2
F3—C4—C5	117.5 (5)	N4—C13—N3	127.6 (5)
C4—C5—C6	116.6 (5)	C15—C14—C18	123.2 (5)
C4—C5—I3	122.2 (3)	N3—C14—C15	120.6 (5)
C6—C5—I3	121.2 (4)	N3—C14—C18	116.1 (5)
C1—C6—C5	122.5 (5)	C14—C15—H15	120.1
F2—C6—C1	118.7 (4)	C14—C15—C16	119.8 (5)
F2—C6—C5	118.8 (5)	C16—C15—H15	120.1
N1—C7—H7	115.6	C15—C16—C17	123.5 (6)
N2—C7—H7	115.6	N4—C16—C15	119.8 (6)
N2—C7—N1	128.8 (6)	N4—C16—C17	116.7 (6)
C9—C8—C12	121.6 (6)	C16—C17—H17A	109.5
N1—C8—C9	120.2 (6)	C16—C17—H17B	109.5
N1—C8—C12	118.2 (5)	C16—C17—H17C	109.5
C8—C9—H9	120.0	H17A—C17—H17B	109.5
C10—C9—C8	120.1 (6)	H17A—C17—H17C	109.5
C10—C9—H9	120.0	H17B—C17—H17C	109.5
C9—C10—C11	123.1 (6)	C14—C18—H18A	109.5
N2—C10—C9	119.9 (5)	C14—C18—H18B	109.5
N2—C10—C11	117.0 (5)	C14—C18—H18C	109.5
C10—C11—H11A	109.5	H18A—C18—H18B	109.5
C10—C11—H11B	109.5	H18A—C18—H18C	109.5
C10—C11—H11C	109.5	H18B—C18—H18C	109.5
H11A—C11—H11B	109.5	C13—N3—C14	115.9 (6)
H11A—C11—H11C	109.5	C13—N4—C16	116.2 (5)

1,2-diiodotetrafluorobenzene and 4,6-dimethylpyrimidine(2c)

Crystal data

$2(\text{C}_6\text{F}_4\text{I}_2) \cdot 2(\text{C}_6\text{H}_8\text{N}_2)$	$Z = 2$
$M_r = 1020.01$	$F(000) = 944$
Triclinic, $P\bar{1}$	$D_x = 2.243 \text{ Mg m}^{-3}$
$a = 8.6005 (4) \text{ \AA}$	Mo $K\alpha$ radiation, $\lambda = 0.71073 \text{ \AA}$
$b = 13.5115 (7) \text{ \AA}$	Cell parameters from 4582 reflections
$c = 14.0306 (6) \text{ \AA}$	$\theta = 3.0\text{--}28.4^\circ$
$\alpha = 77.609 (4)^\circ$	$\mu = 4.20 \text{ mm}^{-1}$
$\beta = 89.057 (4)^\circ$	$T = 150 \text{ K}$
$\gamma = 71.743 (5)^\circ$	Needle, clear light colourless
$V = 1510.03 (13) \text{ \AA}^3$	$0.4 \times 0.08 \times 0.03 \text{ mm}$

Data collection

SuperNova, Single source at offset/far, Eos diffractometer	5954 independent reflections
Radiation source: micro-focus sealed X-ray tube, SuperNova (Mo) X-ray Source	4438 reflections with $I > 2\sigma(I)$
Mirror monochromator	$R_{\text{int}} = 0.052$
Detector resolution: $8.0714 \text{ pixels mm}^{-1}$	$\theta_{\text{max}} = 26.0^\circ$, $\theta_{\text{min}} = 3.0^\circ$
ω scans	$h = -9 \rightarrow 10$
Absorption correction: multi-scan <i>CrysAlis PRO</i> 1.171.39.46 (Rigaku Oxford Diffraction, 2018) Empirical absorption correction using spherical harmonics, implemented in SCALE3 ABSPACK scaling algorithm.	$k = -16 \rightarrow 16$
$T_{\text{min}} = 0.744$, $T_{\text{max}} = 1.000$	$l = -11 \rightarrow 17$
11244 measured reflections	

Refinement

Refinement on F^2	Primary atom site location: dual
Least-squares matrix: full	Hydrogen site location: inferred from neighbouring sites
$R[F^2 > 2\sigma(F^2)] = 0.044$	H-atom parameters constrained
$wR(F^2) = 0.082$	$w = 1/[\sigma^2(F_o^2) + (0.0117P)^2]$ where $P = (F_o^2 + 2F_c^2)/3$
$S = 0.99$	$(\Delta/\sigma)_{\text{max}} = 0.001$
5954 reflections	$\Delta\rho_{\text{max}} = 1.20 \text{ e \AA}^{-3}$

365 parameters	$\Delta_{\min} = -0.89 \text{ e } \text{\AA}^{-3}$
0 restraints	

Special details

Geometry. All esds (except the esd in the dihedral angle between two l.s. planes) are estimated using the full covariance matrix. The cell esds are taken into account individually in the estimation of esds in distances, angles and torsion angles; correlations between esds in cell parameters are only used when they are defined by crystal symmetry. An approximate (isotropic) treatment of cell esds is used for estimating esds involving l.s. planes.

Fractional atomic coordinates and isotropic or equivalent isotropic displacement parameters (\AA^2)

	x	y	z	$U_{\text{iso}}^*/U_{\text{eq}}$
C1	0.3036 (8)	-0.4496 (5)	0.9236 (5)	0.0270 (17)
C2	0.2688 (8)	-0.5395 (5)	0.9775 (5)	0.0274 (17)
C3	0.1876 (9)	-0.5322 (6)	1.0606 (6)	0.0330 (18)
C4	0.1418 (8)	-0.4399 (6)	1.0977 (6)	0.0353 (19)
C5	0.1755 (8)	-0.3500 (6)	1.0460 (6)	0.0356 (19)
C6	0.2552 (8)	-0.3570 (5)	0.9588 (6)	0.0304 (18)
F1	0.1485 (5)	-0.6159 (3)	1.1160 (3)	0.0468 (12)
F2	0.0699 (5)	-0.4360 (4)	1.1821 (3)	0.0533 (13)
F3	0.1359 (5)	-0.2607 (3)	1.0791 (3)	0.0520 (13)
F4	0.2849 (5)	-0.2683 (3)	0.9098 (3)	0.0439 (12)
I1	0.43222 (5)	-0.44923 (4)	0.79534 (4)	0.03036 (13)
I2	0.33362 (6)	-0.68665 (3)	0.93356 (4)	0.03185 (14)
C7	0.1328 (8)	0.0233 (5)	0.6366 (5)	0.0226 (15)
C8	0.1802 (8)	-0.0626 (6)	0.5901 (5)	0.0290 (17)
C9	0.1439 (7)	-0.1548 (5)	0.6317 (5)	0.0235 (16)
C10	0.0641 (8)	-0.1655 (5)	0.7170 (6)	0.0293 (17)
C11	0.0169 (8)	-0.0820 (6)	0.7635 (5)	0.0311 (17)
C12	0.0505 (8)	0.0115 (6)	0.7223 (5)	0.0299 (17)
F5	0.1891 (5)	-0.2390 (3)	0.5872 (3)	0.0376 (11)
F6	0.0287 (5)	-0.2563 (3)	0.7537 (3)	0.0483 (12)
F7	-0.0590 (5)	-0.0919 (4)	0.8470 (3)	0.0520 (13)
F8	0.0013 (5)	0.0907 (3)	0.7715 (3)	0.0434 (12)
I3	0.17965 (6)	0.16801 (4)	0.58570 (4)	0.03172 (13)
I4	0.29582 (5)	-0.05549 (3)	0.45703 (4)	0.02727 (13)
C13	0.5235 (9)	0.1047 (6)	0.7896 (6)	0.037 (2)
H13	0.5641	0.1614	0.7681	0.044*
C14	0.5216 (8)	-0.0589 (5)	0.7792 (5)	0.0240 (15)

C15	0.4169 (8)	-0.0561 (5)	0.8528 (5)	0.0278 (17)
H15	0.3813	-0.1146	0.8766	0.033*
C16	0.3623 (8)	0.0343 (5)	0.8933 (5)	0.0256 (16)
C17	0.2431 (9)	0.0442 (6)	0.9713 (6)	0.041 (2)
H17A	0.1413	0.0976	0.9453	0.061*
H17B	0.2861	0.0646	1.0241	0.061*
H17C	0.2249	-0.0232	0.9950	0.061*
C18	0.5842 (9)	-0.1546 (5)	0.7334 (5)	0.038 (2)
H18A	0.6982	-0.1902	0.7525	0.057*
H18B	0.5713	-0.1314	0.6635	0.057*
H18C	0.5231	-0.2030	0.7551	0.057*
N1	0.4203 (7)	0.1168 (4)	0.8598 (5)	0.0369 (16)
N2	0.5796 (7)	0.0232 (4)	0.7440 (4)	0.0315 (15)
C19	-0.3403 (10)	0.6238 (6)	0.5700 (6)	0.043 (2)
H19	-0.3756	0.6850	0.5952	0.052*
C20	-0.2118 (8)	0.5455 (6)	0.4513 (5)	0.0298 (18)
C21	-0.2348 (8)	0.4517 (5)	0.5011 (6)	0.0335 (19)
H21	-0.1972	0.3903	0.4764	0.040*
C22	-0.3123 (8)	0.4492 (5)	0.5861 (6)	0.0306 (18)
C23	-0.3405 (10)	0.3492 (6)	0.6455 (6)	0.053 (3)
H23A	-0.4521	0.3660	0.6641	0.080*
H23B	-0.2680	0.3222	0.7030	0.080*
H23C	-0.3194	0.2961	0.6069	0.080*
C24	-0.1299 (9)	0.5544 (6)	0.3566 (6)	0.044 (2)
H24A	-0.0348	0.5756	0.3636	0.066*
H24B	-0.2048	0.6069	0.3068	0.066*
H24C	-0.0975	0.4865	0.3384	0.066*
N3	-0.3709 (7)	0.5380 (5)	0.6233 (5)	0.0360 (16)
N4	-0.2672 (7)	0.6343 (5)	0.4870 (5)	0.0375 (16)

Atomic displacement parameters (\AA^2)

	U^{11}	U^{22}	U^{33}	U^{12}	U^{13}	U^{23}
C1	0.023 (4)	0.027 (4)	0.031 (5)	-0.010 (3)	0.000 (3)	-0.002 (3)
C2	0.024 (4)	0.029 (4)	0.027 (5)	-0.008 (3)	-0.003 (4)	-0.003 (3)
C3	0.037 (4)	0.037 (4)	0.021 (5)	-0.012 (4)	0.001 (4)	0.003 (4)
C4	0.029 (4)	0.050 (5)	0.019 (5)	-0.002 (4)	0.001 (4)	-0.007 (4)
C5	0.023 (4)	0.030 (4)	0.043 (6)	0.009 (3)	-0.009 (4)	-0.011 (4)
C6	0.029 (4)	0.026 (4)	0.035 (5)	-0.009 (3)	-0.007 (4)	-0.002 (4)
F1	0.048 (3)	0.056 (3)	0.032 (3)	-0.024 (2)	0.011 (2)	0.008 (2)

F2	0.048 (3)	0.075 (3)	0.028 (3)	-0.006 (2)	0.006 (3)	-0.013 (3)
F3	0.058 (3)	0.045 (3)	0.049 (3)	0.000 (2)	0.001 (3)	-0.026 (3)
F4	0.049 (3)	0.031 (2)	0.054 (3)	-0.019 (2)	-0.004 (3)	-0.005 (2)
I1	0.0269 (2)	0.0336 (3)	0.0298 (3)	-0.0130 (2)	0.0024 (2)	-0.0002 (2)
I2	0.0349 (3)	0.0261 (3)	0.0332 (3)	-0.0109 (2)	-0.0023 (2)	-0.0017 (2)
C7	0.023 (3)	0.025 (4)	0.018 (4)	-0.006 (3)	-0.004 (3)	-0.003 (3)
C8	0.021 (4)	0.040 (4)	0.023 (5)	-0.007 (3)	0.006 (3)	-0.006 (4)
C9	0.016 (3)	0.031 (4)	0.022 (4)	-0.007 (3)	-0.007 (3)	-0.003 (3)
C10	0.020 (3)	0.028 (4)	0.031 (5)	-0.005 (3)	0.001 (3)	0.010 (3)
C11	0.021 (4)	0.049 (5)	0.014 (4)	-0.005 (3)	0.000 (3)	0.004 (4)
C12	0.020 (4)	0.040 (4)	0.028 (5)	-0.004 (3)	0.002 (4)	-0.011 (4)
F5	0.044 (3)	0.033 (2)	0.037 (3)	-0.013 (2)	0.009 (2)	-0.008 (2)
F6	0.046 (3)	0.044 (3)	0.052 (3)	-0.021 (2)	0.009 (3)	0.005 (2)
F7	0.040 (3)	0.072 (3)	0.036 (3)	-0.013 (2)	0.020 (3)	-0.003 (3)
F8	0.043 (3)	0.053 (3)	0.034 (3)	-0.007 (2)	0.011 (2)	-0.019 (2)
I3	0.0308 (3)	0.0307 (3)	0.0345 (3)	-0.0101 (2)	0.0021 (2)	-0.0083 (2)
I4	0.0229 (2)	0.0336 (3)	0.0253 (3)	-0.0082 (2)	0.0052 (2)	-0.0080 (2)
C13	0.047 (5)	0.034 (4)	0.033 (5)	-0.019 (4)	0.008 (4)	-0.006 (4)
C14	0.026 (4)	0.022 (4)	0.016 (4)	-0.004 (3)	-0.009 (3)	0.008 (3)
C15	0.031 (4)	0.024 (4)	0.028 (5)	-0.014 (3)	-0.001 (4)	0.000 (3)
C16	0.021 (3)	0.030 (4)	0.023 (4)	-0.009 (3)	-0.004 (3)	0.000 (3)
C17	0.040 (5)	0.050 (5)	0.033 (5)	-0.016 (4)	0.013 (4)	-0.009 (4)
C18	0.041 (4)	0.038 (5)	0.036 (5)	-0.013 (4)	0.005 (4)	-0.013 (4)
N1	0.047 (4)	0.034 (4)	0.033 (4)	-0.016 (3)	0.007 (4)	-0.010 (3)
N2	0.033 (3)	0.029 (3)	0.031 (4)	-0.009 (3)	0.005 (3)	-0.006 (3)
C19	0.057 (5)	0.038 (5)	0.043 (6)	-0.024 (4)	0.019 (5)	-0.013 (4)
C20	0.022 (4)	0.046 (5)	0.029 (5)	-0.016 (3)	0.005 (4)	-0.016 (4)
C21	0.036 (4)	0.023 (4)	0.047 (6)	-0.012 (3)	0.007 (4)	-0.016 (4)
C22	0.022 (4)	0.029 (4)	0.039 (5)	-0.011 (3)	-0.004 (4)	0.000 (4)
C23	0.066 (6)	0.039 (5)	0.060 (7)	-0.030 (5)	0.026 (6)	-0.004 (5)
C24	0.055 (5)	0.053 (5)	0.034 (5)	-0.028 (4)	0.014 (5)	-0.013 (4)
N3	0.032 (3)	0.036 (4)	0.045 (5)	-0.016 (3)	0.017 (3)	-0.013 (3)
N4	0.048 (4)	0.040 (4)	0.028 (4)	-0.020 (3)	0.011 (4)	-0.008 (3)

Geometric parameters (Å, °)

C1—C2	1.401 (9)	C14—C18	1.511 (8)
C1—C6	1.383 (8)	C14—N2	1.352 (8)
C1—I1	2.097 (7)	C15—H15	0.9300
C2—C3	1.355 (9)	C15—C16	1.402 (8)
C2—I2	2.112 (6)	C16—C17	1.486 (9)
C3—C4	1.395 (9)	C16—N1	1.352 (8)
C3—F1	1.360 (7)	C17—H17A	0.9600
C4—C5	1.386 (10)	C17—H17B	0.9600
C4—F2	1.330 (8)	C17—H17C	0.9600
C5—C6	1.399 (10)	C18—H18A	0.9600
C5—F3	1.328 (7)	C18—H18B	0.9600
C6—F4	1.345 (8)	C18—H18C	0.9600
C7—C8	1.400 (8)	C19—H19	0.9300
C7—C12	1.390 (9)	C19—N3	1.336 (9)
C7—I3	2.093 (6)	C19—N4	1.316 (9)
C8—C9	1.385 (9)	C20—C21	1.382 (9)
C8—I4	2.098 (7)	C20—C24	1.493 (9)
C9—C10	1.373 (9)	C20—N4	1.345 (8)
C9—F5	1.361 (6)	C21—H21	0.9300
C10—C11	1.373 (9)	C21—C22	1.355 (9)
C10—F6	1.349 (7)	C22—C23	1.514 (9)
C11—C12	1.386 (9)	C22—N3	1.360 (8)
C11—F7	1.334 (7)	C23—H23A	0.9600
C12—F8	1.352 (7)	C23—H23B	0.9600
C13—H13	0.9300	C23—H23C	0.9600
C13—N1	1.317 (8)	C24—H24A	0.9600
C13—N2	1.347 (8)	C24—H24B	0.9600
C14—C15	1.359 (9)	C24—H24C	0.9600
C2—C1—I1	123.6 (5)	C16—C15—H15	119.8
C6—C1—C2	118.2 (6)	C15—C16—C17	123.2 (6)
C6—C1—I1	118.2 (5)	N1—C16—C15	118.6 (6)
C1—C2—I2	122.9 (5)	N1—C16—C17	118.2 (6)
C3—C2—C1	119.1 (6)	C16—C17—H17A	109.5
C3—C2—I2	118.0 (5)	C16—C17—H17B	109.5
C2—C3—C4	123.0 (7)	C16—C17—H17C	109.5
C2—C3—F1	122.3 (6)	H17A—C17—H17B	109.5
F1—C3—C4	114.6 (6)	H17A—C17—H17C	109.5

C5—C4—C3	118.9 (7)	H17B—C17—H17C	109.5
F2—C4—C3	122.1 (7)	C14—C18—H18A	109.5
F2—C4—C5	118.9 (7)	C14—C18—H18B	109.5
C4—C5—C6	117.8 (6)	C14—C18—H18C	109.5
F3—C5—C4	121.1 (7)	H18A—C18—H18B	109.5
F3—C5—C6	121.1 (7)	H18A—C18—H18C	109.5
C1—C6—C5	122.9 (7)	H18B—C18—H18C	109.5
F4—C6—C1	120.6 (7)	C13—N1—C16	115.8 (6)
F4—C6—C5	116.5 (6)	C13—N2—C14	113.1 (6)
C8—C7—I3	124.0 (5)	N3—C19—H19	115.3
C12—C7—C8	118.0 (6)	N4—C19—H19	115.3
C12—C7—I3	118.0 (4)	N4—C19—N3	129.4 (7)
C7—C8—I4	122.8 (5)	C21—C20—C24	122.8 (6)
C9—C8—C7	118.6 (6)	N4—C20—C21	119.9 (6)
C9—C8—I4	118.5 (5)	N4—C20—C24	117.4 (7)
C10—C9—C8	122.6 (6)	C20—C21—H21	120.0
F5—C9—C8	119.3 (6)	C22—C21—C20	119.9 (6)
F5—C9—C10	118.1 (6)	C22—C21—H21	120.0
C11—C10—C9	119.5 (6)	C21—C22—C23	123.1 (6)
F6—C10—C9	120.4 (6)	C21—C22—N3	121.4 (6)
F6—C10—C11	120.1 (6)	N3—C22—C23	115.5 (7)
C10—C11—C12	118.7 (7)	C22—C23—H23A	109.5
F7—C11—C10	120.0 (7)	C22—C23—H23B	109.5
F7—C11—C12	121.3 (6)	C22—C23—H23C	109.5
C11—C12—C7	122.6 (6)	H23A—C23—H23B	109.5
F8—C12—C7	121.4 (6)	H23A—C23—H23C	109.5
F8—C12—C11	116.0 (6)	H23B—C23—H23C	109.5
N1—C13—H13	114.9	C20—C24—H24A	109.5
N1—C13—N2	130.2 (6)	C20—C24—H24B	109.5
N2—C13—H13	114.9	C20—C24—H24C	109.5
C15—C14—C18	122.4 (6)	H24A—C24—H24B	109.5
N2—C14—C15	121.8 (6)	H24A—C24—H24C	109.5
N2—C14—C18	115.8 (6)	H24B—C24—H24C	109.5
C14—C15—H15	119.8	C19—N3—C22	113.7 (6)
C14—C15—C16	120.4 (6)	C19—N4—C20	115.7 (6)

pyrimidine -5-amine featuring and 1,3-diiodotetrafluorobenzene (3b)

Crystal data

$4(\text{C}_6\text{F}_4\text{I}_2) \cdot 2(\text{C}_4\text{H}_5\text{N}_3)$	$F(000) = 3248$
$M_r = 1797.66$	$D_x = 2.719 \text{ Mg m}^{-3}$
Monoclinic, Cc	Mo $K\alpha$ radiation, $\lambda = 0.71073 \text{ \AA}$
$a = 12.8944 (5) \text{ \AA}$	Cell parameters from 6459 reflections
$b = 12.7987 (5) \text{ \AA}$	$\theta = 3.0\text{--}28.4^\circ$
$c = 27.0876 (13) \text{ \AA}$	$\mu = 5.75 \text{ mm}^{-1}$
$\beta = 100.731 (4)^\circ$	$T = 150 \text{ K}$
$V = 4392.1 (3) \text{ \AA}^3$	Irregular, clear light colourless
$Z = 4$	$0.1 \times 0.06 \times 0.02 \text{ mm}$

Data collection

SuperNova, Single source at offset, Eos diffractometer	7613 independent reflections
Radiation source: micro-focus sealed X-ray tube, SuperNova (Mo) X-ray Source	6857 reflections with $I > 2\sigma(I)$
Mirror monochromator	$R_{\text{int}} = 0.049$
Detector resolution: $8.0714 \text{ pixels mm}^{-1}$	$\theta_{\text{max}} = 26.0^\circ$, $\theta_{\text{min}} = 3.0^\circ$
ω scans	$h = -15 \rightarrow 15$
Absorption correction: multi-scan <i>CrysAlis PRO</i> 1.171.38.46 (Rigaku Oxford Diffraction, 2015) Empirical absorption correction using spherical harmonics, implemented in SCALE3 ABSPACK scaling algorithm.	$k = -14 \rightarrow 15$
$T_{\text{min}} = 0.654$, $T_{\text{max}} = 1.000$	$l = -26 \rightarrow 33$
17947 measured reflections	

Refinement

Refinement on F^2	Hydrogen site location: mixed
Least-squares matrix: full	H-atom parameters constrained
$R[F^2 > 2\sigma(F^2)] = 0.038$	$w = 1/[\sigma^2(F_o^2) + (0.0085P)^2]$ where $P = (F_o^2 + 2F_c^2)/3$
$wR(F^2) = 0.063$	$(\Delta/\sigma)_{\text{max}} < 0.001$
$S = 1.03$	$\Delta_{\text{max}} = 0.79 \text{ e \AA}^{-3}$
7613 reflections	$\Delta_{\text{min}} = -0.79 \text{ e \AA}^{-3}$
550 parameters	Absolute structure: Refined as an inversion twin.
62 restraints	Absolute structure parameter: $-0.02 (4)$
Primary atom site location: dual	

Special details

Geometry. All esds (except the esd in the dihedral angle between two l.s. planes) are estimated using the full covariance matrix. The cell esds are taken into account individually in the estimation of esds in distances, angles and torsion angles; correlations between esds in cell parameters are only used when they are defined by crystal symmetry. An approximate (isotropic) treatment of cell esds is used for estimating esds involving l.s. planes.

Refinement. Refined as a 2-component inversion twin.

Fractional atomic coordinates and isotropic or equivalent isotropic displacement parameters (\AA^2)

	x	y	z	$U_{\text{iso}}^*/U_{\text{eq}}$
C1	0.7271 (9)	0.7318 (11)	0.6180 (5)	0.019 (3)
C2	0.8129 (10)	0.7977 (12)	0.6248 (5)	0.022 (3)
C3	0.8198 (9)	0.8843 (11)	0.5945 (5)	0.020 (3)
C4	0.7349 (12)	0.9033 (13)	0.5556 (6)	0.032 (4)
C5	0.6486 (10)	0.8370 (12)	0.5486 (6)	0.025 (4)
C6	0.6466 (10)	0.7520 (12)	0.5808 (6)	0.029 (4)
F1	0.8944 (5)	0.7818 (6)	0.6643 (3)	0.027 (2)
F2	0.7357 (7)	0.9827 (7)	0.5239 (4)	0.038 (2)
F3	0.5650 (7)	0.8575 (8)	0.5121 (4)	0.044 (3)
F4	0.5592 (6)	0.6927 (7)	0.5719 (3)	0.036 (2)
I1	0.72052 (5)	0.60314 (7)	0.66590 (3)	0.0210 (2)
I2	0.94665 (6)	0.98626 (8)	0.60707 (4)	0.0325 (3)
C7	0.8152 (9)	0.3953 (11)	0.7523 (5)	0.022 (2)
H7	0.8682	0.4447	0.7528	0.026*
C8	0.6460 (9)	0.3464 (12)	0.7257 (5)	0.023 (3)
H8	0.5789	0.3602	0.7074	0.028*
C9	0.6621 (10)	0.2533 (11)	0.7526 (6)	0.022 (3)
C10	0.7635 (8)	0.2391 (11)	0.7808 (5)	0.017 (3)
H10	0.7779	0.1800	0.8009	0.020*
N1	0.8395 (9)	0.3082 (10)	0.7795 (5)	0.021 (2)
N2	0.5841 (8)	0.1803 (10)	0.7525 (5)	0.030 (3)
H2A	0.5804	0.1614	0.7829	0.036*
H2B	0.5241	0.2081	0.7388	0.036*
N3	0.7211 (9)	0.4162 (9)	0.7247 (5)	0.020 (3)
C11	0.2141 (9)	0.7899 (11)	0.5941 (5)	0.021 (2)
C12	0.3115 (10)	0.8102 (11)	0.6224 (5)	0.018 (2)
C13	0.3747 (9)	0.8921 (11)	0.6131 (5)	0.017 (2)
C14	0.3377 (9)	0.9516 (10)	0.5728 (5)	0.021 (3)

C15	0.2404 (10)	0.9373 (12)	0.5425 (5)	0.022 (3)
C16	0.1789 (9)	0.8558 (11)	0.5542 (5)	0.021 (2)
F5	0.3474 (6)	0.7475 (6)	0.6620 (3)	0.026 (2)
F6	0.3941 (5)	1.0362 (7)	0.5611 (3)	0.035 (2)
F7	0.2055 (6)	0.9999 (7)	0.5034 (3)	0.038 (2)
F8	0.0840 (6)	0.8404 (7)	0.5243 (3)	0.030 (2)
I3	0.12156 (6)	0.66611 (8)	0.61055 (3)	0.0267 (2)
I4	0.52238 (5)	0.92078 (7)	0.65943 (3)	0.0217 (2)
C17	0.2594 (10)	0.6433 (12)	0.2479 (6)	0.025 (3)
H17	0.2071	0.6937	0.2471	0.030*
C18	0.4252 (9)	0.5896 (11)	0.2787 (5)	0.019 (3)
H18	0.4901	0.5990	0.2999	0.022*
C19	0.4103 (10)	0.4999 (12)	0.2501 (6)	0.024 (3)
C20	0.3102 (10)	0.4899 (11)	0.2220 (5)	0.021 (3)
H20	0.2949	0.4292	0.2032	0.025*
N4	0.3520 (9)	0.6639 (11)	0.2778 (5)	0.026 (3)
N5	0.4884 (8)	0.4256 (10)	0.2506 (5)	0.034 (3)
H5A	0.5167	0.4127	0.2816	0.040*
H5B	0.4619	0.3678	0.2369	0.040*
N6	0.2331 (9)	0.5610 (10)	0.2196 (5)	0.021 (3)
C21	0.2589 (10)	1.1305 (12)	0.4098 (5)	0.023 (3)
C22	0.2620 (10)	1.0467 (12)	0.3784 (5)	0.017 (2)
C23	0.3510 (9)	0.9829 (11)	0.3825 (5)	0.018 (2)
C24	0.4351 (10)	1.0098 (11)	0.4171 (5)	0.022 (3)
C25	0.4366 (11)	1.0909 (12)	0.4508 (5)	0.025 (4)
C26	0.3455 (11)	1.1506 (12)	0.4462 (5)	0.024 (4)
F9	0.1765 (5)	1.0244 (7)	0.3418 (3)	0.028 (2)
F10	0.5269 (5)	0.9537 (6)	0.4218 (3)	0.031 (2)
F11	0.5215 (6)	1.1140 (8)	0.4844 (3)	0.036 (2)
F12	0.3446 (7)	1.2302 (7)	0.4788 (3)	0.037 (2)
I5	0.12605 (7)	1.22754 (9)	0.40069 (4)	0.0378 (3)
I6	0.35488 (6)	0.85260 (7)	0.33526 (3)	0.0218 (2)
C32	0.3863 (5)	0.5946 (7)	0.4506 (3)	0.023 (3)
C27	0.3524 (6)	0.5316 (6)	0.4090 (3)	0.016 (3)
C28	0.2577 (6)	0.5532 (6)	0.3768 (3)	0.015 (3)
C29	0.1968 (5)	0.6379 (6)	0.3863 (3)	0.015 (3)
C30	0.2307 (6)	0.7009 (6)	0.4280 (3)	0.025 (3)
C31	0.3255 (6)	0.6793 (7)	0.4601 (3)	0.023 (3)
F13	0.2252 (5)	0.4922 (6)	0.3374 (3)	0.0226 (19)

F14	0.1761 (6)	0.7834 (7)	0.4373 (3)	0.036 (2)
F15	0.3576 (7)	0.7394 (8)	0.5002 (4)	0.045 (3)
F16	0.4764 (6)	0.5751 (7)	0.4816 (3)	0.032 (2)
I7	0.44676 (6)	0.40664 (8)	0.39409 (4)	0.0261 (2)
I8	0.05278 (5)	0.67125 (7)	0.33792 (3)	0.0203 (2)

Atomic displacement parameters (\AA^2)

	U^{11}	U^{22}	U^{33}	U^{12}	U^{13}	U^{23}
C1	0.020 (6)	0.023 (8)	0.015 (8)	0.001 (6)	0.007 (5)	0.001 (6)
C2	0.018 (7)	0.030 (9)	0.015 (9)	-0.004 (6)	-0.003 (6)	0.003 (7)
C3	0.017 (7)	0.021 (9)	0.023 (9)	-0.003 (6)	0.008 (6)	0.002 (6)
C4	0.041 (9)	0.031 (11)	0.028 (10)	-0.003 (8)	0.018 (7)	0.005 (8)
C5	0.029 (8)	0.022 (9)	0.023 (9)	0.003 (6)	0.003 (6)	0.005 (7)
C6	0.025 (7)	0.027 (10)	0.034 (11)	-0.008 (6)	0.005 (6)	-0.003 (7)
F1	0.018 (4)	0.030 (5)	0.031 (5)	-0.005 (3)	0.000 (3)	0.008 (4)
F2	0.048 (5)	0.034 (6)	0.030 (6)	-0.008 (5)	0.004 (4)	0.018 (5)
F3	0.041 (5)	0.052 (7)	0.033 (6)	-0.007 (4)	-0.007 (4)	0.016 (5)
F4	0.031 (4)	0.040 (6)	0.034 (6)	-0.018 (4)	-0.006 (4)	0.009 (4)
I1	0.0228 (4)	0.0168 (5)	0.0230 (6)	-0.0027 (4)	0.0038 (4)	0.0024 (4)
I2	0.0331 (5)	0.0288 (6)	0.0383 (7)	-0.0146 (4)	0.0135 (4)	-0.0012 (5)
C7	0.024 (5)	0.012 (5)	0.030 (6)	-0.004 (4)	0.005 (5)	0.004 (5)
C8	0.014 (6)	0.032 (9)	0.022 (9)	0.004 (6)	0.001 (5)	-0.002 (7)
C9	0.021 (7)	0.022 (9)	0.027 (9)	-0.009 (6)	0.012 (6)	0.003 (7)
C10	0.018 (6)	0.019 (8)	0.011 (8)	0.000 (5)	-0.003 (5)	0.005 (6)
N1	0.023 (5)	0.013 (5)	0.029 (6)	-0.004 (4)	0.005 (4)	0.004 (4)
N2	0.029 (7)	0.037 (8)	0.022 (8)	-0.015 (6)	-0.003 (5)	0.006 (6)
N3	0.029 (7)	0.008 (7)	0.022 (7)	-0.001 (5)	0.005 (5)	0.000 (5)
C11	0.018 (5)	0.020 (6)	0.022 (6)	-0.005 (4)	0.001 (4)	-0.002 (4)
C12	0.022 (5)	0.024 (6)	0.007 (6)	-0.002 (4)	0.000 (4)	0.003 (4)
C13	0.020 (5)	0.024 (6)	0.007 (6)	-0.003 (4)	0.000 (4)	0.002 (4)
C14	0.017 (6)	0.020 (8)	0.029 (9)	-0.005 (6)	0.011 (6)	-0.004 (6)
C15	0.023 (7)	0.026 (9)	0.017 (9)	0.001 (6)	0.003 (6)	0.005 (6)
C16	0.018 (5)	0.021 (6)	0.022 (6)	-0.004 (4)	0.001 (4)	-0.002 (4)
F5	0.029 (4)	0.018 (5)	0.028 (5)	-0.002 (4)	-0.001 (4)	0.006 (4)
F6	0.027 (4)	0.035 (6)	0.040 (6)	-0.018 (4)	0.002 (4)	0.016 (4)
F7	0.037 (5)	0.039 (6)	0.033 (6)	-0.006 (4)	-0.010 (4)	0.018 (5)
F8	0.017 (4)	0.044 (6)	0.027 (6)	-0.005 (4)	-0.003 (4)	0.002 (4)
I3	0.0265 (5)	0.0273 (6)	0.0251 (6)	-0.0133 (4)	0.0016 (4)	0.0003 (5)
I4	0.0168 (4)	0.0233 (6)	0.0242 (6)	-0.0049 (4)	0.0021 (3)	-0.0007 (4)

C17	0.034 (9)	0.018 (9)	0.027 (9)	0.013 (6)	0.012 (7)	0.004 (7)
C18	0.015 (6)	0.027 (9)	0.012 (8)	-0.008 (6)	-0.001 (5)	-0.007 (6)
C19	0.024 (7)	0.023 (9)	0.025 (9)	0.001 (6)	0.006 (6)	0.007 (7)
C20	0.035 (8)	0.022 (9)	0.007 (8)	0.001 (6)	0.005 (6)	0.001 (6)
N4	0.023 (7)	0.034 (9)	0.020 (8)	0.003 (6)	-0.003 (5)	-0.001 (6)
N5	0.034 (7)	0.026 (8)	0.037 (9)	0.010 (6)	-0.003 (6)	-0.009 (7)
N6	0.021 (6)	0.022 (7)	0.021 (7)	-0.004 (5)	0.008 (5)	-0.007 (6)
C21	0.024 (7)	0.026 (9)	0.020 (9)	0.011 (6)	0.010 (6)	0.005 (7)
C22	0.023 (5)	0.016 (6)	0.015 (6)	-0.004 (4)	0.009 (4)	0.002 (4)
C23	0.024 (5)	0.015 (6)	0.015 (6)	-0.005 (4)	0.008 (4)	0.003 (4)
C24	0.025 (7)	0.023 (9)	0.018 (9)	0.009 (6)	0.007 (6)	0.010 (6)
C25	0.028 (8)	0.032 (10)	0.014 (9)	-0.003 (7)	0.006 (6)	-0.005 (7)
C26	0.042 (9)	0.024 (10)	0.010 (8)	0.005 (7)	0.013 (6)	0.002 (7)
F9	0.023 (4)	0.036 (6)	0.023 (5)	0.005 (4)	-0.005 (3)	-0.006 (4)
F10	0.024 (4)	0.031 (5)	0.032 (6)	0.014 (4)	-0.004 (3)	0.001 (4)
F11	0.038 (5)	0.045 (6)	0.022 (6)	-0.003 (4)	-0.005 (4)	-0.011 (4)
F12	0.056 (6)	0.023 (6)	0.034 (6)	0.000 (4)	0.014 (5)	-0.014 (4)
I5	0.0382 (6)	0.0327 (7)	0.0459 (8)	0.0173 (5)	0.0170 (5)	0.0014 (5)
I6	0.0247 (4)	0.0183 (5)	0.0227 (6)	0.0026 (4)	0.0052 (4)	-0.0017 (4)
C32	0.020 (6)	0.029 (7)	0.019 (7)	-0.002 (5)	0.004 (5)	-0.001 (5)
C27	0.012 (5)	0.025 (7)	0.012 (6)	0.007 (4)	0.002 (4)	0.003 (5)
C28	0.009 (5)	0.014 (7)	0.021 (7)	0.000 (4)	0.000 (4)	0.001 (5)
C29	0.013 (5)	0.010 (6)	0.023 (7)	0.002 (4)	0.002 (4)	0.003 (5)
C30	0.017 (5)	0.029 (7)	0.028 (7)	0.006 (5)	0.005 (5)	-0.010 (5)
C31	0.018 (6)	0.033 (8)	0.018 (7)	0.003 (5)	0.004 (5)	-0.008 (6)
F13	0.023 (4)	0.027 (5)	0.015 (5)	0.006 (3)	-0.004 (3)	-0.009 (4)
F14	0.035 (5)	0.031 (6)	0.039 (6)	0.018 (4)	0.000 (4)	-0.016 (4)
F15	0.042 (5)	0.053 (7)	0.036 (7)	0.015 (5)	-0.005 (4)	-0.024 (5)
F16	0.020 (4)	0.037 (6)	0.034 (6)	0.013 (4)	-0.009 (4)	-0.004 (4)
I7	0.0246 (5)	0.0249 (6)	0.0275 (6)	0.0113 (4)	0.0018 (4)	-0.0007 (4)
I8	0.0158 (4)	0.0226 (6)	0.0218 (5)	0.0051 (4)	0.0012 (3)	0.0003 (4)

Geometric parameters (Å, °)

C1—C2	1.377 (18)	C17—H17	0.9300
C1—C6	1.330 (19)	C17—N4	1.339 (19)
C1—I1	2.108 (14)	C17—N6	1.309 (19)
C2—C3	1.391 (19)	C18—H18	0.9300
C2—F1	1.367 (15)	C18—C19	1.38 (2)
C3—C4	1.39 (2)	C18—N4	1.337 (17)
C3—I2	2.071 (13)	C19—C20	1.378 (18)
C4—C5	1.38 (2)	C19—N5	1.383 (16)
C4—F2	1.332 (17)	C20—H20	0.9300
C5—C6	1.40 (2)	C20—N6	1.340 (17)
C5—F3	1.346 (16)	N5—H5A	0.8669
C6—F4	1.343 (15)	N5—H5B	0.8685
C7—H7	0.9300	C21—C22	1.37 (2)
C7—N1	1.341 (18)	C21—C26	1.369 (19)
C7—N3	1.329 (17)	C21—I5	2.093 (13)
C8—H8	0.9300	C22—C23	1.396 (18)
C8—C9	1.39 (2)	C22—F9	1.369 (15)
C8—N3	1.321 (17)	C23—C24	1.340 (18)
C9—C10	1.398 (17)	C23—I6	2.109 (14)
C9—N2	1.373 (15)	C24—C25	1.38 (2)
C10—H10	0.9300	C24—F10	1.370 (14)
C10—N1	1.324 (16)	C25—C26	1.387 (19)
N2—H2A	0.8694	C25—F11	1.321 (15)
N2—H2B	0.8680	C26—F12	1.350 (16)
C11—C12	1.369 (16)	C32—C27	1.3900
C11—C16	1.378 (18)	C32—C31	1.3900
C11—I3	2.082 (12)	C32—F16	1.324 (9)
C12—C13	1.379 (16)	C27—C28	1.3900
C12—F5	1.351 (15)	C27—I7	2.093 (6)
C13—C14	1.345 (17)	C28—C29	1.3900
C13—I4	2.108 (12)	C28—F13	1.326 (10)
C14—C15	1.378 (16)	C29—C30	1.3900
C14—F6	1.375 (14)	C29—I8	2.108 (6)
C15—C16	1.383 (17)	C30—C31	1.3900
C15—F7	1.337 (15)	C30—F14	1.319 (9)
C16—F8	1.350 (15)	C31—F15	1.331 (11)
C2—C1—I1	121.3 (10)	N4—C17—H17	116.0

C6—C1—C2	118.5 (13)	N6—C17—H17	116.0
C6—C1—I1	120.2 (10)	N6—C17—N4	128.1 (13)
C1—C2—C3	123.1 (13)	C19—C18—H18	118.0
F1—C2—C1	119.7 (13)	N4—C18—H18	118.0
F1—C2—C3	117.1 (12)	N4—C18—C19	123.9 (12)
C2—C3—C4	117.3 (12)	C18—C19—N5	122.8 (12)
C2—C3—I2	122.7 (10)	C20—C19—C18	114.0 (12)
C4—C3—I2	120.0 (11)	C20—C19—N5	123.2 (14)
C5—C4—C3	119.7 (14)	C19—C20—H20	117.5
F2—C4—C3	121.5 (14)	N6—C20—C19	125.0 (14)
F2—C4—C5	118.7 (14)	N6—C20—H20	117.5
C4—C5—C6	119.9 (14)	C18—N4—C17	114.7 (13)
F3—C5—C4	119.7 (14)	C19—N5—H5A	108.4
F3—C5—C6	120.3 (13)	C19—N5—H5B	110.7
C1—C6—C5	121.4 (13)	H5A—N5—H5B	108.2
C1—C6—F4	122.4 (14)	C17—N6—C20	114.2 (12)
F4—C6—C5	116.2 (13)	C22—C21—I5	120.5 (11)
N1—C7—H7	117.5	C26—C21—C22	118.6 (12)
N3—C7—H7	117.5	C26—C21—I5	120.9 (11)
N3—C7—N1	124.9 (12)	C21—C22—C23	121.7 (13)
C9—C8—H8	118.3	F9—C22—C21	119.9 (12)
N3—C8—H8	118.3	F9—C22—C23	118.4 (12)
N3—C8—C9	123.4 (12)	C22—C23—I6	121.8 (10)
C8—C9—C10	115.5 (11)	C24—C23—C22	116.9 (13)
N2—C9—C8	123.0 (12)	C24—C23—I6	121.4 (10)
N2—C9—C10	121.5 (13)	C23—C24—C25	124.5 (13)
C9—C10—H10	119.3	C23—C24—F10	120.2 (13)
N1—C10—C9	121.3 (13)	F10—C24—C25	115.3 (12)
N1—C10—H10	119.3	C24—C25—C26	116.6 (14)
C10—N1—C7	118.1 (12)	F11—C25—C24	122.2 (13)
C9—N2—H2A	111.0	F11—C25—C26	121.2 (14)
C9—N2—H2B	108.4	C21—C26—C25	121.7 (14)
H2A—N2—H2B	108.5	F12—C26—C21	120.5 (13)
C8—N3—C7	116.6 (13)	F12—C26—C25	117.8 (14)
C12—C11—C16	117.2 (12)	C27—C32—C31	120.0
C12—C11—I3	121.8 (10)	F16—C32—C27	120.8 (7)
C16—C11—I3	121.0 (9)	F16—C32—C31	119.2 (7)
C11—C12—C13	123.6 (12)	C32—C27—C28	120.0
F5—C12—C11	118.4 (12)	C32—C27—I7	119.6 (5)

F5—C12—C13	117.9 (11)	C28—C27—I7	120.4 (5)
C12—C13—I4	121.6 (9)	C27—C28—C29	120.0
C14—C13—C12	116.5 (11)	F13—C28—C27	119.7 (6)
C14—C13—I4	122.0 (9)	F13—C28—C29	120.3 (6)
C13—C14—C15	123.7 (12)	C28—C29—I8	120.3 (4)
C13—C14—F6	120.8 (11)	C30—C29—C28	120.0
F6—C14—C15	115.4 (12)	C30—C29—I8	119.7 (4)
C14—C15—C16	117.4 (13)	C29—C30—C31	120.0
F7—C15—C14	121.8 (13)	F14—C30—C29	121.4 (7)
F7—C15—C16	120.8 (12)	F14—C30—C31	118.6 (7)
C11—C16—C15	121.5 (12)	C30—C31—C32	120.0
F8—C16—C11	120.7 (12)	F15—C31—C32	120.1 (7)
F8—C16—C15	117.8 (12)	F15—C31—C30	119.9 (7)

Appendix 6

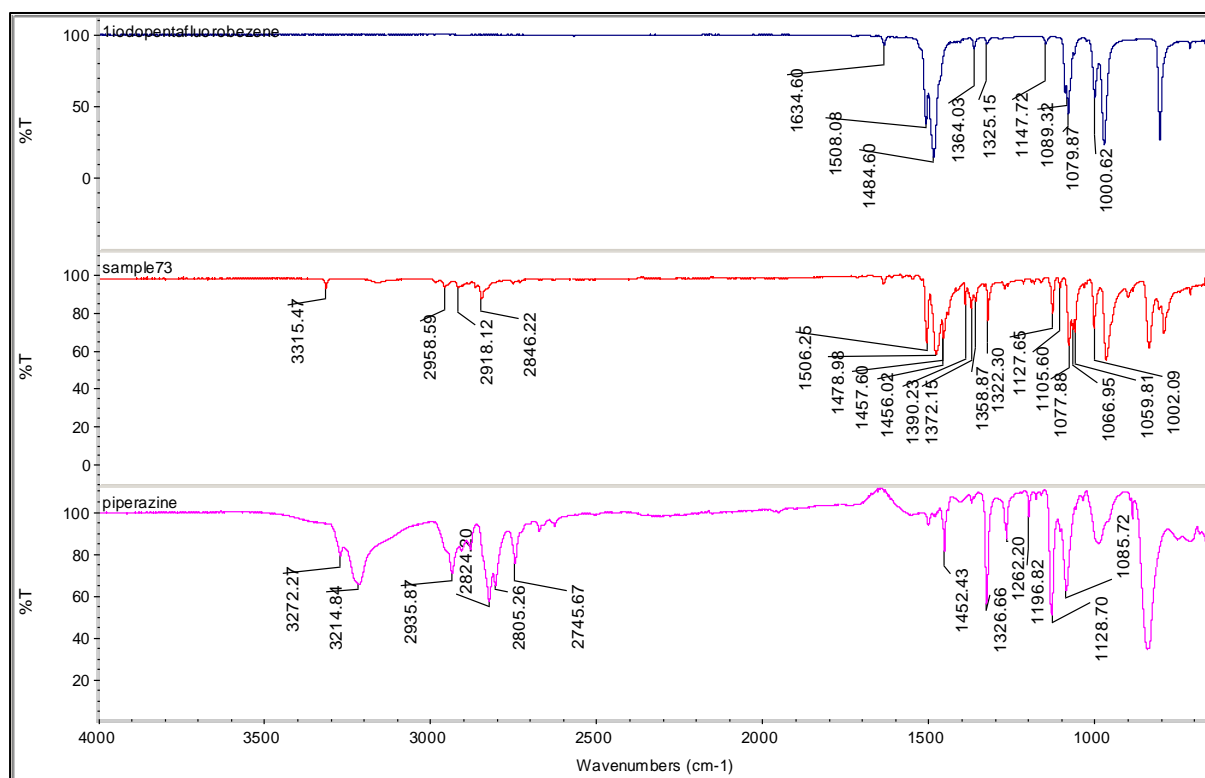
(Supplementary information)

Chapter 6:- Crystallographic and QTAIM studies of variety of halogen bonds containing compounds using piperazine

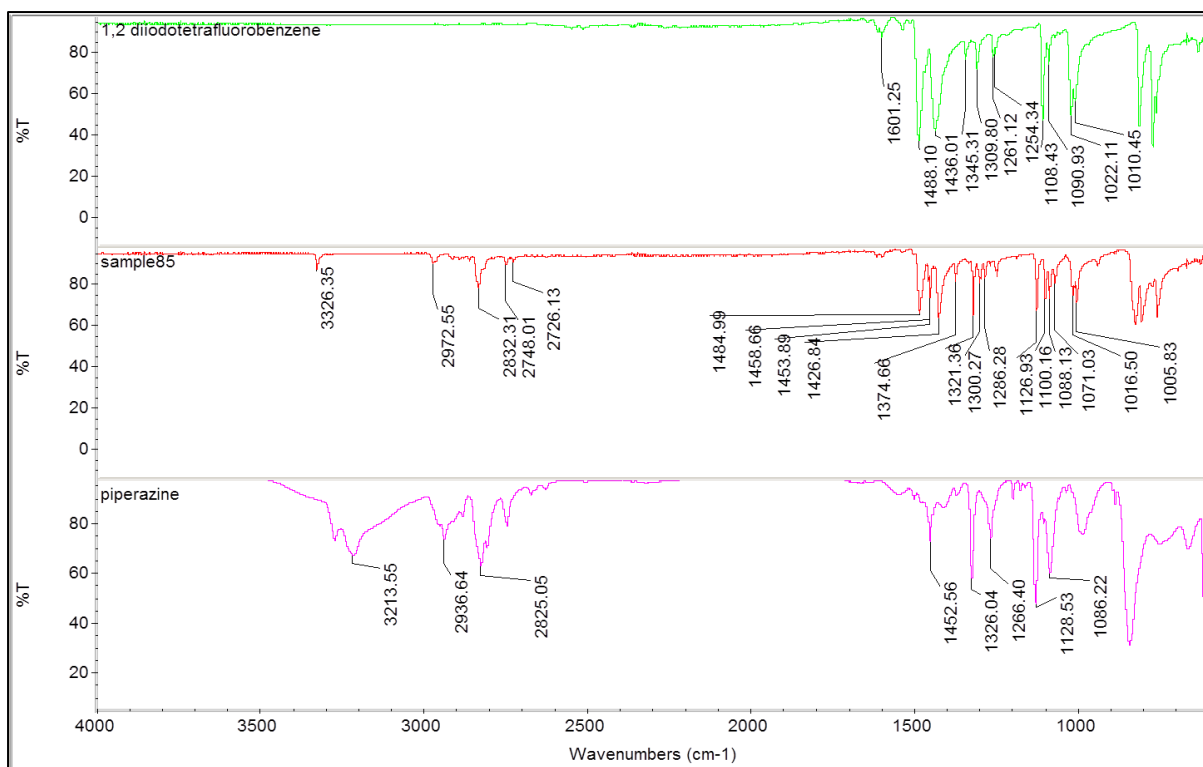
Sultan Alkaabi, Alan K. Brisdon*,

Department of Chemistry, University of Manchester, Oxford Road, Manchester M13 9PL, England.

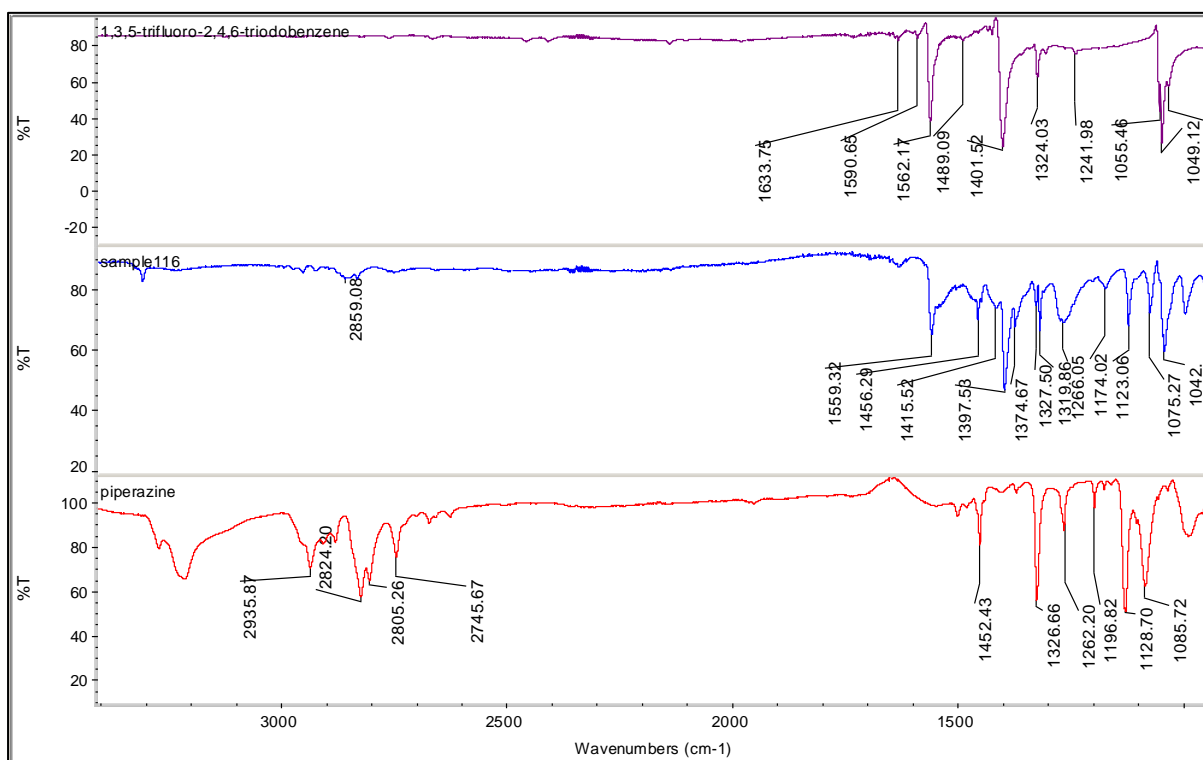
Correspondence email: *alan.brisdon@manchester.ac.uk



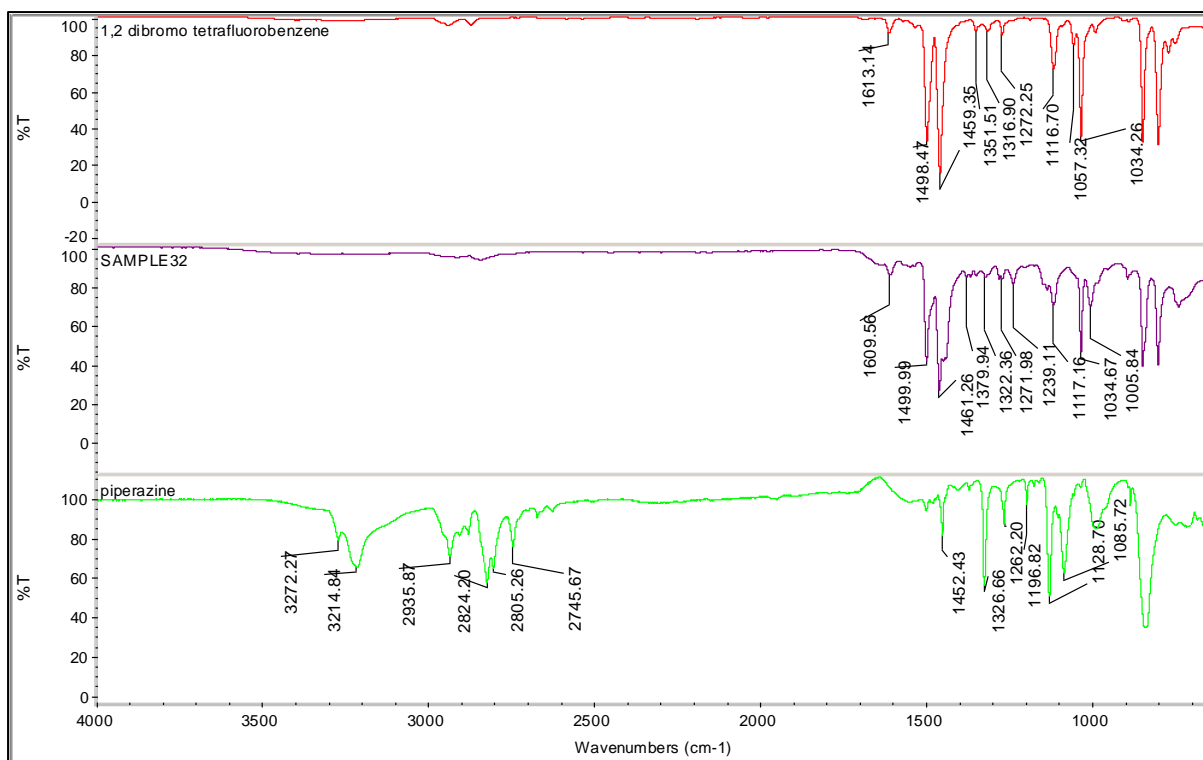
S 6.1 IR spectra showing the two starting materials and adduct **1a**



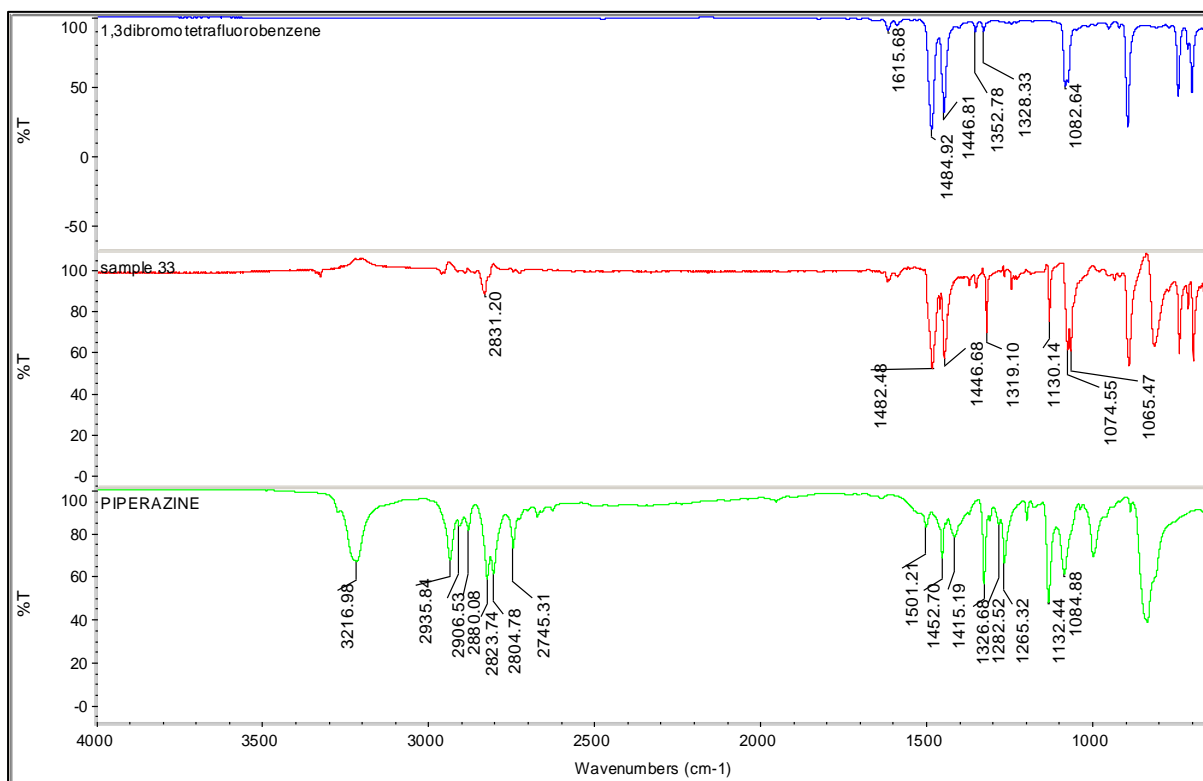
S 6.2 IR spectra showing the two starting materials and adduct **2a**



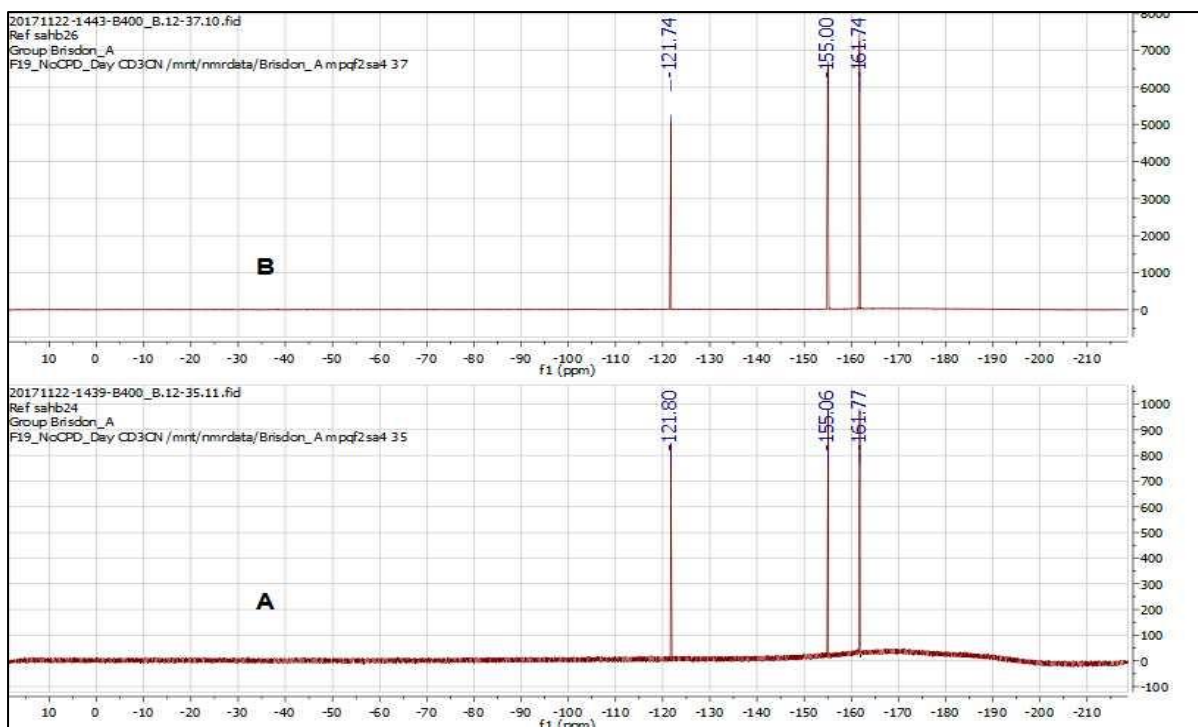
S 6.3 IR spectra showing the two starting materials and **3a**



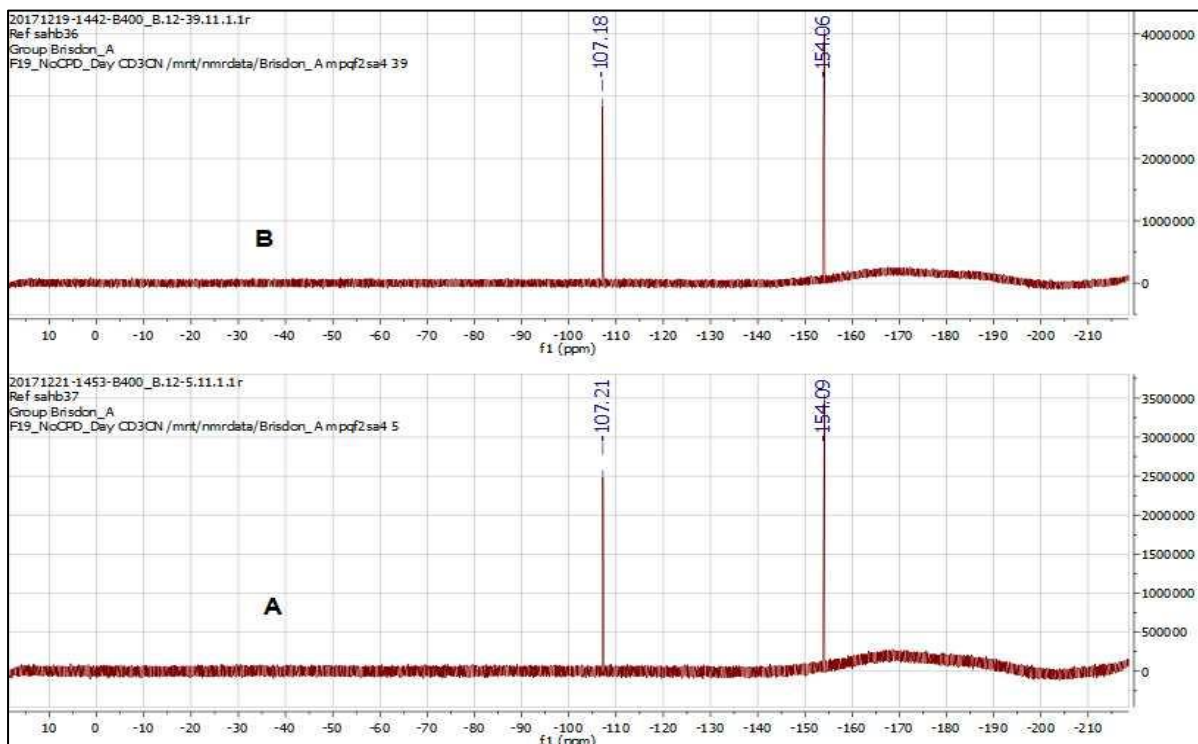
S 6.4 IR spectra showing the two starting materials and **4a**



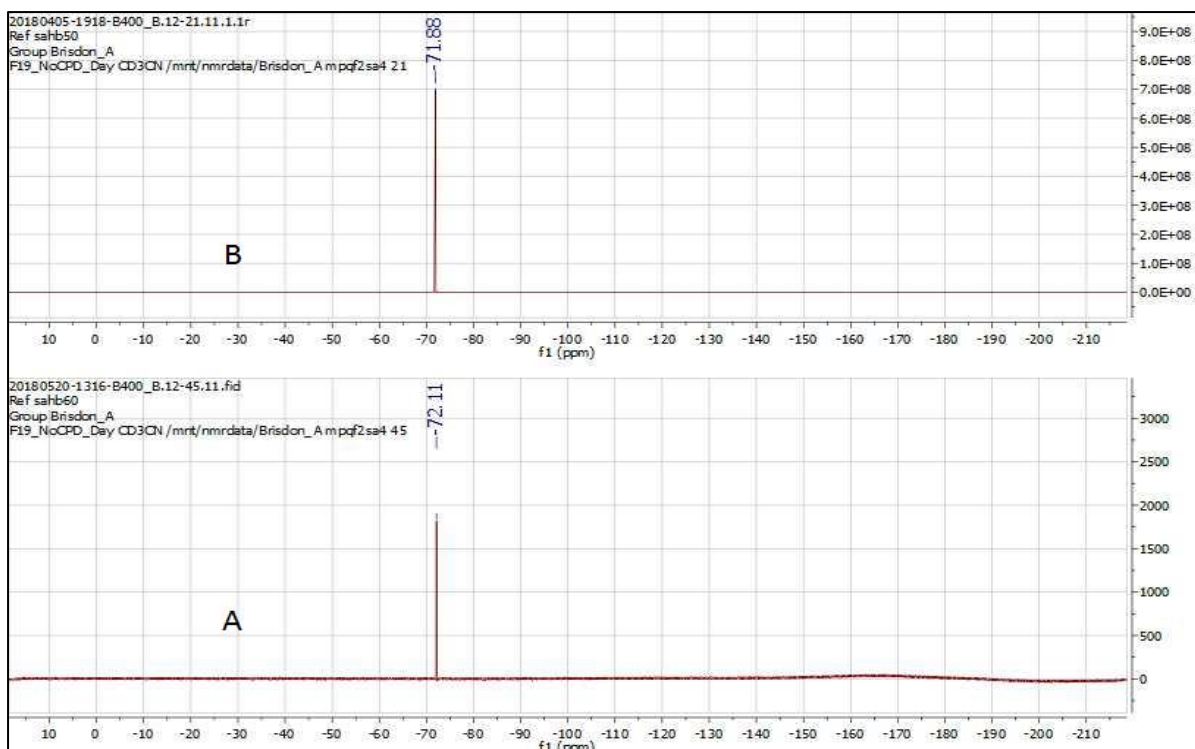
S 6.5 IR spectra showing the two starting materials and **5a**



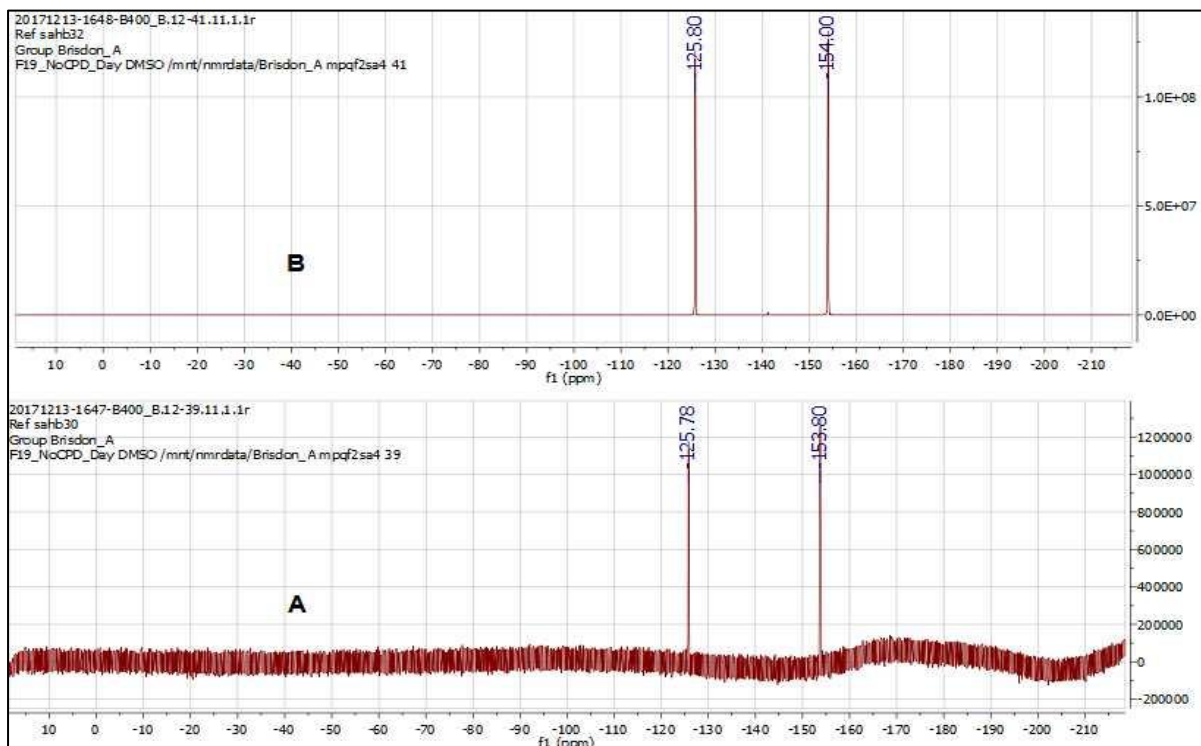
S 6.6 ^{19}F NMR spectra for (A) the adduct **1a** and (B) iodopentafluorobenzene dibromotetrafluorobenzene using in acetonitrile- d_3



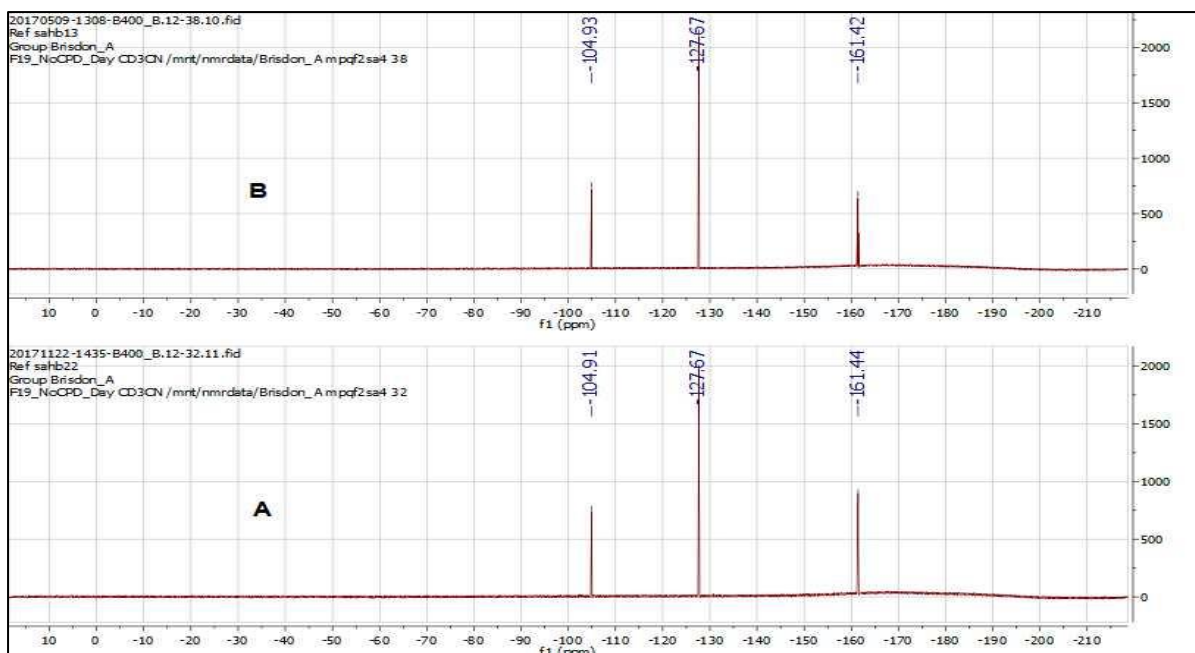
S 6.7 ^{19}F NMR spectra for (A) the adduct, **2a**, and (B) 1,2-diiodotetrafluorobenzene in acetonitrile- d_3



S 6.8 ^{19}F NMR spectra for (A) the adduct, **3a** and (B) 1,3,5-trifluoro-2,4,6-triiodobenzene in acetonitrile- d_3



S 6.9 ^{19}F NMR spectra for (A) the adduct, **4a** and (B) 1,2-dibromotetrafluorobenzene, in DMSO



S 6.10 ^{19}F NMR spectra for (A) the adduct, **5a** and (B) 1,3-dibromotetrafluorobenzene in acetonitrile-d

Computing details

Data collection: *CrysAlis PRO* 1.171.39.46 (Rigaku OD, 2018) for (1a); *CrysAlis PRO* 1.171.38.46 (Rigaku OD, 2015) for (2a, 3a, 4a and 5a); cell refinement: *CrysAlis PRO* 1.171.39.46 (Rigaku OD, 2018) for (1a); *CrysAlis PRO* 1.171.38.46 (Rigaku OD, 2015) for (2a, 3a, 4a and 5a); data reduction: *CrysAlis PRO* 1.171.39.46 (Rigaku OD, 2018) for (1a); *CrysAlis PRO* 1.171.38.46 (Rigaku OD, 2015) for (2a, 3a, 4a and 5a); program(s) used to solve structure: ShelXT (Sheldrick, 2015); program(s) used to refine structure: *SHELXL* (Sheldrick, 2015); molecular graphics: Olex2 (Dolomanov *et al.*, 2009); software used to prepare material for publication: Olex2 (Dolomanov *et al.*, 2009).

Iodofluorobenzene– piperazine (1a)

Crystal data

$\text{C}_6\text{F}_5\text{I}\cdot\text{C}_2\text{H}_5\text{N}$	$F(000) = 632$
$M_r = 337.03$	$D_x = 2.296 \text{ Mg m}^{-3}$
Monoclinic, $P2_1/c$	Mo $K\alpha$ radiation, $\lambda = 0.71073 \text{ \AA}$
$a = 5.3154 (2) \text{ \AA}$	Cell parameters from 2195 reflections
$b = 10.5471 (4) \text{ \AA}$	$\theta = 3.8\text{--}27.7^\circ$
$c = 17.4651 (7) \text{ \AA}$	$\mu = 3.32 \text{ mm}^{-1}$
$\beta = 95.136 (4)^\circ$	$T = 150 \text{ K}$
$V = 975.20 (6) \text{ \AA}^3$	Plate, clear light colourless
$Z = 4$	$0.08 \times 0.06 \times 0.01 \text{ mm}$

Data collection

SuperNova, Single source at offset/far, Eos diffractometer	1918 independent reflections
Radiation source: micro-focus sealed X-ray tube, SuperNova (Mo) X-ray Source	1575 reflections with $I > 2\sigma(I)$
Mirror monochromator	$R_{\text{int}} = 0.050$
Detector resolution: 8.0714 pixels mm^{-1}	$\theta_{\text{max}} = 26.0^\circ$, $\theta_{\text{min}} = 3.0^\circ$
ω scans	$h = -6 \rightarrow 4$
Absorption correction: multi-scan <i>CrysAlis PRO</i> 1.171.39.46 (Rigaku Oxford Diffraction, 2018) Empirical absorption correction using spherical harmonics, implemented in SCALE3 ABSPACK scaling algorithm.	$k = -13 \rightarrow 11$
$T_{\text{min}} = 0.746$, $T_{\text{max}} = 1.000$	$l = -21 \rightarrow 20$
5525 measured reflections	

Refinement

Refinement on F^2	Primary atom site location: dual
Least-squares matrix: full	Hydrogen site location: mixed
$R[F^2 > 2\sigma(F^2)] = 0.035$	H atoms treated by a mixture of independent and constrained refinement
$wR(F^2) = 0.061$	$w = 1/[\sigma^2(F_o^2) + (0.0091P)^2]$ where $P = (F_o^2 + 2F_c^2)/3$
$S = 1.03$	$(\Delta/\sigma)_{\text{max}} = 0.001$
1918 reflections	$\Delta_{\text{max}} = 0.63 \text{ e } \text{\AA}^{-3}$
139 parameters	$\Delta_{\text{min}} = -0.80 \text{ e } \text{\AA}^{-3}$
0 restraints	

Special details

Geometry. All esds (except the esd in the dihedral angle between two l.s. planes) are estimated using the full covariance matrix. The cell esds are taken into account individually in the estimation of esds in distances, angles and torsion angles; correlations between esds in cell parameters are only used when they are defined by crystal symmetry. An approximate (isotropic) treatment of cell esds is used for estimating esds involving l.s. planes.

Fractional atomic coordinates and isotropic or equivalent isotropic displacement parameters
(\AA^2)

	<i>x</i>	<i>y</i>	<i>z</i>	$U_{\text{iso}}^*/U_{\text{eq}}$
I1	0.78998 (6)	0.70705 (3)	0.57092 (2)	0.02181 (11)
F1	0.3611 (5)	0.7297 (2)	0.68966 (15)	0.0288 (7)
F2	0.0752 (5)	0.5564 (2)	0.75463 (15)	0.0309 (7)
F3	0.1369 (5)	0.3063 (2)	0.72597 (16)	0.0342 (7)
F4	0.4957 (6)	0.2284 (2)	0.63434 (17)	0.0333 (8)
F5	0.7746 (5)	0.4008 (3)	0.56637 (16)	0.0321 (7)
N1	1.1175 (8)	0.8800 (4)	0.5108 (2)	0.0214 (9)
H1	1.240 (9)	0.828 (4)	0.507 (3)	0.026*
C1	0.5709 (9)	0.5709 (4)	0.6246 (3)	0.0200 (11)
C2	0.3969 (9)	0.6060 (4)	0.6742 (3)	0.0206 (11)
C3	0.2491 (9)	0.5183 (5)	0.7083 (3)	0.0235 (12)
C4	0.2830 (9)	0.3911 (5)	0.6945 (3)	0.0230 (12)
C5	0.4598 (9)	0.3532 (4)	0.6473 (3)	0.0221 (11)
C6	0.6017 (9)	0.4417 (4)	0.6126 (3)	0.0206 (11)
C7	1.1818 (9)	0.9844 (4)	0.5641 (3)	0.0239 (12)
H7A	1.3226	1.0320	0.5471	0.029*
H7B	1.2324	0.9507	0.6149	0.029*
C8	0.9580 (9)	1.0702 (4)	0.5678 (3)	0.0225 (12)
H8A	0.8189	1.0237	0.5867	0.027*
H8B	1.0012	1.1400	0.6027	0.027*

Atomic displacement parameters (\AA^2)

	U^{11}	U^{22}	U^{33}	U^{12}	U^{13}	U^{23}
I1	0.02237 (19)	0.01808 (18)	0.0247 (2)	-0.00159 (13)	0.00035 (14)	0.00319 (14)
F1	0.0343 (19)	0.0158 (16)	0.0366 (18)	0.0021 (12)	0.0046 (15)	-0.0038 (12)
F2	0.0331 (19)	0.0334 (18)	0.0278 (17)	0.0020 (13)	0.0111 (15)	-0.0016 (13)
F3	0.037 (2)	0.0290 (18)	0.0371 (18)	-0.0081 (13)	0.0074 (15)	0.0067 (14)
F4	0.040 (2)	0.0128 (16)	0.047 (2)	-0.0023 (12)	0.0045 (16)	-0.0034 (13)
F5	0.0303 (18)	0.0268 (17)	0.0413 (19)	-0.0001 (13)	0.0147 (15)	-0.0056 (14)
N1	0.021 (2)	0.014 (2)	0.029 (3)	0.0022 (17)	0.002 (2)	-0.0005 (19)

C1	0.019 (3)	0.019 (3)	0.020 (3)	-0.0023 (19)	-0.008 (2)	0.004 (2)
C2	0.026 (3)	0.015 (3)	0.021 (3)	0.006 (2)	0.000 (2)	-0.003 (2)
C3	0.024 (3)	0.033 (3)	0.014 (3)	0.002 (2)	0.003 (2)	0.001 (2)
C4	0.021 (3)	0.027 (3)	0.020 (3)	-0.012 (2)	0.000 (2)	0.007 (2)
C5	0.026 (3)	0.014 (3)	0.025 (3)	-0.003 (2)	-0.002 (2)	-0.002 (2)
C6	0.022 (3)	0.018 (3)	0.022 (3)	0.001 (2)	0.005 (2)	0.000 (2)
C7	0.024 (3)	0.021 (3)	0.027 (3)	-0.003 (2)	0.000 (2)	0.000 (2)
C8	0.029 (3)	0.018 (3)	0.022 (3)	-0.001 (2)	0.005 (2)	-0.005 (2)

Geometric parameters (Å, °)

I1—C1	2.120 (5)	C1—C2	1.373 (6)
F1—C2	1.350 (5)	C1—C6	1.391 (6)
F2—C3	1.343 (5)	C2—C3	1.383 (6)
F3—C4	1.335 (5)	C3—C4	1.378 (6)
F4—C5	1.352 (5)	C4—C5	1.364 (6)
F5—C6	1.348 (5)	C5—C6	1.374 (6)
N1—C7	1.462 (6)	C7—C8	1.501 (6)
N1—C8 ⁱ	1.491 (6)	C8—N1 ⁱ	1.491 (6)
C7—N1—C8 ⁱ	110.5 (4)	F3—C4—C5	120.7 (4)
C2—C1—I1	121.6 (3)	C5—C4—C3	119.9 (4)
C2—C1—C6	117.0 (4)	F4—C5—C4	120.0 (4)
C6—C1—I1	121.3 (4)	F4—C5—C6	119.8 (4)
F1—C2—C1	120.1 (4)	C4—C5—C6	120.2 (4)
F1—C2—C3	117.7 (4)	F5—C6—C1	120.0 (4)
C1—C2—C3	122.2 (4)	F5—C6—C5	118.5 (4)
F2—C3—C2	120.5 (4)	C5—C6—C1	121.5 (4)
F2—C3—C4	120.3 (4)	N1—C7—C8	109.9 (4)
C4—C3—C2	119.2 (5)	N1 ⁱ —C8—C7	108.8 (4)
F3—C4—C3	119.3 (4)		

Symmetry code: (i) $-x+2, -y+2, -z+1$.

1,2-diiodotetrafluorobenzene– piperazine(2a)

Crystal data

$C_3F_2I \cdot C_2H_5N$	$F(000) = 452$
$M_r = 244.00$	$D_x = 2.486 \text{ Mg m}^{-3}$
Monoclinic, $P12_1/m1$	Mo $K\alpha$ radiation, $\lambda = 0.71073 \text{ \AA}$
$a = 5.2637 (6) \text{ \AA}$	Cell parameters from 1732 reflections
$b = 20.651 (3) \text{ \AA}$	$\theta = 3.4\text{--}27.8^\circ$
$c = 6.1156 (7) \text{ \AA}$	$\mu = 4.86 \text{ mm}^{-1}$
$\beta = 101.244 (11)^\circ$	$T = 150 \text{ K}$
$V = 652.01 (14) \text{ \AA}^3$	Plate, clear light colourless
$Z = 4$	$0.28 \times 0.02 \times 0.01 \text{ mm}$

Data collection

SuperNova, Single source at offset, Eos diffractometer	1303 independent reflections
Radiation source: micro-focus sealed X-ray tube, SuperNova (Mo) X-ray Source	1156 reflections with $I > 2\sigma(I)$
Mirror monochromator	$R_{\text{int}} = 0.031$
Detector resolution: $8.0714 \text{ pixels mm}^{-1}$	$\theta_{\text{max}} = 26.0^\circ$, $\theta_{\text{min}} = 3.4^\circ$
ω scans	$h = -6 \rightarrow 6$
Absorption correction: multi-scan <i>CrysAlis PRO</i> 1.171.38.46 (Rigaku Oxford Diffraction, 2015) Empirical absorption correction using spherical harmonics, implemented in SCALE3 ABSPACK scaling algorithm.	$k = -25 \rightarrow 23$
$T_{\text{min}} = 0.723$, $T_{\text{max}} = 1.000$	$l = -7 \rightarrow 7$
2520 measured reflections	

Refinement

Refinement on F^2	Primary atom site location: dual
Least-squares matrix: full	Hydrogen site location: mixed
$R[F^2 > 2\sigma(F^2)] = 0.033$	H atoms treated by a mixture of independent and constrained refinement
$wR(F^2) = 0.092$	$w = 1/[\sigma^2(F_o^2) + (0.0456P)^2 + 0.4181P]$ where $P = (F_o^2 + 2F_c^2)/3$
$S = 1.09$	$(\Delta/\sigma)_{\text{max}} = 0.001$
1303 reflections	$\Delta_{\text{max}} = 1.41 \text{ e \AA}^{-3}$
85 parameters	$\Delta_{\text{min}} = -0.69 \text{ e \AA}^{-3}$
0 restraints	

Special details

Geometry. All esds (except the esd in the dihedral angle between two l.s. planes) are estimated using the full covariance matrix. The cell esds are taken into account individually in the estimation of esds in distances, angles and torsion angles; correlations between esds in cell parameters are only used when they are defined by crystal symmetry. An approximate (isotropic) treatment of cell esds is used for estimating esds involving l.s. planes.

Fractional atomic coordinates and isotropic or equivalent isotropic displacement parameters (\AA^2)

	x	y	z	$U_{\text{iso}}^*/U_{\text{eq}}$
I1	1.34028 (7)	0.65670 (2)	-0.28107 (6)	0.01772 (17)
F1	0.9979 (6)	0.61889 (16)	0.0577 (6)	0.0235 (8)
F2	0.7265 (7)	0.68448 (18)	0.3115 (5)	0.0246 (8)
C1	1.1410 (10)	0.7165 (3)	-0.0897 (8)	0.0146 (11)
C2	1.0037 (11)	0.6833 (3)	0.0506 (9)	0.0179 (12)
C3	0.8653 (10)	0.7170 (3)	0.1828 (8)	0.0170 (11)
N1	0.6398 (9)	0.5592 (2)	-0.4724 (8)	0.0192 (11)
H1	0.750 (12)	0.579 (3)	-0.475 (11)	0.023*
C4	0.5320 (11)	0.5338 (3)	-0.6961 (9)	0.0216 (13)
H4A	0.6599	0.5070	-0.7474	0.026*
H4B	0.4881	0.5694	-0.8000	0.026*
C5	0.7068 (11)	0.5057 (3)	-0.3124 (9)	0.0195 (12)
H5A	0.7773	0.5229	-0.1656	0.023*
H5B	0.8375	0.4784	-0.3576	0.023*

Atomic displacement parameters (\AA^2)

	U^{11}	U^{22}	U^{33}	U^{12}	U^{13}	U^{23}
I1	0.0176 (3)	0.0186 (3)	0.0170 (2)	0.00138 (14)	0.00373 (16)	-0.00300 (14)
F1	0.0283 (19)	0.0135 (17)	0.0313 (19)	0.0013 (14)	0.0118 (15)	0.0016 (15)
F2	0.0296 (19)	0.0226 (19)	0.0248 (18)	-0.0001 (16)	0.0131 (15)	0.0053 (15)
C1	0.014 (3)	0.019 (3)	0.011 (2)	0.001 (2)	0.003 (2)	-0.003 (2)
C2	0.022 (3)	0.010 (3)	0.020 (3)	-0.001 (2)	0.001 (2)	0.000 (2)
C3	0.017 (3)	0.023 (3)	0.011 (2)	0.000 (2)	0.002 (2)	0.002 (2)
N1	0.019 (3)	0.017 (3)	0.023 (2)	-0.003 (2)	0.008 (2)	0.002 (2)
C4	0.026 (3)	0.024 (3)	0.016 (3)	0.004 (3)	0.009 (2)	0.001 (2)
C5	0.020 (3)	0.018 (3)	0.019 (3)	-0.003 (2)	0.000 (2)	-0.001 (2)

Geometric parameters (Å, °)

I1—C1	2.114 (5)	C3—C3 ⁱ	1.364 (12)
F1—C2	1.332 (7)	N1—C4	1.471 (7)
F2—C3	1.352 (6)	N1—C5	1.474 (7)
C1—C1 ⁱ	1.386 (11)	C4—C5 ⁱⁱ	1.508 (8)
C1—C2	1.403 (8)	C5—C4 ⁱⁱ	1.508 (8)
C2—C3	1.377 (8)		
C1 ⁱ —C1—I1	125.70 (14)	F2—C3—C2	120.0 (5)
C1 ⁱ —C1—C2	119.2 (3)	F2—C3—C3 ⁱ	119.8 (3)
C2—C1—I1	115.1 (4)	C3 ⁱ —C3—C2	120.3 (3)
F1—C2—C1	121.6 (5)	C4—N1—C5	110.4 (5)
F1—C2—C3	117.8 (5)	N1—C4—C5 ⁱⁱ	109.5 (4)
C3—C2—C1	120.5 (5)	N1—C5—C4 ⁱⁱ	109.6 (5)

Symmetry codes: (i) $x, -y+3/2, z$; (ii) $-x+1, -y+1, -z-1$.

1,3,4-trifluoro-2,4,6-triiodobenzene– piperazine(3a)

Crystal data

C ₆ F ₃ I ₃ ·C ₂ H ₅ N	Z = 2
$M_r = 552.83$	$F(000) = 492$
Triclinic, $P\bar{1}$	$D_x = 3.079 \text{ Mg m}^{-3}$
$a = 8.6231 (9) \text{ \AA}$	Mo $K\alpha$ radiation, $\lambda = 0.71073 \text{ \AA}$
$b = 9.1223 (11) \text{ \AA}$	Cell parameters from 1899 reflections
$c = 9.3224 (9) \text{ \AA}$	$\theta = 3.3\text{--}28.1^\circ$
$\alpha = 67.187 (10)^\circ$	$\mu = 7.87 \text{ mm}^{-1}$
$\beta = 72.699 (9)^\circ$	$T = 150 \text{ K}$
$\gamma = 63.128 (11)^\circ$	Irregular, clear light colourless
$V = 596.28 (13) \text{ \AA}^3$	$0.05 \times 0.03 \times 0.01 \text{ mm}$

Data collection

SuperNova, Single source at offset, Eos diffractometer	2342 independent reflections
Radiation source: micro-focus sealed X-ray tube, SuperNova (Mo) X-ray Source	1952 reflections with $I > 2\sigma(I)$
Mirror monochromator	$R_{\text{int}} = 0.047$
Detector resolution: 8.0714 pixels mm^{-1}	$\theta_{\text{max}} = 26.0^\circ$, $\theta_{\text{min}} = 3.0^\circ$
ω scans	$h = -10 \rightarrow 10$
Absorption correction: multi-scan <i>CrysAlis PRO</i> 1.171.38.46 (Rigaku Oxford Diffraction, 2015) Empirical absorption correction using spherical harmonics, implemented in SCALE3 ABSPACK scaling algorithm.	$k = -11 \rightarrow 9$
$T_{\text{min}} = 0.883$, $T_{\text{max}} = 1.000$	$l = -11 \rightarrow 11$
4283 measured reflections	

Refinement

Refinement on F^2	Primary atom site location: dual
Least-squares matrix: full	Hydrogen site location: mixed
$R[F^2 > 2\sigma(F^2)] = 0.042$	H atoms treated by a mixture of independent and constrained refinement
$wR(F^2) = 0.078$	$w = 1/[\sigma^2(F_o^2) + (0.0132P)^2]$ where $P = (F_o^2 + 2F_c^2)/3$
$S = 0.99$	$(\Delta/\sigma)_{\text{max}} = 0.001$
2342 reflections	$\Delta_{\text{max}} = 0.97 \text{ e } \text{\AA}^{-3}$
139 parameters	$\Delta_{\text{min}} = -1.41 \text{ e } \text{\AA}^{-3}$
0 restraints	

Special details

Geometry. All esds (except the esd in the dihedral angle between two l.s. planes) are estimated using the full covariance matrix. The cell esds are taken into account individually in the estimation of esds in distances, angles and torsion angles; correlations between esds in cell parameters are only used when they are defined by crystal symmetry. An approximate (isotropic) treatment of cell esds is used for estimating esds involving l.s. planes.

Fractional atomic coordinates and isotropic or equivalent isotropic displacement parameters
(\AA^2)

	<i>x</i>	<i>y</i>	<i>z</i>	$U_{\text{iso}}^*/U_{\text{eq}}$
I1	0.82567 (7)	0.38442 (7)	0.70161 (6)	0.01802 (15)
I2	0.69893 (7)	0.60882 (8)	0.02429 (6)	0.02227 (16)
I3	0.22594 (7)	1.04894 (7)	0.44503 (6)	0.02104 (16)
F1	0.8612 (6)	0.3909 (6)	0.3456 (5)	0.0255 (12)
F2	0.4103 (6)	0.9173 (6)	0.1484 (5)	0.0227 (12)
F3	0.4839 (6)	0.7327 (6)	0.6762 (5)	0.0224 (11)
C1	0.6814 (9)	0.5608 (10)	0.5125 (8)	0.0115 (17)
C2	0.7256 (10)	0.5351 (10)	0.3677 (9)	0.0158 (18)
C3	0.6362 (10)	0.6529 (11)	0.2443 (8)	0.0149 (18)
C4	0.4977 (10)	0.7979 (11)	0.2695 (9)	0.0186 (19)
C5	0.4405 (9)	0.8315 (11)	0.4137 (9)	0.0167 (18)
C6	0.5368 (10)	0.7069 (11)	0.5336 (8)	0.0166 (19)
N1	1.0237 (9)	0.1576 (10)	0.9483 (8)	0.0242 (18)
H1	1.095 (11)	0.210 (12)	0.940 (9)	0.029*
C7	1.1577 (10)	0.0069 (11)	0.8966 (9)	0.0186 (19)
H7A	1.2438	-0.0611	0.9683	0.022*
H7B	1.2182	0.0459	0.7924	0.022*
C8	0.9294 (11)	0.1011 (11)	1.1064 (9)	0.022 (2)
H8A	0.8418	0.2007	1.1384	0.026*
H8B	1.0115	0.0349	1.1819	0.026*

Atomic displacement parameters (\AA^2)

	U^{11}	U^{22}	U^{33}	U^{12}	U^{13}	U^{23}
I1	0.0197 (3)	0.0171 (3)	0.0156 (3)	-0.0055 (2)	-0.0067 (2)	-0.0021 (2)
I2	0.0279 (3)	0.0222 (3)	0.0161 (3)	-0.0065 (3)	-0.0038 (2)	-0.0085 (2)
I3	0.0176 (3)	0.0205 (3)	0.0213 (3)	-0.0022 (2)	-0.0031 (2)	-0.0084 (2)
F1	0.025 (3)	0.022 (3)	0.023 (3)	0.001 (2)	-0.004 (2)	-0.011 (2)
F2	0.026 (3)	0.018 (3)	0.017 (2)	-0.003 (2)	-0.014 (2)	0.002 (2)
F3	0.022 (2)	0.029 (3)	0.014 (2)	-0.006 (2)	-0.0032 (19)	-0.008 (2)
C1	0.015 (4)	0.011 (4)	0.012 (4)	-0.009 (3)	0.000 (3)	-0.003 (3)
C2	0.021 (4)	0.009 (4)	0.019 (4)	-0.003 (4)	-0.008 (4)	-0.006 (4)
C3	0.021 (4)	0.015 (4)	0.013 (4)	-0.009 (4)	-0.003 (3)	-0.004 (4)
C4	0.022 (4)	0.013 (5)	0.018 (4)	-0.008 (4)	-0.009 (4)	0.005 (4)
C5	0.012 (4)	0.017 (5)	0.022 (4)	-0.006 (4)	-0.004 (3)	-0.005 (4)
C6	0.023 (4)	0.019 (5)	0.011 (4)	-0.010 (4)	-0.002 (3)	-0.007 (4)

N1	0.028 (4)	0.025 (5)	0.022 (4)	-0.011 (4)	-0.002 (3)	-0.009 (4)
C7	0.014 (4)	0.023 (5)	0.016 (4)	-0.002 (4)	-0.003 (3)	-0.008 (4)
C8	0.028 (5)	0.014 (5)	0.018 (4)	-0.004 (4)	-0.006 (4)	-0.002 (4)

Geometric parameters (Å, °)

I1—C1	2.131 (7)	C5—C6	1.395 (10)
I2—C3	2.108 (7)	N1—H1	0.91 (8)
I3—C5	2.062 (8)	N1—C7	1.484 (11)
F1—C2	1.348 (9)	N1—C8	1.475 (10)
F2—C4	1.356 (8)	C7—H7A	0.9700
F3—C6	1.347 (8)	C7—H7B	0.9700
C1—C2	1.372 (10)	C7—C8 ⁱ	1.496 (11)
C1—C6	1.387 (11)	C8—C7 ⁱ	1.496 (11)
C2—C3	1.375 (9)	C8—H8A	0.9700
C3—C4	1.370 (11)	C8—H8B	0.9700
C4—C5	1.391 (11)		
C2—C1—I1	122.1 (6)	C1—C6—C5	123.4 (7)
C2—C1—C6	117.7 (7)	C7—N1—H1	99 (6)
C6—C1—I1	120.2 (5)	C8—N1—H1	117 (5)
F1—C2—C1	119.0 (6)	C8—N1—C7	110.6 (7)
F1—C2—C3	119.2 (7)	N1—C7—H7A	109.7
C1—C2—C3	121.8 (7)	N1—C7—H7B	109.7
C2—C3—I2	121.7 (6)	N1—C7—C8 ⁱ	109.7 (7)
C4—C3—I2	119.9 (5)	H7A—C7—H7B	108.2
C4—C3—C2	118.3 (7)	C8 ⁱ —C7—H7A	109.7
F2—C4—C3	119.2 (7)	C8 ⁱ —C7—H7B	109.7
F2—C4—C5	117.2 (7)	N1—C8—C7 ⁱ	109.4 (7)
C3—C4—C5	123.6 (7)	N1—C8—H8A	109.8
C4—C5—I3	121.6 (5)	N1—C8—H8B	109.8
C4—C5—C6	115.1 (7)	C7 ⁱ —C8—H8A	109.8
C6—C5—I3	123.3 (6)	C7 ⁱ —C8—H8B	109.8
F3—C6—C1	119.6 (6)	H8A—C8—H8B	108.2
F3—C6—C5	117.1 (7)		

Symmetry code: (i) $-x+2, -y, -z+2$.

1,2-dibromotetrafluorobenzene– piperazine(4a)

Crystal data

Br ₂ C ₆ F ₄ ·C ₂ H ₅ N	Z = 2
$M_r = 350.95$	$F(000) = 332$
Triclinic, $P\bar{1}$	$D_x = 2.362 \text{ Mg m}^{-3}$
$a = 5.1117 (6) \text{ \AA}$	Mo $K\alpha$ radiation, $\lambda = 0.71073 \text{ \AA}$
$b = 5.9696 (9) \text{ \AA}$	Cell parameters from 1113 reflections
$c = 16.3344 (18) \text{ \AA}$	$\theta = 3.5\text{--}25.5^\circ$
$\alpha = 90.915 (10)^\circ$	$\mu = 8.24 \text{ mm}^{-1}$
$\beta = 90.677 (9)^\circ$	$T = 150 \text{ K}$
$\gamma = 98.075 (11)^\circ$	Irregular, clear light orange
$V = 493.39 (11) \text{ \AA}^3$	$0.1 \times 0.05 \times 0.02 \text{ mm}$

Data collection

SuperNova, Single source at offset, Eos diffractometer	1938 independent reflections
Radiation source: micro-focus sealed X-ray tube, SuperNova (Mo) X-ray Source	1437 reflections with $I > 2\sigma(I)$
Mirror monochromator	$R_{\text{int}} = 0.069$
Detector resolution: $8.0714 \text{ pixels mm}^{-1}$	$\theta_{\text{max}} = 26.0^\circ$, $\theta_{\text{min}} = 3.5^\circ$
ω scans	$h = -5 \rightarrow 6$
Absorption correction: multi-scan <i>CrysAlis PRO</i> 1.171.38.46 (Rigaku Oxford Diffraction, 2015) Empirical absorption correction using spherical harmonics, implemented in SCALE3 ABSPACK scaling algorithm.	$k = -7 \rightarrow 5$
$T_{\text{min}} = 0.441$, $T_{\text{max}} = 1.000$	$l = -19 \rightarrow 20$
3471 measured reflections	

Refinement

Refinement on F^2	Primary atom site location: dual
Least-squares matrix: full	Hydrogen site location: mixed
$R[F^2 > 2\sigma(F^2)] = 0.058$	H atoms treated by a mixture of independent and constrained refinement
$wR(F^2) = 0.110$	$w = 1/[\sigma^2(F_o^2) + (0.0188P)^2]$ where $P = (F_o^2 + 2F_c^2)/3$
$S = 1.03$	$(\Delta/\sigma)_{\text{max}} < 0.001$
1938 reflections	$\Delta_{\text{max}} = 0.83 \text{ e \AA}^{-3}$
127 parameters	$\Delta_{\text{min}} = -0.73 \text{ e \AA}^{-3}$
0 restraints	

Special details

Geometry. All esds (except the esd in the dihedral angle between two l.s. planes) are estimated using the full covariance matrix. The cell esds are taken into account individually in the estimation of esds in distances, angles and torsion angles; correlations between esds in cell parameters are only used when they are defined by crystal symmetry. An approximate (isotropic) treatment of cell esds is used for estimating esds involving l.s. planes.

Fractional atomic coordinates and isotropic or equivalent isotropic displacement parameters (\AA^2)

	<i>x</i>	<i>y</i>	<i>z</i>	$U_{\text{iso}}^*/U_{\text{eq}}$
Br1	0.20720 (14)	0.78129 (13)	0.31263 (5)	0.0206 (2)
Br2	0.28448 (15)	0.94413 (13)	0.11391 (5)	0.0269 (3)
F1	0.5217 (8)	0.3956 (7)	0.3420 (3)	0.0264 (11)
F2	0.8424 (8)	0.2058 (7)	0.2424 (3)	0.0297 (12)
F3	0.9203 (8)	0.3517 (8)	0.0870 (3)	0.0359 (13)
F4	0.6722 (8)	0.6869 (8)	0.0313 (3)	0.0308 (12)
C2	0.4587 (9)	0.7186 (7)	0.1580 (3)	0.0181 (17)
C1	0.4213 (8)	0.6444 (7)	0.2378 (3)	0.0181 (17)
C6	0.5518 (9)	0.4713 (8)	0.2663 (2)	0.0184 (18)
C5	0.7198 (9)	0.3723 (7)	0.2150 (3)	0.0232 (19)
C4	0.7572 (8)	0.4465 (8)	0.1352 (3)	0.0220 (19)
C3	0.6266 (9)	0.6197 (8)	0.1067 (2)	0.0194 (18)
N1	-0.1345 (12)	0.9770 (11)	0.4233 (4)	0.0180 (15)
H1	-0.295 (13)	0.975 (11)	0.389 (4)	0.022*
C7	-0.2150 (13)	0.8204 (13)	0.4901 (4)	0.0202 (18)
H7A	-0.2865	0.6729	0.4676	0.024*
H7B	-0.3512	0.8768	0.5222	0.024*
C8	-0.0225 (14)	1.1997 (13)	0.4559 (5)	0.0231 (18)
H8A	-0.1546	1.2636	0.4874	0.028*
H8B	0.0298	1.3003	0.4111	0.028*

Atomic displacement parameters (\AA^2)

	U^{11}	U^{22}	U^{33}	U^{12}	U^{13}	U^{23}
Br1	0.0211 (4)	0.0220 (5)	0.0190 (5)	0.0039 (3)	0.0026 (3)	-0.0035 (3)
Br2	0.0299 (5)	0.0248 (5)	0.0267 (5)	0.0064 (4)	-0.0027 (4)	0.0059 (4)
F1	0.035 (3)	0.028 (3)	0.018 (3)	0.007 (2)	0.003 (2)	0.006 (2)
F2	0.037 (3)	0.027 (3)	0.029 (3)	0.015 (2)	0.000 (2)	0.003 (2)
F3	0.037 (3)	0.047 (3)	0.027 (3)	0.019 (2)	0.011 (2)	-0.009 (2)
F4	0.039 (3)	0.037 (3)	0.017 (3)	0.004 (2)	0.011 (2)	0.002 (2)
C2	0.014 (4)	0.014 (4)	0.025 (5)	0.000 (3)	0.004 (3)	0.003 (3)
C1	0.018 (4)	0.013 (4)	0.022 (5)	-0.004 (3)	0.002 (3)	-0.006 (3)
C6	0.028 (4)	0.016 (4)	0.009 (4)	-0.006 (3)	0.003 (3)	-0.001 (3)
C5	0.022 (4)	0.017 (5)	0.032 (5)	0.009 (3)	-0.007 (4)	0.000 (4)
C4	0.018 (4)	0.028 (5)	0.022 (5)	0.009 (4)	0.010 (3)	0.003 (4)
C3	0.029 (5)	0.022 (5)	0.007 (4)	0.005 (4)	0.005 (3)	0.008 (3)
N1	0.016 (3)	0.024 (4)	0.014 (4)	0.005 (3)	-0.002 (3)	-0.002 (3)
C7	0.020 (4)	0.022 (5)	0.019 (5)	0.005 (3)	0.008 (3)	0.004 (4)
C8	0.024 (4)	0.022 (5)	0.023 (5)	0.004 (3)	-0.002 (4)	-0.002 (4)

Geometric parameters (\AA , $^\circ$)

Br1—C1	1.900 (3)	C4—C3	1.3900
Br2—C2	1.864 (3)	N1—H1	0.98 (7)
F1—C6	1.327 (5)	N1—C7	1.473 (9)
F2—C5	1.329 (5)	N1—C8	1.461 (9)
F3—C4	1.331 (5)	C7—H7A	0.9700
F4—C3	1.315 (5)	C7—H7B	0.9700
C2—C1	1.3900	C7—C8 ⁱ	1.511 (10)
C2—C3	1.3900	C8—C7 ⁱ	1.511 (10)
C1—C6	1.3900	C8—H8A	0.9700
C6—C5	1.3900	C8—H8B	0.9700
C5—C4	1.3900		
C1—C2—Br2	122.8 (3)	C4—C3—C2	120.0
C1—C2—C3	120.0	C7—N1—H1	105 (4)
C3—C2—Br2	117.2 (3)	C8—N1—H1	115 (4)
C2—C1—Br1	122.2 (3)	C8—N1—C7	110.8 (6)
C2—C1—C6	120.0	N1—C7—H7A	109.8
C6—C1—Br1	117.8 (3)	N1—C7—H7B	109.8
F1—C6—C1	121.9 (4)	N1—C7—C8 ⁱ	109.2 (6)

F1—C6—C5	118.1 (4)	H7A—C7—H7B	108.3
C5—C6—C1	120.0	C8 ⁱ —C7—H7A	109.8
F2—C5—C6	119.7 (4)	C8 ⁱ —C7—H7B	109.8
F2—C5—C4	120.3 (4)	N1—C8—C7 ⁱ	110.0 (6)
C6—C5—C4	120.0	N1—C8—H8A	109.7
F3—C4—C5	119.4 (4)	N1—C8—H8B	109.7
F3—C4—C3	120.6 (4)	C7 ⁱ —C8—H8A	109.7
C3—C4—C5	120.0	C7 ⁱ —C8—H8B	109.7
F4—C3—C2	122.2 (4)	H8A—C8—H8B	108.2
F4—C3—C4	117.8 (4)		

Symmetry code: (i) $-x, -y+2, -z+1$.

1,3-dibromotetrafluorobenzene– piperazine(5a)

Crystal data

Br ₂ C ₆ F ₄ ·C ₂ H ₅ N	Z = 2
$M_r = 350.95$	$F(000) = 332$
Triclinic, $P\bar{1}$	$D_x = 2.276 \text{ Mg m}^{-3}$
$a = 5.1595 (5) \text{ \AA}$	Mo $K\alpha$ radiation, $\lambda = 0.71073 \text{ \AA}$
$b = 6.0243 (7) \text{ \AA}$	Cell parameters from 1140 reflections
$c = 16.7733 (14) \text{ \AA}$	$\theta = 3.4\text{--}24.5^\circ$
$\alpha = 90.556 (8)^\circ$	$\mu = 7.94 \text{ mm}^{-1}$
$\beta = 90.548 (7)^\circ$	$T = 150 \text{ K}$
$\gamma = 100.778 (9)^\circ$	Plate, clear light colourless
$V = 512.09 (9) \text{ \AA}^3$	$0.2 \times 0.1 \times 0.02 \text{ mm}$

Data collection

SuperNova, Single source at offset, Eos diffractometer	2018 independent reflections
Radiation source: micro-focus sealed X-ray tube, SuperNova (Mo) X-ray Source	1476 reflections with $I > 2\sigma(I)$
Mirror monochromator	$R_{\text{int}} = 0.043$
Detector resolution: $16.1428 \text{ pixels mm}^{-1}$	$\theta_{\text{max}} = 26.0^\circ, \theta_{\text{min}} = 3.4^\circ$
ω scans	$h = -6 \rightarrow 6$
Absorption correction: multi-scan <i>CrysAlis PRO</i> 1.171.38.46 (Rigaku Oxford Diffraction, 2015) Empirical absorption correction using spherical harmonics, implemented in SCALE3 ABSPACK scaling algorithm.	$k = -7 \rightarrow 6$
$T_{\text{min}} = 0.336, T_{\text{max}} = 1.000$	$l = -20 \rightarrow 20$
3358 measured reflections	

Refinement

Refinement on F^2	Primary atom site location: iterative
Least-squares matrix: full	Hydrogen site location: mixed
$R[F^2 > 2\sigma(F^2)] = 0.050$	H atoms treated by a mixture of independent and constrained refinement
$wR(F^2) = 0.123$	$w = 1/[\sigma^2(F_o^2) + (0.037P)^2]$ where $P = (F_o^2 + 2F_c^2)/3$
$S = 1.09$	$(\Delta/\sigma)_{\max} = 0.001$
2018 reflections	$\Delta_{\max} = 0.67 \text{ e } \text{\AA}^{-3}$
216 parameters	$\Delta_{\min} = -0.67 \text{ e } \text{\AA}^{-3}$
210 restraints	

Special details

Geometry. All esds (except the esd in the dihedral angle between two l.s. planes) are estimated using the full covariance matrix. The cell esds are taken into account individually in the estimation of esds in distances, angles and torsion angles; correlations between esds in cell parameters are only used when they are defined by crystal symmetry. An approximate (isotropic) treatment of cell esds is used for estimating esds involving l.s. planes.

Fractional atomic coordinates and isotropic or equivalent isotropic displacement parameters (\AA^2)

	x	y	z	$U_{\text{iso}}^*/U_{\text{eq}}$	Occ. (<1)
Br1	0.21212 (13)	0.30377 (12)	0.68378 (4)	0.0316 (3)	
F3	0.603 (3)	0.277 (3)	0.9720 (8)	0.078 (5)	0.728 (3)
F1	0.534 (3)	-0.0701 (19)	0.6697 (5)	0.031 (2)	0.728 (3)
F2	0.875 (2)	-0.052 (2)	0.9319 (4)	0.066 (3)	0.728 (3)
C2	0.560 (2)	0.0201 (17)	0.7422 (4)	0.022 (2)	0.728 (3)
C1	0.421 (3)	0.189 (2)	0.7623 (5)	0.028 (4)	0.728 (3)
C6	0.432 (2)	0.273 (2)	0.8400 (5)	0.038 (3)	0.728 (3)
C5	0.582 (2)	0.1890 (19)	0.8975 (4)	0.049 (3)	0.728 (3)
C4	0.722 (2)	0.0204 (18)	0.8773 (4)	0.044 (3)	0.728 (3)
C3	0.710 (2)	-0.0640 (15)	0.7997 (4)	0.033 (3)	0.728 (3)
F4	0.296 (2)	0.430 (2)	0.8616 (8)	0.052 (3)	0.728 (3)
Br2	0.8954 (3)	-0.2916 (3)	0.77228 (10)	0.0339 (4)	0.728 (3)
H1	-0.248 (12)	0.508 (10)	0.607 (4)	0.023 (18)*	
C7	-0.2175 (12)	0.3167 (11)	0.5094 (4)	0.0283 (15)	
H7A	-0.3519	0.3676	0.4773	0.034*	
H7B	-0.2924	0.1705	0.5312	0.034*	
N1	-0.1292 (11)	0.4802 (10)	0.5744 (3)	0.0278 (13)	
C8	0.0199 (12)	0.2973 (11)	0.4583 (4)	0.0256 (15)	
H8A	0.1528	0.2441	0.4903	0.031*	
H8B	-0.0334	0.1894	0.4152	0.031*	

F1A	0.368 (7)	0.431 (6)	0.852 (2)	0.052 (3)	0.272 (3)
F4A	0.525 (10)	-0.076 (8)	0.6523 (14)	0.061 (11)	0.272 (3)
F3A	0.821 (5)	-0.276 (4)	0.7558 (14)	0.047 (8)	0.272 (3)
Br2A	0.7037 (15)	0.2919 (14)	0.9811 (4)	0.0548 (15)	0.272 (3)
F2A	0.917 (5)	-0.097 (4)	0.9040 (11)	0.045 (6)	0.272 (3)
C6A	0.528 (7)	-0.018 (5)	0.7286 (11)	0.047 (10)	0.272 (3)
C1A	0.415 (8)	0.162 (6)	0.7543 (14)	0.034 (11)	0.272 (3)
C2A	0.470 (8)	0.252 (6)	0.8305 (14)	0.051 (3)	0.272 (3)
C3A	0.639 (6)	0.164 (5)	0.8809 (10)	0.039 (7)	0.272 (3)
C4A	0.753 (5)	-0.016 (4)	0.8552 (9)	0.025 (5)	0.272 (3)
C5A	0.698 (5)	-0.107 (4)	0.7790 (10)	0.029 (6)	0.272 (3)

Atomic displacement parameters (\AA^2)

	U^{11}	U^{22}	U^{33}	U^{12}	U^{13}	U^{23}
Br1	0.0266 (4)	0.0374 (5)	0.0311 (4)	0.0067 (3)	-0.0028 (3)	0.0088 (3)
F3	0.109 (12)	0.110 (8)	0.031 (5)	0.065 (9)	-0.023 (5)	-0.018 (4)
F1	0.037 (5)	0.036 (4)	0.020 (3)	0.009 (4)	0.000 (3)	0.005 (3)
F2	0.076 (6)	0.098 (8)	0.038 (5)	0.056 (5)	-0.021 (5)	0.000 (5)
C2	0.015 (4)	0.024 (4)	0.022 (4)	-0.008 (3)	0.000 (3)	0.000 (3)
C1	0.023 (7)	0.033 (6)	0.027 (5)	0.002 (6)	-0.005 (4)	0.006 (4)
C6	0.040 (6)	0.050 (6)	0.028 (4)	0.016 (5)	-0.003 (4)	-0.002 (4)
C5	0.052 (7)	0.063 (7)	0.036 (5)	0.026 (6)	-0.006 (5)	-0.004 (4)
C4	0.043 (7)	0.064 (7)	0.030 (4)	0.028 (6)	-0.012 (4)	-0.004 (4)
C3	0.035 (6)	0.039 (6)	0.027 (4)	0.013 (5)	-0.002 (4)	0.004 (4)
F4	0.059 (7)	0.070 (4)	0.038 (4)	0.038 (5)	-0.009 (4)	-0.010 (3)
Br2	0.0283 (8)	0.0331 (7)	0.0415 (8)	0.0083 (5)	-0.0013 (6)	0.0050 (5)
C7	0.026 (4)	0.037 (4)	0.025 (3)	0.013 (3)	0.004 (3)	0.007 (3)
N1	0.028 (3)	0.033 (3)	0.023 (3)	0.009 (3)	0.007 (3)	-0.001 (3)
C8	0.024 (4)	0.030 (4)	0.024 (3)	0.009 (3)	-0.009 (3)	-0.001 (3)
F1A	0.057 (8)	0.070 (4)	0.038 (5)	0.038 (5)	-0.011 (5)	-0.010 (4)
F4A	0.062 (19)	0.10 (2)	0.035 (9)	0.038 (16)	-0.008 (8)	-0.005 (8)
F3A	0.053 (16)	0.071 (12)	0.028 (11)	0.039 (11)	-0.011 (8)	-0.013 (8)
Br2A	0.078 (4)	0.068 (3)	0.028 (2)	0.039 (3)	-0.020 (2)	-0.0118 (17)
F2A	0.059 (12)	0.045 (11)	0.038 (10)	0.024 (9)	-0.015 (10)	0.001 (9)
C6A	0.04 (2)	0.066 (17)	0.038 (8)	0.027 (17)	-0.006 (9)	-0.001 (8)
C1A	0.02 (2)	0.054 (17)	0.026 (8)	0.011 (17)	-0.001 (10)	0.005 (9)
C2A	0.057 (8)	0.069 (4)	0.038 (5)	0.038 (5)	-0.010 (5)	-0.009 (4)
C3A	0.043 (14)	0.051 (11)	0.026 (7)	0.021 (11)	0.000 (8)	-0.002 (7)
C4A	0.018 (10)	0.035 (9)	0.021 (7)	0.005 (8)	0.007 (6)	0.006 (6)

C5A	0.018 (12)	0.044 (11)	0.025 (7)	0.007 (10)	0.007 (7)	0.003 (7)
-----	------------	------------	-----------	------------	-----------	-----------

Geometric parameters (Å, °)

Br1—C1	1.909 (5)	C7—C8	1.523 (8)
Br1—C1A	1.886 (11)	N1—C8 ⁱ	1.468 (8)
F3—C5	1.349 (13)	C8—N1 ⁱ	1.468 (8)
F1—C2	1.322 (9)	F1A—C2A	1.333 (18)
F2—C4	1.333 (6)	F4A—C6A	1.322 (18)
C2—C1	1.3900	F3A—C5A	1.355 (19)
C2—C3	1.3900	Br2A—C3A	1.844 (14)
C1—C6	1.3900	F2A—C4A	1.332 (13)
C6—C5	1.3900	C6A—C1A	1.3900
C6—F4	1.326 (9)	C6A—C5A	1.3900
C5—C4	1.3900	C1A—C2A	1.3900
C4—C3	1.3900	C2A—C3A	1.3900
C3—Br2	1.868 (6)	C3A—C4A	1.3900
C7—N1	1.473 (8)	C4A—C5A	1.3900
F1—C2—C1	119.6 (7)	N1 ⁱ —C8—C7	109.1 (5)
F1—C2—C3	120.2 (7)	F4A—C6A—C1A	120.9 (18)
C1—C2—C3	120.0	F4A—C6A—C5A	117.6 (18)
C2—C1—Br1	120.2 (5)	C1A—C6A—C5A	120.0
C6—C1—Br1	119.8 (5)	C6A—C1A—Br1	120.8 (12)
C6—C1—C2	120.0	C6A—C1A—C2A	120.0
C1—C6—C5	120.0	C2A—C1A—Br1	119.0 (12)
F4—C6—C1	121.5 (7)	F1A—C2A—C1A	118.8 (17)
F4—C6—C5	118.5 (7)	F1A—C2A—C3A	121.1 (17)
F3—C5—C6	120.3 (8)	C1A—C2A—C3A	120.0
F3—C5—C4	119.7 (7)	C2A—C3A—Br2A	117.7 (10)
C4—C5—C6	120.0	C4A—C3A—Br2A	122.3 (10)
F2—C4—C5	119.6 (6)	C4A—C3A—C2A	120.0
F2—C4—C3	120.3 (6)	F2A—C4A—C3A	119.1 (12)
C3—C4—C5	120.0	F2A—C4A—C5A	120.9 (12)
C2—C3—Br2	119.7 (4)	C3A—C4A—C5A	120.0
C4—C3—C2	120.0	F3A—C5A—C6A	122.3 (13)
C4—C3—Br2	120.3 (4)	F3A—C5A—C4A	117.7 (13)
N1—C7—C8	108.4 (5)	C4A—C5A—C6A	120.0
C8 ⁱ —N1—C7	110.2 (5)		

Symmetry code: (i) -x, -y+1, -z+1.